Flow Cytometry in Hematopathology

A Visual Approach to Data Analysis and Interpretation

Doyen Nguyen, MD
Lawrence W. Diamond, MD
Raul C. Braylan, MD

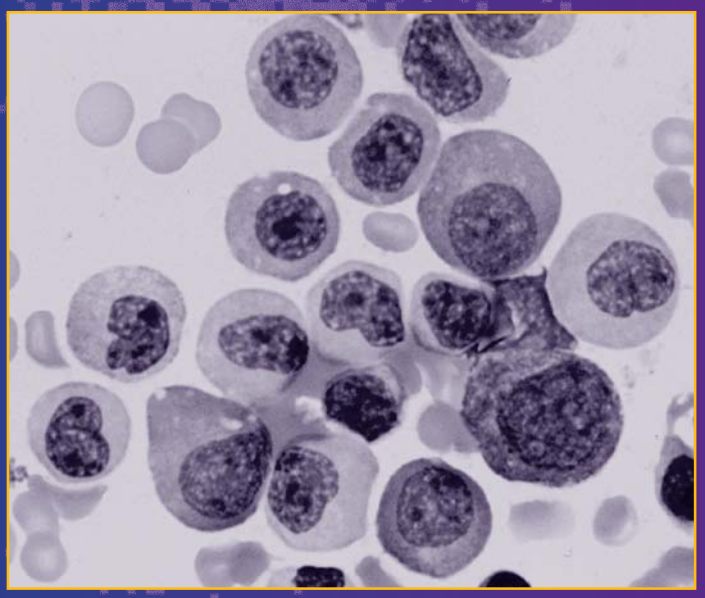

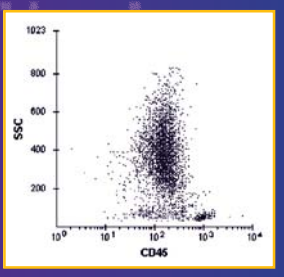

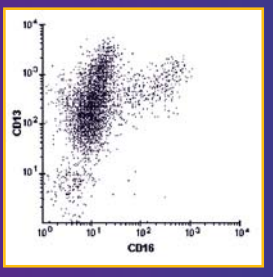

HUMANA PRESS

CD-ROM Included

Flow Cytometry in Hematopathology:

A Visual Approach to Data Analysis and Interpretation

DN and LWD: With all of our love to Vladimir, Petrushka, Fidelio, Feivel, Amadeus, Cherubino, Tamino, Wolfgang (“Bum Jr”), Belmonte, Apollo, Sergei, “Post Auto”, Paddington, “Cookie Jar”, Sasha, Misha, Clipper, Beaker, Lanipo and Hiapo.

Flow Cytometry in Hematopathology:

A Visual Approach to Data Analysis and Interpretation

Doyen Nguyen, MD

Lawrence W. Diamond, MD

Raul C. Braylan, MD

University of Florida College of Medicine
Gainesville, FL

999 Riverview Drive, Suite 208
Totowa, New Jersey 07512

www.humanapress.com

Cover Illustration: Myelodysplastic syndrome. FCM dot plots with an altered CD13/CD16 myeloid maturation curve and low SSC in the myeloid population. Photomicrograph taken by Doyen Nguyen confirming hypogranular bone marrow myeloid precursors. Material from a case seen at the University of Florida.

Production Editor: Jessica Jannicelli.
Cover design by Patricia F. Cleary.

For additional copies, pricing for bulk purchases, and/or information about other Humana titles, contact Humana at the above address or at any of the following numbers: Tel.: 973-256-1699; Fax: 973-256-8341, E-mail: humana@humanapr.com; or visit our Website: http://humanapr.com

This publication is printed on acid-free paper. ♾
ANSI Z39.48-1984 (American National Standards Institute) Permanence of Paper for Printed Library Materials.

Printed in the United States of America. 10 9 8 7 6 5 4 3 2 1

Library of Congress Cataloging-in-Publication Data

Nguyen, Doyen T.
Flow cytometry in hematopathology : a visual approach to data analysis and interpretation / Doyen Nguyen, Lawrence W. Diamond, Raul C. Braylan.
p. cm. — (Current clinical pathology)
Includes bibliographical references and index.
1. Blood—Diseases—Diagnosis. 2. Flow cytometry. 3. Hematopoietic stem cell disorders—Diagnosis. 4. Immunophenotyping. I. Diamond, Lawrence W. II. Braylan, Raul C. III. Title. IV. Series.

RB45.N49 2002
616.4′1075—dc21

2002032239

Contents

Chapter 5 FCM interpretation and reporting

Preface

Flow cytometry immunophenotyping of hematopoietic disorders is a complex and demanding exercise that requires a good understanding of cell lineages, developmental pathways, and physiological changes, as well as broad experience in hematopathology. The process includes several interrelated stages, from the initial medical decision regarding which hematologic condition is appropriate for FCM assay, to the final step of diagnosis whereby the FCM data is correlated with other relevant clinical and laboratory information. The actual FCM testing involves three major steps: pre-analytical (specimen processing, antibody staining), analytical (acquiring data on the flow cytometer) and post-analytical (data analysis and interpretation). The literature, including the latest FCM textbooks, provides ample information on the technical principles of FCM such as instrumentation, reagents and laboratory methods, as well as quality control and quality assurance. Similarly, correlations of morphologic findings and phenotypic profiles have been well covered in many publications. In contrast, much less attention has been given to the other equally important aspects of FCM immunophenotyping, especially data analysis. The latter is a crucial step by which a phenotypic profile is established.

To bridge this gap in the literature, the focus of this book is more on FCM data analysis than laboratory methods and technical details. For the reader to become familiar with our data analysis strategy, an overview of our approach to the pre-analytical and analytical steps is also presented, with an emphasis on the pre-analytical aspects, which have been rarely touched upon in the literature.

The process of data analysis follows a practical and systematic approach, utilizing the visual patterns of the dual parameter displays rather than calculating a "percent positive" for each individual antibody. The FCM graphic displays presented throughout the book, together with the clinical case studies contained in the companion CD-ROM should facilitate the readers to gain an in-depth appreciation of this visual approach to data analysis. Via the case studies, the topics discussed in the textbook can be illustrated in greater detail, and the FCM diagnostic subtleties will become more apparent.

The book is designed for all laboratory professionals involved in the immunophenotyping of hematologic disorders, including pathologists, PhDs and technologists working in FCM laboratories, residents and fellows in pathology and hematopathology training programs, as well as clinical hematologists with a special interest in this subspecialty. In terms of organization, this book breaks away from the traditional mold used in other books. The chapters are not arranged by specific diagnosis (i.e. the end point of a diagnostic work-up) but by how the data presents at the time of the diagnostic consultation. This organization reflects the real life problem-solving methods applied daily in the laboratory, whereby the strategies employed differ depending on whether the cell population in the sample analyzed is heterogeneous or nearly homogeneous.

The few available books covering FCM phenotypes in hematologic malignancies have tended to focus more on leukemias than lymphomas. In this book, equal emphasis is given to both categories of disease, thereby providing considerably more information on lymphomas and chronic lymphoproliferative disorders. Furthermore, DNA cell cycle analysis is also included in the FCM study of mature lymphoid malignancies, in which the DNA data have

been proven to be of prognostic significance, thus permitting a more objective and reproducible grading of these tumors.

The approach to the classification of hematologic neoplasms employed in this book also departs from that used in the various existing classifications. The antigenic profiles of leukemias and lymphomas have been incorporated into the more recent classification schemes. However, the phenotypes of many disorders, in particular malignant lymphomas, have been derived from paraffin-based immunostaining instead of FCM studies, thus not taking into consideration the large amounts of valuable information provided by FCM immunophenotyping (e.g. a better appreciation of the pattern of antigenic density distribution and coexpression). The approach taken in this book is to simplify the classification (which should facilitate the comparison of results between different institutions) by utilizing the graphical patterns of phenotypic expression and the results of DNA cell cycle analysis where appropriate, together with other relevant clinical/laboratory data including the morphology of the submitted specimen. A more detailed discussion on the morphology of the bone marrow and peripheral blood manifestations of hematologic disorders can be found in our previous book (and its companion CD-ROM) entitled "Diagnostic Hematology: A Pattern Approach", ISBN 0 7506 4247 5 (Arnold Publishers, distributed in the USA by Oxford University Press).

For practical reasons, most of the FCM graphics in the book are presented as black and white illustrations. The dot plots in many of the case studies contained in the CD-ROM are, on the other hand, presented in color to facilitate the viewing of the cell cluster(s) of interest, especially for educational purposes. The use of color dot plots is popular in some laboratories. In our opinion, laboratory staff involved in FCM data analysis should be familiar with both black and white and color FCM displays however, rather than relying solely on the color format.

The list of suggested readings is not meant to be exhaustive. Many of the references were chosen mainly for the readers to obtain more depth on certain topics, e.g. the maturation and differentiation of hematopoietic cells.

Acknowledgments

The authors would like to acknowledge David Novo, president of De Novo Software (www.denovosoftware.com) for providing several copies of his FCS Express software to create the FCM illustrations in the book and the case studies contained in the CD-ROM. We would also like to thank our medical colleagues, in particular Wolfgang Huebl, for the contribution of hematologic samples and/or unusual cases. The authors also thank the many FCM technologists they have been associated with for their excellent work, in particular Mikhail Mazharov and the crew at the University of Florida Shand's Hospital hematopathology laboratory, especially John B. Anderson, Heath I. Bailey, Sandra M. Campbell, Catherine R. Charleston, William D. Dixon, Gabriel R. Luchetta, and Darin J. Ryder.

List of Abbreviations

7-AAD	7-amino-actinomycin D
AIDS	Acquired immunodeficiency syndrome
ALCL	Anaplastic large cell lymphoma
ALL(s)	Acute lymphoblastic leukemia(s)
AML(s)	Acute myeloid leukemia(s)
APC	Allophycocyanin
ATLL	Adult T-cell leukemia-lymphoma
BC	Blast crisis
CD	Cluster designation
cKappa	Cytoplasmic kappa
cLambda	Cytoplasmic lambda
CLL	Chronic lymphocytic leukemia
CLL/PL	Chronic lymphocytic leukemia with increased prolymphocytes
CML	Chronic myeloid leukemia
CMMoL	Chronic myelomonocytic leukemia
CMV	Cytomegalovirus
CSF	Cerebrospinal fluid
CV	Coefficient of variation
DI	DNA index
DLCL	Diffuse large cell lymphoma
DNA	Deoxyribonucleic acid
EBV	Epstein-Barr virus
EDTA	Ethylenediamine tetra-acetic acid
ET	Essential thrombocythemia
FAB	French-American-British
FCC	Follicular center cell
FCM	Flow cytometry
FITC	Fluorescein isothiocyanate
FNA	Fine needle aspiration
FRFH	Florid reactive follicular hyperplasia
FSC	Forward scatter
G-CSF	Granulocyte colony stimulating factor
HCL	Hairy cell leukemia
H&E	Hematoxylin and eosin
HIV	Human immunodeficiency virus
HTLV	Human T-cell lymphotropic virus
IM	Infectious mononucleosis
LCL(s)	Large cell lymphoma(s)
LGL(s)	Large granular lymphocyte(s)
LL	Lymphoblastic lymphoma
LPC	Lymphoplasmacytoid
LPD(s)	Lymphoproliferative disorder(s)
MALT	Mucosa-associated lymphoid tissue
MBCL	Monocytoid B-cell lymphoma

MCL	Mantle cell lymphoma
MDS	Myelodysplastic syndrome(s)
MF	Mycosis fungoides
MGUS	Monoclonal gammopathy of undetermined significance
MM	Multiple myeloma
MNC(s)	Mononuclear cell(s)
MoAb(s)	Monoclonal antibody (antibodies)
MPD(s)	Myeloproliferative disorder(s)
MPO	Myeloperoxidase
MRD	Minimal residual disease
N/C	Nuclear/cytoplasmic
NHL(s)	Non-Hodgkin's lymphoma(s)
NK	Natural killer
NOS	Not otherwise specified
NSE	Nonspecific esterase
PCR	Polymerase chain reaction
PE	Phycoerythrin
PerCP	Peridinium chlorophyll protein complex
PLL	Prolymphocytic leukemia
PMT(s)	Photomultiplier tube(s)
PRV	Polycythemia rubra vera
PTCL(s)	Peripheral T-cell lymphoma(s)
RBC(s)	Red blood cell(s)
SCID	Severe combined immunodeficiency
SLL	Small lymphocytic lymphoma
SLVL	Splenic lymphoma with villous lymphocytes
SSC	Side scatter
TCR	T-cell receptor
TRAP	Tartrate-resistant acid phosphatase
WBC(s)	White blood cell(s)

CHAPTER

1

Approach to flow cytometry: General considerations

With the increased availability of antibodies and fluorochromes and the improvements in instrument hardware and software, flow cytometry (FCM) immunophenotyping has become a popular and useful diagnostic tool in the hematopathology laboratory. The utility of FCM immunophenotyping is multifold, as it facilitates (1) the distinction between neoplastic and benign conditions, (2) the diagnosis and classification of lymphomas and leukemias, (3) the assessment of other neoplastic and pre-neoplastic disorders such as plasma cell dyscrasias and myelodysplastic syndromes, and (4) the detection of minimal residual disease in patients with acute leukemia or chronic lymphoid leukemia.

The advantage of FCM is a high degree of efficiency and sensitivity. The technique is also likely to be more reproducible than microscopy. The high level of sensitivity facilitates the detection of rare neoplastic cells (based on their specific characteristics) in a heterogeneous population. The ability to assess multiple parameters simultaneously sets FCM apart from other technologies.

In many institutions, there is a tendency to perform immunological studies only when the lesion is considered difficult to diagnose by conventional morphology. It is preferable, however, that FCM testing be carried out routinely, even when the morphology is apparently typical, since the findings help to confirm the diagnosis and may provide prognostic or other useful biological information. In addition, the data are valuable for follow-up purposes, especially when samples of tumor recurrences are very small (e.g., cerebrospinal fluid [CSF], needle aspirates) where morphologic examination may fail to detect neoplastic cells.

Proper data analysis is a critical step in FCM immunophenotyping. In this process, the phenotypic profile of the cells of interest is derived from the light scatter and fluorescence intensity signals recorded from each individual cell on a cell-to-cell basis (the data thus collected is referred to as list mode data). Although the literature contains numerous publications on the characteristic immunophenotypes associated with different hematologic malignancies, few publications describe how the data analysis was performed.

1.1 Reasons for the necessity of proper data analysis

The common practice in most institutions has been to describe antigenic expression as the percentage of positive cells. The popular approach to FCM analysis has been as follows: (1) The cells are gated first by light scatter, then the antibody fluorescence analyzed on single parameter histograms or dual parameter plots; (2) for each marker, a cursor is moved and set to measure the fraction of cells with fluorescence greater than that of the control sample (in which cells are exposed to an irrelevant immunoglobulin); (3) the results are then reported as percent positive per antibody tested. The origins of this approach to data reporting can be traced back to the microscopic evaluation of immunostaining performed on glass slides (smears, cytospin preparations) and the reporting techniques used for lymphocyte subset analysis (e.g., CD4 in human immunodeficiency virus [HIV]-infected patients).

Immunostaining on glass slides initially used fluorescent probes but has subsequently evolved to the peroxidase- and alkaline phosphatase-based immunocytochemistry techniques.

In this method, the neoplastic cells on the smears or tissue sections are identified visually by routine morphologic criteria. Although dual staining may be achieved by immunohistochemistry in selected situations, the technique is usually limited to a single antibody per slide.

In many laboratories, the larger share of the FCM workload is composed of T- (or other) cell subset determinations on peripheral blood samples that do not harbor malignant cells. In this setting, a change in the number of cells in each subset is clinically important. Furthermore, the cells analyzed are discrete subpopulations of normal lymphoid cells with relatively bright fluorescence. Therefore, it is appropriate to report each subset as a percent positive for each antibody and, where applicable, to calculate the CD4;CD8 ratio. The numerical values thus generated are reminiscent of those obtained for chemistry tests, in which the abnormalities consist of altered levels of the normal components in the blood.

In samples suspected of harboring a hematopoietic malignancy, however, determining the exact number of neoplastic cells is less important than determining whether or not neoplastic cells are present and, if present, the type of hematopoietic neoplasm they represent. Unfortunately, this information is not always apparent from the "percent-positive" data format. The percent-positive format assumes, incorrectly, that within a leukemia or lymphoma, all of the tumor cells uniformly either lack or exhibit the same degree of clear-cut expression for a given antigen. However, in contrast to benign lymphocytes, neoplastic hematopoietic cells of the same clone often do not express the same amount of a given antigen on their cell surface and, therefore, display variability in the fluorescence intensity for that marker. The degree of variability depends on the particular surface antigen. For instance, reporting a case of leukemia as being 40% CD20 positive is ambiguous. This number could represent either (1) a case in which 40% of the cells formed a distinct population with a fluorescence intensity well above the negative control or (2) a single population in which 100% of the cells displayed a shifted fluorescence intensity, but only 40% of the cells were brighter than the background. The latter occurrence is frequently observed when the tumor cell expression for a surface antigen is weak.

1.1.1 The pitfalls of the FCM data format of "percent positive" per antibody tested

In the context of a leukemia-lymphoma workup, it is important to express the immunophenotyping data in ways that avoid ambiguity and offer the optimal information for correlation with other clinical and laboratory data. Expressing the FCM data as "percent positive" per antibody tested is rarely relevant and may even be misleading, as shown in the examples presented below. The use of an arbitrary cutoff value (20% being the most common) for a marker to be considered as positive has contributed to many erroneous interpretations. Although the 20% level has been employed at numerous institutions, none of the publications have described how this number became established. The following real-life examples illustrate why the approach of reporting FCM results as percent positive and omitting the fluorescence data is inappropriate in leukemia-lymphoma immunophenotyping.

Flow cytometry results on a bone marrow from a patient with suspected chronic myeloid leukemia in blast crisis (CML-BC), from an institution where the FCM laboratory is not part of the hematopathology laboratory. The specimen was processed by Ficoll-Hypaque. Other procedure-related information is not available.

CD19	31%	CD34	30%	CD2	11%
CD20	20%	CD14	7%	CD3	13%
CD10	29%	Kappa	8%	CD7	6%
CD13	32%	Lambda	10%	CD5	19%
CD33	26%	HLA-DR	29%		

Based on this format of data reporting and the 20% threshold, the case was interpreted as a biphenotypic blast crisis of CML (positive for CD19, CD10, CD13, CD33). However, when the list mode data was visualized on dual parameter dot plots, correlating the forward scatter (FSC) and antibody fluorescence, it became clear that (1) the neoplastic cells constituted 30% of the cell population in the FCM sample and (2) they were of medium cell size and had the following phenotype: CD19 moderate, CD20 dim, CD10 moderate, CD34 weak, HLA-DR moderate. Other antigens, (i.e., CD13, CD33, CD14, CD2, CD3, CD5, CD7, kappa, and lambda) were not expressed by the tumor cells. The CD13 (32%) and CD33 (26%) were present on mononuclear myeloid precursors (promyelocytes, myelocytes, and metamyelocytes) and not on the neoplastic population. The correct phenotype is that of a precursor B-cell lymphoblast instead of biphenotypic. Correlation with the bone marrow aspirate morphology further confirmed a lymphoid blast crisis of CML.

A limited (follow-up) panel was performed on the peripheral blood of a patient with known chronic lymphocytic leukemia (CLL), to assess the efficacy of anti-CD20 therapy as part of a clinical trial. The lymphocyte count was 3.1×10^7/L. The blood film was unremarkable except for a mild increase in large granular lymphocytes. The FCM data were reported as follows:

CD2	75%	CD19	23%	Kappa	17%
CD3	62%	CD20	18%	Lambda	8%

Based on these results, it was concluded that there was no residual CLL in the patient's peripheral blood. However, subsequent re-evaluation of the list mode data, using the simple correlated displays of FSC and antibody fluorescence, was sufficient to demonstrate the presence of a small population of monoclonal B-cells (CD19 moderate, CD20 weak) with weak kappa expression, in a background of benign T-cells and polyclonal B-cells. Contrary to the initial interpretation, residual CLL was present in the patient's peripheral blood.

It is apparent from the above examples that reporting FCM data as percent positive per antibody tested can negate the usefulness of FCM and easily lead to confusing or erroneous interpretations, which may impact therapeutic decisions.

Some laboratories do include fluorescence data in the FCM reports. However, the data may still be expressed in a suboptimal (and, therefore, inappropriate) manner, as shown in the following case example.

Below are the FCM results on a peripheral blood specimen studied at a teaching hospital:

CD2	48% moderate	CD19	47% moderate
CD3	45% moderate	CD20	26% moderate
CD4	21% moderate	CD22	47% moderate
CD7	47% moderate	sIgM	48% moderate
CD8	20% moderate	Kappa	3% moderate
CD13	3% moderate	Lambda	2% moderate
CD33	1% moderate	CD10	36% moderate
CD34	1% weak	CD45	100% strong
TdT	55% moderate	HLA-DR	55% moderate

The results indicated a proliferation of immature cells (TdT^+). The hospital's conclusion was that the case represented an acute lymphoblastic leukemia (ALL) with a mixed (B-cell and T-cell) lineage. Because of the data-reporting format, it is unclear whether the immature cells are of B- or T-cell lineage, however. Although fluorescence intensities were mentioned, data interpretation in this particular laboratory was actually based on percent positive with an arbitrary 20% cutoff. When proper visual data analysis was subsequently applied to the raw data,

it became apparent that the blood sample contained a clearly identifiable neoplastic population of precursor B-ALL, admixed with a high number of normal T-cells.

1.2 General aspects of FCM data analysis and interpretation

The above-described situations indicate the necessity of a comprehensive approach to FCM data analysis and interpretation. In the authors' experience, the optimal method is for the laboratory medical staff to apply a visual approach to FCM data analysis rather than relying on percentages. In other words, data interpretation is based on a visual appraisal of the FCM graphics, assessing the complex patterns formed by the shape and relative position of the cell clusters observed on various dot plots such as FSC vs fluorescence, side scatter (SSC) vs CD45, and correlated fluorescence dot plots. Any other approach to FCM data interpretation, using a scoring system or percent positive per antibody, underutilizes the full potential of FCM.

Laboratory professionals, as well as clinicians, should realize that visual FCM data analysis is a process reminiscent of the microscopic examination of morphologic material (e.g., bone marrow aspirate smears, lymph node sections) in which the data form a pattern and are reported in a qualitative and quantitative (where appropriate) format. Although microscopic examination encompasses all elements in the sample, reporting the data focuses only on the abnormal component. Similarly, the FCM interpretative report should be based on the cells of interest, even though the list mode data should be collected unselected (i.e., it includes all cells in the sample).

Collecting list mode data ungated ensures that no abnormal cells are lost, because in many instances, the nature of the abnormal population is not yet known at the time the specimen is run. Restricting the initial data collection to certain preset criteria (i.e., a "live gating" approach such as the use of a live light scatter gate) may easily result in "throwing the critical cells away." A specific example is missing a small number of circulating hairy cells when the analysis is live-gated on cells with the light scatter characteristics of normal lymphocytes. An additional advantage of the ungated approach is that the presence of other cells serves as internal positive and negative controls.

After the data have been acquired ungated, certain gating procedures can be applied during the analysis step. Some of the most useful gating strategies include (1) gating on B-cells, to determine clonality (Figure 1.1) and the coexpression of other critical antigens, and (2) gating on CD45 to characterize leukemic blasts (Figure 1.2). These strategies require the use of multicolor (two color, at the very least) antibody combinations. The recommendations by the US–Canadian Consensus on the Use of Flow Cytometry Immunophenotyping in Leukemia and Lymphoma have stressed the necessity of a multiparameter approach to FCM analysis, using multiple fluorochromes in addition to forward and side light scatter.

Since the publication of the Consensus recommendations, there has been a slow increase in the awareness on the visual approach to FCM data analysis. The literature contains very little information on this approach, however. The purpose of this book is to fill this void.

The FCM dot plots and histograms displayed in this book, using FCS Express™ software, are derived from clinical samples analyzed on Becton-Dickinson instruments, using commercially available antibody reagents (*see* Chapter 2). Other current state-of-the-art instruments are equipped with a similar capability for multicolor FCM testing and mechanisms for color compensation. The principles of FCM data analysis presented in this book are applicable to all brands of flow cytometers.

Interpretation of the FCM immunophenotyping results is one step in the diagnosis of malignant lymphoma and leukemia. Although, in many cases the diagnosis is apparent following a visual inspection of the FCM immunophenotyping data together with the DNA cell cycle histogram, in other instances the antigenic profile and the pattern of the cell clusters suggest only

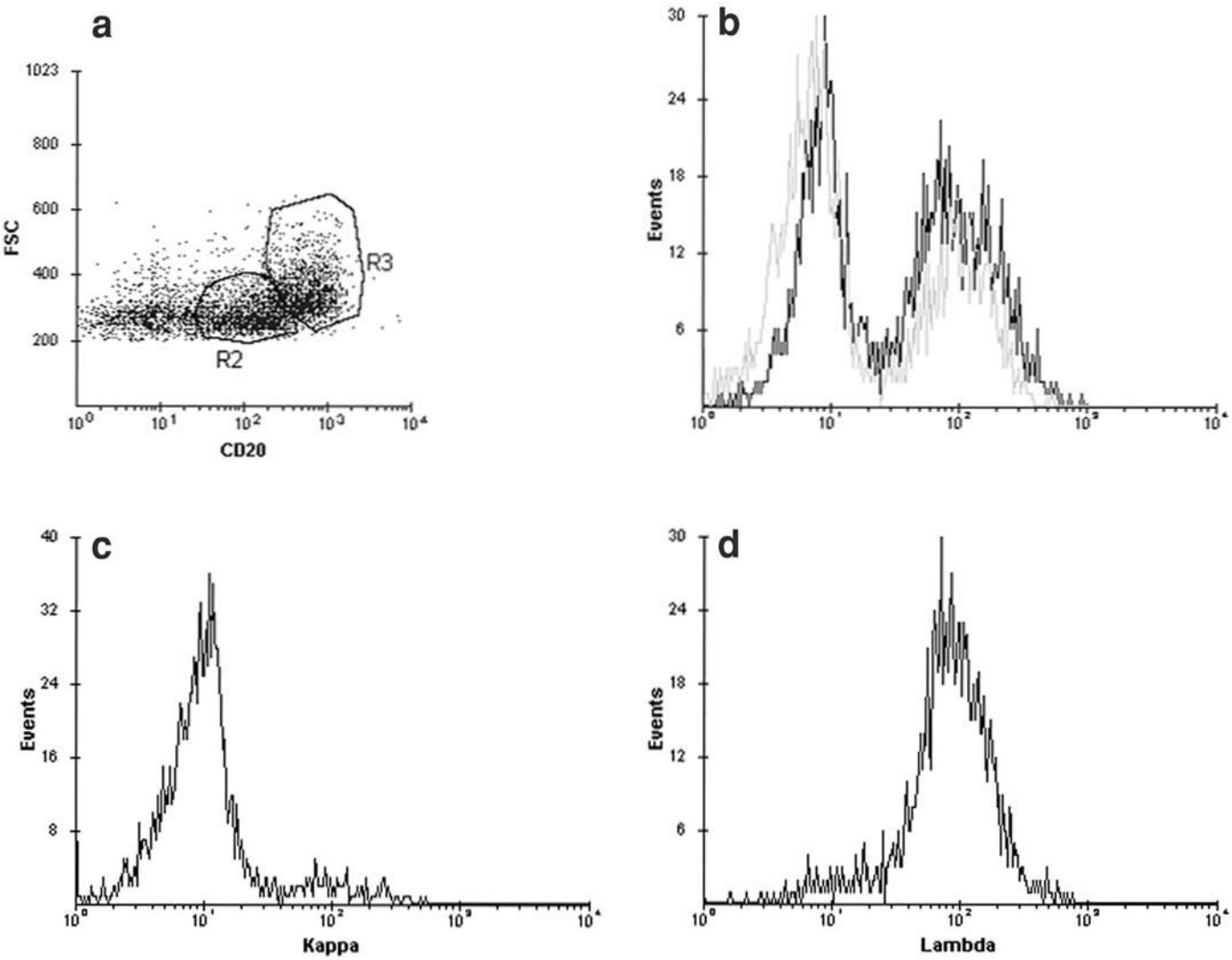

Figure 1.1 (a) Lymph node sample with two B-cells populations differing in FSC signals and CD20 intensities. (b) Overlay kappa/lambda histograms gated on R2: The B-cells with dimmer CD20 and lower FSC are polyclonal. (c,d) Gated on R3: The B-cells with brighter CD20 and higher FSC are monoclonal for lambda.

a differential diagnosis instead of a specific disorder. In such cases, it is critical that the diagnostic interpretation takes into account the other clinical and laboratory data, such as the hemogram findings and the cytologic/morphologic features. The synthesis of the pertinent results requires the responsible medical staff to be well versed in the different subdisciplines of hematopathology. Irrespective of whether a case is straightforward or complex, the authors advocate a routine systematic approach to FCM diagnostic interpretation. This will ensure that no relevant information is omitted.

A correlation between the FCM findings and the available morphologic data should be performed in all cases. Wright–Giemsa-stained cytospins made from the cell suspension of the tissue or fluid submitted for FCM study must be reviewed, to correlate the findings with those derived from the FCM plots. This is especially helpful when abnormal (neoplastic) cells are few or the FCM data cannot be clearly interpreted.

For peripheral blood specimens, the FCM data are correlated with the hemogram and cytologic features from a fresh blood film. Similarly, FCM interpretation on bone marrow speci-

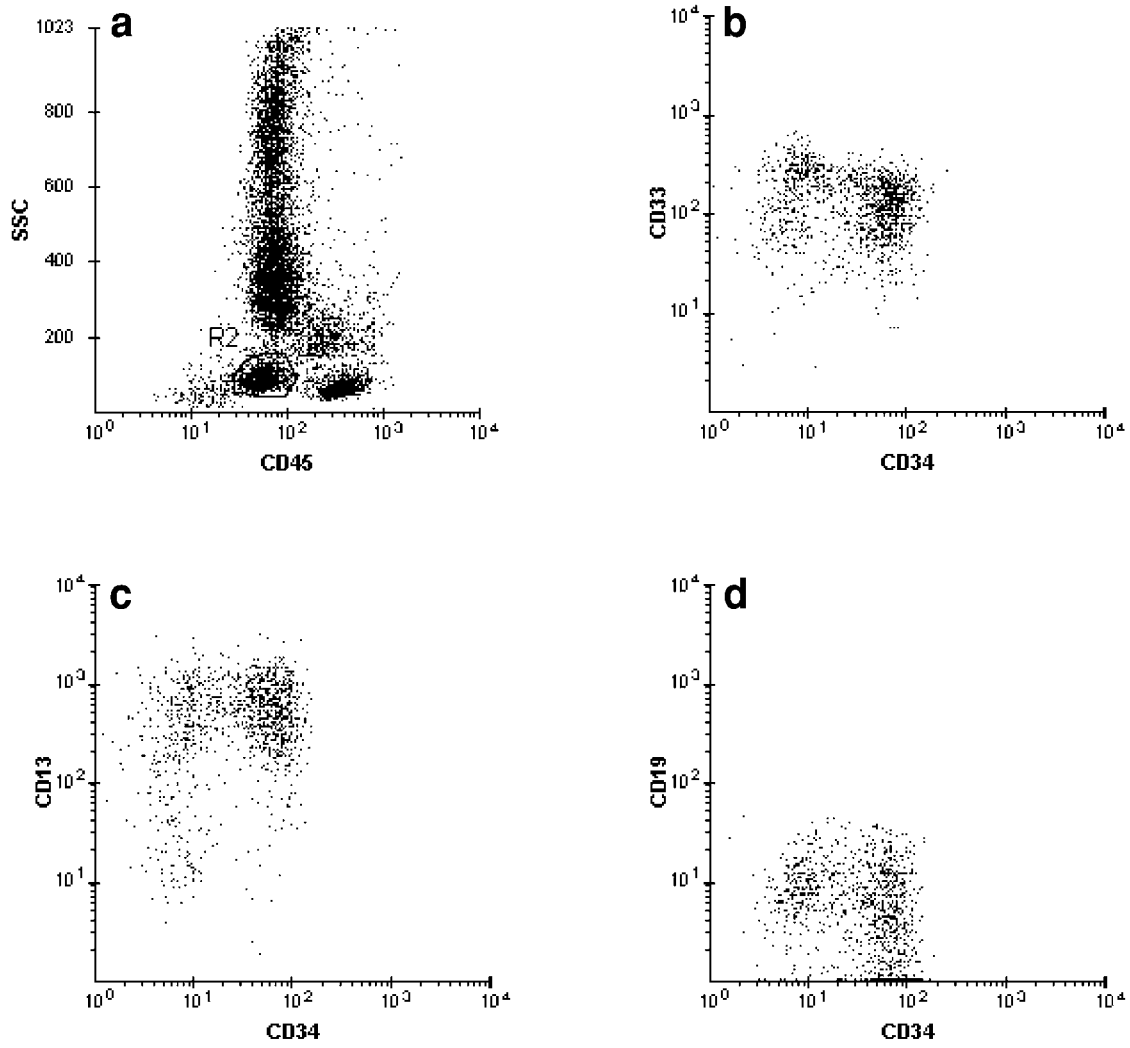

Figure 1.2 (a) Peripheral blood sample with a distinct cluster (R2) in the blast region. (b–d) Gated on R2: Blasts are positive for CD13 and CD33. CD19 is negative. CD34 is expressed with a bimodal distribution.

mens should include a review of the hemogram, peripheral blood film, bone marrow aspirate smear or imprint, and cytochemistries, where appropriate. It cannot be emphasized enough that hemogram findings, along with fresh peripheral blood and bone marrow smears, must accompany the specimen when bone marrow is sent to a referral laboratory for immunophenotyping, so that a proper, thorough diagnostic evaluation of the case can be conducted. For interpretation on solid tissue (e.g., lymph node), the FCM data are correlated with the morphologic features on the imprints and hematoxylin and eosin (H&E) sections (where available).

In addition to the above-mentioned minimum correlation with the morphologic findings, it is also important to review immunoelectrophoresis results in suspected lymphoplasmacytoid neoplasms or plasma cell dyscrasias. Knowledge of the pertinent clinical history, especially the type of therapy (e.g., immunotherapy, growth factors), is also useful to further refine FCM diagnostic interpretation. This necessitates a dialogue between the medical staff caring for the patient and the FCM laboratory. Because of the time delay associated with molecular genotyping and cytogenetics, these techniques play a minimal role at the time of rendering the diagnosis. Correlation of those results with the FCM data is useful, however, for confirming the diagnosis or providing additional information.

1.3 Other applications of FCM in hematopathology

In addition to being a diagnostic tool, FCM analysis has also been used for prognostic purposes. The main caveat, when determining the prognostic significance of biological parameters of neoplastic cells, is that the validity of the results is influenced by various factors such as laboratory methodologies, clinical staging procedures, and therapeutic protocols. Despite such drawbacks, studies have shown that the DNA index may be of prognostic significance in childhood ALL and the S-phase fraction is useful in grading a lymphoproliferative disorder/non-Hodgkin's lymphoma (LPD/NHL). In addition, there have also been attempts to correlate certain antigenic features with the patient's response to therapy or survival. For instance, the intensity of CD45 expression appears to influence the outcome in pediatric ALL. In most leukemias and lymphomas, however, there is only limited evidence that the expression of any particular antigen serves as a reliable predictor of prognosis.

An important application of FCM analysis is the detection of minimal residual disease, especially in acute leukemia. In this regard, FCM was thought not to be as sensitive a technique as polymerase chain reaction (PCR)-based methodologies. However, this apparent lack of sensitivity is most likely due to the fact that the number of cells acquired in a standard FCM clinical assay is far less than that used in PCR analysis. According to recent reports, 1 leukemic cell in 10^4–10^5 bone marrow mononuclear cells can be detected by FCM when a large number of cells are analyzed, thus achieving a sensitivity level comparable to that of molecular analysis. These two techniques complement each other and are best applied in tandem to reduce any potential false-negative results. The FCM approach has the advantage of being less labor intensive and achieving a faster turnaround time. Furthermore, the ability of FCM to separate viable from dying cells permits a more accurate quantitation of minimal residual disease (MRD) levels. Irrespective of the methodology, it appears that the clinically significant MRD level is 0.01% (i.e., 10^{-4}). The presence of residual leukemic cells above this level at the end of therapy or an increase in MRD levels in consecutive bone marrow samples during clinical remission has been shown to be associated with a higher risk of relapse and a poorer overall survival, and it tends to correlate with adverse cytogenetic abnormalities. Thus, evaluation of MRD provides valuable information regarding the aggressiveness of the leukemia and its sensitivity to a given therapeutic regimen. It is expected that routine monitoring of MRD by FCM should facilitate early therapeutic intervention, thereby reducing the morbidity/mortality associated with overt clinical relapse.

1.4 Overview of lineage-associated markers

The cellular markers commonly used in the immunophenotyping of hematologic neoplasms can be broadly categorized into the following groups: B-cell, T-cell, natural killer (NK)-cell, myeloid/monocytic, erythroid, and non-lineage-associated markers (including activation markers such as CD38 and HLA-DR). The establishment of these markers was derived from studies on the differentiation and maturation of hematopoietic cells. Noncommitted hematopoietic stem cells express CD34. There is considerable heterogeneity within the population of $CD34^+$ progenitors, however, and those in the later stages also express HLA-DR and CD38. Another marker of immature cells is TdT, present predominantly, although not exclusively, among lymphoid precursors.

The earliest B-cell precursors can be identified by cCD22, the hallmark of the B-cell lineage. Cytoplasmic CD22 is present even before any detectable rearrangement of the immunoglobulin genes. Also found on early B-cell precursors are CD19 and CD10. The subsequent maturation and differentiation of the B-cell precursors in the bone marrow is characterized by a gradual decrease in CD10 together with a gradual gain in CD20. The appearance of surface

immunoglobulin expression, along with the disappearance of immature markers (TdT, CD34), defines a mature B-cell. Normal mature B-cells enter the circulation and are characterized by the presence of well-expressed surface immunoglobulins, along with CD20 and CD22. The further differentiation into different subtypes of mature B-cells and plasma cells occurs mainly in peripheral lymphoid tissues.

The identifier of a T-cell lineage is cCD3, which appears in the earliest T-cell precursors (i.e., prothymocytes) in the thymus. CD2 and CD7 are also present on the early T-cell precursors. During thymic maturation, the T-cell precursors undergo rearrangement of the T-cell receptor (TCR). This process is accompanied by the appearance of other T-cell lineage-associated markers (CD5, CD4, CD8). In most T-cells, the resulting functional TCR molecule is composed of $\alpha\beta$ heterodimers. A minor population of T-cells express $\gamma\delta$ TCR instead, accounting for about 3–5% of $CD3^+$ T-cells in the blood. The $\gamma\delta$ T-cells emigrate from the fetal thymus to reside in cutaneous and mucosal (especially gastrointestinal) sites. The majority of $\gamma\delta$ T-cells are CD4 and CD8 negative; approximately one-third are CD8 positive. Immunological recognition of a mature T-cell is based on the absence of TdT expression or other early thymic markers (e.g., CD1) and the overt expression of surface CD3.

Following antigen stimulation and cellular activation, a number of other antigens may be newly expressed on activated B- or T-cells. Common activation markers include HLA-DR, CD25, and CD30. Some non-lineage-associated antigens are adhesion molecules, which serve to facilitate cell-to-cell interaction.

Cells of the myeloid lineage may be identified by the expression of CD13, C33, and CD117. The maturation process of myeloblasts into promyelocytes is accompanied by a loss of CD34 and HLA-DR, followed by the expression of CD15, CD11b, and CD16 at the myelocyte and metamyelocyte stages. Intense CD14 is a characteristic of monocytes. An additional identifying feature of monocytes is the expression of other myeloid markers (CD33, CD64), which differ in intensity and distribution from that on myeloid cells.

Erythroid precursors are characterized by downregulated CD45 and high expression of CD71 (transferrin receptor). Antiglycophorin antibodies are of limited usefulness because they react primarily with cells that can be easily identified morphologically as erythroblasts from the basophilic stage onward.

It is important to be aware that some markers, although considered to be associated with a specific lineage, may be expressed by neoplastic cells of a different lineage. For example, CD15 is typically associated with myeloid processes, but it can also be present in a substantial number of T-ALL and precursor B-ALL, as well as monocytic leukemias. Similarly CD7, a T-cell-associated antigen, is often present in acute myeloid leukemia (AML). Such instances have given rise to the concept of aberrant immunophenotypes. The use of the label "lineage infidelity" warrants some caution, however, since not all lineage-associated antigens share the same degree of specificity. For example, antigens such as CD11b, CD16, and CD15 do not constitute sufficient evidence of myeloid differentiation. Furthermore, the concept of aberrancy is based on our current understanding of the normal sequence of phenotypic development, which may still be incomplete and evolving.

The great majority of currently known hematopoietic antigens are not lineage associated. An example of a non-lineage-associated marker routinely used in FCM immunophenotyping is CD56 (neural cell adhesion molecule). Although CD56 is considered to be associated with the NK lineage, it is present in several other types of disorders including plasma cell tumors, small-cell neuroendocrine tumors, and a significant number of AML. Although there is no marker pathognomonic of NK differentiation, true NK cells and NK-like T-cells can be identified based on the combined pattern of expression of one or more "NK markers" (CD16, CD56, or CD57) together with some of the T-cell-associated antigens.

CHAPTER 2

FCM immunophenotyping and DNA analysis: Practical aspects that can affect data analysis and interpretation

In the optimal setting, the FCM lymphoma–leukemia immunophenotyping laboratory is an integral component of the diagnostic hematopathology service. Flow cytometric analysis involves three stages: preanalytical (specimen handling and processing, including antibody staining), analytical (running the sample through the flow cytometer and acquiring data), and postanalytical (data analysis and interpretation). The quality and performance of the preanalytical and analytical steps impact on the resulting fluorescence data and thereby the interpretation. Deficiencies such as suboptimal instrument performance, poor reagent quality (antibodies and/or fluorochromes), or poor specimen quality can all result in inadequate resolution of positive and negative immunofluorescence.

Integrating the FCM and hematopathology laboratories facilitates both the preanalytical steps (because the specimen can be processed simultaneously for other related technologies) and the postanalytical steps (during which the FCM results are correlated with other data prior to establishing a diagnosis). The methodologies used in the authors' laboratories follow closely the recommendations of the US–Canadian Consensus on the Use of Flow Cytometry Immunophenotyping in Leukemia and Lymphoma. The general aspects of the methodologies for the preanalytical and analytical steps are presented in this chapter. Discussions on quality control are not included, however, as they have been presented at length in previous textbooks and manuals.

2.1 Sample selection

The laboratory has little control over certain factors, such as specimen collection and transportation, which can adversely affect the sample prior to its arrival. Although rigorous quality control applied to the various intralaboratory procedures can ensure the accuracy and reproducibility of the FCM results, poor specimen collection remains a major source of potential unsatisfactory FCM analysis. The time elapsed between specimen acquisition and delivery to the laboratory, and the environmental conditions during transport are critical factors affecting the viability of the cells in the sample. As a rule, specimens cannot be held for more than 48 hours in the fresh state after collection. This time window is much narrower for samples harboring a tumor with a high turnover rate (e.g., Burkitt's lymphoma). For these reasons, specimen requirements and acceptance guidelines should be thoroughly communicated to the clinical services as well as to referring institutions. Exposure to extreme temperatures and the presence of blood clots (or gross hemolysis) are conditions that can render a blood or bone marrow specimen unacceptable for analysis.

Fresh specimens for FCM processing and analysis fall into two broad categories: liquid samples (peripheral blood, bone marrow, body fluids) and solid tissue (lymph nodes, tonsils/adenoids, spleen, bone marrow biopsies, and extra nodal infiltrates).

2.1.1 Liquid specimens

Peripheral blood can be collected in either ethylenediamine tetra-acetic acid (EDTA) or heparin. Collection in EDTA is preferred, however, since a hemogram and a blood smear can

be obtained from the same sample. The volume of blood required depends on the white blood cell (WBC) count; 10 mL of blood is adequate in most instances. The blood specimen is preferably maintained at room temperature. Referred blood specimens from outside institutions should be accompanied by a hemogram and a fresh blood smear (i.e., free of storage artifacts), either unstained or stained with Wright–Giemsa, for cytologic evaluation. For quality control, however, the FCM laboratory should also make a smear from the FCM blood sample.

Similarly, EDTA is the anticoagulant of choice for bone marrow specimens sent to the FCM–hematopathology laboratory. Bone marrow smears, cytochemistries where appropriate, and FCM studies can be all performed from the same tube. Ideally, the hematopathology staff should be personally involved with the collection of the bone marrow specimen to ensure that each test (e.g., FCM, cytogenetics, morphology) is allocated a proper amount of representative marrow. Two of the authors routinely performed the bone marrow procedure themselves; the recommended approach has been previously described (Nguyen and Diamond, *Diagnostic Hematology: A Pattern Approach*). As a result, one of the most frequent problems encountered in the laboratory (i.e., the marked discrepancy between the cellular bone marrow smears made at the bedside and those from the severely hemodilute marrow sample submitted for FCM analysis) was minimized. Referred bone marrow aspirate samples received from outside institutions should be accompanied by a fresh bone marrow smear containing an adequate number of spicules. Preferably, a fresh blood smear and hemogram should also be included, so that a complete diagnostic evaluation of the bone marrow can be carried out properly. Approximately 3–5 mL of representative marrow aspirate is usually sufficient for a comprehensive FCM analysis, unless the marrow is severely hypocellular. Bone marrow aspirates have a much higher cell density than peripheral blood specimens. The addition of nutrient media containing serum proteins to the aspirate will help to maintain cell viability in bone marrow samples that cannot be processed soon after collection.

Once received in the laboratory, the bone marrow sample is poured out onto a Petri dish to check if spicules are present. A small portion of the spicules is taken to prepare an "in-house" marrow smear for quality control. Two scalpels are applied to mince the remaining spicules to release cellular elements (especially neoplastic lymphoid cells and plasma cells) that tend to adhere to the spicules.

In the case of an aspicular aspirate ("dry tap"), the FCM marrow sample should consist of at least two 2-cm-long core biopsies submitted in sterile tissue culture media, preferably RPMI supplemented with fetal calf serum and a mixture of antibiotics. Cell suspensions can be obtained from the biopsies by the same mechanical dissociation procedure applied to solid tissue.

In body cavity effusions, it is important to collect samples with good cell viability. This can be achieved by draining off the existing effusion, and later obtaining the reaccumulated "fresh" effusion.

For deep-seated lesions (e.g., mediastinal or retroperitoneal) the preferred specimen for FCM analysis is a fine needle aspiration rather than a core biopsy. Multiple passes (at least 3–4), performed by an experienced person, usually provide a higher cell yield than a tissue core biopsy, and minimize sampling error. Specimens of CSF, being scanty and usually bloodless, do not require much initial processing. A cell count can be obtained and cytospins prepared directly from the submitted sample.

2.1.2 Solid tissue specimens

Solid tissue specimens (e.g., lymph nodes, spleen, tonsil/adenoids, or extranodal sites) should be submitted as thin slices, less than 2 mm thick, in a generous amount of sterile tissue culture media at 4°C (i.e., on ice). This helps to reduce the rate of autolysis and degradation of cellular proteins and DNA. For in-house cases, where specimens are delivered immediately

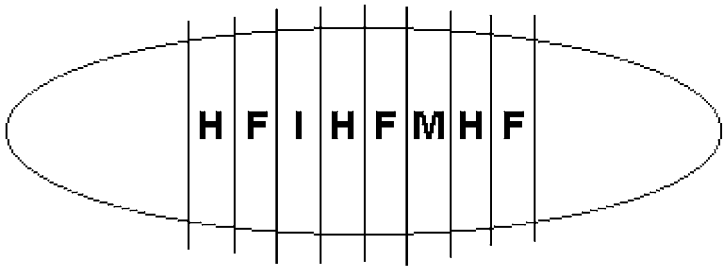

Figure 2.1 Diagram of lymph node slicing and the allocation of the slices to different studies. F: FCM analysis, H: histology, I: immunohistochemistry, M: molecular studies. Each slice is less than 2 mm thick.

to the laboratory, it is only required to keep the tissue moistened with a culture media- (or saline-) soaked gauze. There are no set rules for the required amount of sample because this is dependent on several factors, including the cellularity in the sample, the fragility of the cells, and the susceptibility to apoptosis. More is always better, especially in the case of extranodal specimens where there may be a significant proportion of nonlymphoid tissue or fibrocollagenous stroma. It is important, however, to submit a generous amount of fresh solid tissue to the FCM–hematopathology laboratory, so that an adequate amount of sample may be allocated to various other procedures in addition to the preparation of cell suspensions for FCM analysis. These procedures, potentially necessary for the complete characterization of a particular lymphoid tumor, include the following:

- Snap-freezing for immunohistochemistry or molecular genetics.
- Fixation in a 1;1 mixture of RPMI and ethanol for molecular genetics.
- Wright–Giemsa-stained air-dried touch imprints for cytologic evaluation. The cut surface of the tissue slice should be blotted to remove excess fluid prior to making imprints.
- Fixation for histology, preferably with B-5 or a fixative with a heavy metal component (e.g., barium chloride) for morphologic correlation. For referral cases from an outside pathology laboratory, only a small fraction of the sample submitted to the FCM laboratory is used for histology, since the outside institution has already handled routine histology.

To ensure that the sample is representative, the slices sent to the FCM laboratory should be adjacent to those submitted for routine histology (Figure 2.1). A practice to be avoided is that of submitting the tip of the lymph node for FCM while allocating the central portion for routine histology. It is also not advisable to hold the fresh tissue for FCM analysis until after the histologic sections are ready, because the time delay often adversely affects the viability of the sample.

Cell suspensions are obtained from the solid tissue by mechanical dissociation whereby the tissue is minced with two scalpels in a Petri dish containing a small volume of culture media, then passed through a fine-wire-mesh screen. Alternative techniques such as repeated aspiration of the tissue using an 18-gage needle or scraping the cut surface of the tissue section with a scalpel blade or glass slide at a 45° angle, can also be employed.

2.2 Preparing nucleated cell suspensions

Separating nucleated cells from red blood cells in liquid specimens is achieved by red cell lysis (using ammonium chloride or other solutions). The ghost red cells are removed in the subsequent washing steps. White cells can be stained with antibodies prior to or following red cell lysis. In rare instances, red cells fail to lyse. This may be the result of increased numbers

of reticulocytes (e.g., specimens harboring a red cell disorder such as hemoglobinopathy or thalassemia) or increased lipids in the serum. The unlysed red cells can be electronically removed from analysis, however, by using antiglycophorin antibody and a gating procedure. The red cell lysis procedure is preferred to density gradient methods (e.g., Ficoll-Hypaque) because it allows cells to be maintained close to their native state. Density gradient methods are based primarily on the buoyant density of normal lymphocytes. Because neoplastic cells do not necessarily share the same density as normal lymphocytes, the density gradient methods, despite their ability to remove erythrocytes, mature granulocytes, and dead cells, can result in excessive loss of critical cells. This effect is especially undesirable for samples with a low content of neoplastic cells. In addition, selective population losses in the CD8 subsets can also occur with density gradient techniques.

2.3 Cell yield and viability

Following the red cell lysis step, the cell yield is determined with an automated cell counter. Cytospins are made from the cell suspension to serve as morphologic controls, to ensure that the critical cells have been retained for analysis. When necessary, it is helpful to prepare additional cytospins for cytochemical stains (e.g., myeloperoxidase, nonspecific esterase, tartrate-resistant acid phosphatase). The viability of the cell suspension can be assessed by FCM, based on the uptake of DNA-binding dyes such as propidium iodide or 7-amino-actinomycin D (7-AAD) by dead cells. A manual alternative technique is trypan blue exclusion. As a rule, the cell yield and viability tend to be lower in aggressive tumors composed of large cells than in low-grade tumors composed of small cells. The larger neoplastic cells are more fragile and therefore more susceptible to damage and cell loss during the washing and centrifugation steps of specimen processing. Solid tissue specimens often have lower viability than liquid specimens. There is no set rule concerning the viability level below which a specimen yields uninterpretable data and therefore becomes unacceptable for FCM analysis. A lower viability can be tolerated for specimens composed of nearly all neoplastic cells than for those with a scanty proportion of tumor cells.

2.4 Sample staining

Sample staining should be carried out as soon as possible after the nucleated cell suspension has been prepared. Delaying this step will only reduce viability and induce cell clumping, especially if the tubes holding the cell suspensions are stored in an upright position. With the exception of cases with low cell yield, a portion of the cell suspension should be kept aside for potential repeats or add-on testing.

2.4.1 Surface antigens

The multicolor direct immunofluorescence staining technique using commercially available antibodies is employed for the simultaneous detection of multiple cell surface markers. Cell surface antigen staining is performed on viable unfixed cells. All staining is performed at 4°C to minimize capping and antigen shedding. Appropriate isotype controls are included. The usual number of cells recommended for immunostaining is 10^6 cells for each test (i.e., each tube of antibody reagent cocktail). In situations with low cell yield, it is possible to perform the staining with as few as $(1–2) \times 10^5$ cells/tube, however. The procedure should be carried out gently so as to minimize any further cell loss.

An efficient and cost-saving strategy is the use of a microtiter plate-based method, which reduces the number of cells required for each test and the volume of reagents while maintaining

the same proportions as in the conventional tube method. Each well of the microtiter plate requires only one-fifth of the reagents and cells. Batches of antibody reagent panels in microtiter plates can be prepared in advance, stored frozen, and thawed for use as needed. The microtiter plate method is further enhanced by the use of automated cell handlers. Computer-controlled devices to resuspend and introduce cells into the fluidic system of the flow cytometer are currently available, thus achieving a highly efficient and virtually "hands-off" operation.

2.4.2 Intracellular antigens

Although the testing for intracellular antigens is performed up front in some laboratories, the authors' preference is to have these done as "add-on" tests when it is medically necessary (*see* Section 2.8). The staining procedure is more laborious than cell surface antigen staining and calls for cell fixation and permeabilization. Cells are fixed to maintain structural integrity and are permeabilized to allow antibodies to reach the appropriate intracellular targets. The fixative should preserve the epitope of the intracellular antigen in question without causing aggregation of the cell suspension. Intracellular targets include TdT, cytoplasmic light chains, cCD3, cCD22, myeloperoxidase, and bcl-2. The first two are the most frequently tested. For increased sensitivity, the detection of intracellular antigens is done in conjunction with cell surface antigens [e.g., CD38 (for cytoplasmic immunoglobulins), CD19, or CD10 (for TdT)]. To evaluate surface and intracellular antigens simultaneously, the cell surface molecule is stained first, followed by the fixation and permeabilization step, then staining of the intracellular antigen. As with all staining procedures, appropriate background controls are included. In addition, a cell line expressing the targeted intracellular antigen is run in parallel with the patient's sample.

It may be necessary to determine empirically the optimal staining conditions for the various surface antigen–intracellular antigen combinations to ensure the stability of the antigen–antibody–fluorochrome complexes on the cell surface and the preservation of the targeted intracellular antigens. Because the success of intracellular antigen staining depends on the use of small-sized fluorochromes, antibodies targeted against intracellular antigens are conjugated to fluorescein isothiocyanate (FITC). Other fluorochromes may be used for simultaneous surface antigen labeling. This approach also permits simultaneous analysis of a surface antigen and DNA content analysis (using propidium iodide [PI] fluorescence), as there is a good separation between the emission signals of FITC and PI.

2.4.3 DNA content

In the author's laboratory, DNA ploidy and cell cycle analysis are routinely assessed in malignant lymphomas and acute lymphoblastic leukemia-lymphoma. If the proportion of ALL cells is low (e.g., partial involvement of the peripheral blood or bone marrow), then DNA analysis can be performed in tandem with TdT or cell surface antigen (e.g., CD19) staining. Similarly, if the number of neoplastic cells in a tissue involved by lymphoma is low, DNA analysis can be gated on the critical cells by utilizing a surface label and/or the cell size (FSC) parameter.

DNA staining is performed on fresh cell suspensions. The recommended number of cells for DNA staining is 10^6 because a large number of cells needs to be analyzed to obtain robust measurements of the S-phase, an area that contains relatively fewer cells than the other phases of the cell cycle. The staining procedure is started promptly after the nucleated cell suspension is ready to minimize degradation of DNA. DNA degradation can alter the stoichiometry of dye binding to DNA, thereby affecting interpretation. The authors do not recommend DNA analysis on formalin-fixed, paraffin-embedded tissues. Although this approach makes retrospective studies possible, it often results in poorer quality analysis and an apparently higher

S-phase as an artifact. Furthermore, the archival material precludes simultaneous DNA and cell surface antigen staining.

Propidium iodide, which binds to double-stranded nucleic acids by intercalating between the base pairs, has been the DNA–fluorochrome of choice for clinical applications. Combining PI staining with RNAse treatment has produced consistent high-quality results in the authors' laboratory. The permeabilization step utilizes a fixative, either ethanol or paraformaldehyde. Ethanol fixation provides excellent preservation of DNA for long periods of time, but may cause cell shrinkage and loss of cell surface staining. It is best suited for stand-alone DNA staining. Paraformaldehyde fixation is more appropriate for simultaneous antigen detection (using FITC-conjugated antibodies) and DNA analysis, because it can preserve cell light scatter properties and antigen staining. The concentration of paraformaldehyde and the duration of fixation are critical factors to be considered, as a slight excess may induce DNA crosslinking, thereby increasing the coefficient of variation (CV) of the DNA histograms. The availability of newer DNA fluorescent dyes (e.g., those developed based on the anthraquinones) should help to facilitate the combined DNA–antigen staining procedure.

To identify which peak in the histogram is DNA diploid, a DNA diploid standard (normal lymphocytes, or other DNA-content standards such as chicken or trout erythrocytes) can be run with the patient's cell suspension, in which case two aliquots are prepared for each sample. The smaller aliquot, which contains the diploid standard mixed in with the patient's sample, is used for ploidy determination. The second aliquot is allocated for cell cycle measurements and therefore contains a larger number of cells. Because the presence of added diploid cells may interfere with cell cycle calculations, no DNA standard is added to the second aliquot.

2.5 Data acquisition

The data acquired from the flow cytometer consist of light scatter and fluorescence measurements on single cells suspended in a liquid stream passing single file through a monochromatic light beam produced by a laser. Each cell is an event of a particular light intensity, recorded in an appropriate channel proportional to that intensity.

The light scatter measurements reflect the physical properties of the cells (cell size or internal complexities), whereas the fluorescence data give information on the membrane or intracellular molecules (proteins, DNA) depending on the antibodies and dyes used for labeling the cells. As each dye-labeled cell passes through the light beam, the fluorochrome bound to the cell absorbs light, is excited to a higher energy state, and quickly returns to its relaxed state by emitting a fluorescence signal of a longer wavelength. The fluorescence signals are collected and amplified by photodetectors.

2.5.1 Calibration

The various elements of the flow cytometer, namely light scatter detectors and fluorescence detectors, which include the voltage settings and spectral compensations of the photomultiplier tubes, must be monitored daily to ensure proper data acquisition. Standardized fluorescent beads are used for calibrating the instrument to determine that there have not been significant variations in the instrument settings from day to day. In this procedure, the electronics (i.e., the high-voltage settings of the photomultiplier tubes) are adjusted to place the fluorescence peaks of the beads in the same channels every time, thereby documenting any minor change in the settings. Another set of beads is used to monitor the mean channel and the CV for the FSC, SSC, and each of the fluorescence signals. These parameters are considered to be operating within acceptable limits if the CVs are <3.0 for FSC and SSC and <2.0 for each of the fluorescence signals.

2.5.2 Color compensation

The initial setup of compensation settings is an empirical process, which depends on the fluorochrome combination and the particular instrument (i.e., the optical filters and photomultiplier tubes [PMTs]). Because of the broad emission spectra of fluorochromes, the light collected by an optical filter of a specific wavelength range reaching a PMT, consists of not only the signals from the intended fluorochrome but also signals from other fluorescent dyes. With color compensation, a fraction of the contaminating signals (as measured by their respective PMTs) gets subtracted from the measured signal electronically. The most appropriate material for the initial setup and subsequent monitoring of color compensation is a normal control cell preparation, which consists of mononuclear cells from the buffy coat of a unit of donated blood. Each buffy coat can yield approximately 50–100 vials of 2×10^7 mononuclear cells that can be stored frozen, then thawed for daily use. The control cells are stained with mutually exclusive markers bearing the fluorochromes of interest, such as FITC–CD4, phycoerythrin (PE)–CD8, and peridinium chlorophyll protein complex (PerCP)–CD20. Once compensation has been adjusted for each of the PMTs, the three aliquots are mixed into a single tube and analyzed. Any further modifications to the PMT high voltage or gain setting will require recompensation.

2.5.3 List mode data collection

The goal of data acquisition is to collect measurements (light scatter, fluorescence) from each cell individually. The presence of doublets or aggregates can corrupt the acquired data. The adverse effect of doublet contamination is most serious when the cells of interest are few and the likelihood for confusion with a doublet event is high. The doublets may either originate from the cell suspension or result from an inappropriately high rate of sample throughput. In the latter instance, a doublet is the result of two single particles being so close to each other in the sample core stream that the flow cytometer sees them as a single event. The diameter of the core stream and thereby the alignment of the cells is affected by the sample delivery rate into the flow cell; the higher the sample delivery rate, the wider the core stream and the lower the precision and accuracy of the data collected. Doublets and cell aggregates in the cell suspension can be the result of either delay in analysis or suboptimal tissue dissociation, in which case they are also present on the corresponding cytospins.

When running the sample for DNA analysis, the concentration of cells should be kept high (between 5×10^5 and 2×10^6/mL) and the flow rate low to achieve a low CV. The lower the CV is, the better the measurement of both ploidy and the calculations of the different phases of the cell cycle. In the authors' laboratory, the maximum threshold for the flow rate is 200 cells/second. If the sample contains two different populations with very close DNA contents, the resolution can be improved by lowering the flow rate further. The optimal number of events to be acquired is between 30,000 and 70,000 cells, to achieve adequate statistics for cell cycle determinations. More cells should be acquired when the fraction of neoplastic cells is low. The data are collected ungated (i.e., no data, including debris, is discarded). The extent of debris signals present in the channels below the G0 peak is a clue to the magnitude of the debris in the channels underlying the S-phase and G2 peak.

A slightly higher flow rate, 400–500 cells/second, is acceptable for immunophenotyping. In the authors' laboratory, 20,000–30,000 events are routinely collected ungated from each sample tube after exclusion of the nonviable cells. Low levels (below 1%) of abnormal cells can be detected by an experienced observer when the phenotype is quite specific, such as that displayed by hairy cells. In other instances, where the phenotype is not so pathognomonic, acquiring a higher number of cells will improve the sensitivity of detection. The ungated data collection ensures that no critical cells are missed. After the initial acquisition of ungated data,

in selected cases additional data can be collected (e.g., live-gating to enrich a small population of potentially monoclonal B-cells). All other necessary gating procedures, such as gating on CD45 to identify leukemic blasts, are performed during the subsequent analysis of the originally ungated list mode data. For cases with poor red cell lysis, as evidenced by the presence of abundant red blood cells (RBCs) on the cytospin and a sizable cluster of CD45-negative cells with very low FSC, the data collection should be on 20,000 "non-RBC" events.

A different approach to data collection is applied for the assessment of minimal residual disease because the sensitivity of the detection depends on the number of cells analyzed. According to previous studies on MRD (many using PCR-based methods), it appears that the clinically significant level of MRD is at 10^{-4} and above. For assessing MRD by FCM, detailed information on the phenotypic characteristics of the patient's leukemic cells should be available from a previous FCM analysis at the time of diagnosis. Using a set of appropriate markers, the data are acquired with a "live gate." Greater than 10^5 cells need to be collected in order to achieve a sensitivity of detecting one leukemic cell per 10^4 normal cells.

2.5.4 Exclusion of nonviable cells

Flow cytometric identification of nonviable cells is preferably done with propidium iodide incorporation, especially for solid tissue specimens, as the viability is often lower than that in liquid specimens (Figure 2.2). Another possible but more costly reagent is 7-AAD. An alternative method is to gate dead cells out by the forward scatter parameter. Although dead and dying cells appear larger under the microscope, they have a lower refractive index than viable cells and therefore scatter less light in the forward direction. As a result, they can be removed electronically by excluding the lower FSC channels, where dead cells and debris accumulate. This FSC gating approach is less accurate than PI exclusion, however, especially on samples with cell populations of heterogeneous cell size, because the larger dead cells will fall in the same region as the smaller viable cells.

2.6 Antibody panel design

For the analysis of leukemias and lymphomas, the antibodies are assembled into panels. There has been no agreement between laboratories on a uniform and standardized panel. It is not unusual for the panels in use in a particular laboratory to be based on practical (cost concerns and number of samples) rather than medical considerations. The design of antibody panels reflects one of two opposite approaches to the FCM workup of leukemias and lymphomas: comprehensive vs stepwise. In the first approach, the sample is analyzed with a large panel from the start. The number of antibodies in the panel is sufficiently extensive to permit a full characterization of the neoplasm, including any aberrant expression of the cell surface antigens. In the second approach, the FCM study starts with a limited panel. Then, based on the initial results, further analysis with appropriate antibodies is performed on the remaining sample, if necessary. Not infrequently, more than one round of additional testing may be required before reaching a final diagnosis. The stepwise strategy is more economical in terms of reagent cost, but the turnaround time is slower. The high frequency of additional testing can be disruptive to the laboratory workflow, especially in a laboratory with a high volume of FCM specimens. This can end up being expensive in terms of the technologists' efficiency. A more important factor to consider is the decreased cell viability in the sample between the initial and subsequent additional steps, which, in turn, can affect the results adversely. The comprehensive approach, because of its large battery of reagents, is more costly. Using the microtiter plate technique and/or processing a large number of specimens can offset the cost, however.

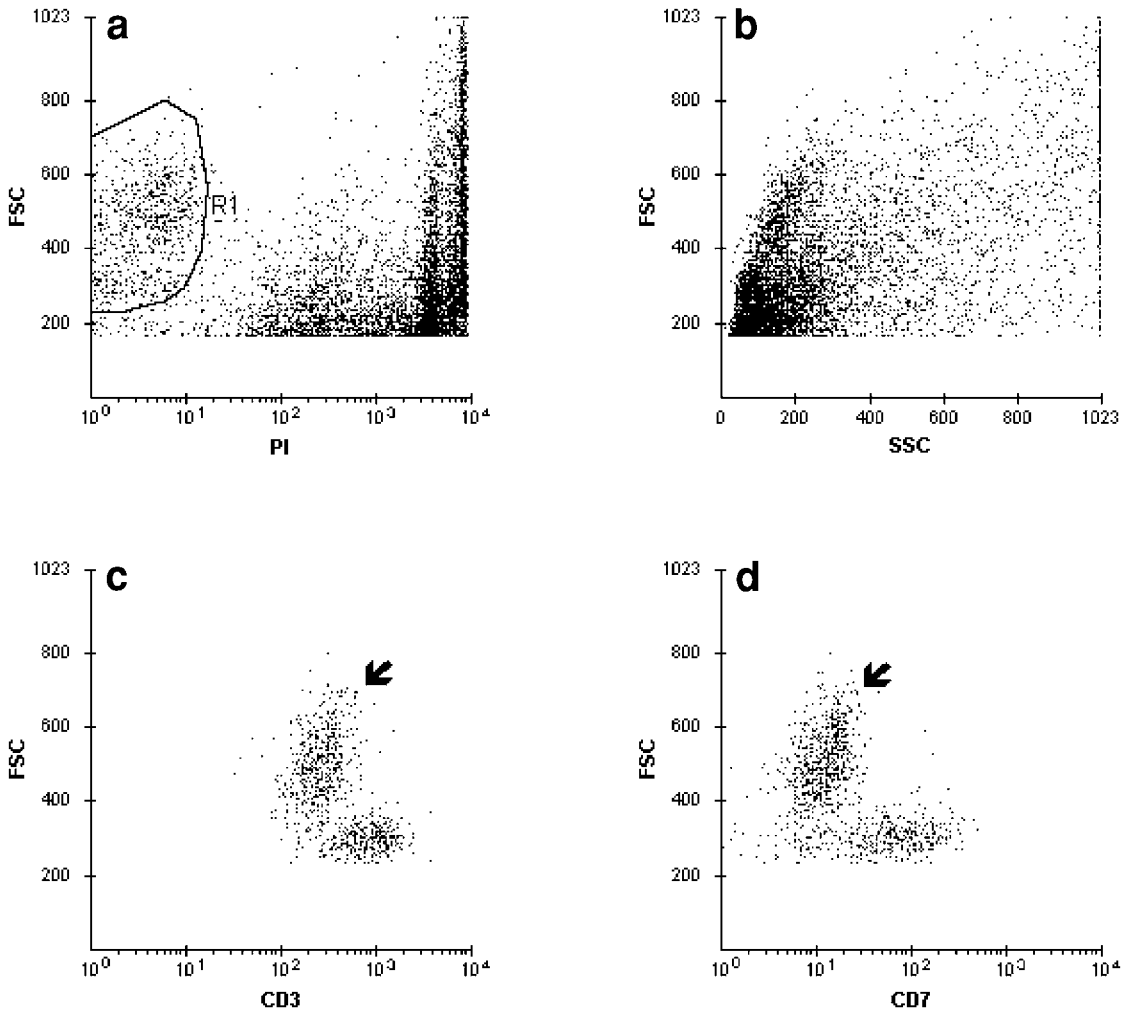

Figure 2.2 Liver with involvement by peripheral T-cell lymphoma. (a) The high uptake of PI by dead and dying cells facilitates the separation of viable (R1 gate) from nonviable cells. The viability in this sample is 15%. (b) The high content of nonviable cells imparts a disarrayed appearance to the ungated FSC/SSC dot plot. (c,d) Gated on R1: The tumor (arrow) demonstrates high FSC, downregulated CD3 and a loss of CD7 expression. Residual T-cells (low FSC, $CD3^+$, $CD7^+$) are present.

The clinical impression or the morphologic features of the specimens should not dictate the design and selection of an antibody panel. Despite efforts to improve the communication between the clinical and laboratory services, the clinical information on the FCM request forms is often scanty, vague, and potentially misleading. Furthermore, to have an antibody panel for each specific group of hematologic neoplasms (e.g., an ALL panel, AML panel, B-cell LPD panel, and T-cell LPD panel) would be inappropriate and defeat the purpose of FCM immunophenotyping. For instance, the presence of many large mononuclear cells in the blood or bone marrow does not necessarily indicate acute leukemia. Involvement by a large cell lymphoma can give a similar morphologic picture and, consequently, lead to the selection of the incorrect antibody panel (i.e., an acute leukemia panel instead of a lymphoma panel). Conversely, small ALL cells in sheets in the bone marrow can be easily mistaken as involvement by a mature B-cell LPD. Errors in panel selection can be circumvented by the comprehensive approach to FCM analysis, and in the absence of economic constraints, it is preferable to apply such an approach. A certain degree of redundancy of some critical antibodies (e.g., CD34 and

CD20) between different tubes is necessary to optimize the sensitivity of FCM analysis and thereby permit the detection of aberrant antigenic expression on neoplastic cells. In the context of a scanty specimen with a low cell yield, however, the morphologic findings or clinical information can be useful for guiding the selection of a limited battery of reagents.

2.6.1 Antibody selection

Given the current large repertoire of reagents available from various manufacturers, careful antibody selection and panel design is important to achieve the best possible diagnostic information. Several technical factors need to be considered, including the type of antibody (monoclonal vs polyclonal), antibody isotype (IgG1, IgG2, IgM), antibody clone, dye conjugation, and preparation by the manufacturer (i.e., the stoichiometry between antibody and fluorochrome). Except for the analysis of immunoglobulins, FCM immunophenotyping relies on monoclonal antibodies. Compared to the polyclonal antibodies used in the early days of immunophenotyping, monoclonal reagents are cleaner, with less background and crossreactivity. Monoclonal antibodies targeted against the same antigen structure but produced by different manufacturers do not necessarily have similar antibody reactivity, however. A specific example is the difference in reactivity between CD14–Leu M3 (Becton Dickinson), CD14–Mo2 (Coulter) and CD14–My4 (Coulter). Another factor to consider when constructing a panel is that antibodies (and fluorochrome conjugation) are more than likely to be optimized (and thus best suited for a particular brand of flow cytometer) if the reagents and instruments are from the same manufacturer.

One advantage of monoclonal antibodies is consistency in titer and affinity from one lot of antibody of the same clone to the next. Subtle changes in the preparation may alter the reactivity however, which, in turn, may affect the usefulness of the antibody in characterizing a particular disorder. A specific example is anti-CD20. This reagent has a wide dynamic range in fluorescence intensity, a useful feature to discriminate CLL/SLL (small lymphocytic lymphoma) from other B-cell neoplasms, as well as distinguishing neoplastic B-cells from a background of benign B-cells. A seemingly minor change in the preparation of the same clone of CD20 antibody can severely alter the fluorescence dynamic range, with the resulting loss of this important discriminating function.

2.6.1.1 Anti-light chain antibodies

The high specificity of monoclonal antibodies, each recognizing distinctly defined epitopes, can be a disadvantage in the detection of immunoglobulins. Immunoglobulins have many epitopes and are, therefore, more easily detectable by polyclonal Fab'_2 fragments than by monoclonal reagents. The immunoglobulins in some mature B-cell malignancies may not be produced correctly; one or more epitopes may be deleted or altered. Staining with a monoclonal antibody may yield a false-negative result if the reagent happens to be specific for the missing or modified epitope, whereas polyclonal antibodies, especially those with broader specificities, will give a positive result by reacting with the other epitopes of the immunoglobulin.

The reactivities of anti-immunoglobulin (kappa, lambda) antibodies can vary widely between manufacturers. To select the optimal brand of kappa and lambda reagents, several candidate pairs are tested at various dilutions with samples from a variety of known disorders, including reactive lymphoid hyperplasia in the lymph nodes or tonsils, CLL/SLL, mantle cell lymphoma (MCL), follicular center cell (FCC) lymphoma, and a neoplasm not producing immunoglobulin (e.g., AML). The samples with reactive hyperplasia, in which both light chains are expressed, are used for titration, to determine the optimal dilution for each reagent. For any given brand of kappa and lambda, the optimal dilution is usually the same for both antibodies. In some instances, however, because of preparation and lot-to-lot variation, one of

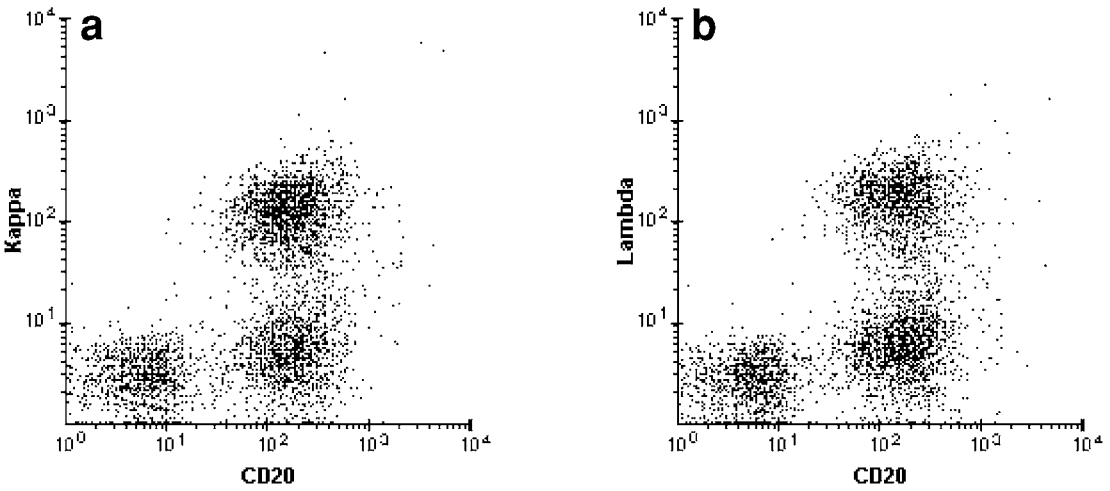

Figure 2.3 Titration of anti-kappa and anti-lambda antibodies using a reactive lymph node. (a,b) CD20-positive B-cells are polyclonal for kappa and lambda. For this particular pair of reagents, kappa had to be one step more dilute than lambda to achieve the desired results.

the two light chain antibodies may need to be diluted more than the other so as to give identical fluorescence signals (Figure 2.3). Based on this comparative evaluation of different brands of kappa and lambda, a given brand is considered optimal if the fluorescence signals fall in the expected range for any given disorder, namely weak intensity in CLL/SLL and moderate to strong in MCL, along with the least background staining.

With some brands of kappa/lambda reagents, it may not be possible to achieve the appropriate fluorescence intensity. The signals, irrespective of the dilutions, are inappropriately bright for samples with CLL/SLL (Figure 2.4) and may fall in the same fluorescence range observed in FCC and MCL. The intensity of surface light chain expression is one of several criteria critical in the diagnosis and subclassification of mature B-cell malignancies. Therefore, in selecting the optimal polyclonal kappa and lambda antibodies, the appropriate fluorescence signal is a more important consideration than the ability to detect extremely dim light chain expression. Lack of detectable light chains in a mature B-cell population invariably signifies an abnormal or neoplastic B-cell population, with the exception of benign plasma cells and reactive large germinal center cells. For this reason, it is also not necessary to conjugate the light-chain antibodies to a fluorochrome with a high quantum yield such as PE. Furthermore, because the kappa antibody serves as a control for lambda and vice versa, it is advisable to conjugate these antibodies to the same type of fluorochrome (i.e., FITC). Preferably, the antibody panel should contain two sets of kappa and lambda reagents from different manufacturers, each pair combined with a different B-cell marker in the following configuration: kappa (1)–FITC/CD20–PE and lambda (1)–FITC/CD20–PE; kappa (2)–FITC/CD19–PE and lambda (2)–FITC/CD19–PE. In the authors' experience, this strategy is more sensitive than the popular combination of kappa–FITC/lambda–PE (available as a kit from most manufacturers), especially when the monoclonal B-cells coexist with a larger population of benign B-cells. Another advantage of this approach is the possibility of assessing the relationship between CD19 and CD20, a valuable feature in the characterization of low-grade B-cell neoplasms (*see* Section 3.6.2).

2.6.2 Fluorochrome conjugation

For certain antibodies, conjugation to a particular fluorochrome can affect how much information can be derived from the test results. A specific example is the conjugation of FITC to CD10, used in combination with CD20–PE.

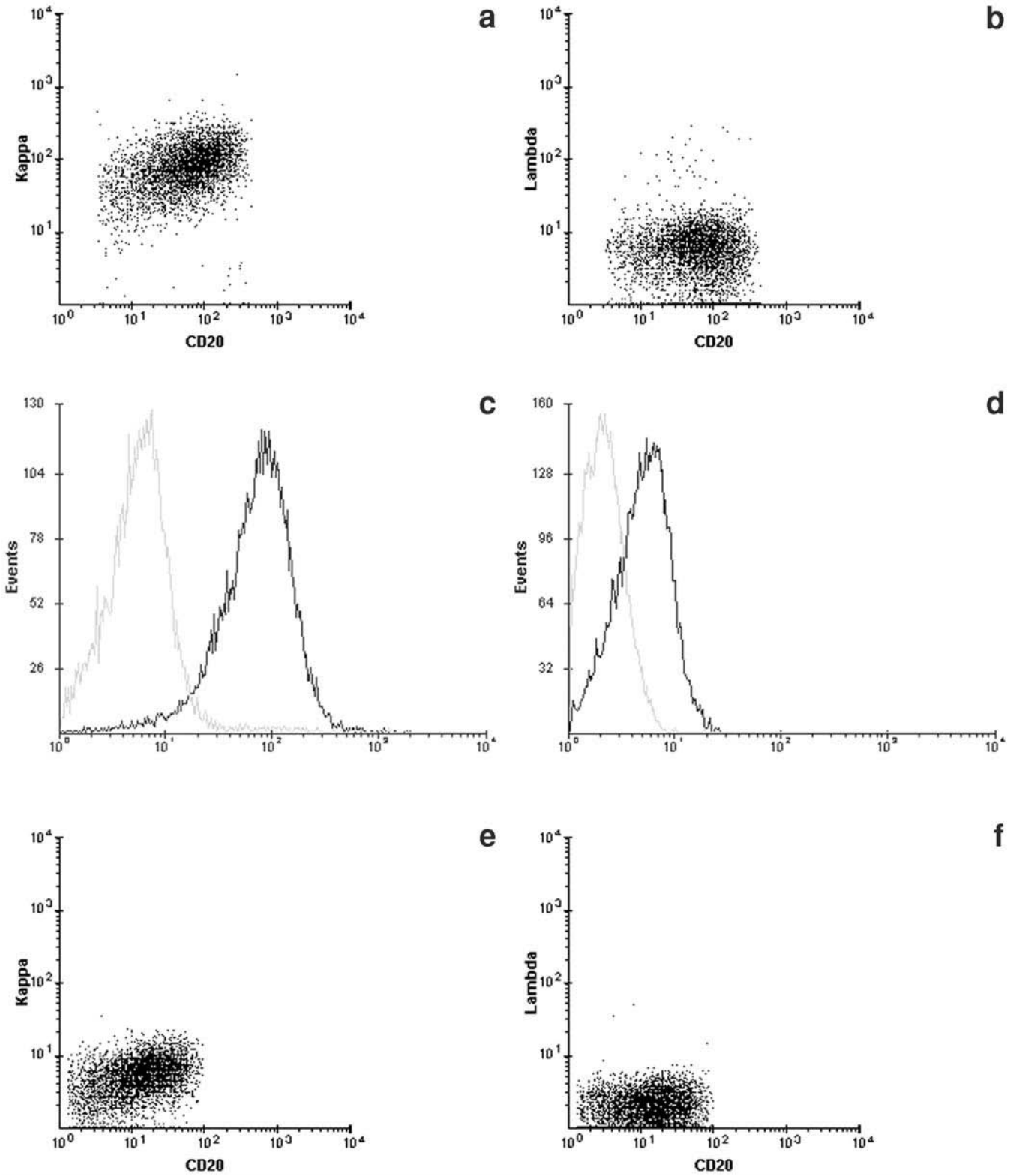

Figure 2.4 Selection of kappa and lambda reagents tested on the same specimen. (a,b) First set of antibodies: The intensity of the positive kappa light chain on CLL cells is inappropriately bright. The peak fluorescence of kappa is one decalog brighter than that of lambda (c). (e,f) The second set of reagents from a different manufacturer yields appropriate results (i.e., dim positive kappa on CLL cells). The same results are seen on the corresponding kappa/lambda overlay histogram (d).

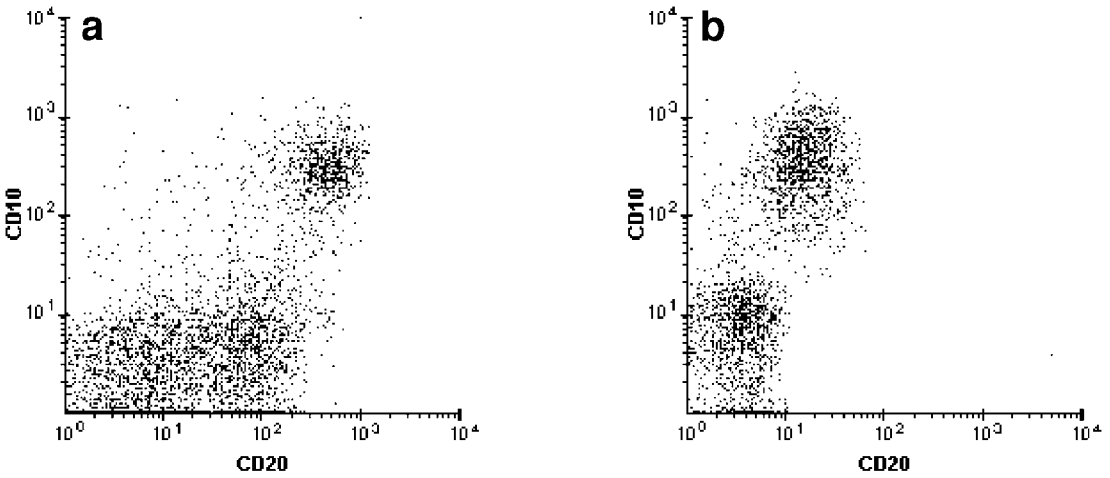

Figure 2.5 (a) The conjugation of CD10 to PE results in an apparent increase in CD10 brightness on the benign germinal center cells (lymph node with FRFH). The resulting CD10/CD20 staining pattern becomes similar to, rather than distinctive from, that seen in a lymph node with FCC lymphoma (b). In (b), CD20 is downregulated because the patient has been treated with anti-CD20.

The pattern of cell clusters on the CD10–FITC/CD20–PE dot plot is useful for distinguishing the following: (1) normal precursor B-cells (hematogones) from precursor-B ALL cells and (2) follicular lymphoma from florid reactive follicular hyperplasia (FRFH), either of which can present with no detectable light chain. In FRFH, the different cell clusters are seen in close continuity with each other (*see* Section 4.1.1.1). When CD10 is conjugated to PE, however, the dot plot pattern does not yield the same useful information because the apparent CD10 expression on reactive germinal center cells becomes much more intense. The resulting cell cluster is well separated from other cell clusters (Figure 2.5), an appearance similar to FCC lymphoma. On the other hand, CD10–PE, when combined with kappa–FITC and lambda–FITC, can be useful for detecting residual/relapsed follicular lymphoma in patients treated with anti-CD20 agents.

The selection of fluorochromes to be conjugated to the monoclonal antibodies (MoAbs) is based on the principle that a fluorochrome with a high quantum yield must be used if the antigen sought after is expressed at a low level. Otherwise, the MoAb can be conjugated to a fluorochrome with lower quantum yield, such as FITC. For antigens known to be present at high density (e.g., CD45), the corresponding MoAb can be conjugated to PerCP. For example, CD13 and CD33 should be conjugated to PE so as to maximize the separation of cells expressing these antigens. This principle does not apply to the surface light chains on B-cells, however, because weak expression of monoclonal light chains is a useful diagnostic criterion for the subclassification of B-cell LPD/NHL.

The higher the number of fluorochromes for simultaneous analysis, the lower the number of tubes in the antibody panel and the lower the total number of cells required for the entire FCM study; reagents and cells are thus utilized more efficiently. Five-parameter analysis (i.e., with three fluorochromes) is currently the norm. Four-color labeling is more desirable if there are no associated technical difficulties. The four-color assay is most suitable for evaluating MRD, where the sample may be scanty and the number of critical cells rare. However, the sensitivity, precision, and accuracy of four-color vs three-color testing have not yet been formally compared.

When testing solid tissue samples that often contain a significant number of dead cells, it is prudent that one of the dyes be used for excluding nonviable cells. In designing reagent cock-

tails for multicolor staining, it is important to be aware that one antibody can interfere with the reactivity of another; this can be due to either the isotype of the antibody and/or the type of dye, to which the antibody is conjugated. The electronic process of color compensation is based on the assumption that there is no steric hindrance, enhancement of binding, or dye-to-dye interaction (such as energy transfer or quenching) between the antibodies present in the cocktail. In general, IgG antibodies are preferable to IgM because there is less likelihood for nonspecific binding and steric hindrance. Similarly, a very large size fluorochrome can cause steric interference.

The authors prefer the single molecule type of fluorochrome, namely FITC, PE, allophycocyanin (APC), and PerCP to the large tandem conjugates such as PE–Texas Red or PE–Cy5. Proper energy transfer (i.e., the enhancement of the fluorescence of the acceptor molecule) simultaneous to the quenching of fluorescence of the donor, is critical to the function of a tandem conjugate. When there is inefficient energy transfer between the donor and the acceptor molecules, or nonspecific binding to the Fc receptor of monocytes (e.g., PE–Cy5), the use of tandem conjugates may lead to misleading results. The argument for using tandem conjugates is the possibility to perform four-color immunophenotyping on instruments equipped with a single laser (488 nm). Potential problems, namely steric interference and the difficulties in achieving optimal color compensation among the four fluorochromes, must be carefully considered in this approach, however.

2.7 Comprehensive antibody panels

In the authors' laboratory, the antibody panels have been designed based on a comprehensive approach to FCM analysis. The rationale is to optimize the detection and characterization of the critical cells for determining (1) the lineage of the cells of interest (e.g., myeloid, B-cell, T-cell) (2) their maturity status (3) the clonality, where appropriate (4) the specific subtype of hematopoietic malignancy and (5) the status of the normal elements present. The use of large comprehensive panels also facilitates the detection of two or more unrelated neoplastic processes present in the same specimen. Appropriate isotype controls are included in the panels. The evaluation of the FCM data also relies on internal controls, however (e.g., T-cells serve as internal control for B-cells and vice versa) (Figure 2.6).

2.7.1 Disease-oriented antibody panels

Over the years, the panels have evolved to incorporate new monoclonal antibodies of diagnostic significance. Recently, the authors have modified the design of the panels from a disease-oriented approach to one based on specimen type. The former strategy includes panels directed toward acute leukemia, lymphoproliferative disorders, or both types of disease. The differences between the acute leukemia and lymphoproliferative panels are that the former includes myeloid markers (e.g., CD13, CD64) whereas the latter contains additional antibodies (e.g., CD25, CD103) necessary for subclassifying LPDs and lymphomas. Antibodies needed to identify the lymphoid lineages as well as maturity status are present in both panels.

The more comprehensive panel combines all of the antibodies of the acute leukemia and lymphoproliferative panels and is most useful when no relevant clinical information is available and the number of critical cells is so low as to escape routine microscopic screening (or the nature of the abnormal cells undetermined by morphologic criteria). The maturity status of the neoplastic cells (e.g., blasts vs large lymphoma cells in the blood or bone marrow) may not be apparent on morphologic examination, because critical cytologic features such as nuclear chromatin can be easily altered by a slight degree of suboptimal staining and processing.

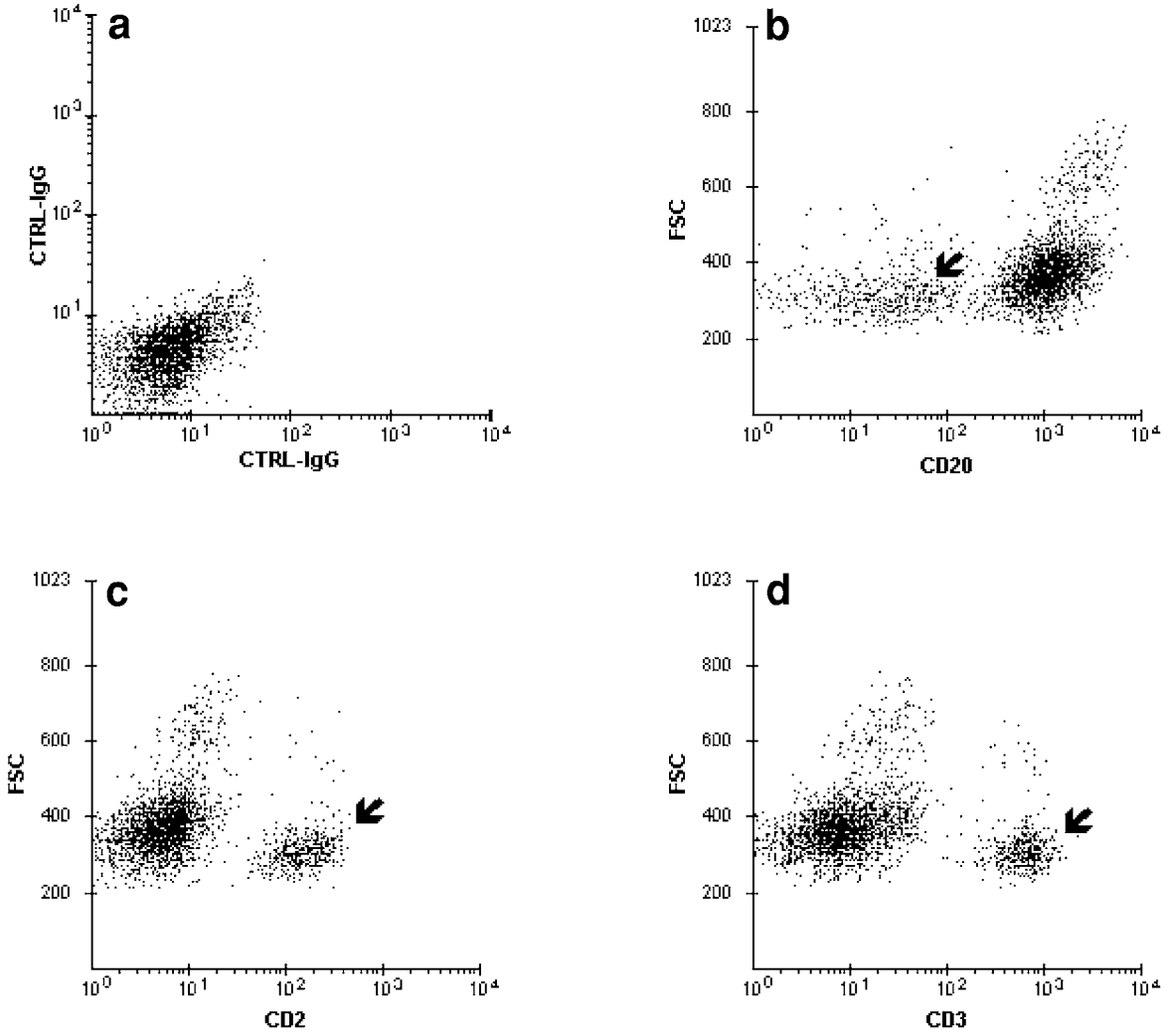

Figure 2.6 Isotype-matched negative controls (a) and internal controls (b–d). The normal residual T-cells (arrows) serve as a negative internal control for CD20 and a positive control for CD2 and CD3. The tumor cells, which comprise the larger cell cluster, are positive for CD20 and negative for CD2 and CD3.

2.7.2 Antibody panels oriented by specimen type

The main drawback to the disease-oriented strategy is that in order to select the proper panel (acute leukemia vs lymphoproliferative), morphologic screening of the specimen by an adequately experienced professional is required. In the authors' experience from several laboratories (United States and Europe), incorrect panel selection because of morphologic misinterpretation is not an infrequent occurrence. To circumvent these issues, the authors have replaced the above antibody panels with panels oriented by specimen type. Thus, the two new panels are a blood/bone marrow/spleen (BBS) panel and a tissue/fluid (TF) panel. This strategy is based on the following rationale: (1) There is an equal predilection for immature hematopoietic malignancies (namely AML and ALL) as well as mature lymphoid neoplasms (B-cell or T-cell LPD/NHL) to involve the blood, bone marrow, and/or spleen and (2) solid tissue and body fluids are much more often involved by lymphoid malignancies (irrespective of the maturity status of the neoplastic cells) than by myeloid neoplasms. In addition, disorders such as plasma cell tumors and hairy cell leukemia (HCL) occur infrequently in the tissue and fluid compartments. The BBS panel, similar to the combined panel under the disease-

Table 2.1 A three-color version of the BBS panel

FITC	PE	PerCP
CD34	CD117	CD45
CD34	CD33	CD45
CD16	CD13	CD45
CD16	CD11b	CD45
CD71	HLA-DR	CD45
CD19	CD34	CD45
CD10	CD20	CD45
CD5	CD19	CD45
CD19	CD23	CD45
CD103	CD20	CD45
CD20	CD11c	CD45
CD25	CD20	CD45
CD4	CD8	CD45
CD7	CD3	CD45
CD2	CD56	CD45
CD138	CD38	CD45
Kappa $F(ab')_2$	CD19	CD45
Lambda $F(ab')_2$	CD19	CD45
Kappa $F(ab')_2$	CD20	CD45
Lambda $F(ab')_2$	CD20	CD45
IgG1	IgG1	CD45
IgG2	IgG2	CD45

Note: For blood and bone marrow samples, viability is tested first. Occasionally, if viability is low, PI is added to the tubes.

oriented strategy, contains a large battery of surface antibodies up front, to permit a full characterization of the neoplasm. The TF panel is smaller, because several of the myeloid-associated markers, as well as CD103 and CD138, are not included. In the unusual event where the data reveal involvement of the tissue or fluid by AML, HCL, or plasma cell tumors, then the necessary antibodies are run as add-on tests using portions of the cell suspensions that are routinely set aside for such eventualities.

A three-color version of the BBS panel (Table 2.1) and TF panel (Table 2.2) are shown to illustrate our approach to FCM analysis and to facilitate the readers with the viewing of the FCM illustrations and case studies, many of which are derived from specimens analyzed using the three-color approach. The guidelines [e.g., the use of two sets of kappa and lambda from different manufacturers (one paired with CD20 and the other with CD19)] applied in the three-color version are retained as the panels get modified to a four-color version.

The construction of the cocktails has been aimed at getting the maximum diagnostic information from the antibodies, especially those with a wide dynamic range. A specific example is the previously mentioned CD10–FITC/CD20–PE combination. Another important cocktail is CD11c–FITC/CD20–PE. Because of the wide dynamic range of CD11c, the pattern and the position of the critical cells on the dot plot permits one to distinguish HCL from other CD11c-positive B-cell LPDs (*see* Section 3.6.3.2). This combination is especially helpful because a small number of B-cell LPDs may exhibit CD103 (B-ly7 clone) reactivity identical to HCL. In general, markers with a wide dynamic range are more useful, as cell populations positive for the same marker can be easily distinguished by their different fluorescence reactivities with that marker. Compared to other B-cell antibodies (e.g., CD19, CD22, FMC-7), CD20 has an optimal wide dynamic range. Therefore, most of the antibodies needed for the characterization of B-cell LPD/NHL are anchored to CD20 instead of CD19. The panels do not include FMC-7 or CD22 since, in the authors' experience, these provide no additional diagnostic information to CD19 and CD20.

The main utility of FMC-7 is its absence; lack of FMC-7 expression is a typical finding in CLL. However, this feature is rather redundant for the diagnosis of CLL in light of the char-

Table 2.2 A three-color version of the TF panel

FITC	PE	3rd Color
CD5	CD19	PI
CD19	CD23	PI
CD20	CD11c	PI
CD10	CD20	PI
CD25	CD2	PI
CD4	CD8	PI
CD7	CD3	PI
CD16	CD56	PI
Kappa $F(ab')_2$	CD19	PI
Lambda $F(ab')_2$	CD19	PI
Kappa $F(ab')_2$	CD20	PI
Lambda $F(ab')_2$	CD20	PI
IgG1	IgG1	PI
IgG2	IgG2	PI
CD71	CD33	CD45–PerCP
CD34	CD19	CD45–PerCP

Note: The antibodies listed in the TF and BBS panels are obtained from the same manufacturer supplying the flow cytometers (the authors' laboratory is equipped with Becton Dickinson instruments) with the exception of CD103 (B-ly7), CD138, and the two sets of kappa and lambda.

acteristic CD20 fluorescence pattern and the relationship of CD20 to CD19 (*see* Section 3.6.2) in this disorder. On a dual fluorescence display of FMC-7 and CD20, a clear linear relationship can be demonstrated (Figure 2.7).

2.8 Tailored panels and add-on testing

In addition to these large routine panels, smaller panels can be tailored to analyze follow-up specimens of patients with a recent diagnosis of hematopoietic malignancy if the original graphical FCM data from the diagnostic sample is available for review. The smaller panel is especially applicable if the follow-up specimen (e.g., CSF, fine needle aspiration [FNA]) has a low cell yield. For instance, a so-called "clonal excess detection" panel can be applied to follow patients with B-cell LPD/NHL. The minimal clonal excess panel should contain CD19, CD20, kappa, and lambda. When appropriate, CD10, CD103, or CD5/CD23 are included. The antibody combinations for the tubes are similar to their counterparts in the standard panels.

Because of it scantiness, CSF is handled differently from other specimens. Most CSF samples are submitted as follow-up specimens, to rule out involvement by acute leukemia (primarily ALL) or, less commonly, high-grade LPD/NHL. The cytospins may be reviewed first to determine if FCM is applicable. In general, when suspicious cells are present, the selection of the key antibodies to analyze the CSF is based on the FCM results from an earlier diagnostic specimen (e.g., lymph node, bone marrow). Often the neoplastic cells can be detected using three or four antibody combinations in a single tube.

Antibodies to detect intracellular antigens (TdT, myeloperoxidase [MPO], cytoplasmic light chains, cCD3, cCD22, bcl-2) are not included in the authors' standard panels. The analysis is performed as an add-on test because antibody staining for intracellular antigens is more time-consuming than that for surface antigens. Because T-cell LPD/NHLs occur infrequently in the Western world, testing for the surface antigens TCR α/β and TCR γ/δ is also performed only on a case-by-case basis.

To maintain the optimal efficiency in a busy FCM–hematopathology laboratory, the following guidelines can be applied to "automate" the decision of when and which intracellular antigen staining to perform:

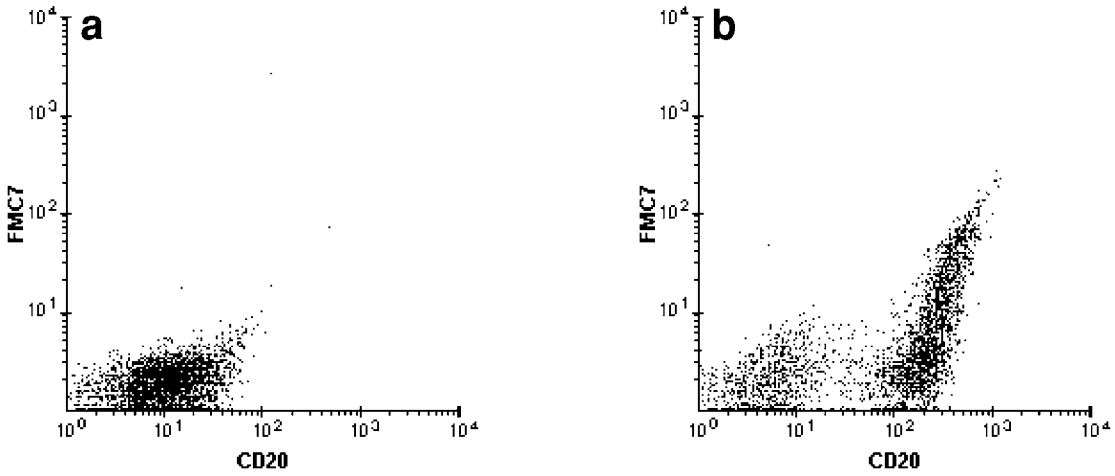

Figure 2.7 Relationship of FMC-7 to CD20. (a) Downregulated CD20 and absent FMC-7 in CLL/SLL; (b) FMC-7 and CD20 coexpression in Burkitt's lymphoma.

TdT: Reactivity with either TdT or CD34 indicates that the neoplasm is composed of immature cells. Therefore, testing for TdT may be omitted for maturity assessment if the leukemia is already $CD34^+$. TdT testing is most appropriate when the results from the standard panels indicate a lymphoid neoplasm with no CD34, no surface light chain expression, and no evidence of plasma cell differentiation. In that case, TdT is necessary to establish the maturity status of the tumor cells, which affects the diagnosis and therapy. A useful approach to assess TdT in ALL is to combine the TdT assay with DNA analysis. Aneuploidy is not only helpful as a prognostic marker but the TdT/DNA combination will also serve as a useful fingerprint for the detection of residual/relapsed disease in the patient's follow-up specimens. An additional approach to monitoring MRD is the combination of TdT with T-cell (e.g., CD7 or CD3) or B-cell (e.g., CD19 or CD10) markers. The combination TdT/CD19 is also useful for distinguishing hematogones from residual/relapsed precursor B-ALL (*see* Section 3.5.2).

Whereas the immature neoplastic cells in ALL can be confused morphologically with mature neoplastic lymphoid cells in LPD/NHL, blasts in AML are morphologically distinctive from the maturing myeloid precursors. Therefore, testing for TdT in AML is not necessary irrespective of whether CD34 is expressed or not. The expression of TdT in AML is noncontributory for diagnostic and prognostic purposes. Furthermore, because of the high frequency of antigenic shift in AML, it is unlikely that TdT can be useful as a fingerprint at relapse.

MPO antibody: The demonstration of MPO activity or CD13 and CD33 expression constitutes firm evidence of myeloid differentiation. MPO activity can be detected cytochemically (MPO cyto) or immunologically (MPO Ab). Therefore, MPO Ab testing may not always be necessary if the leukemia is either positive for MPO cyto or expresses both CD13 and CD33. Acute leukemias expressing only one of these two antigens (either CD13 or CD33) but with no lymphoid markers are invariably AML, in which case MPO Ab testing may also be omitted.

In contrast, if the blast population does not demonstrate a clear lineage (e.g., only one lymphoid and one myeloid marker are expressed), then testing for MPO Ab would be helpful. At the same time, staining for the appropriate cytoplasmic lymphoid marker, either cCD22 or cCD3, should also be performed. The frequency of cases where additional testing for MPO Ab and cCD3 or cCD22 is needed is relatively low.

Cytoplasmic CD3, CD22, or mu chain: With the use of multiple antibodies in the panel and the multicolor approach, the need to stain for cCD3 and cCD22 rarely arises in our laboratory. In most cases of T-ALL, the presence of CD2, CD5, and CD7 is sufficient to infer the T-cell lineage. Previously, cytoplasmic IgM (cmu) was used for subclassifying precursor B-ALL. It is no longer necessary to perform this staining because the presence or absence of cmu has been shown to be of no relevance to prognosis and therapy. Testing for cCD3 may be helpful when the neoplastic cells

express fewer than three pan T-cell-associated markers and lack surface CD3 and other lineage markers. Occasional high-grade T-cell lymphomas, in which only CD2 and CD5 or CD2 and CD7 are present, fall into this category.

Bcl-2: Testing for bcl-2 in combination with CD20 is appropriate when the results from the TF panel indicate a slightly larger cell population, intensely CD20 positive and CD10 positive, and with poor or no surface light-chain expression. In these cases, the differential diagnosis is FCC lymphoma vs FRFH. In addition to the pattern of CD10–FITC/CD20–PE coexpression (*see* Section 4.1.1.1), bcl-2 testing helps to resolve the differential diagnosis. This testing is particularly useful in cases of needle aspirates or when tissue samples are small and bcl-2 staining by immunohistochemistry may not be easily interpretable.

Cytoplasmic light chains: This assay is performed to assess plasma cell clonality and is most often done in combination with surface CD38 or CD138 staining. Therefore, testing for cytoplasmic kappa (cKappa) and cytoplasmic lambda (cLambda) are performed when (1) the results from the standard panel reveal an increase in the number of plasma cells (e.g., a distinct population with bright CD38 and negative CD45) or (2) the surface phenotype of plasma cells is abnormal (e.g., downregulated CD38 or expression of CD56). In some instances, analysis of cytoplasmic light chains can be performed up front with the standard panel when the submitted specimen is accompanied by detailed and relevant clinical information suggesting the possibility of myeloma. Staining for cytoplasmic light chains can also be paired with CD20 or CD19 to detect lymphoid malignancies with plasmacytic differentiation.

2.8.1 Minimal residual disease

Detection of MRD by FCM analysis takes advantage of the immunophenotypic abnormalities frequently exhibited by leukemic blasts. The abnormalities may be overt, such as the expression of a marker from a different cell lineage, or subtle, in the form of downregulated or upregulated expression of a number of antigens when compared to normal counterparts. For instance, leukemic cells of most precursor-B ALL can be distinguished from bone marrow B-cell progenitors based on the differences in the expression of several antigens, including CD45, CD19, CD20, CD10, CD38, and CD34. Recently, CD58, also known as lymphocyte function-associated antigen-3 (LFA-3), has been described as a useful marker for differentiating B-lineage ALL from benign B-cell progenitors. Several four-color combinations of these various markers can be thus applied to the monitoring of MRD in precursor B-ALL. In the case of T-ALL, the combination of a pan-T-cell antigen with either TdT or CD34 (e.g., TdT/CD3) has proven to be useful, since the combined expression of TdT/CD3 or CD34/CD3 is virtually not encountered in normal bone marrow cells. Minimal residual disease detection in ALL of either lineage is also facilitated by the presence of an aberrant myeloid antigen, CD56, or aneuploidy.

The evaluation of MRD in AML by FCM relies on the phenotypic aberrancies (*see* Section 3.5.1.1) present on the patient's leukemic blasts at the time of diagnosis, based on which combinations of appropriate markers can be selected. Because of the relatively frequent phenotypic changes associated with long-term clonal evolution in AML, the use of such combinations is more suitable for detecting residual disease at the end of induction or consolidation therapy rather than later relapses.

2.9 FCM immunophenotyping data representation

The standard format for displaying FCM data uses two-dimensional (2D) projections with *x*- and *y*-axes. Based on the current commercially available software for FCM data analysis, the most common approach for displaying immunophenotyping data derived from an antibody panel is the automatic tube-by-tube approach. The parameters available from one tube are displayed, followed by those from the next tube, and so on in a sequential manner. The

parameters are shown in various permutations for the *x*- and *y*-axes, (e.g., FL1 vs FL2, FL1 vs FL3, FL2 vs FL3, light scatter [FSC or SSC] vs antibody fluorescence, and single-parameter fluorescence histograms). This approach to data display is rather inefficient because not every permutation is informative and there is a high number of graphics being generated.

With some effort and careful planning, however, the FCM software currently available from most manufacturers can be used to create analysis panels based on a medical rationale, which provides a more logical approach to analyzing immunophenotyping data than the tube-by-tube approach. It may be judicious to install the analysis panels on workstation(s) connected via a network, so that the immunophenotyping data from any given case can be analyzed at any workstation and not only the computer associated with a particular flow cytometer.

2.9.1 Analysis panels

In the authors' laboratory, one analysis panel has been created for each of the standard antibody panels (BBS, TF). The organization of the FCM displays in the BBS analysis panel follows the rationale that in the BBS compartment, acute leukemias (lymphoid and myeloid) and B-cell NHL/LPD occur more frequently than T-cell disorders. The TF analysis panel reflects a similar reasoning (i.e., that mature B-cell malignancies are more frequent than their T-cell counterparts). Because acute leukemias are considered life-threatening, the corresponding displays are among the first to appear on the analysis panels, which allows the technologist to flag the case and start any necessary "add-on" antibody testing.

The preferred format for data representation adopted by the authors is the dot plot whereby each dot corresponds to one event. The printout of the dot plots, especially if in black and white, is best done at the 25–50% level of the actual cells acquired to facilitate the visual resolution of closely placed cell clusters.

The analysis panels should be designed to include, in addition to the familiar dual fluorescence dot plots, displays that correlate the cell size (FSC) and antibody fluorescence data. The information derived from these two types of dot plots complement each other. The dot plots for FSC and antibody fluorescence can be used for displaying ungated cell populations (i.e., in the case of the BBS analysis panel, granulocytes are included). The dual fluorescence dot plots correlating antibody expressions can be focused on mononuclear cells, in order to identify and characterize the critical cells. Where appropriate, a gate can be drawn around the neoplastic cells (Figure 2.8) so as to estimate their relative proportion. In addition, the BBS analysis panel also includes dot plots gated solely on the granulocytic clusters to evaluate the expression of myeloid antigens (namely CD13, CD16, and CD11b) on the maturing myeloid precursors. The observed pattern of antigenic coexpression is often altered in myeloid processes, such as some myelodysplastic syndromes and myeloproliferative disorders (*see* Sections 4.2.2.2 and 4.5.2). A version of the list of dot plots included in the BBS and TF analysis panels are given in Table 2.3.

2.9.2 Color display

The immunophenotyping data can be displayed in color (e.g., each cell cluster in an SSC/CD45 display can be assigned a color), which may facilitate the identification of cell populations in other 2D projections of the data. Once a given population is depicted with a particular color on the anchor SSC/CD45 dot plot, it will appear in the same color in other dot plots. It is then possible to follow that population from one tube to the next throughout the panel. To use color displays effectively requires that the antibody panel be built around a single anchor marker such as CD45–PerCP. In other words, the antibody panel cannot have two anchor markers, such as CD45–PerCP in some tubes and CD20–PerCP in other tubes.

In a TF panel, if color is assigned to different populations using FSC as the anchor "marker," then in correlated dual fluorescence data displays such as CD71/CD20 (Figure 2.9), the color

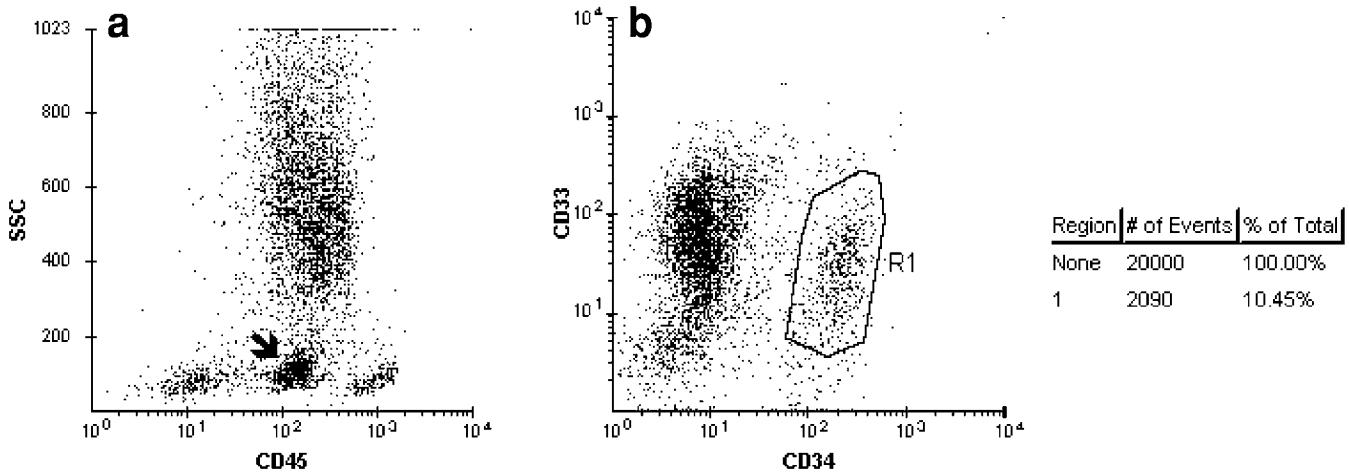

Figure 2.8 Bone marrow with residual AML. (a) The neoplastic cells form a distinct cluster in the blast region (arrow), and coexpress CD33 and CD34 (b). The blast content can be derived from a gate (R1) drawn around the $CD33^+$ $CD34^+$ cluster.

Table 2.3 List of plots routinely displayed (in B&W) for the BBS/TF analysis panels

	y-axis	*x*-axis
1. Ungated	FSC	PI
2. On viable cells	SSC	CD45
	FSC	SSC
	FSC	Myeloid markers, CD10, HLA-DR, CD38
	CD14	CD64
3. On MNCs (preferably)	FSC	Lymphoid markers
4. On MNCs (preferably)	CD19, CD33, CD117	CD34
	CD5, CD23, κ(1), λ(1)	CD19
	CD10, CD11c, CD103, CD25, κ(2), λ(2)	CD20
	CD7, CD4, CD25	CD3
	CD4	CD8
	CD25	CD2
	CD2, CD16	CD56
	CD138	CD38
	CD38	CD45
	CD14	CD64
5. On granulocytes	CD13	CD16
	CD11b	CD16
	CD10	CD20
6. Kappa and lambda histograms are gated on the subpopulations of B-cells according to the patterns seen on the FSC/CD20 and FSC/CD19 dot plots		

Note: MNCs: mononuclear cells; κ: kappa; λ: lambda.

of the population of interest provides information about its cell size (i.e., small cells vs large cells). In such instances, the use of color provides a third parameter (FSC) to the 2D data projection. This does not preclude displaying the fluorescence data in correlation with the cell size, however. In most laboratories, the emphasis has been on dual fluorescence 2D projections (e.g., FL1 vs FL2) and little attention has been given to the correlated FSC and fluorescence data display. The valuable information (sometimes subtle), which can be derived from the pattern and the relationship of the clusters present on the correlated FSC and antibody fluorescence dot plots, has therefore been overlooked (Figure 2.10).

The main utility of displaying the FCM graphics in color is to reduce the number of FCM graphics to be printed for diagnostic review. The use of color also helps to identify different

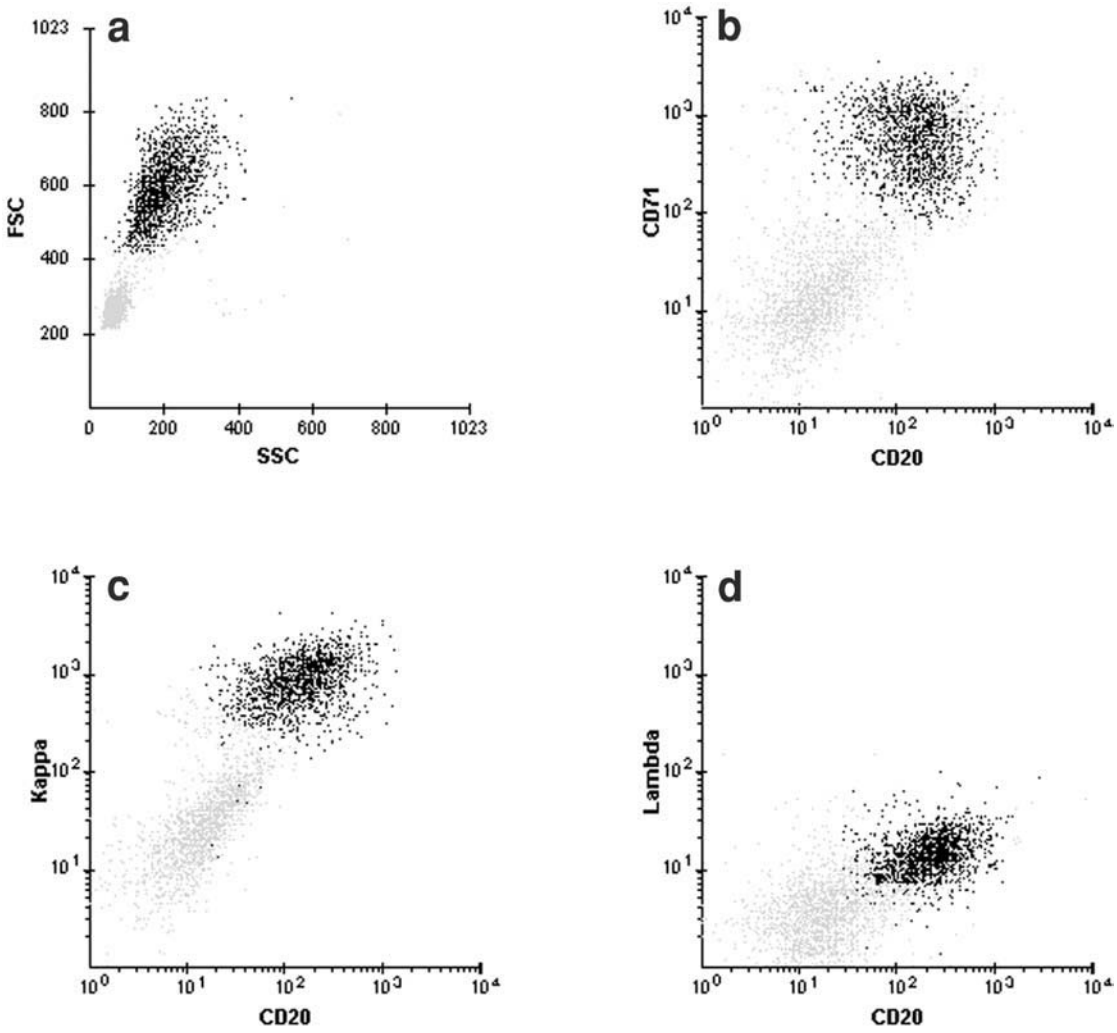

Figure 2.9 Lymph node with high-grade B-NHL. (a) Two distinct cell populations differing in cell size (FSC), for which the use of colors can be applied. (b–d) Cells with high FSC (black) are neoplastic B-cells monoclonal for kappa and expressing high levels of CD71. Cells with low FSC (gray) are benign T-cells negative for the markers displayed.

cell populations, especially those sharing similar reactivity for a given marker. A typical example is the expression of activation markers such as HLA-DR or CD38 by cells of various lineages. For instance, on the dot plot FSC/HLA-DR or HLA-DR/CD34 from a bone marrow specimen, there is an apparent continuous population with heterogeneous HLA-DR intensity, from negative to extremely bright. On the color displays, it can be more easily appreciated that the apparent continuous population is actually composed of several cell populations of approximately the same cell size merging into each other (Plate 1). In other instances, what appears to be two adjacent cell clusters is actually one cell population with bimodal reactivity for a given marker. With appropriate color display, potential confusion of one vs two populations may be avoided (Plate 2).

Many commercially available FCM software packages assign a hierarchy to the colors selected by the user, the color selected first being on the top of the hierarchy. Where two cell clusters overlap with each other, the one with the higher-ranked color will obscure the other, partly or completely, depending on the degree of overlap. For example, on the SSC/CD45 dot plot, the colors red and light green are assigned to the monocytic and myeloid populations,

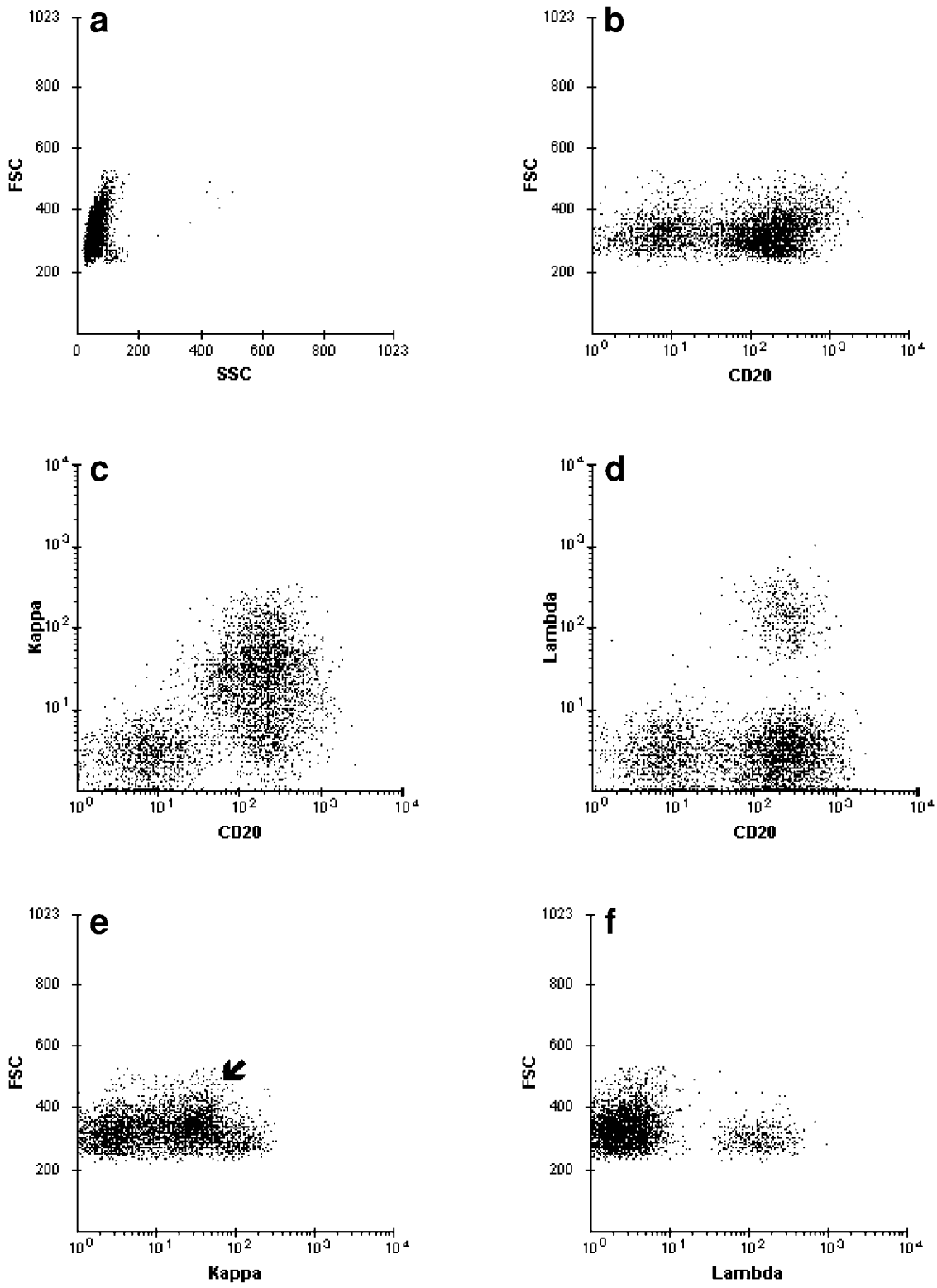

Figure 2.10 Utility of FSC vs fluorescence displays. The lymphoid cells are of similar cell size (a,b) despite their antigenic heterogeneity. (b–d) The benign and neoplastic B-cells share similar intensities of CD20 and CD19 (not shown). It is thus difficult to evaluate monoclonality and quantify the malignant cells on the dual fluorescence dot plots. (e,f) The monoclonal cell cluster (arrow) is more clear-cut on the FSC/kappa (evaluated together with FSC/lambda) display.

respectively, with the latter being the higher-ranked color. In another dot plot (e.g., CD33/CD34), these two populations largely overlap each other. Despite the fact that red is a bold and darker color than light green, very few, if any, red signals can be seen through the lighter green cluster (Plate 3). The effect is equivalent to that caused by an opaque light green color. In such instances, there is no advantage compared to a monochrome (black-and-white) display. This hierarchical "opacity" is the main limitation to the usefulness of the color display. In some cases, the use of colors may be distracting, causing subtle findings to be paradoxically missed. In the authors' opinion, it is important to be versed in inspecting the immunophenotyping data irrespective of whether the graphics are in color or black-and-white.

2.10 Approach to DNA data analysis

The purpose of DNA analysis is to determine the DNA content (i.e., the ploidy level) of the cells of interest and their growth rate (i.e., the relative proportion of cells in each phase of the cell cycle). The cell cycle can be compartmentalized based on the amount of DNA in the nucleus at a given time in the cycle. Cells with the 2N amount of DNA are either noncycling (G_0 phase) or in the presynthetic growth (G_1) phase of the cell cycle, during which RNA and some proteins are accumulated. This is followed by the synthetic (S) phase during which DNA is being replicated. Cells in the S-phase have an intermediate amount of DNA between 2N and 4N. After DNA duplication, the cells enter the postsynthetic (G_2) growth phase and, finally, undergo mitosis (M). By FCM, cells in G_2- and M-phases are considered together, as they both have a 4N amount of DNA.

The authors' approach to DNA analysis is to first inspect the dot plot of FSC and PI fluorescence, correlating the DNA content and cell cycle measurements with the relative cell size. DNA fluorescence measurements, which have a relatively limited biological dynamic range (typically, fourfold to eightfold) are made using linear amplification. In addition, the FSC/PI fluorescence dot plot is useful for detecting small aneuploid population(s), which may be missed on the single parameter DNA histogram, and evaluating the presence of debris and aggregates. The conventional approaches to correct for doublets and aggregates have been based primarily on the altered pulse shape produced by the doublets or clumps when illuminated by a focused laser beam (e.g., the gating strategy of integrated vs peak PI red fluorescence). In this gating strategy, doublets of G_0/G_1 cells can be eliminated because they produce an integrated fluorescence equivalent to a G_2/M cell, but a peak fluorescence equal to a G_0/G_1 cell. This exclusion technique does not eliminate the type of doublet caused by two G_0/G_1 cells passing through the laser side-by-side, however. An alternative approach to this electronic exclusion is to use commercially available DNA analysis software whereby mathematical algorithms can be applied to subtract doublets based solely on the DNA content distribution.

2.10.1 DNA ploidy

The ploidy status of the cells of interest is determined by the position of its G_0/G_1 peak relative to the G_0/G_1 peak of diploid cells. By convention, the aneuploid peak must be separable from the diploid peak (i.e., the histogram is bimodal, with a trough between the diploid and aneuploid populations) (Figure 2.11). The DNA index, which reflects the DNA content in the aneuploid population, is the ratio of the peak fluorescence of the aneuploid G_0/G_1 peak to that of the diploid G_0/G_1 cells. The resolution of two cell populations depends on the CV of the DNA analysis and the percentage of aneuploid cells in the sample. The closer to diploid the aneuploid cells are and the lower the proportion of aneuploid cells, the lower the CV must be to achieve separation. Most lymphomas are diploid or near diploid; frank aneuploidy and poly-

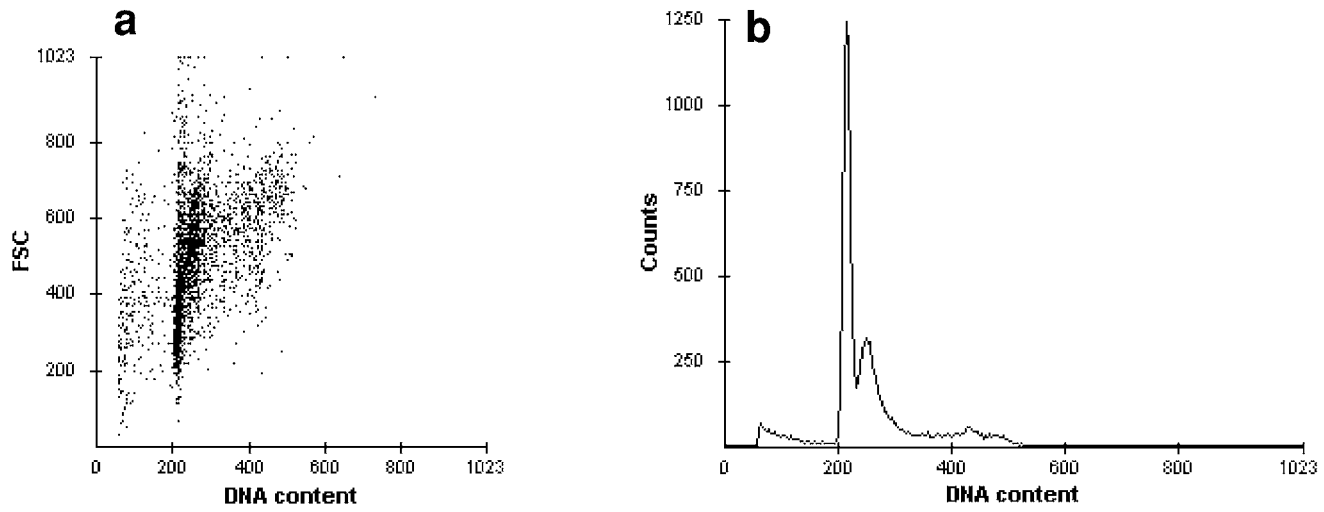

Figure 2.11 Lymph node with high-grade B-NHL. Cells were fixed in ethanol, treated with RNAse, and stained with PI. Doublets were excluded. (a) The aneuploid cells are larger than the diploid cells. Most of the S-phase signals are associated with the aneuploid cells. (b) The same data shown on the DNA content histogram. Using a diploid control (not shown), it was established that the left peak represents diploid cells. The tumor is aneuploid (DNA index [DI]: 1.16) and highly proliferative (S% 23.9).

ploidy are less frequent (Figure 2.12). Therefore, if the specimen contains a large non-neoplastic population, this diploid component may obscure the near-diploid neoplastic cells on the single parameter DNA histogram and interfere with calculations of the tumor cell S-phase. In most instances, this problem can be resolved by performing dual parameter analysis of DNA and antigens (Figure 2.13). It is also important to be aware of artifact-induced aneuploidy (e.g., ethanol-fixed, PI-stained whole blood or bone marrow may produce extra peaks on the DNA histograms because of the presence of granulocytes).

In ALL, aneuploidy (especially in combination with TdT) is a useful marker for detecting low-level involvement of a sanctuary site (e.g., CSF), as well as for monitoring residual disease in a post-treatment hypocellular marrow or impending relapse in a regenerative marrow (Figure 2.14). In addition, DNA ploidy may be of prognostic significance in ALL. Data on pediatric ALL have revealed that a DNA index (DI) greater than 1.16, which corresponds to the presence of more than 53 chromosomes, is associated with longer remission. Although there is a good correlation between FCM aneuploidy and cytogenetic aneuploidy, karyotypic abnormalities (e.g., small deletions, balanced translocations) that result in a pseudodiploid karyotype are not detectable by flow cytometry.

2.10.2 S-phase

Calculation of the cell cycle phases requires the deconvolution of the DNA histogram into three areas (G_0/G_1, S, and G_2/M) and integration of each individual area. The main difficulty in this process is to separate cells in early S-phase from those in G_0/G_1, and cells in late S-phase from those in G_2/M. Various computing methods have been applied to calculate the fraction of cells in each phase of the cell cycle. Commercially available programs can be applied to complex histograms (e.g., the presence of debris or overlapping peaks) or those with very high proliferative fractions. For discrete populations with a rather evenly distributed S-phase, low content of debris, and low to intermediate S-phase fractions (<15 %), a simple rectangle method for S-phase calculation is suitable to most cases of malignant lymphoma.

Because the presence of normal cells in the sample can affect the cell cycle phase calculations on the neoplastic cells, the calculations need to be corrected by subtracting the normal

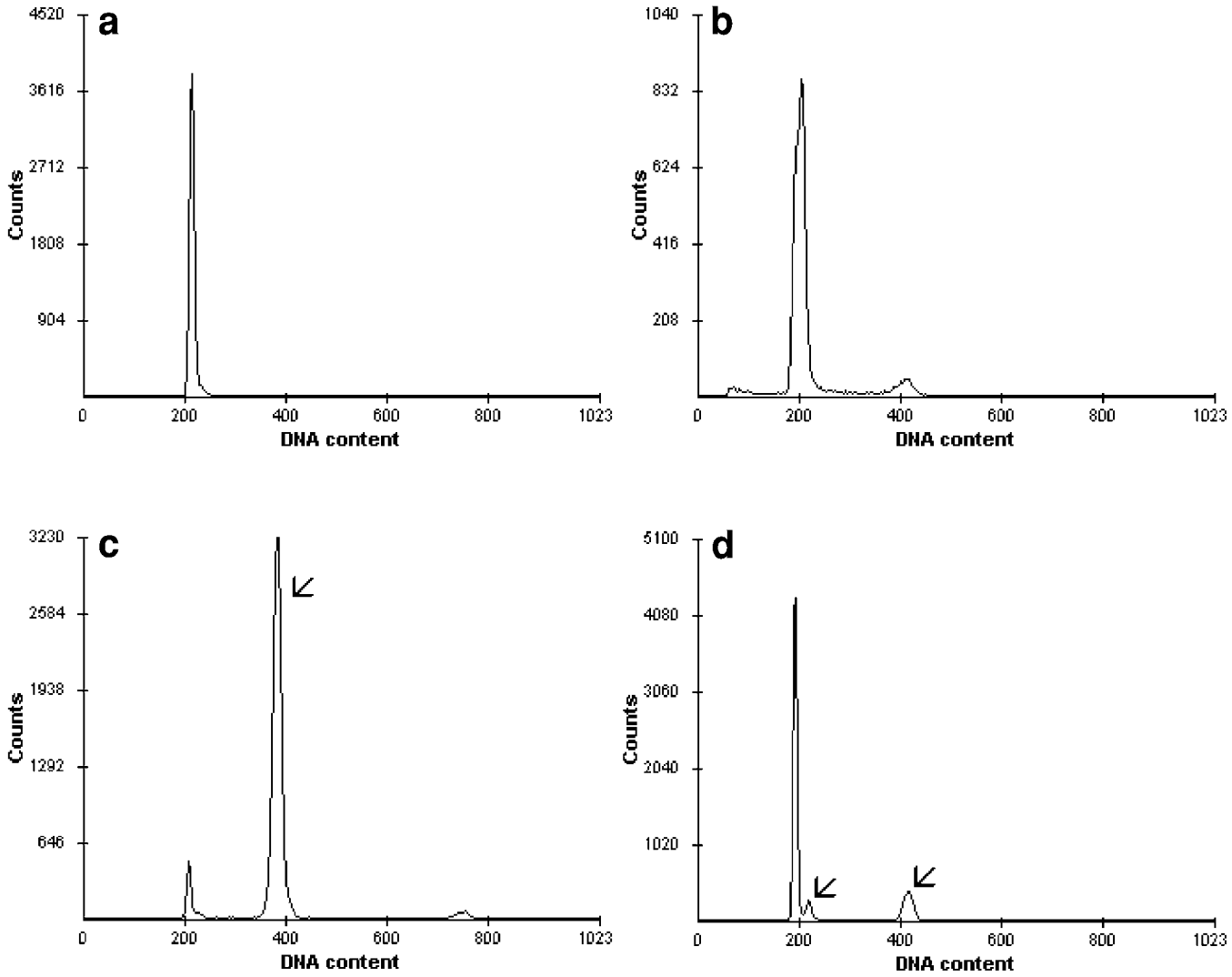

Figure 2.12 Examples of DNA histograms on different lymphomas. (a) FCC II lymphoma: diploid and low S-phase fraction (S% 2). (b) PTCL: Diploid, S-phase fraction in the intermediate range (S% 10). (c) PTCL: The tumor (arrow) is near tetraploid (DI: 1.84) with an S-phase fraction of 6%. (d) FCC II lymphoma: The tumor (arrows) is polyploid and the S-phase low (DI: 1.1 and 2.1, S% 2).

cells from the G_0/G_1 peak. If the neoplastic cells cannot be identified by a specific marker, one can assume that normal cells, in specimens other than the bone marrow, are mostly quiescent and do not contribute significantly to the cycling pool. This assumption can be applied irrespective of how close the DNA peak of the neoplastic is to that of the normal cells. The normal cells can often be separated by their light scatter characteristics. Another approach, especially if the normal and neoplastic populations closely overlap, is dual parameter DNA–antigen analysis whereby an uncontaminated tumor cell cycle fraction can be calculated (Figure 2.13). This is the method of choice when the aneuploid cells are the minor component and/or the normal cells are bone marrow hematopoietic precursors, whereby the S and G_2/M signals from the tumor cells on the single parameter DNA histogram are obscured by the "noise" from the larger normal component. If DNA–antigen dual analysis is not feasible, immunohistochemical staining for cell cycle-dependent proteins (e.g., Ki-67) can be performed on paraffin sections instead.

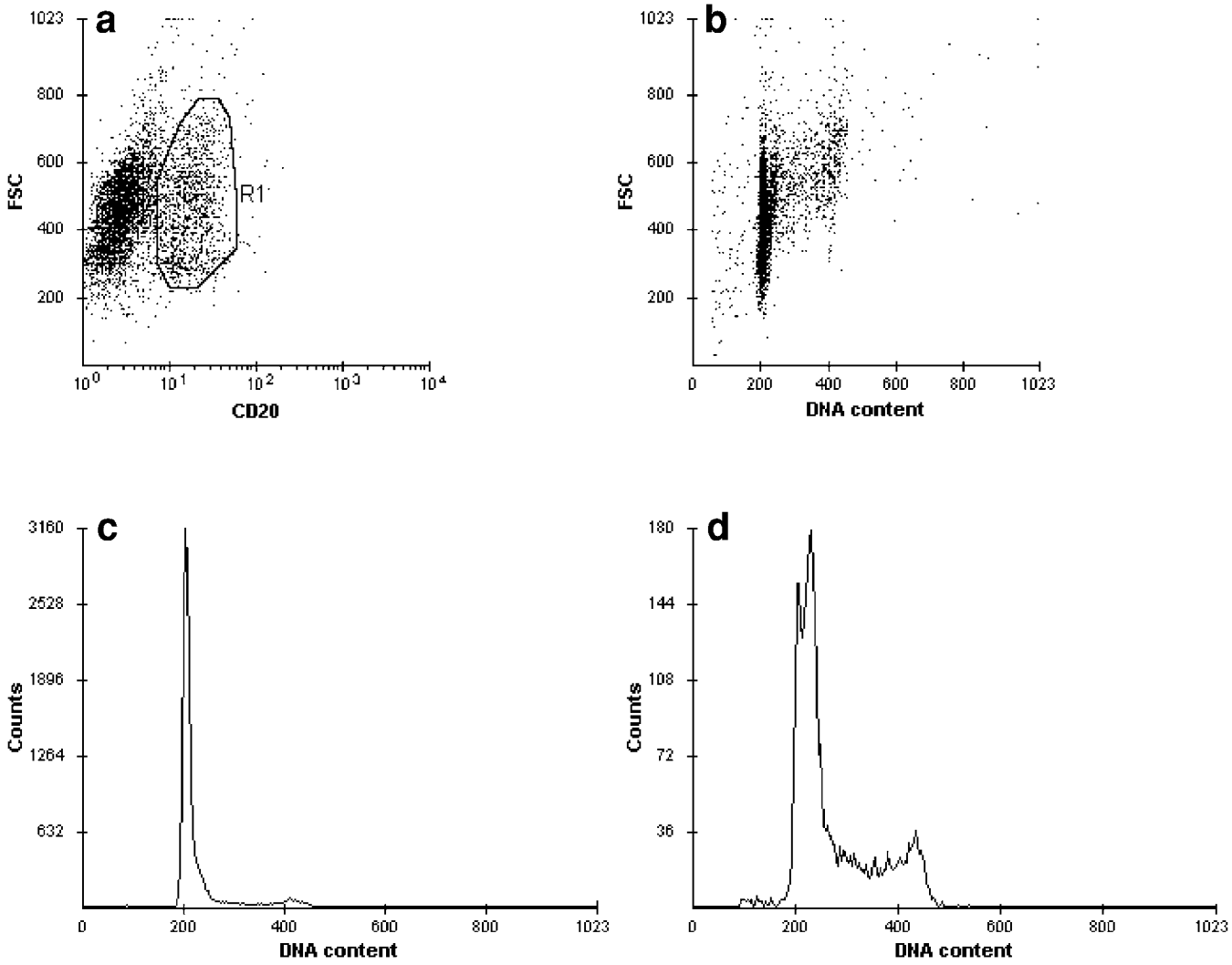

Figure 2.13 Combined analysis of light scatter, CD20, and DNA content to detect and characterize the presence of high-grade B-cell NHL in the peripheral blood. (a) The neoplastic B-cells (R1) are of heterogeneous cell size and comprise 16% of the total cell population. (b) DNA analysis on all cells in the sample. The S-phase signals are associated with large cells. The near-diploid component is more discernible on the FSC/DNA dot plot than on the single parameter DNA histogram (c). (d) DNA analysis on $CD20^+$ cells only (R1 gate): The tumor is near diploid (DI: 1.1) and extremely proliferative. The tumor-associated S-phase fraction (S% 54) is much higher than that determined on the entire sample (c).

In lymphomas, the S-phase fraction has been proven to correlate well with the biological grade (i.e., clinical course) of the disease. Highly proliferative lymphomas confer a shorter remission duration and poorer overall survival than lymphomas with a low S-phase. On the other hand, the incidence of clinical "complete remission" is higher in lymphomas with a high S-phase fraction because highly proliferative tumors are more amenable to aggressive therapy. Thus, the S-phase fraction is extremely useful for grading lymphomas and assessing progression/transformation from low-grade to aggressive lymphoma, irrespective of the histological classification scheme. From studies correlating the S-phase fraction in lymphomas with the clinical survival and/or relapse-free interval, an S-phase threshold can be derived to establish the grading and prognostic categories. The accepted S-phase threshold for lymphoma grading is 5%. Because FCM parameters, similar to any other laboratory data, contain some error margin, it is preferable to devise three rather than two prognostic groups. Low-grade lymphomas

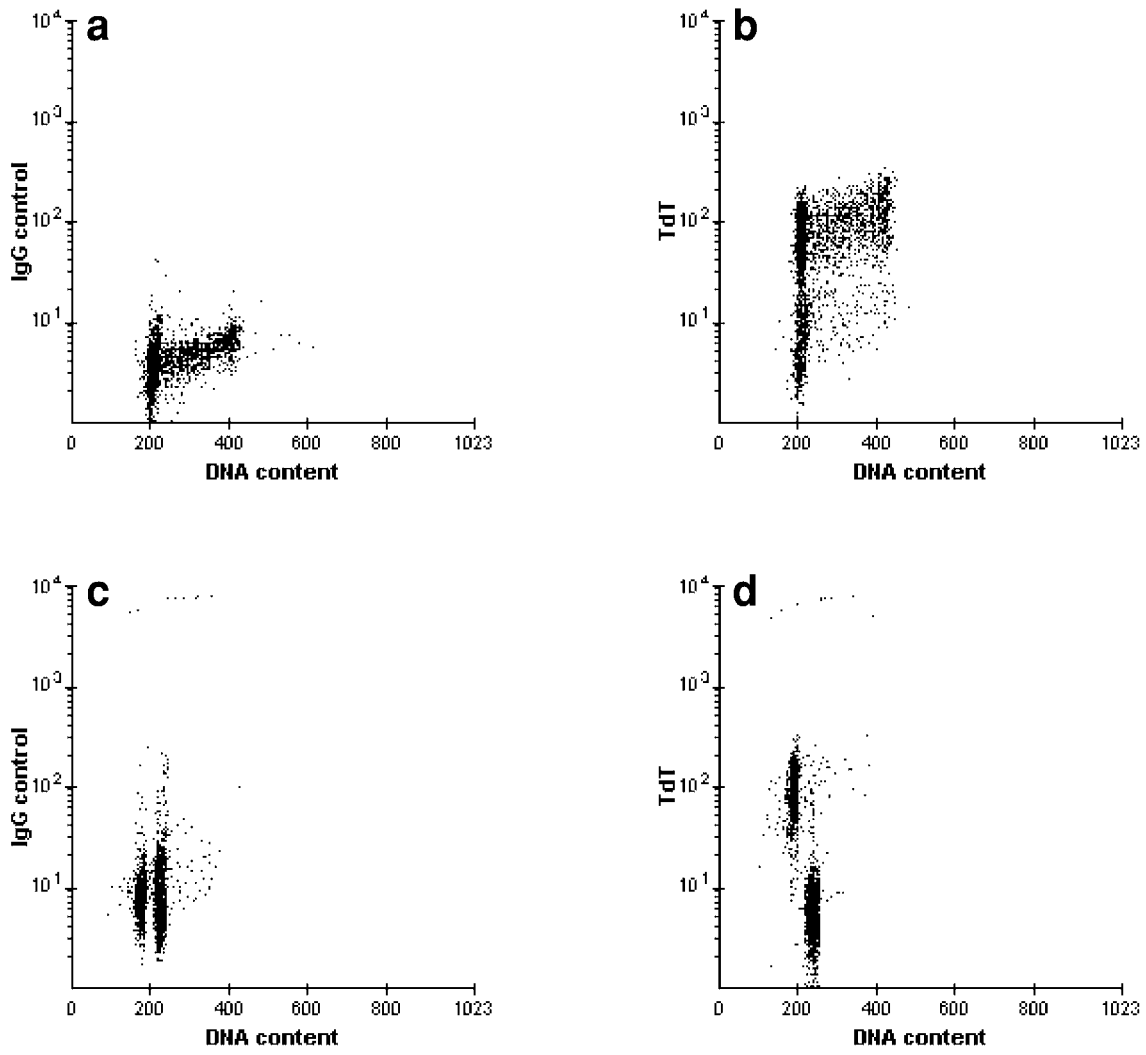

Figure 2.14 Combined analysis of TdT and DNA content applied to two different cases of precursor B-ALL with appropriate controls (a,c) included. (b) Blasts in the first case are TdT-positive and diploid. The proliferative fraction is high. (d) Blasts in the second case are TdT-positive and hypodiploid (DI: 0.77). The S-phase fraction is low.

invariably demonstrate proliferative fractions well below the 5% level. The S-phase fraction in more aggressive disease is scattered over a wide range, however. In this group, high-grade lymphomas such as Burkitt's lymphoma or B-cell lymphoma with plasmablastic differentiation (i.e., immunoblastic lymphoma) have S-phases in the range of 20% and beyond. In between the two extremes of low- and high-grade is the category of intermediate-grade lymphomas in which the S-phase fraction usually falls between 5% (or the vicinity thereof) and 15%.

CHAPTER

3

FCM data analysis on nearly homogeneous samples

During data acquisition, the flow cytometer measures the light-scattering properties and fluorescence characteristics of each cell in sequence. The main purpose of the next step, data analysis, is to identify the cells of interest. This process involves distinguishing any abnormal cell population present from normal cell types and, when an abnormal population is found, determining its lineage, maturity, and other characteristics (cell size, antigens expressed, fluorescence pattern of the antigenic expression). The antigenic profile of the abnormal population may lead to a specific diagnosis.

Once a neoplastic population is characterized, the multiparameter data can be used to quantify its proportion relative to other cells in the sample. In leukemia-lymphoma immunophenotyping, the percentage of neoplastic cells is a less important feature than the fluorescence intensity of specific antigens on their surface, especially since the percentage of abnormal cells is easily altered by sampling-related factors such as severe hemodilution in bone marrow or fine needle aspirates. Furthermore, tumor cells are often more fragile than normal cells and therefore preferentially lost during transport, storage, or specimen processing.

The ability to distinguish the cells of interest from other normal cell types depends on (1) the relative frequency of the neoplastic cells in the final FCM sample (i.e., after processing) and (2) how much they differ from the normal cells. In most instances, clinical samples consist of heterogeneous cell populations and the critical cells are often not the predominant component. In some cases, the sample is overrun by a nearly homogenous neoplastic cell population, producing a cell culture-like picture such that even the crude and suboptimal technique of single-color FCM can determine the phenotype of the malignant cells.

The FCM dot plots produced by heterogeneous samples are inherently complex (with multiple cell clusters) and therefore potentially difficult to evaluate, especially by untrained observers. In contrast, samples with very high numbers of neoplastic cells generate more straightforward-appearing FCM graphics, in which the abnormal cell cluster is virtually the sole component. Several hematopoietic neoplasms can produce this type of FCM picture, including (a) most acute leukemias and (b) various LPD/NHL with extensive involvement at the time of presentation, such as CLL/SLL, prolymphocytic leukemia (PLL), MCL, and Burkitt's lymphoma.

In this chapter, the focus is on nearly homogenous specimens, because they serve as a useful starting point for inexperienced laboratory staff to familiarize themselves with the visual approach to FCM data analysis. Because the tumor population is already obvious, the task of data analysis in homogeneous specimens is primarily concerned with characterizing the phenotype of the abnormal population. It is easy to appreciate the light scatter properties and antigenic characteristics of a homogenous abnormal cell population, reflected by its location and shape on the various dot plots. Because the graphics in homogeneous specimens are simplified, the logical sequence that should be applied to the review of all FCM cases, both simple and more complex, can be easily understood. It should be noted that a small population of normal cells (mostly residual benign lymphocytes) is almost always present, even in specimens with extensive neoplastic involvement. This minor population serves as an internal control. Its location and shape on the dot plots should not be overlooked.

Lineage assignment of leukemias and lymphomas is facilitated by the fact that the neoplastic cells conserve many antigens present on normal lymphoid or myeloid cells. There have been several attempts to subclassify lymphoid malignancies according to the different stages of B-cell and T-cell ontogeny, based on the speculation that the phenotype of the neoplastic cells represents an arrest at a given stage of B-cell or T-cell differentiation. The classification of ALL in earlier studies has been based on such assumptions. However, when applied to lymphoid neoplasms beyond the simple classification of early and mature stages, these assumptions are of limited practical value in the diagnosis (or prognosis) of leukemia and malignant lymphoma. Furthermore, despite antigenic similarities between malignant and benign lymphoid cells, many antigens are expressed on neoplastic cells differently from their expression on normal lymphocytes (e.g., weaker fluorescence intensity).

3.1 FCM parameters

The physical characteristics and antigenic features of a cell population are determined based on the light scatter and fluorescence parameters.

3.1.1 Forward scatter

The light scattered by a cell in the forward direction near the axis of the incident beam is a complex function of refractive index and cell diameter. The signal collected by the FSC detectors is approximately proportional to cell size. In clinical samples, this parameter has proven to be a good discriminator in mononuclear cells and is especially useful in the characterization of mature lymphoid neoplasms. Lymphomas composed of cells with high FSC signals tend to be more aggressive and more proliferative than those comprised of small cells (low FSC).

In the analysis panels used by the authors, FSC is represented on the *y*-axis of the FSC vs SSC and FSC vs fluorescence dot plots. A linear scale of 0, 200, 400, 600, 800, and 1000 is employed, and instrument settings are established such that signals falling within the 200–400 range are considered low FSC, 400–600 is considered intermediate, and from around 600 upward is considered high. These, in turn, correspond to low, medium (Figure 3.1), and large cell size (Figure 3.2), respectively. For example, normal small lymphoid cells appear as a compact cluster with low FSC, whereas monocytes display medium FSC (Figure 3.3). Debris and platelet clumps, when present, generate FSC signals below 200. Within any cell population, irrespective of its benign or malignant nature, there is a certain degree of variation in cell size. As a result, the lower-range FSC signals of a cell cluster with medium cell size can overlap slightly with the upper-range FSC signals of a cluster with small cell size.

Note that the range limits provided here for the FSC parameter are only rough estimates. In the visual approach to FCM data analysis, the relative position of various cell clusters and the resulting pattern are of greater significance than the absolute numerical values of any of the light scatter or fluorescence signals.

Assignment of cell size for a given cell population is based on the FSC signals generated by the majority of the cells in the cluster. For example, in many cases of low-grade B-cell NHL, some of the FSC signals fall into the 400–410 range (i.e., medium cell size), but the bulk of the cell population falls within the small size range (Figure 3.4).

The shape of the cluster distribution along the FSC axis also provides information on the degree of cell size heterogeneity within the population. A stretched-out cell cluster, with FSC signals spanning from the lower limit of the low FSC to the upper limit of the medium FSC range, is an indication that the cell population is of variable size (Figure 3.5). A microscopic review of the corresponding cytospin will confirm that the population in question is composed of cells ranging from small to large. The picture of variable FSC is typically seen in follicu-

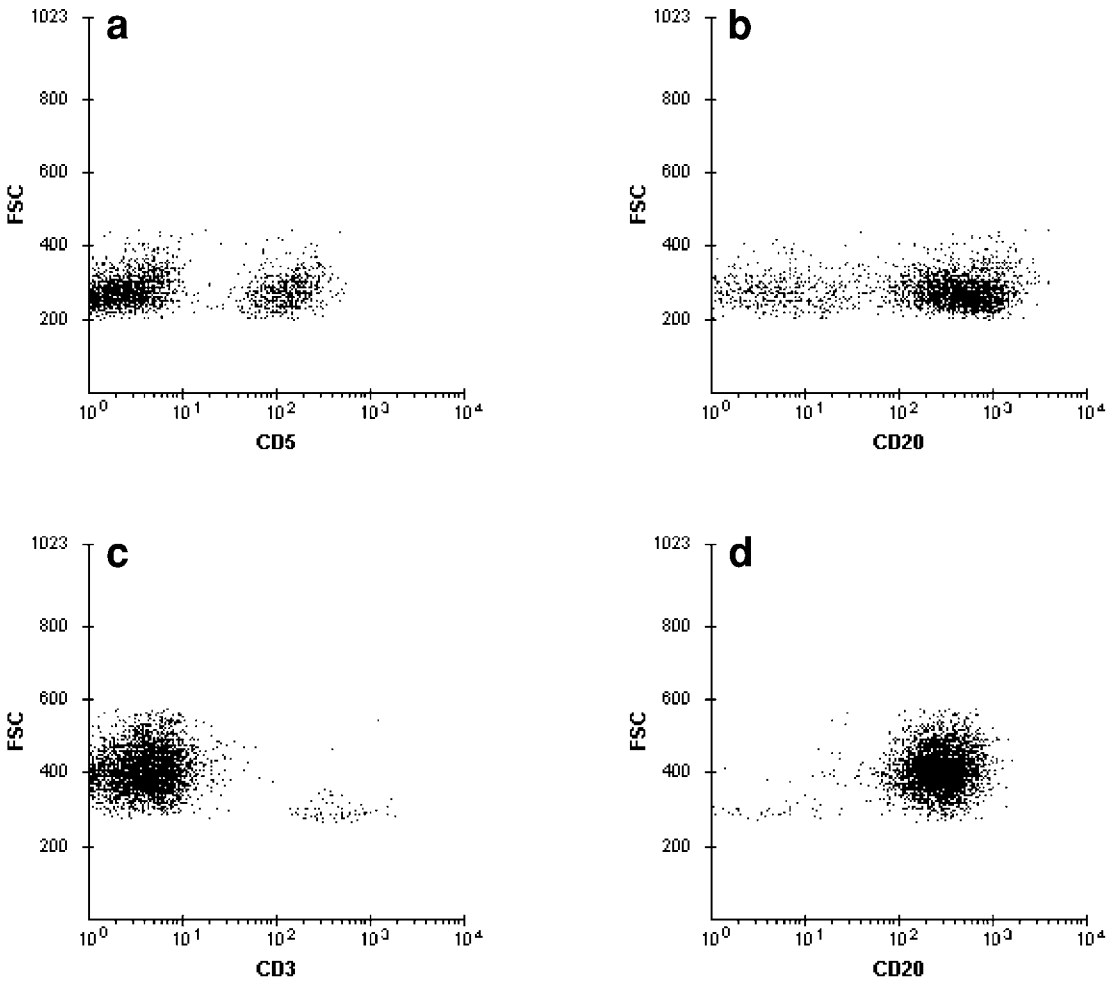

Figure 3.1 (a,b) Lymph node with FCC I lymphoma. The cell size (FSC) of the neoplastic cells ($CD20^+$) is small, similar to that of residual T-cells ($CD5^+$). (c,d) Lymph node with Burkitt's lymphoma. The malignant B-cells are larger (medium FSC) than the residual T-cells.

lar lymphomas containing a substantial number of large cells (i.e., FCC II and FCC III lymphomas) as well as in those CLL with an increased number of activated cells.

Occasionally, the neoplastic population in composed of two nearly distinct clusters with different FSC signals. The cell size distribution is then referred to as bimodal (Figure 3.6). This is not a common phenomenon, but can be seen in some cases of CLL/PL (also referred to as "CLL in prolymphocytic transformation" because of the increased number of prolymphocytes).

In general, there is a good correlation between the cell size as determined by FSC and that estimated by light microscopy. Light scatter determinations are derived from live cells in suspension, close to their native state. The morphologic material for light microscopy, on the other hand, can be laden with undesirable artifacts, either from suboptimal fixation/processing of tissue sections or slow drying of smear/imprints, which can easily lead to cell shrinkage. Optimal quality morphologic material is therefore required for correlation. Cells that display medium FSC signals often appear large on air-dried smears and imprints. A typical example is monocytes. This phenomenon is not a discrepancy; it is simply due to the fact that on cytologic preparations these cells, basically spherical structures, have been flattened into circles with an apparent greater surface area.

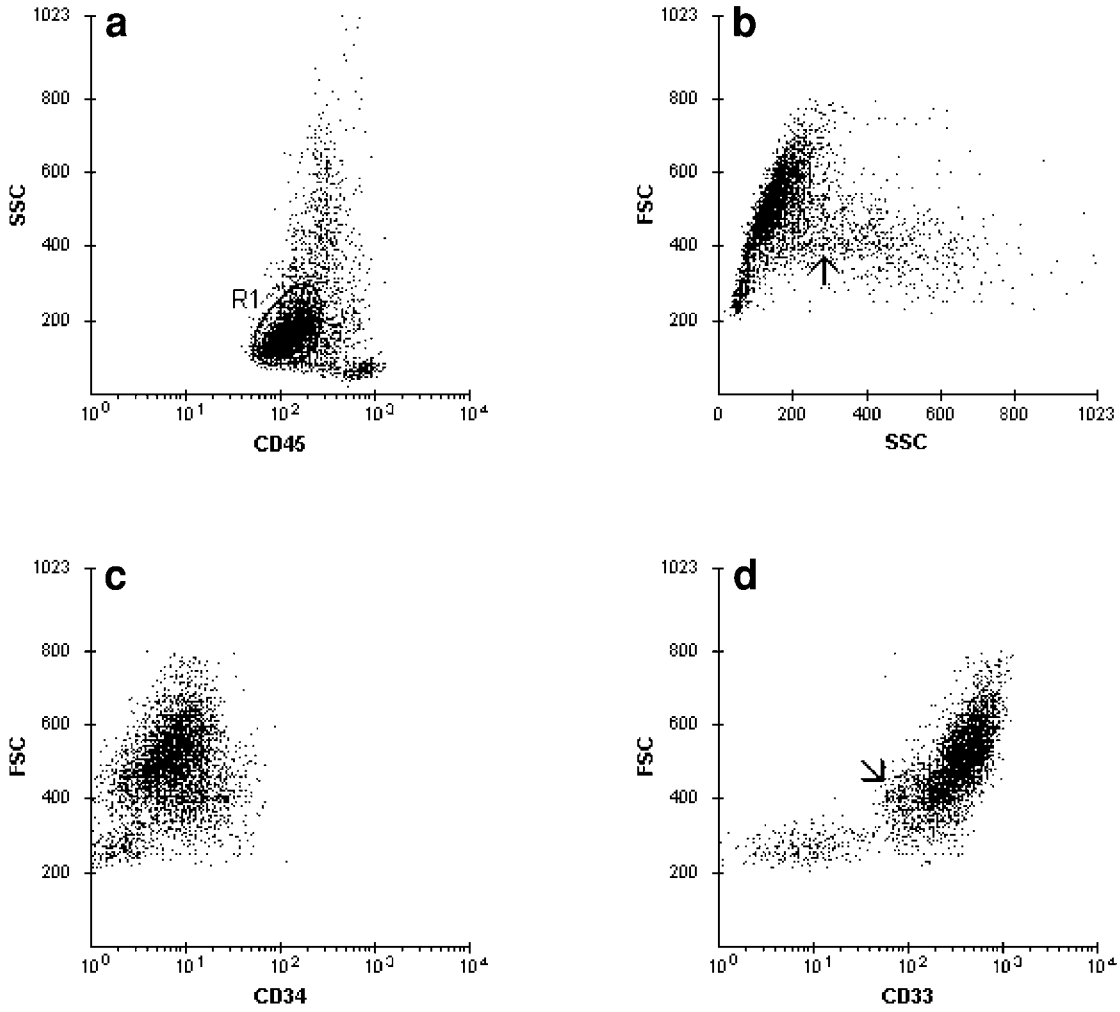

Figure 3.2 AML involving the kidney. (a) A prominent cluster (R1) in the blast region. (b–d) Blasts display large cell size, CD33 expression, and lack of CD34. The expression of CD33 is brighter than that on granulocytes (arrow).

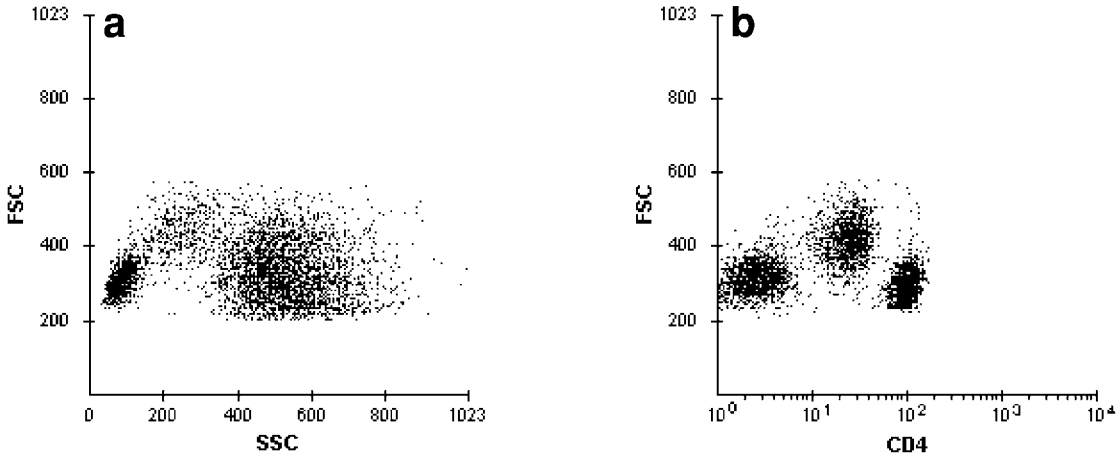

Figure 3.3 Normal peripheral blood. (a) Three distinct populations differing in cell size and granularity: lymphocytes (low FSC, low SSC), monocytes (medium FSC, low SSC), and granulocytes (medium FSC, high SSC). (b) Gated on mononuclear cells (i.e., no granulocytes): B-cells, T-cells, and monocytes. CD4 expression on monocytes is less intense than that on T-cells.

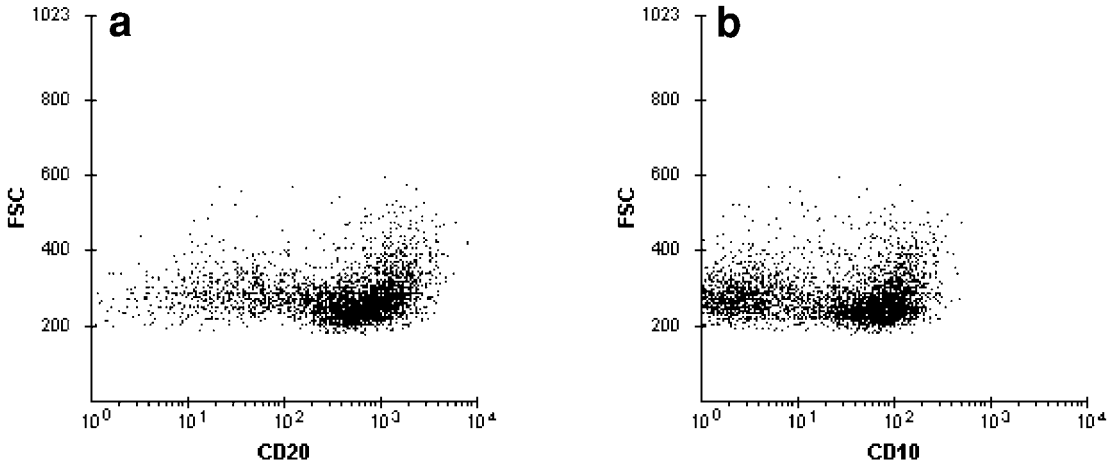

Figure 3.4 Lymph node with FCC lymphoma. (a,b) The tumor population ($CD20^+$ $CD10^+$) is of small cell size. Only a small number of the FSC signals fall in the medium cell size range.

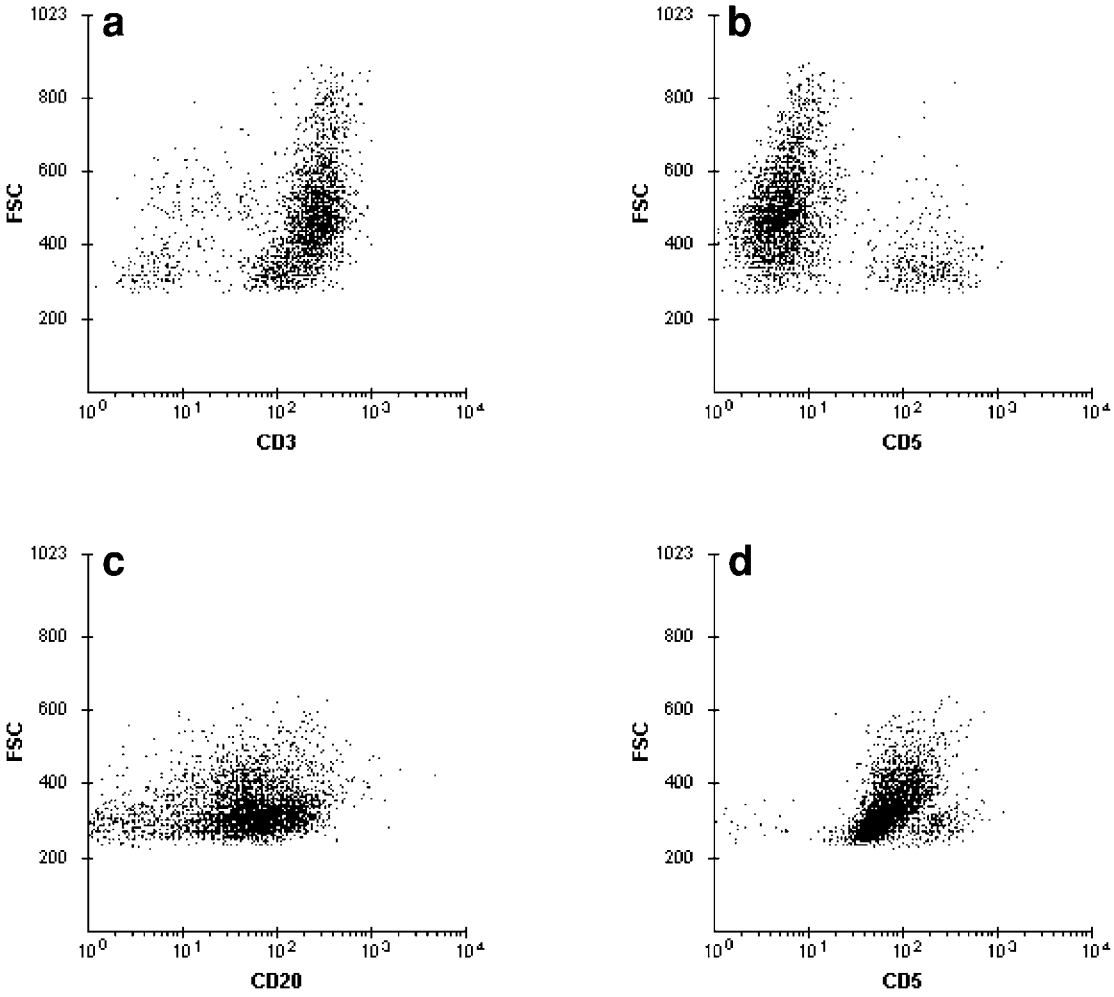

Figure 3.5 (a,b) Extranodal PTCL. The neoplastic cells ($CD3^+$, $CD5^-$) display variable FSC, from low to high. (c,d) Peripheral blood with activated CLL. The tumor population ($CD20^+$ $CD5^+$) is of small to medium cell size. Because of the increased proportion of activated cells, the intensity of CD20 is brighter than that seen in typical CLL.

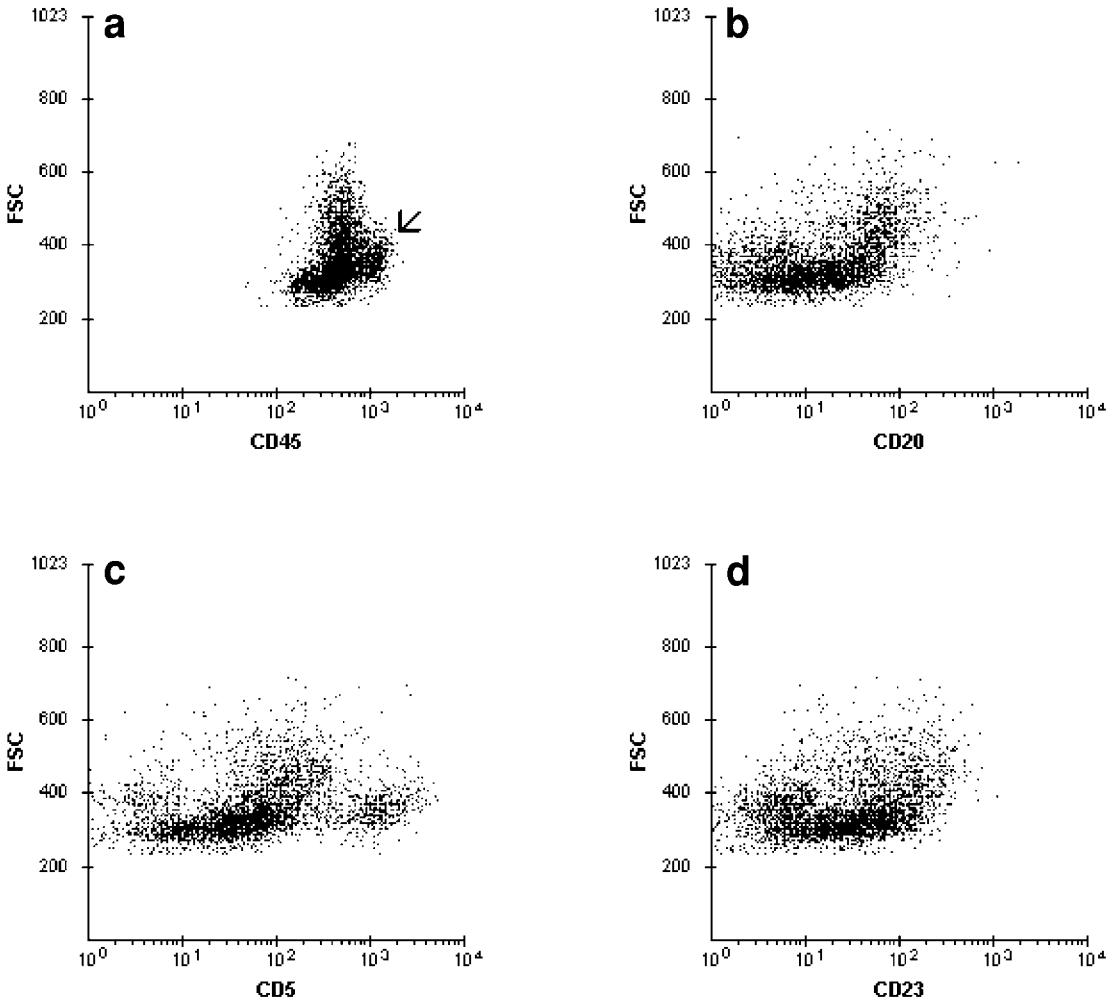

Figure 3.6 Peripheral blood: CLL with increased prolymphocytes (morphology shown in Plate 8). (a–d) The leukemic population demonstrates bimodal FSC. The phenotypic profile (downregulated CD20, coexpression of CD5 and CD23) of typical CLL is still retained; however, CD20 and CD5 are brighter in the more activated component (larger cells). CD45 is also downregulated in comparison to the small population of normal lymphocytes (arrow).

The feature of FSC as a good discriminator of cell size in mononuclear cells can be exploited by displaying correlated dual-parameter FSC/fluorescence plots for each of the antibodies tested. Often, the cells of interest can be followed from one display to another by virtue of their location on the FSC axis (i.e., cell size) (Figure 3.7). Furthermore, the location, size, and shape of the neoplastic cluster and its relationship to the background normal cell population(s) seen on the various FSC vs antibody fluorescence dot plots can often be specific for a given type of leukemia or lymphoma.

3.1.2 Side scatter

Side-scatter signals are collected by optical detectors located perpendicular to the excitation beam. The SSC signals reflect the cell internal structure such as cytoplasmic organelles, which may be loosely termed "granularity." The cell diameter and index of refraction can also affect this signal, however. The authors prefer to collect and display SSC data on a linear scale from 0 to 1024.

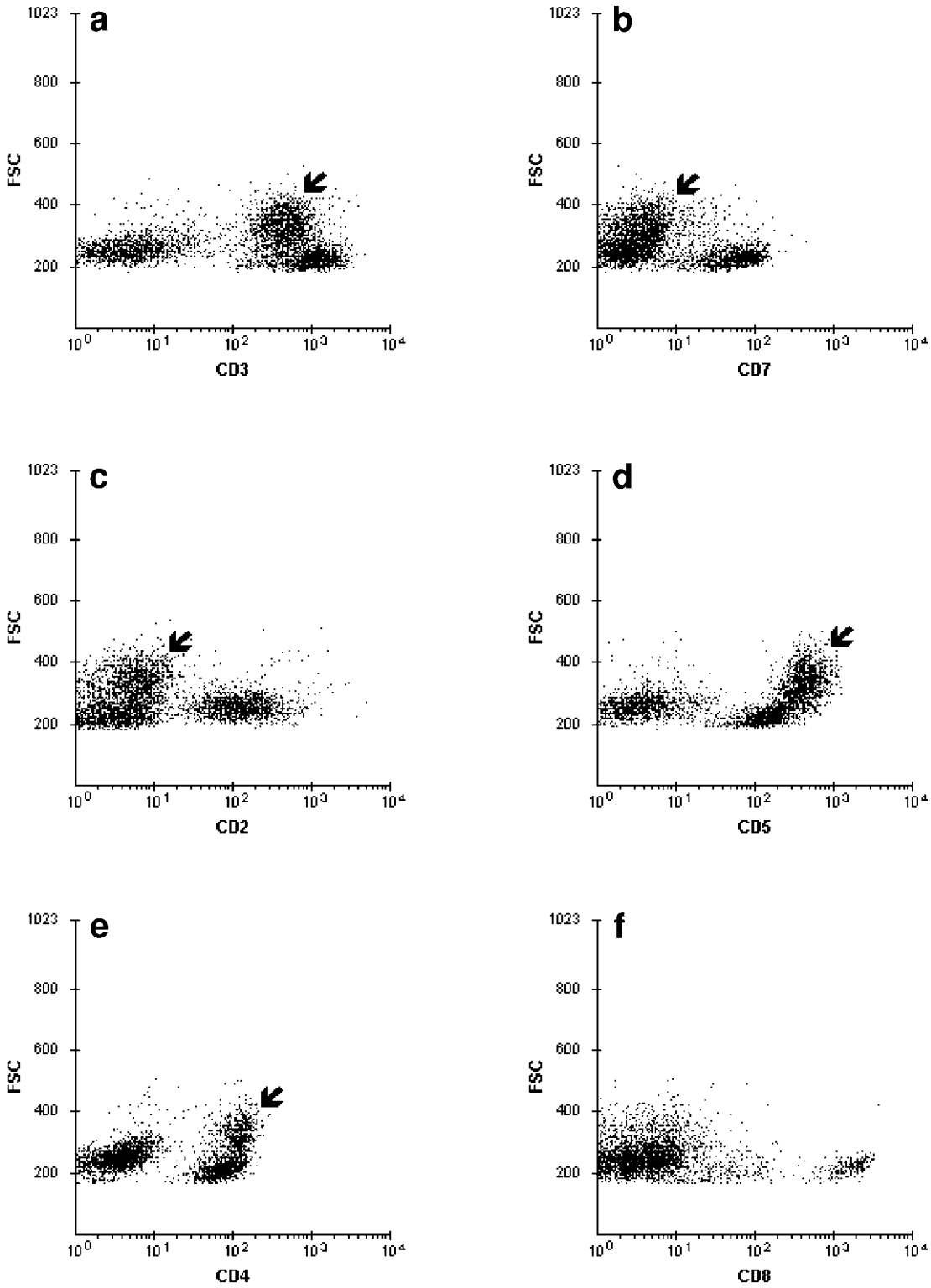

Figure 3.7 Lymph node involvement by mycosis fungoides. (a–f) Using the FSC parameter, the neoplastic cell population (arrow) can be followed from one display to the next, to evaluate its antigenic expression and relationship to other cell clusters, in particular the residual normal T-cells. The tumor cells demonstrate downregulated CD3 (a), upregulated CD5 (d), positivity for CD4 (e), and lack of CD7 (b), CD2 (c), and CD8 (f) expression.

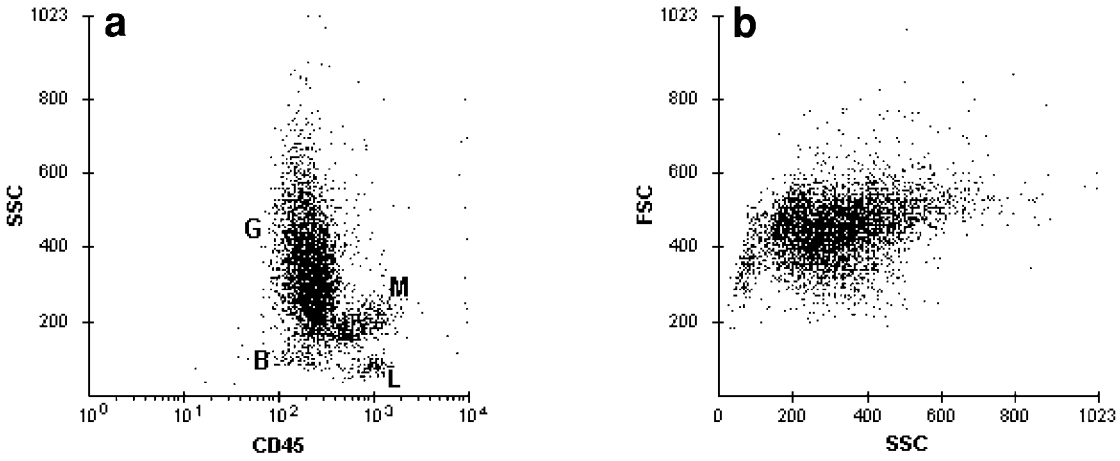

Figure 3.8 Peripheral blood with 1% circulating blasts. (a) The various cell populations are well separated on the SSC/CD45 dot plot. B: blasts; G: granulocytes; L: lymphocytes; M: monocytes. (b) Only lymphocytes, monocytes, and granulocytes can be seen on the FSC/SSC display.

With the exception of SSC vs CD45, dot plots of SSC vs antibody fluorescence have no applicability in FCM data analysis because SSC is a poor discriminator of mononuclear cells. The analysis panels therefore only include two dot plots displaying the SSC parameter: FSC/SSC and SSC/CD45–PerCP (Figure 3.8). These two graphics are useful for separating the mononuclear cell fraction from the myeloid cells. Granulocytes have much higher SSC signals, usually 300 and higher. In addition, the SSC/CD45 dot plot is excellent for defining various subpopulations in the bone marrow or peripheral blood (*see* Section 4.1.2).

3.1.3 Fluorescence

Assessing fluorescence intensity is an important step in characterizing and classifying hematopoietic malignancies. This is even more critical when dealing with closely related disorders that share the expression of several antigens (e.g., CLL/SLL and MCL). The level of fluorescence detected is dependent on (1) the fluorochrome employed, (2) the binding capacity of the particular fluorochrome–antibody conjugate, and (3) the number of antigenic epitopes on the cell surface. To this end, efforts have been spent on quantitative FCM, with an aim to standardize and measure absolute fluorescence intensity. It is still not clear that this approach is widely applicable, however, or whether absolute fluorescence intensity measurements are criteria sufficient to characterize abnormal populations. In practice, a cell population is recognized as abnormal because of the pattern of one or more aberrancies (e.g., downregulated expression or overexpression) in comparison to normal cells, rather than absolute fluorescence measurements. Therefore, for diagnostic purposes, fluorescence intensity determinations utilize relative units rather than absolute ones. The relative intensities are usually estimated based on the difference between the mean, median, or modal channel (channel number with the most events) of normal and neoplastic cells, and the results are reported in a semiquantitative/qualitative manner (e.g., negative, positive, dim, and bright).

Because of the wide range of fluorescence intensities spanning over four decades (i.e., 10,000;1), flow cytometers employ logarithmic amplifier systems for compressing the data over 1024 channels into a log scale of four decades of 256 channels each. On the dot plots, fluorescence intensities are often displayed on a scale of 10^0, 10^1, 10^2, 10^3, and 10^4. In general, the first decalog (between 10^0 and 10^1) represents negative fluorescence, and signals

falling in the second, third, and fourth decalogs represent weak (+), moderate (++), and strong (+++) fluorescence intensity, respectively.

The intensity of a given antigen on the cells of interest is determined by visually comparing the pattern produced by the critical cells reacting with the corresponding antibody to that obtained with the isotype-matched control. Placing of the cursor is not useful because, in clinical samples, there is often an overlap between the negative and positive cells. It is important not to rely solely on isotype controls, however, as they may not necessarily match the biochemical properties of every antibody in the panel, despite an identical concentration and protein–fluorochrome ratio. The background normal cells in the sample are important internal controls. In a large panel, there will always be cells or antibodies serving as negative controls. It is also important not to be too rigid about the above-mentioned scale division.

In straightforward situations, the fluorescence intensity of a given marker on the negative population falls within the first decalog, and the cells of interest form a clear-cut cluster in the positive region. This is most easily seen when the sample is comprised almost entirely of abnormal cells. The lack of staining of this population with a given antibody serves as its own negative control when compared to the positive staining with another antibody (Figure 3.9). In many instances, however, an increase in the cell size of the malignant cells is accompanied by a higher degree of background staining, as the large cells tend to be more "sticky" (presumably from increased Fc receptors) or have more autofluorescence. The fluorescence signals of the negative isotype control may then extend well into the region usually considered to be positive staining (i.e., into the second decalog and occasionally beyond). A mental correction of this right shift is necessary to assign the appropriate fluorescence intensity to the positive population. For example, if the expression of a given antigen on the abnormal cells falls within the third decalog (moderate) but the negative population is right-shifted well into the second decalog (Figure 3.10), the fluorescence intensity on the positive population should be appropriately reported as weak instead of moderate. It is important not to confuse this phenomenon with poor instrument calibration. When the background shift is caused by increased "stickiness" or autofluorescence, it should not be present in other specimens (e.g., neoplasms with small cell size, or normal specimens) run the same day. The reverse phenomenon can also be seen; that is, the negative population does not fill the entire first decalog but is significantly shifted close to 10^0. This situation is relatively infrequent, however. It may be seen in samples composed of a nearly pure population of small malignant lymphoid cells (Figure 3.11).

A common phenomenon associated with large B-cell lymphomas with intense expression of CD20 is the shedding of CD20, which then coats the residual T-cells. As a result, the T-cell cluster appears to be CD20-positive when viewed on any of the dot plots that feature CD20 (e.g., FSC/CD20, CD5/CD20). This phenomenon is also observed in FCC lymphomas (*see* Section 3.6.3.1).

A difficult but sometimes important task in assessing fluorescence intensity is to distinguish very weak (dim) positive staining from negative cells. This occurs frequently when evaluating surface light chain expression, especially in CLL. With regard to light chains, this difficulty can be resolved in most instances by including two different sets of kappa and lambda reagents in the FCM panel (Figure 3.12). Irrespective of the methods applied to describe fluorescence intensity, either quantitative or qualitative, the distinction between dim positive and negative staining ultimately involves arbitrary criteria. In general, the population is considered positive for an antigen if its histogram is shifted by a certain number of fluorescence channels in comparison to an internal negative control. Regardless of the exact number of channels chosen to define the minimum shift arbitrarily, it is important that this shift can be clearly visualized when the histograms or the cluster displays are superimposed on one another (Figure 3.13).

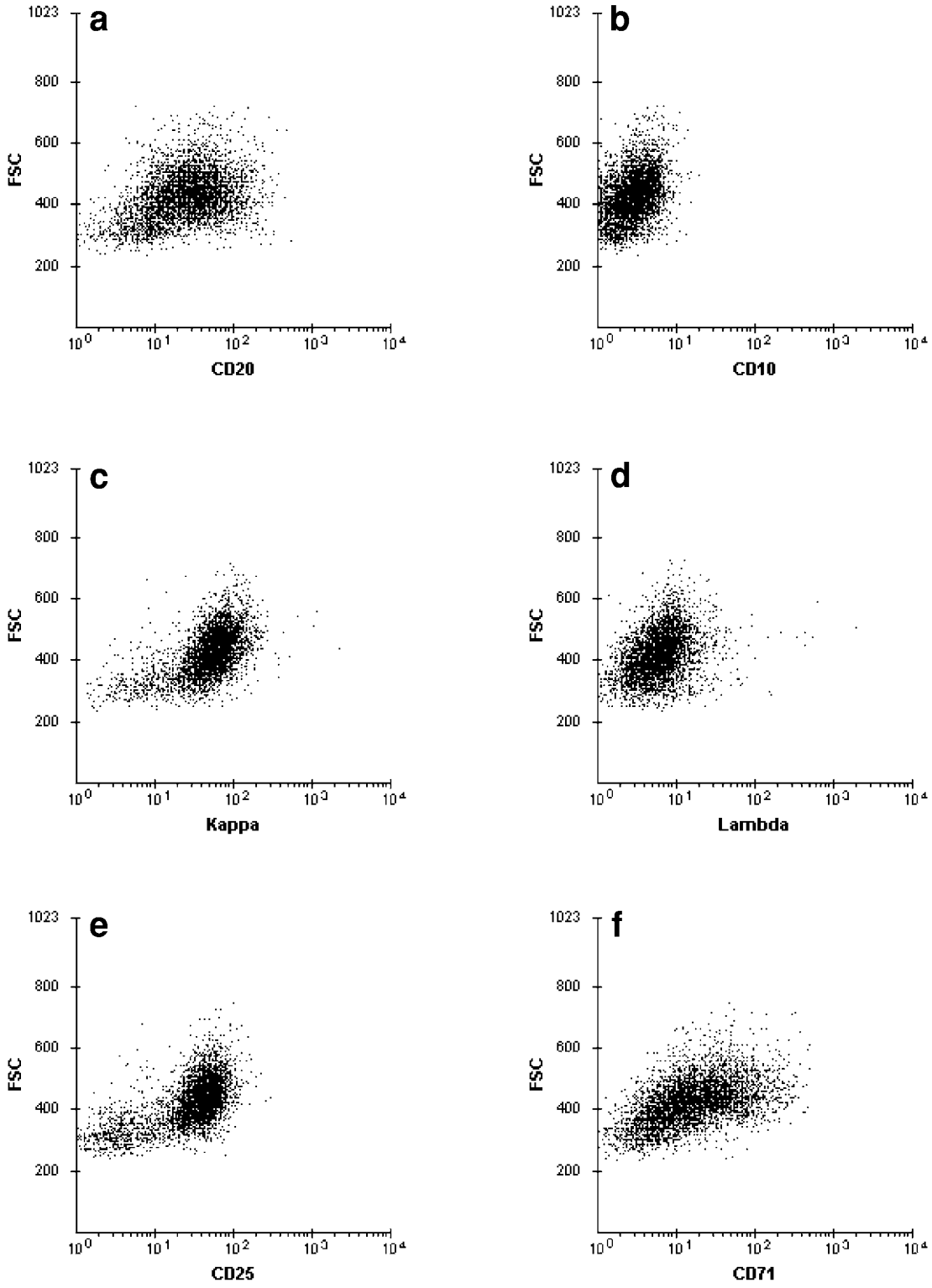

Figure 3.9 Lymph node with large cell lymphoma. The neoplastic cells comprise 81% of the cells in the sample. (b,d) The fluorescence signals of the negative markers, CD10 and lambda, fall in the first decalog. These serve as negative internal controls. The tumor cells are of medium cell size and react with CD20 (a), CD25 (e), kappa (c), and CD71 (f).

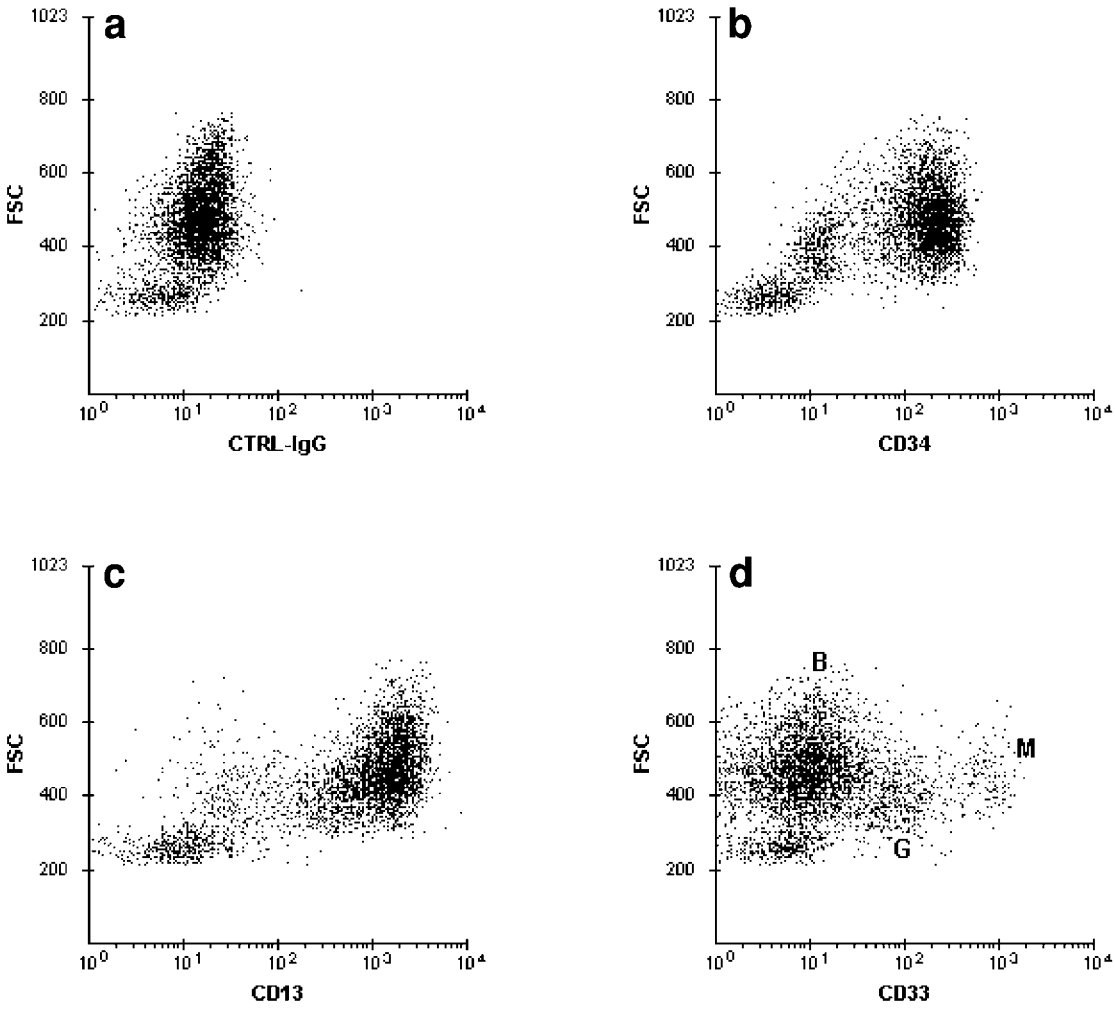

Figure 3.10 Bone marrow with AML. (a) Isotype negative control with increased baseline fluorescence extending into the second decalog. Other isotype-matched negative controls (not shown) yielded the same picture. (b–d) This increase is taken into account when judging the fluoresecence intensity of the various markers on the leukemic blasts. Blasts (B) are thus $CD34^{+}$, $CD13^{++}$ and $CD33^{-}$. Residual granulocytes (G) and moncytes (M) are present.

3.1.3.1 Heterogeneous fluorescence intensity (bimodal, variable)

In a benign cell population, the fluorescence intensity of most cell surface antigens is relatively uniform from one cell to another, thus yielding a rather compact cell cluster on the FCM dot plots (Figure 3.14). In a neoplastic proliferation, however, the quantitative and qualitative expression of certain antigens can vary widely from cell to cell. Because of this heterogeneous staining intensity, the malignant cell cluster may appear stretched out, emulating the shape of a saucer or a "figure eight" corresponding to variable (Figures 3.13 and 3.15) and bimodal (Figure 3.16) distributions, respectively. Such patterns of antigenic expression may serve as a diagnostic clue or fingerprint for follow-up purposes. It can be difficult to convey this useful, but complex graphical data to the clinical staff, who for the most part, are unfamiliar with the complexities of FCM data and are mainly interested in "bottom-line" information. The extent of the heterogeneity in the fluorescence staining, especially if bimodal, also makes it problematic how to report the fluorescence intensity in semiquantitative terms

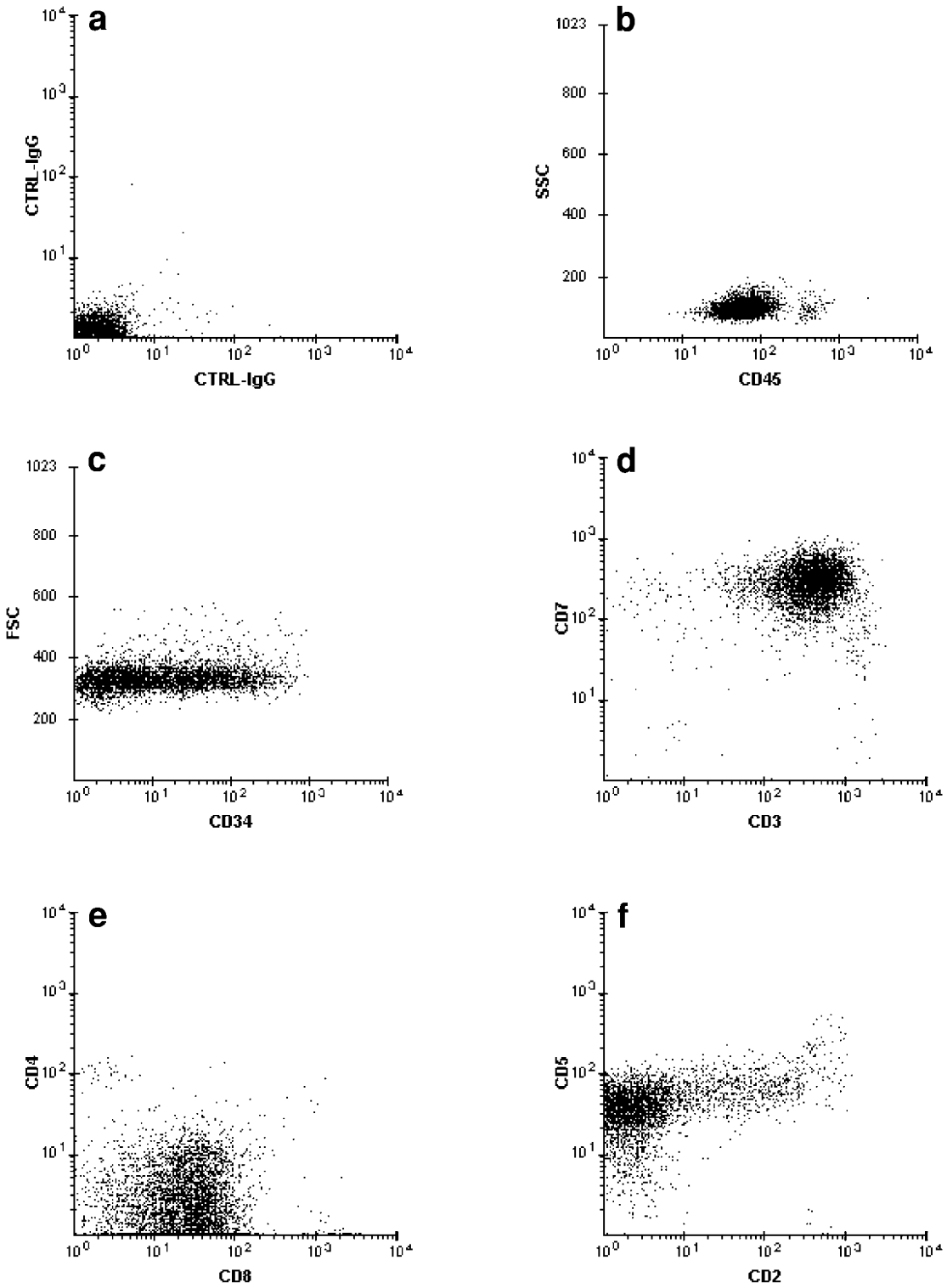

Figure 3.11 Peripheral blood with T-ALL. (a) Isotype-matched negative controls: The fluorescence signals are "shifted" close to 10^0. (b) Blasts comprise more than 90% of the cells in the sample. (c–f) The fluorescence of the isotype controls is taken into consideration for the grading of the intensities of the markers expressed on the blasts. Blasts are thus $CD7^{+++}$, $CD3^{+++}$, $CD5^{++}$, $CD4^{+}$, and $CD8^{++}$. CD2 is present only on a small subset of the blasts. The intensity of CD34 is extremely heterogeneous, ranging from negative to bright.

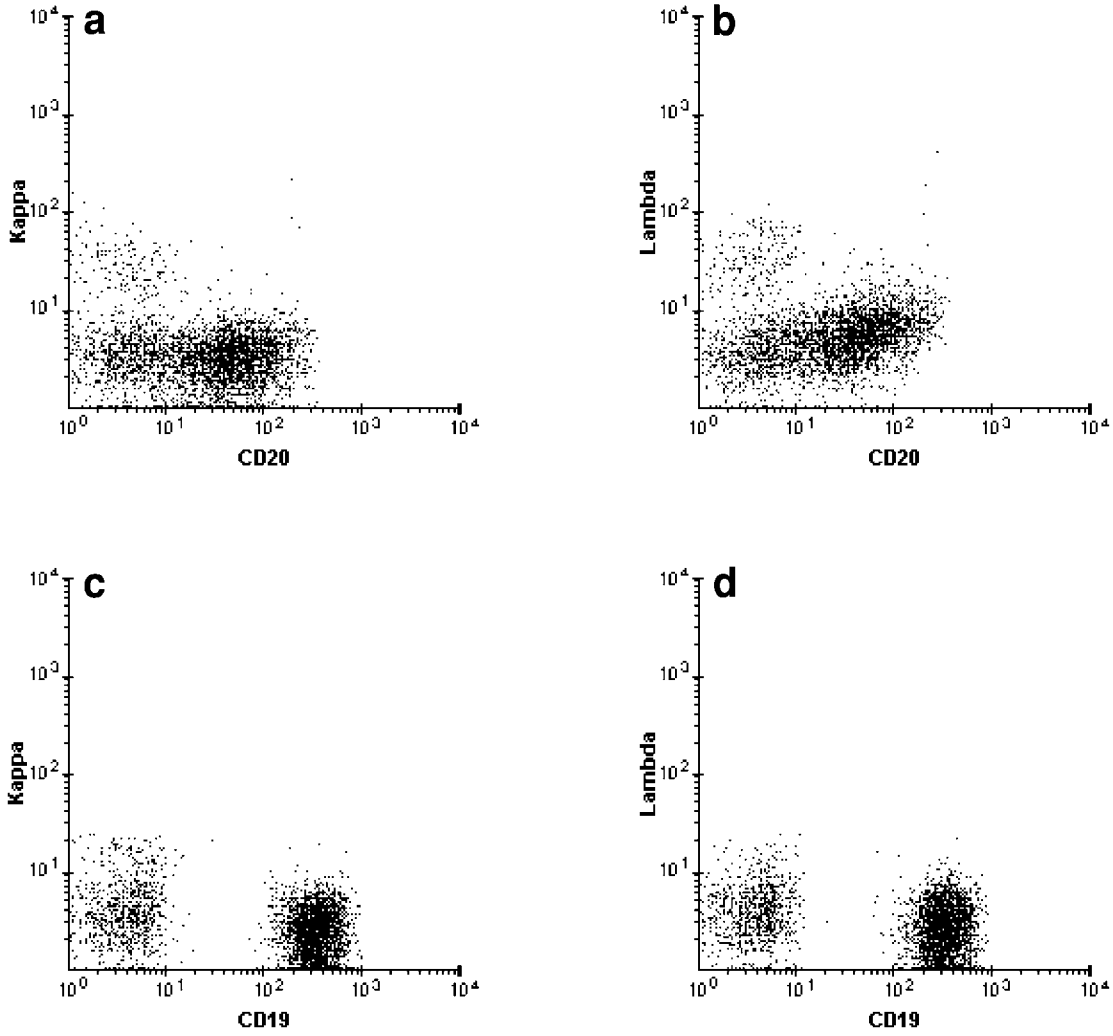

Figure 3.12 Peripheral blood with CLL. Two sets of kappa/lambda reagents (from different manufacturers) used for evaluating monoclonality. (a,b) Weak lambda light chain detectable on the leukemic cells. (c,d) With the second set of reagents, no surface light chain is detected. Other typical features of CLL (downregulated CD20, CD20 weaker than CD19) can also be appreciated.

(e.g., weak, moderate, strong). In the authors' experience, the brighter half of the bimodal distribution provides the more clinically relevant information in most instances, as shown in the following example. The fluorescence intensity we report is that of the brighter half, usually adding the term "bimodal" as a modifier.

Example A case of precursor B-ALL demonstrated a bimodal distribution for CD34 (Figure 3.17), with the fluorescence intensity starting from the negative region (first decalog) and extending well into the positive weak region (second decalog). In this case, the clinically relevant information concerned the maturity status of the abnormal population. Therefore, CD34 was reported as "weak, variable." Positive staining for TdT further confirmed that the tumor cells were blasts. Alternatively, the intensity of CD34 may be reported as "weak, hemipositive," although this terminology does not clearly indicate whether the fluorescence intensity is bimodal or variable. It is important not to describe the data simply as "+/–", however, because this format has also been used to mean equivocal results.

Until now, there has been no uniform system for describing or reporting fluorescence distributions. This, together with the lack of standard antibody panels across institutions, has made interlaboratory comparison of FCM data difficult. For clinical purposes (e.g., to moni-

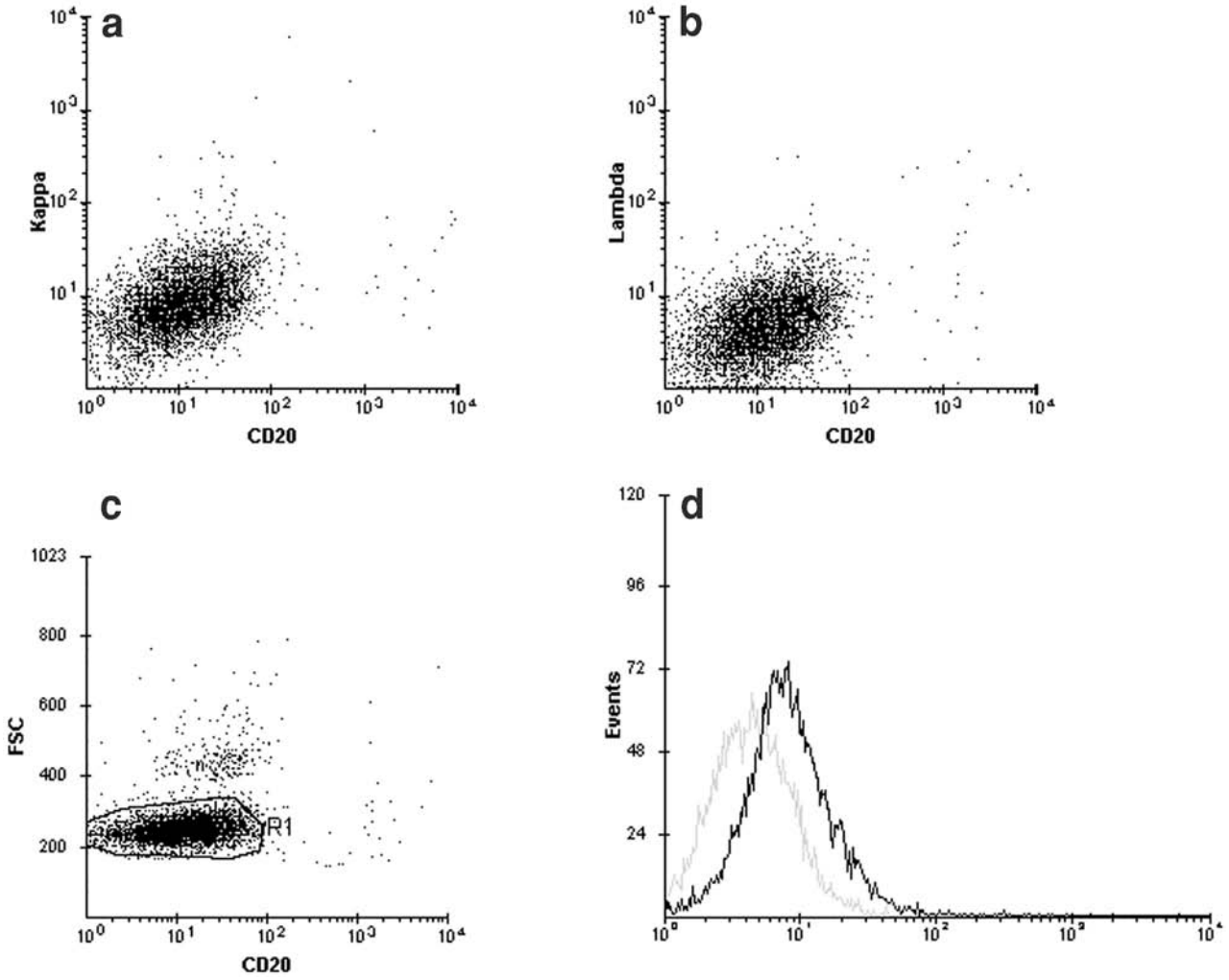

Figure 3.13 Bone marrow with CLL/SLL. (a–d) The intensity of the positive light chain (kappa) is extremely weak, but it is still readily visualized especially on the overlay kappa/lambda histograms (gated on R1). Downregulation of CD20, variable fluorescence distribution of CD20 (starting in the negative region), and the small cell size are other features typical of CLL.

tor patients on whom FCM assays have been performed by more than one institution) review and comparison of the FCM list mode data is currently the most appropriate method for long-term follow-up.

It is important to be aware that the appearance of a bimodal distribution in fluorescence intensity may represent two distinctive but closely related populations (e.g., some cases of AML with monocytic differentiation), instead of one single population, especially if the "figure eight" has a narrow waist. This can be suspected when the same bimodal distribution is seen across several antigens or when the two subpopulations are clearly separate based on the coexpression of certain key markers (Figure 3.18). In such instances, it is more correct to characterize the overlapping halves of the bimodal distribution as two separate clusters: the population of critical cells (i.e., blasts, in the case of AML with monocytic differentiation) and a "related" population (i.e., promonocytes, monocytes).

Using the approach of reporting the average fluorescence intensity based on the mean fluorescence peak channel, it can be difficult to achieve an adequate description of the fluorescence intensity when faced with a complex distribution. In such instances, the authors have sometimes employed the term "variable" as a modifier to the semiquantitative results to denote

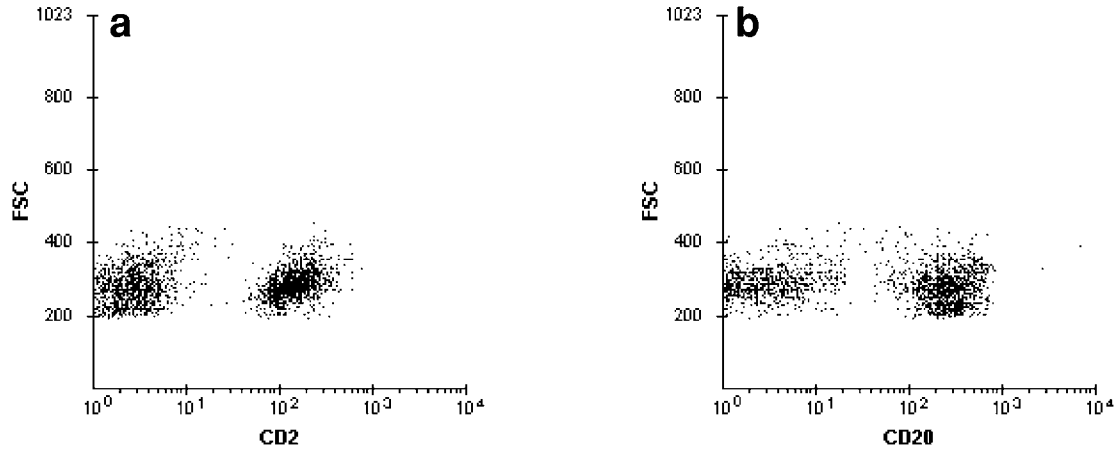

Figure 3.14 Benign lymph node. (a,b) Normal T- and B-cell populations with relatively homogeneous fluorescence distribution for CD2 and CD20, respectively. The benign lymphoid cells are of small cell size.

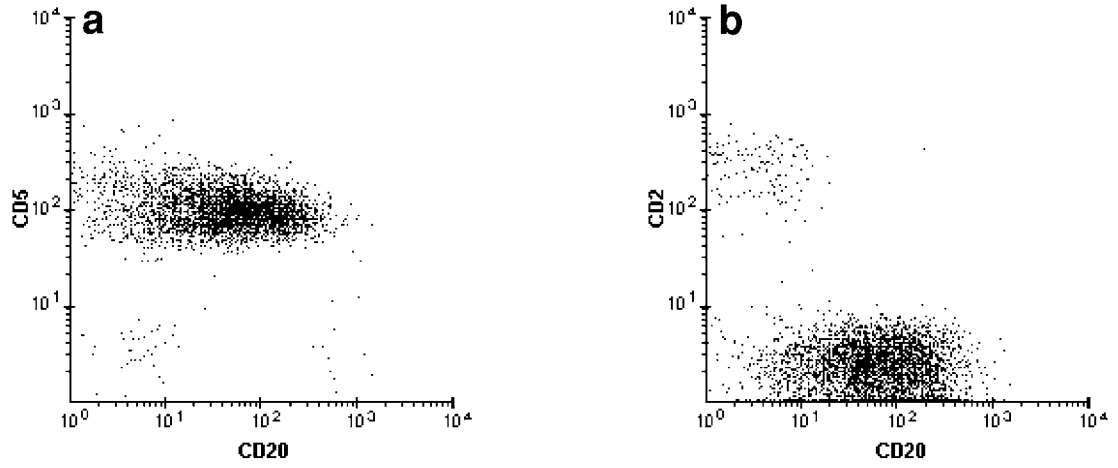

Figure 3.15 Peripheral blood with CLL. (a,b) The leukemic cells coexpress CD20 and CD5. CD20 expression is of a variable distribution and the resulting cell cluster stretches over more than one decalog. A minute population of residual T-cells ($CD2^+$) is present.

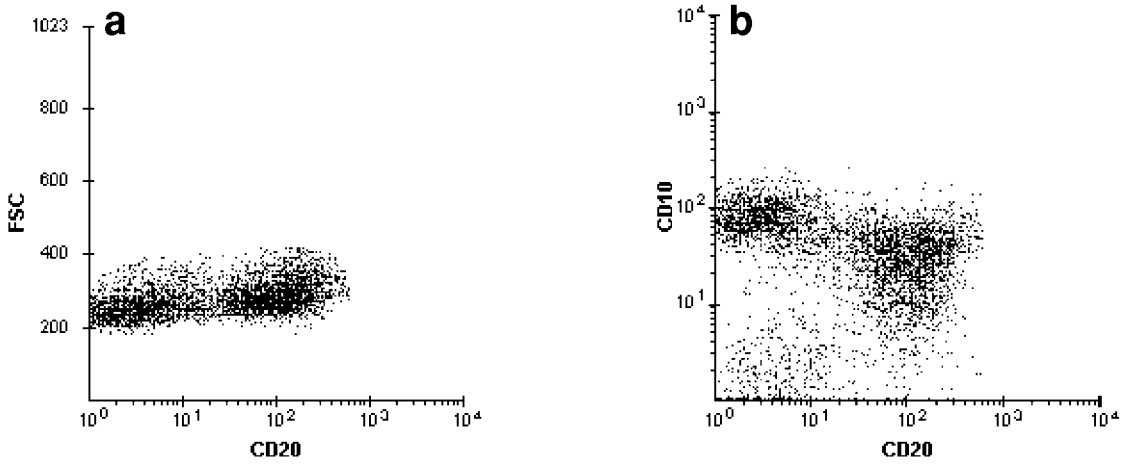

Figure 3.16 An unusual case of FCC II lymphoma. (a,b) The tumor cell population is mostly of small cell size. Most unusual is the bimodal expression of CD20; it is markedly downregulated to absent in about half of the neoplastic cells and well expressed in the other half. The latter display slightly dimmer and more variable CD10 expression.

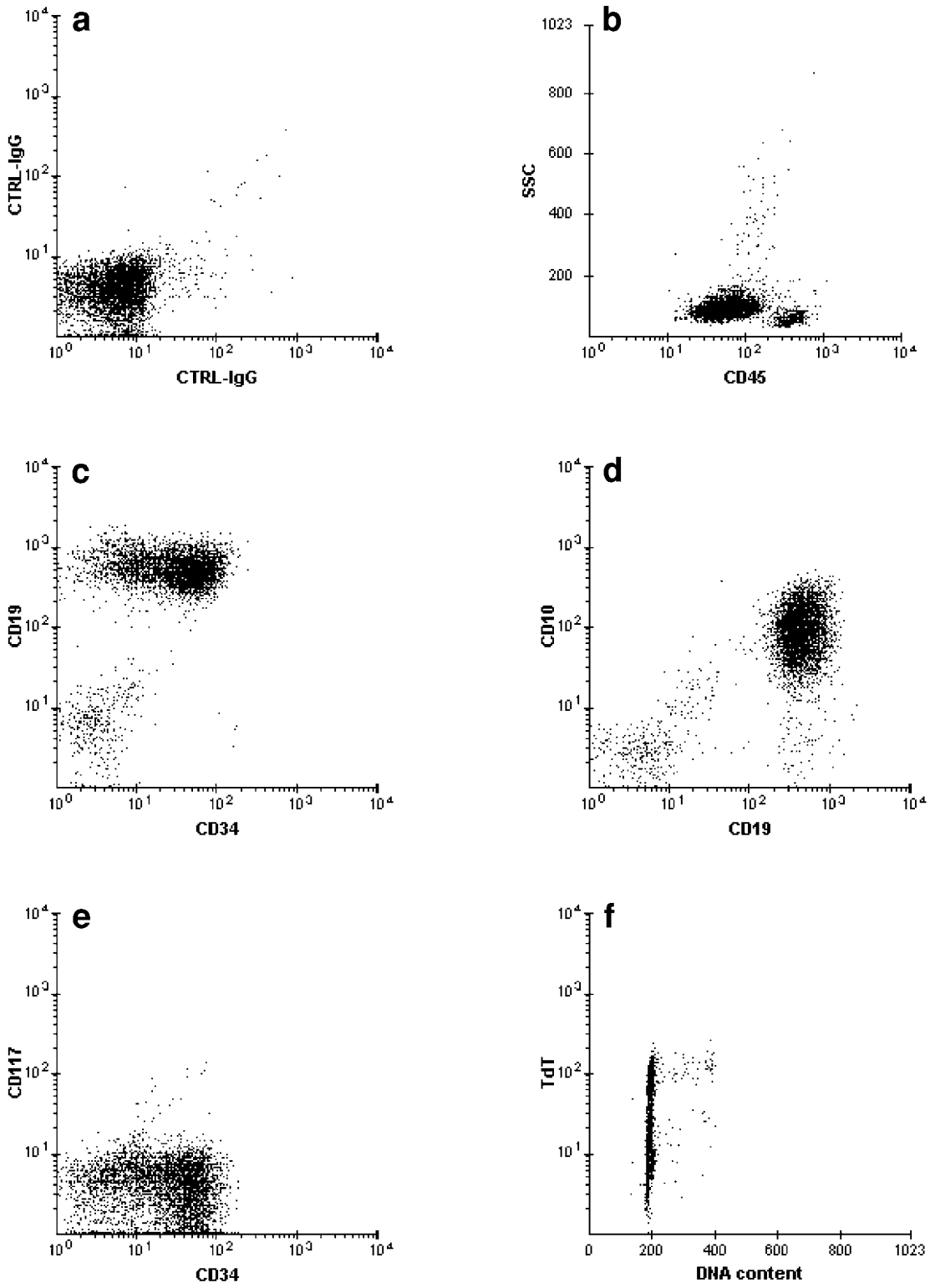

Figure 3.17 Bone marrow with precursor B-ALL. (a) Isotype-matched negative controls. (b) The blast population accounts for 90% of the cells in the sample. (c–e) Blasts are $CD19^{++}$, $CD10^{++}$, $CD117^{-}$, and $CD34^{+}$ (bimodal). (f) The tumor cells are diploid and express TdT.

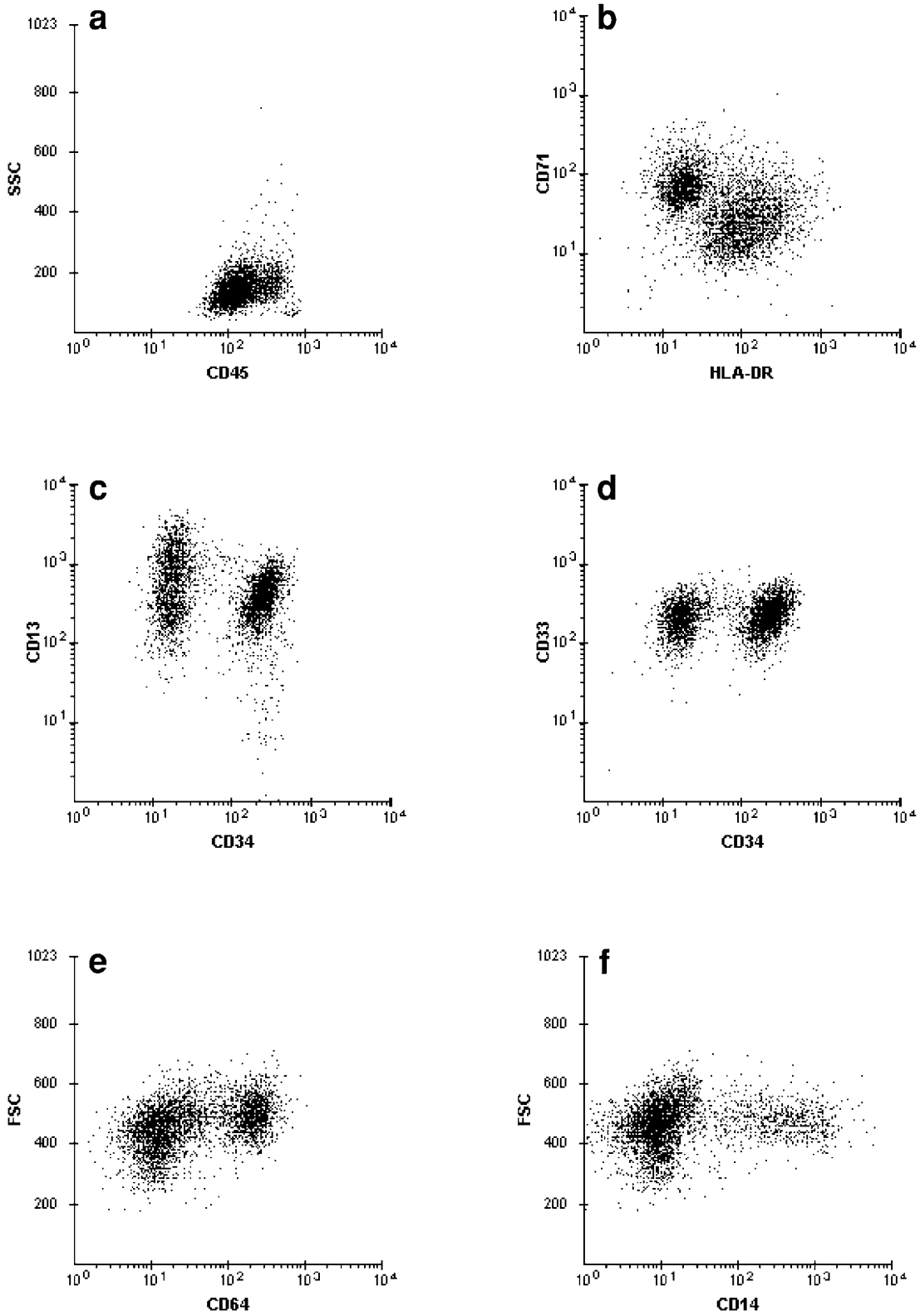

Figure 3.18 AML with monocytic differentiation. (a) A large cluster with bimodal CD45 in the blast region. (b–f) The leukemic population is actually composed of two related components: Blasts and monocytic elements differing in the expression of CD34 (positive in blasts), CD64 (brighter in monocytes), CD14 (negative in blasts), CD71 (dimmer in blasts), and HLA-DR (brighter in blasts). The two subpopulations overlap in cell size and CD13/CD33 expression. CD117 (not shown) is also bimodal.

the heterogeneous staining pattern. Depending on the type of cells and the antigen expressed, the fluorescence signals may begin in the negative region (and/or span over two decalogs or more) (Figure 3.11c). A specific example is the pattern of CD20 expression in CLL/SLL. The appearance of the neoplastic cell cluster on the FSC/CD20 dot plot is virtually pathognomonic for this disorder (Figure 3.13c). In such cases, the intensity of CD20 is best described as "weak, variable." Note that this pattern of CD20 expression can be altered if the analysis is performed following anti-CD20 therapy or if the manufacturers introduce changes (quantitatively or qualitatively) to the composition of any of their reagent cocktails containing CD20 antibody.

3.2 Fluorescence dynamic range

As alluded to in Chapter 2, the graphical pattern of reactivity to certain antibodies or antibody combinations is extremely useful for discriminating cell populations with similar antigenic profiles. In certain diseases, the fluorescence intensity on the malignant cells is different from that on the normal counterparts, or the distribution of the antigen density (and thereby the fluorescence intensity) within the abnormal population is more heterogeneous than the normal cells, resulting in a distinctively shaped cluster. To take advantage of such useful features, it is important to know the range of intensity of a given marker on different hematopoietic elements. In general, a marker with a wide dynamic range (e.g. CD45) offers good discrimination between different cell populations and therefore is most useful diagnostically, especially if it is also lineage-associated (e.g., CD20).

An advantageous feature of CD20 is that its expression on malignant B-cells is usually distinctive from that on the benign counterparts, whereas the density of CD19 on benign and neoplastic B-cells is similar. On dot plots correlating CD19 with other parameters such as FSC, benign and malignant B-cells may overlap and form a single cell cluster. In contrast, with CD20, one often sees the benign and malignant B-cell populations as separate clusters, thus facilitating gating procedures for the identification of other antigens (especially surface light chains) on the cells of interest. Because of this characteristic, CD20 is the marker of choice for pairing with other antibodies to further characterize B-cell neoplasms. In a small number of cases, the discriminatory function is demonstrated by CD19 instead. Therefore, to take advantage of this feature, the authors' laboratory uses two different sets of light chain reagents: one set paired with CD20, the other with CD19 (Figure 3.19). This approach has proven to be extremely helpful in diagnosing and classifying mature B-cell neoplasms.

3.3 Strategy to the visual review of FCM immunophenotyping data

Visual FCM data analysis can be performed most efficiently if the inspection of the FCM graphics follows a sequence based on medical logic. The layout of the FCM displays in the analysis panels mentioned in Section 2.9.1 helps to facilitate this process. For samples derived from the blood, bone marrow, or spleen (i.e., the BBS panel), the following strategy has proven to be helpful to the authors.

Visual inspection begins with the SSC/CD45 dot plot to determine if an overt blast cluster is present and to decide whether or not the sample is composed of multiple cell clusters or overrun by a single, and thereby abnormal, population. The following discussion pertains to the latter situation, in which the dot plots are easier to evaluate than their complex counterparts in specimens harboring neoplastic cells along with several other cell types (*see* Chapter 4).

If the shape and location of the abnormal cell cluster on the SSC/CD45 display suggest that it is a blast population (Figure 3.20a), then the visual evaluation is focused on the dot plots

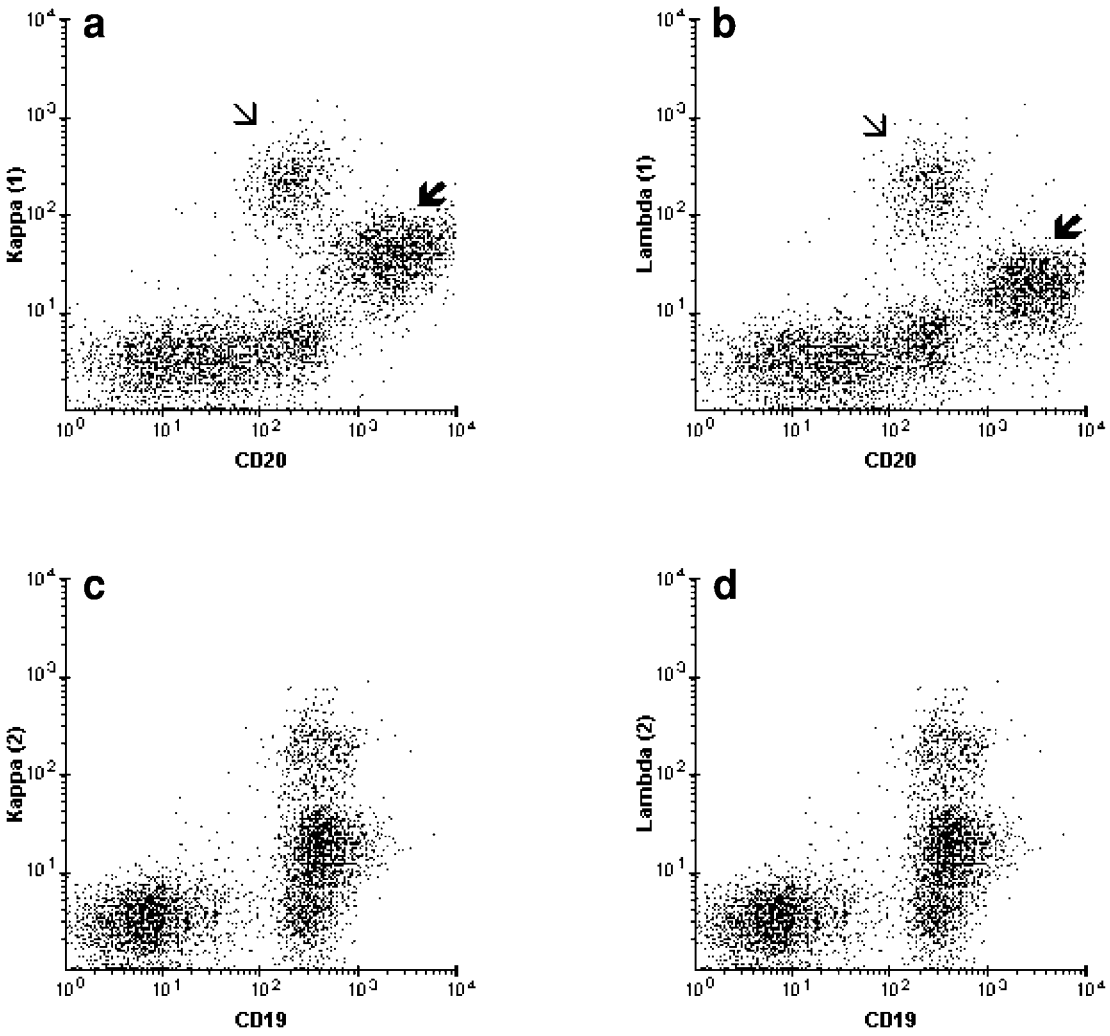

Figure 3.19 Coexisting benign and neoplastic B-cells in a case of FCC lymphoma. (a,b) These two populations are well separated based on CD20 expression. The population with weaker CD20 expression is polyclonal (thin arrow), whereas the one with brighter CD20 is monoclonal for kappa (arrow). (c,d) The benign and neoplastic B-cells cannot be separated from each other based on CD19 expression.

that display CD34, CD117, myeloid antigens (namely CD13 and CD33), HLA-DR, CD19, T-cell antigens, and TdT. TdT is mainly evaluated in T-cell lymphoblastic lymphoma–leukemia because T-lymphoblasts express CD34 at a much lower frequency than their precursor B counterparts.

If the appearance of the abnormal cell cluster suggests a mature lymphoid disorder (Figure 3.20b), then the cell size (FSC) should be evaluated next. This parameter is of greater importance in mature lymphoid malignancies than in acute leukemia because of its usefulness in subclassifying LPD/NHL. The evaluation continues with the inspection of the light chain expression, along with that of CD19, CD20, and other key antigens (e.g., CD5, CD10, CD23, CD103) necessary for characterizing the tumor. If the light chain expression is polyclonal, then the T-cell and NK-cell markers are evaluated instead.

For solid tissue or body fluid samples (i.e., the TF panel) the visual analysis relies more on the FSC/SSC than the SSC/CD45 dot plot because, in most instances, the cellular elements are comprised primarily of mature lymphoid cells, irrespective of whether the population is

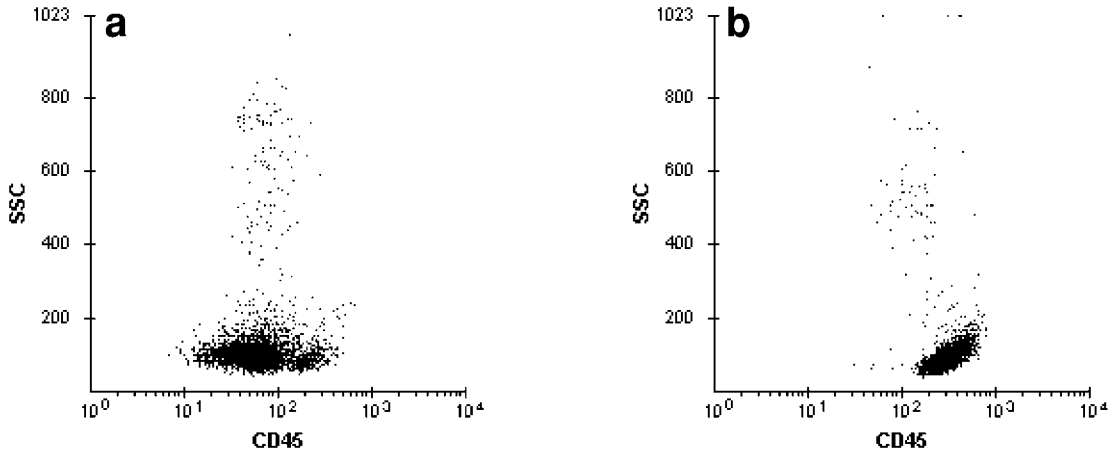

Figure 3.20 (a) Peripheral blood with acute leukemia. The prominent cell cluster in the blast region accounts for 80% of the cells in the sample. (b) Peripheral blood with a B-cell LPD. The specimen is virtually composed entirely of lymphoid cells.

homogeneous or heterogeneous. The visual inspection follows the sequence described for LPD/NHL.

3.4 Common SSC/CD45 patterns

The SSC/CD45 dot plot is most useful for identifying blast populations. Although some of the patterns are virtually pathognomonic for certain acute leukemias, further corroborating evidence from the remaining FCM data is necessary for the final interpretation. Normal lymphocytes, which serve as an internal control, are invariably present as a cluster with very low SSC and bright CD45.

3.4.1 Assessment of the blast population


Case study 1

The blast population most often occupies the position shown in Figures 3.11b, 3.20a, and 3.21a with SSC in the low to moderate range, and CD45 of weak to moderate intensity. CD45 expression on blasts is invariably one decalog or more weaker than that in normal lymphocytes. Leukemic blasts with bright CD45 similar to that of lymphocytes are rarely encountered.

Because the SSC signals correlate with internal cytoplasmic complexities, it can be inferred that a blast cluster with low SSC corresponds morphologically to blast cells with very scant cytoplasm (Plate 4). In most instances, blasts with very low SSC prove phenotypically to be ALL (Figure 3.21). Some AMLs may display an SSC/CD45 similar to that associated with ALL (Figure 3.22).

A substantial increase in normal B-cell progenitors is a common occurrence in regenerative bone marrow, especially that from pediatric subjects. The expansion of these cells does not overrun other normal hematopoietic elements, however. Therefore, the possibility that normal precursor B-cells could manifest as the only cell cluster seen on the SSC/CD45 display is essentially nonexistent. The differential diagnosis of normal B-cell progenitors vs leukemic blasts may need to be considered, however, if the various bone marrow cell populations are well represented on the SSC/CD45 dot plot and a small but conspicuous cluster with very low SSC is seen in the blast location.

When evaluated in the context of positive myeloid antigen expression, the shape of the blast cluster on the SSC/CD45 dot plot can be an important clue to subclassifying AML. For

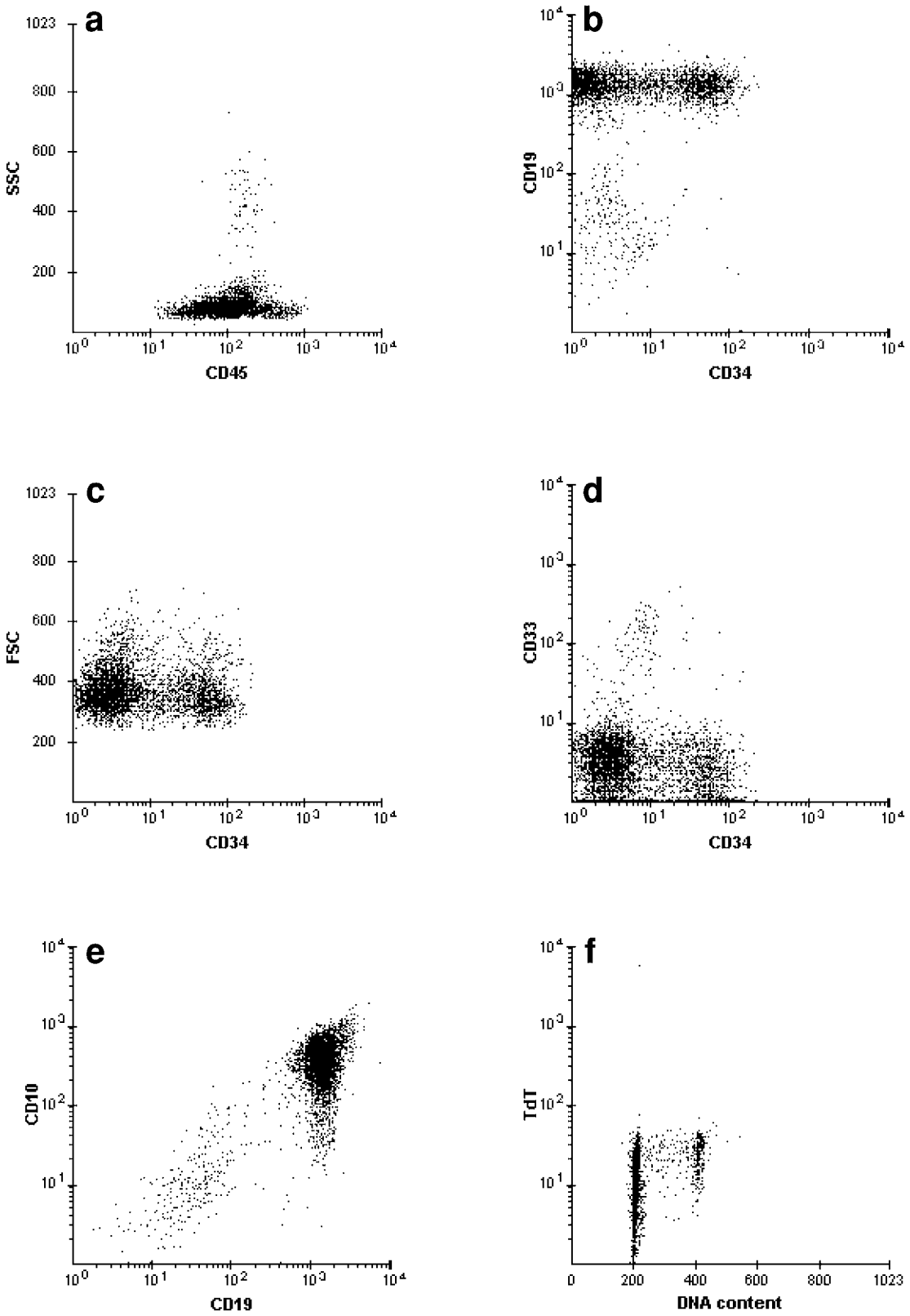

Figure 3.21 Bone marrow with precursor B-ALL. (a) The blast cluster accounts for 92% of the cells in the sample. (b–e) Blasts display medium cell size, weak CD34 with a bimodal distribution, and bright coexpression of CD10 and CD19. CD33 is negative. (f) TdT is also expressed.

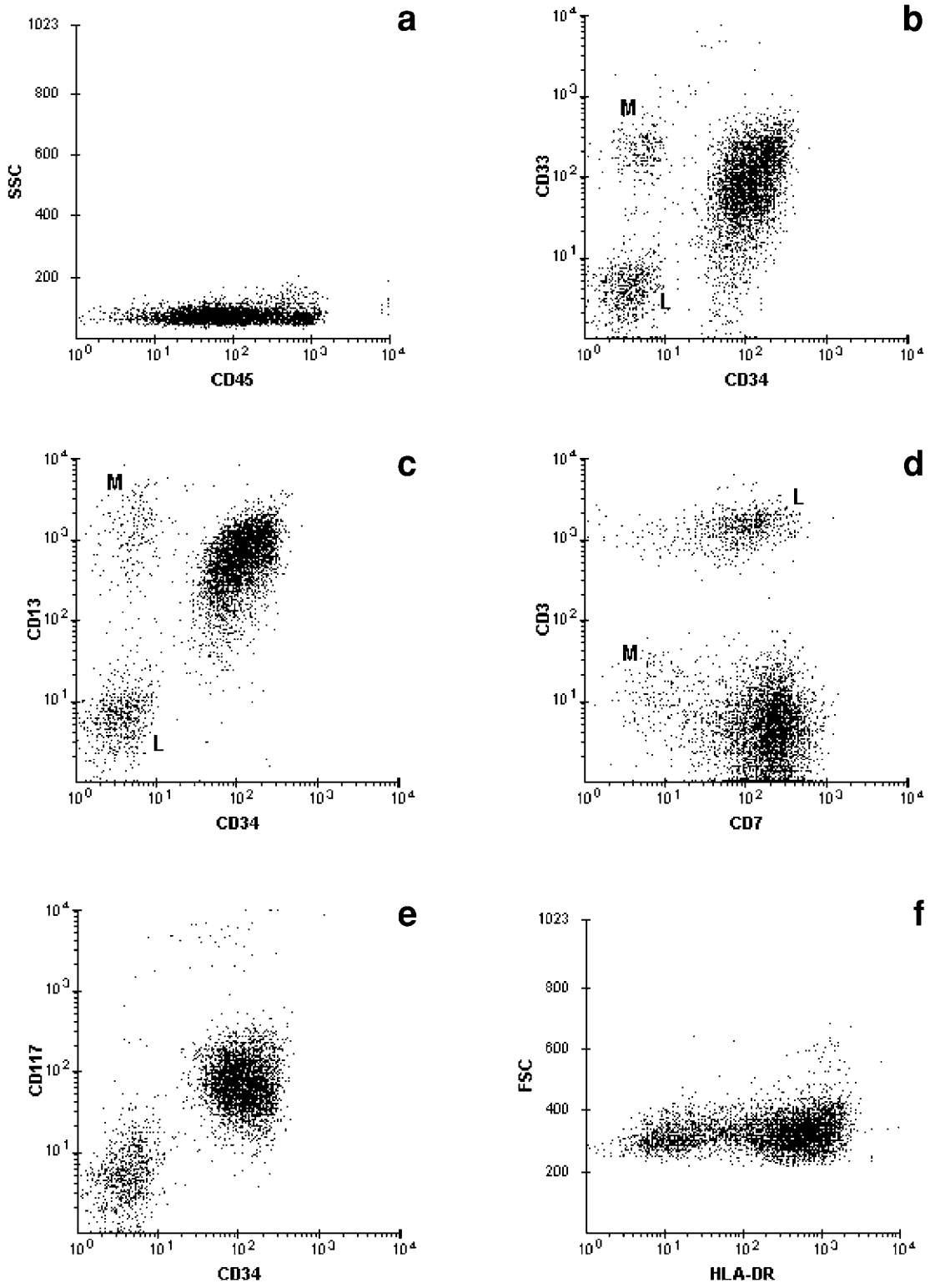

Figure 3.22 Peripheral blood with AML-M0. (a) The blast population displays very low SSC and heterogeneous CD45 expression; the SSC/CD45 pattern is similar to that associated with ALL. (b–f) Ungated data to include the small populations of residual monocytes (M) and lymphocytes (L). Blasts comprise 85% of the cells in the sample. CD13, CD33, CD34, CD117, HLA-DR, and CD7 are well expressed.

this purpose, the bone marrow sample must be representative (i.e., minimally contaminated with granulocytes and monocytes from the peripheral blood). The finding of a prominent blast cluster (expressing myeloid antigens) and virtually no other cell populations on SSC/CD45 indicates AML with minimal evidence of maturation, which can be either AML-M0 or AML-M1 depending on the results of myeloperoxidase cytochemistry (Plate 5).

A virtually single major population with weak to moderate CD45 and SSC signals encompassing a wide range (180–800) from moderate to high is strongly suggestive of AML-M3 (Figure 3.23). The bone marrow in two other conditions may occasionally produce a similar appearance on the SSC/CD45 dot plot (Figure 3.24): (1) CML or CML-like MPD and (2) a vigorous response to granulocyte colony-stimulating factor (G-CSF) therapy (*see* Section 4.5). These can be easily distinguished from AML-M3 based on the remaining FCM graphics such as the pattern of the AML-M3 cell cluster on the CD13/CD16 and CD11b/CD16 dot plots (Figures 3.23 and 3.24). The pattern of CD15/CD34 expression, in which the neoplastic cells lose CD34 prior to acquiring low levels of CD15, has also been reported as another characteristic of AML-M3. Other additional corroborating evidence for promyelocytic leukemia includes the absence of reactivity for HLA-DR, coexpression of CD13 and CD33, and heterogeneous CD13 (as compared to CD33) intensity (Figure 3.23). The constellation of these features correlates highly with t(15;17) and the PML-RARα gene rearrangement, as well as the morphology of AML-M3 blasts.

Case study 2

In AML-M3v, the shape of the cluster on the SSC/CD45 dot plot depends on the degree of hypogranularity. The morphology in most cases displays a variable degree of hypogranularity along with a small proportion of typical M3 blasts and possibly some evidence of maturation to the later myeloid stages. The resulting shape of the blast population on the SSC/CD45 dot plot can be that of a triangle or a teardrop whereby the bulk of the cell cluster represents hypogranulated blasts (Figure 3.25). Typical AML-M3, when relapsed following ATRA (alpha-trans-retinoic acid) therapy, may also manifest as M3v. In unusual cases of M3v composed of markedly hypogranular to agranular blasts, the appearance of the blast cluster can be indistinguishable from that seen in AML with minimal maturation. In addition, CD34 and HLA-DR may be expressed, but the expression of these antigens is of weak intensity and variable distribution (Figure 3.26). Other "aberrancies" such as weak/partial expression of CD11b, CD117 or CD2 occur much more rarely.

Case studies 3 and 4

In AML with monocytic differentiation (i.e., AML-M4 and M5), the shape and location of the blast cluster on the SSC/CD45 dot plot depend on the degree of monocytic differentiation and the relative content of the mature monocytic elements. The type of specimen (i.e., bone marrow vs peripheral blood) also needs to be taken into account because the neoplastic population in the blood may be seen as two distinct clusters (blasts plus monocytes), whereas the corresponding bone marrow yields a single merging cluster. The appearance is usually that of a large cluster shifting upward and to the right (i.e., toward the monocytic region) (Figure 3.27b). Alternatively, the leukemic cells can form a widened cluster extending from the blast region into the monocytic region, thus displaying a variable CD45 expression (Figure 3.27c). If the analysis is on a representative bone marrow sample and the neoplastic cluster displays bimodal CD45 (i.e., merging of the cellular events from the blast region and monocytic regions), then it is important to ensure that the tumor is not actually composed of two separate populations (*see* Section 3.1.3.1).

Occasionally, the internal complexities of the malignant cells in AML-M5 are sufficient to generate high SSC signals, in which case the shape and location of the tumor cell cluster can mimic that observed in AML-M3 (Figures 3.27d and 3.28). The remaining FCM data, however, especially the reactivity of the malignant cells to HLA-DR, CD11b, CD14, CD64, and CD56, provides additional evidence of monocytic differentiation (*see* Section 3.5.1). Cytochemical staining for nonspecific esterase (NSE) can also be added to the immunophenotyp-

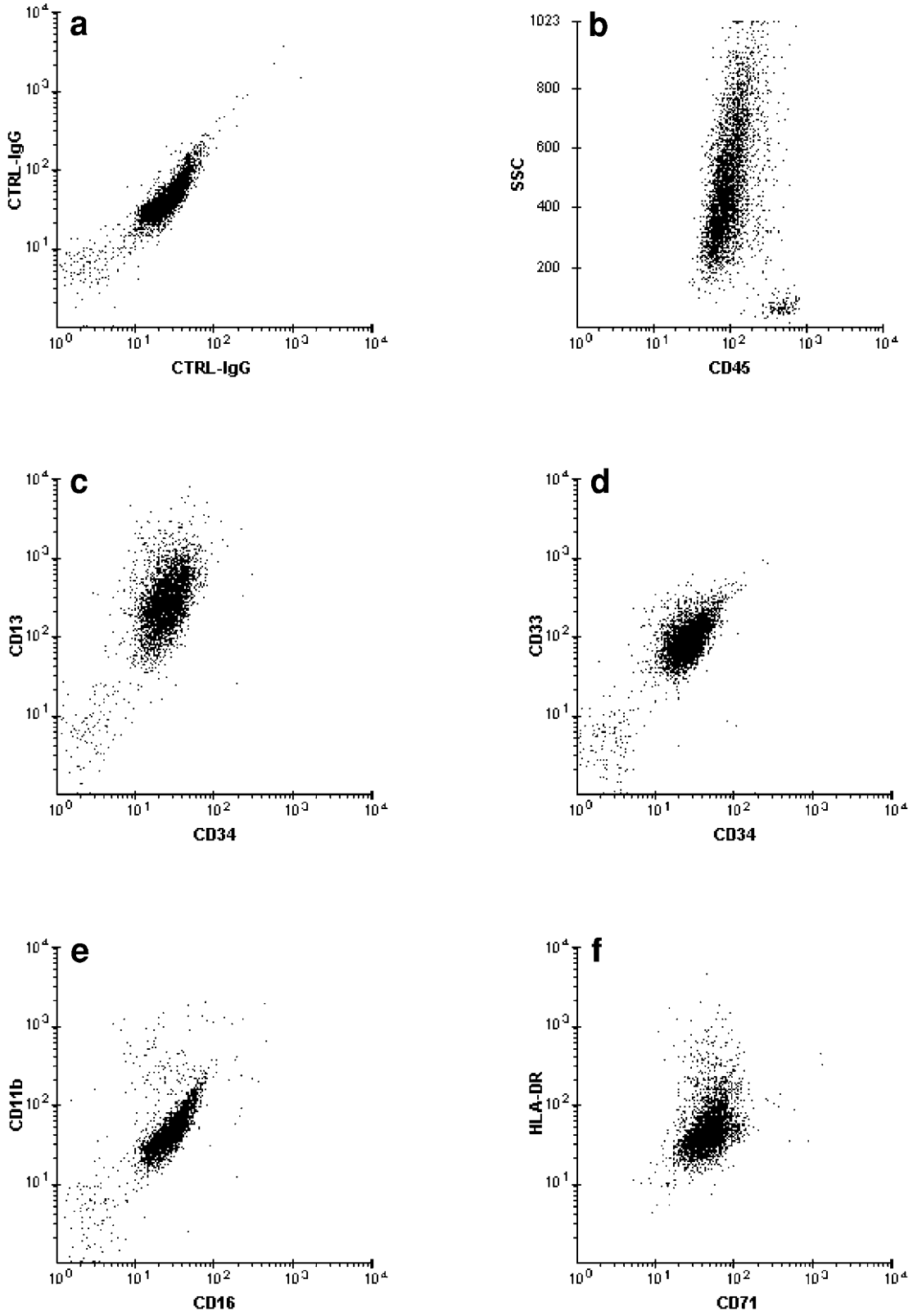

Figure 3.23 Phenotypic characteristics of AML-M3. (a) Isotype-matched negative control showing increased baseline fluorescence. (b–f) The sample is composed of virtually a single predominant blast cluster, with high SSC, and lack of both CD34 and HLA-DR. CD11b, CD16, and CD15 (not shown) are also negative. The intensity of CD13 (c) is relatively more heterogeneous than that of CD33 (d).

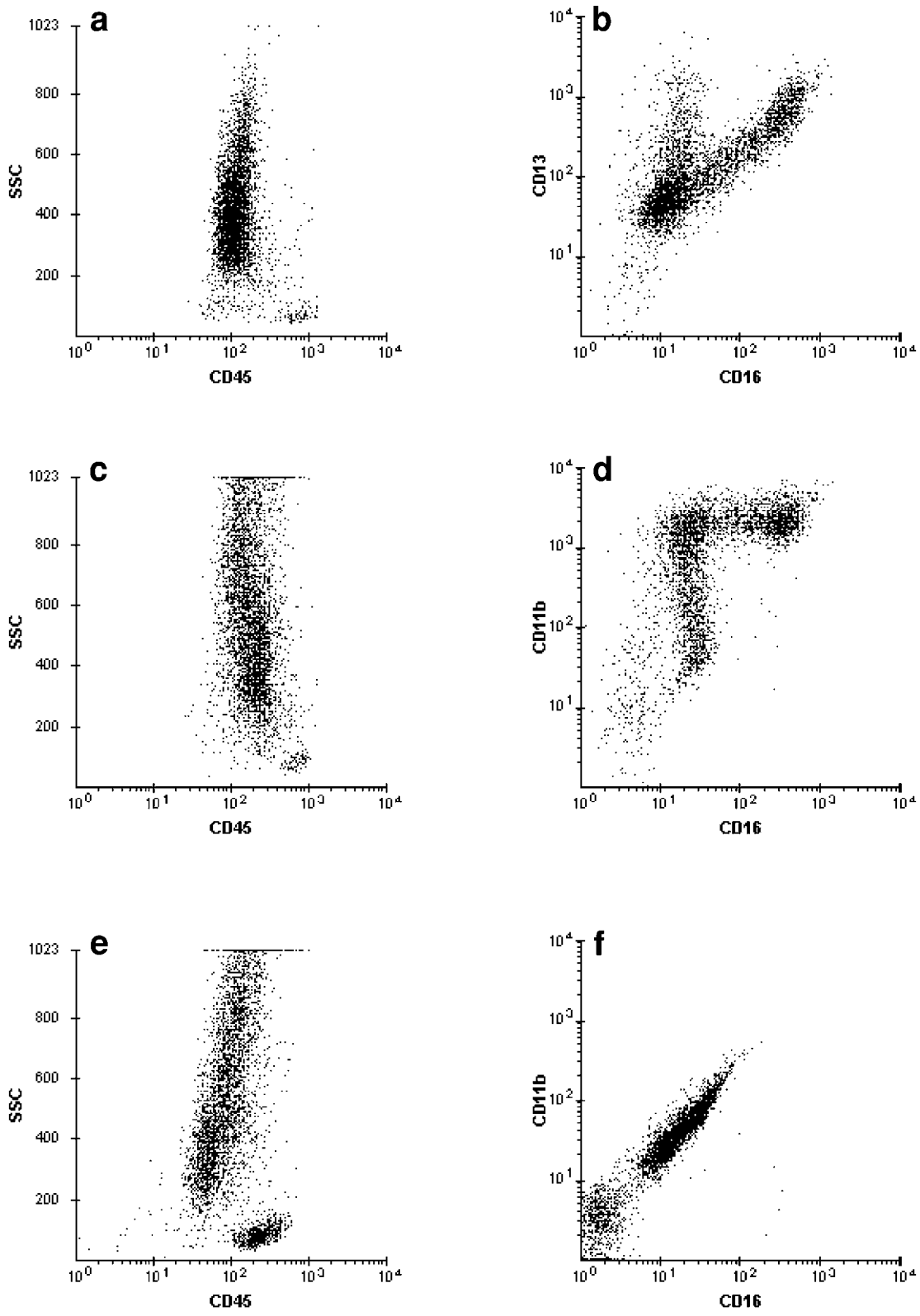

Figure 3.24 Conditions that may produce a bone marrow SSC/CD45 pattern similar to that of AML-M3. (a,b) G-CSF effect; (c,d) CML-like MPD; (e,f) AML-M3 (*see also* Figure 3.23). The single predominant cluster of myeloid precursors (a,c) mimics the appearance of the AML-M3 blast cluster. There is reactivity for CD16 and CD11b (b,d). In contrast, CD16 and CD11b are negative in AML-M3 (f).

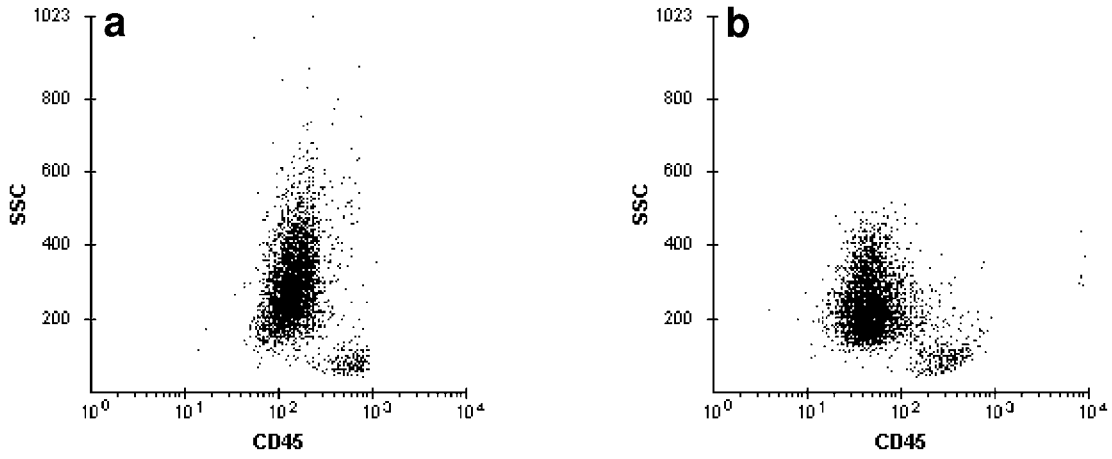

Figure 3.25 Bone marrow with AML-M3v from two different patients. (a,b) A predominant blast cluster with moderate SSC.

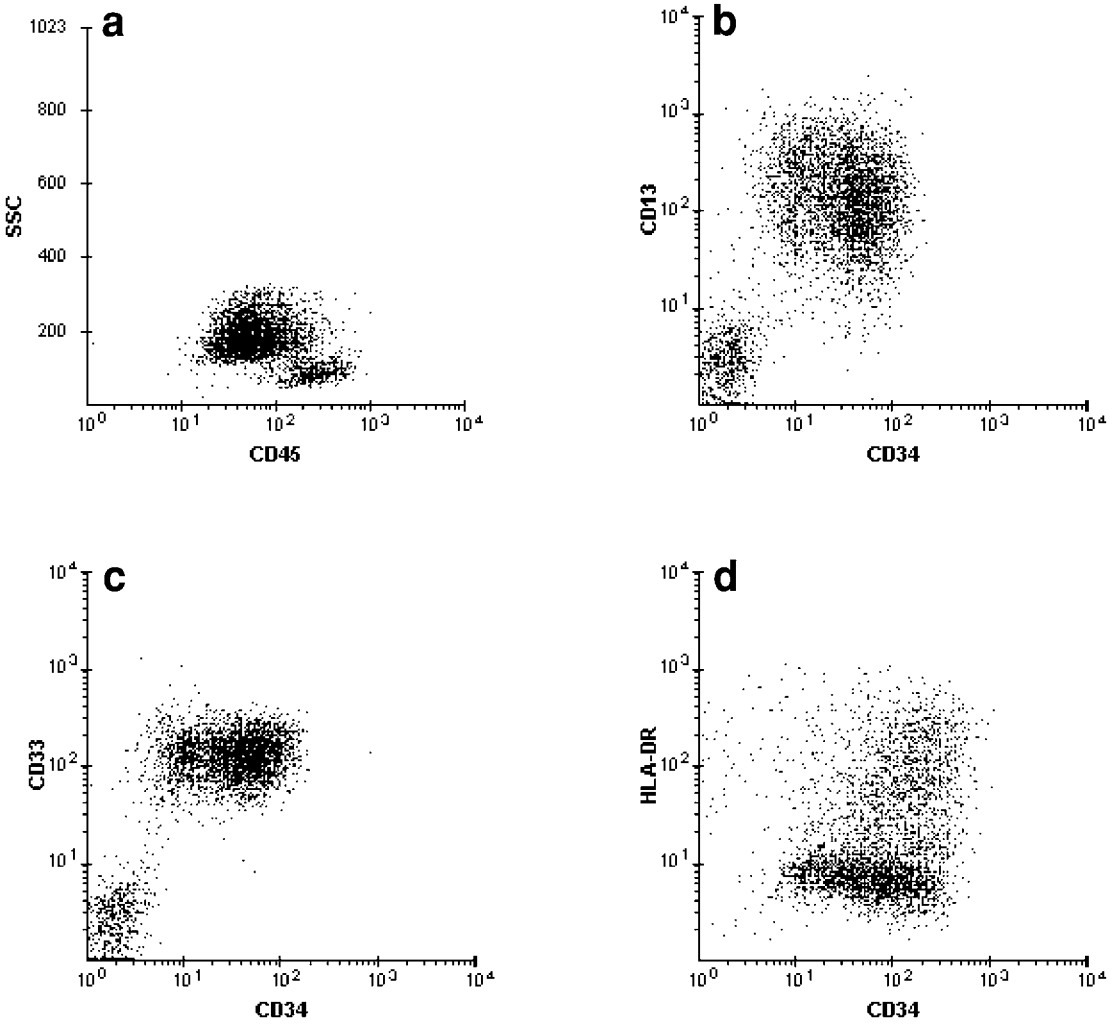

Figure 3.26 Peripheral blood with agranular AML-M3v (morphology shown in Plate 6). This case displays several unusual features: a relatively low SSC (a), expression of CD34 with a variable distribution best appreciated in (d), and variable expression of HLA-DR in a small subset of the leukemic cells. Other typical features of AML-M3, namely heterogeneous CD13 (b) and homogeneous CD33 (c), are retained, however. The t(15;17) and PML-RARα gene rearrangement were demonstrated in this case.

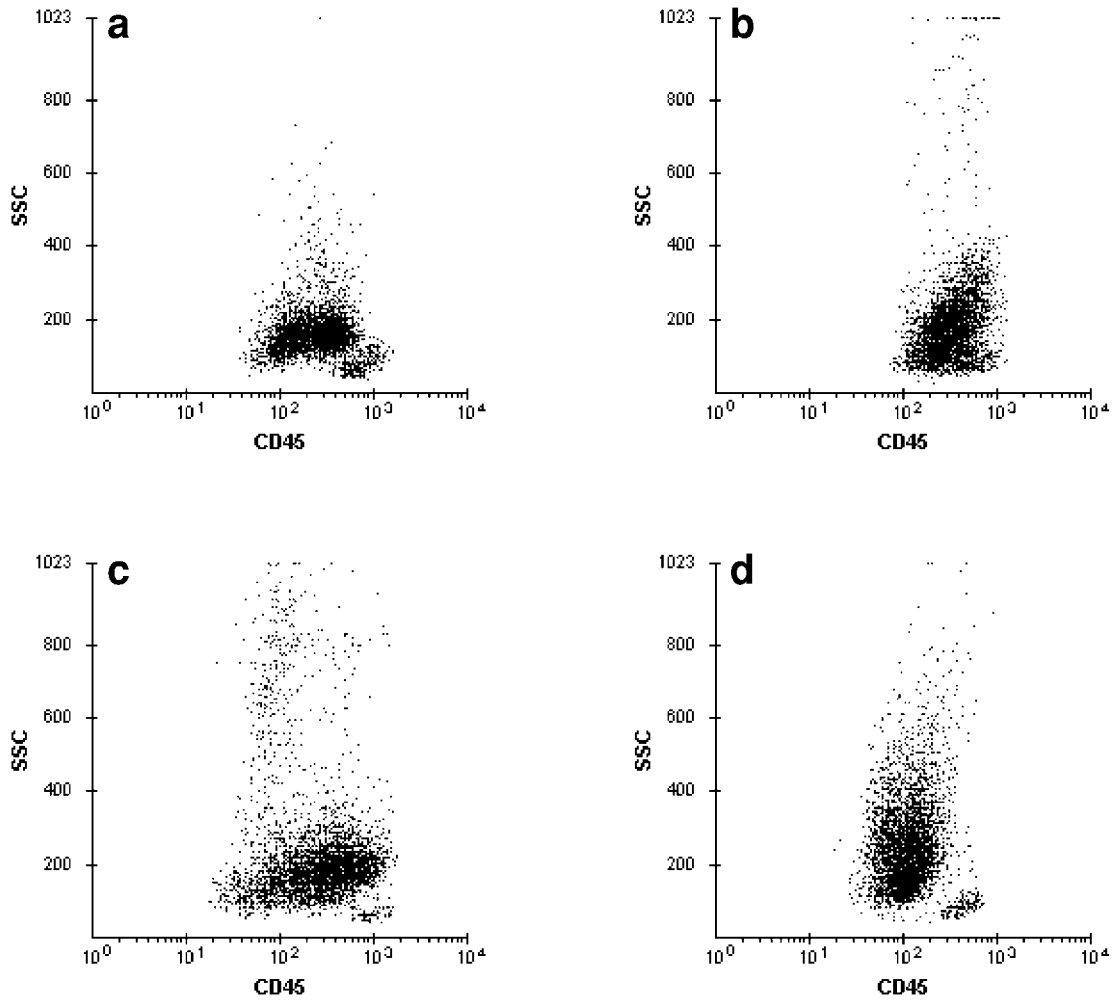

Figure 3.27 Various SSC/CD45 patterns in AML with monocytic differentiation from four different patients. (a) Peripheral blood: The neoplastic population with bimodal CD45 is formed by the merging and overlapping of the blast and monocytic clusters. (b) Bone marrow: The blast cluster is shifted toward the monocytic region. (c) Bone marrow: The leukemic population spans from the blast region into the monocytic region. (d) Bone marrow: The appearance of the blast cluster mimics that seen in AML-M3v.

ing results if an AML with monocytic differentiation is to be subclassified as AML-M4 or M5 according to the French–American–British (FAB) criteria.

3.4.2 Immature neoplastic cells with downregulated CD45

Case study 5

CD45 is markedly downregulated or negative in a substantial number of acute leukemias, many of which are precursor B-ALL. On the SSC/CD45 dot plot, the blast population is seen in the far-left position (Figure 3.29). Other cell types can also appear in this location, however, including erythroid precursors, plasma cells (Figure 3.30), and nonhematopoietic metastases. Occasional high-grade mature B-cell neoplasms (especially those with plasmablastic differentiation) or rare mature T-cell LPD/NHL may also exhibit downregulated CD45.

Large numbers of unlysed red cells manifest as a prominent cluster in the CD45-negative region; these should have been excluded from the data acquisition based on a quick screening of the cytospins prior to running the samples on the flow cytometer, however.

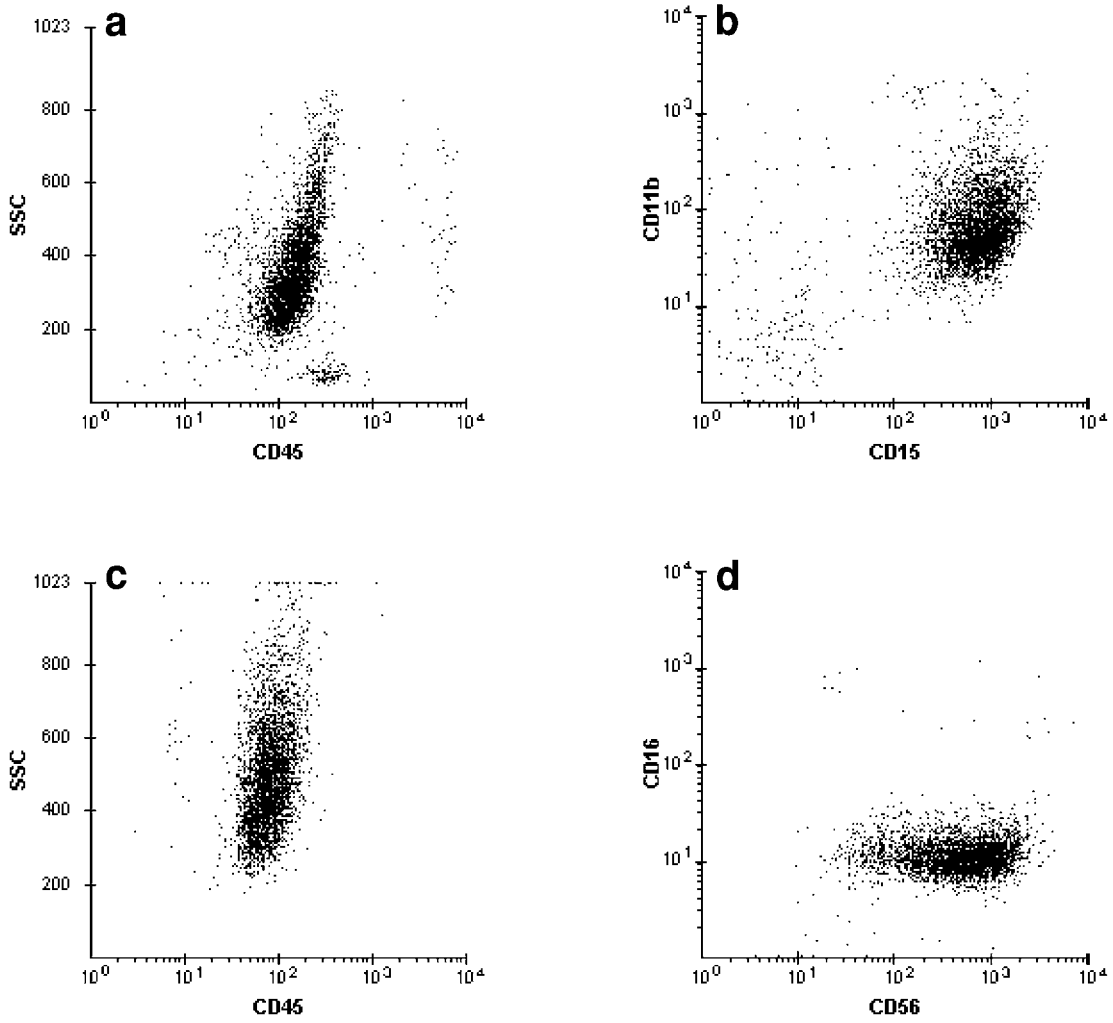

Figure 3.28 Two unusual cases of AML with monocytic differentiation. The SSC is unusually high (a,c), resulting in a picture reminiscent of AML-M3. CD11b and CD15 are brightly expressed in the first case (b), whereas CD56 is positive in the second (d).

A prominent cluster with low SSC and a bimodal CD45 distribution spanning over two decalogs or more from the negative into the positive range is an uncommon finding. This may represent one of the following:

- The merging of two distinctive populations. The cluster on the left with markedly downregulated CD45 may be comprised of erythroid precursors, and the cluster on the right may be comprised of blasts. Alternatively, they may represent two different clones of blasts (e.g., ALL and AML) with similar SSC characteristics.
- One single neoplastic population with bimodal CD45. An occasional ALL or AML may display this pattern (Figure 3.31).

Case study 6

3.4.3 SSC/CD45 in mature lymphoid disorders

The SSC/CD45 dot plot is of limited usefulness in mature lymphoid disorders because different types of NHL/LPD generate closely similar SSC signals and CD45 intensities. In specimens with extensive involvement by any NHL/LPD, the usual finding on the SSC/

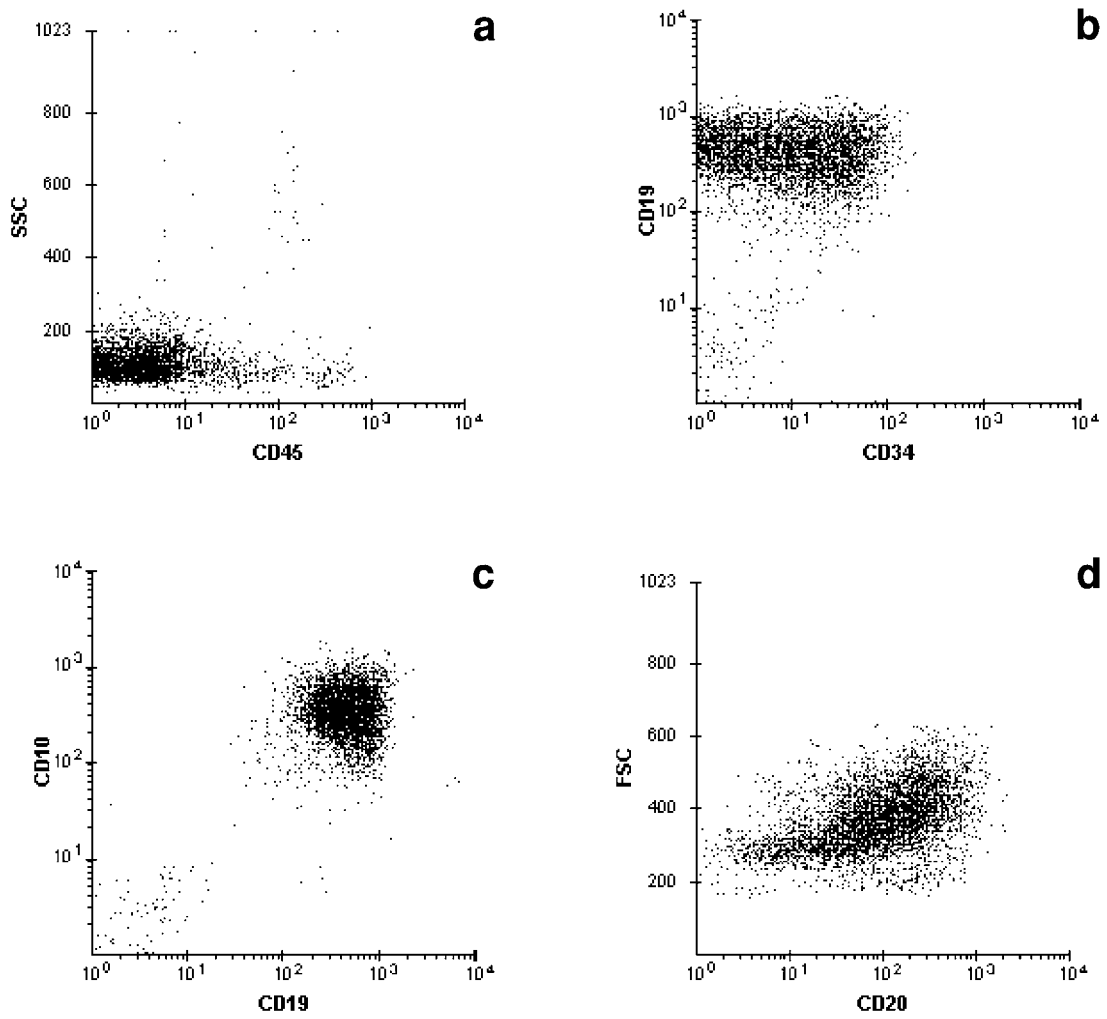

Figure 3.29 Bone marrow with CD45-negative precursor B-ALL. Blasts are of medium cell size (d) and display markedly downregulated CD45 (a) and bright coexpression of CD19 and CD10 (c). CD34 is weak and of variable distribution (b). An unusual feature is the bright expression of CD20 (d).

CD45 dot plot is a prominent cluster with low SSC and moderate to strong CD45 expression (Figure 3.20b). Although the intensity of CD45 on the neoplastic cells is closely similar to that of normal lymphoid cells, it may be slightly downregulated and the distribution more heterogeneous. This feature is most commonly seen in CLL, with the neoplastic cells forming a cluster occupying the hematogone region (Figure 3.32). The light scatter characteristics and CD45 intensity of hairy cells, as well as neoplastic cells in a substantial number of large cell lymphomas, are similar to those of monocytes (*see* Sections 3.6.3.2 and 3.6.3.4). Thus, in extensive involvement of the bone marrow or blood, the resulting cell cluster seen on the SSC/CD45 dot plot may simulate the SSC/CD45 picture of a neoplastic monocytic disorder. A small number of aggressive LPD/NHL may lack detectable CD45 (*see* Section 3.6.3.4).

3.5 Other dot plot patterns useful in acute leukemia diagnosis

The correlated displays CD13/CD34, CD33/CD34, or CD117/CD34 are useful for quantifying the proportion of leukemic myeloblasts (Figures 3.18 and 3.22). Similarly, the propor-

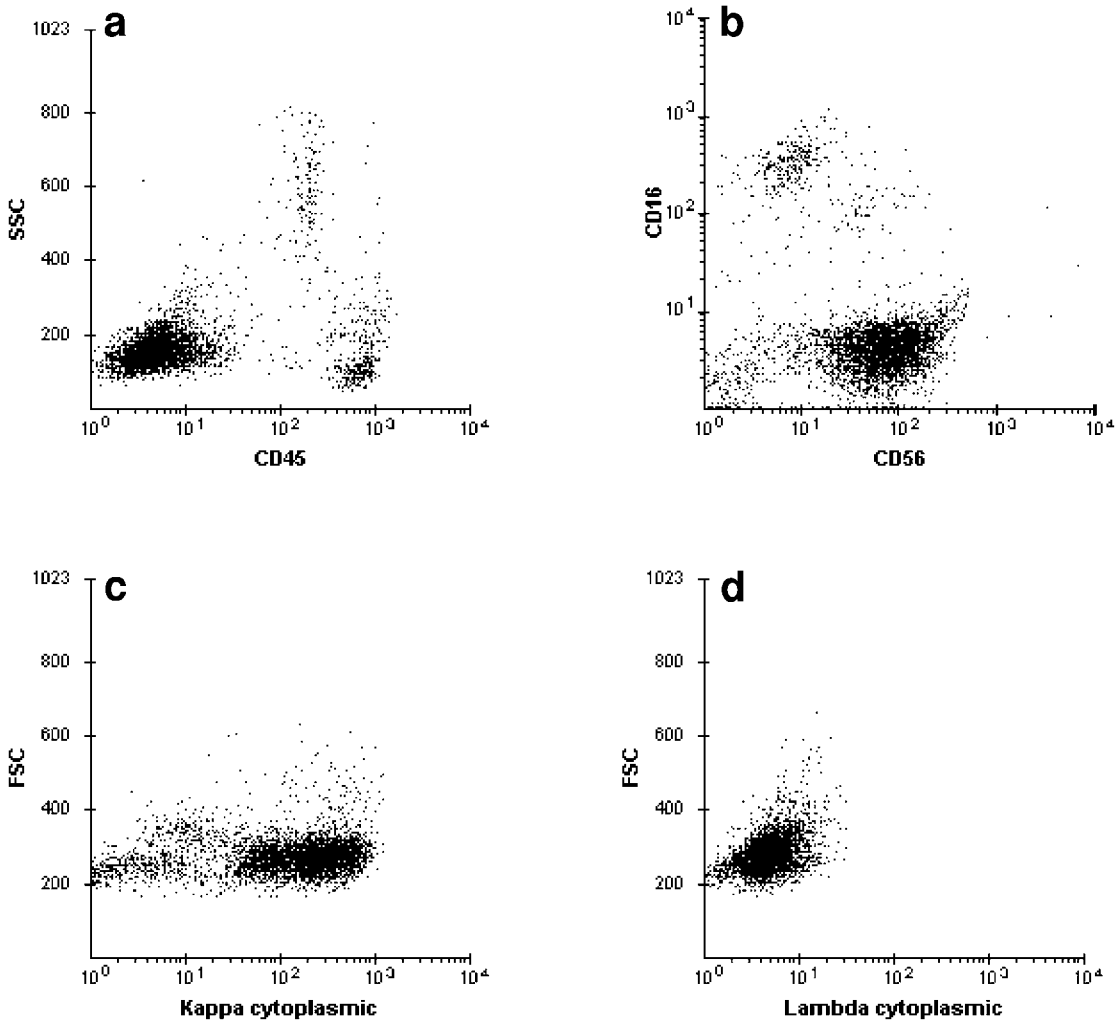

Figure 3.30 Plasma cell leukemia (morphology shown in Plate 42). (a) A predominant neoplastic cluster in the CD45-negative region. (b–d) The tumor is positive for CD56 and cytoplasmic kappa.

tion of precursor B-ALL blasts can be derived from the CD19/CD34 dot plot (Figures 3.17, 3.21, and 3.29), or TdT/CD19, especially if the blasts are CD34 negative. In most T-ALLs, the blast proportion can be determined based on TdT/CD7 coexpression or, alternatively, CD4/CD8 coexpression (Figure 3.11). In a substantial number of AMLs, especially those with monocytic differentiation, the blasts are negative for CD34. Many of these demonstrate reactivity for CD117, however. In contrast, the blasts in ALL typically lack CD117.

3.5.1 Useful antigenic features in AML

In the context of a prominent blast population with myeloid antigen expression, the results of other markers such as HLA-DR, CD14 (when correlated with CD64), CD16, or CD56 can be helpful for subclassifying AML. Although the blast population may demonstrate a bimodal or variable distribution for CD34, CD13, or CD33, this feature does not add much to the subclassification of AML.

The diagnostic importance of HLA-DR lies in its lack of expression, typically seen in AML-M3 blasts. In contrast, blasts in non-M3 AML express moderate to very bright levels of HLA-DR. Two potential pitfalls are to be avoided, however:

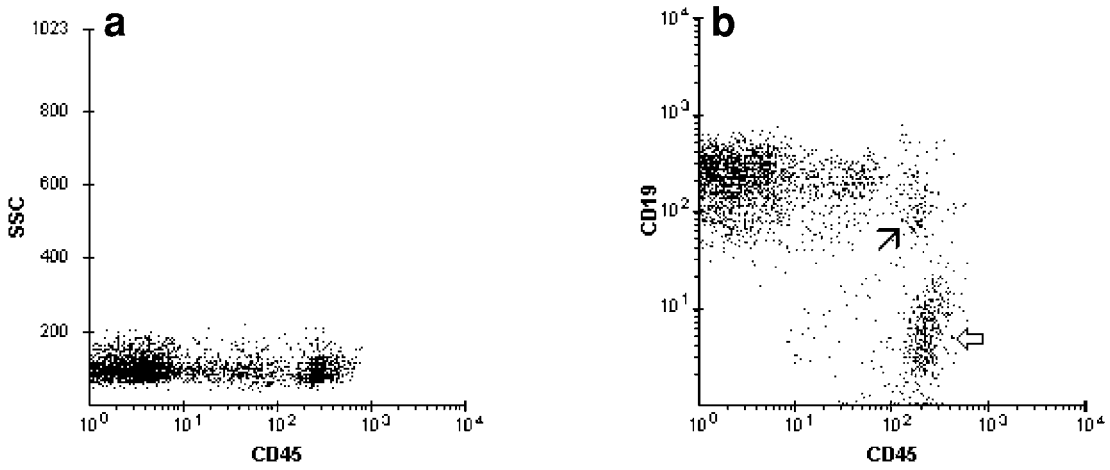

Figure 3.31 Precursor B-ALL with bimodal CD45. (a,b) Two subpopulations of blasts: The major one is CD45-negative and the minor one is CD45-positive. Some normal B-cells (arrow) and T-cells (open arrow) are present.


Case study 7

1. Absence of HLA-DR can occur in some cases of AML-M1 (Figure 3.33). The phenotypic profile is similar to that of AML-M3 in that the neoplastic cells are negative for both HLA-DR and CD34. However, the shape of the blast cluster on the SSC/CD45 dot plot is not that associated with AML-M3 (Figures 3.23 and 3.25). The pattern of reactivity to CD13 and CD33 is also different. Furthermore, these cases also lack the cytogenetic abnormalities of AML-M3 and do not respond to ATRA therapy. Additional phenotypic aberrancies may be present, such as markedly downregulated to absent CD13 but bright CD33, in contrast to AML-M3 in which both CD13 and CD33 are well expressed.
2. HLA-DR expression may occur in AML-M3. These are often AML-M3v, in which the blasts are severely hypogranular or agranular (Plate 6) and, therefore, may be morphologically mistaken for non-M3 blasts or lymphoma cells. The intensity of HLA-DR is distinctively weaker (Figure 3.26) than that seen in non-M3 blasts, however. Other phenotypic features such as a lack of expression of CD117, CD11b, and CD16, plus the cytogenetic abnormalities and biological behavior are otherwise identical to typical AML-M3.

The CD14/CD64 dot plot is useful for determining monocytic differentiation. There exist noticeable differences in reactivity between different clones of anti-CD14 antibodies. The observations described here pertain primarily to the Leu-M3 clone of anti-CD14, which labels predominantly mature monocytes. Some of the other clones of anti-CD14 also label myeloid cells, but at a lesser level of reactivity than that with monocytes. Similarly, CD64 expression is less intense on granulocytes than monocytes. On the correlated dot plot, mature monocytes appear as a homogeneous cluster with bright CD14 and CD64 (Figure 3.34).

In some cases of chronic myelomonocytic leukemia (CMMoL), the granulocytic elements are so few that the resulting SSC/CD45 dot plot displays a single major cluster in the monocytic position (Figure 3.35) [i.e., a picture similar to that of AML with monocytic differentiation (Figures 3.27 and 3.36)]. Conversely, residual/relapsed AML with monocytic differentiation may contain a substantial number of myeloid cells, and the resulting SSC/CD45 can thus mimic that of CMMoL. In such instances, the pattern of CD14/CD64 reactivity is a clue to distinguish these two different disorders. The neoplastic population in CMMoL is composed mostly of mature elements coexpressing bright CD14 and CD64. In contrast, the coexpression of CD14 and CD64 on neoplastic cells in AML with monocytic differentiation often manifests as a diffuse "trailing" cluster (Figure 3.36). This vertical "trail"

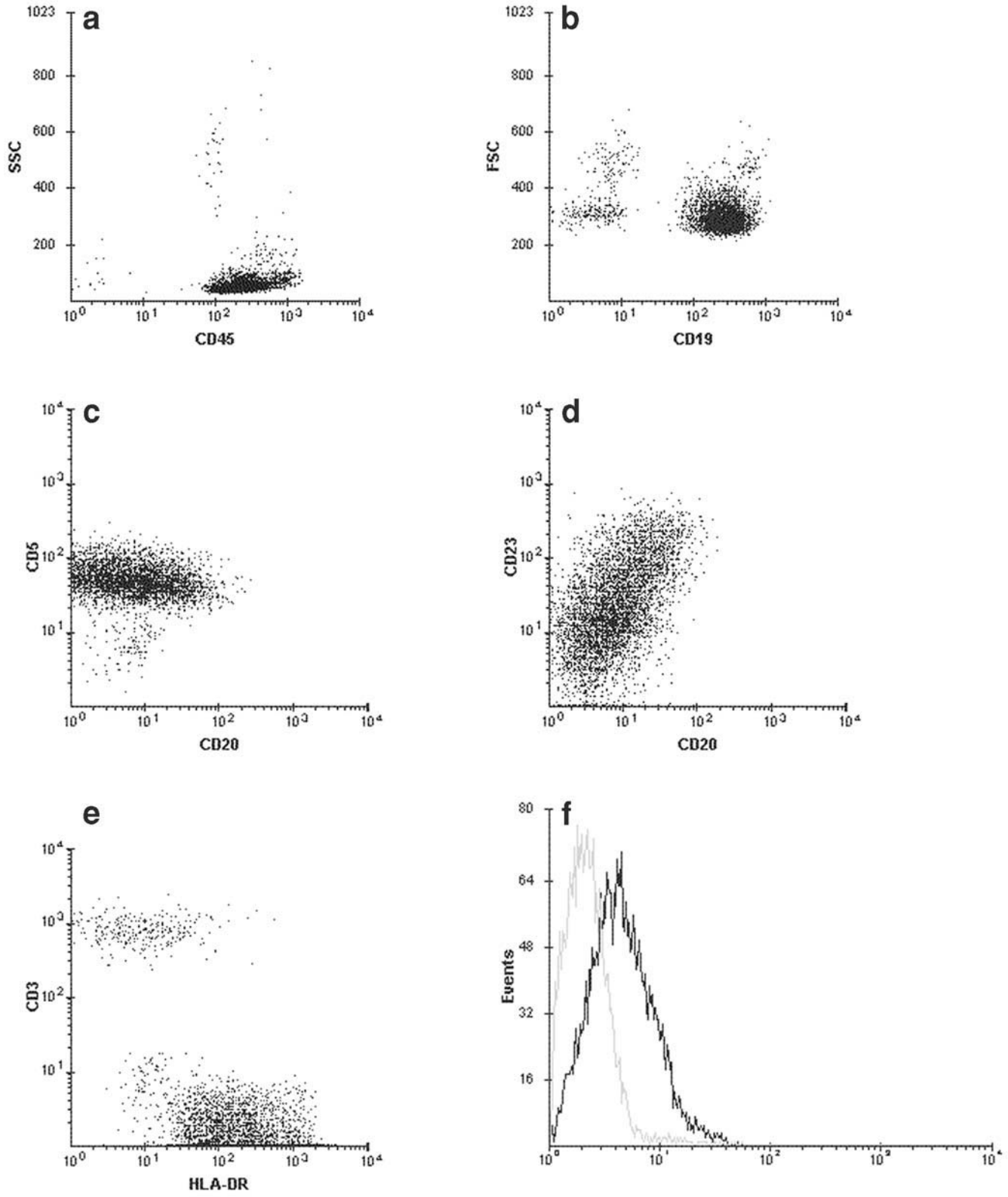

Figure 3.32 Bone marrow with CLL. (a) A predominant cluster in the hematogone region, with CD45 less intense than that on normal lymphocytes. (b–f) The leukemic cells display the typical phenotypic features of CLL: small cell size, weak and heterogeneous CD20 expression, CD20 less intense than CD19, dim lambda-positive surface light chain (f), and reactivity for CD5 and CD23. In this case, CD23 is downregulated and of variable distribution. HLA-DR is expressed.

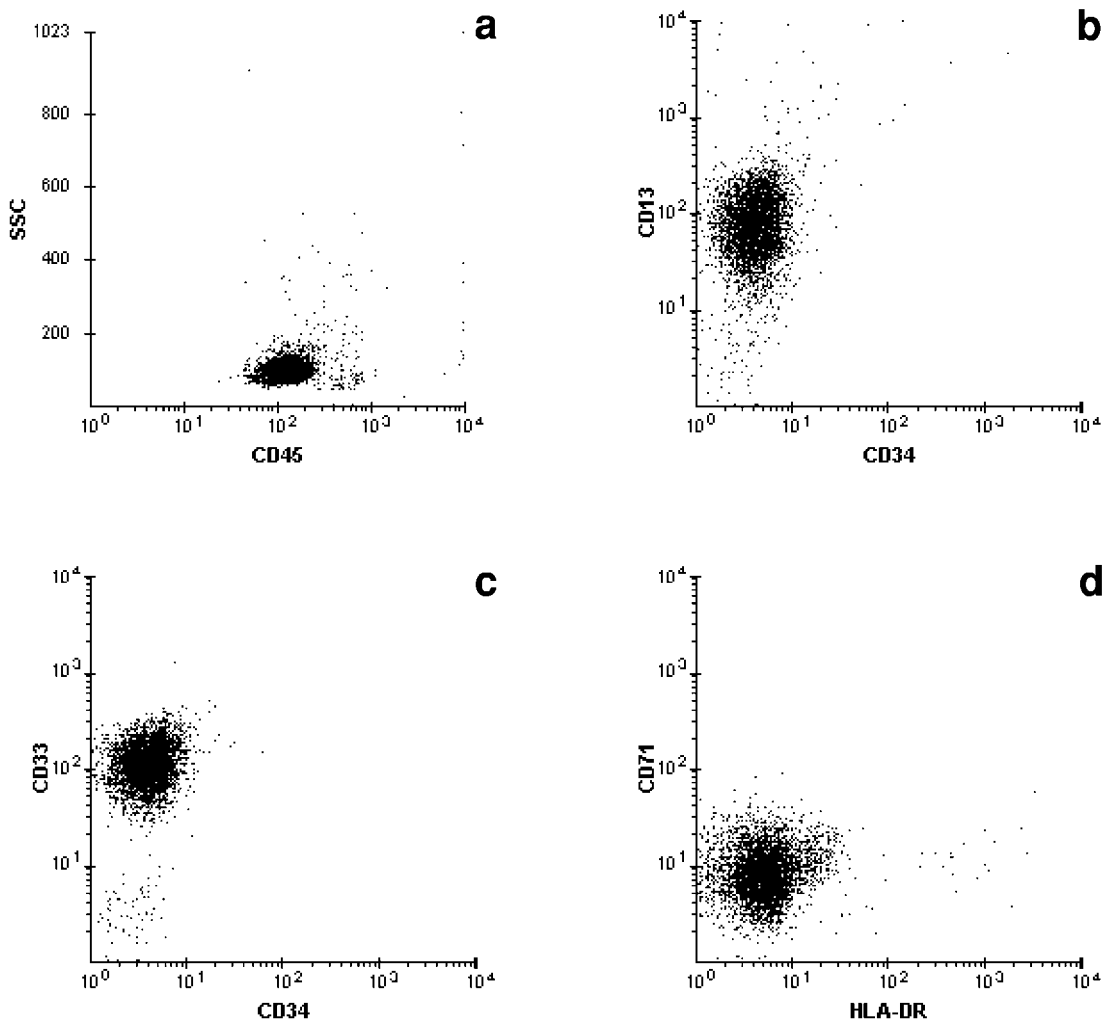

Figure 3.33 An unusual case of AML-M1. (a) A single predominant cluster in the blast region with low SSC. (b–d) Blasts are CD13^{++}, CD33^{++}, and negative for CD34. HLA-DR is minimally present on a tiny subset of the blasts. Cytogenetics and molecular genetics did not reveal a PML-RARα rearrangement.

pattern reflects the marked heterogeneity in CD14 expression (ranging from negative to bright) and thereby the variable degree of monocytic differentiation/maturation among the neoplastic cells. This, in turn, translates morphologically as a spectrum of blasts, promonocytes, and monocytes (Plate 7) in which the more immature elements predominate. The most immature cells often produce a loosely formed cell cluster located at the lower end (i.e., CD64 bright, CD14 negative or markedly downregulated) of the vertical trail (Figure 3.36d). In some cases, the entire tumor population lacks CD14 expression (Figure 3.37). The morphologic picture in the latter instance is usually that of AML-M5a. In others, a third pattern is observed whereby the blast and monocytic components (although seen together as one cell population on the SSC/CD45 dot plot) separate from each other into (1) a blast cluster negative for CD14 and CD64 and (2) a CD14/CD64-positive "trail" of monocytic elements (Figure 3.36a,b). Such cases may be referred to as AML with a monocytic component. The terminology "AML with monocytic differentiation" and "AML with a monocytic component" can be used interchangeably, however, since these two subgroups share a similar biological behavior.

Case studies 8 and 9

CD56 expression may occur in acute leukemias, either of lymphoid or myeloid lineages. In myeloid leukemias, CD56 reactivity tends to be associated with monocytic differentiation

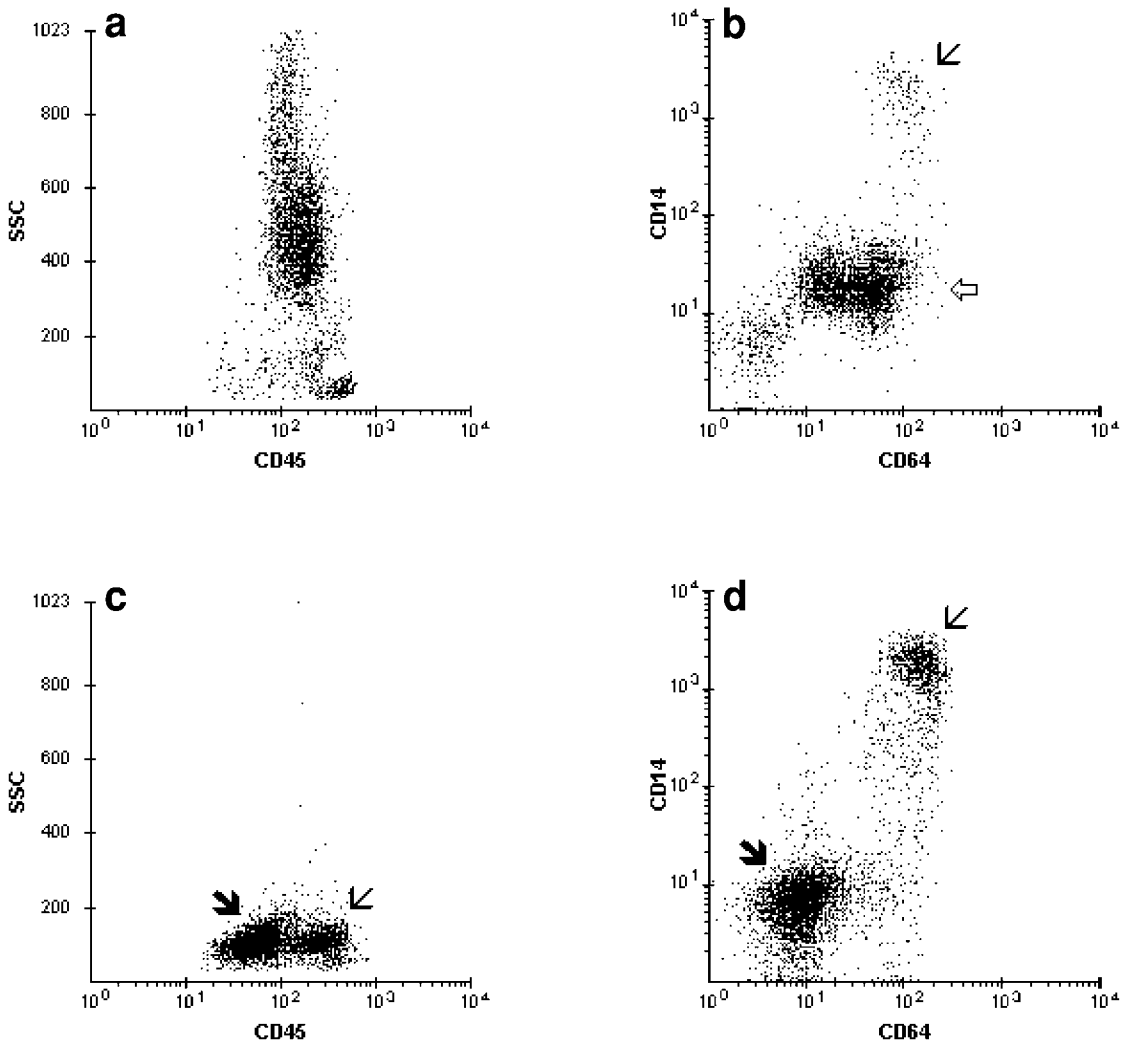

Figure 3.34 Coexpression of CD14 (Leu-M3) and CD64 on monocytes. (a,b) Normal bone marrow with a small population of monocytes forming a relatively compact cluster positive for CD64 and CD14 (thin arrow). Myeloid precursors (open arrow) are $CD14^-$ and $CD64^+$. There is increased baseline fluorescence (not shown) in this case. (c,d) Peripheral blood with AML-M4. Distinct blast (arrow) and monocytic clusters. (d) Gated on MNCs: Mature monocytes (thin arrow) are prominent and coexpress bright CD14 and CD64. A small subset of the monocytic elements display variable CD14 expression, seen as a short ill-defined trail attached to the CD14/CD64-positive cluster. Blasts are $CD14^-$ and $CD64^-$.

Case study 10

(Figure 3.37f). This feature is also present in other abnormal monocytic proliferations such as CMMoL (Figure 3.35). Because these phenotypic abnormalities are by themselves not diagnostic of abnormal monocytic proliferations and may be seen in other non-M3 AMLs (Figure 3.38), the data need to be evaluated in the context of other immunophenotypic findings.

CD16 and CD11b are normally present on late myeloid cells and may be expressed in AML. Although it is not possible to correlate the presence or absence of CD11b and/or CD16 with any particular FAB subtypes of AML, it is of interest to note that both CD16 and CD11b are absent in AML-M3 (Figures 3.23 and 3.24).

3.5.1.1 Myeloid phenotypic abnormalities and MRD detection

In comparison to ALL, the evaluation of MRD in AML is more challenging and requires a larger panel of antibodies. More than one clone of AML cells may be present at the time of

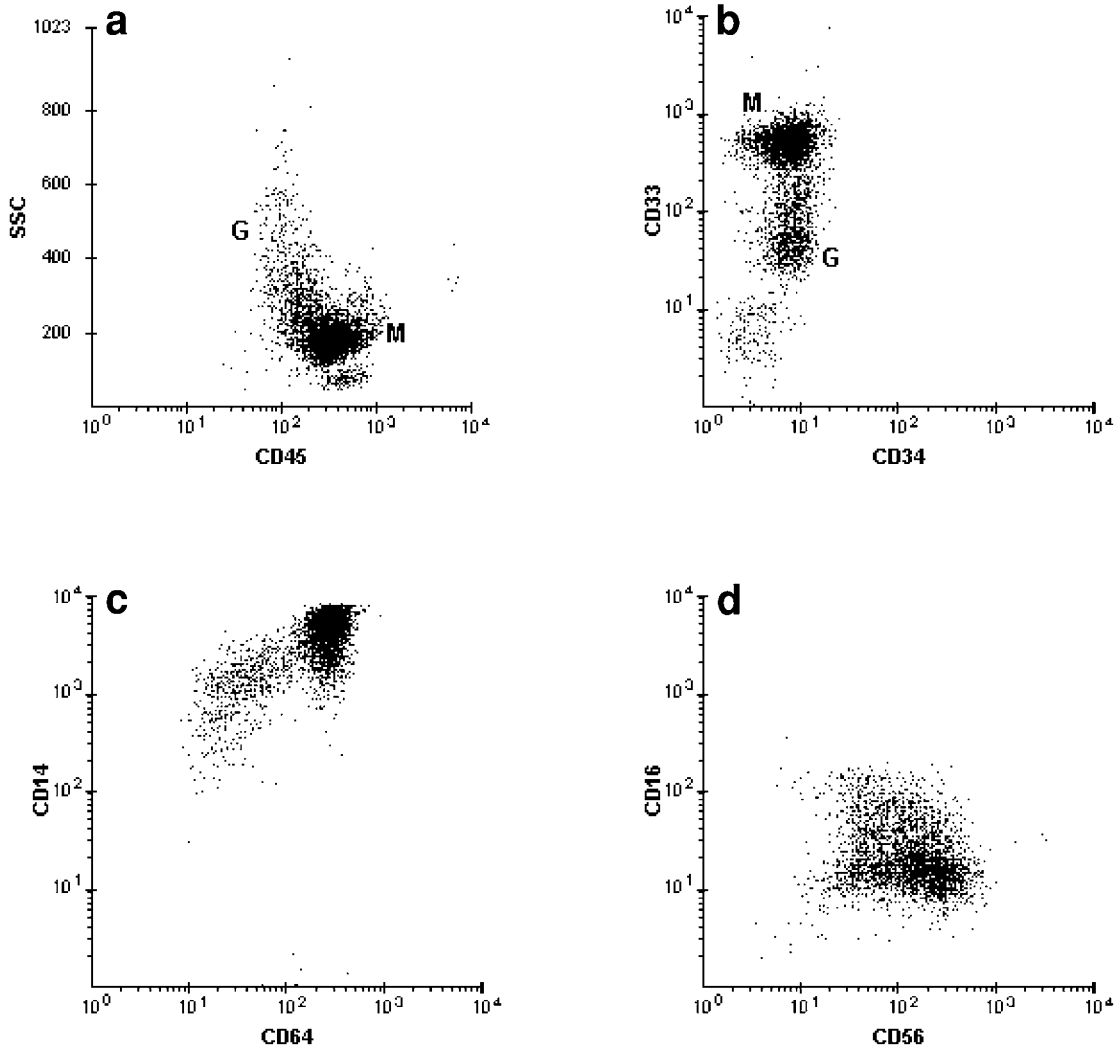

Figure 3.35 Peripheral blood with CMMoL. (a) A single predominant cluster in the monocytic region. Granulocytes (G) are markedly reduced. (b) Brighter CD33 on mononocytes (M) than on granulocytes. (c,d) Gated on the monocytic cluster: the neoplastic monocytes are CD64^{++}, CD14^{+++}, and CD56^{++}. An unusual finding is the presence of a small subpopulation with weak CD16 reactivity and less intense CD14 and CD64.

diagnosis, and the residual/relapsed disease can consist of any of the original clones. Changes in the antigenic expression, associated with long-term clonal evolution, may also complicate the detection of early relapse.

A substantial number of AMLs exhibit antigenic abnormalities at the time of diagnosis, based on which custom-built panels can be designed for the analysis of follow-up specimens. The frequently encountered abnormalities include the following:

- Reactivity for a B- or T-cell associated marker.
- Expression of a late myeloid antigen (e.g., CD11b, CD14, or CD15). When coexisting with CD34, such antigenic expression is considered asynchronous.
- Lack of either CD13 or CD33.
- Absent HLA-DR.
- Downregulated CD45.
- Coexpression of CD56. A rare case of AML with monocytic differentiation may lack both CD13 and CD33 and demonstrate reactivity for only CD14 and CD56.

Case study 11

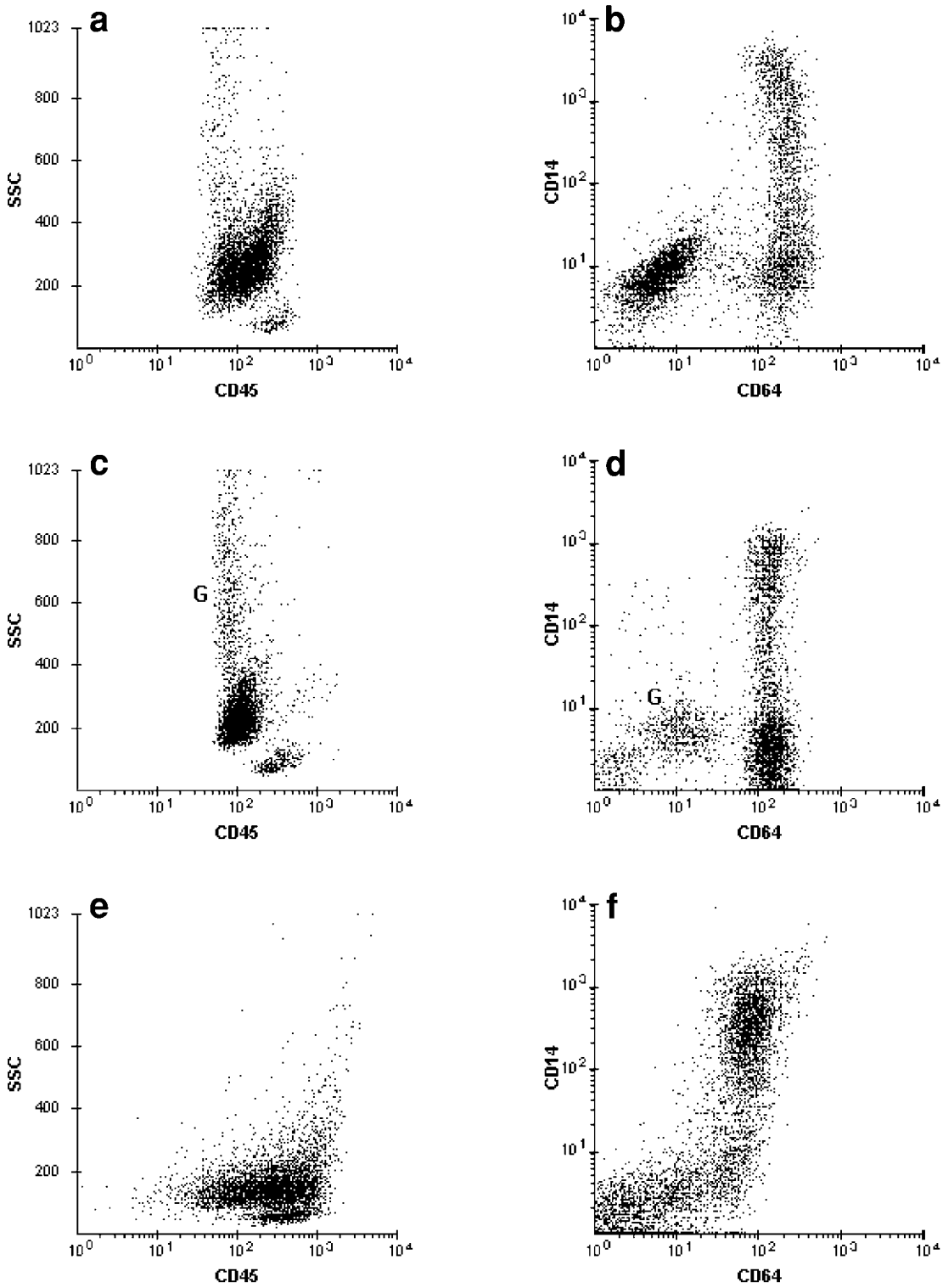

Figure 3.36 AML with monocytic differentiation. Case 1: (a) Merging blast and monocytic clusters. (b) Blasts are $CD14^-$, $CD64^-$. Monocytic cells display variable CD14 expression (CD14/CD64 trail). Case 2: (c) A prominent cluster in the monocytic region. Some residual granulocytes (G) are present. (c) CD14/CD64 trail. The majority of the monocytic cells are $CD14^-$ and $CD64^{++}$, which correspond to the most immature cells. Case 3: (e) A predominant cluster extending from the blast to the monocytic region. (f) The blast component is partially CD64-positive and lacks CD14. There is a large proportion of more mature elements in the monocytic component.

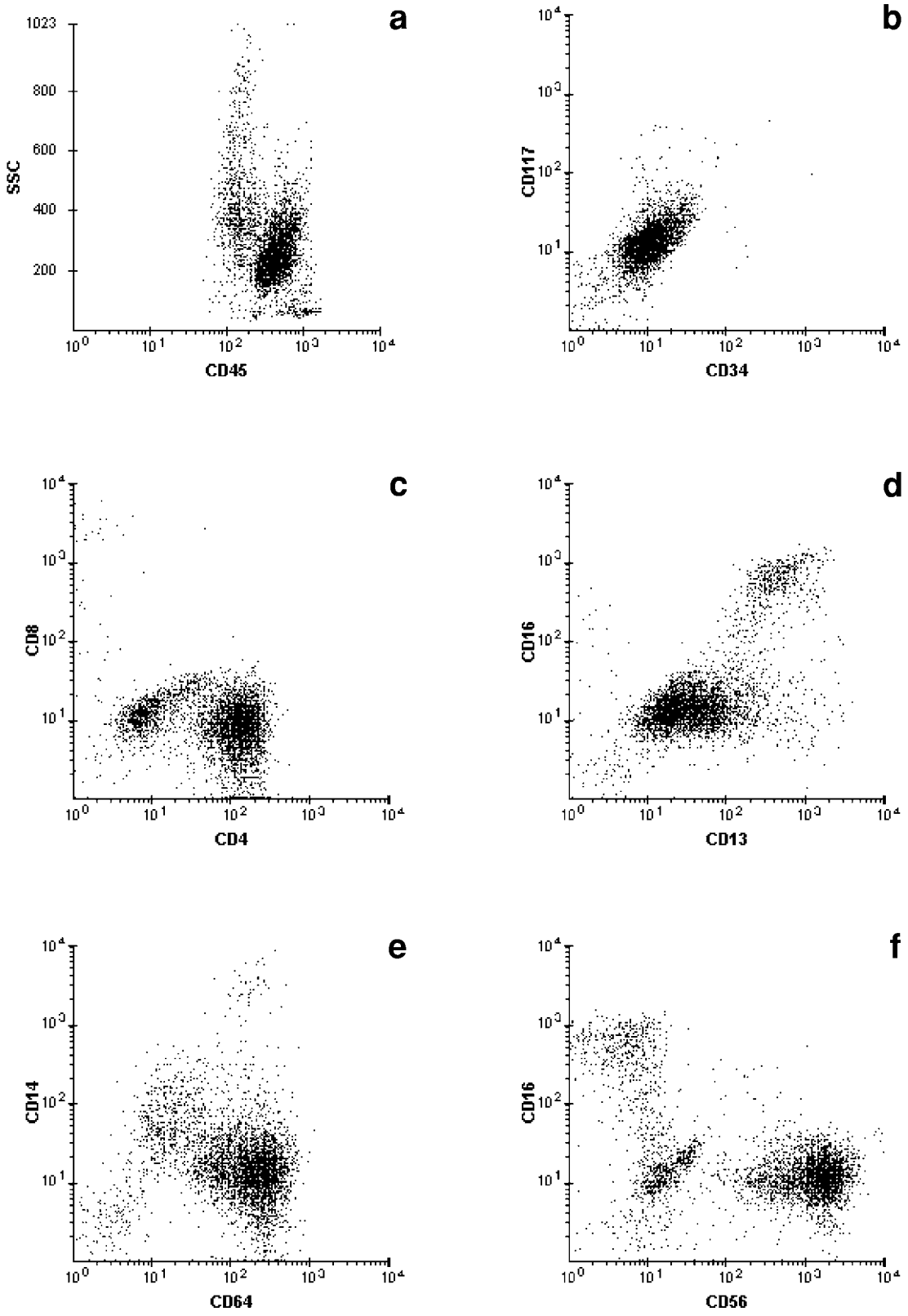

Figure 3.37 AML with monocytic differentiation (morphology shown in Plate 21). The SSC/CD45 picture (a) is similar to that of CMMoL as the blast cells occupy the monocytic region and display moderate SSC. (b–f) Blasts are negative for CD34, CD117, CD14, and CD16. CD4, CD13, CD64, and CD56 are expressed. Residual granulocytes are $CD13^{++}$ and $CD16^{++}$.

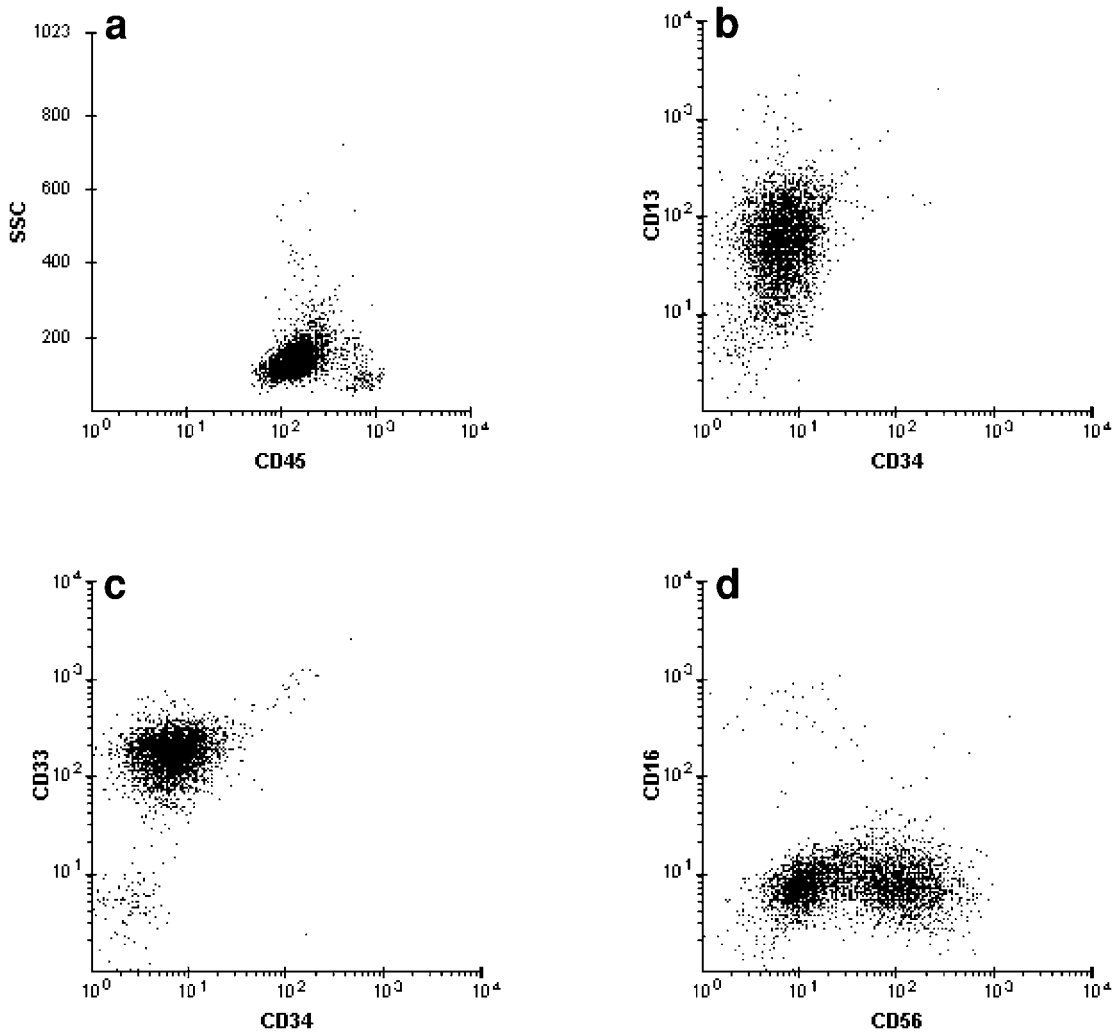

Figure 3.38 AML-M1 with CD56 expression. (a) Virtually a single predominant cluster with low SSC in the blast region. (b–d) Blast are $CD34^{-}$, $CD13^{++}$, $CD33^{++}$, $CD16^{-}$ and $CD56^{++}$. The distribution of CD56 is bimodal. The results of other markers (not shown) include reactivity for HLA-DR and CD117, and lack of CD14 and CD64.

- Abnormal light scatter characteristics, such as low FSC and SSC seen in the rare AML with basophilic differentiation.

3.5.2 Precursor B-ALL vs bone marrow precursor B-cells (hematogones)

Normal B-cell precursors (hematogones) in the bone marrow and precursor B-ALL share similar phenotypic features, namely TdT, CD19, and CD10. At the time of diagnosis, most cases of precursor B-ALL present with an overwhelming proportion of immature B-cells with the resulting suppression of other hematopoietic elements in the bone marrow. This feature is, by itself, sufficient to indicate that the proliferation is neoplastic. In the follow-up bone marrow specimens, however, the distinction between residual/relapsed precursor B-ALL and normal B-cell progenitors may not be straightforward, especially because these two populations may coexist. On the other hand, the presence of precursor B-cells in the peripheral blood or extramedullary sites points toward a malignant process.

Evaluation of one or more of the following parameters may help to distinguish precursor B-ALL from a proliferation of normal B-cell precursors.

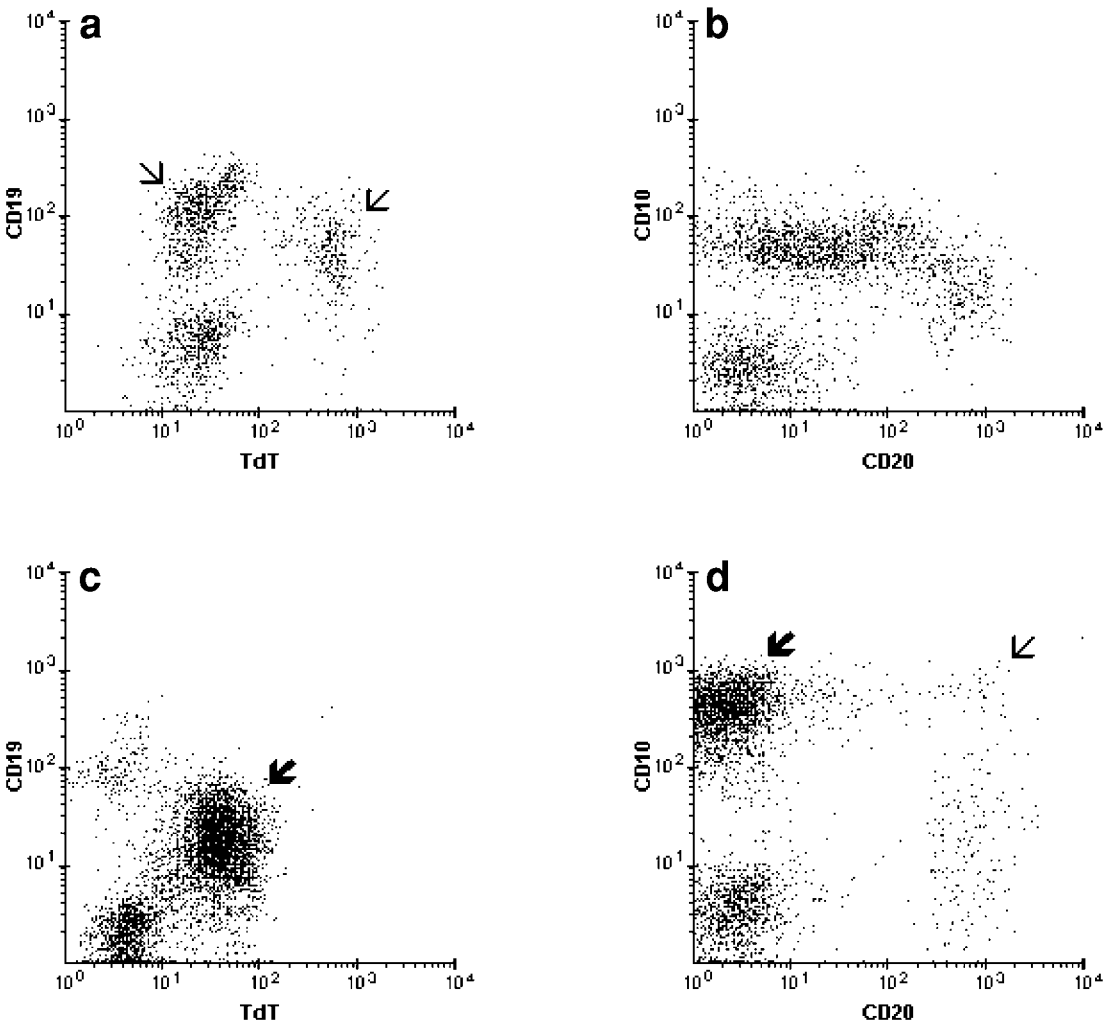

Figure 3.39 Bone marrow B-cell precursors vs precursor B-ALL. (a,b) Gated on the hematogone and lymphocyte regions of the SSC/CD45 dot plot (not shown) of a normal pediatric bone marrow. Precursor B-cells (thin arrows) separate into two subpopulations: one positive for TdT and the other negative. CD20 expression is markedly heterogeneous. The brightest CD20 and dimmer CD10 are seen on the least immature B-cell progenitors. (c,d) Precursor B-ALL (ungated data). The leukemic cells (arrow) coexpress CD19 and TdT. CD20 is negative. A minute population of hematogones (thin arrow) is present.

1. DNA aneuploidy. This parameter, when present, indicates the neoplastic nature of the cell population. The analysis can be done in conjunction with TdT (Figure 2.14d).
2. The pattern of coexpression of TdT and CD19 (Figure 3.39). On the correlated TdT/CD19 dot plot, ALL cells form a single compact cluster. In contrast, normal precursor B-cells manifest as two separate clusters, one expressing TdT (and also CD34) and the other lacking TdT.
3. The pattern of CD10 and CD20 coexpression (Figure 3.39). The population of hematogones is markedly heterogeneous in terms of CD20 intensity (from negative to bright) and therefore produces a "trail" pattern on the CD10/CD20 dot plot. The CD10/CD20 trail is J-shaped (Figure 3.39b) whereby the less immature B-cell progenitors have brighter CD20 but weaker CD10. The majority of precursor B-ALLs lack CD20 expression. Among those expressing CD20, the distribution of CD20 on the leukemic blasts is less heterogeneous than that seen on hematogones (Figure 3.29). A sporadic case may display a CD10/CD20 pattern nearly mimicking that of normal B-cell precursors, however.
4. Light scatter characteristics. Hematogones produce lower SSC and FSC signals than ALL cells.


Case study 12

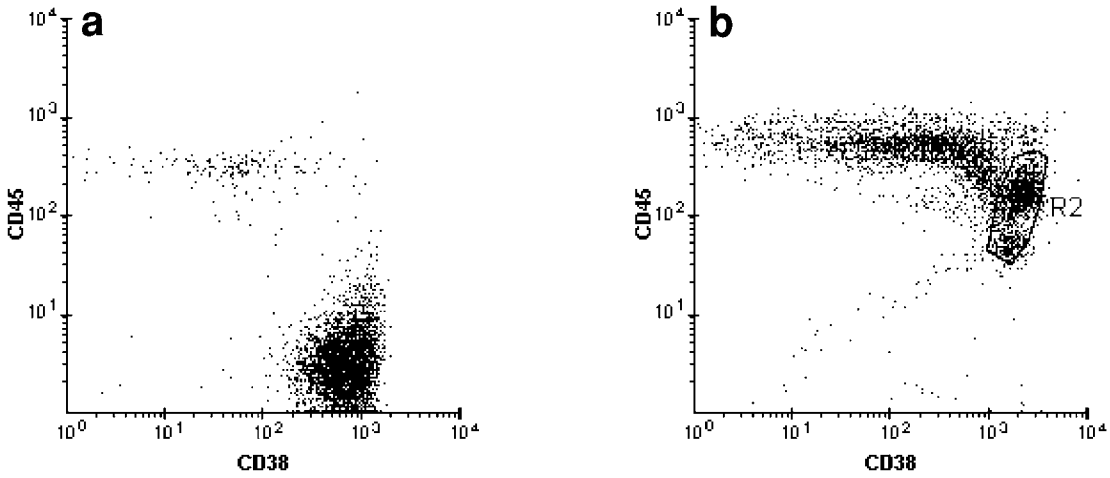

Figure 3.40 (a) Precursor B-ALL. The leukemic cells are CD45^{-} and CD38^{++}. (b) Data on MNCs only (granulocytes excluded). CD38 expression on bone marrow B-cell precursors (R2) is brighter than that on ALL cells.

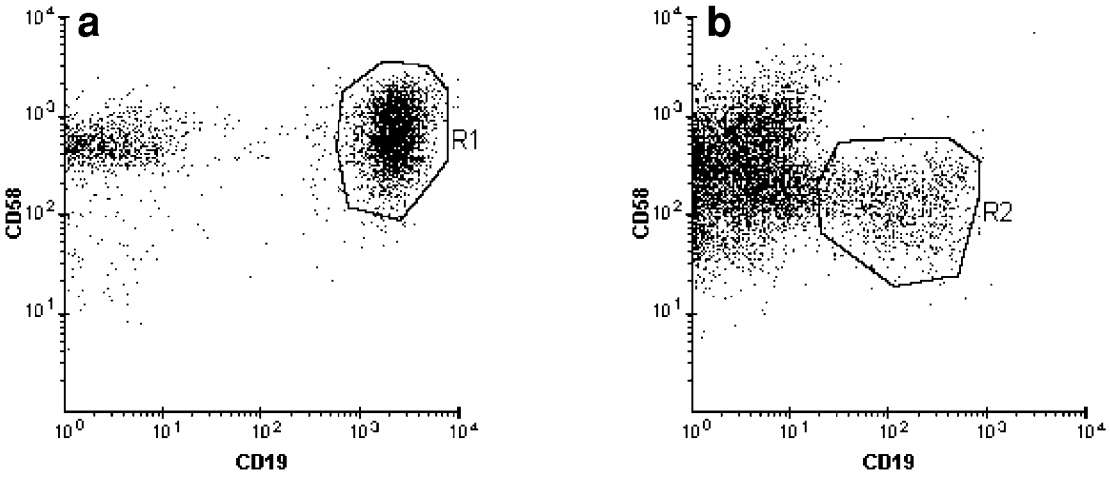

Figure 3.41 (a) Precursor B-ALL. CD58 on the leukemic blasts (R1). (b) Normal pediatric bone marrow (ungated data) with a conspicuous population of B-cell progenitors (R2) expressing lower levels of CD58.

5. CD38 expression (Figure 3.40). The intensity of CD38 on normal B-cell progenitors is one of the brightest among hematopoietic precursors. By comparison, CD38, although bright, is less intense in most precursor B-ALLs.
6. The pattern of CD58/CD19 coexpression (Figure 3.41). Leukemic blasts demonstrate much higher levels of CD58 than normal B-cell progenitors. This highly discriminating feature has made CD58 a useful marker for the detection of MRD in precursor B-cell ALL.

In some instances, the distinction between malignant and normal precursor B-cell populations may still be extremely difficult, especially in a regenerative marrow where the rare (residual/relapsed) blast cells are masked by an overwhelming number of normal B-cell progenitors. Such instances pose a serious dilemma that can only be resolved by close clinical follow-up and repeat analysis.

3.6 Evaluation of mature lymphoid malignancies

Mature lymphoid neoplasms (LPD/NHL) can be categorized on the basis of the cell lineage (B-cell vs T-cell vs NK cell) and biological grade (low grade vs aggressive). In addition to the S-phase fraction, the FSC parameter and the expression of the transferrin receptor (CD71), a marker of cellular activation/proliferation, contribute to the grading of mature lymphoid malignancies. In general, higher tumor grade is associated with higher S-phase, increased cell size, or bright CD71 (Figure 3.42).

3.6.1 Assessment of surface light chain expression

Visual evaluation of surface light chain expression is required to establish the monoclonality of a B-cell proliferation. The optimal approach is to analyze the surface light chain data gated on B-cells. Other methods, such as determining the percentage of kappa-positive and lambda-positive cells with a calculation of the kappa;lambda ratio on all cells can easily result in a misinterpretation of polyclonality. In heterogeneous specimens where the B-cell subpopulation consists nearly entirely of neoplastic cells or in homogeneous samples composed virtually of a single population of abnormal B-cells (e.g., CLL with marked lymphocytosis), the B-cell gate can encompass the entire CD20 or CD19 population (Figure 3.43). If the B-cell population is heterogeneous, consisting of two or more clusters of different cell sizes or CD20 intensities, then several selective gates may be necessary to identify and quantify the monoclonal population (*see* Section 4.4.1).

In determining the fluorescence intensity of the expressed light chain, it is helpful to take into account the following:

- The position of the peak of the positive light chain on the fluorescence scale.
- The background intensity of the negative light chain and the degree of overlapping, if present, between the kappa and lambda fluorescence clusters.
- The extent of the difference between the mean peak fluorescence channels of kappa and lambda.

Using this approach, the intensity of the positive light chain is determined relative to that of the negative one, not just based on where it falls on the fluorescence scale. This is especially applicable when there is an increase of background fluorescence on the negative cluster (Figure 3.43d), either due to the increased nonspecific binding of immunoglobulins by the neoplastic cells (usually associated with increased cell size) or a high level of serum immunoglobulins. In general, if there is obvious overlap in the fluorescence intensity distributions of the light chains, then the intensity of the positive light chain is weak (Figures 3.12, 3.13, 3.32, 3.42, and 3.43). This usually corresponds to a difference of less than one decalog between the mean peak fluorescence channels of the negative and positive histograms.

The above-described technique is best applied when there are an adequate number of B-cell events. If the malignant B-cell population is minimal (1% or less), additional data collection of B-cells may be necessary.

A mature B-cell population negative for both light chains is, by definition, abnormal, except if the specimen analyzed is a solid lymphoid organ (tonsils, lymph nodes) with marked FRFH. In such cases, there may be a subpopulation of activated benign B-cells lacking expression of either light chain (germinal center cells). Inspection of other dot plots will reveal diagnostic clues for FRFH (*see* Section 4.1.1.1). Except for this exception, a mature B-cell population negative for both light chains can be proven to be neoplastic by other corroborating parameters, such as aneuploidy or an overwhelming proportion of the abnormal cells in the sample

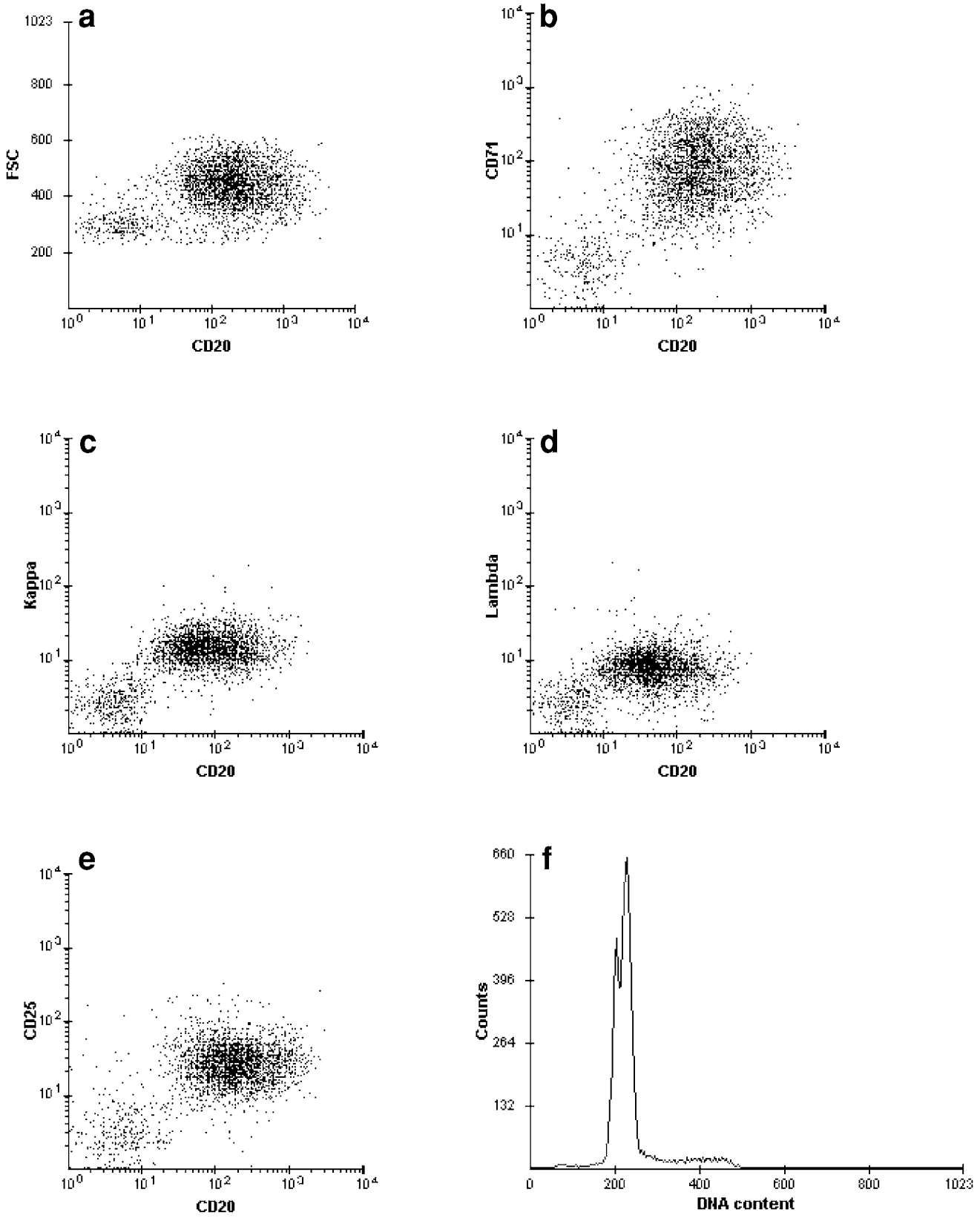

Figure 3.42 High-grade B-cell NHL. The neoplastic cells display the characteristics of an aggressive lymphoma, including increased FSC (a), bright CD71 expression (b), and an elevated S-phase fraction (S% 20) with aneuploidy (DI 1.1) (f). CD25 is also well expressed (e). Surface light chain (kappa) is very weakly expressed (c,d).

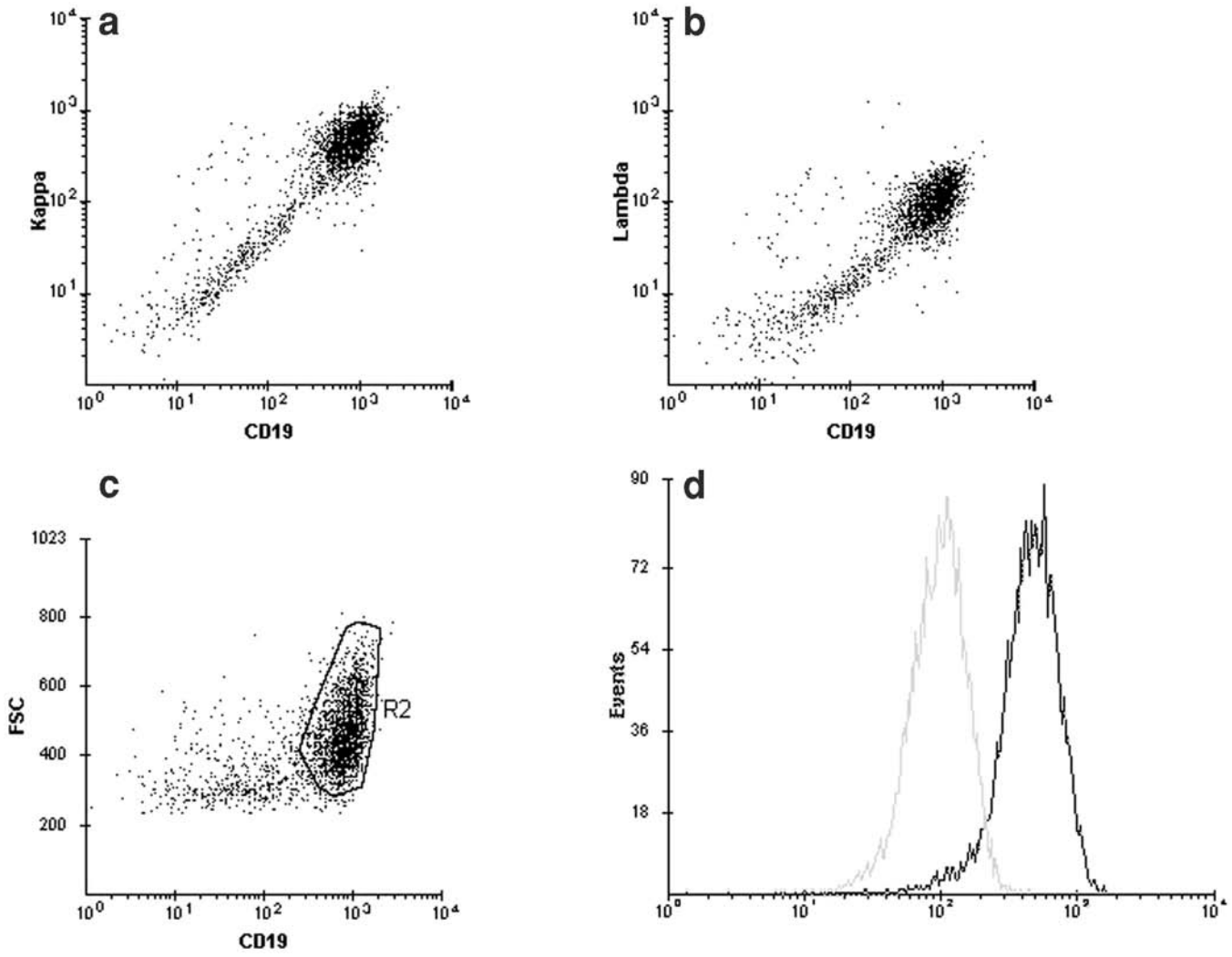

Figure 3.43 Lymph node (FNA) with diffuse large cell lymphoma (DLCL). (a–d) The tumor cells are of variable cell size (medium to large) and comprise 90% of the cells in the sample. CD19 is well expressed. The background fluorescence of the negative light chain (lambda) is increased. The neoplastic cells are thus kappa^{+}, and not kappa^{++}, as they would be if the results were simply read off the fluorescence scale (kappa/lambda overlay gated on R2).

analyzed. Lack of surface light chain expression has been found in a number of NHL/LPD, including CLL/SLL, diffuse large-cell lymphoma (DLCL), and FCC (Figure 3.44) lymphomas. Potential diagnostic confusion between FRFH and FCC lymphomas can be avoided by comparing the respective patterns of CD10/CD20 or bcl-2/CD20 coexpression (*see* Section 4.1.1.1).

3.6.2 Assessment of pan B-cell antigens

The evaluation of pan B-cell antigens takes advantage of the wide dynamic range of CD20 and is most useful in mature B-cell neoplasms with low FSC. A comparison of the relative intensities of CD19 and CD20 (both conjugated to same type of fluorochrome) can provide an additional clue for subclassifying small B-cell LPD/NHL. The following possibilities can be encountered, based on the relationship of CD20 and CD19 fluorescence intensities:

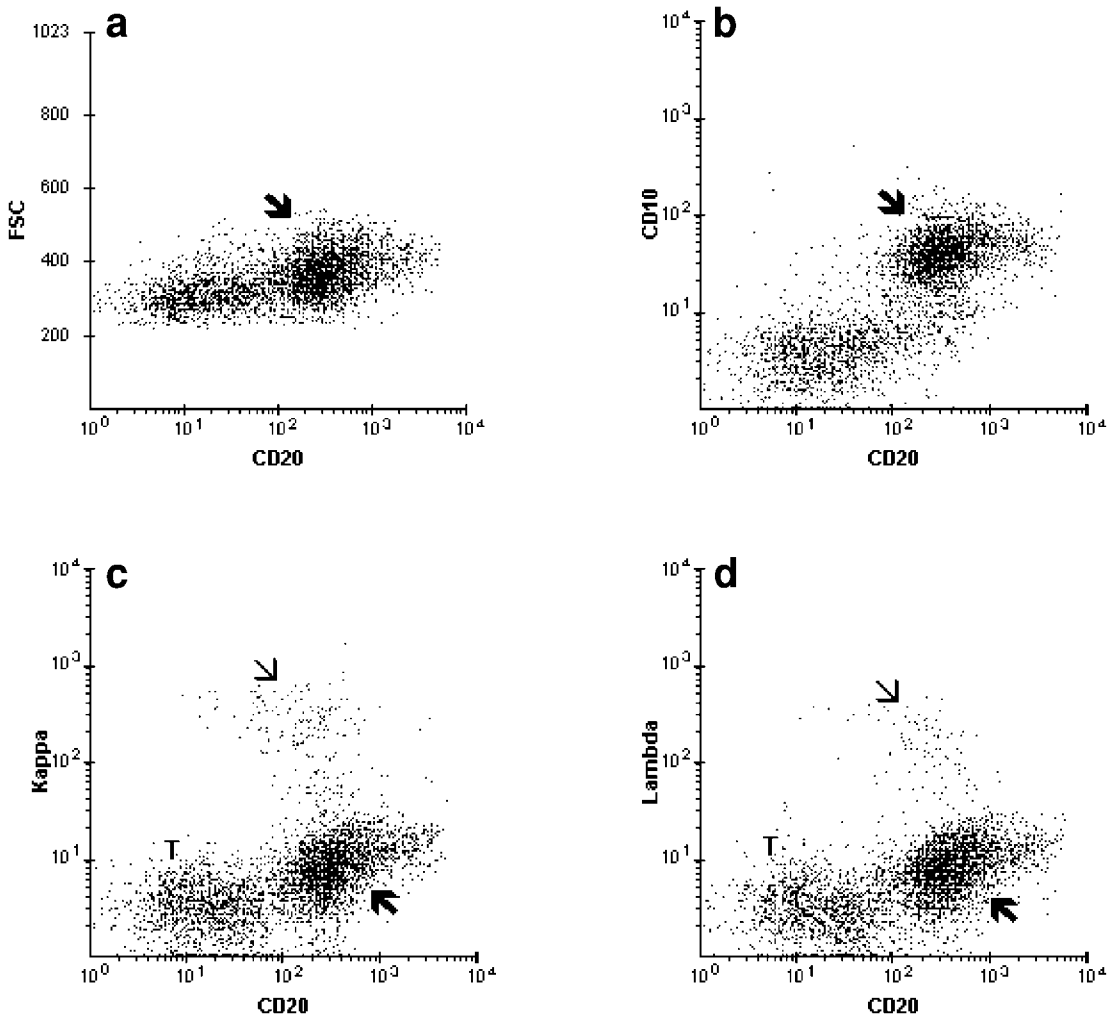

Figure 3.44 FCC lymphoma in the thyroid. The neoplastic cells (arrow) are slightly larger than benign T-cells (a), coexpress CD10 and CD20 (b), but lack detectable surface light chain (c,d). A minute population of polyclonal B-cells (thin arrow) and residual T-cells (T) are present. Note the shifting of the T-cell cluster into the CD20-positive region; this is due to CD20 coating, commonly seen in FCC lymphoma.

1. CD20 intensity < CD19 (Figure 3.32). This pattern, together with small cell size, is virtually pathognomonic of CLL, in which CD20 is downregulated and displays a heterogeneous fluorescence distribution. The fluorescence signals for CD20 often begin in the negative region (Figure 3.13). CD19 is usually of moderate intensity. It is still important, however, to evaluate this pattern in the context of other features (i.e., CD5 and CD23 expression) as well as the intensity of the monoclonal light chain. Other closely related entities, such as CLL/PL, as well as some cases of LPC lymphoma–leukemia, often exhibit a phenotypic profile similar to CLL, with subtle differences in the intensity of CD20 and/or surface light chains. These CLL-related disorders contain a variable increase in activated cells. When significant, the activated cells are reflected as an increased FSC, with either a bimodal (Figure 3.6) or variable distribution (Figure 3.5c,d). Morphologically, the tumor demonstrates a spectrum of small lymphocytes, plasmacytoid lymphocytes, and/or prolymphocytes (Plate 8). A dimorphic picture may result if small lymphocytes and prolymphocytes predominate. Because of the increase in activated cells, the intensity of CD20 (Figure 3.5c) or the surface light chain can become relatively brighter than that seen in CLL (Figures 3.45 and 3.46). The pattern of CD20 < CD19 and the variable distribution of CD20 density are often retained, however. CD38 becomes brighter, whereas CD5 or CD23 may be less intense. These more acti-

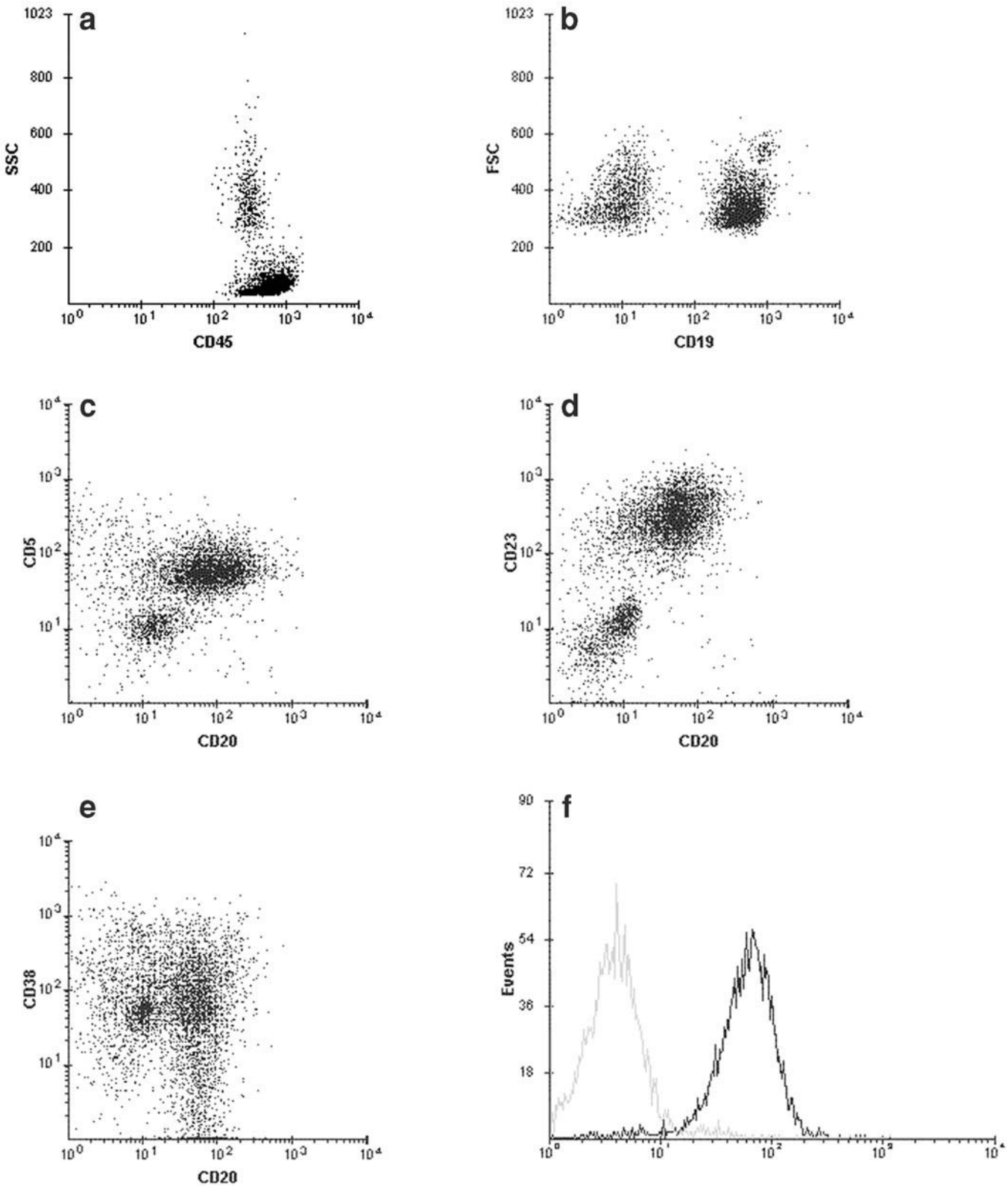

Figure 3.45 Peripheral blood with activated CLL. (a,b) Leukemic cells with slightly decreased CD45 and mildly increased FSC. (c–e) Gated on MNCs: Coexpression of CD5, CD23, and CD20. CD20 is brighter than usual, but still of variable distribution and less intense than CD19. CD38 is expressed. (f) Gated on B cells: The difference between the mean peak fluorescence channels of the negative (lambda) and positive (kappa) histograms is greater than one decalog (i.e., kappa intensity is not weak).

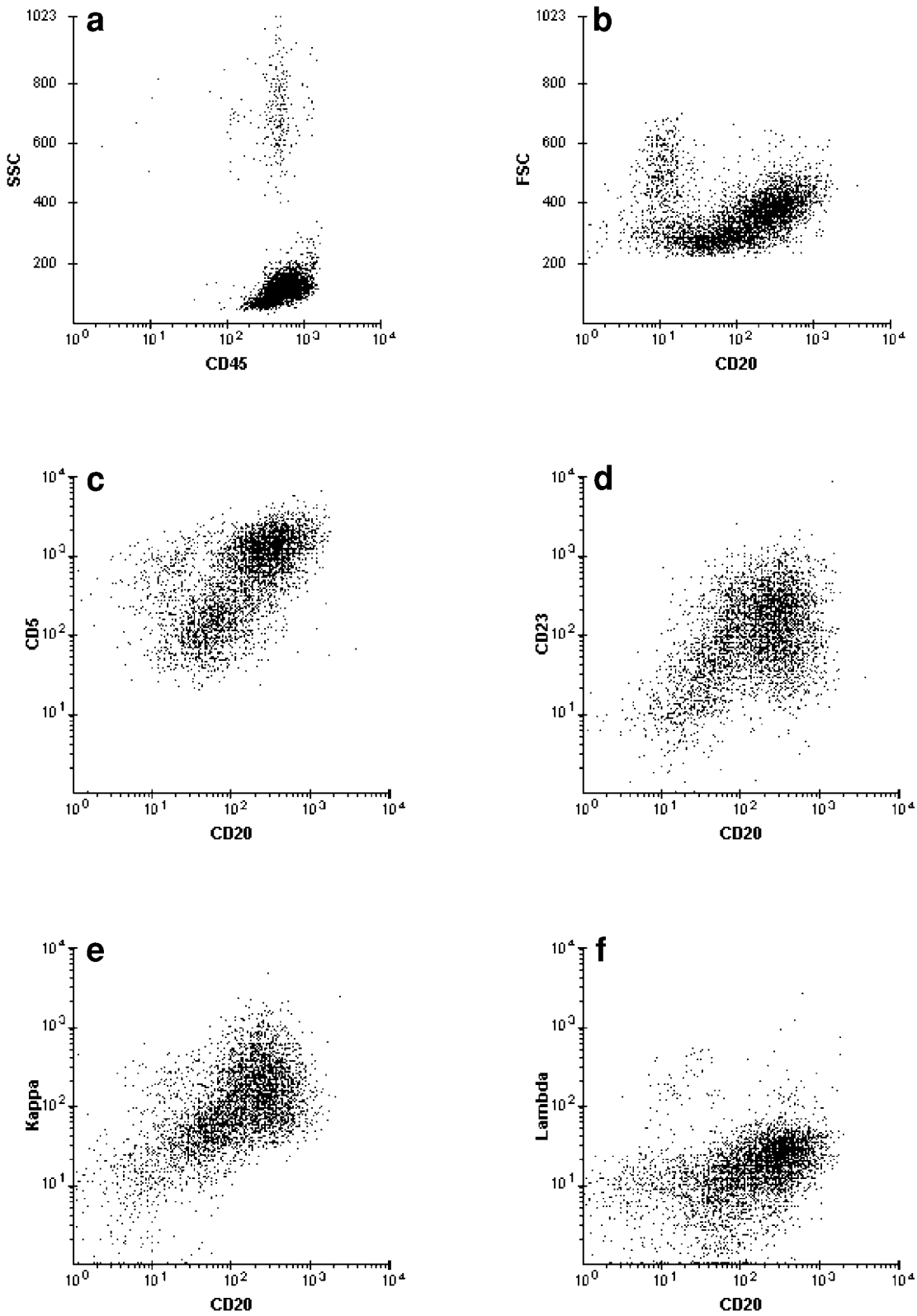

Figure 3.46 Peripheral blood with CLL/PL. (a,b) A predominant lymphoid cluster with SSC shifting toward the monocytic region, bimodal FSC and bimodal CD20. (c–f) Gated on MNCs: The expression of CD5, CD23 and kappa is also bimodal (i.e., more intense on the activated lymphoid cells with higher FSC and brighter CD20).

vated forms of CLL have also been referred to as "mixed CLL," "atypical CLL," or "CLL in prolymphocytic transformation." Correlation of the morphologic findings from the different sites of involvement (e.g., peripheral blood and lymph node), together with the review of the corresponding FCM studies and serum protein data, will provide a better understanding of CLL and its related disorders. In patients with multiple FCM studies, it is not unusual to observe a progression from CLL to the more activated form over the course of time. Furthermore, the FCM picture of the lymph node may reveal a larger activated component than that seen in the blood or bone marrow. This apparent discrepancy is translated morphologically as the presence of prominent proliferation centers in the lymph node, whereas the blood or bone marrow is involved mostly by small lymphoid cells.

Case studies 13 and 14

2. The fluorescence intensities of CD19 and CD20 are closely similar (CD19 = CD 20) and usually in the moderate range. This pattern is the least informative, being present in various low-grade B-cell LPD/NHLs, such as FCC lymphoma, MCL, mucosa-associated lymphoid tissue (MALT) lymphoma, and the above-mentioned CLL-related disorders.
3. CD19 intensity < CD20. This feature is frequently encountered in FCC and mantle cell lymphoma. Its main utility is primarily in the context of a $CD5^+$ $CD23^-$ small B-cell LPD/NHL (Figure 3.47). Because the combination $CD5^+$ $CD23^-$ is found not only in MCL but also in a number of LPC disorders, the CD19 intensity < CD20 pattern is a helpful clue for recognizing MCL. Unlike the fluorescence signals of downregulated CD20 in CLL, the downregulated CD19 usually falls within the second or third decalog, rather than the first decalog.

Case study 15

Downregulated expression or loss of CD19 and/or CD20 (Figure 3.48) can also occur in large, mature B-cell neoplasms, especially those with a very high S-phase. Many of these demonstrate plasmablastic (also referred to as immunoblastic) differentiation morphologically.

3.6.3 Useful antigenic features in mature B-cell malignancies

The differential diagnosis of B-cell LPD/NHL can be further narrowed on the basis of the expression of certain antigens or variations in density thereof, in addition to the relationship of CD20 and CD19 intensities described earlier. A substantial number of small B-cell LPD/NHL bear no distinctive antigenic characteristic, however (i.e., a nondescript B-cell phenotype) and are thus referred to as B-cell LPD/NHL, NOS (not otherwise specified). The useful antigenic features are described next.

3.6.3.1 CD10 expression: Follicular center cell lymphomas

In the context of a mature B-cell malignancy, coexpression of CD10 and a pan B-cell antigen infers follicular center cell differentiation. CD10 intensity varies from case to case (Figure 3.49). According to the literature, approximately 20–25% of well-documented FCC lymphomas lack any detectable CD10 expression, however. CD20 is well expressed unless the specimen analyzed is obtained following anti-CD20 immunotherapy. Occasionally, the neoplastic population may display marked heterogeneity in the expression of CD20 (e.g., a bimodal distribution) (Figure 3.16). On FCM dot plots derived from lymph node specimens, the tumor cell cluster is usually obvious (Figure 3.49a,b) whereas in the blood or bone marrow, the lymphomatous population can be inconspicuous because the involvement can be as low as 1% (or less). Lack of a detectable light chain is observed in a small number of FCC lymphomas (Figure 3.44).

Case studies 16 and 17

The FSC parameter in FCC lymphomas varies considerably from case to case (depending on the relative preponderance of small and large follicular center cells) ranging from small (Figure 3.49), through variable (Figure 3.50), to large. Discrepancy between the FSC results and the morphology may occur as a result of tissue sampling, when the sample allocated for FCM analysis

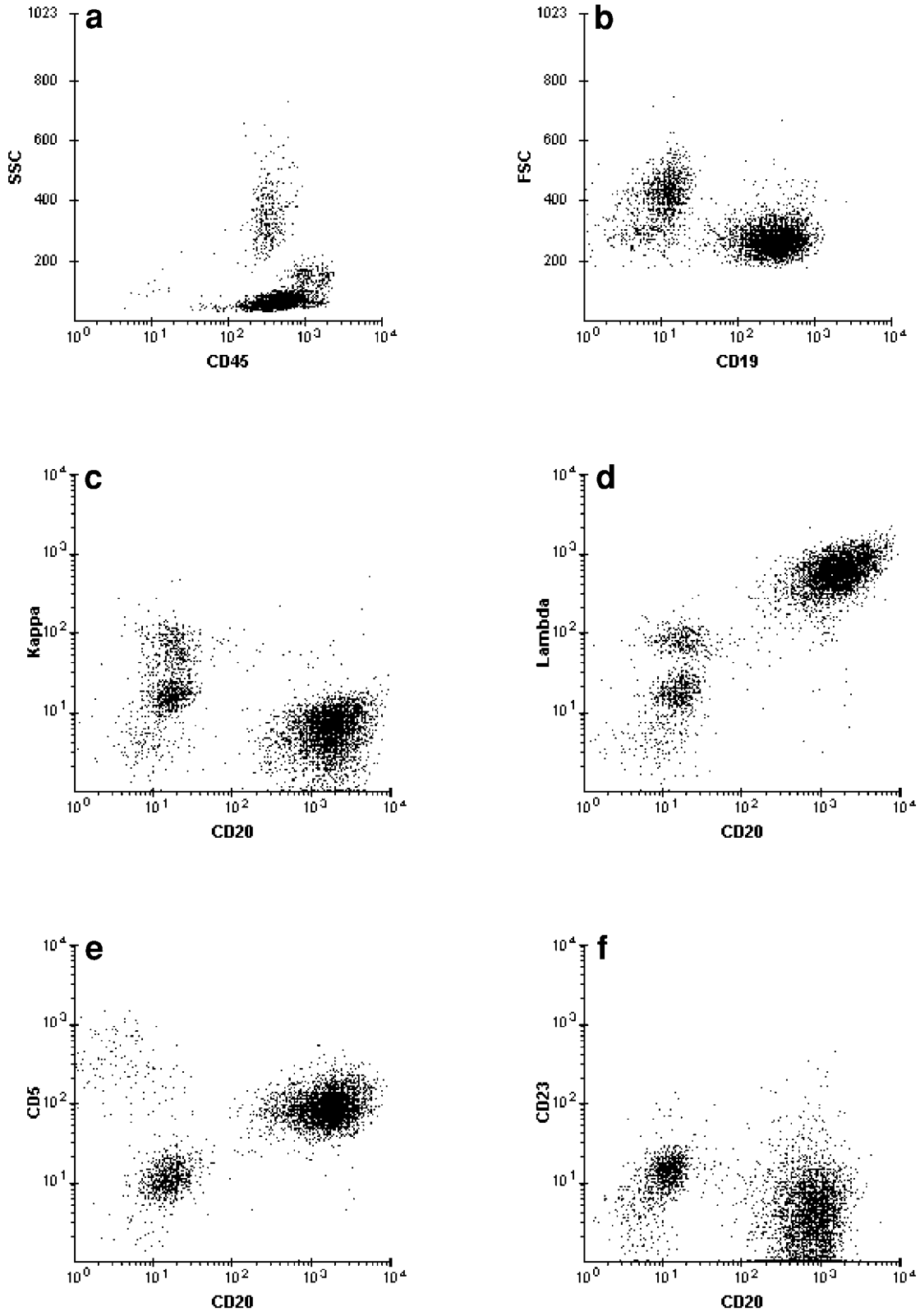

Figure 3.47 Peripheral blood involvement by MCL (morphology shown in Plate 35). (a–f) A predominant lymphoid cluster with CD45 downregulated into the hematogone region. The cell size is small. The leukemic cells are CD19^{++}, CD20^{+++}, CD5^{+}, CD23^{-}, lambda^{++}. CD19 is less intense than CD20. A small number of T-cells and granulocytes are present.

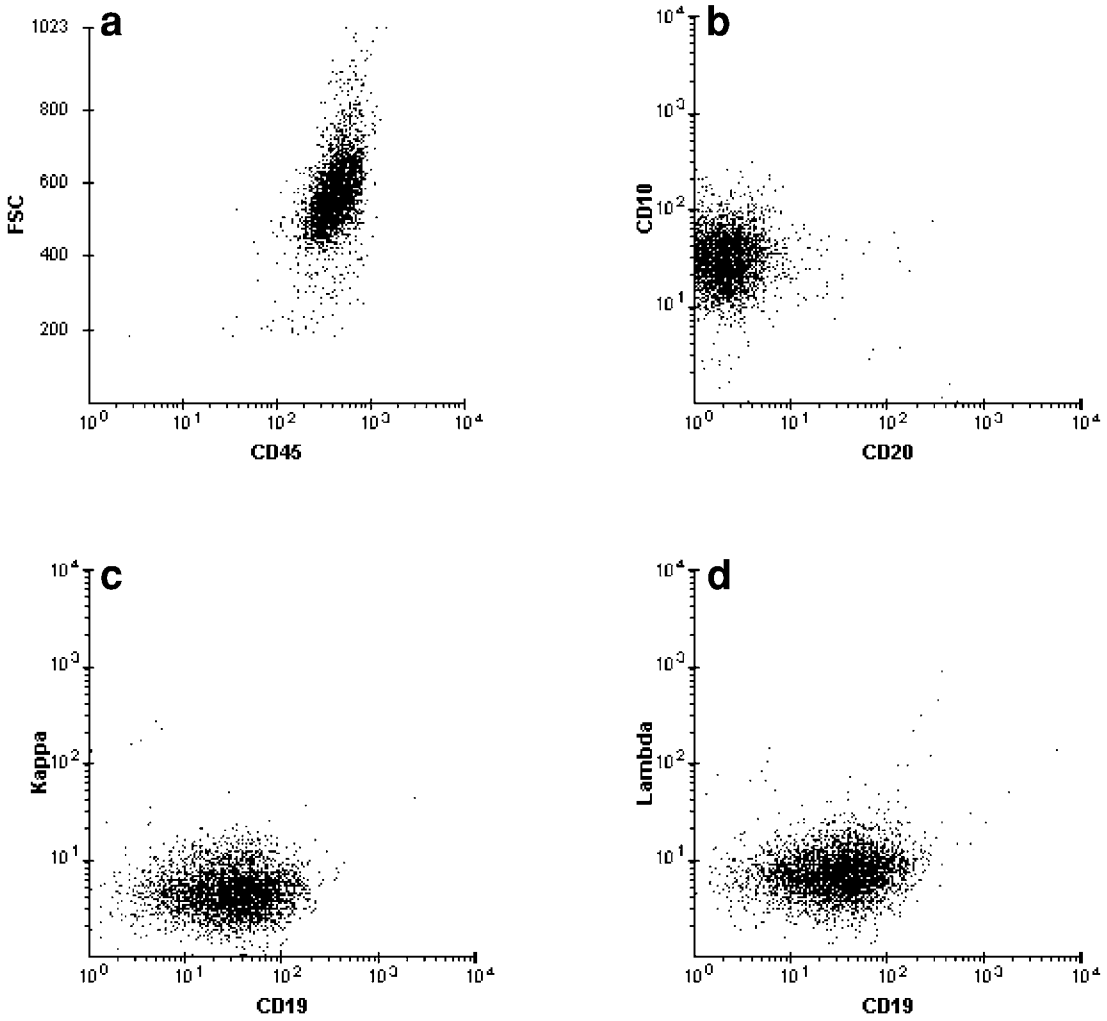

Figure 3.48 Pelvic mass with plasmablastic large cell lymphoma (LCL). (a–d) Neoplastic cells are large. CD20 is not detectable. Lambda is extremely dimly expressed. CD10 is present.


Case study 18

is taken from areas containing a preponderance of small cells while the remaining tissue contains foci with high numbers of large cells. Otherwise, there is generally a good correlation between the cell size and each subtype of FCC lymphoma (small, mixed, and large [i.e., FCC I, II, and III, respectively]). In the natural course of the disease, low-grade FCC lymphoma ultimately transforms into either FCC III or DLCL, both of which are traditionally considered to be aggressive lymphomas. Although the S-phase fraction in these transformed FCC lymphomas is higher than that observed in FCC I and FCC II, it is much lower than that observed in *de novo* non-FCC large cell lymphoma. In a substantial number of FCC III, the S-phase fraction is either low (Figure 3.51) and similar to that of low-grade LPD/NHL, or may only slightly exceed the typical 5% threshold. Furthermore, the waxing and waning clinical course of transformed FCC lymphoma contrasts with the rapidly progressive behavior of *de novo* LCL.

CD10 is also present in Burkitt's lymphoma. Although the FCM immunophenotyping data in Burkitt's lymphoma and CD10-positive DLCL (many of which represent transformation from low-grade FCC lymphoma) may be indistinguishable (Figures 3.52 and 3.53), the extremely high S-phase (usually exceeding 20%) is an important clue for recognizing Burkitt's lymphoma by FCM analysis (Figure 3.52e,f).

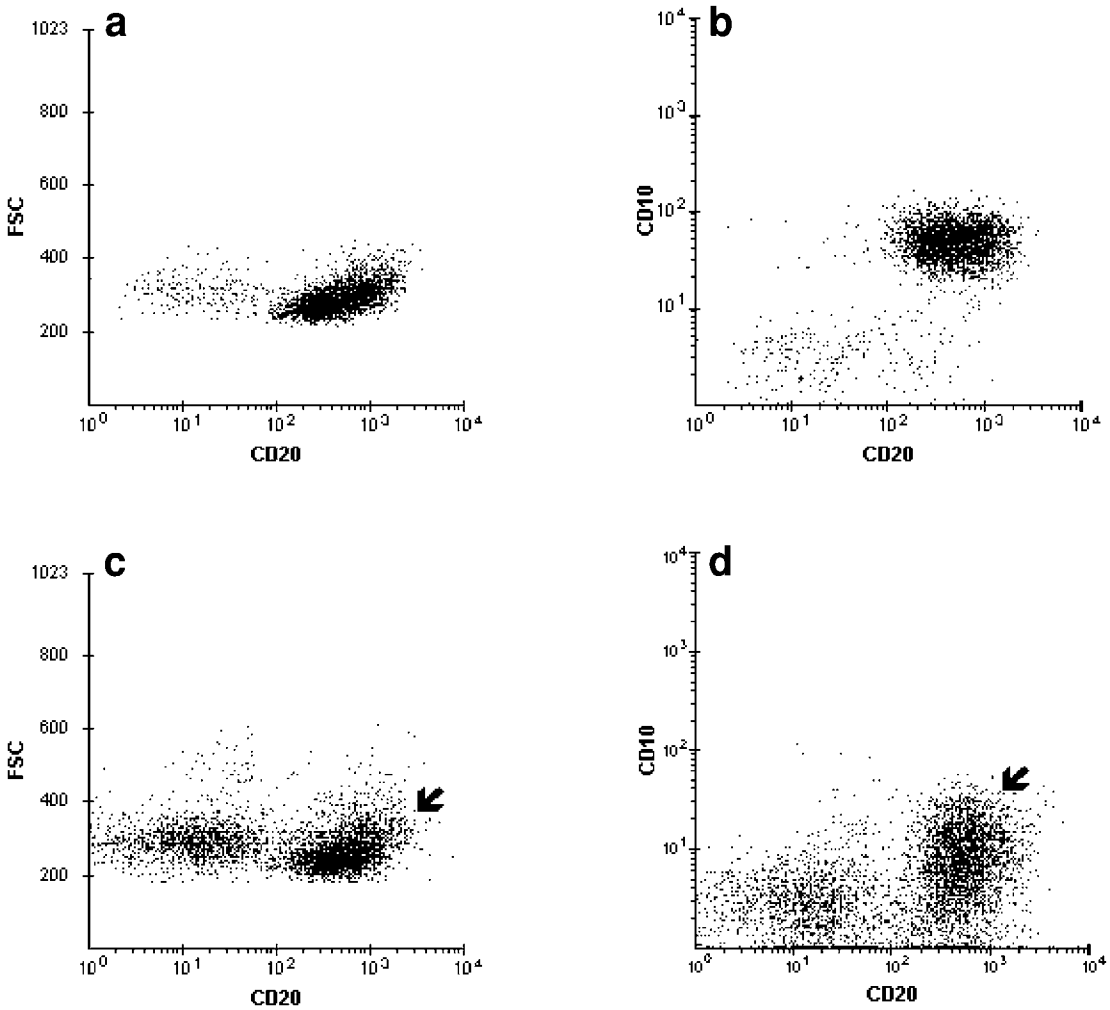

Figure 3.49 Variations in CD10 intensity. Two different cases of FCC I lymphoma. (a,b) Case 1: The tumor is of small cell size and displays bright CD20 and CD10. (c,d) Case 2: The neoplastic cells (arrow) are small. The intensity of CD10 is weak and variable.

3.6.3.2 Pattern of CD20 and CD11c coexpression


Case study 19

CD11c is expressed in various B-cell neoplasms, including hairy cell leukemia. CD25, typically found in HCL, may be found in non-HCL B-cell LPD (most often CLL and CLL-related disorders) as well, although usually at a very weak intensity. In HCL, however, both CD20 and CD11c are intensely expressed, resulting in a coexpression pattern distinctive from that in other diseases (Figure 3.54). Furthermore, the cell size of hairy cells is larger than lymphocytes and the SSC similar to that of monocytes. The constellation of these findings, together with the coexpression of CD25 and CD103, is essentially pathognomonic for HCL and serves as a fingerprint for the detection of a very low level of hairy cells in the peripheral blood. Rarely, CD10 may be also found on hairy cells. In most of the non-HCL B-cell LPD/NHL with CD11c expression, the intensity distribution for CD11c is heterogeneous, thus producing a "trail" pattern on the CD11c/CD20 dot plot (Figure 3.55).

In the authors' experience, cases of LPD that may be misinterpreted as HCL, are those in which the blood or bone marrow smears display lymphoid cells with hairy or villous projections. Slow drying of the air-dried smears can easily induce such cytologic features, however,

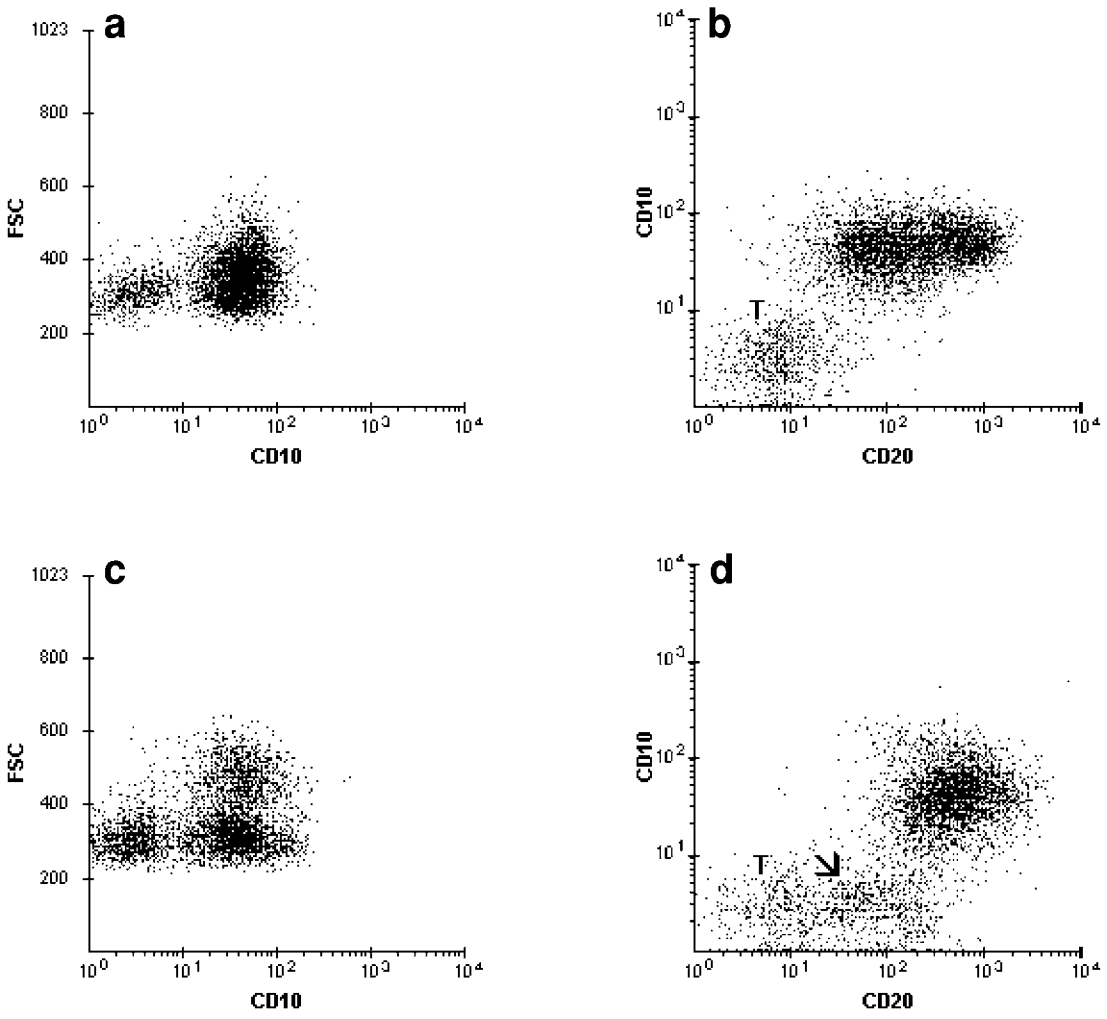

Figure 3.50 Two different cases of FCC lymphoma with an increased number of large FCC cells. (a,b) Case 1: The tumor is of variable cell size, ranging from small to medium. CD10 and CD20 are well expressed. Note the unusual variable distribution in CD20 intensity. (c,d): The tumor is of bimodal cell size with coexpression of CD10 and CD20. A small but conspicuous population of benign (CD10-negative) B-cells is present (arrow) in addition to the residual T-cells (T).

and the artifacts are most visible in cells with ample cytoplasm and a relatively low content of organelles/granularity. Lymphoid cells such as plasmacytoid lymphocytes, activated lymphocytes, or prolymphocytes fall into this category. The pattern of CD11c/CD20 coexpression is one of several clues, which if evaluated carefully, can prevent potential misinterpretation. This is especially true since some of these LPDs with "hairy/villous" cytology (*see* Section 5.2.1.7) may express weak CD25 (Figure 3.55) or, in rare instances, the B-ly7 clone of CD103 (Figure 3.56). The distribution of CD103 intensity, because of its limited dynamic range, is similar between HCL and the occasional case of $CD103^{+}$ non-HCL LPD. The extremely bright CD20 and CD11c coexpression in HCL is a differentiating characteristic, however. Other additional features, such as increased WBC count with abundant circulating abnormal cells, and a cellular bone marrow aspirate also permit one to recognize that the LPD with "hairy" cytology is not HCL. This can be further confirmed by the patient's lack of response to the HCL therapeutic regimen.

(text continues on page 95)

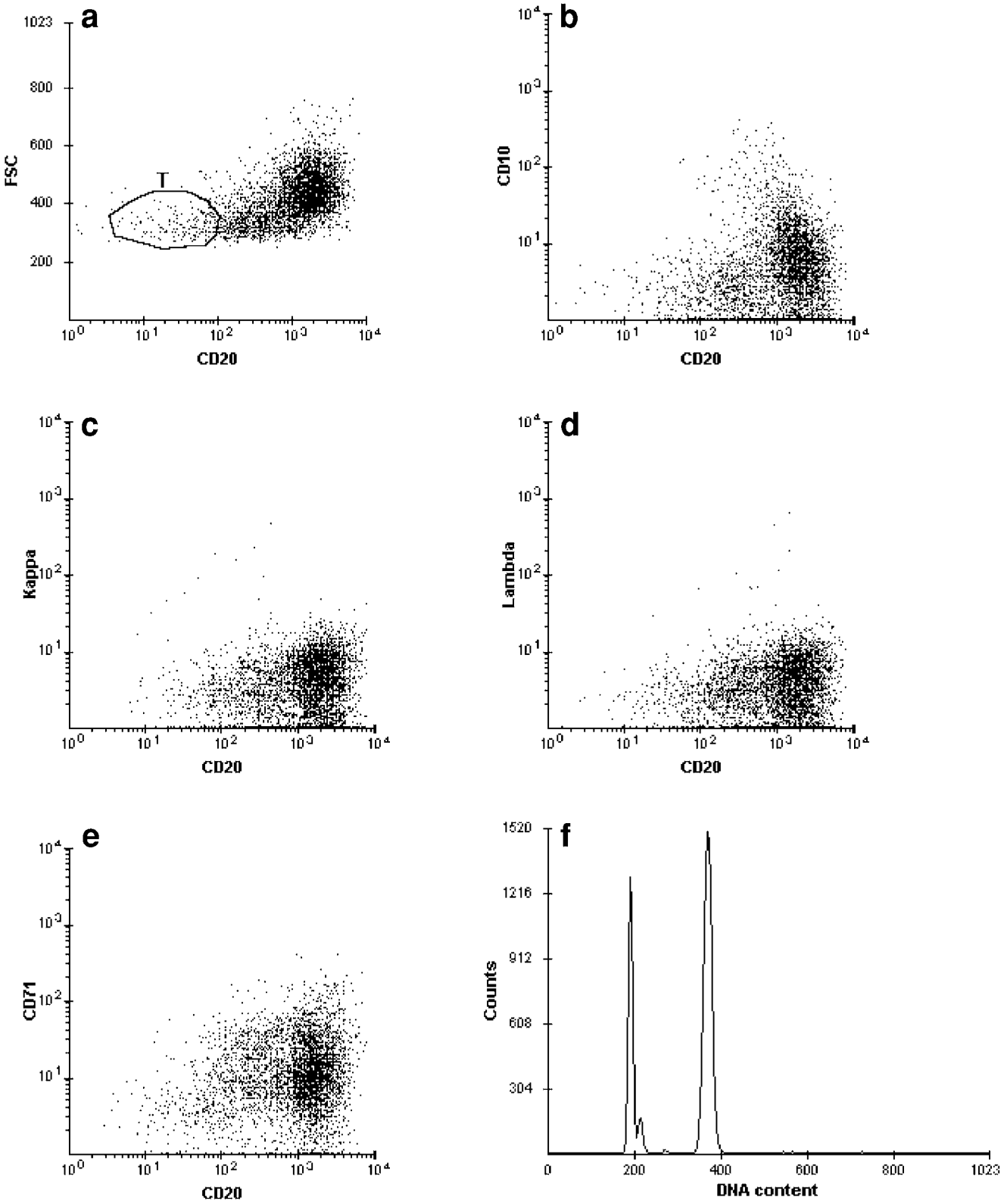

Figure 3.51 Follicular lymphoma with a preponderance of large cells (FCC III). (a) The tumor displays bimodal FSC and bimodal CD20 with brighter CD20 on the larger cells. A minute residual T-cell population (T) is present. (b–d) Weak and down-regulated CD10 expression on the brighter CD20 cells. The smaller cells with dimmer CD20 are negative for CD10. The surface light chain is not detectable. (e,f) Low proliferative activity as evidenced by the very dim CD71 expression and low S-phase (S% 0.84). The DNA index is 1.9.

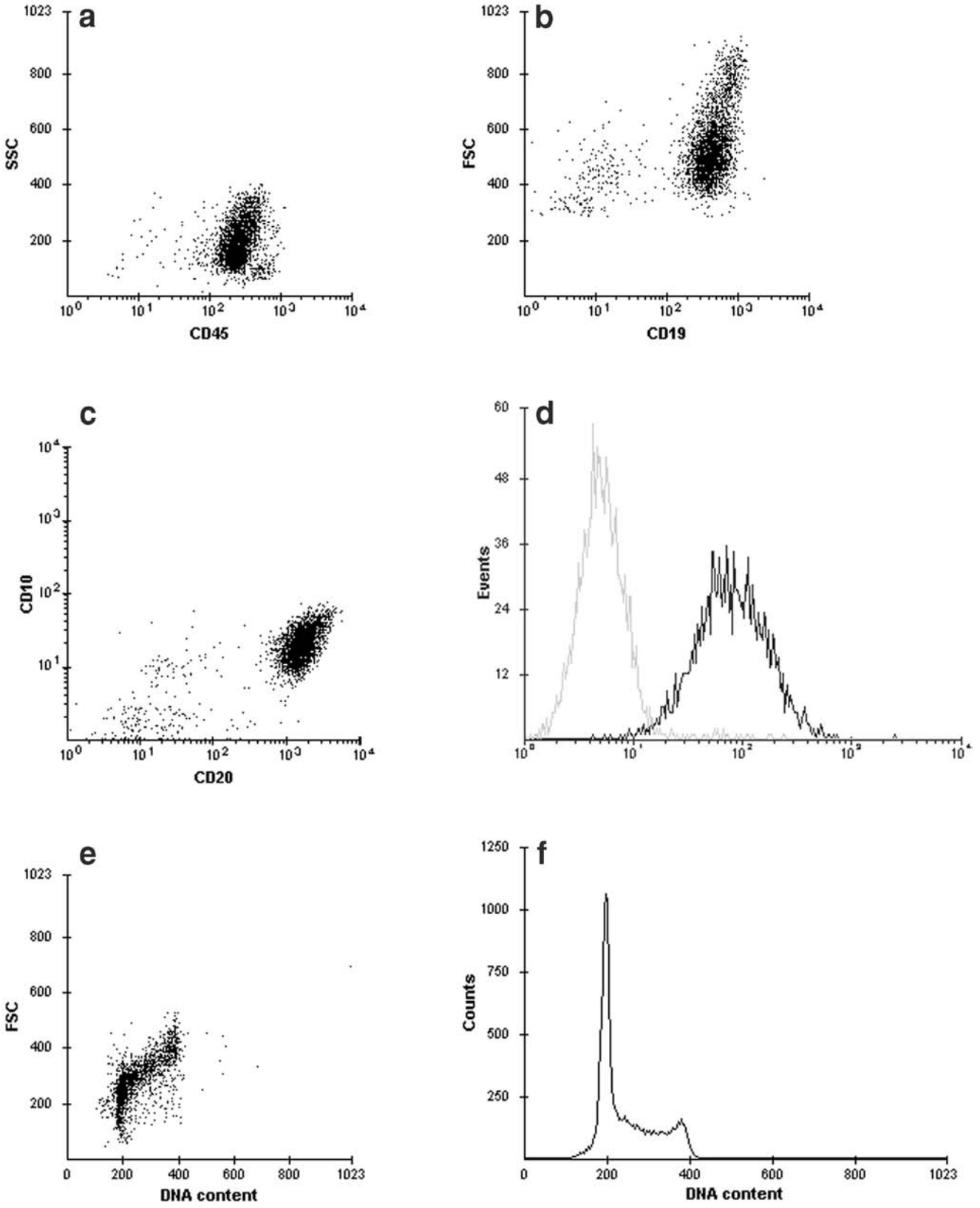

Figure 3.52 Bone marrow with Burkitt's lymphoma–leukemia. (a) Virtually a single predominant cluster in the monocytic region with moderate SSC. (b–d) The neoplastic cells are of variable (medium to large) cell size and express CD10, CD19, CD20 (CD20 brighter than CD19), and lambda light chain. (e,f) The tumor is diploid with a very high proliferative fraction (S% 51.3).

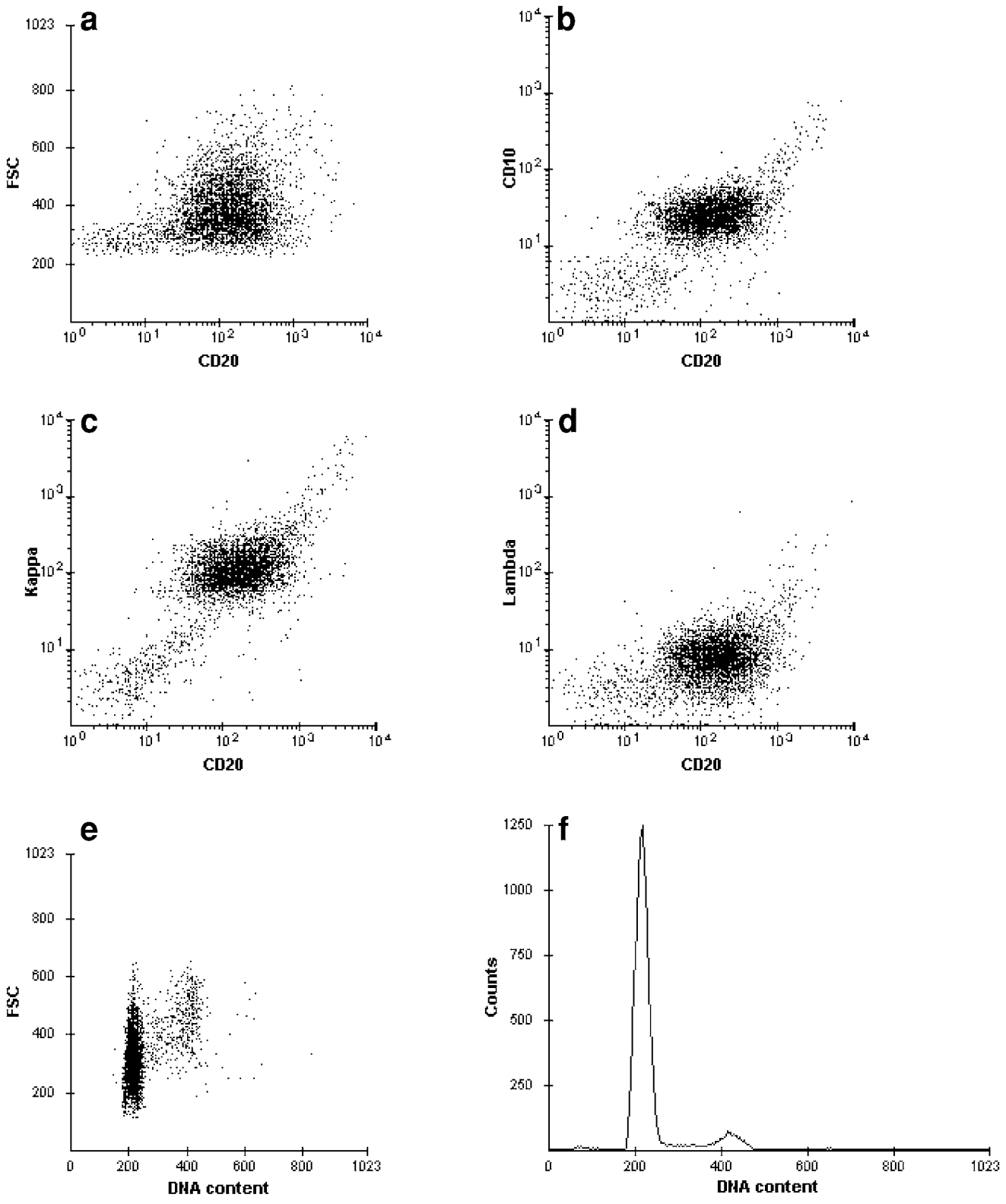

Figure 3.53 Lymph node with CD10-positive DLCL. (a–f). The neoplastic cells are CD20^{++}, CD10^{+}, and kappa^{++} and display increased FSC. The tumor is near diploid (more discernable on the FSC/DNA content dot plot than on the single parameter histogram) with an S-phase fraction of 7%.

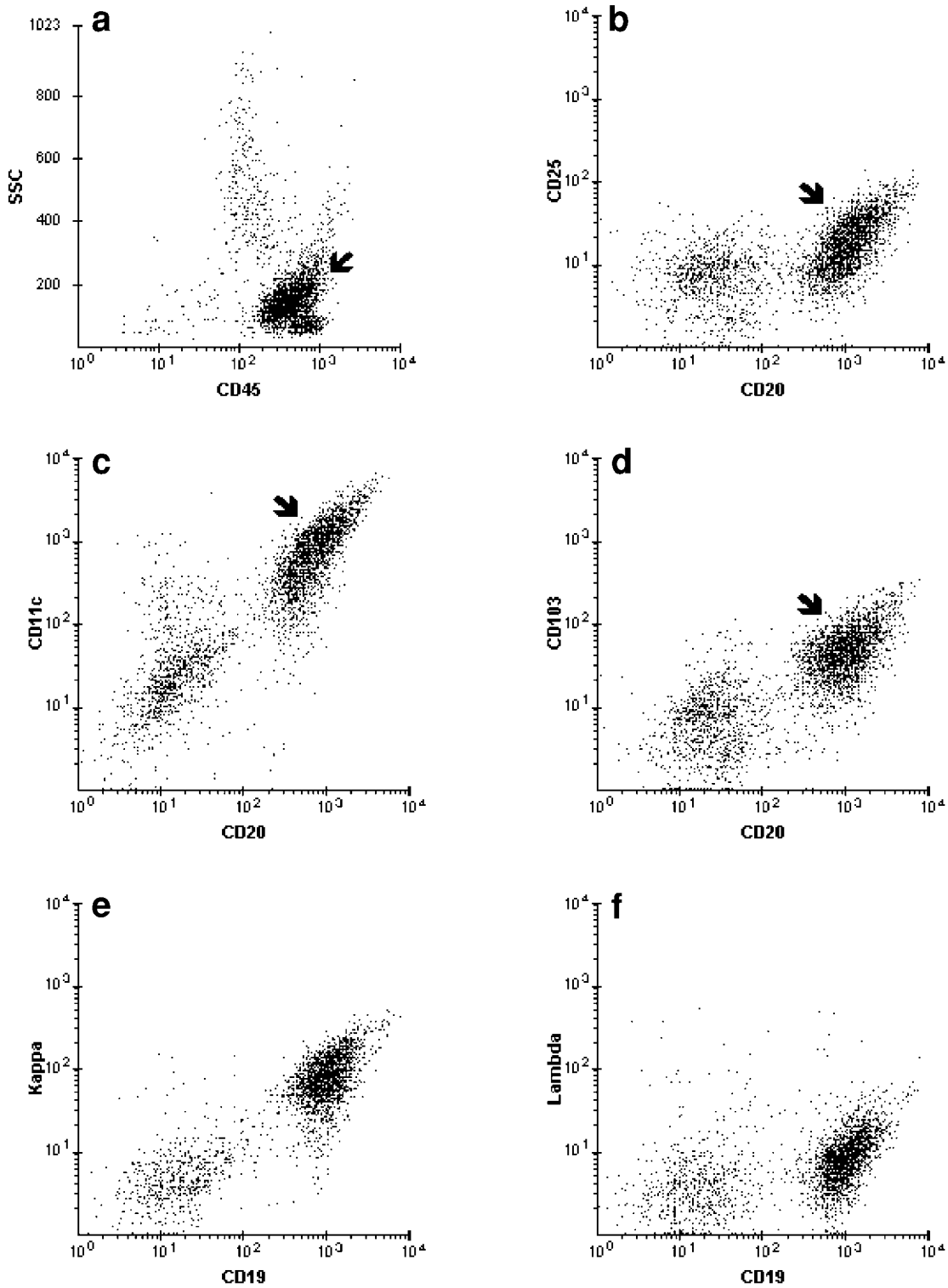

Figure 3.54 Bone marrow core biopsy with HCL. (a) The neoplastic cells (arrow) are seen in the monocytic region. (b–f) CD25 and CD103 are well expressed on hairy cells. There is intense coexpression of CD20 and CD11c. The tumor is monoclonal for kappa. Some residual T-cells (with evidence of CD20 coating) are present.

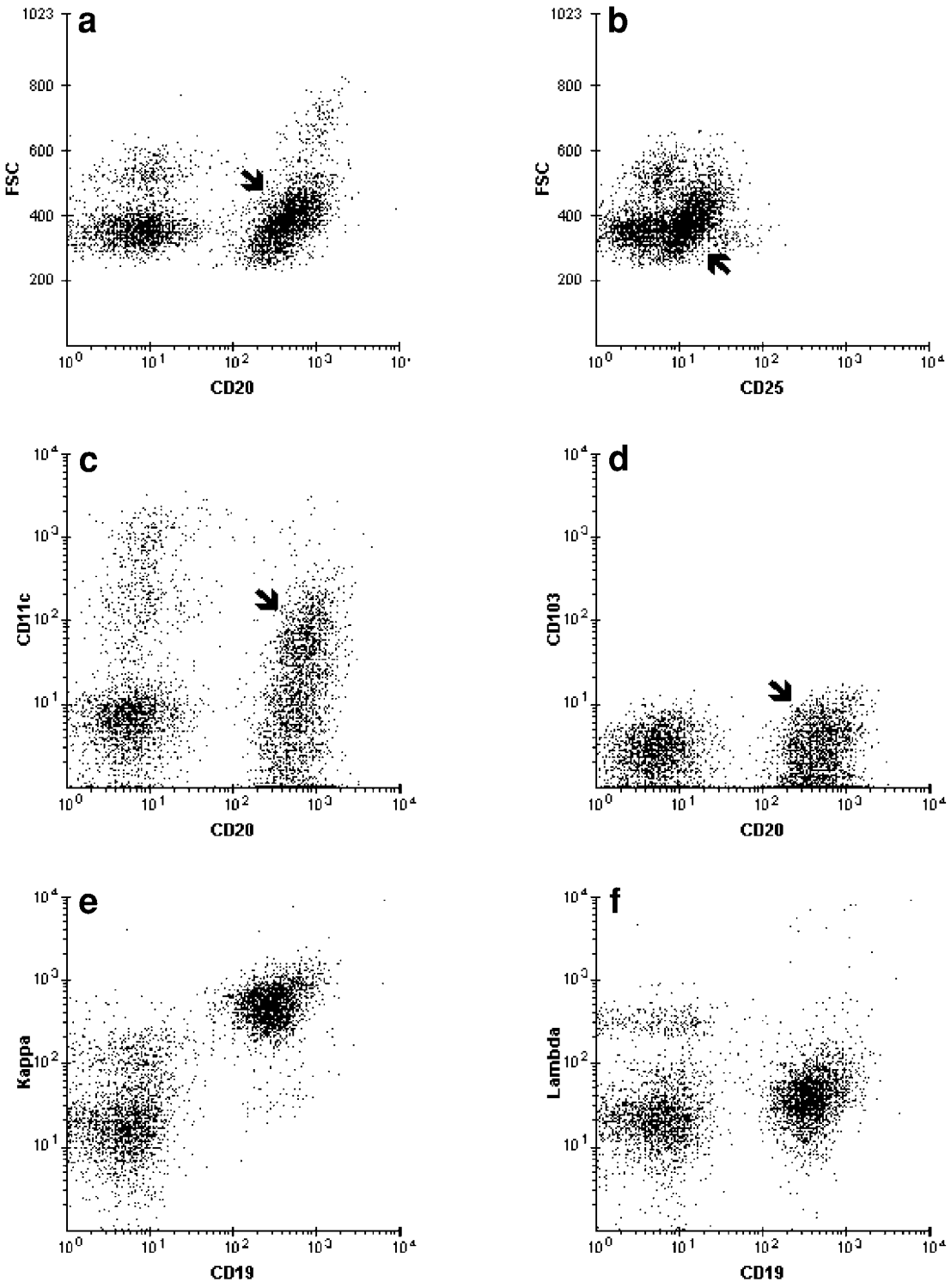

Figure 3.55 Peripheral blood with CD25-positive B-cell LPD NOS, morphologically LPC leukemia. (a–f) The leukemic cells (arrow) are small to medium size, with CD20, CD19, CD25, and kappa reactivity, but lack CD103. CD5 and CD10 are negative (not shown). CD11c is heterogeneous, from negative to positive (a CD11c/CD20 staining pattern different from that in HCL). There is indirect evidence of hypergammaglobulinemia (e,f).

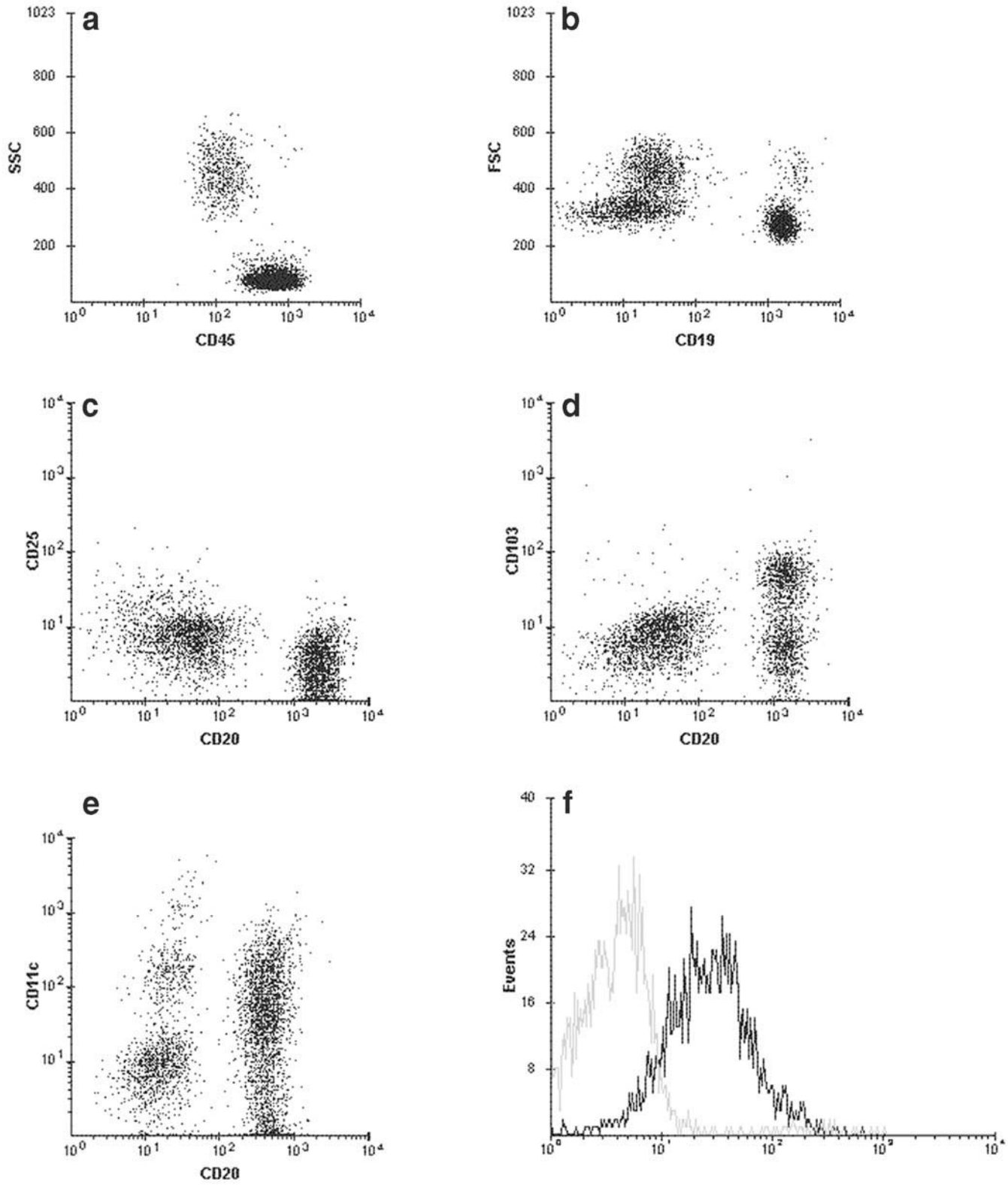

Figure 3.56 Peripheral blood with CD103-positive LPD NOS, morphologically LPC leukemia. (a–e) A prominent lymphoid cluster composed of normal T-cells and neoplastic B-cells. The tumor cells are small and express bright CD19 and CD20. CD25 is absent. CD103 is present and of variable distribution (from negative to positive). CD11c is markedly heterogeneous. (f) Gated on B-cells: The surface light chain (lambda) is weak.

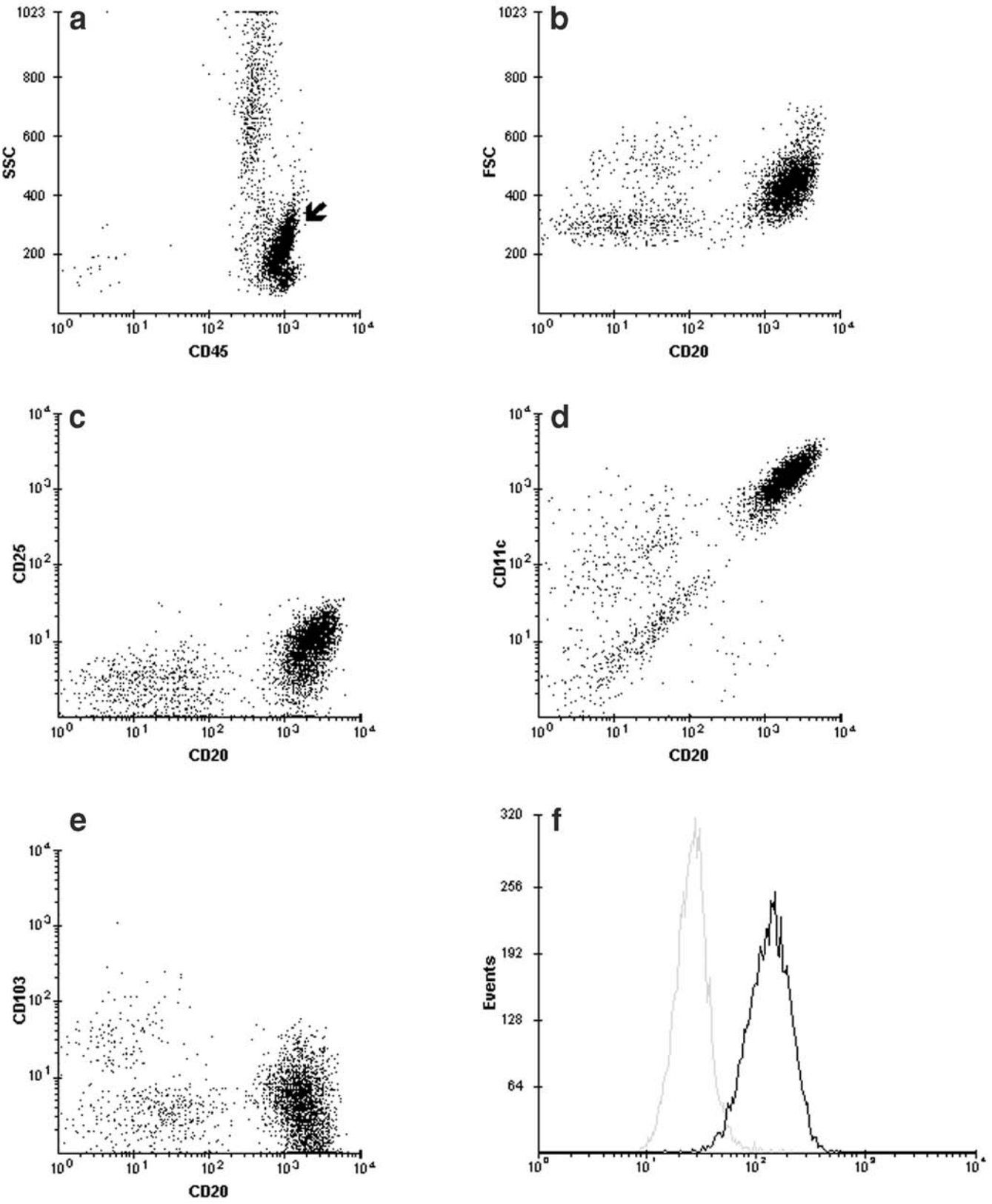

Figure 3.57 Peripheral blood with B-cell LPD NOS, morphologically PLL (shown in Plate 32). (a,b) Leukemic cells (arrow) with medium FSC occupying the monocytic region. (c–e) Gated on MNCs: weak CD25, minimal CD103 on a subset. CD5 and CD10 (not shown) are negative. The intense coexpression of CD20 and CD11c mimics that of HCL. (f) Gated on CD20-positive cells: Lambda is positive (weak). The background fluorescence of the negative kappa light chain is increased.

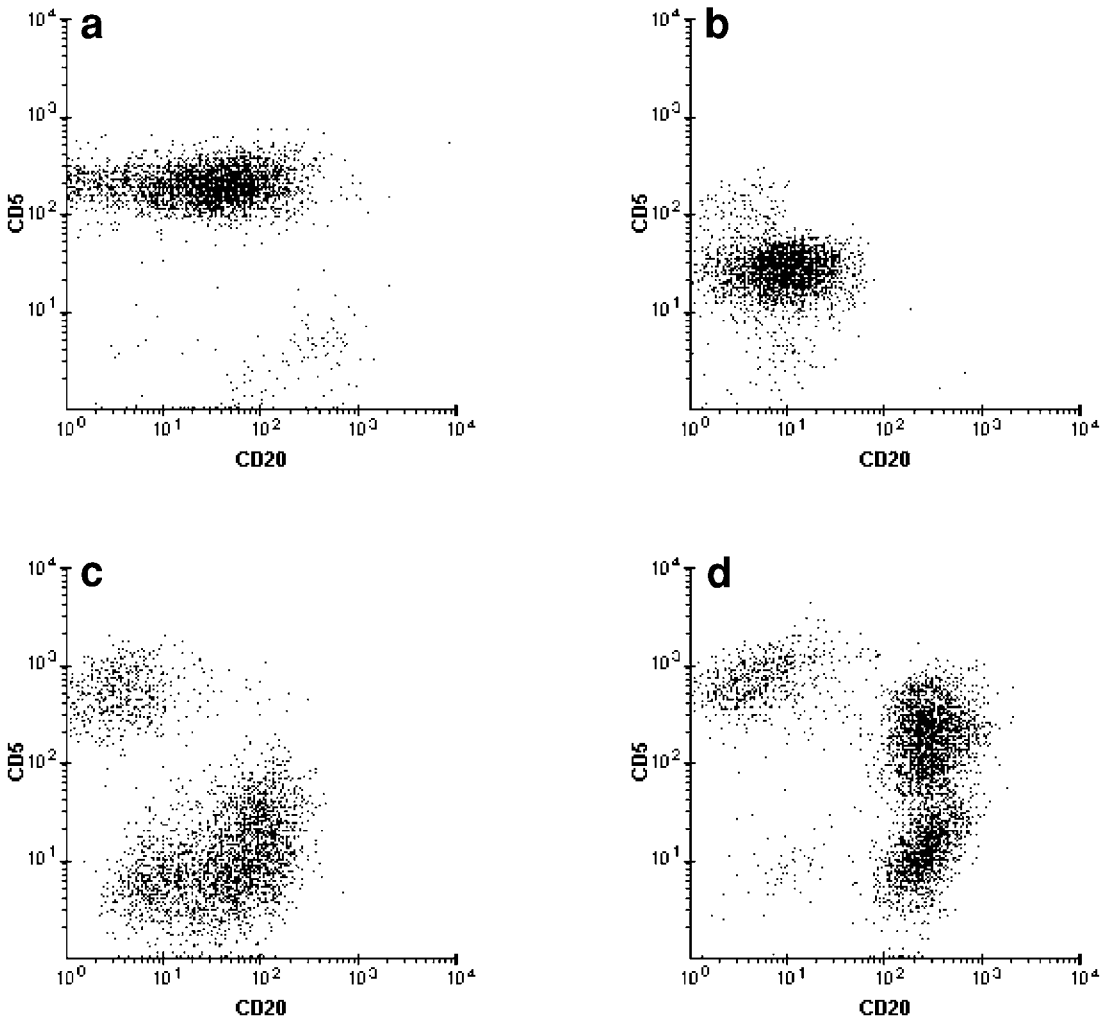

Figure 3.58 Variations in CD5 expression. Four different lymph node samples. (a) CLL/SLL: CD5 as bright as that on T-cells. (b) CLL/SLL: CD5 less intense than that on T-cells. (c) LPC lymphoma: Two subpopulations, one CD5-negative and the other with downregulated CD5. (d) MCL: Bimodal CD5 expression (an unusual finding).

It cannot be stressed enough that the reactivity for CD25 and CD103 and the very intense coexpression of CD11c/CD20 need to be evaluated together because one or two of these three features may be present in non-HCL B-cell LPD (Figures 3.55–3.57).

3.6.3.3 CD5 expression

Normally present on T-cells, the presence of CD5 in B-cell tumors is the most well-recognized "aberrancy." Among the CD5-positive B-cell malignancies, the intensity of CD5 varies from case to case (Figure 3.58). It is often weaker than that in normal T-cells. Distinguishing the various entities within this subgroup of $CD5^+$ B-cell LPD/NHL, which includes CLL/SLL, CLL-related disorders, MCL, and $CD5^+$ large cell lymphoma, requires the evaluation of other parameters, including cell size, the presence or absence of CD23, and the intensity of CD20 and surface light chain (*see* Section 3.6.2 and Section 4.4.1.1). The differential diagnosis of $CD5^+$ B-cell disorders is presented in Chapter 5.

3.6.3.4 Aberrant B-cell profile

Compared to T-cell malignancies, B-cell disorders have a lower frequency of aberrancies in pan B-cell antigens or surface immunoglobulin expression. The antigenic abnormalities include the absence of CD19 or CD20 (Figure 3.48) and lack of surface light chains despite detectable surface heavy chain expression (Figure 3.59). In the latter scenario, it is judicious to ensure that both markers of immaturity (CD34 and TdT) are negative since the combination of positive surface heavy chain (IgM) and absent surface light chain has been reported as a characteristic of transitional ALL, a rare subtype of ALL. These phenotypic abnormalities tend to occur in CLL, lymphoplasmacytic neoplasms, and high-grade B-cell LPD/NHL (i.e., with large cell size, aneuploidy, and high S-phase), especially those with a plasmablastic cytology, such as that observed in acquired immunodeficiency syndrome (AIDS)-related NHL (including primary effusion lymphomas). CD45 expression in these high-grade B-cell lymphomas is often weak or absent (Figure 3.60). Other sporadic aberrancies include the expression of a myeloid or a T-cell-associated antigen (Figure 3.61) other than CD5.

Case studies 20–22

When evaluating follow-up specimens in patients with B-cell LPD/NHL, it is important to be aware that the apparent lack of CD20 expression may have been induced by anti-CD20 therapy.

3.6.4 Identification of abnormal T-cells

The absence of one or more T-cell antigens in otherwise mature T-cells strongly suggests a PTCL. Less known, however, is the quantitative variation in antigenic density that often occurs in lymphoid tumors. These changes, as well as the abnormal coexpression of antigens, may be difficult to appreciate in immunohistology preparations.

Because there exist no T-cell antigens equivalent to the surface light chains, identifying the malignant nature of a T-cell proliferation may be problematic. Furthermore, antigenic abnormalities such as the lack of CD3, coexpression of CD4 and CD8, or the aberrant expression of CD10 can be found in both immature T-cell malignancies and postthymic T-cell neoplasms. Lack of HLA-DR is typically seen in T-ALL. This feature is not a reliable indicator of immature T-cells since it can be found in a number of mature T-cell malignancies (e.g., Sezary syndrome). Reactivity for TdT or CD34 is therefore the most reliable feature to separate these two groups of disorders. Another helpful clue is the appearance of the neoplastic population on the SSC/CD45 dot plot.

Therefore, identification of a post-thymic T-cell process relies on one or more of the following features:

1. An aberrant antigenic profile. The determination of clonality in suspected T-cell LPD/NHL is mainly based on the detection of an abnormal phenotype (i.e., phenotypes not observed in normal mature T-cells). A well-recognized aberrancy is the lack of expression of one or more pan T-cell antigens namely CD3, CD5, or CD7) (Figure 3.62). In many mature T-cell disorders, the aberrancy can be subtler. Instead of an obvious loss of antigenic expression, the abnormality can manifest as a quantitative variation or a heterogeneous distribution in antigen density. Although these subtle changes are difficult to appreciate on immunohistochemistry preparations, they can be readily detected by FCM, using a combination of CD5 or CD7 together with CD3 antibodies. On these dot plots, the neoplastic T-cells can be distinctively separated from normal T-cells on the basis of the altered fluorescence intensity, either downregulated or upregulated, of one or more pan T-cell antigens (Figures 3.63 and 3.64). A rare aberrancy observed in post-thymic T-cell neoplasms is the expression of CD1. This marker is normally present on thymocytes and is expressed in many T-ALLs. Aberrant CD20 expression may also occur infrequently (Figure 3.65).
2. CD4/CD8 abnormalities. The CD4;CD8 ratio does not indicate clonality. A marked increase or decrease in the ratio, generally considered to be > 10;1 or < 1;10 suggests a malignant T-cell proliferation (Figures 3.63 and 3.66), however, especially if the sample analyzed is peripheral blood.

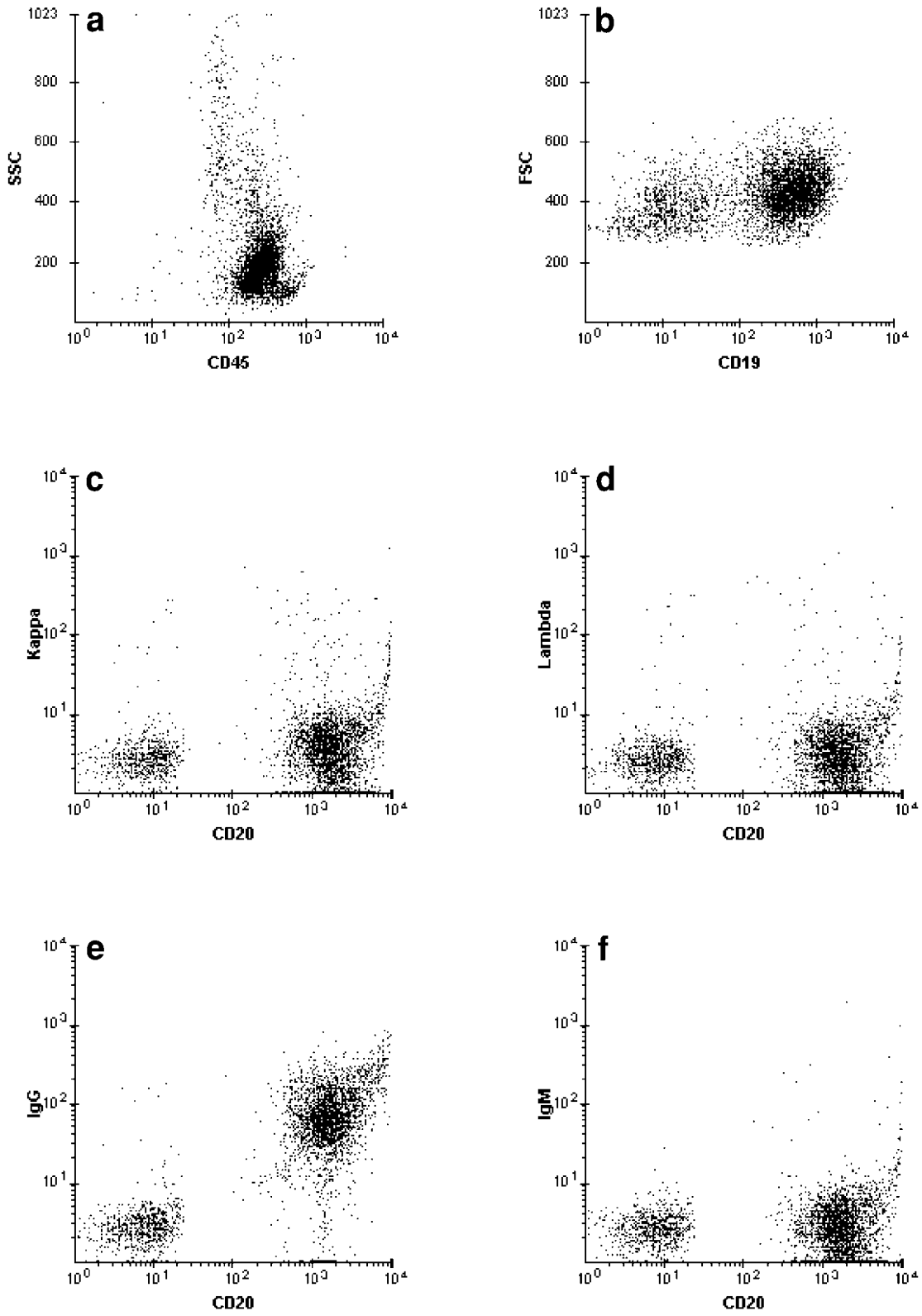

Figure 3.59 Bone marrow with high-grade B-cell NHL. (a,b) The tumor cells are of medium cell size and form a cluster in the monocytic region. (c–f) Gated on MNCs: The neoplastic cells ($CD20^{+++}$, $CD19^{++}$) express IgG only. IgM, IgD and IgA (not shown), and both light chains are negative.

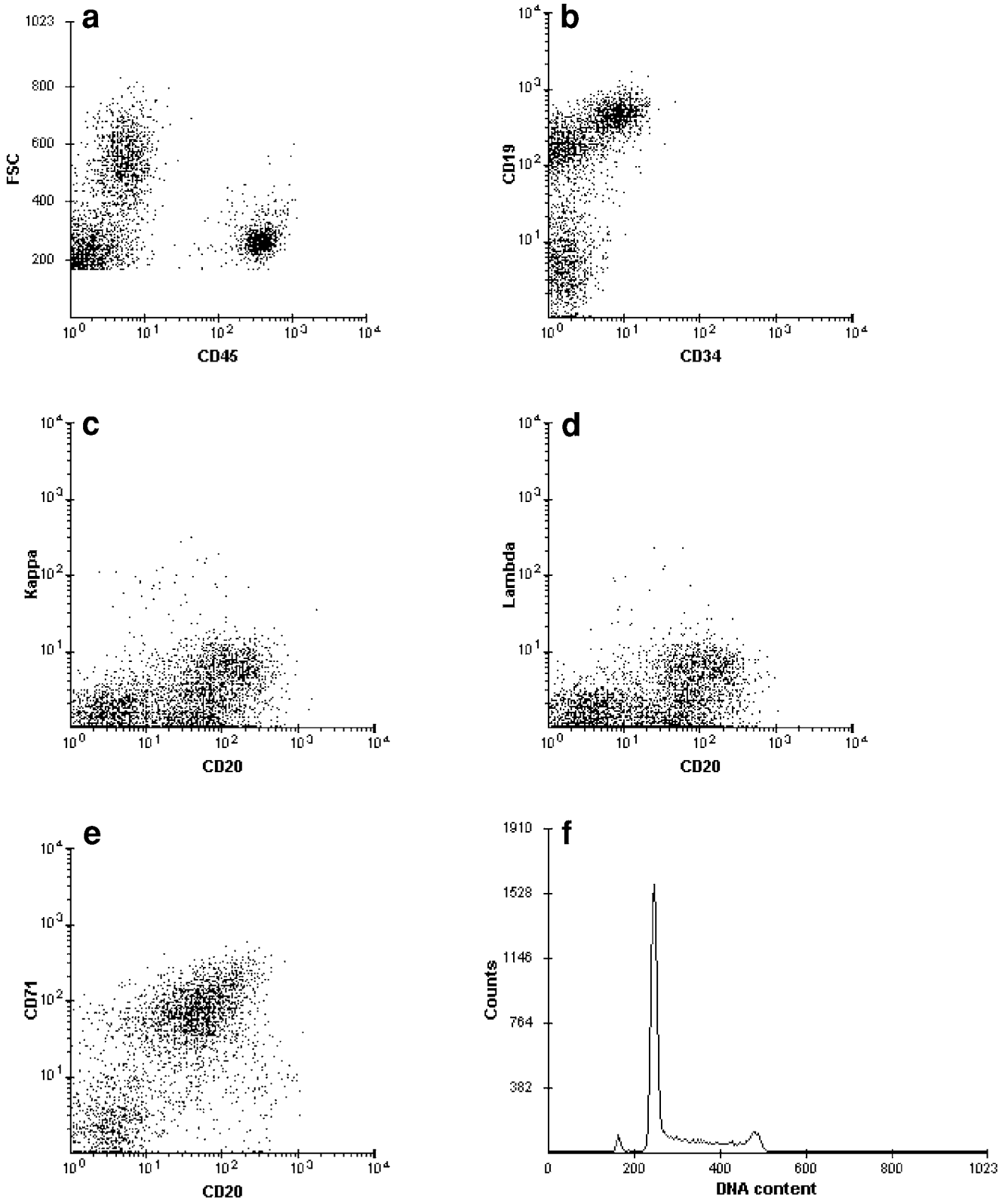

Figure 3.60 Lymph node with CD45-negative high-grade B-cell lymphoma. (a–f) The tumor displays bimodal FSC and no detectable CD45. Residual T-cells ($CD45^{++}$) are present. Neoplastic cells are positive for CD20, CD10 (not shown), and CD19. CD34, TdT (not shown), and both light chains are negative. The tumor is aneuploid (DI: 1.77) and highly proliferative, with bright CD71 and a high S-phase fraction (S% 34.7).

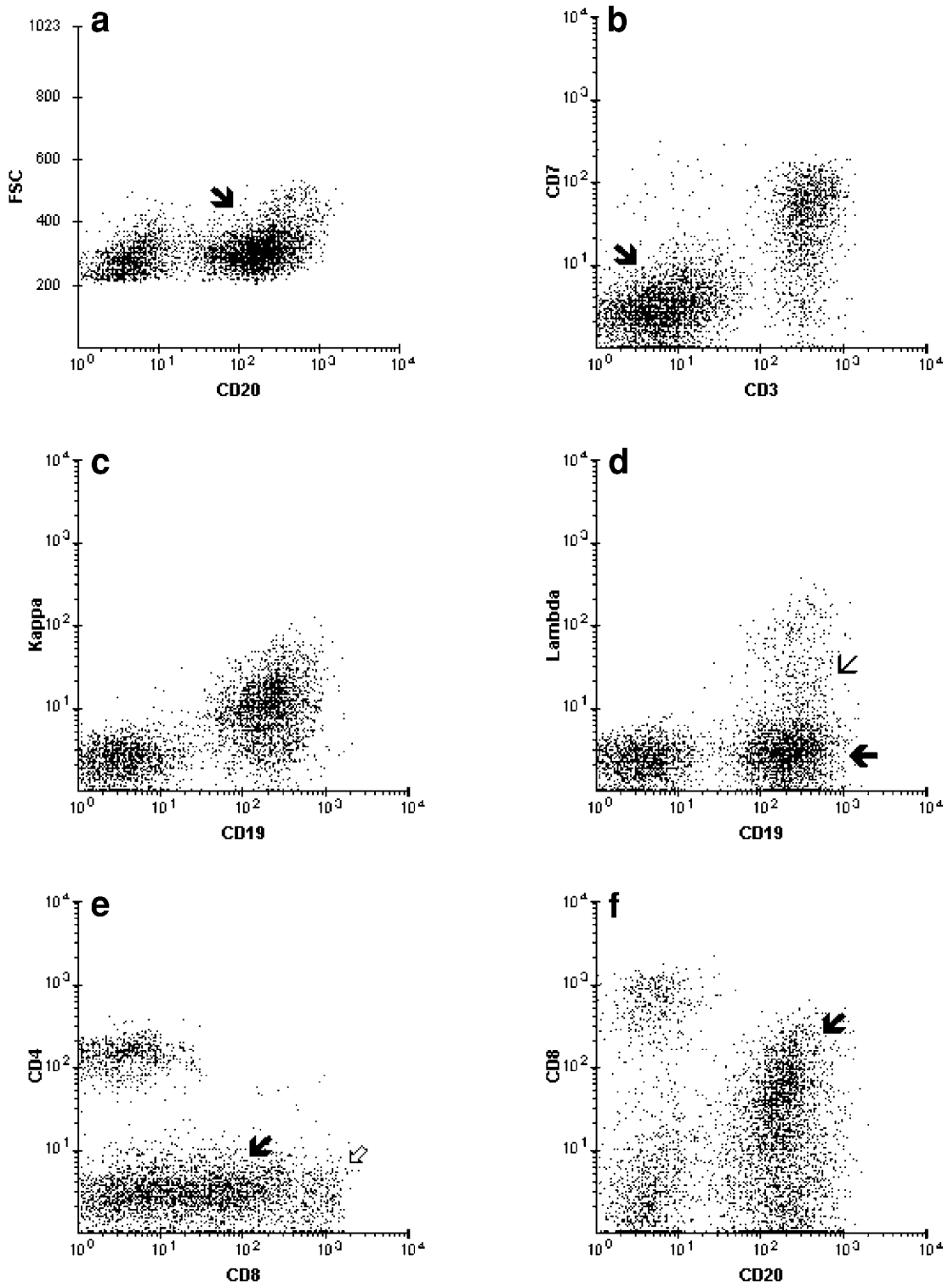

Figure 3.61 Low-grade B-cell NHL NOS with aberrant CD8 reactivity. (a–f) The neoplastic population (arrow) is composed mostly of small cells. The cells are $CD20^{++}$, $CD19^{++}$, and $kappa^{+}$. An unusual feature is the weak and variable expression of CD8. Small populations of benign B-cells (thin arrow) and normal CD4 and CD8 (open arrow) T-cells are present.

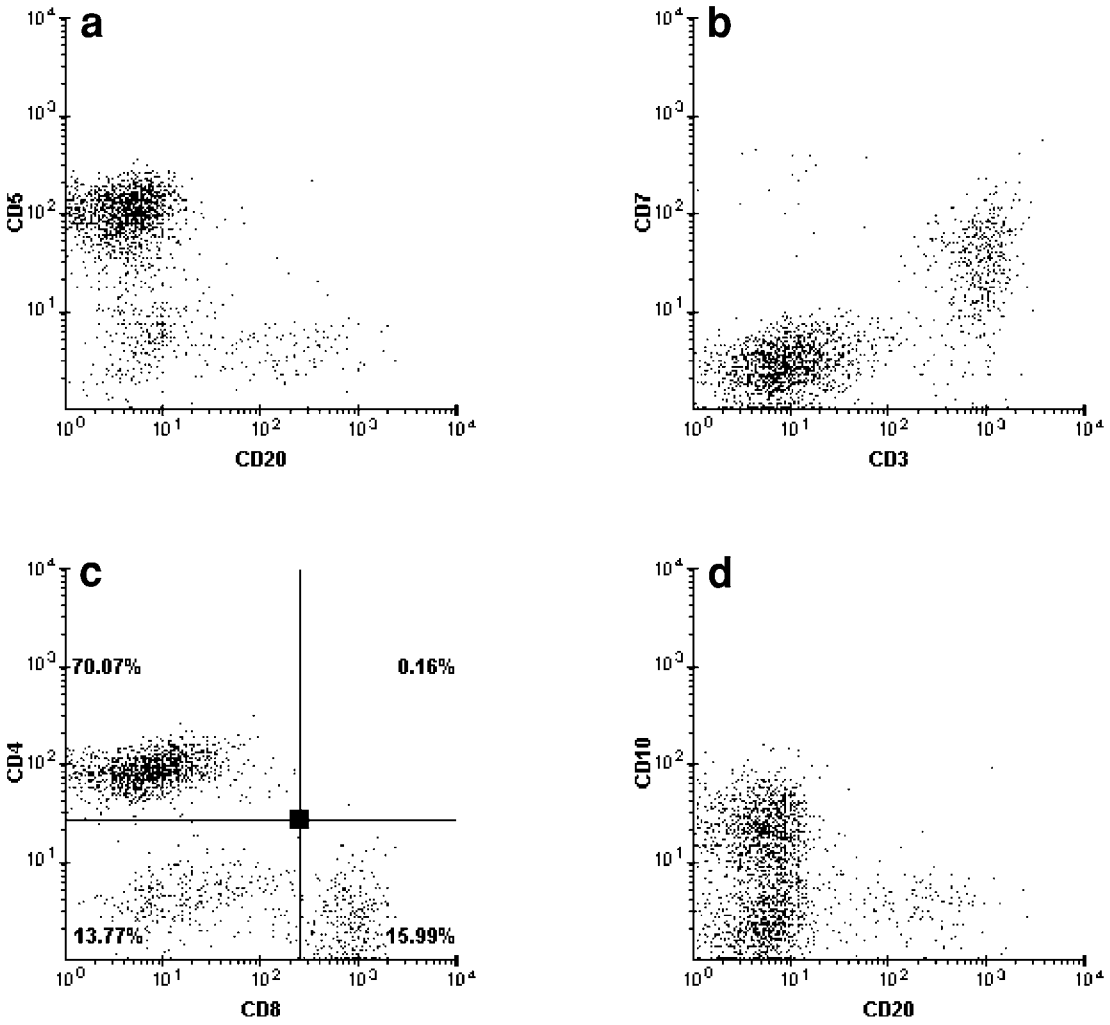

Figure 3.62 Lymph node (FNA) with PTCL. (a–d) The neoplastic cells display an aberrant T-cell phenotype with lack of CD3 and CD7. CD5, CD4, and CD2 (not shown) are well expressed. CD10 is dim and of variable distribution. NK-cell markers (not shown) are negative.

Other corroborating clinical and laboratory findings, such as an absolute lymphocytosis, persistent lymphadenopathy, or detectable rearranged T-cell genes still need to be considered before labeling the process as neoplastic. Another feature suggestive of malignancy is either coexpression of CD4 and CD8 (Figure 3.65) or lack of both CD4 and CD8 (Figure 3.64) in a sizable lymphoid population. In normal tissues outside the thymus, $CD4^+$ $CD8^+$ and $CD4^-$ $CD8^-$ cells are present in insignificant numbers. Either feature is more common in T-cell lymphoblastic leukemia-lymphoma than in post-thymic T-cell disorders. Coexpression of CD4 and CD8 is a normal finding if the specimen analyzed is the thymus (i.e., thymoma), however, since this is the expected phenotype of thymocytes (Figure 3.67). Furthermore, caution should be taken when analyzing peripheral blood specimens from pediatric patients. In certain congenital immunodeficiencies such as severe combined immunodeficiency (SCID), the lymphocytes may lack CD3 expression or be negative for both CD4 and CD8. The presence of lymphopenia and the clinical setting are important clues to the underlying immunodeficiency.

Case studies 23–25

3. The proportion of the cells of interest. The phenotype of some mature T-cell malignancies may not display any aberrancy (i.e., the tumor cells may have a profile identical to either normal CD4 T-cells or normal CD8 T-cells). The process can still be recognized as neoplastic if the population is present in overwhelming numbers. A specific example is T-PLL, in which the peripheral blood

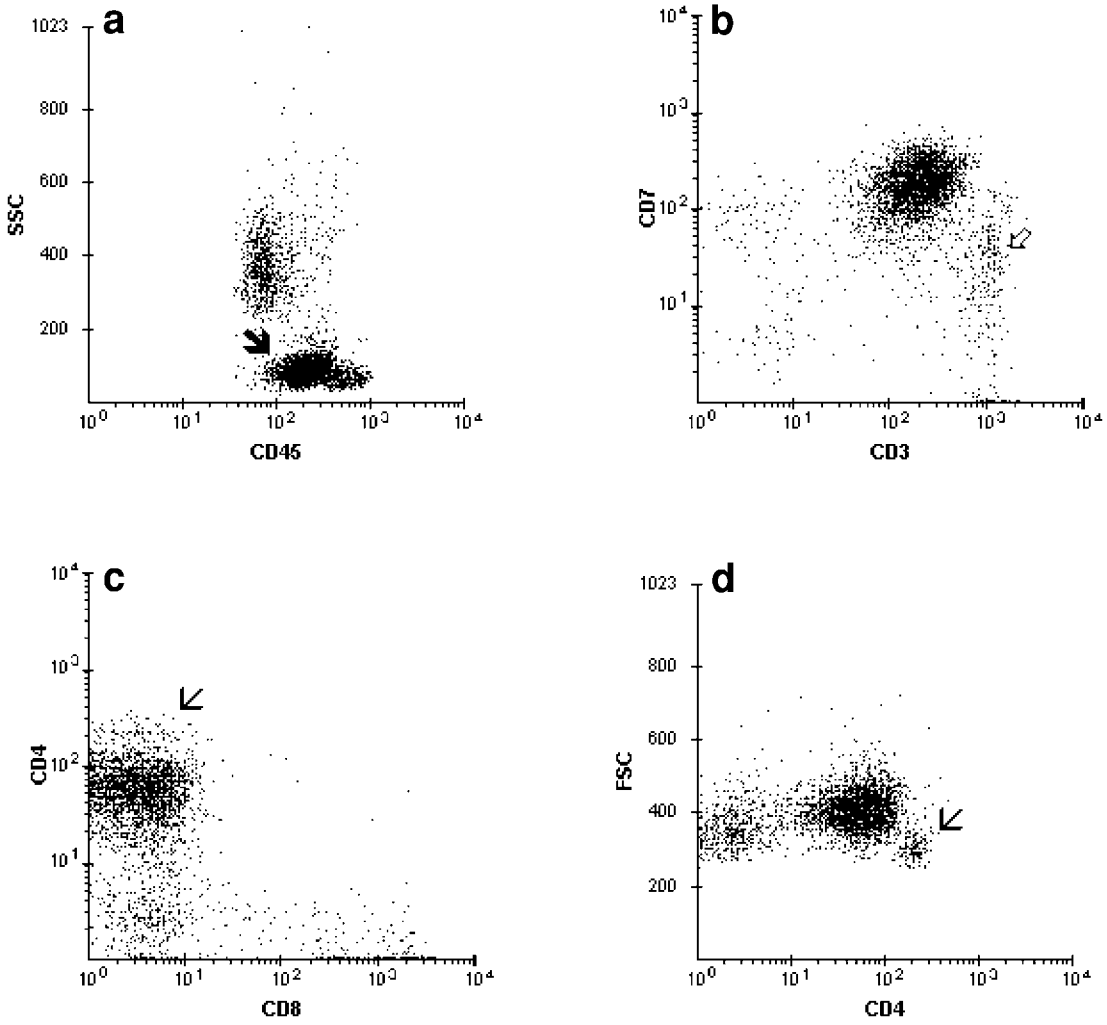

Figure 3.63 PTCL in leukemic phase. Subtle antigenic aberrancies. (a) Downregulated CD45. The tumor (arrow) occupies the hematogone region. (b) Slightly downregulated CD3 as compared to normal T-cells (open arrow). (c,d) Slightly downregulated CD4 compared to normal T-cells (thin arrow), which can be better appreciated on the FSC/CD4 than the CD4/CD8 dot plot. CD4;CD8 ratio is markedly increased. The tumor cells are of medium cell size.

is essentially composed of a single population of phenotypically "normal" CD4 T-cells. The cell size (FSC in the moderate range) is another clue that these are abnormal T-cells (Figure 3.68).

4. DNA and cell cycle parameters. Aneuploidy and/or an increased S-phase are additional parameters supportive of a malignant process.

3.6.5 Useful antigenic features in mature T-cell malignancies

In addition to the above-described phenotypic abnormalities for recognizing mature T-cell malignancies, the presence of certain phenotypic features, such as coexpression of CD25 or NK-cell markers, permits one to identify the specific subtype of T-cell neoplasm. Some of these disorders, such as T-PLL, aggressive true NK-leukemia, the NK-like T-cell leukemias, and many cases of adult T-cell leukemia–lymphoma (ATLL), display extensive involvement of the blood at the time of diagnosis.

Expression of CD25, together with the absence of one or more pan T-cell antigens, is virtually pathognomonic for ATLL (Figure 3.69). Although most cases of ATLL are CD4-

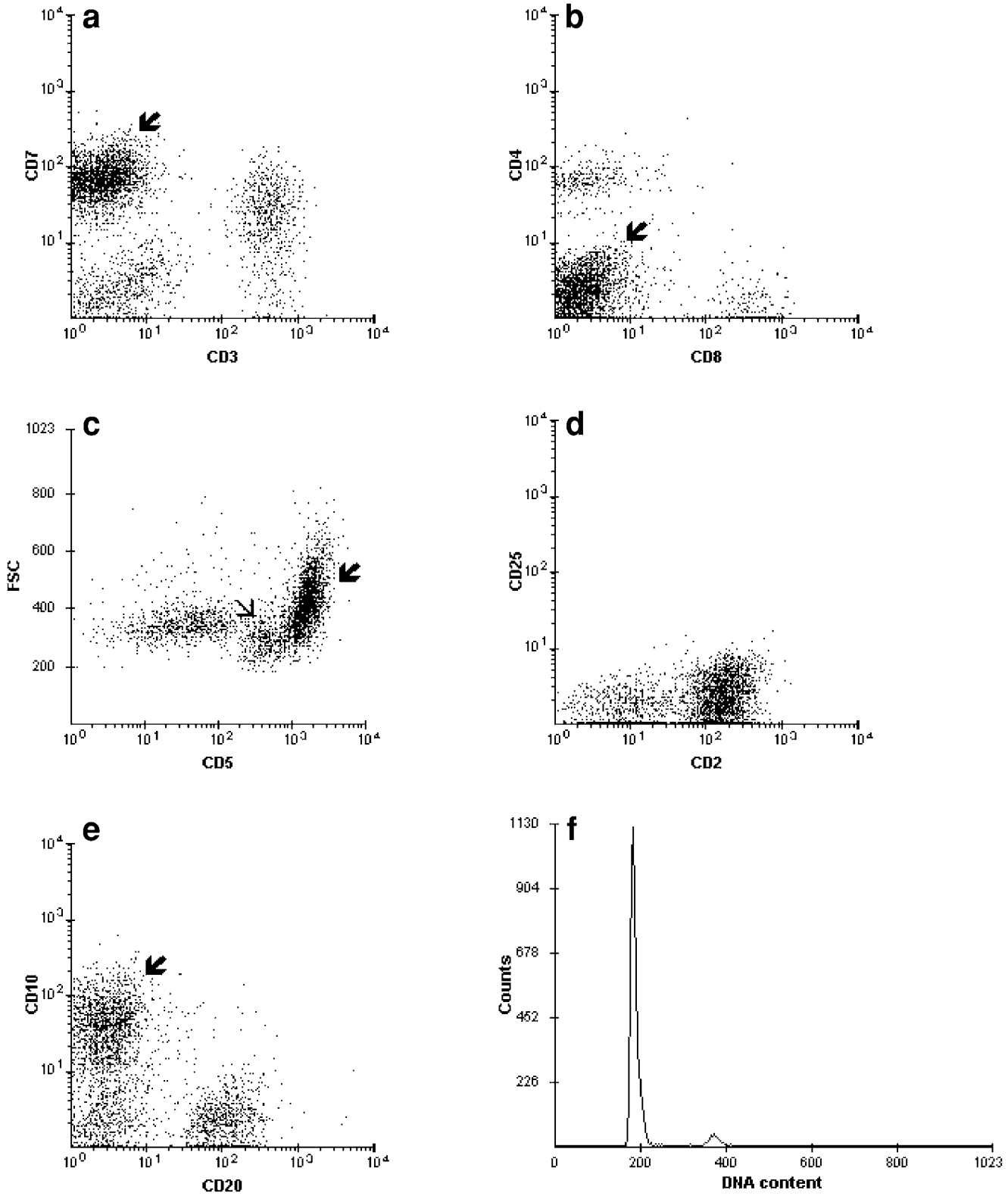

Figure 3.64 Lymph node with PTCL. The neoplastic cells (arrow) are of medium cell size and display an aberrant T-cell phenotype: lack of CD3 (a), CD4 and CD8 both absent (b), upregulated CD5 (c) as compared to the normal T-cells (thin arrow), and expression of CD10 (e). The intensity of CD2 and CD7 is similar to that on normal T-cells. NK markers (not shown) are negative. (f) The tumor is diploid with a low S-phase fraction (S% 3.8).

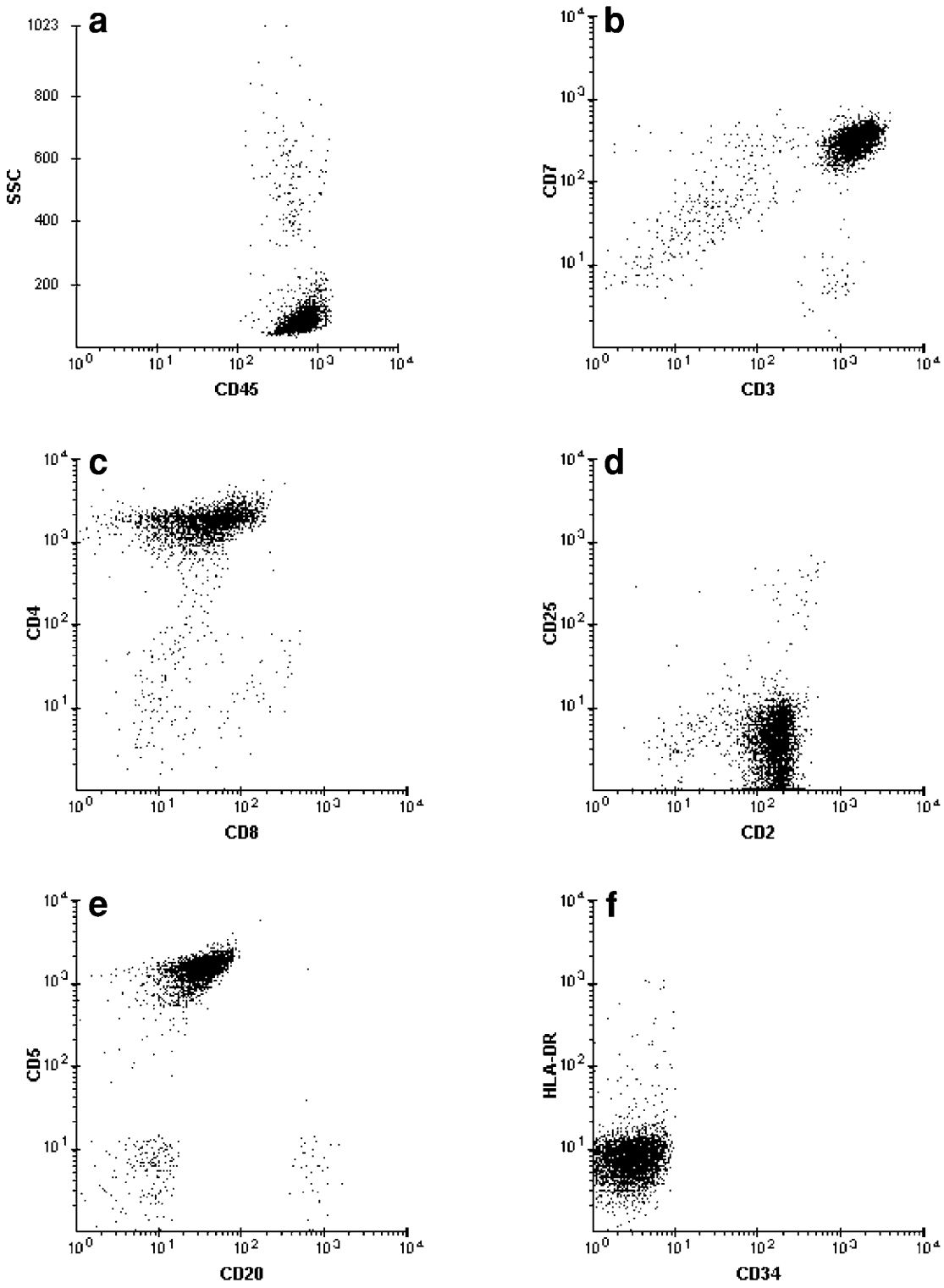

Figure 3.65 Peripheral blood with T-PLL (morphology shown in Plate 44). (a) Virtually a single predominant cluster in the lymphoid region. (b–f) CD3, CD7, CD2, and CD4 are well expressed on the leukemic cells. The leukemic cells also display weak CD8 and weak, aberrant CD20 expression. CD25 is negative. HLA-DR is absent. CD34 and TdT are negative (not shown).

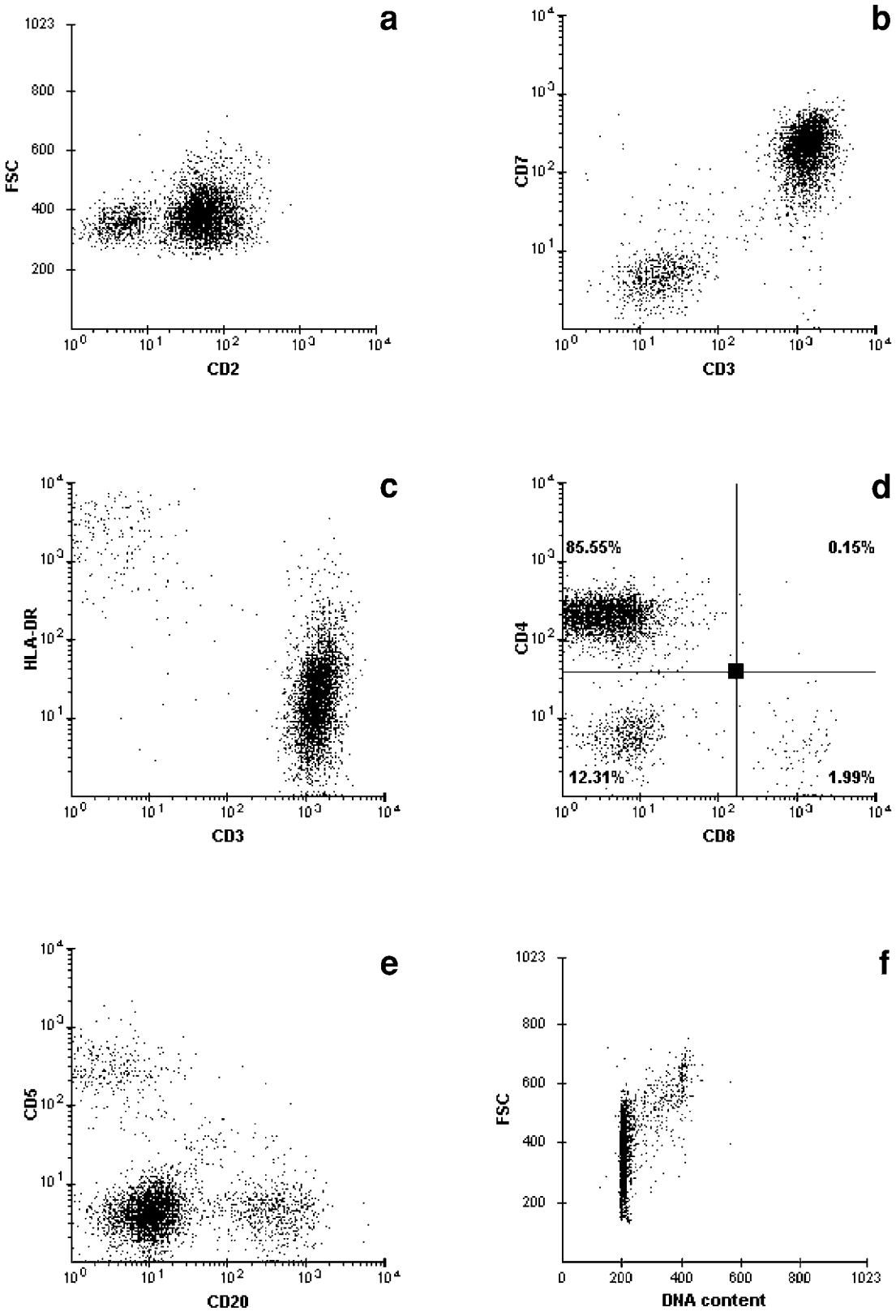

Figure 3.66 Lymph node involvement by mycosis fungoides. (a–d) The tumor cells are medium size and express CD2, CD3, CD7, and CD4 at the same level as normal T-cells. CD4;CD8 ratio is markedly increased. HLA-DR is weakly expressed. (e) The only antigenic aberrancy is the loss of CD5. (f) The tumor is diploid with a moderate S-phase fraction (S% 9.5).

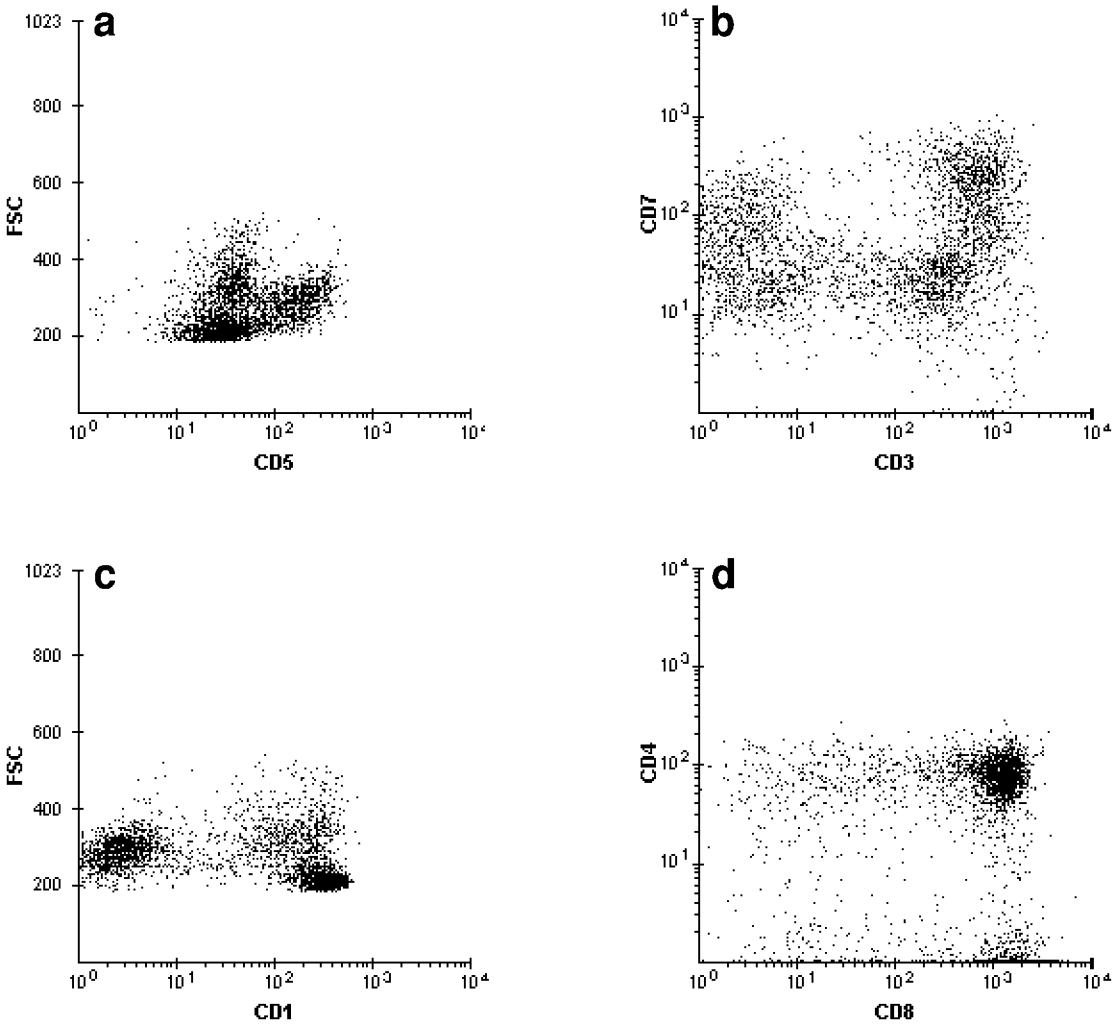

Figure 3.67 Thymocytes, from a case of thymoma. (a–c) The degree of heterogeneity in the expression of T-cell antigens (including CD1) varies from one marker to another and reflects the presence of various subpopulations of thymocytes at various stages of maturation and differentiation. (d) The great majority coexpress bright CD4 and CD8. Similar to CD4 and CD8, the intensity of CD2 (not shown) is bright and homogeneous.


Case study 26

positive, a small number coexpress CD4 and CD8. The typical spectrum of small to large lymphoid cells with the "flower cell" cytology of the tumor cells on the blood smear, plus the laboratory evidence of human T-cell lymphotropic virus (HTLV)-I infection, are additional supportive features for this diagnosis.


Case study 27

T-prolymphocytic leukemia is recognized by its extremely high WBC count and an apparent normal helper T-cell phenotype (Figure 3.68). The overwhelming number of neoplastic cells results in a markedly elevated CD4;CD8 ratio. This feature is the main phenotypic abnormality in T-PLL.


Case studies 28–30

The blood and bone marrow manifestations of aggressive NK disorders, which include true NK and NK-like T-cell malignancies, may be confused with an acute leukemia morphologically. The FCM characteristics are clear-cut, however, and indicate a mature population with medium to high FSC and coexpression of several T-cell markers along with one or more NK markers (CD16, CD56 or CD57). The results for CD16 may vary because of the wide difference among various anti-CD16 antibodies. In general, the aggressive NK or NK-like T-cell

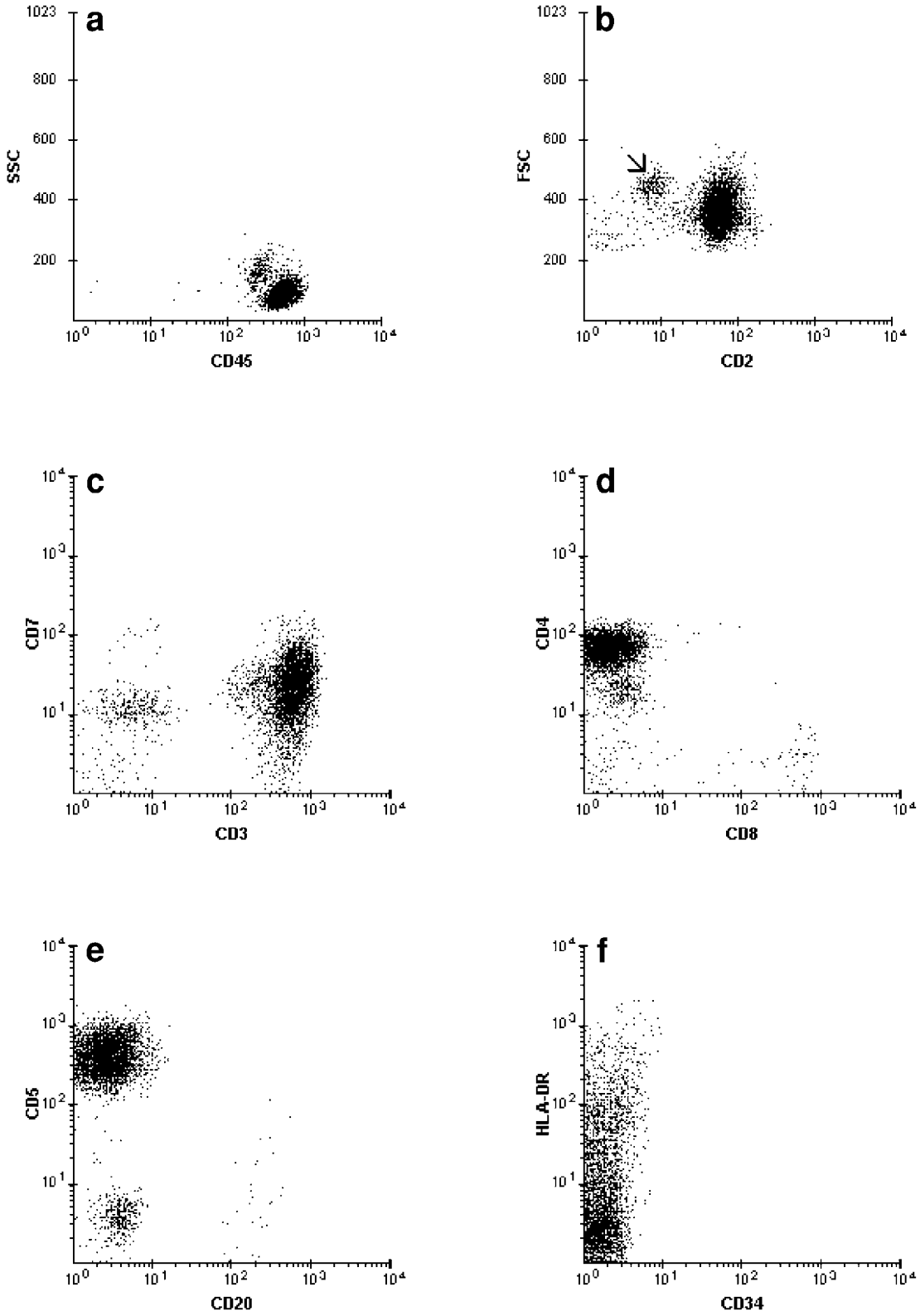

Figure 3.68 Peripheral blood with T-PLL. (a) A predominant lymphoid cluster. (b–f) The leukemic cells are of medium size, smaller than monocytes (arrow), and display no antigenic aberrancy. CD3, CD7, CD5, CD2, and CD4 are of similar intensities to those on normal T-cells. HLA-DR is of weak and variable intensity.

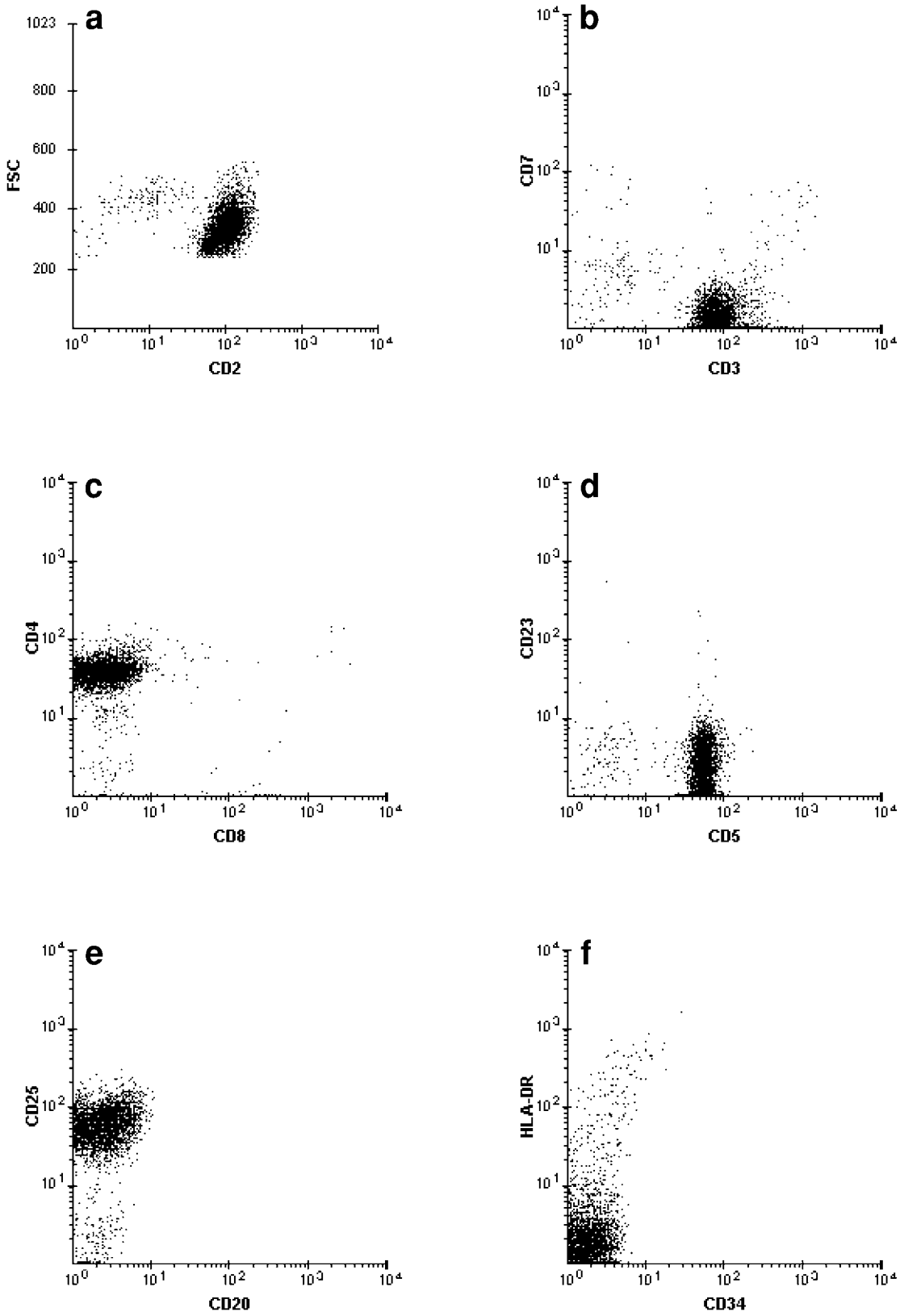

Figure 3.69 Peripheral blood with ATLL (morphology shown in Plate 43). (a–f) The leukemic cells are of medium cell size, but smaller than monocytes. CD2, CD3, CD4, CD5, and CD25 are well expressed. CD7 is absent. HLA-DR is negative.

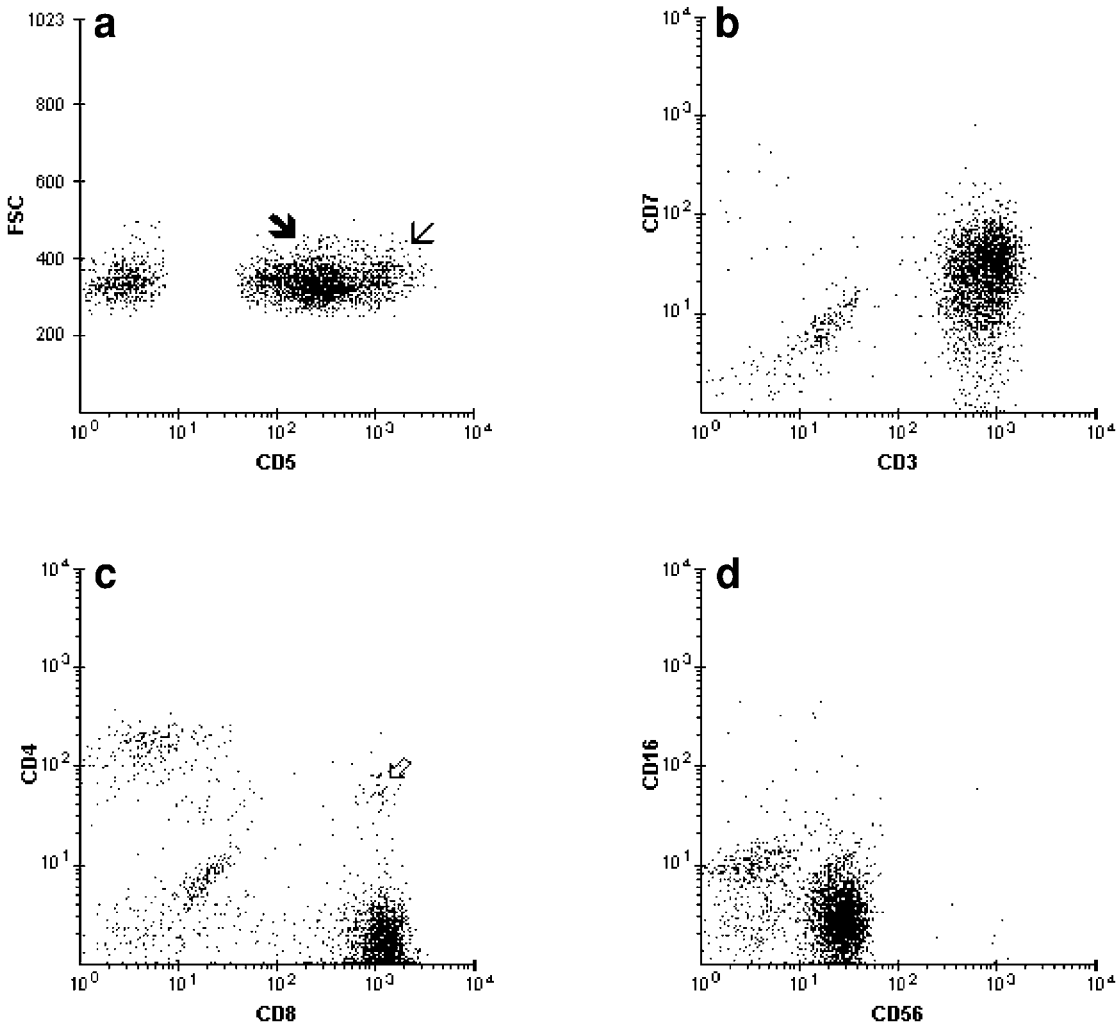

Figure 3.70 NK-Like T-cell leukemia. (a–d) The leukemic cells (arrow) display low FSC and weaker CD5 than normal T-cells (thin arrow). CD3, CD7, and CD8 are expressed at the same level as normal T-cells. CD56 is positive. Despite the small cell size, this case was biologically aggressive with marked leukocytosis and a short clinical course. There is a minute $CD4^{++}/CD8^{++}$ T-cell population (open arrow).

malignancies are usually associated with CD56 expression, whereas CD57 is more common in the low-grade counterparts (*see* Sections 4.1.2.3 and 4.4.2). A small number of cases may express CD57 instead of CD56, however. The increased cell size, high proliferative fraction, and multiorgan involvement are clear-cut indicators of the aggressive biology of this group of lymphoma–leukemias.

CD8 and CD5, when expressed, are often downregulated compared to normal suppressor T-cells (Figure 3.70). True NK cells differ from NK-like T-cells by the lack of a CD3/TCR complex and the germline configuration of the TCR genes. In other words, true NK cells do not express TCR-αβ, TCR-γδ, or surface CD3 (Figure 3.71). The truncated mRNA for the ε-chain of CD3 is present in true NK cells, however, thus producing isolated CD3 ε-chains that react with the polyclonal anti-CD3 antibodies used in immunohistochemistry. As a result, the distinction between true NK and NK-like T-cells may not be possible with paraffin immunostaining.

The following is the summary of the phenotypes often encountered in the aggressive NK disorders:

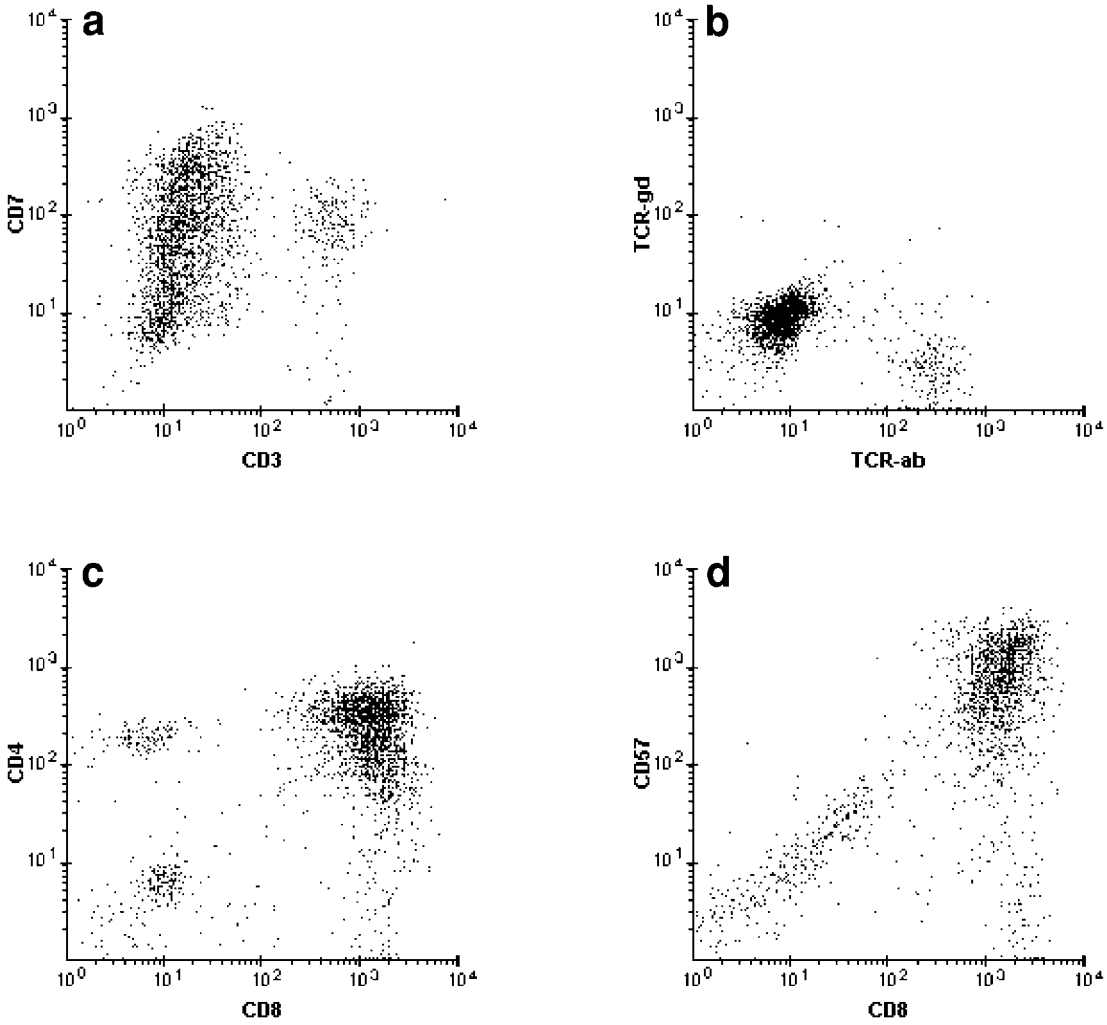

Figure 3.71 Aggressive true NK-cell leukemia. (a–d) The neoplastic cells are negative for CD3, TCR-αβ, and TCR-γδ. CD7 is expressed but of heterogeneous distribution. This case has two unusual features: coexpression of CD4 and CD8 and reactivity for CD57 instead of CD56. CD34 and TdT are negative (not shown). Residual normal T-cells (positive for CD3, CD7, and TCR-αβ) are present.

- Positive CD56/CD2/CD7, downregulated or absent CD8/CD5, absent CD3/TCR-αβ/TCR-γδ/CD4. These features indicate a true NK cell proliferation.

Case study 31

- Positive CD56/CD2/CD7/CD3/TCR-γδ, downregulated CD5, absent TCR-αβ/CD4/CD8 (Figure 3.72). This NK-like T-cell, TCR-γδ phenotype occurs mainly in the rare γδ-T-cell lymphoma–leukemia (also known as hepatosplenic lymphoma).

Case study 32

- Positive CD56/CD2/CD7/CD3/TCR-αβ, downregulated CD5 and CD8, absent TCR-γδ/CD4. This NK-like T-cell, TCR-αβ phenotype (Figure 3.70) is found in the majority of aggressive NK-like T-cell malignancies. A rare case may express CD57 instead of CD56.

3.7 Dot plot patterns in histiocytic proliferations and nonhematopoietic malignancies

The main nonhematopoietic neoplasm that passes through the flow cytometer is small cell carcinoma (neuroendocrine neoplasms) because the tumor cells are more likely to occur as individual cells and the cell size is in the range of that seen in aggressive lymphoid malignancies. Small cell carcinoma (Figure 3.73) is often accompanied by extensive necrosis. The resulting

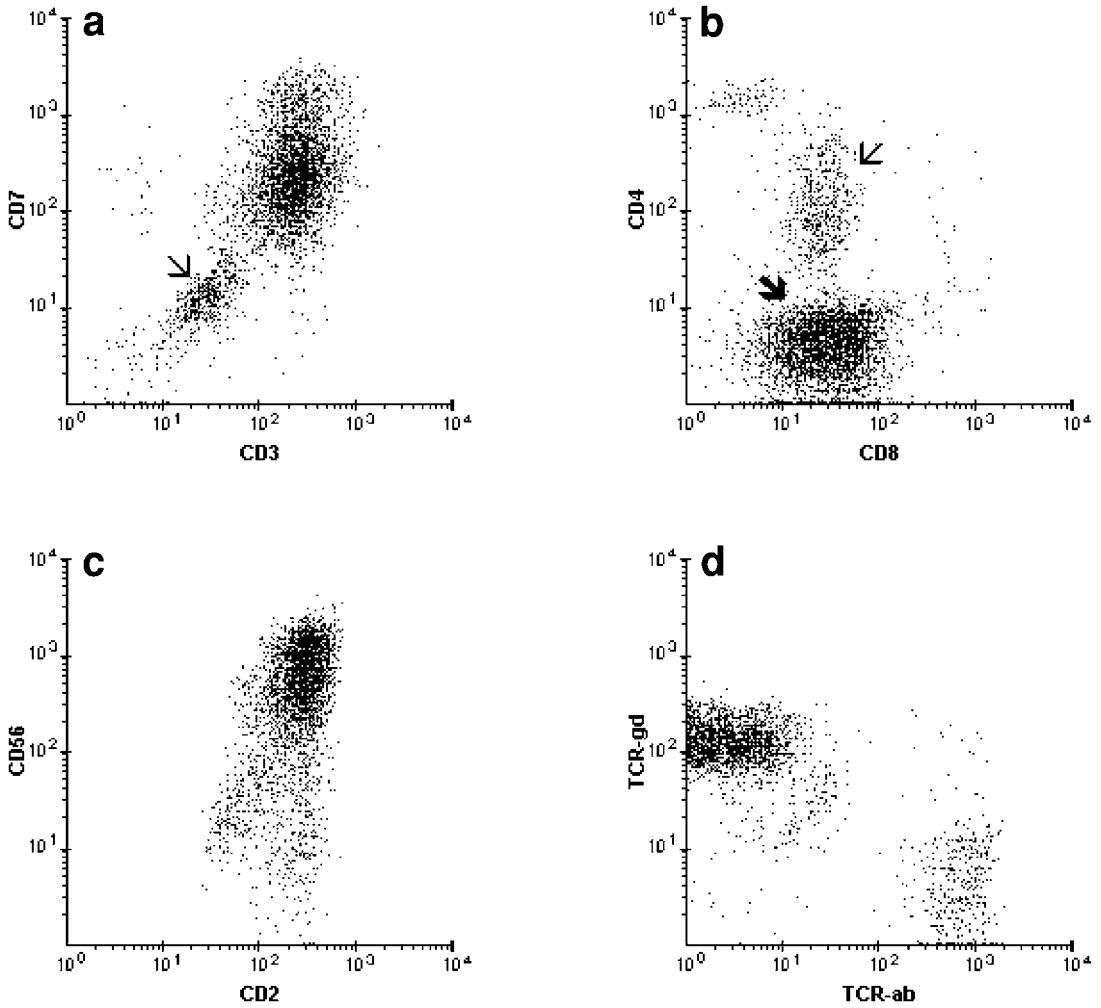

Figure 3.72 Bone marrow with γδ-T-cell lymphoma-leukemia (morphology shown in Plate 50). (a,b) The neoplastic cells (arrow) coexpress CD7 and CD3. CD4 is negative and CD8 is very dim. There is increased background fluorescence. Monocytes (thin arrow) are $CD4^+$ and $CD8^-$. (c,d) The tumor displays bright CD2, CD56, and TCR-γδ expression.

FCM dot plots may show an uninterpretable and disarrayed distribution. In many cases, the tumor cells can be recognized by their variable and extremely high FSC signals, along with CD56 expression. CD117 may also be present (Figure 3.73c).

Specimens harboring a proliferation of histiocytes/macrophages are very rarely encountered in the FCM laboratory. The graphical FCM data, when viewed in the context of myeloid/monocytic antigenic expression, can provide helpful clues for recognizing these unusual situations, including the following:

- A markedly high level of background fluorescence (Figure 3.74).
- The pattern of FSC, SSC, and CD45. On the SSC/CD45 dot plot, the histiocytic population occupies the position of monocytes, but with high SSC similar to that produced by granulocytes (Figures 3.74 and 3.75). The FSC signals are much higher than that of monocytes or granulocytes.
- CD1, when present, points toward the diagnosis of Langerhan's cell histiocytosis, also known as histiocytosis X (Figure 3.75).

Case study 33

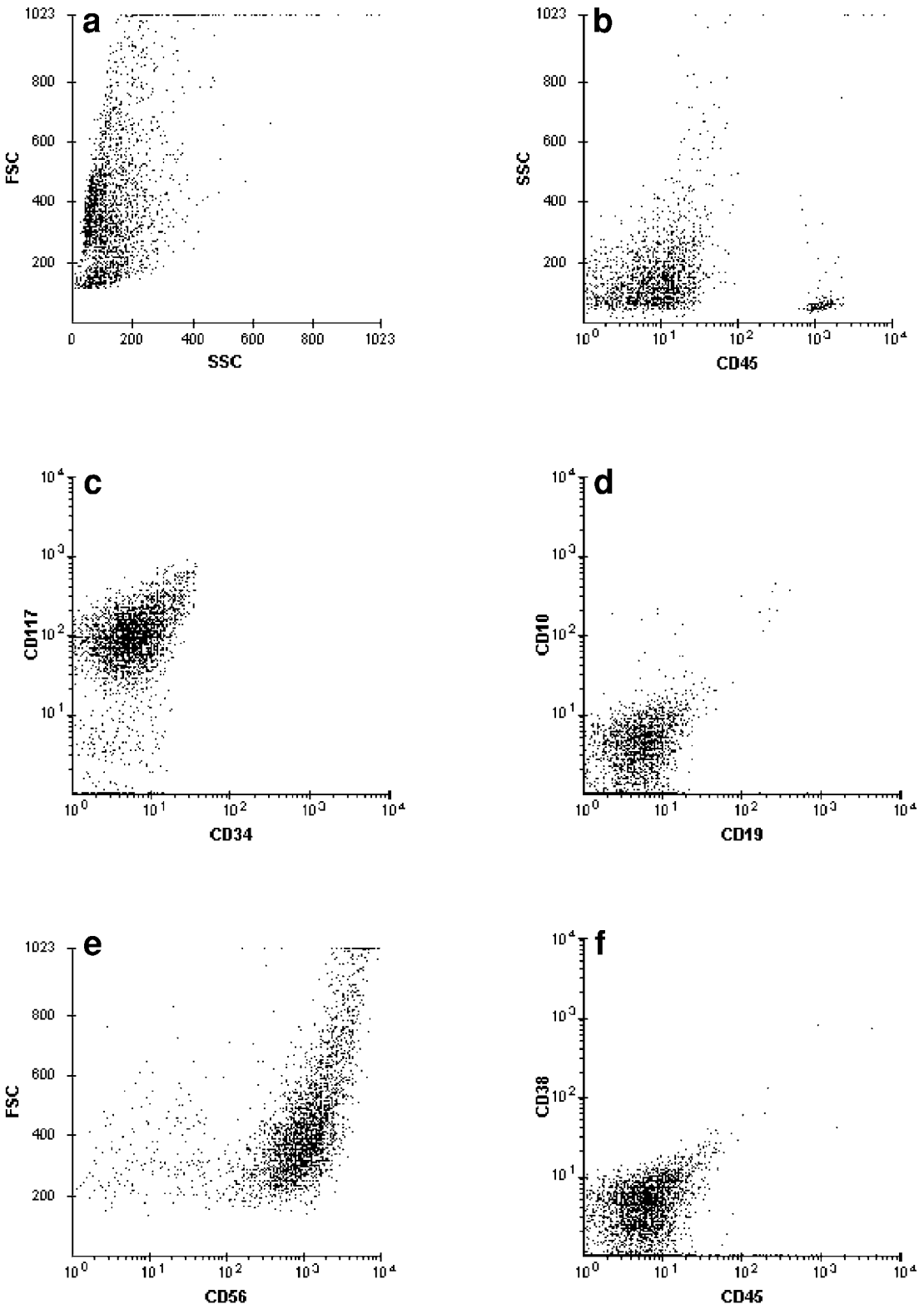

Figure 3.73 Bone marrow with small cell carcinoma. (a) Abnormal FSC/SSC picture. (b–f) The tumor cells form a prominent cluster in the CD45-negative region with variable FSC signals from low to high. CD10, CD19, and all of the remaining lymphoid and myeloid markers (not shown) are negative, except for CD117 and CD56.

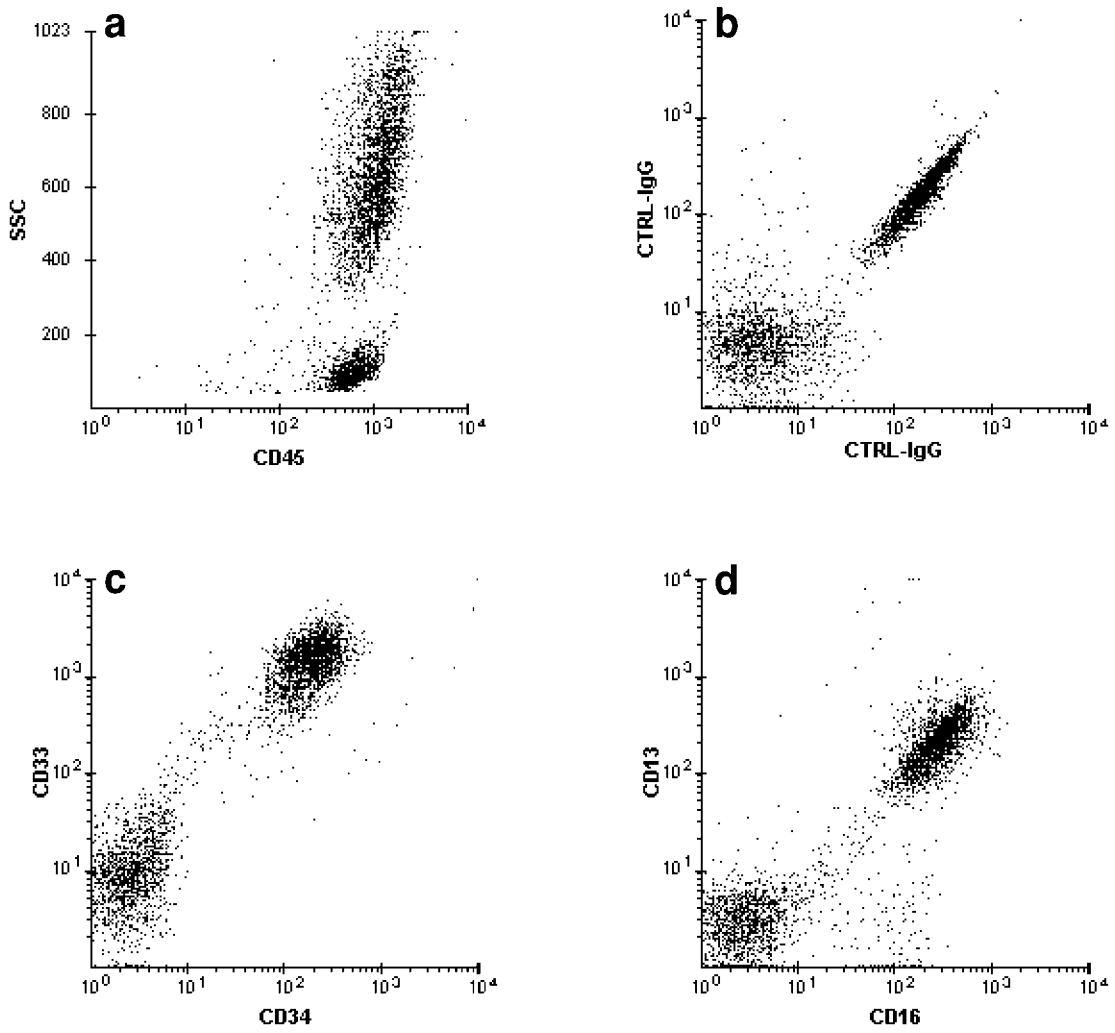

Figure 3.74 Macrophages in a "nadir" (postchemotherapy) bone marrow. (a) Only lymphocytes and a population with very high SSC located in the monocytic region. (b) Isotype-matched negative controls: High level of background fluorescence. (c,d) Only CD33 is expressed. CD34, CD13, CD16, and all of the remaining lymphoid and myeloid markers (not shown) are negative.

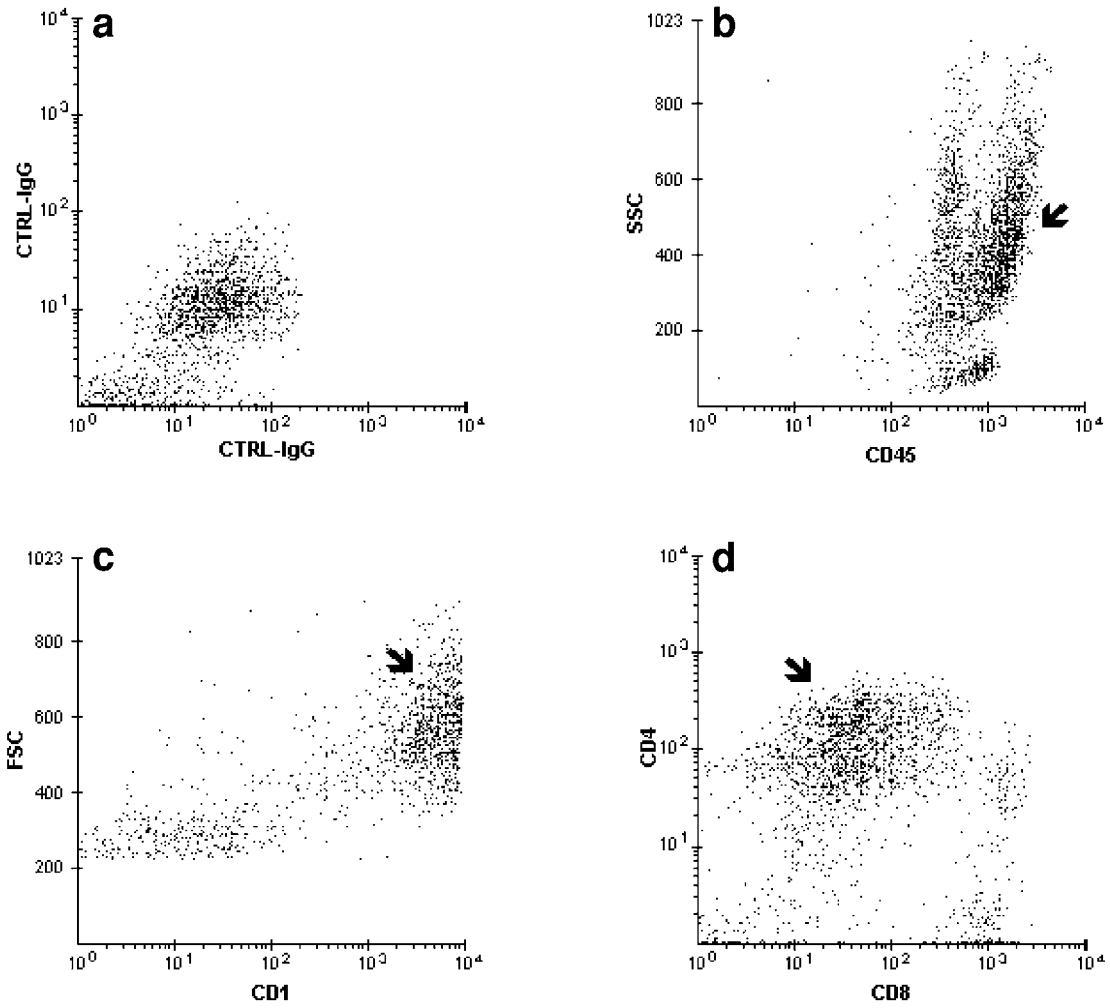

Figure 3.75 Langerhan's cell histiocytosis. (a) Isotype-matched negative controls: Slightly increased background fluorescence. (b) A monocytic-like cell cluster with high SSC (arrow). (c,d) The cells of interest display very intense CD1 expression. CD4 is positive and CD8 essentially negative.

Plates

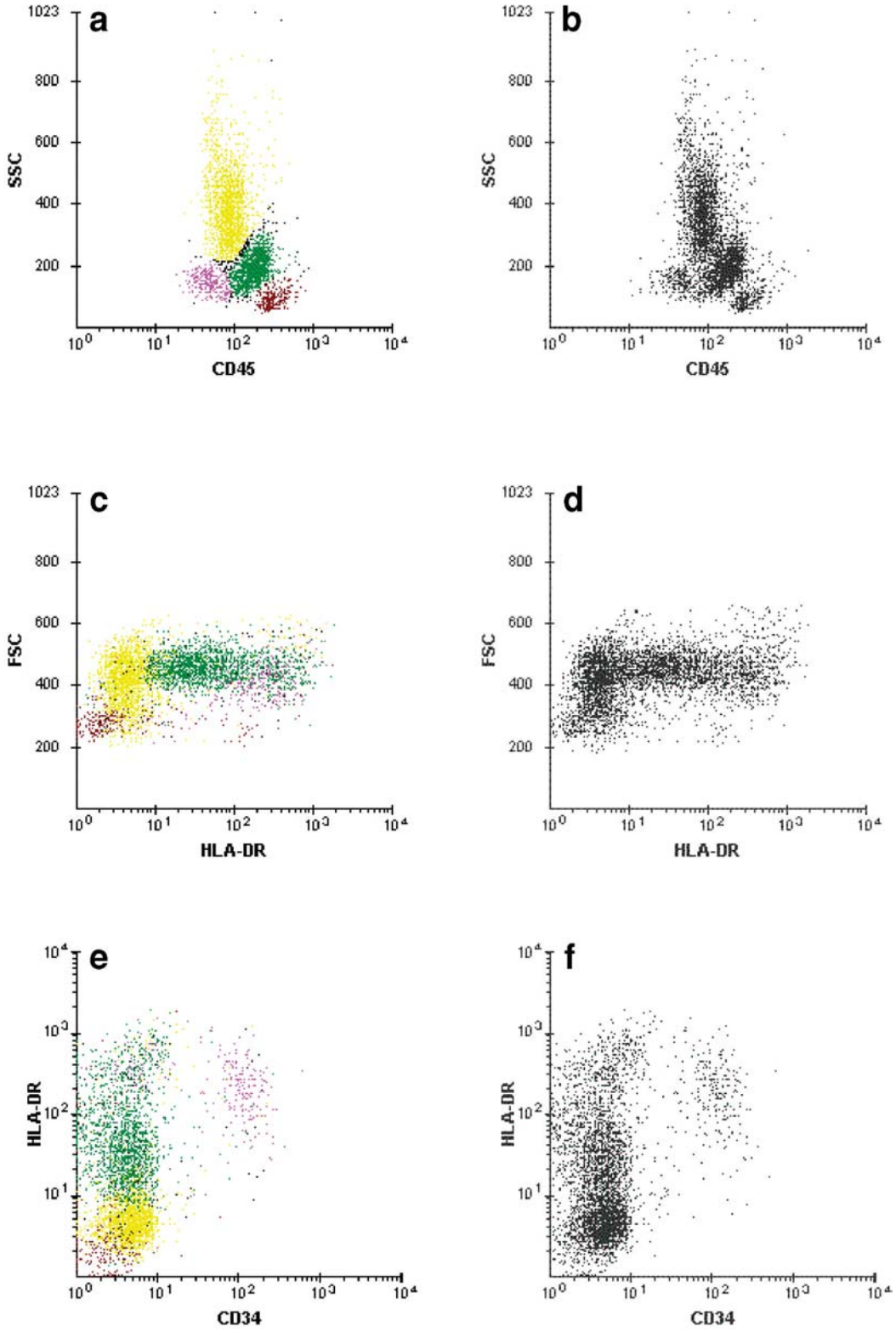

Plate 1 Peripheral blood with chronic myelomonocytic leukemia (CMMoL). (a,b) The various cell clusters can be well appreciated on either the black-and-white (B&W) or color display. Pink: blasts (4%); green: monocytes; yellow: granulocytes; brown: lymphocytes. The HLA-DR$^+$ population (d) is actually composed of the blast and monocytic populations (c). Lymphocytes, granulocytes, and monocytes on the color display (e) appear as one continuous population on the B&W dot plot (f).

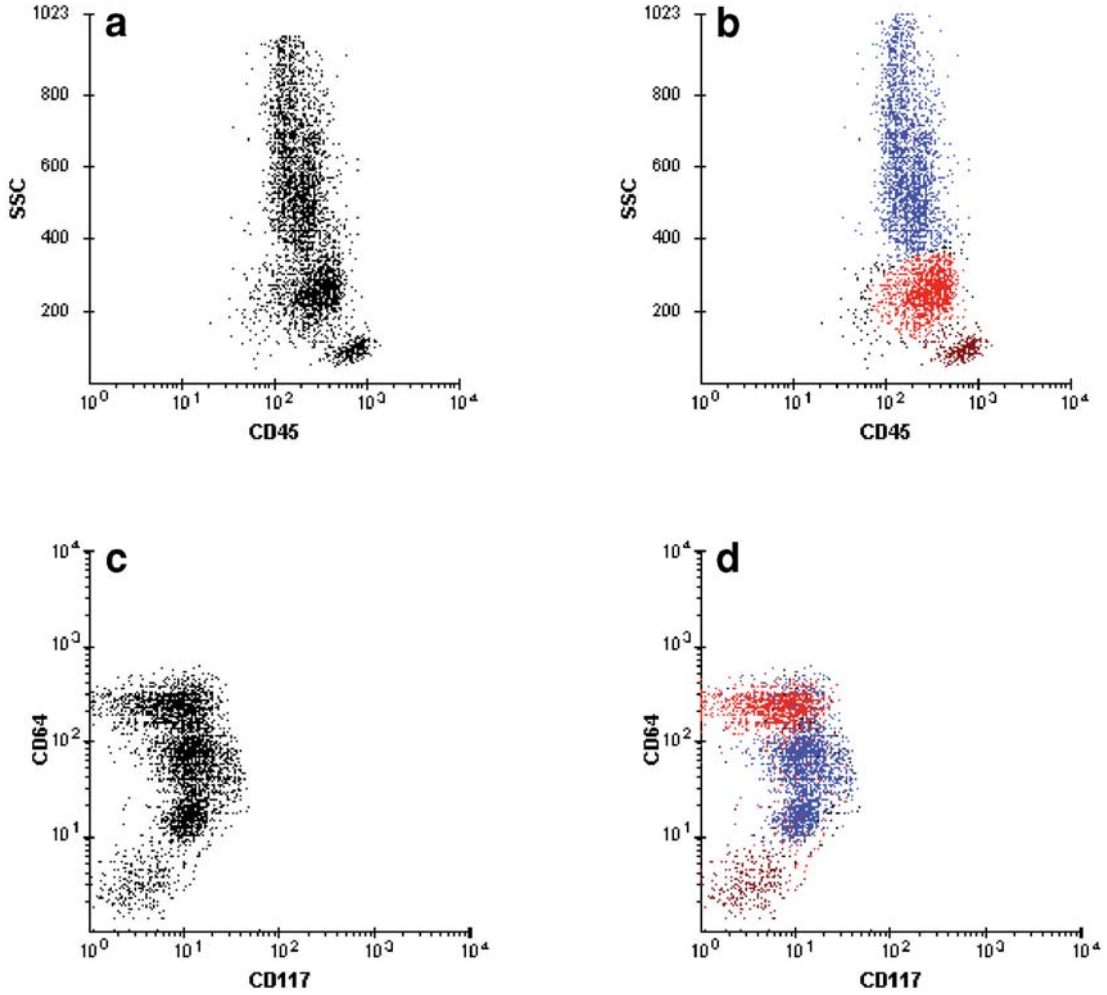

Plate 2 Bone marrow with CMMoL. (a,b) Monocytes (red), granulocytes (blue), and lymphocytes (brown) can be well appreciated on either the color or B&W display. (c,d) The granulocytes, because of the bimodal reactivity for CD64, may be mistaken as two different populations on the B&W display.

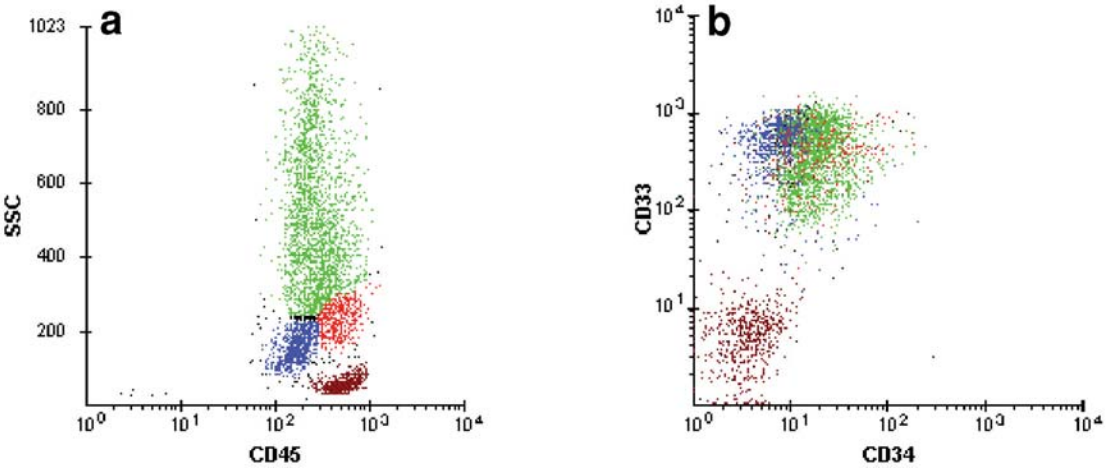

Plate 3 Limitation due to color hierarchy. (a) Bone marrow with AML; in descending hierarchy, the colors are blue (blasts), green (granulocytes), red (monocytes), and brown (lymphocytes). (b) Very few of the red dots are seen through the green cluster.

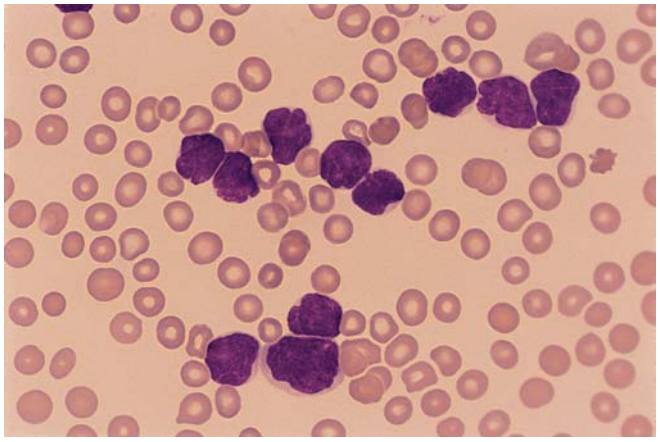

Plate 4 Circulating blasts with scant cytoplasm in precursor B-ALL. The cytology (small cell size and condensed chromatin) in this case mimics that of a mature lymphoid malignancy.

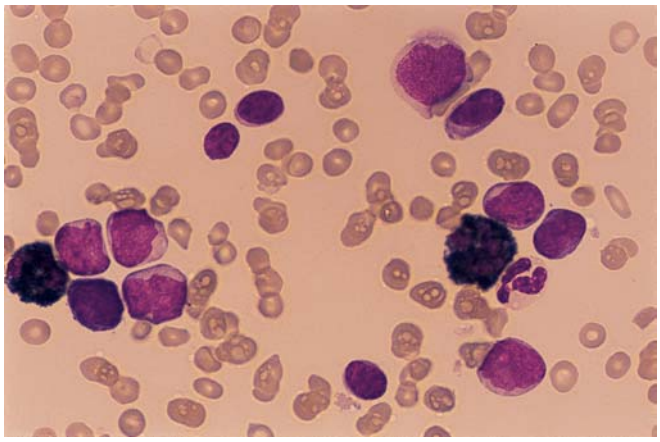

Plate 5 Myeloperoxidase cytochemistry (MPO cyto) in AML-M0. Blasts and a small number of hypogranular neutrophils are negative for MPO cyto. Staining is present in most neutrophils.

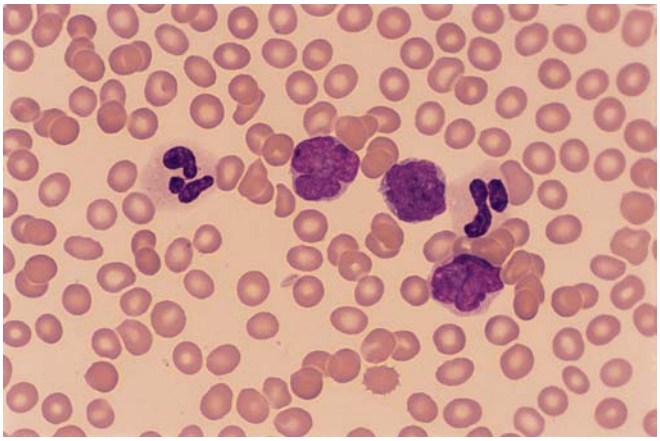

Plate 6 Agranular AML-M3v. The cytology (lack of granules, scant cytoplasm, coarse chromatin) in this case simulates that of circulating large lymphoma cells.

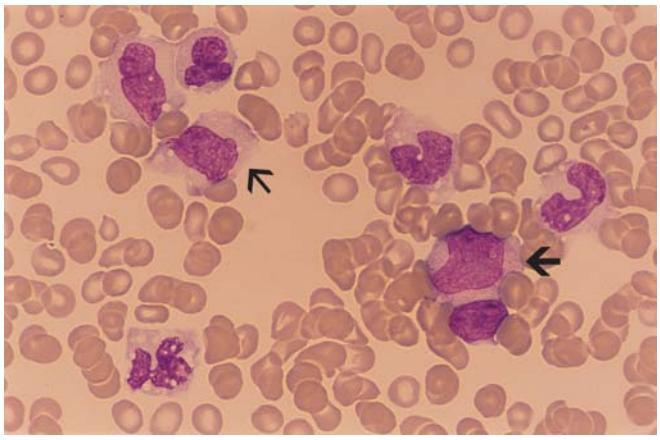

Plate 7 AML with monocytic differentiation, showing a spectrum of blasts (arrow), promonocytes (thin arrow), and monocytes in the blood.

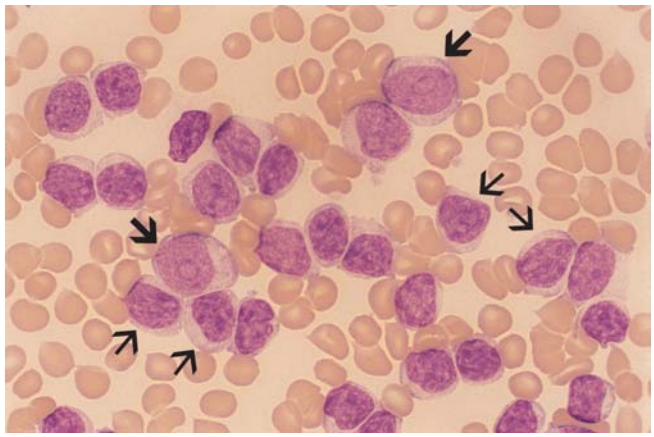

Plate 8 Activated CLL with increased prolymphocytes (arrow) and plasmacytoid lymphocytes (thin arrow) (i.e., CLL/PL by current morphologic criteria). The nucleolus is smaller and the chromatin is coarser in plasmacytoid lymphocytes than in prolymphocytes.

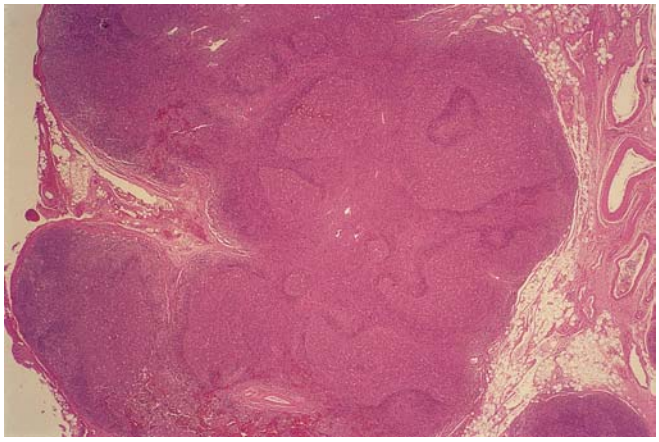

Plate 9 Florid reactive follicular hyperplasia.

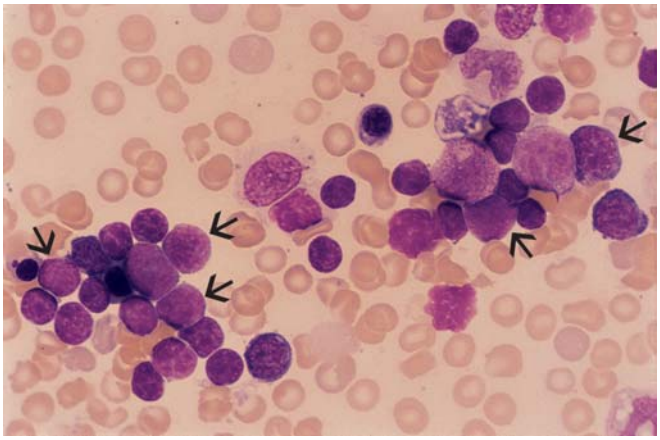

Plate 10 Hematogones (arrow) following bone marrow transplant for ALL.

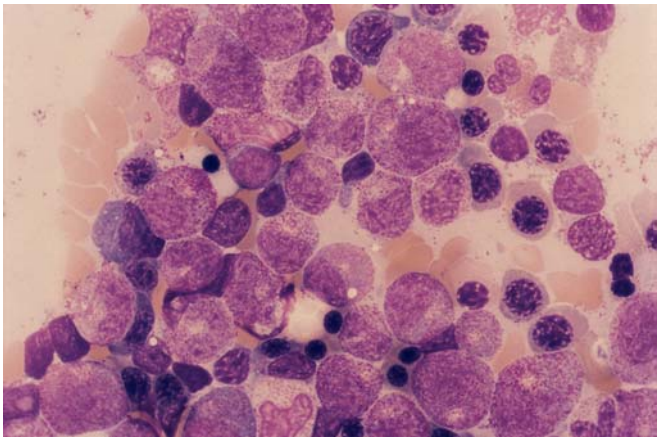

Plate 13 Intense granulation in myeloid precursors secondary to G-CSF therapy.

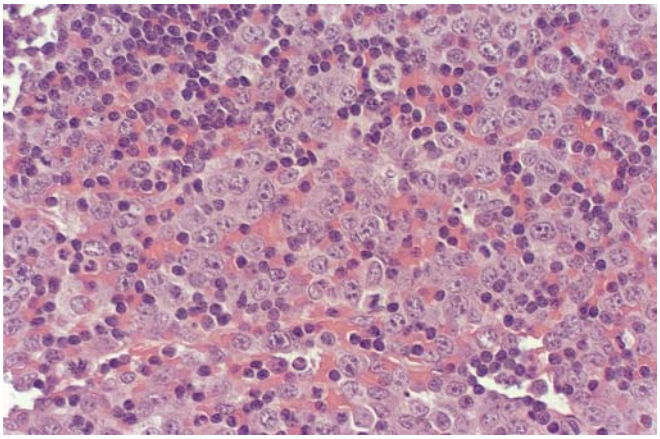

Plate 11 EBV viral lymphadenitis. Sheets of transformed cells, mimicking the picture of large-cell lymphoma.

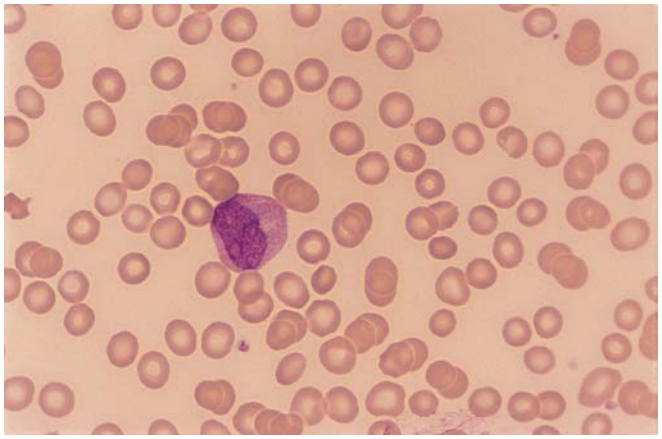

Plate 14 T-ALL. Circulating blast with conspicuous azurophilic granules.

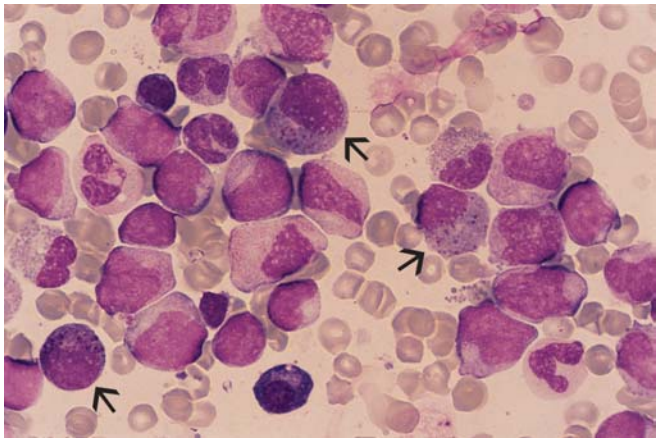

Plate 12 AML-M4E. Basophilic granules present in abnormal eosinophilic precursors (arrow).

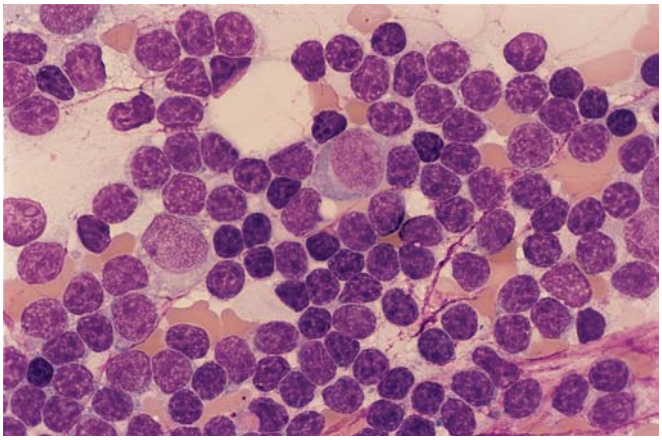

Plate 15 Precursor B-cell ALL. The blasts in this case are cytologically indistinguishable from CLL cells.

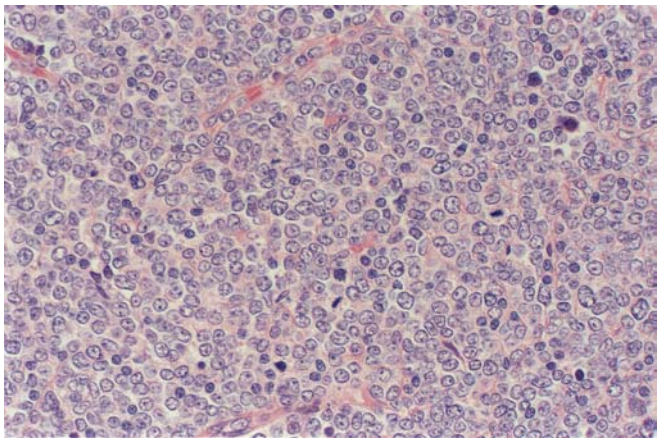

Plate 16 Nodal involvement by AML, morphologically simulating large cell lymphoma.

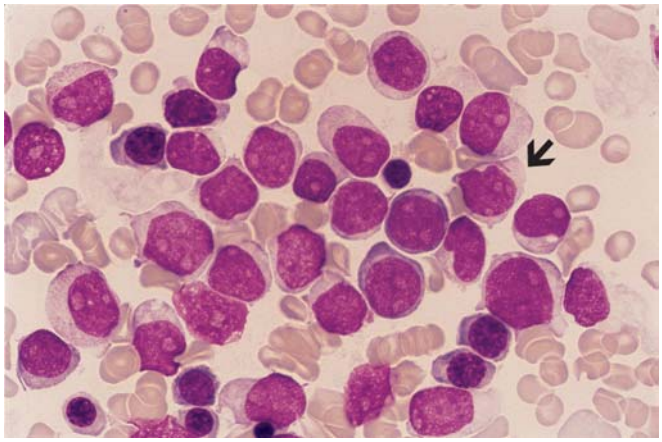

Plate 19 Blast with Auer rod (arrow) in AML-M1.

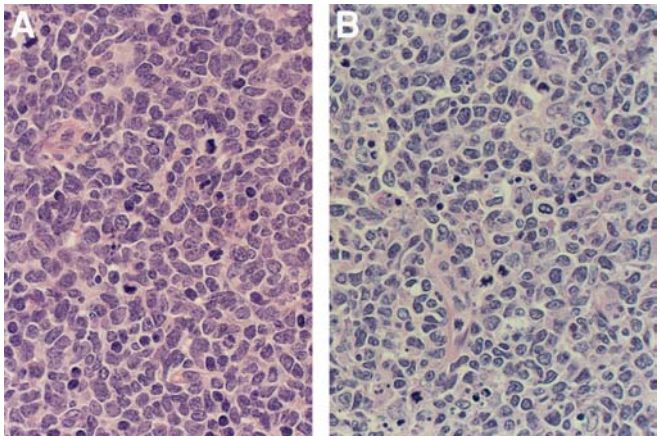

Plate 17 Lymphoblastic lymphoma (A) and "blastic" MCL (B), showing similarities in cell size, nuclear chromatin, and mitotic activity. Increased apoptotic figures in (B).

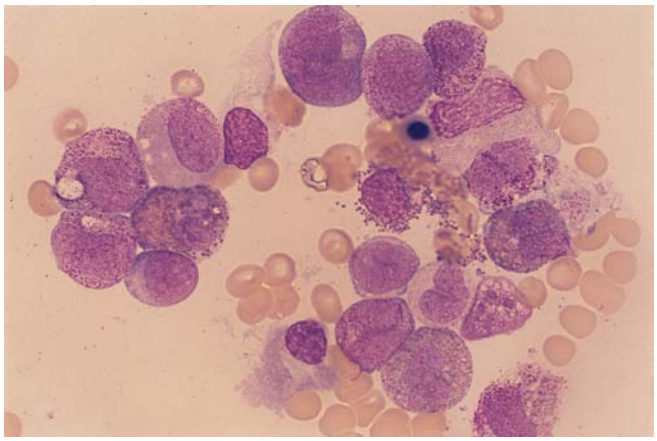

Plate 20 AML-M2Eo. Normal-appearing eosinophilic precursors.

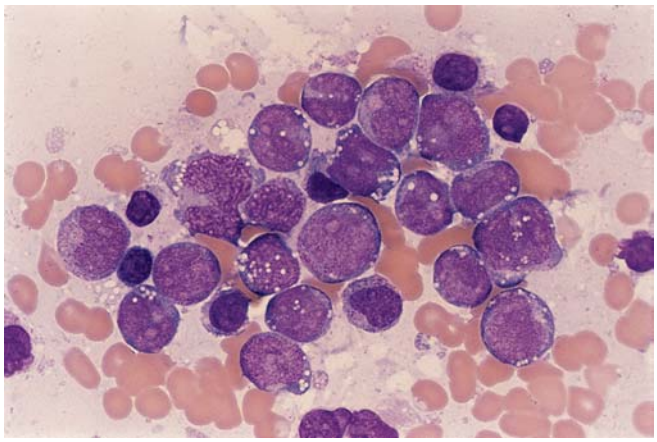

Plate 18 Agranular M3v. Blasts with vacuolated cytoplasm and a few azurophilic granules, cytologically similar to blasts in AML with monocytic differentiation.

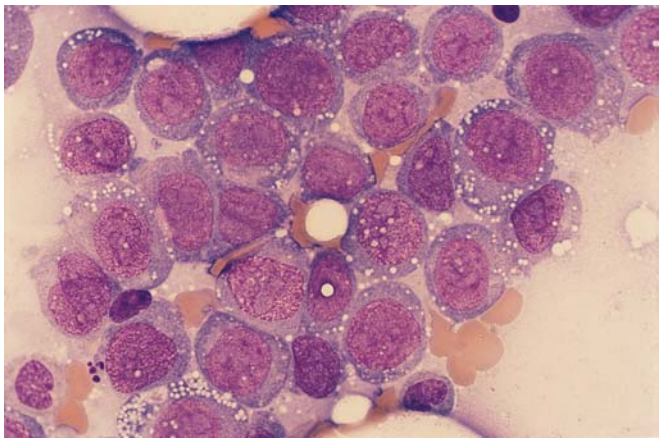

Plate 21 Blasts with vacuolated cytoplasm in AML with monocytic differentiation (*see* Figure 3.37), classified as FAB M5a.

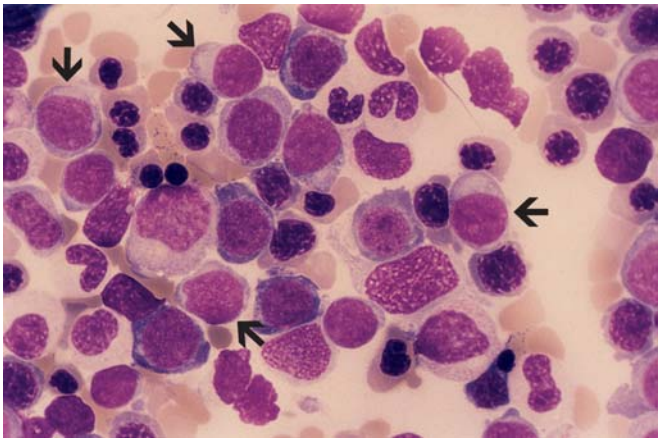

Plate 22 AML-M6. Blasts (arrow) and abundant erythroid precursors. Hypogranular granulocytes and basophilic stippling present.

Plate 23 Hypoplastic MDS, morphologically similar to aplastic anemia. The combination of 7% blasts by FCM analysis and the cytogenetic abnormality of 7q– support the diagnosis of MDS.

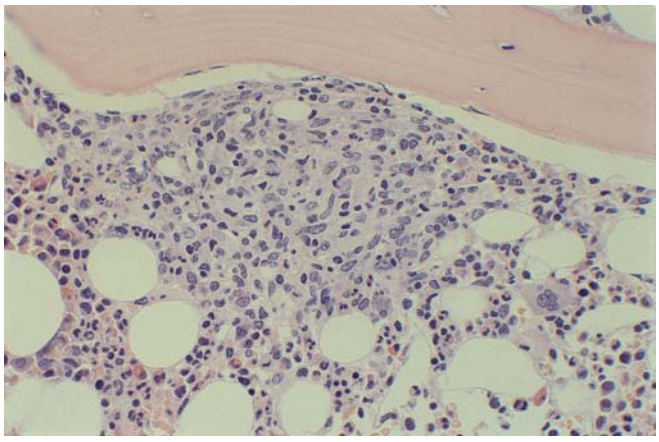

Plate 24 Paratrabecular infiltration by PTCL.

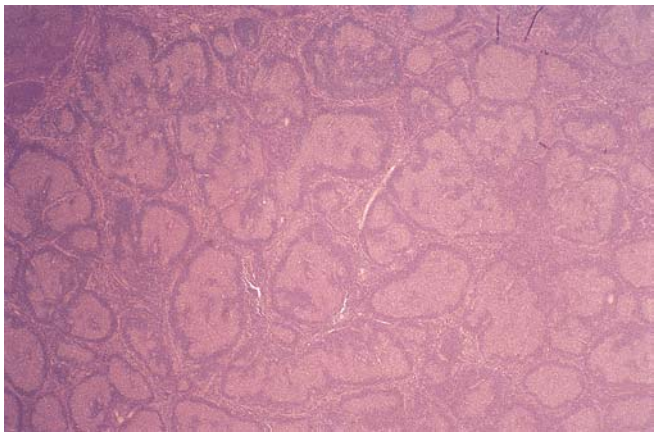

Plate 25 Follicular lymphoma with a so-called floral pattern at low-power magnification.

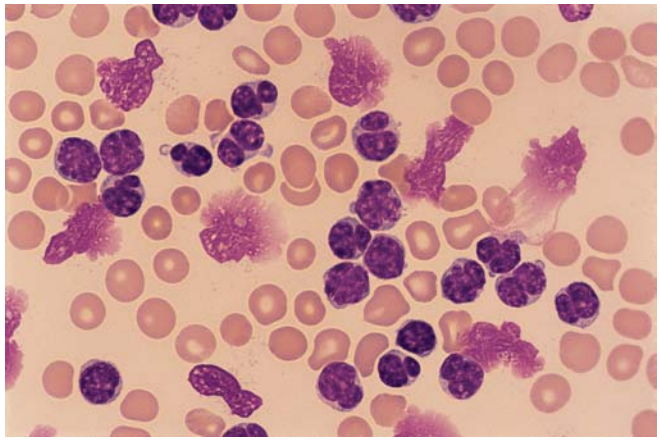

Plate 26 Storage-induced nuclear irregularities in CLL, simulating the blood picture of FCC or mantle cell lymphoma in leukemic phase.

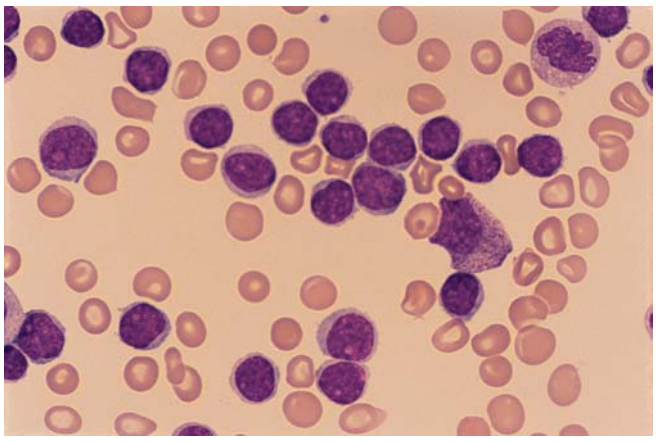

Plate 27 Fresh blood smear from the same specimen as Plate 26. A few activated lymphoid cells with a small distinct nucleolus are present.

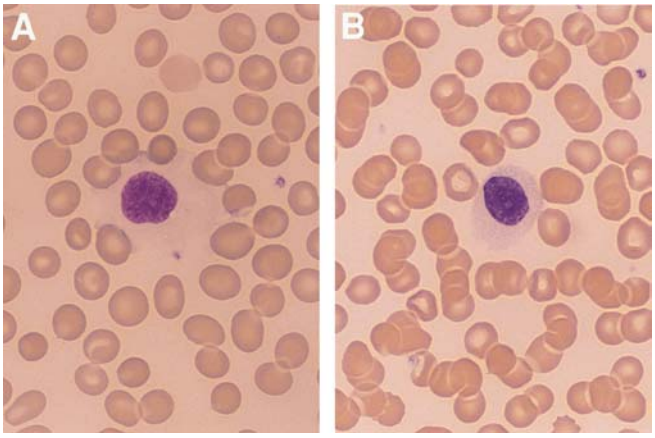

Plate 28 (A) Hairy cell with abundant pale cytoplasm and bland appearing nucleus. (B) In the thicker areas of the smear (which dry more slowly), the cell shrinks and appears smaller with more condensed chromatin.

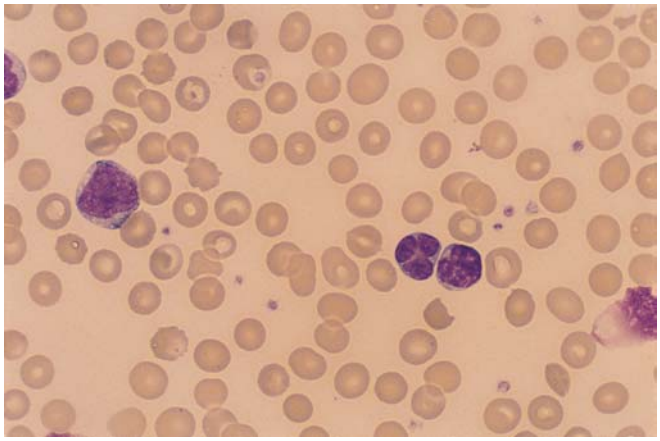

Plate 29 An occasional clefted lymphoid cell in a case of CLL/PL (under chemotherapy) protracted to multiple therapeutic regimens.

Plate 30 SLL with increased and confluent pseudofollicles.

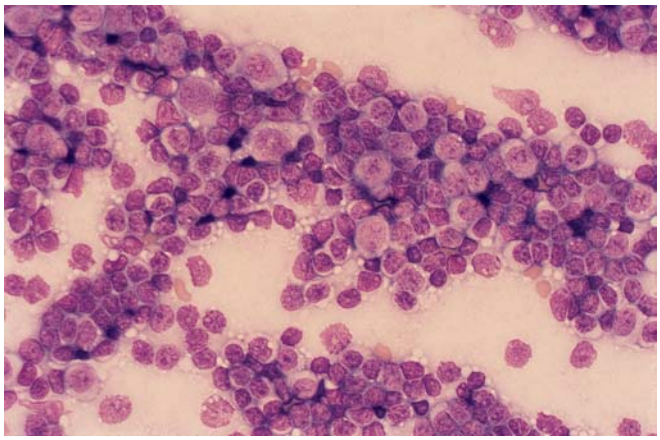

Plate 31 Imprint from the same specimen as Plate 30. A mixture of small lymphocytes, plasmacytoid lymphocytes, and prolymphocytes. The same picture in the blood is known as CLL/PL.

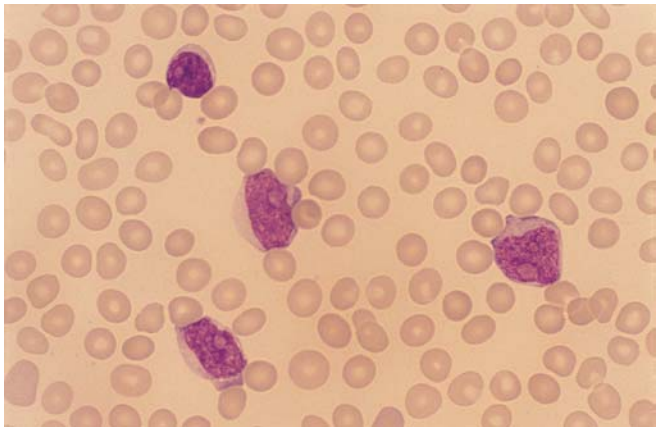

Plate 32 B-PLL (*see* Figure 3.56). To untrained eyes, the neoplastic cells may be confused with leukemic blasts.

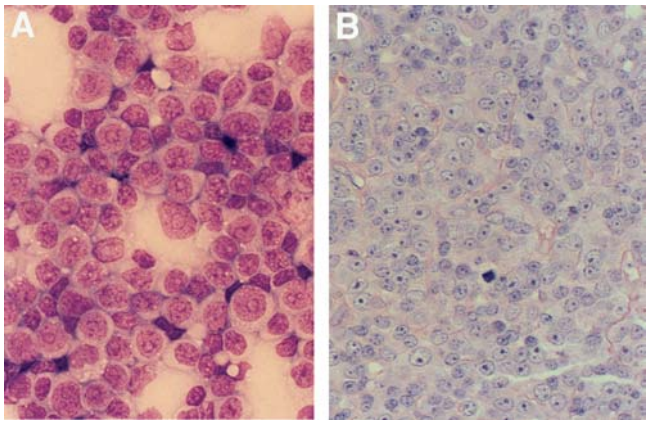

Plate 33 Nodal involvement by B-PLL from the same patient as Plate 32. H&E section and imprint showing sheets of transformed cells consistent with prolymphocytes.

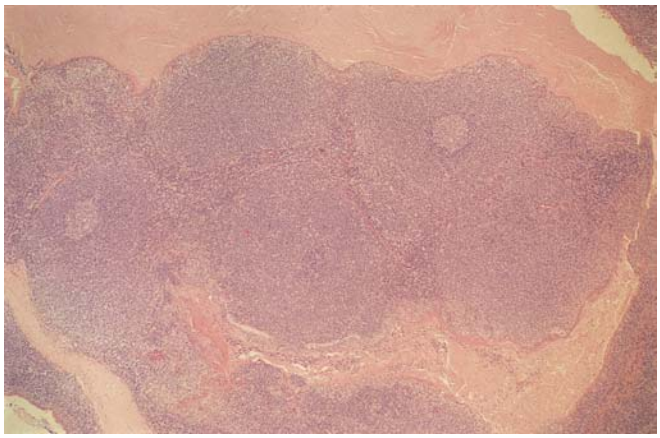

Plate 34 Mantle cell lymphoma. Nodular pattern with small residual germinal centers present.

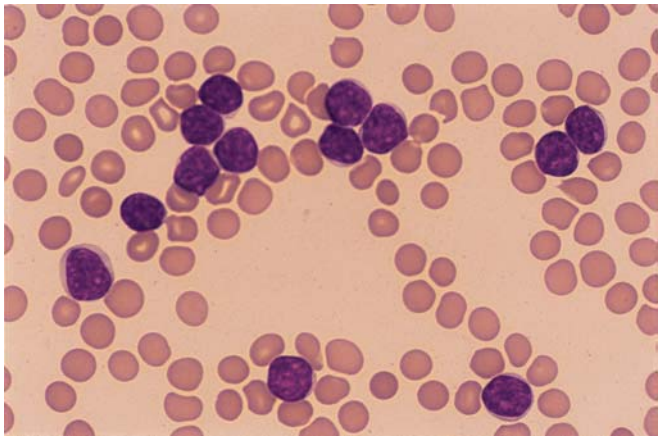

Plate 35 MCL in leukemic phase (*see* Figure 3.47). The neoplastic cells in this case are bland appearing with round nuclei, similar to CLL cells.

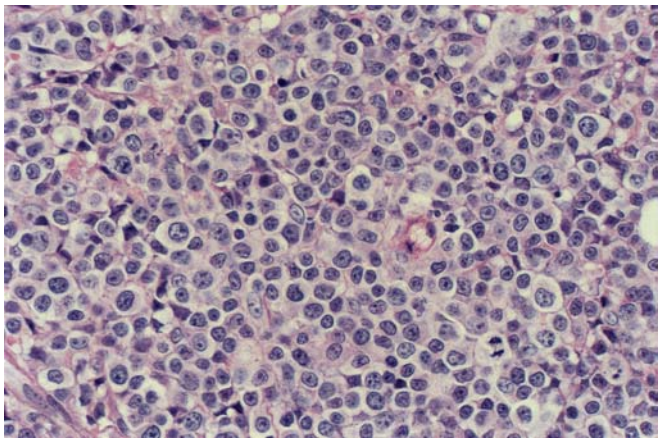

Plate 36 $CD5^+$ large cell lymphoma. The tumor cells display a plasmablastic appearance.

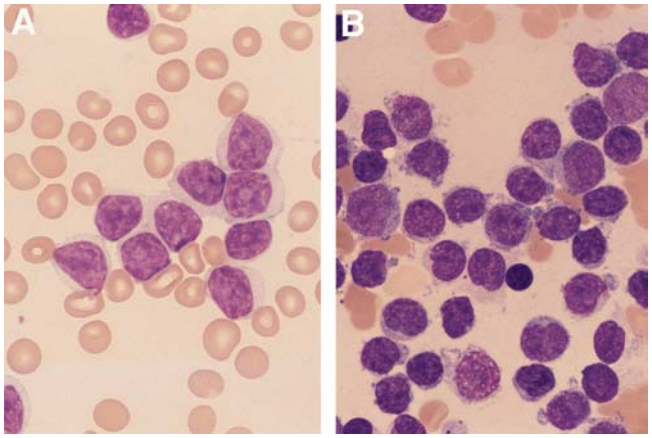

Plate 37 LPC lymphoma–leukemia. The cytology is better appreciated on the blood film (A) than on the bone marrow smear (B), where slow drying has resulted in hairs and blebs and a smaller cell size.

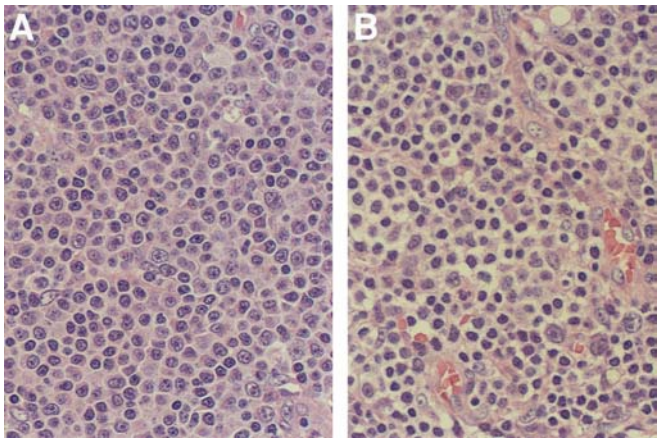

Plate 38 LPC lymphoma–leukemia. Optimal section (A); suboptimal section (B) with clearing artifacts often misinterpreted as clear pale cytoplasm.

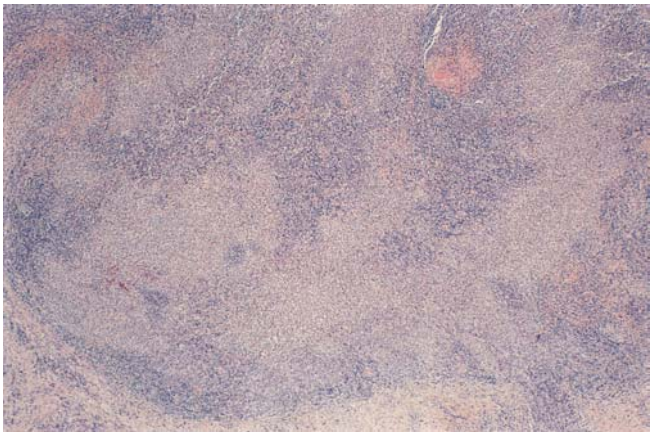

Plate 39 MBCL. Interfollicular infiltration by large irregular clusters of pale cells.

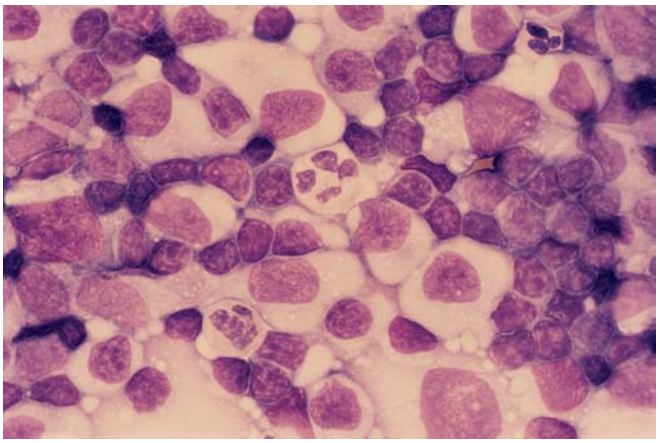

Plate 40 Imprint from the same specimen as Plate 39. Neoplastic cells showing a hairy-cell-like cytology (abundant pale cytoplasm, bland reticulated chromatin). Neutrophils are commonly associated with monocytoid B-cells.

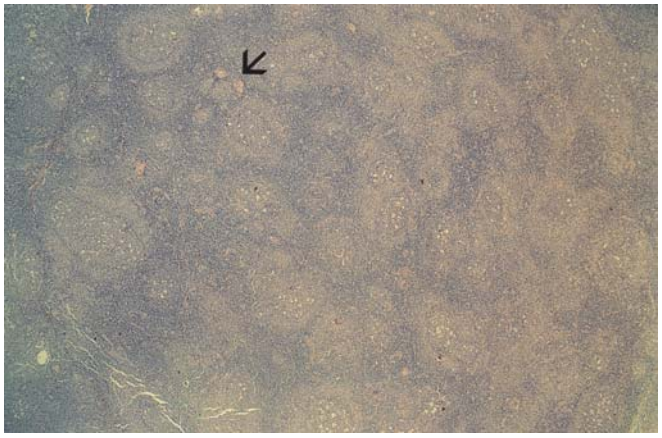

Plate 41 Marginal zone pattern in SLL. The pale rings around residual reactive follicles are composed of loosely packed prolymphocytes and plasmacytoid lymphocytes. Occasional typical pseudofollicles (arrow) are also present.

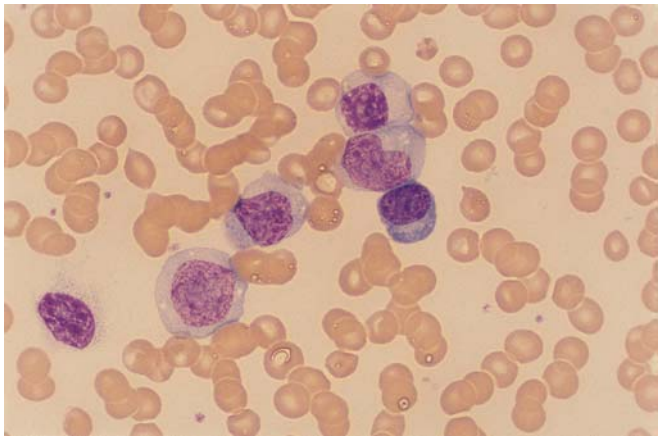

Plate 42 Plasma cell leukemia. Predominantly immature-appearing plasma cells.

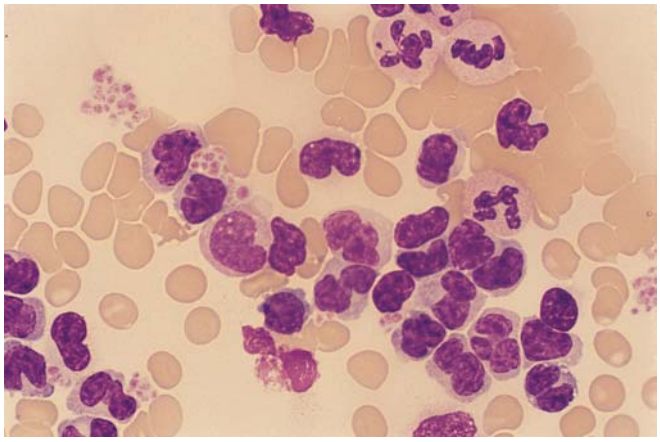

Plate 43 ATLL. Leukocytosis composed of lymphoid cells with marked nuclear irregularities.

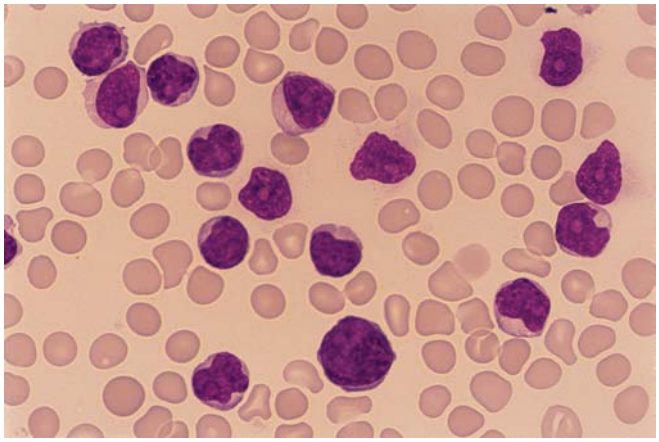

Plate 44 T-PLL. The tumor cells display a small distinct nucleolus and are smaller than those in B-PLL.

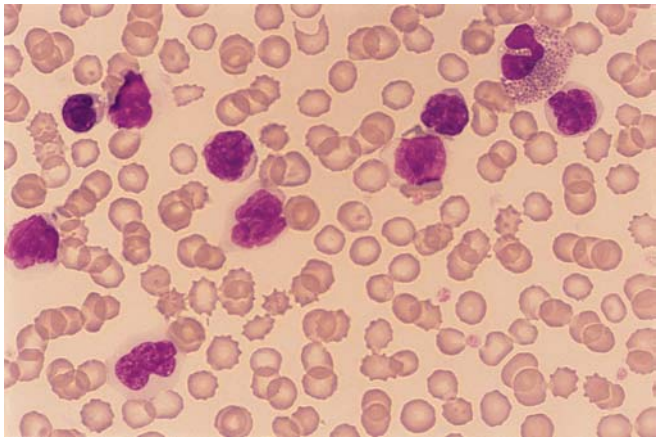

Plate 45 Advanced stage of Sezary syndrome, with abundant circulating tumor cells. The blood picture closely mimics ATLL. The patient has had a splenectomy.

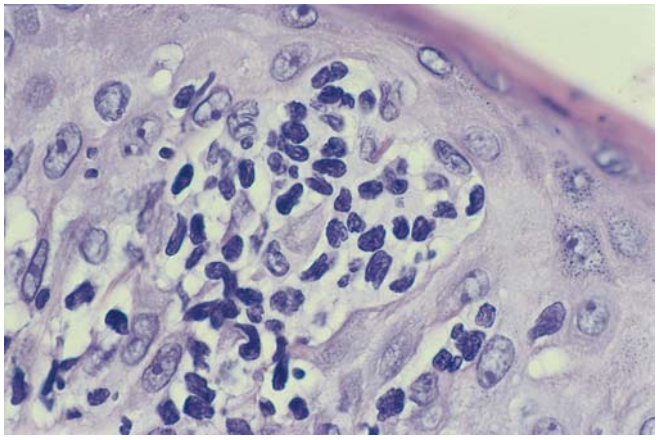

Plate 46 Earlier skin biopsy on the same patient as Plate 45. The epidermis is infiltrated by collections of neoplastic lymphoid cells (Pautrier's abscess).

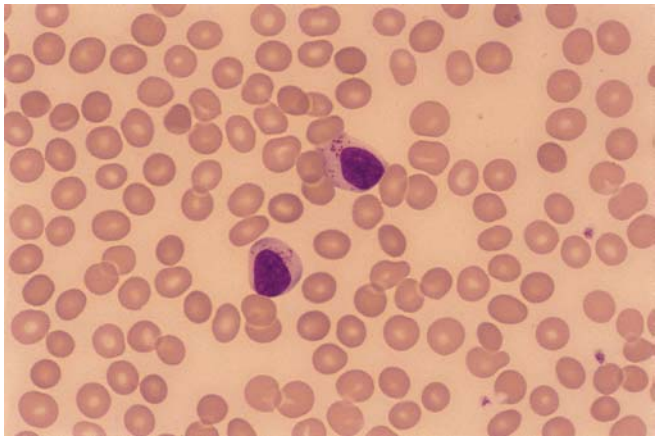

Plate 47 Indolent LGL leukemia (NK-like T-cell phenotype) with bland-appearing neoplastic large granular lymphocytes.

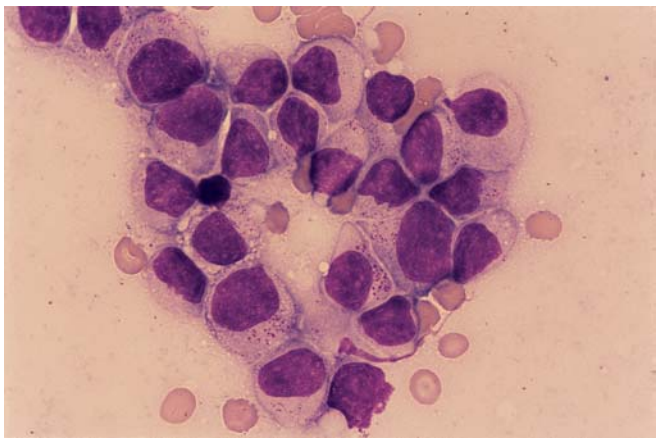

Plate 48 Aggressive NK lymphoma. Neoplastic cells with abundant azurophilic granules.

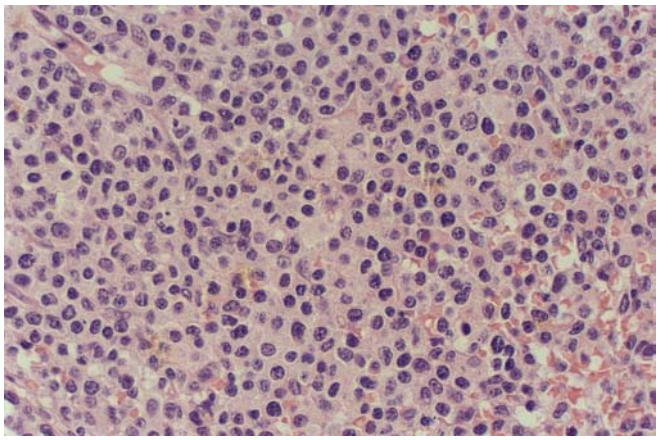

Plate 49 H&E section from the same specimen as Plate 48. Neoplastic cells with ample pale cytoplasm.

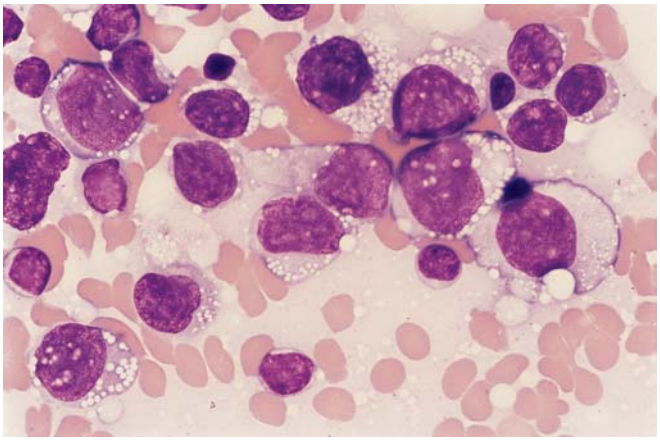

Plate 50 Bone marrow involved by γδ-T-cell lymphoma–leukemia. The cytology mimics that of AML with monocytic differentiation.

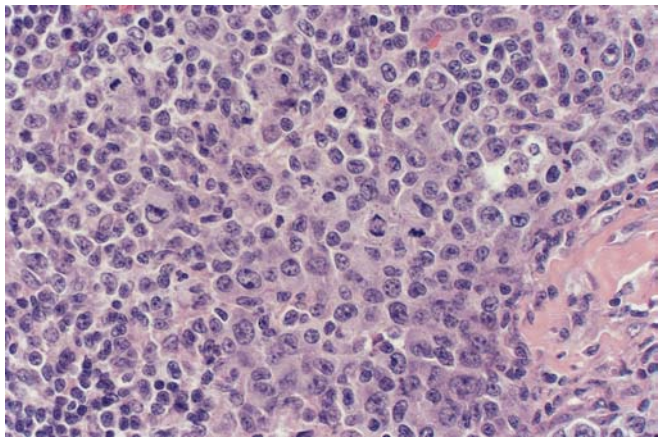

Plate 51 $CD30^+$ lymphoma. The tumor population is relatively monotonous. ALK-1 is expressed.

CHAPTER

4 FCM data analysis on heterogeneous specimens

Most clinical specimens, whether normal/reactive or harboring neoplastic cells, are heterogeneous. The highest degree of heterogeneity is seen in bone marrow samples. Solid lymphoid tissues such as tonsils and lymph nodes are less heterogeneous because the granulocyte/monocyte component is usually insignificant. The benign nonpurulent effusion, when not overloaded with a large number of macrophages or mesothelial cells, is the least complicated type of specimen consisting of B- and T-cells in a similar proportion to that seen in the blood. The FCM 2D projections in heterogeneous samples are inherently complex, displaying multiple clusters, some of which may be overlapping. The task in analyzing these dot plots is twofold: first, to determine whether the sample is benign/reactive or contains a neoplastic population (which may or may not be evident at first glance) and, second, to characterize the tumor cells, if present. In some malignant conditions such as myelodysplastic syndrome (MDS), CML, or CMMoL, an overt neoplastic cluster (i.e., increased blasts) may not be present. The FCM graphics often demonstrate several features useful for recognizing these disorders however, such as an altered proportion of the granulocytic or monocytic component and qualitative antigenic abnormalities on the myeloid (e.g., altered maturation curves), monocytic, or erythroid elements.

The visual FCM data can become highly complex if the specimen harbors more than one malignant process (e.g., high-grade MDS and multiple myeloma [MM], or CLL and HCL). In order not to overlook potentially subtle abnormalities, it is necessary to be familiar with the appearance of the various cell clusters (shape, size, density, relative position) on certain key dot plots in different types of normal or benign reactive specimens.

Visual FCM data analysis in heterogeneous samples follows a similar sequence to that applied to the nearly homogeneous specimens (*see* Chapter 3). Depending on the type of specimen, it begins with either the SSC/CD45 dot plot for blood or bone marrow (BBS panel) or the FSC/SSC dot plot for solid tissue or body fluids (TF panel). For blood and bone marrow samples, data analysis also includes an evaluation of the maturing granulocytes (granularity and antigenic maturation) or other elements (e.g., B-cells, erythroid precursors) in addition to identifying any neoplastic population present.

4.1 Identifying normal FCM samples

A normal FCM sample is one in which no detectable clonal/neoplastic proliferation exists as determined by the light scatter and fluorescence parameters.

4.1.1 Benign/reactive solid lymphoid tissue (e.g., lymph nodes, tonsils)

In general, the FCM dot plots derived from reactive lymph nodes display findings similar from case to case, irrespective of the specific morphologic subtype of the reactive process. Polyclonality and the absence of phenotypic aberrancies characterize a benign sample. It is important to be aware, however, that the absence of abnormalities by FCM analysis does not necessarily exclude the existence of lymphoma (or other tumors that may not be recovered in the cell suspension). If the lymphomatous involvement is focal, either sampling error or selec-

tive loss of neoplastic cells (especially when present in low numbers) during tissue preparation can easily result in a false picture of "negative" dot plots. Furthermore, lymph nodes involved by Hodgkin's disease also yield "negative" FCM data because the malignant cells are usually not present in the final cell yield. In Hodgkin's disease, the composition of the background lymphocytes and their expression of lymphoid surface antigens are indistinguishable from that seen in reactive lymph nodes.

In benign/reactive lymph nodes, the relative proportion of mature B- and T-cells varies widely from case to case. On the FSC/SSC or FSC/CD45 dot plots, both B- and T-cell populations are merged into a single cluster of variable cell size (Figure 4.1a,b). On the dot plots showing reactivity to B- and T-cell antibodies, the B- and T-cell clusters are well segregated based on the clear-cut expression of their respective lineage markers (Figures 4.1 and 4.2). The expression of HLA-DR (Figure 4.2f) and/or CD38 (Figure 4.1e) reflects evidence of activation in a proportion of lymphocytes. CD25 expression may be present on a small number of reactive T-cells (Figure 4.2b).

A ratio of helper to suppressor T-cells can be derived from the CD4/CD8 dot plot (Figure 4.2b). In the lymph node, this ratio can be higher than that in the peripheral blood, and may occasionally exceed 10**;**1 (Figure 4.3). CD103 (B-ly7) can be detected in a subset of T-cells (Figure 4.2c) of the suppressor family.

Polyclonality in B-cells can be best appreciated from a side-by-side evaluation of the kappa/CD20 and lambda/CD20 dot plots, displaying the normal bimodal distribution of kappa and lambda (Figure 4.4). The bimodal distribution is most evident as a "double camel hump" (Figure 4.4b) seen on the corresponding single parameter histograms for kappa and lambda when gated on B-cells. In patients with marked polyclonal hypergammaglobulinemia, immunoglobulin coating of B-cells may obscure the normal bimodal distribution and produce a broad distribution with a single peak instead.

A small number of benign B-cells positive for CD5 (with a weaker intensity than that on T-cells) may be seen in some reactive lymphadenopathies (Figure 4.5). A more frequent finding is the expression of CD10 in a subset of reactive B-cells. The corresponding lymph node sections invariably demonstrate follicular hyperplasia (Plate 9). These CD10-positive reactive B-cells are larger and display the brightest CD20 intensity (Figure 4.6a). They correspond to the activated larger germinal center cells. In marked FRFH, the increased number of these cells is seen as a sizable cluster with coexpression of CD10, intense CD38, and CD20. This may lead to potential confusion with FCC lymphoma, especially because the larger cells in most cases of FRFH lack surface light-chain expression (Figures 4.6 and 4.7d) similar to that seen in a substantial number of FCC lymphomas (*see* Section 3.6.3.1, Figure 3.44). Characteristically, germinal center cells do not contain intracellular bcl-2 protein, however.

4.1.1.1 Pattern of CD10/CD20 coexpression. Distinction between FRFH and FCC lymphoma

Close evaluation of the CD10/CD20 dot plot will reveal the subtle differences between FRFH and the majority of FCC lymphomas (Figures 3.44, 3.49, and 3.50). In this regard, the choice of fluorochromes (*see* Section 2.6.2) to be conjugated with CD10 and CD20 are important in bringing out these differences. The reactivities to CD20 and CD10 by the various lymphoid cell populations in FRFH produce a pattern reminiscent of a "horizontal hockey stick" whereby the cluster of reactive B-cells with coexpression of CD10 and CD20 is the foot of the "hockey stick" (Figures 4.6 and 4.8). The "horizontal hockey stick" is formed by several closely adjoined cell clusters (i.e., T-cells, B-cells with and without CD10 expression). In contrast, the neoplastic cell cluster in FCC lymphoma is well separated from the other lymphoid cell populations (Figures 3.44b, 3.49d, and 3.50) and the intensity of CD10 on malignant fol-

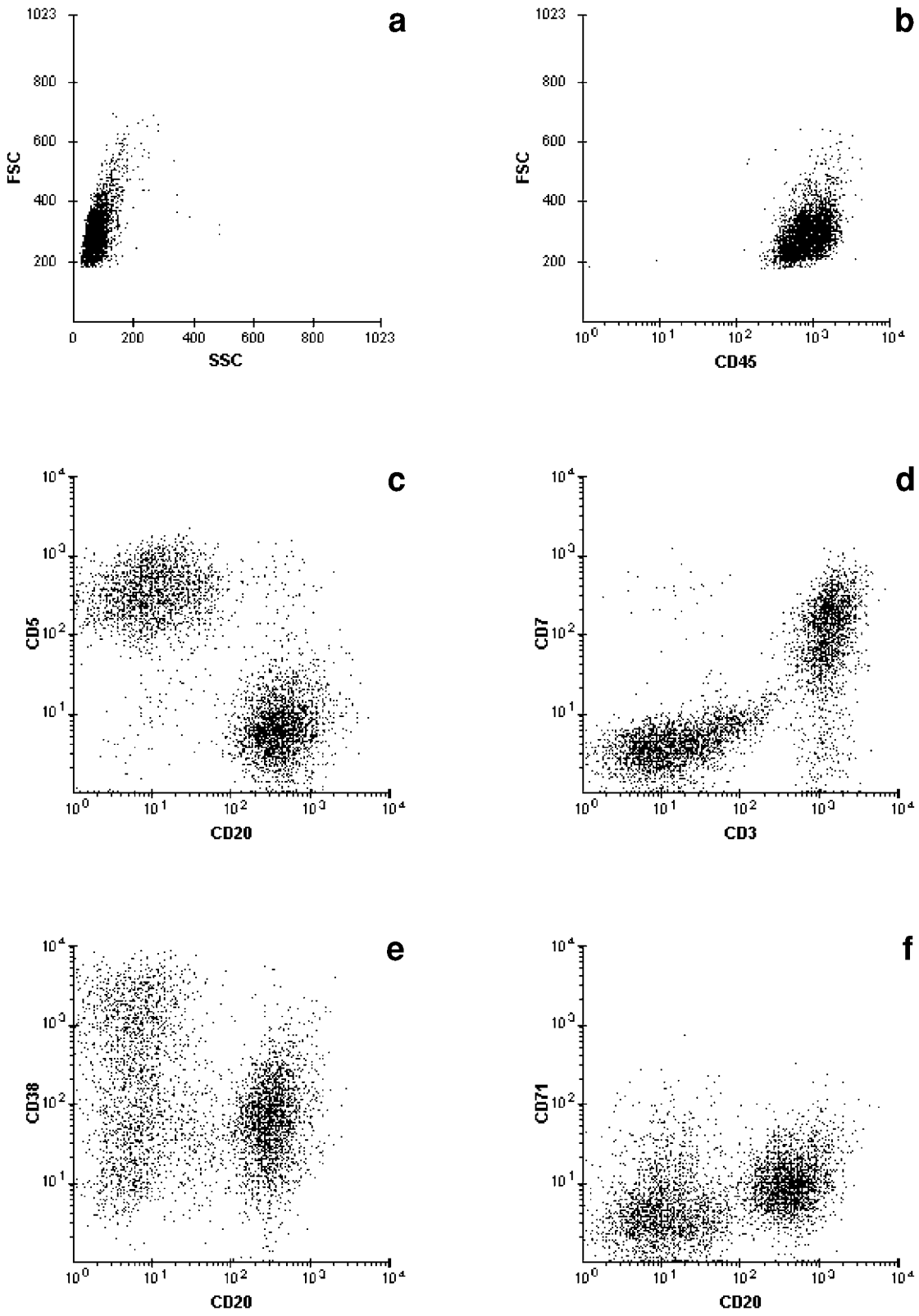

Figure 4.1 Benign lymph node. (a,b) A single lymphoid cluster with low to medium FSC and bright CD45. (c,d) Normal B- and T-cells. (e,f) Variable expression of CD38 in B- and T-cells. CD71 is minimally expressed, indicative of low proliferative activity.

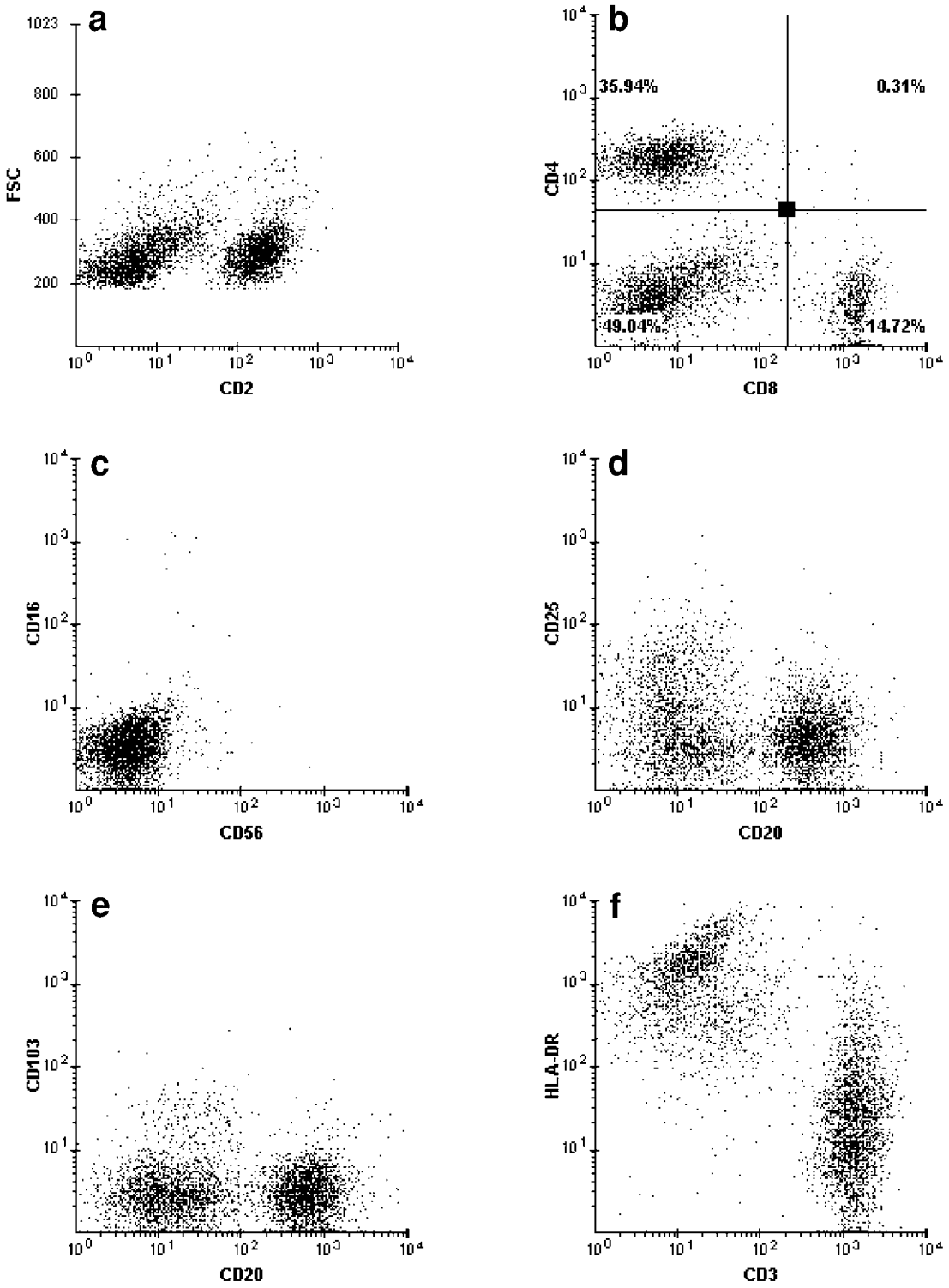

Figure 4.2 Benign lymph node (continuation of Figure 4.1). (a) B- and T-cells, mostly of small cell size. (b) CD4;CD8 ratio is within the normal range. (c,d) Dim CD25 on a subset of T-cells. Lymphoid cells with NK markers are virtually absent. (e,f) A small subset of T-cells express CD103 (B-ly7). HLA-DR is intense on the B-cells, but more heterogeneously distributed on the T-cells.

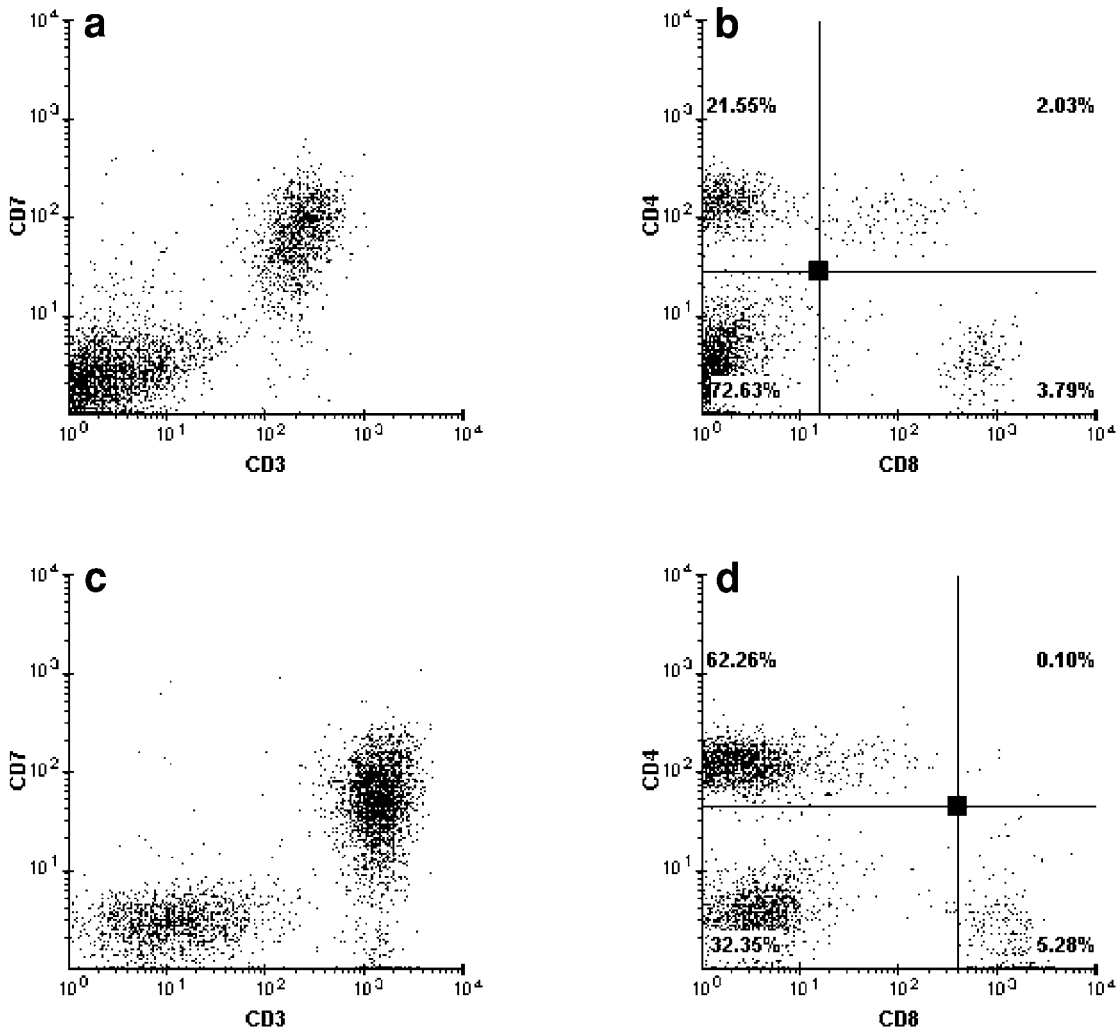

Figure 4.3 Increased CD4;CD8 ratio in lymph nodes. (a,b) Case 1: FRFH. T-Cells with normal expression of CD3 and CD7. CD2 and CD5 (not shown) are also well expressed. CD4;CD8 ratio is 5.7;1. (c,d) Case 2: Castleman's disease. Normal T-cells coexpressing CD3 and CD7. CD4;CD8 ratio is 11.8;1.

licular center cells is overall stronger than that on the reactive counterparts. The "horizontal hockey stick" pattern is less obvious if the combination of reagents employed consists of CD10–PE and CD20–PerCP, as the high quantum yield of PE blurs the subtle difference in CD10 intensities between FRFH and FCC lymphoma (Figure 2.5). In very florid hyperplasia, the $CD10^+$ subpopulation of reactive B-cells can be so prominent that a definite distinction from FCC lymphoma may not be achievable on the basis of the CD10/CD20 data alone. Testing for bcl-2, by either immunohistochemistry on paraffin-embedded sections or by FCM analysis using CD20–PE and bcl-2–FITC, can resolve the differential diagnosis. The patterns of the combined reactivities to bcl-2 and CD20 demonstrate a clear-cut difference between FRFH and FCC lymphoma (Figure 4.9).


Case study 34

In some cases of FCC lymphoma, the lymph node contains a high number of residual benign B-cells. Because the neoplastic cells express CD20 more intensely than the normal B-cells, the resulting pattern on the CD10/CD20 dot plot may simulate that seen in FRFH, especially if CD10 expression on the tumor cells is poorly expressed (Figure 4.10). However, the finding of monoclonal surface light chain or bcl-2 expression on the brightest CD20 cells provides the evidence that the follicular process is neoplastic.


Case study 35

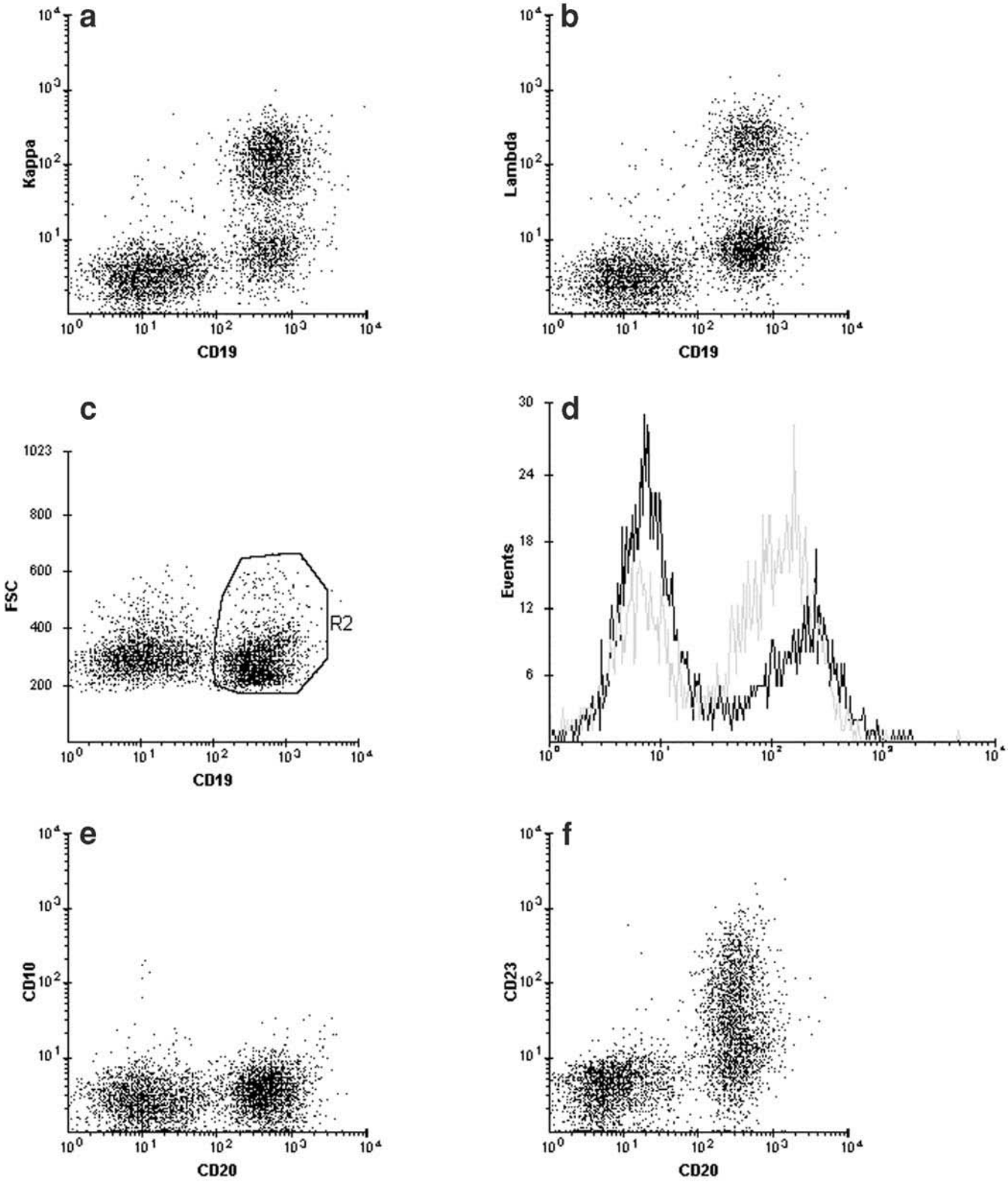

Figure 4.4 Benign lymph node (same sample as that in Figure 4.1). (a,b) Polyclonal B-cells, easily appreciated by a side-by-side comparison of the kappa/CD19 and lambda/CD19 dot plots. (c,d) Overlay kappa/lambda histograms gated on B-cells (R2) only, showing the double camel hump pattern of polyclonal light-chain expression. (e,f) B-cells are CD23-positive and CD10-negative.

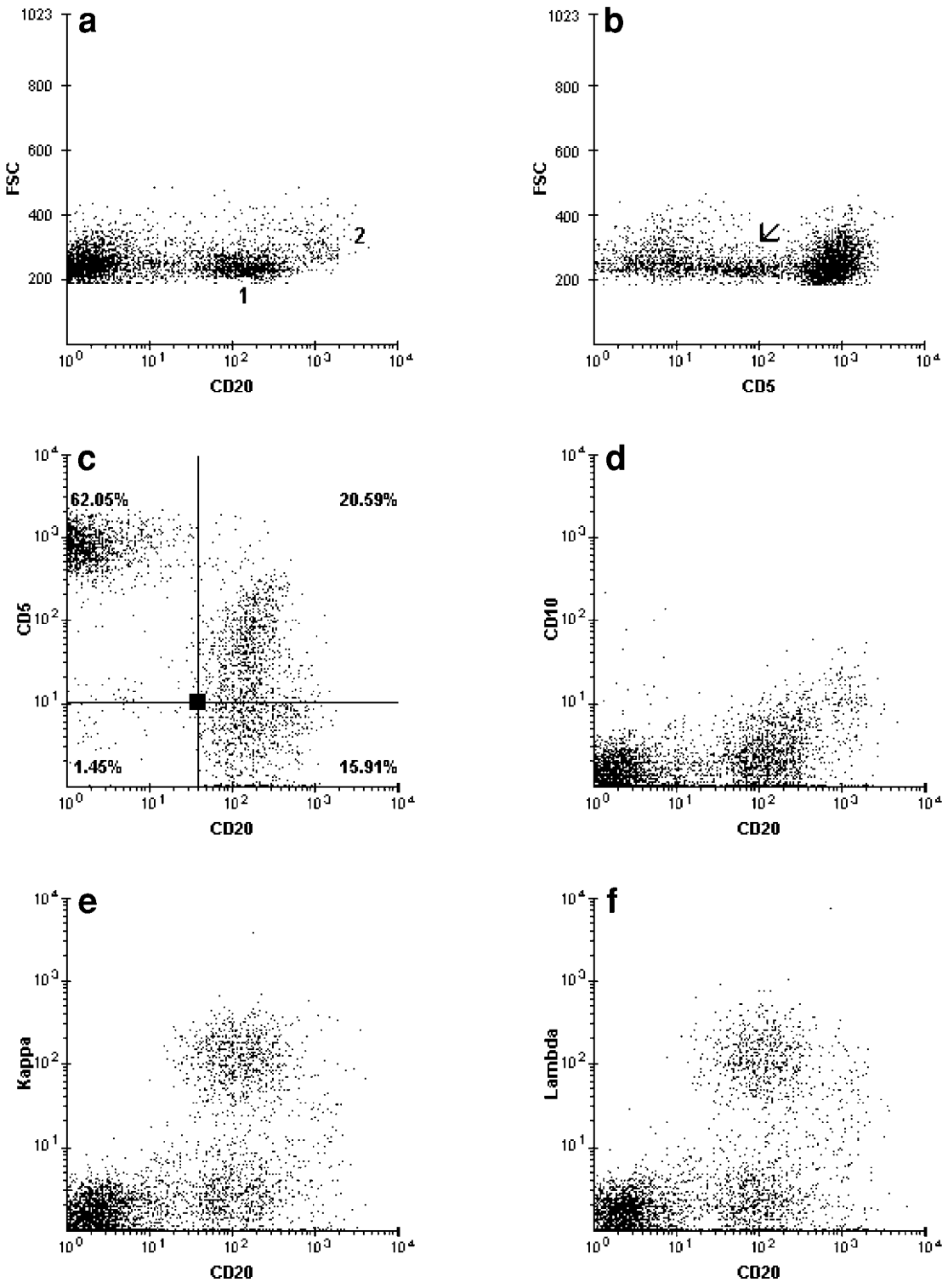

Figure 4.5 Reactive lymph node with CD5-positive B-cells. (a) Two subpopulations (#1 and #2) of B-cells differing in CD20 intensity. (b) A small population of lymphocytes with dim CD5 (arrow). (c,f) B-cells are polyclonal: The subpopulation with dimmer CD20 is CD10-negative; a subset thereof is CD5-positive, comprising 21% of the cells in the sample. The subpopulation with brighter CD20 expresses weak CD10.

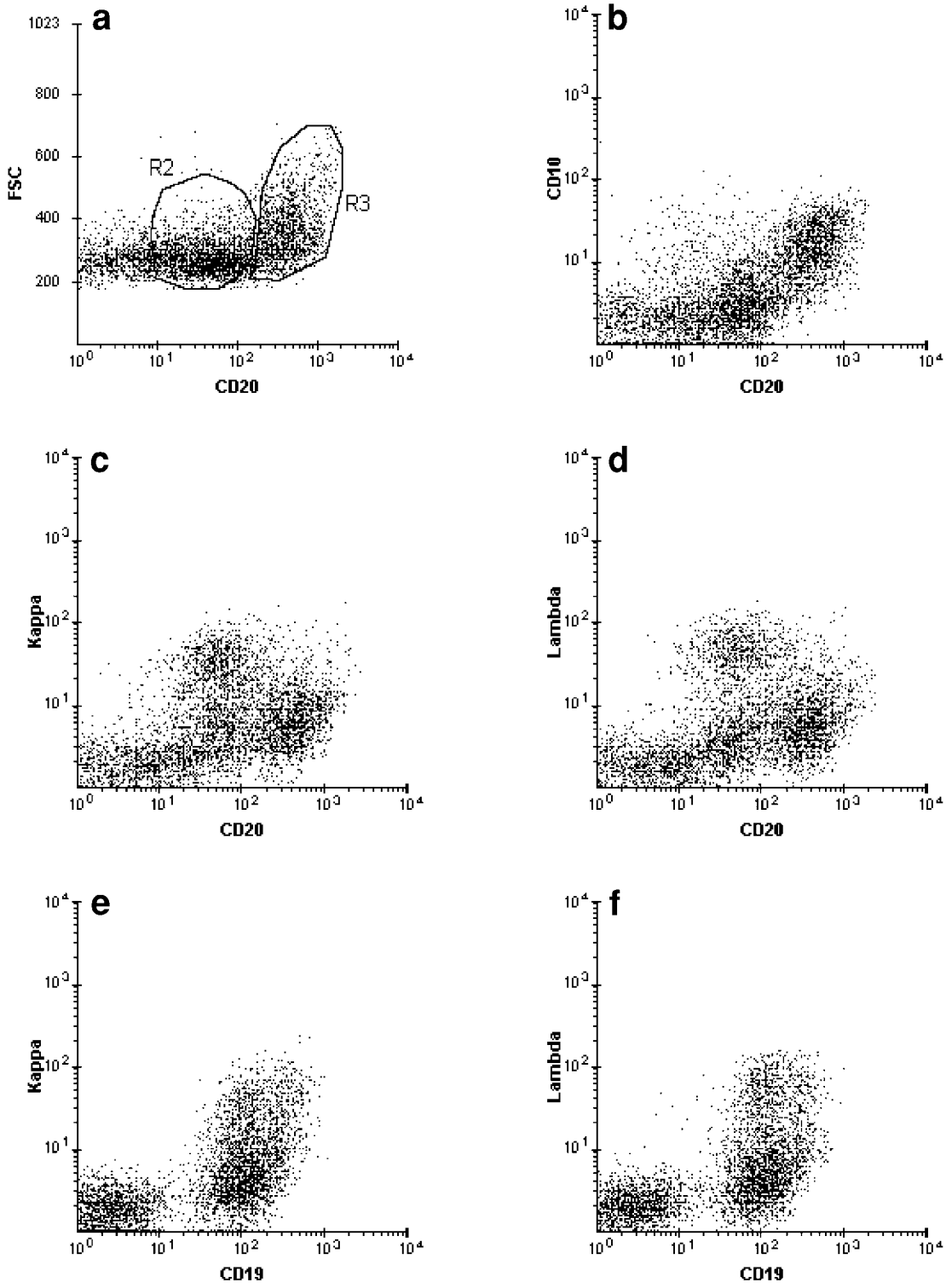

Figure 4.6 Lymph node with FRFH. (a) Two subpopulations of B-cells: One with smaller cell size and dimmer CD20 (R2) and the other composed of larger cells with brighter CD20 (R3). (c) CD10/CD20 "hockey stick" pattern. The brighter CD20 cells coexpress CD10. (c,d) The dimmer CD20 cells are polyclonal. The brighter CD20 cells have no detectable light chain. (e,f) Using CD19, it is not possible to discriminate between the two subpopulations.

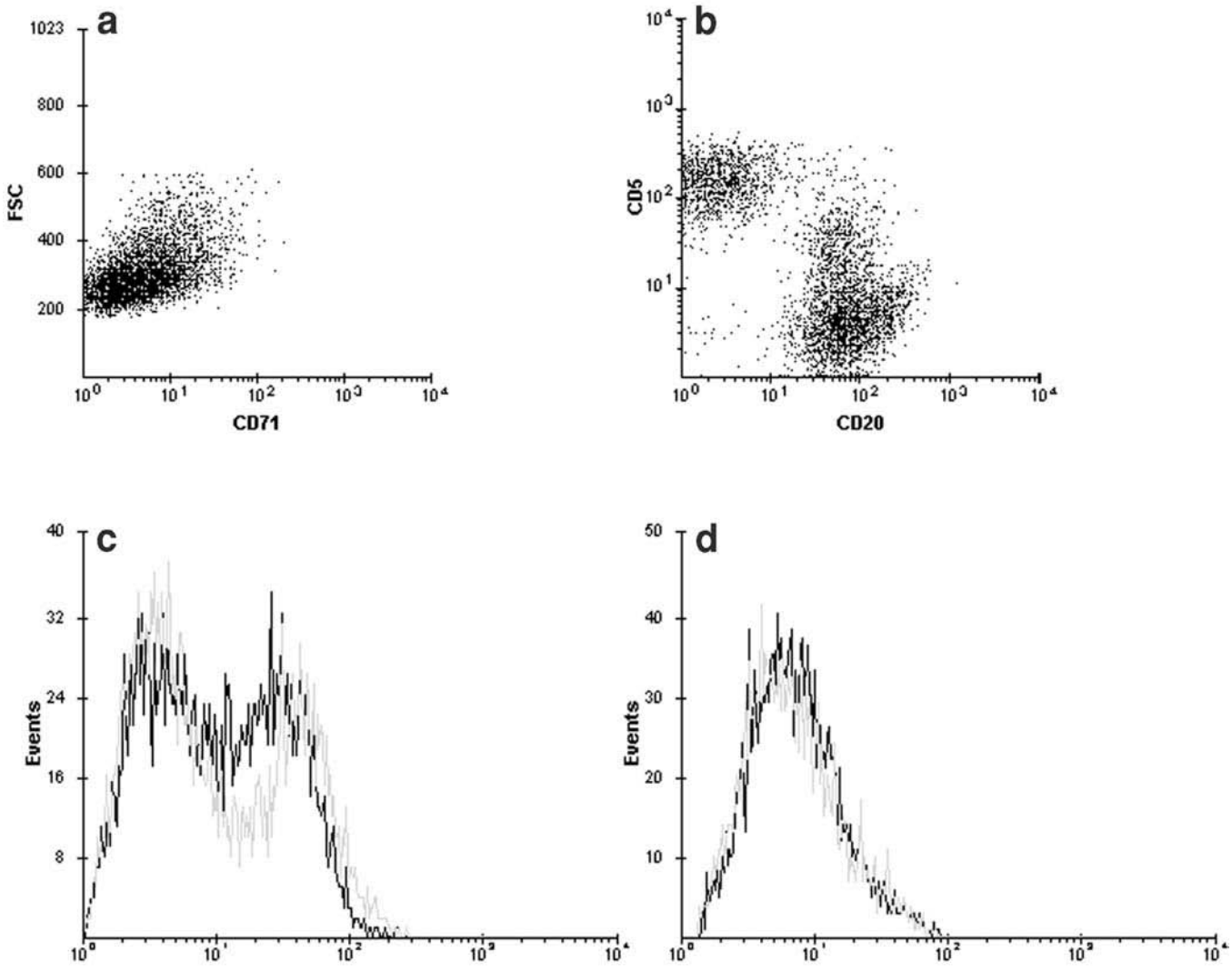

Figure 4.7 Lymph node with FRFH (continuation of Figure 4.6). (a) Dim CD71 expressed on the larger cells. (b) A subset of the dimmer CD20 cells is positive for CD5. (c) Gated on R2 (from Figure 4.6): Overlay kappa/lambda histograms showing the double camel hump pattern of polyclonal light chain expression. (d) Gated on R3 (from Figure 4.6): A single peak in the negative region (this region extends beyond the first decalog).

4.1.2 Normal peripheral blood and normal bone marrow

The peripheral blood and bone marrow are discussed together since marrow aspirates contain all of the blood elements. The following discussion does not pertain to specimens sent in for the evaluation of minimal residual disease because a standard data acquisition of 20,000 cells may not detect small numbers of residual leukemic cells, especially when they are present at levels below 1%.

A normal-appearing specimen by FCM analysis is defined by the absence of abnormalities. The following should not be present in normal specimens: (1) an increased number of blasts; (2) a marked preponderance of a specific cell population (lymphocytes, monocytes, granulocytes, red cell precursors, or eosinophils); (3) abnormal B-cells, T-cells, or plasma cells; (4) abnormal "antigenic" maturation in the granulocytic elements; and (5) nonhematopoietic elements. Because the size of the different cell clusters only reflects their relative proportion in the blood or bone marrow, the WBC count or bone marrow cellularity should be taken into

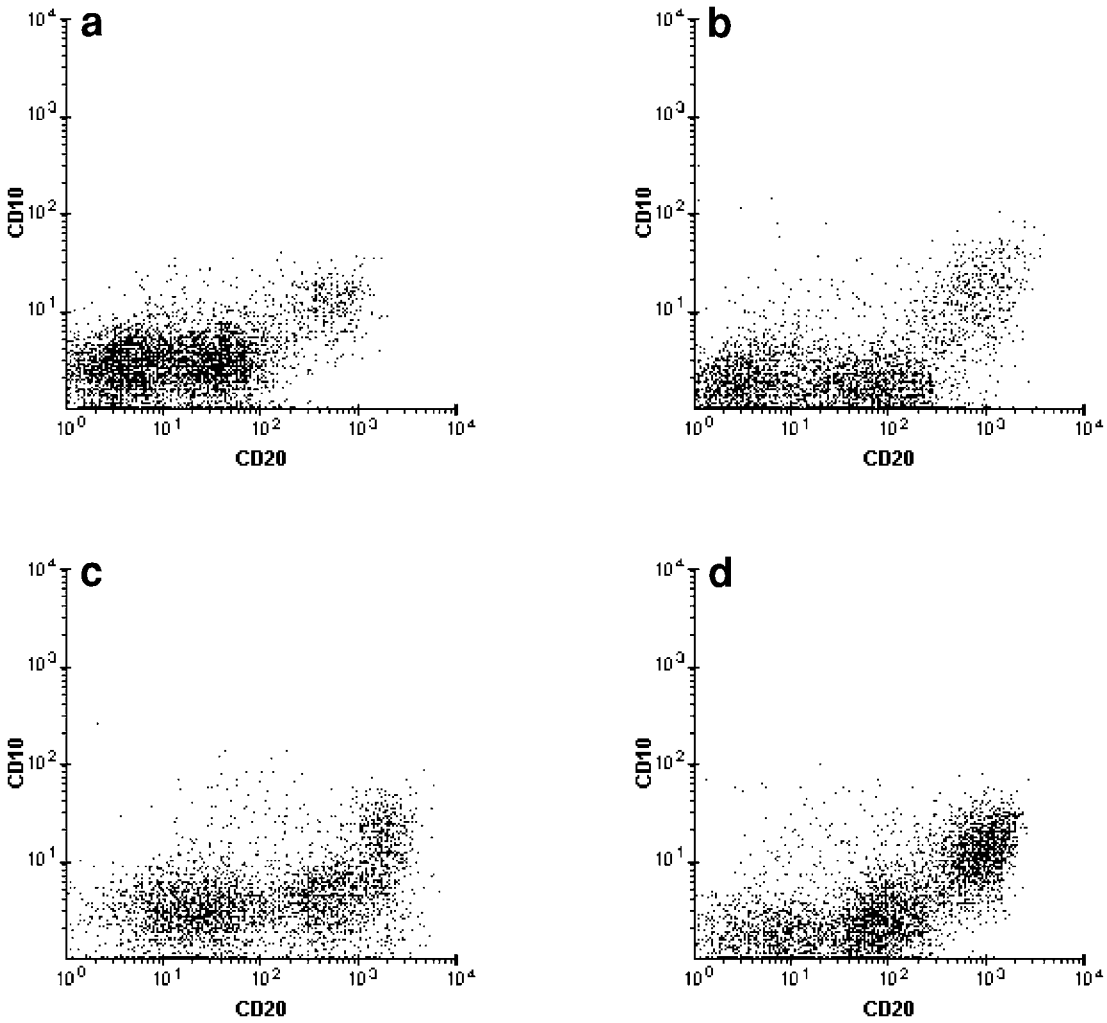

Figure 4.8 CD10/CD20 reactivity in four different lymph nodes with FRFH. (a–d) The proportion of the brighter CD20 cells with CD10 expression varies with the degree of follicular hyperplasia in the sample.

account. The bone marrow FCM data in some neoplastic disorders such as low-grade MDS (e.g., refractory anemia) or myeloproliferative disorder (MPD) (e.g., polycythemia rubra vera [PRV] or essential thrombocythemia [ET]) can be indistinguishable from that in a normal subject.

The different cell clusters in the blood or bone marrow can be best appreciated on the SSC/CD45 dot plot where granulocytes, lymphocytes, and monocytes are well separated based on their respective granularity and CD45 intensity (Figure 4.11). Lymphocytes and monocytes demonstrate high densities of CD45, whereas the intensity of CD45 on granulocytes is lower by one decalog. In a representative normal bone marrow specimen, the monocytic component is not conspicuous. The appearance of the granulocytic cluster in the bone marrow reflects the heterogeneity of the myeloid precursors, which consist of both mature and immature elements ranging from promyelocytes to neutrophils. The bone marrow granulocytic cluster is actually composed of two merging clusters with a variable degree of overlap, whereby the more granular elements (with higher SSC signals) display lower CD45 (Figure 4.11a). Eosinophils, when present in sufficient numbers, manifest as a cluster with extremely high SSC and a CD45 intensity slightly brighter than that on myeloid cells (Figure 4.12).

The cell size of the various elements in the blood or bone marrow can be appreciated on ungated FCM graphics correlating FSC and antigenic fluorescence (e.g., FSC/CD45). An ade-

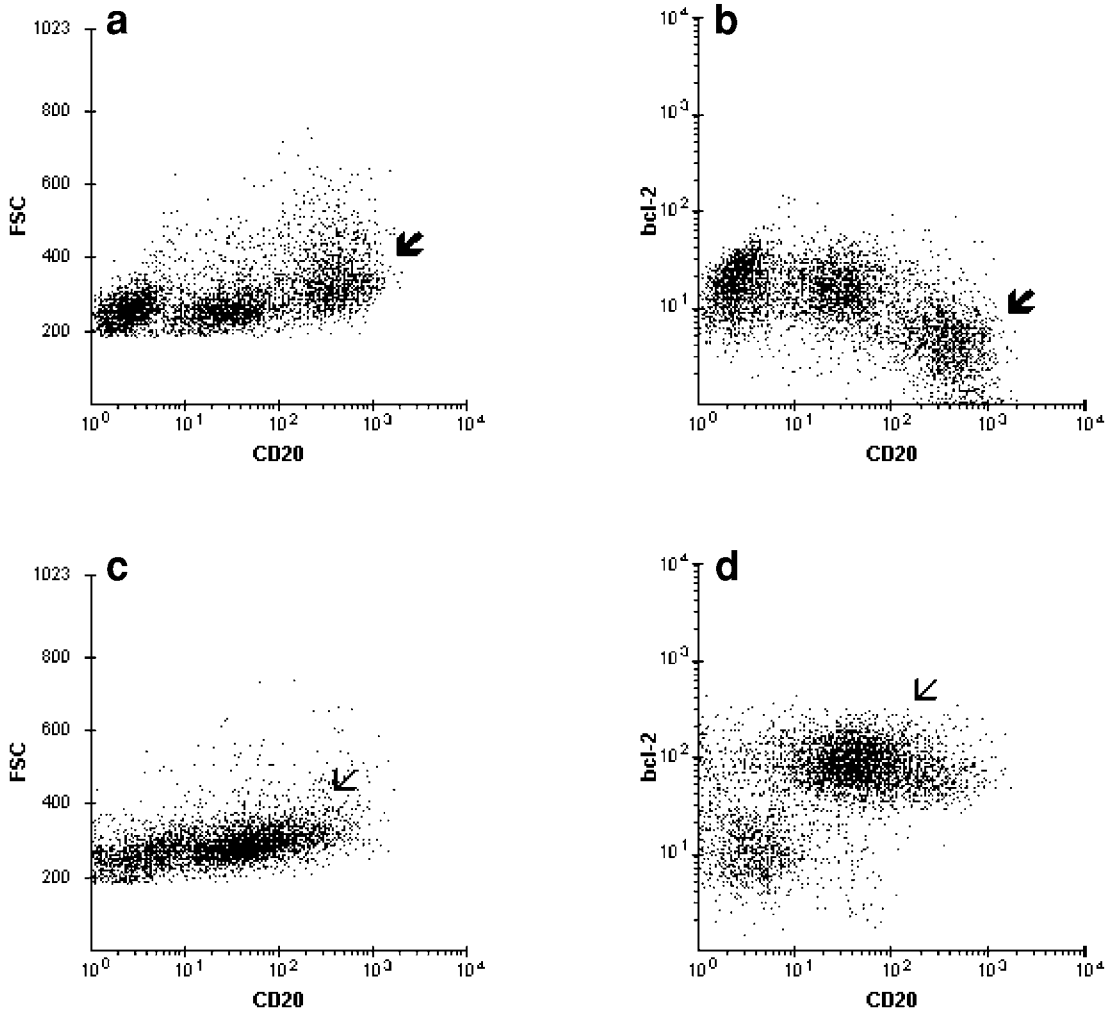

Figure 4.9 FRFH vs FCC lymphoma. Bcl-2 reactivity. (a,b) FRFH: Two subpopulations of B-cells differing in FSC signals and CD20 intensity. The brighter CD20 subpopulation (arrow) is bcl-2-negative. The other benign B- and T-cells are weakly bcl-2 positive. (c,d) FCC lymphoma: The neoplastic cells (thin arrow) are of small cell size and demonstrate bright bcl-2 expression.

quate bone marrow sample without gross abnormalities typically produces a "tunnel-like" pattern on the FSC/CD45 dot plot (Figure 4.13).

Based on the SSC/CD45 dot plot, the cellular events to be evaluated in the subsequent graphics can be separated into two broad groups: granulocytes and mononuclear cells. The latter group includes events from the regions associated with blasts, bone marrow B-cell precursors, lymphocytes, and monocytes, as well as signals from the CD45-negative to the borderline region which may represent blasts (*see* Section 3.4.2), erythroid precursors, plasma cells, platelets, or nonhematopoietic elements.

4.1.2.1 Blast region

In normal specimens, the blast region is essentially empty, with only a few scattered events present (Figure 4.11a). Enumeration of the blast events can be achieved by drawing a gate around this region. A better approach, if blasts express CD34 (the majority of leukemic blasts do), is to determine the blast content from the CD117/CD34, CD33/CD34 (or CD13/CD34),

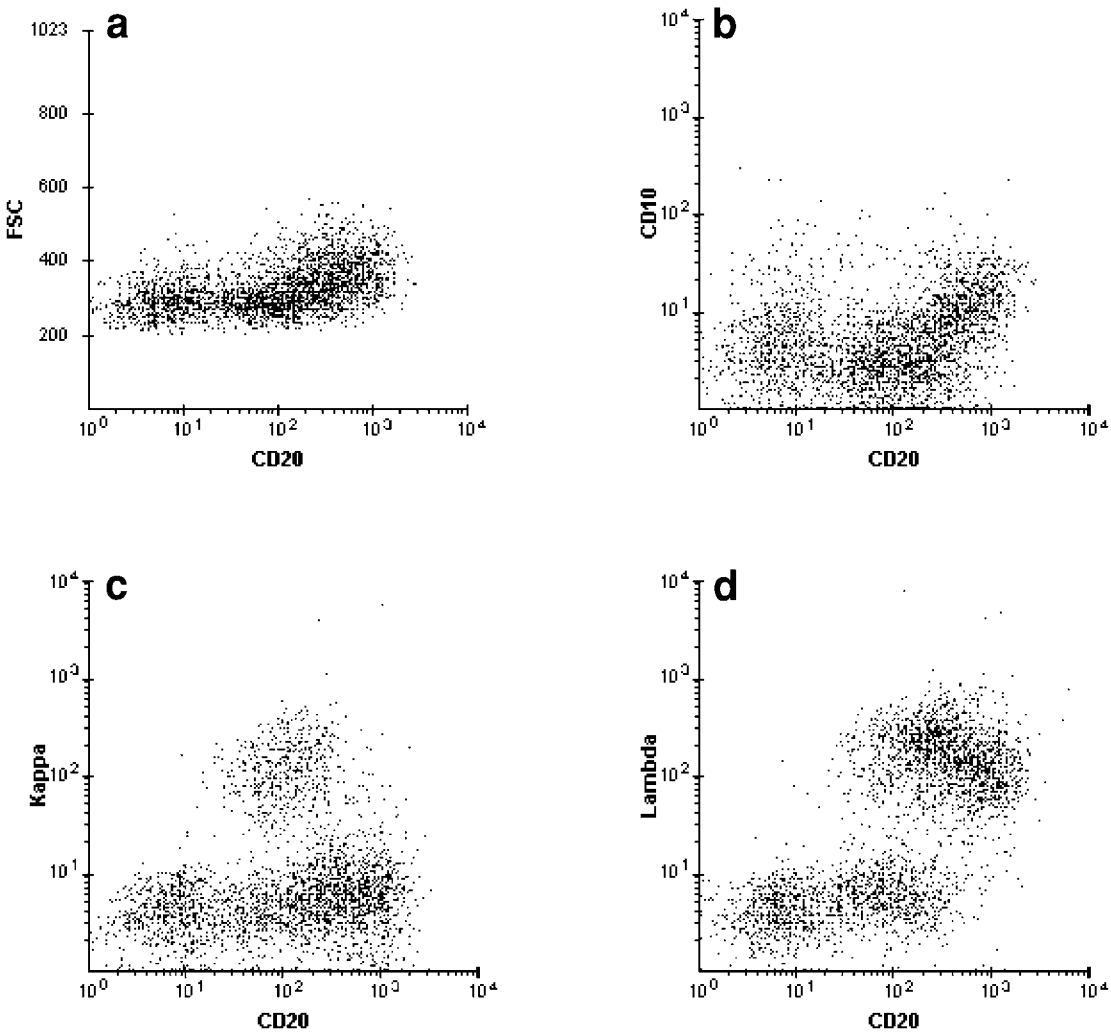

Figure 4.10 FCC with a CD10/CD20 pattern simulating FRFH. (a) Two populations of CD20 cells. The larger cells display brighter CD20. (b) Dim CD10 expression on the brighter CD20 cells. (c,d) The dimmer CD20 cells are polyclonal. The brighter CD20 cells are monoclonal for lambda and are thus neoplastic. In this case, the unusual combination of a substantial number of residual benign B-cells and the poorly expressed CD10 on the tumor cells result in a CD10/CD20 pattern mimicking that seen in FRFH.

or CD19/CD34 dot plots (Figure 4.14). Note that CD117 may occasionally be found on cells other than blasts, such as plasma cells, abnormal maturing granulocytes, and small cell carcinoma (*see* Section 3.7).

In the blood, the presence of a discrete cluster of blasts, however tiny it may be, is a significant finding (Figure 4.15). In the bone marrow, the threshold generally employed is that which has been traditionally accepted for clinical remission of acute leukemias (i.e., less than 5% myeloblasts). However, because of the manner in which the bone marrow is collected in most institutions, the aspirate sample allocated for FCM analysis is often much more hemodilute than the sample spread on the smears. Therefore, a bone marrow blast level of less than 5% in the FCM sample does not necessarily exclude a neoplastic condition. Such hemodilution-related artifacts can be circumvented by performing FCM analysis on cells extracted from bone marrow core biopsies. A better approach for obtaining representative marrow is to collect ample amounts of aspirate in EDTA and to let the specimen stand until the spicules rise to the top, where they can be easily collected (*see* the book *Diagnostic Hematology: A Pattern*

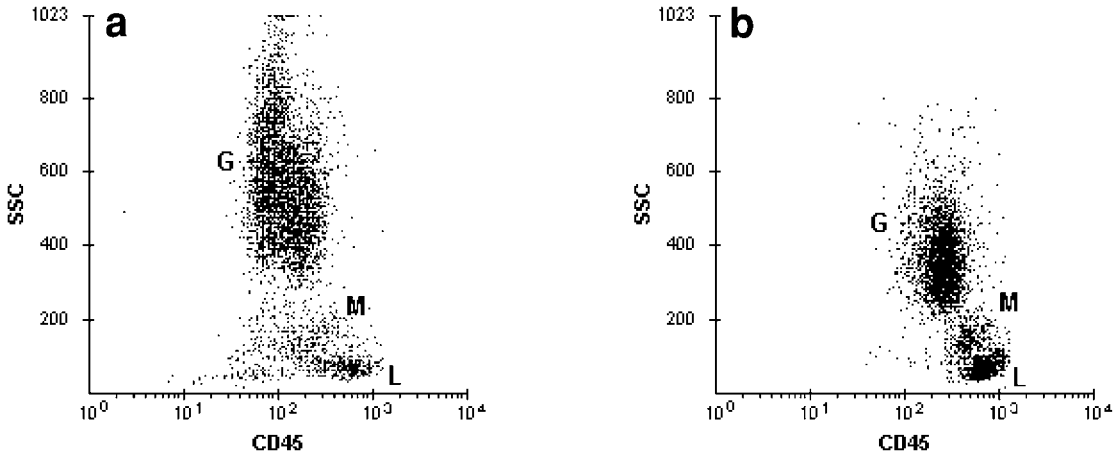

Figure 4.11 (a) Normal bone marrow composed predominantly of granulocytic (G) precursors. The monocytic (M) and lymphoid (L) cell clusters are small. The blast level is less than 1%. A conspicuous erythroid cluster is not evident because most of the nucleated red cells (13–15% on the aspirate smears) have been lysed. (b) Normal peripheral blood with granulocytes, monocytes, and lymphocytes.

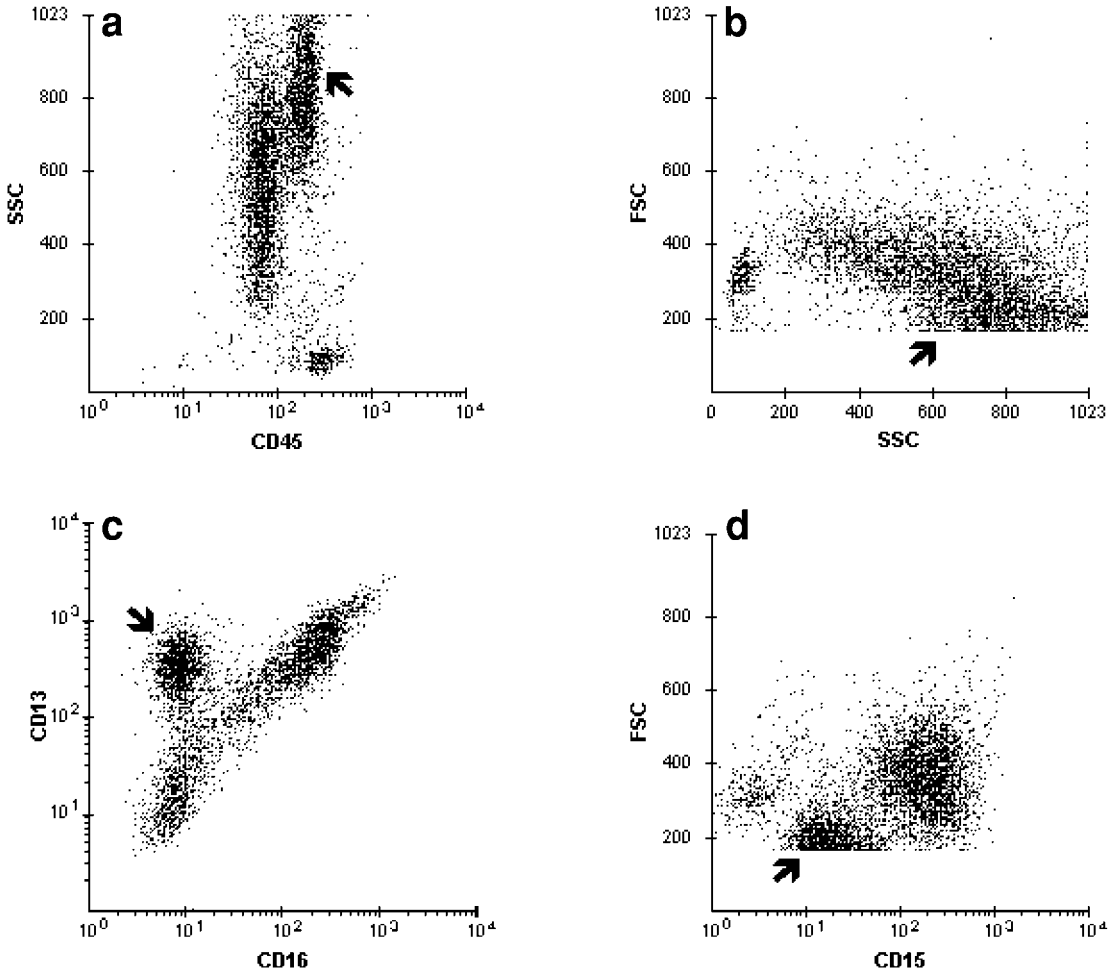

Figure 4.12 Bone marrow eosinophilia. (a,b) The eosinophilic precursors (arrow) display slightly brighter CD45 than the granulocytes, and the characteristic combination of low FSC and high SSC. (c,d) Eosinophils are CD16-negative. CD13 is expressed. CD15 is dimmer than that on myeloid cells. The intensity of several of the myeloid antigens on eosinophils overlaps with that on granulocytes and is thus best evaluated on the FSC vs fluorescence dot plots.

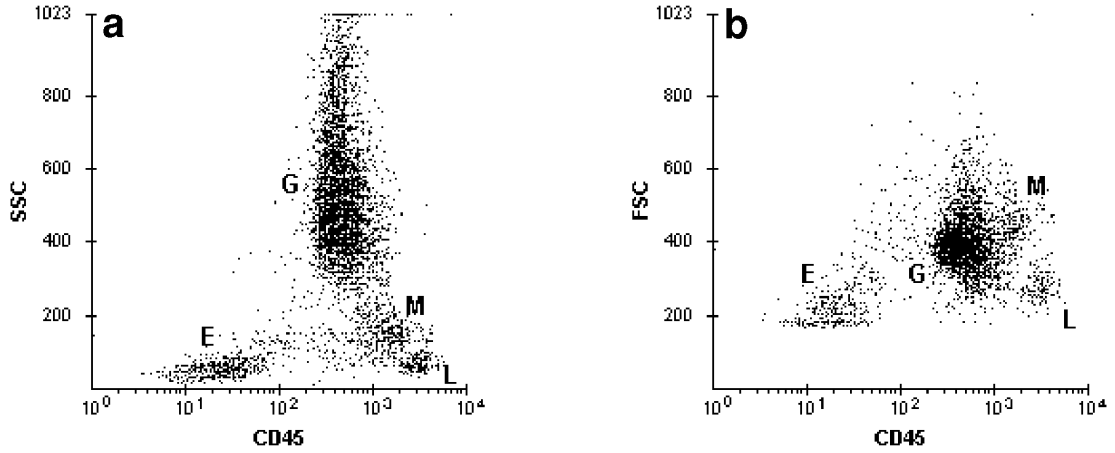

Figure 4.13 (a) Normal bone marrow with erythroid precursors (E), granulocytes (G), lymphocytes (L), and monocytes (M). The relative cell size can be appreciated on the FSC/CD45 dot plot (b).

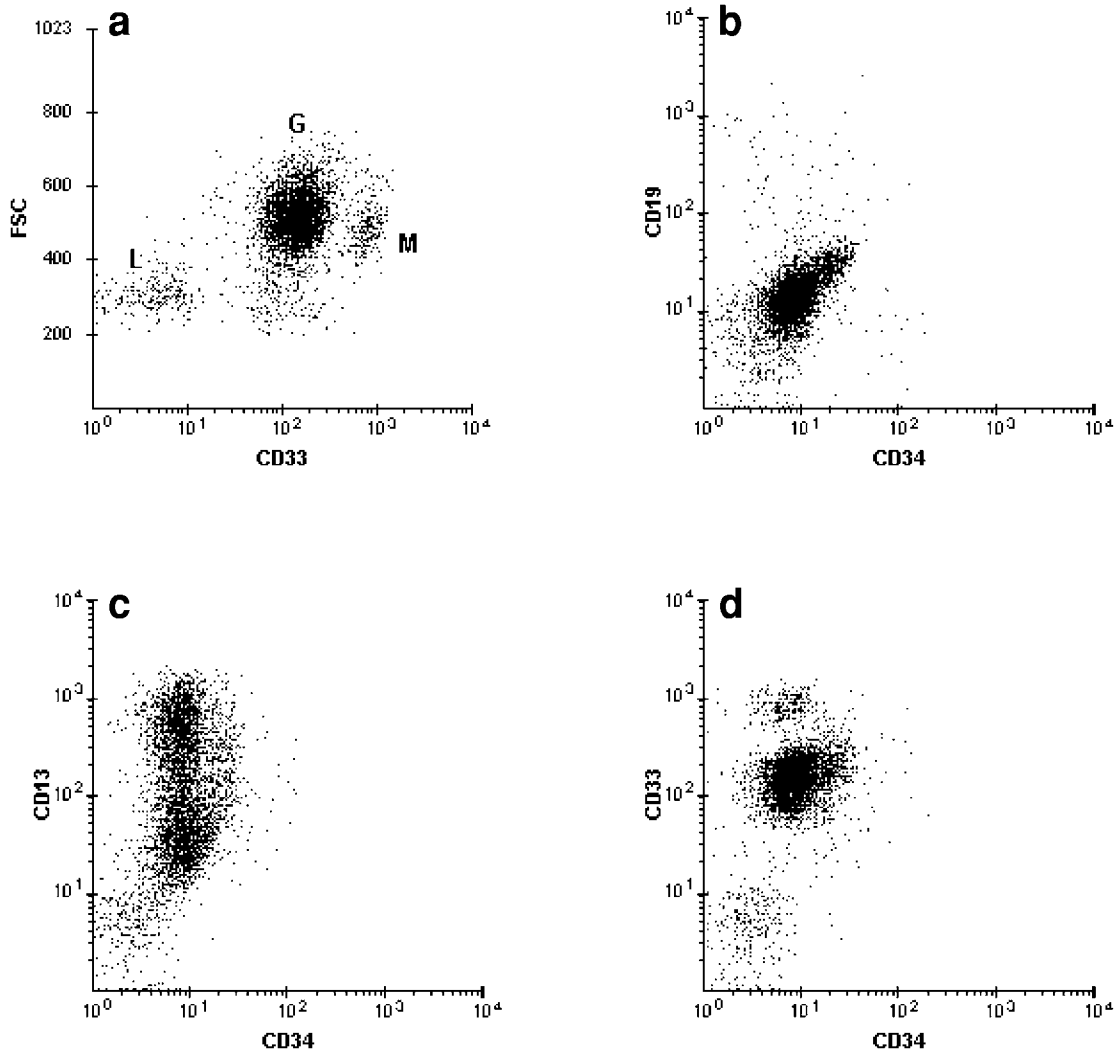

Figure 4.14 Normal bone marrow (same sample as in Figure 4.11a). (a) Lymphocytes (L), monocytes (M), and myeloid (G) precursors form distinct clusters on the FSC/CD33 dot plot. (b–d) CD34-positive events are minimal. The blast level is 0.5%.

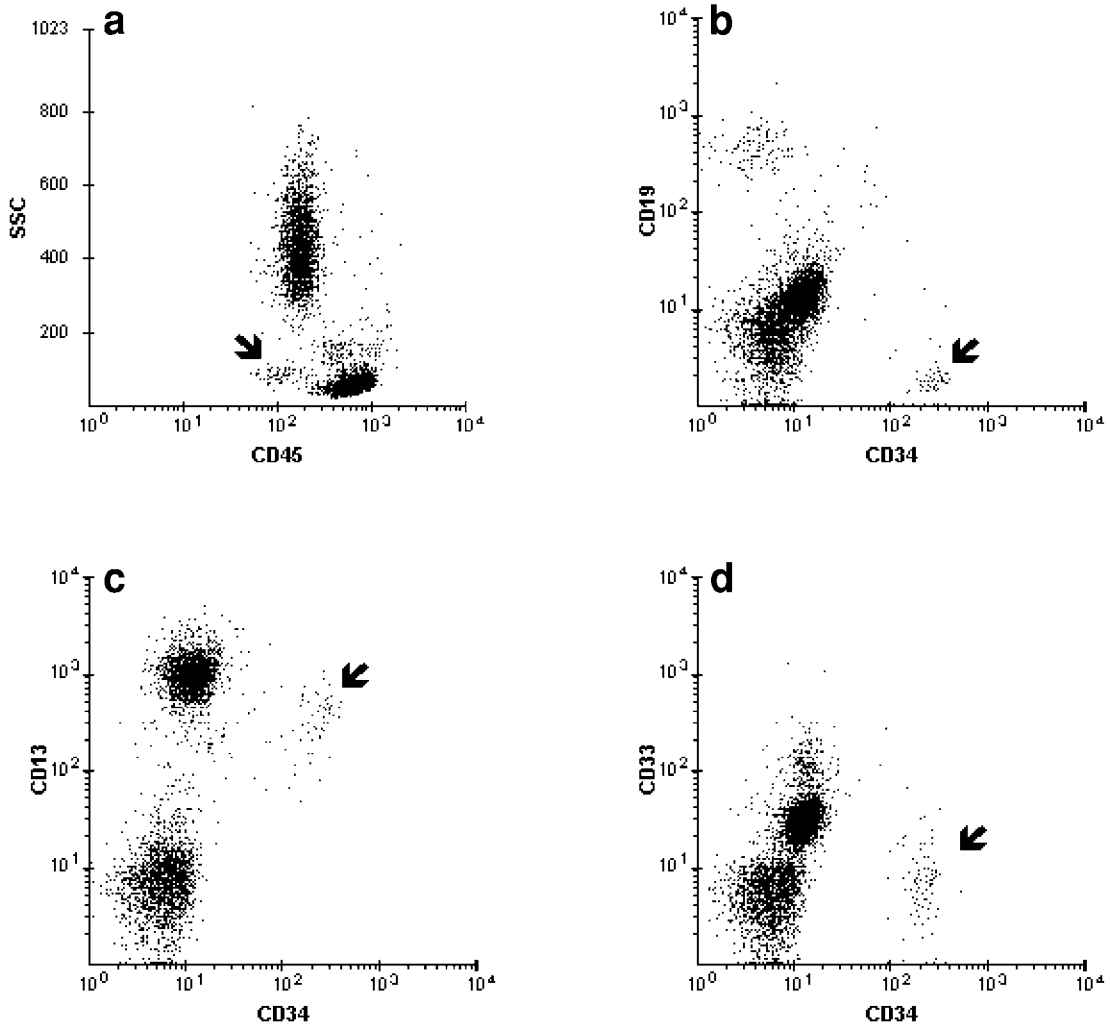

Figure 4.15 Peripheral blood with 1% circulating blasts (arrow). (a) A tiny cluster in the blast region. (b–d) Blasts display an abnormal phenotype $CD34^{++}$, $CD13^{++}$, and $CD33^{-}$. CD19 is negative. CD117 (not shown) is expressed.

Approach for the details on this bone marrow collection procedure). The spicules are then allocated in appropriate amounts for FCM and any other necessary studies.

The presence of a discrete blast cluster in the bone marrow, even without phenotypic aberrancies (*see* Section 3.5.1.1) and at a level considered within the normal range, can still be cause for concern. Knowledge of the antecedent clinical history and close follow-up are warranted in such cases to exclude or confirm either preneoplastic conditions (MDS) or minimal residual AML.

4.1.2.2 Bone marrow B-cell precursors (hematogones)

In close proximity to the blast region on the SSC/CD45 dot plot is the location for bone marrow B-cell precursors (hematogones). These cells can be easily recognized by the extremely low SSC and a CD45 intensity intermediate between that of lymphocytes and blasts (Figure 4.16). This characteristic appearance, along with the low FSC, distinguishes hematogones

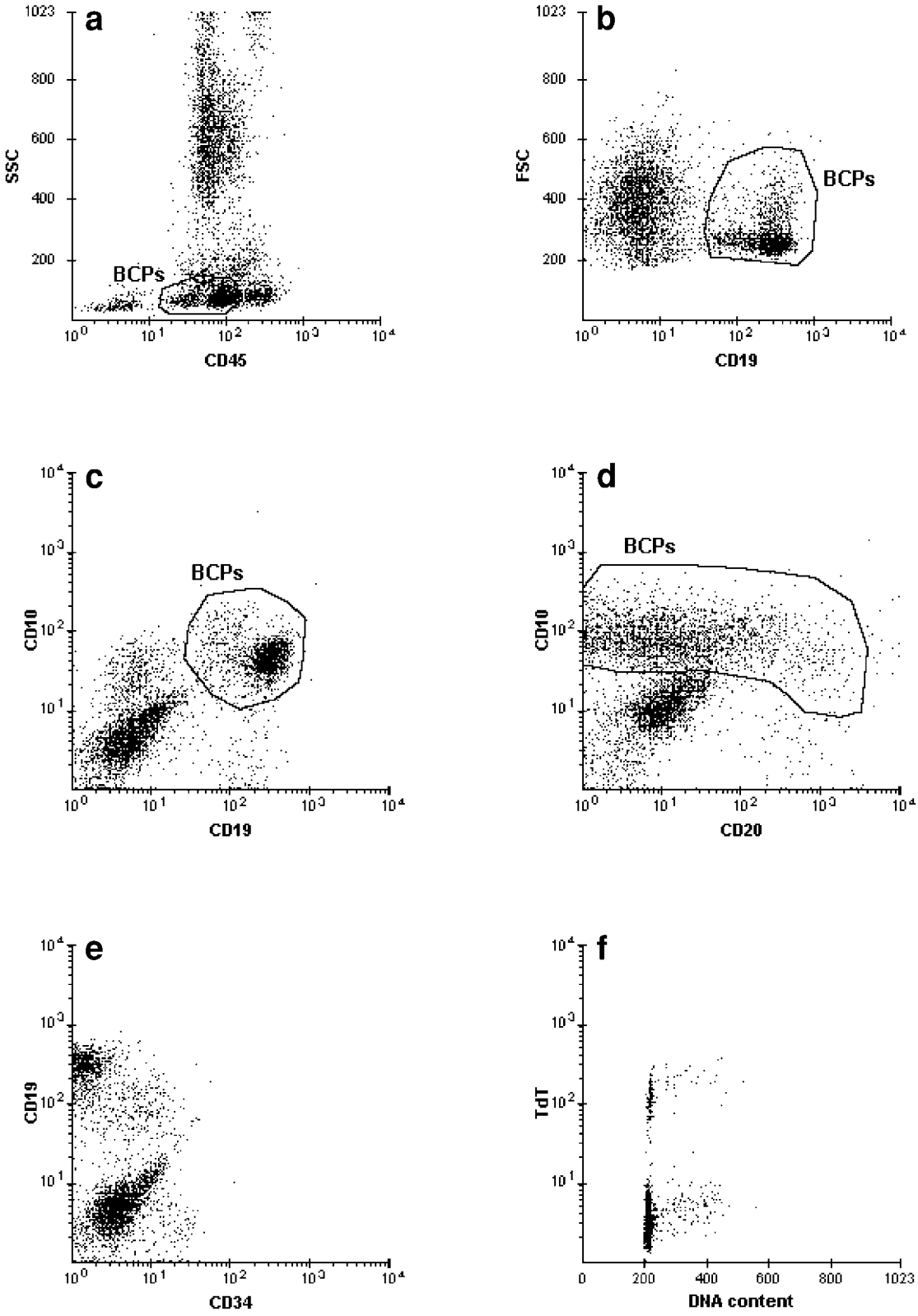

Figure 4.16 Pediatric bone marrow with 29% B-cell progenitors (BCPs). (a–e) BCPs display a variable degree of heterogeneity in cell size and CD45, CD19, CD20, and CD10 expression. This reflects the presence of various subpopulations of BCPs at various stages of maturation and differentiation. TdT is present in a subpopulation.

(when present in significant numbers) from ALL cells. Increased numbers of normal B-cell precursors is most common in the pediatric age group (Plate 10), especially in bone marrows affected with solid tumors (e.g., neuroblastoma) or non-neoplastic hematologic conditions, such as idiopathic thrombocytopenic purpura (ITP) or maturation arrest of hematopoietic precursors, as well as in regenerative marrows following chemotherapy/transplantation for acute leukemia. It is not unusual to find leukemic blasts and hematogones coexisting in the same sample, especially in residual or early relapsed disease. The distinction of B-cell progenitors from residual AML cells is straightforward because their antigenic characteristics do not overlap (Figure 4.17). In contrast, in the setting of residual/relapsed ALL, it may be necessary to use other approaches (*see* Section 3.5.2) to differentiate hematogones from residual ALL cells, especially since both components often coexist in a regenerative marrow.

Case studies 36 and 37

4.1.2.3 Lymphocytes

The evaluation of B- and T-cells in the blood and bone marrow follows the same steps applied to the lymph node, using the appropriate B- and T-cell dot plots gated on mononuclear cells. The B-cell component is small and simpler than that in the lymph node, since normal blood and bone marrow contain no follicular mature B-cells with CD10/CD20 coexpression.

Non-neoplastic alterations affecting blood or bone marrow lymphocytes involve primarily the T-cell component, most commonly manifesting as an inverted CD4;CD8 ratio and/or activation changes. This can be observed in immunosuppressive states, including those secondary to chemotherapy or underlying malignancies. Decreased numbers of CD4 cells and/or increased numbers of CD8 cells, when seen in advanced stages of CLL and other LPD/NHL, may imply a poor prognosis. An inverted CD4;CD8 ratio also occurs in viral infections (e.g., Epstein–Barr Virus [EBV], cytomegalovirus [CMV]) as a result of the reactive proliferation of suppressor T-cells (Figure 4.18). Samples from the sites involved (peripheral blood, lymph node) by viral infections are rarely submitted for FCM analysis except when the clinical picture is unusual (e.g., older age group) or the lymph node morphology simulates that of a large cell lymphoma (Plate 11). In such instances, the absence of T-cell antigen aberrancies, together with appropriate serological data are helpful clues to support the benign nature of the CD8 proliferation. This can be further confirmed by the subsequent self-limited clinical course.

Case study 38

In HIV-infected subjects, an inverted CD4;CD8 ratio is the result of the destruction of CD4 cells and, in the early stages, a compensatory increase in CD8 cells. In some cases, indirect evidence of a marked polyclonal hypergammaglobulinemia may be seen on the FCM graphics (Figures 4.19 and 4.20). The loss of the suppressor subset of CD4 T-cells, which normally regulates B-cell production of immunoglobulins, most likely accounts for this abnormality.

Case studies 39 and 40

Lymphocytes expressing NK markers are most easily detectable in the blood and consist of true NK-cells and NK-like T-cells. In addition to the expression of one or more NK antigens, this group can also be recognized by a weaker CD8 intensity (Figure 4.21) than normal suppressor T-cells. The majority of lymphocytes expressing NK-associated antigens are large granular lymphocytes, which, under normal conditions, account for a small proportion (10–15%) of the total lymphoid population. Increased large granular lymphocytes (LGLs) can be observed in altered immune conditions, including autoimmune disorders, chemotherapy, and underlying malignancy. Reactive LGL proliferations can persist over long periods of time. The distinction between reactive and neoplastic LGL proliferations can be problematic, unless the number of LGLs is so overwhelming as to suggest malignancy or the LGLs are CD3+ LGLs (in which case molecular techniques can be applied to assess TCR gene rearrangements). Correlation among the FCM data, lymphocyte count, blood smear morphology, and clinical findings is therefore often necessary.

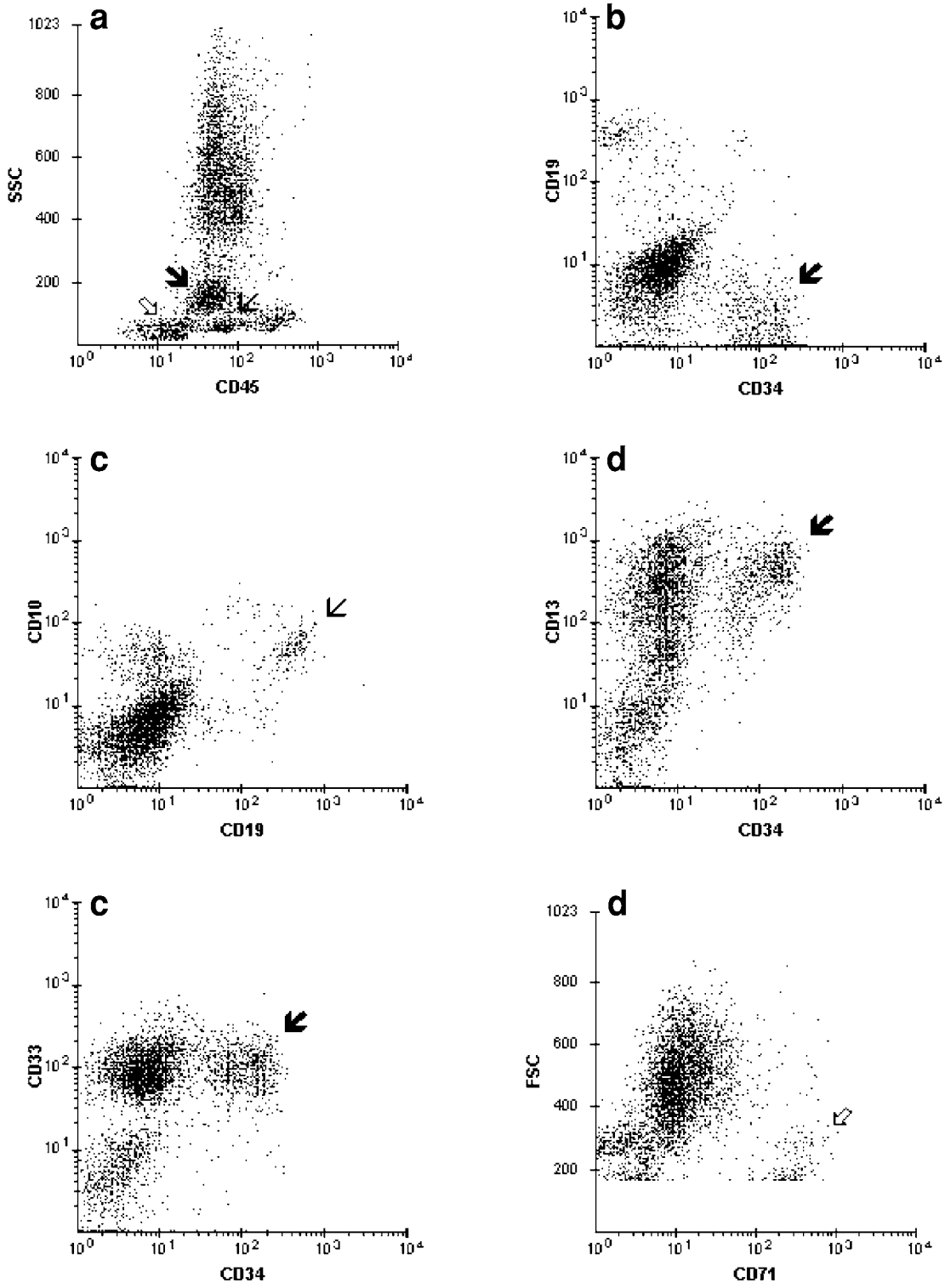

Figure 4.17 Coexisting leukemic blasts and B-cell progenitors. (a–f) Blasts (arrow), hematogones (thin arrow), and erythoid precursors (open arrow) are present in addition to the lymphocytes and granulocytes. Blasts, coexpressing CD34, CD13, and CD33, comprise 18% of the cells in the sample; CD19 is negative on the blasts. CD19 and C10 are present on hematogones. Erythroid precursors display intense CD71; most are of small cell size.

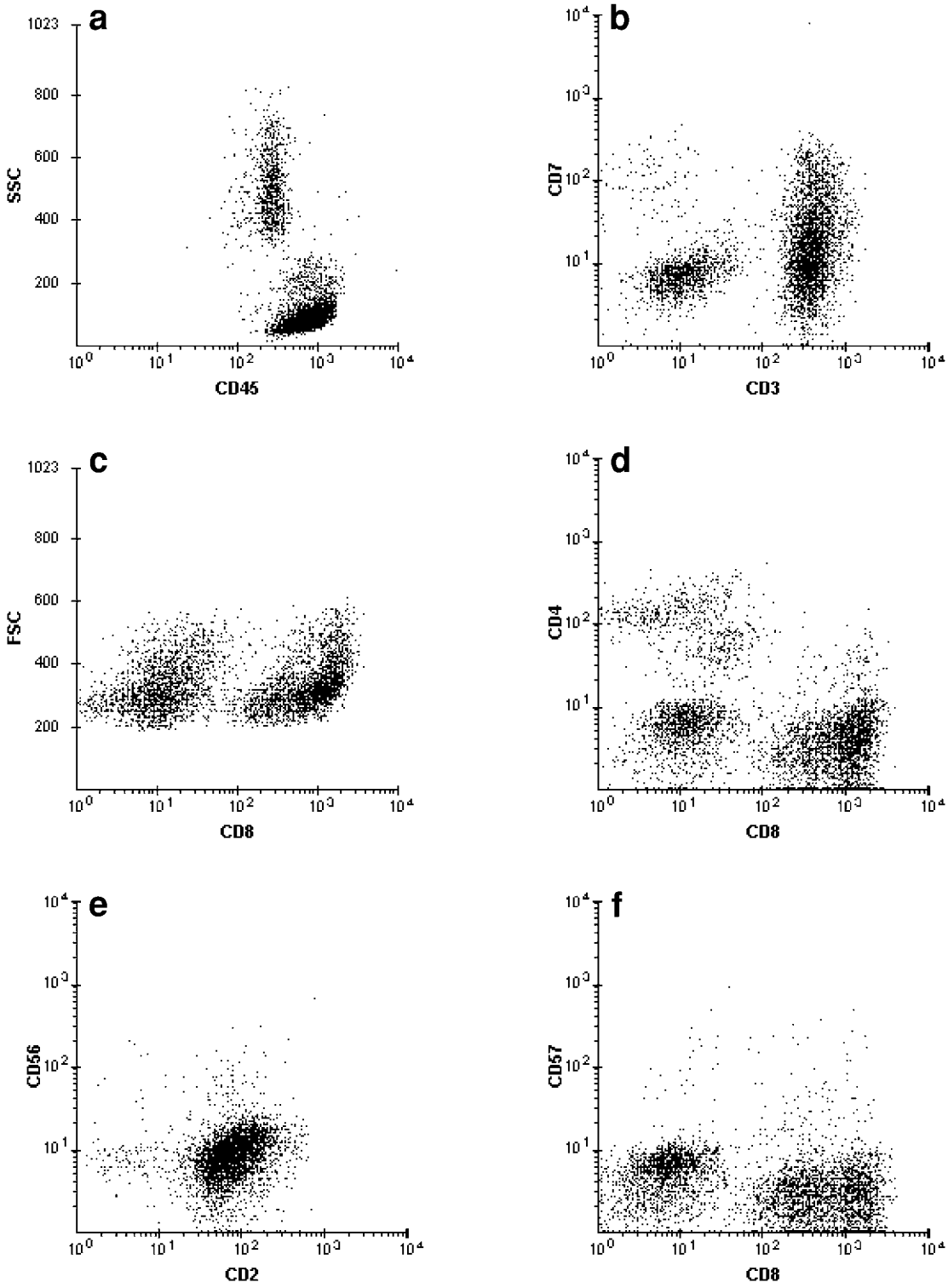

Figure 4.18 Peripheral blood with EBV viral lymphocytosis in a young adult male. (a) A prominent lymphoid cluster. The SSC/CD45 picture is reminiscent of that seen in an LPD. (b–f) The lymphoid cells are of variable cell size and coexpress CD3, CD7, CD2, CD5 (not shown), and CD8. The expression of CD7 and CD8 is heterogeneous. CD56, CD57, and CD16 (not shown) are not expressed. EBV serology was positive in this case.

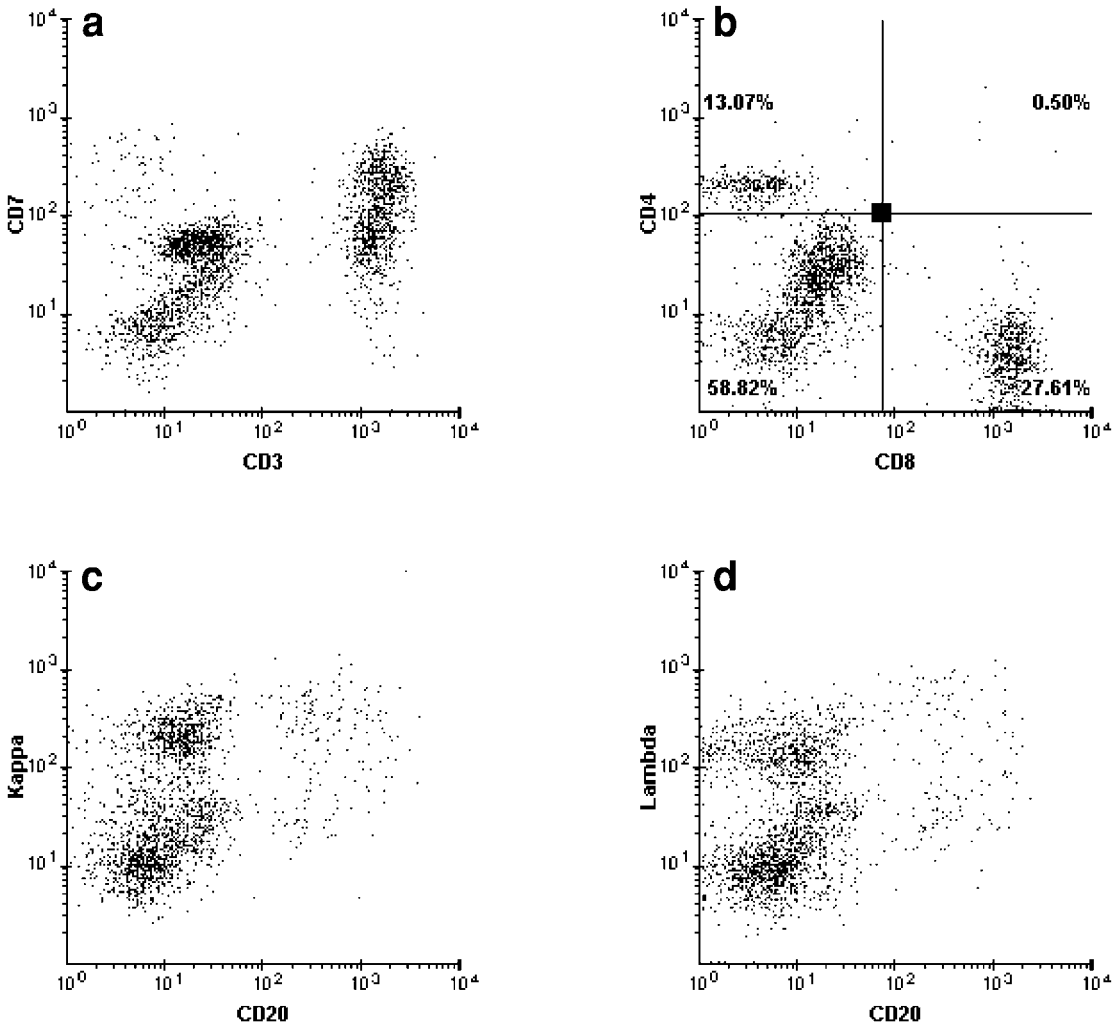

Figure 4.19 Peripheral blood from an HIV-positive patient. (a–d) Gated on MNCs: Normal T-cells with reversed CD4;CD8 ratio (0.47;1). There is also indirect evidence of marked polyclonal hypergammaglobulinemia (the CD20-negative cells are coated with immunoglobulins and appear to be positive for kappa and lambda). A small number of polyclonal B-cells are present.

4.1.2.4 Monocytes

In addition to its specific location on the SSC/CD45 dot plot, the monocytic population also demonstrates bright coexpression of CD14 (Leu-M3) and CD64 (Figures 3.34 and 4.22). The CD14/CD64 dot plot is useful for evaluating the maturation of the monocytic elements, especially in neoplastic monocytic proliferations (*see* Section 3.5.1). Other myeloid antigens such as CD13, CD33, and CD11b are also present on monocytes. The intensities of some of these antigens differ between monocytes and myeloid cells (e.g., brighter CD33 on monocytes than on granulocytes), thus facilitating the distinction between these cell types on the ungated dot plots correlating FSC with the respective myeloid antigens (Figures 4.14a and 4.22b).

4.1.2.5 Plasma cells

In the bone marrow, the brightest $CD38^+$ cells are plasma cells. Under normal conditions, the proportion of plasma cells in the FCM sample rarely exceeds 1% for several reasons,

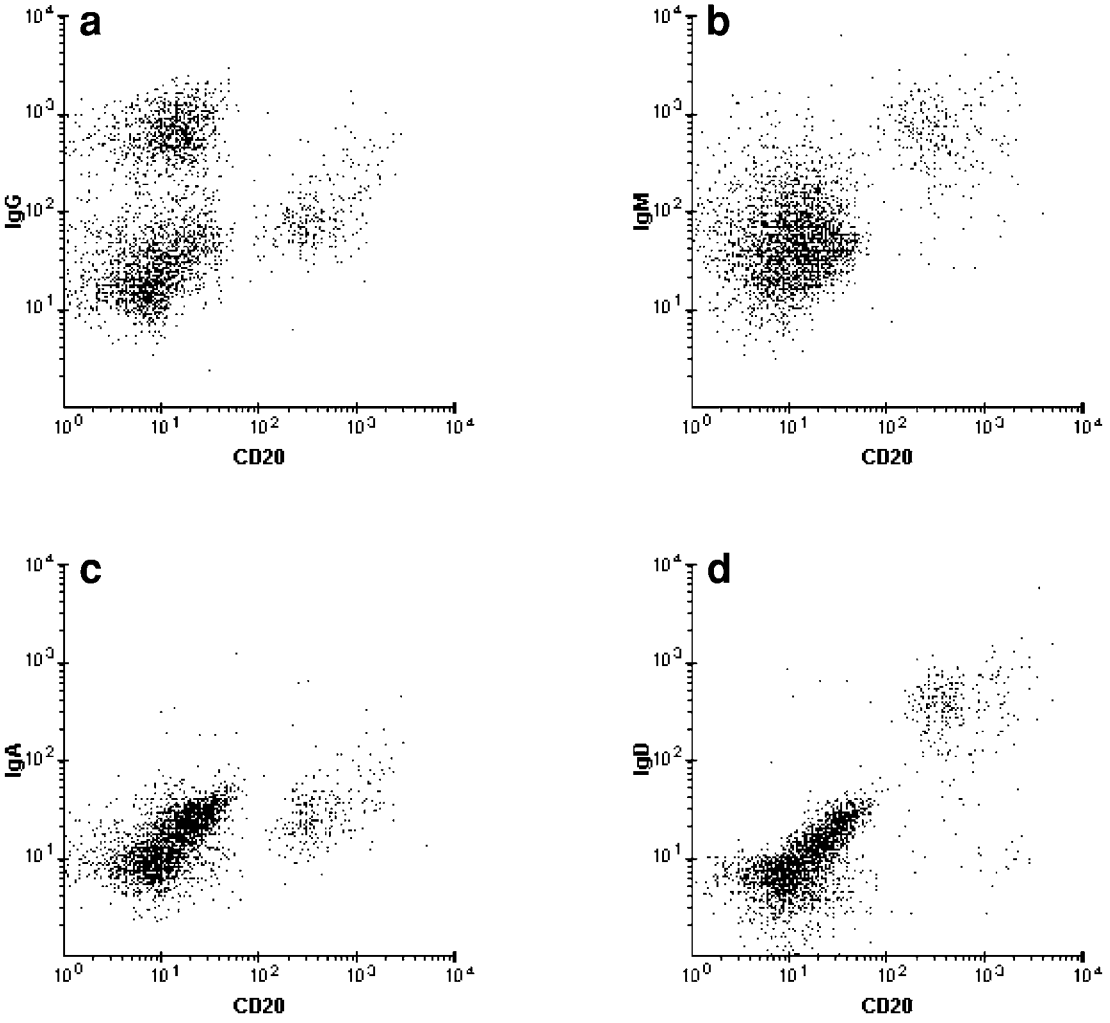

Figure 4.20 Peripheral blood from an HIV-positive patient (continuation of Figure 4.19). (a–d) Gated on MNCs: Marked hypergammaglobulinemia. B-cells are IgM- and IgD-positive. IgA and IgG are negative.

Case study 40

including: (1) the aspirates allocated for FCM analysis are often hemodilute, (2) the distribution of plasma cells in the bone marrow is focal, (3) plasma cells tend to adhere to the spicules and, therefore, are not well released into the cell suspension, and (4) plasma cells may be relatively fragile and therefore easily lost during cell processing. A 5- to 20-fold discrepancy in the proportion of plasma cells between the FCM sample and the aspirate smear is a common occurrence. Therefore, the finding of a plasma cell population above 1% as determined from the CD138/CD38 or CD45/CD38 dot plot (Figure 4.23) may suggest some degree of plasmacytosis, whereby an evaluation of other surface antigens or cytoplasmic light chains will permit the exclusion of a plasma cell dyscrasia. Polyclonal plasmacytosis in solid lymphoid organs is an uncommon occurrence and may be associated with altered immune conditions.

In addition to the very intense CD38 expression, benign plasma cells also display the following immunophenotypic characteristics:

- Polyclonal cytoplasmic light chain expression.
- Lack of surface immunoglobulins.
- Downregulated to absent CD45.

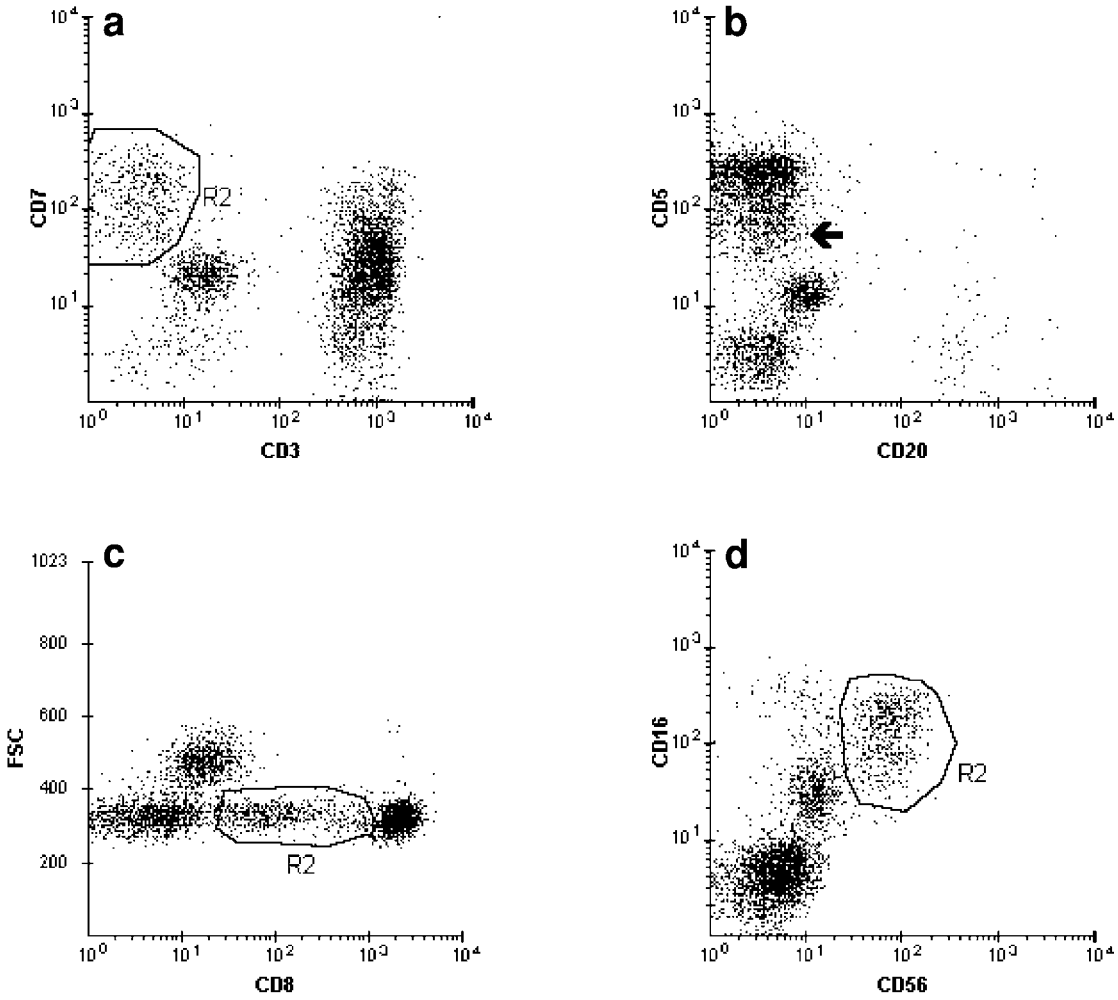

Figure 4.21 NK cells in the peripheral blood. (a–d) Gated on MNCs (which account for 50% of the total cell population). NK cells (R2) are negative for CD3 and express CD7, CD5, CD2 (not shown), CD8, CD16, and CD56. CD5 (arrow) as well as CD2 (not shown) are slightly weaker than on T-cells. CD8 is heterogeneous and dimmer than that on suppressor T-cells. In this sample, NK cells comprise 6% of the cells analyzed.

- Well-expressed CD138.
- The combination of CD19 reactivity and a lack of CD56 (as well as the lower FSC and SSC values) differ from that seen on neoplastic plasma cells.

4.1.2.6 Erythroid precursors

By FCM analysis, the erythroid component in normal bone marrow specimens often appears insignificant because many of the late erythroid precursors (i.e., polychromatophilic and later) are eliminated during the red cell lysis step. This effect can be appreciated by comparing the marrow aspirate smear to the cytospin made after sample preparation. There is variability in the degree of red cell lysis across laboratories, however.

The few antibodies currently available for evaluating erythroid cells include CD71 (transferrin receptor) and anti-glycophorin A (Gly-A). The maturation process from the early erythroid precursor to the erythrocyte stage is accompanied by a decrease in CD45 and an increase in glycophorin A. With normal maturation, the erythroid population consists predominantly of

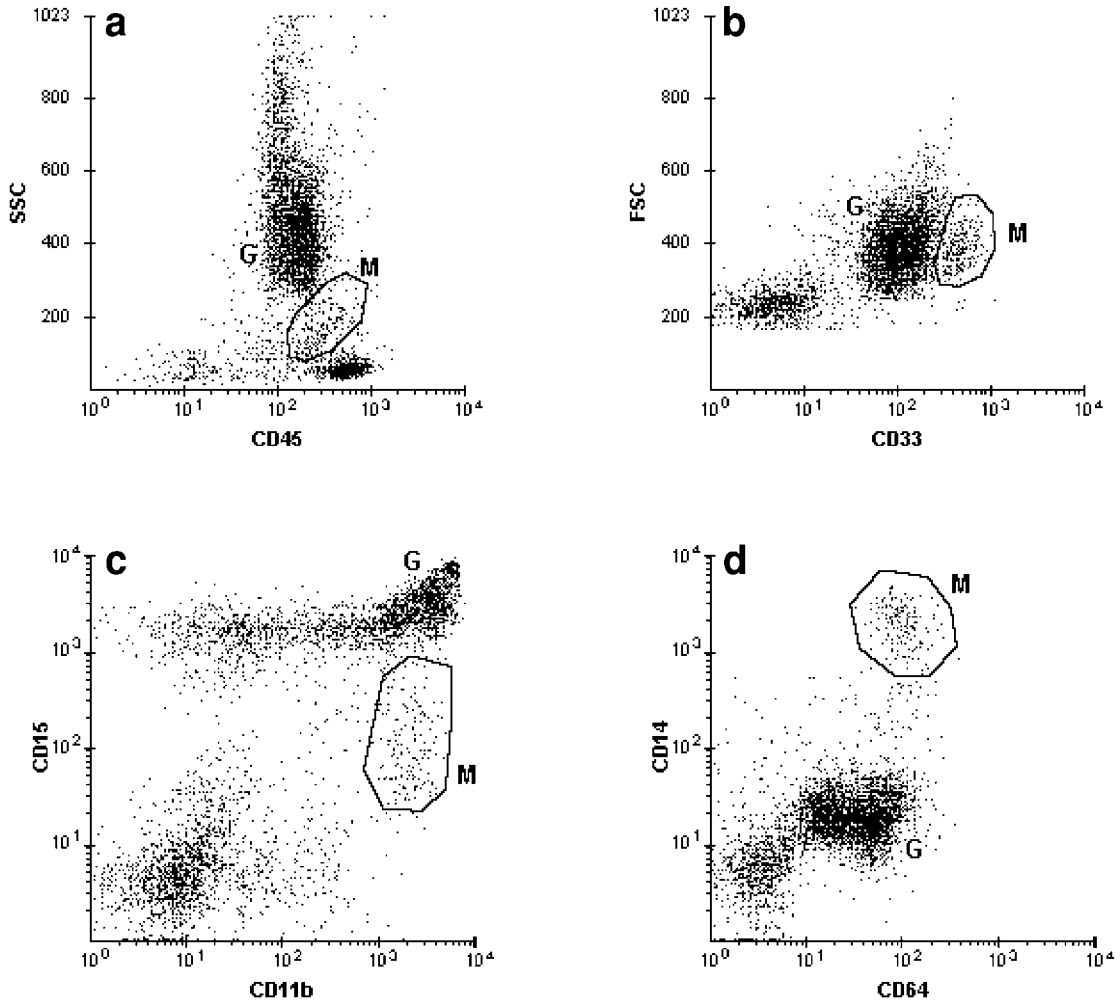

Figure 4.22 Normal bone marrow. Monocytes (M) can be recognized by their location on the SSC/CD45 dot plot (a). The cell size is in the medium range (b). CD33 is brighter than that on granulocytes (G), whereas CD15 is dimmer (c). CD14 is intense (d).

late erythroid precursors; early forms (i.e., basophilic erythroblasts and earlier) are few. On the CD71/Gly-A dot plot, normal erythroid precursors produce a cluster brightly coexpressing the two antigens (Figure 4.24).

In benign conditions with erythroid hyperplasia such as B12/folate deficiency or red cell hemolysis, the erythroid cluster seen on the SSC/CD45 dot plot becomes more conspicuous. Such processes can be best appreciated on the FSC/CD71 dot plot (Figure 4.25). Other preneoplastic or neoplastic conditions with erythroid hyperplasia, such as low-grade MDS or PRV, in which most abnormalities are in the erythroid series, can yield a similar picture. These disorders may display no other FCM abnormalities because the blast level is usually within the normal range and myeloid antigenic maturation is often devoid of overt abnormalities.

Given the effect of the red cell lysis step, the finding of a substantial cluster in the CD45 borderline negative region of the SSC/CD45 dot plot from a blood specimen does not indicate circulating nucleated red cells but rather platelet clumps/giant platelets (Figure 4.26). Reactivity for CD41 and a cell size much smaller than lymphoid cells, as well as the tendency to pick up PE nonspecifically, further confirm the identity of the platelet population.

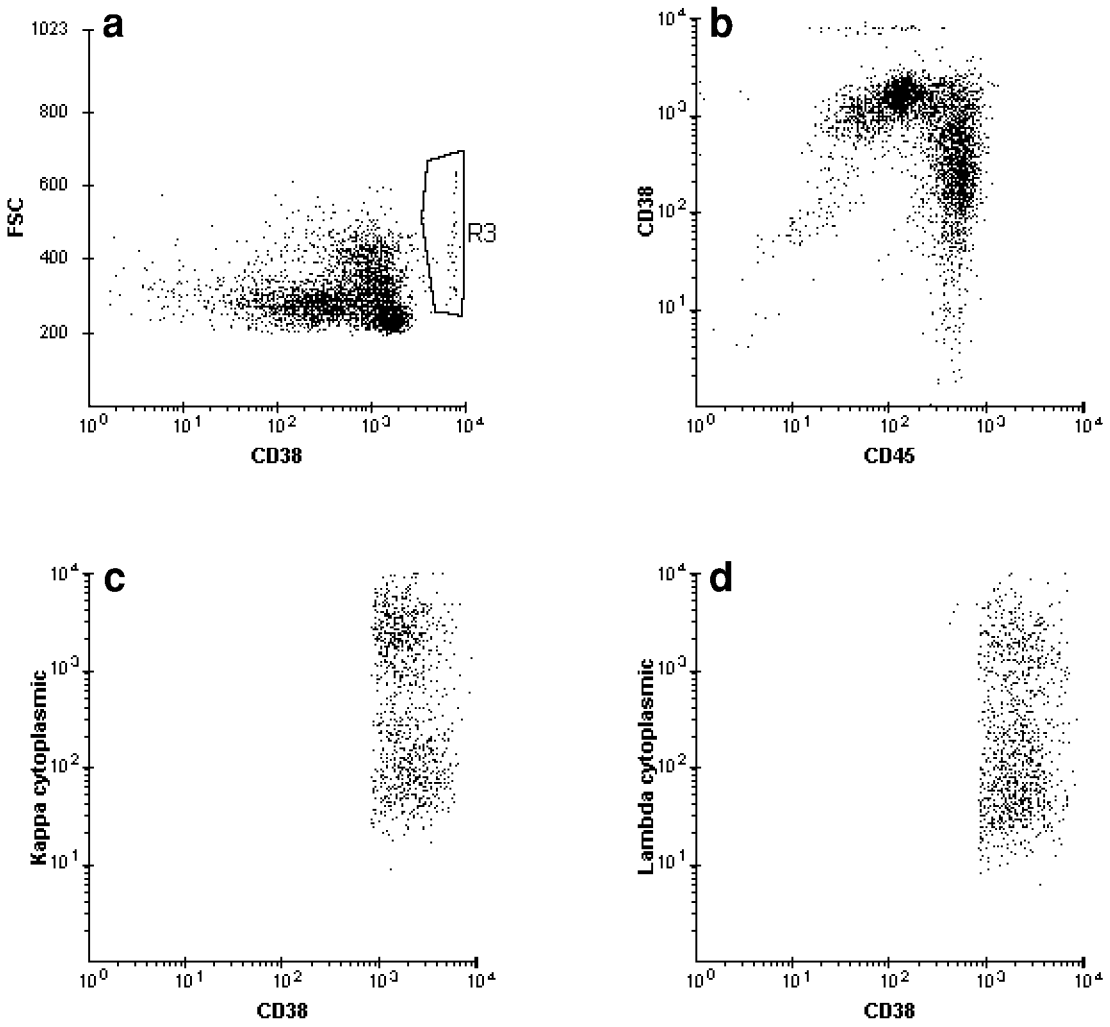

Figure 4.23 Normal bone marrow with mild plasmacytosis. (a,b) A small population (R3) with the brightest CD38 expression and FSC in the medium range. CD45 is weak. (c,d) Gated on the brightest CD38 cells: Both cytoplasmic kappa and lambda are detected. In this sample, plasma cells comprise 1% of the cells analyzed. The corresponding fresh bone marrow aspirate smears contain 10% plasma cells.

4.1.2.7 Maturing myeloid cells

Flow cytometry data analysis on maturing myeloid cells consists of assessing the granularity and antigenic maturation. Overt hypogranularity (an infrequent finding, Figure 4.26a) or hypergranularity (e.g., secondary to G-CSF; *see* Section 4.5.1) can be detected on the SSC/CD45 dot plot. The maturation process is best evaluated on the CD13/CD16 and CD11b/CD16 displays, with the data gated on the granulocyte cluster only. On these two graphics, the myeloid component in the peripheral blood, being composed mostly of mature elements, forms a single well-defined cluster with bright coexpression of CD13, CD11b, and CD16 (Figure 4.27). This appearance is altered if the blood contains a substantial number of circulating intermediate myeloid precursors (e.g., associated with G-CSF effect), in which case the patterns on the CD13/CD16 and CD11b/CD16 dot plots resemble those seen in a hemodilute bone marrow. In contrast to peripheral blood granulocytes, the bone marrow myeloid precursors generate a continuous curvilinear population with heterogeneous coexpression of CD13, CD16, and CD11b, thus reflecting the antigenic maturation of the myeloid elements (Figure 4.27). The

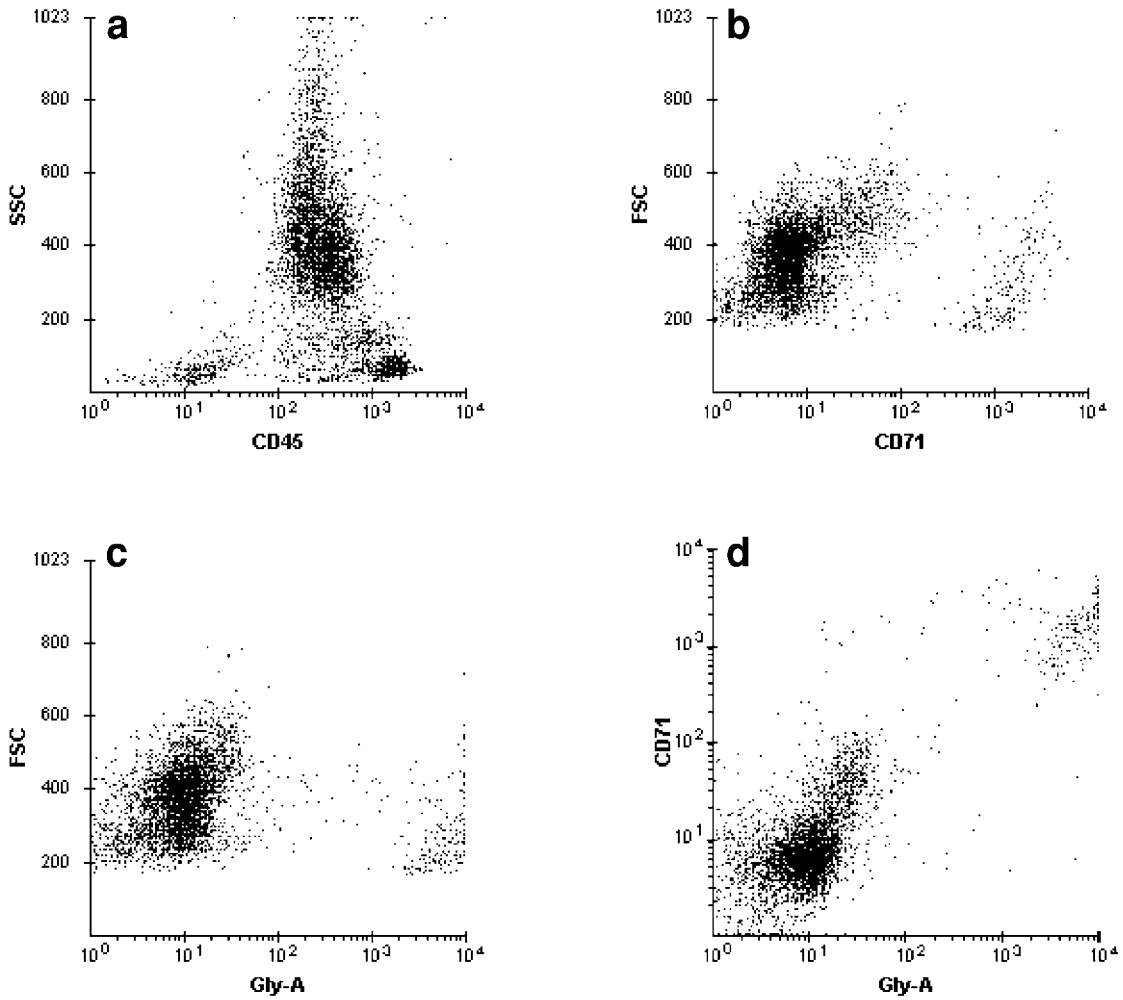

Figure 4.24 Erythroid precursors in a normal bone marrow. (a–d) The erythroid population forms a cluster in the CD45-negative to borderline region. Most of the precursors are of small cell size and display the brightest coexpression of CD71 and glycophorin A.

CD13/CD16 maturation curve is reminiscent of a "wide open checkmark," whereas the CD11b/CD16 curve appears more angular and conical-like to horseshoe-like. Alternatively, the shape of the single parameter CD16 and CD11b histograms (gated on granulocytes) can be used to assess myeloid maturation. In the authors' experience, there exists a good correlation between the antigenic maturation and the morphologic maturation seen on the bone marrow aspirate smears. Abnormalities in the maturation curves can be observed in both neoplastic (e.g., AML, MDS) and benign conditions (e.g., G-CSF therapy). Another useful marker to study myeloid cells is CD10. CD10 is well expressed in mature granulocytes, but at lower levels than on normal B-cell progenitors (Figure 4.27).

4.2 Abnormal samples with a detectable immature neoplastic population

An immature neoplastic population refers to an increased number of cellular events in the blast region on the SSC/CD45 dot plot (Figure 4.28), which can represent one of several diagnostic possibilities, including acute leukemia (*de novo*, relapsed, or residual), MPD with increased blasts, or high-grade MDS. The expression of immaturity markers (CD34, CD117,

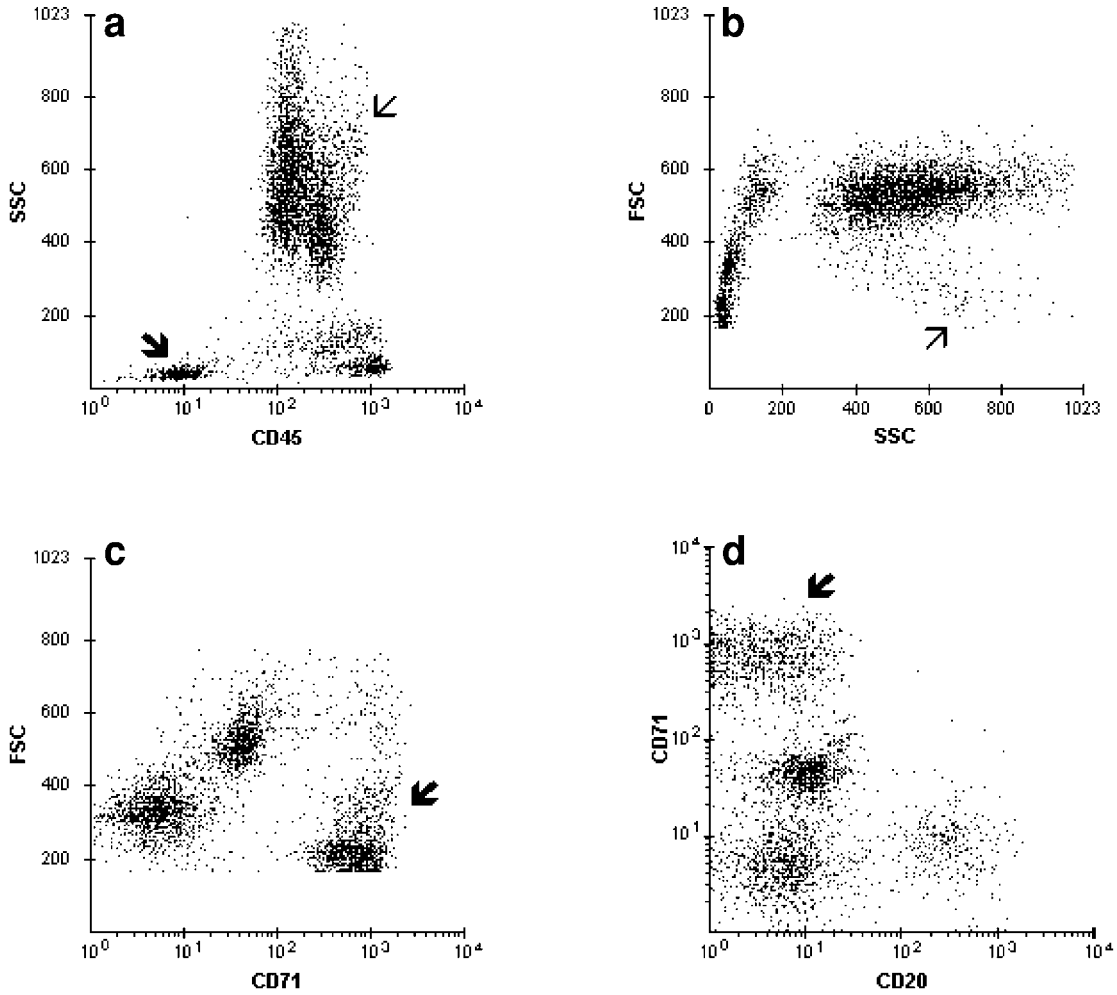

Figure 4.25 Normal bone marrow with a mildly increased number of erythroid precursors and slight eosinophilia. (a,b) A conspicuous erythroid cluster (arrow) present in the CD45-negative region. A small ill-defined cluster of eosinophils (thin arrow) is also visible, best seen on the FSC/SSC dot plot. (c,d) Gated on MNCs: The erythroid precursors range from small to large (most are small) and display the brightest CD71 expression. In this sample, erythroid cells comprise 12% of the cells analyzed. The fresh bone marrow smears contain 33% erythroid cells (myeloid;erythroid ratio1.5;1) and 7% eosinophils.

or TdT), myeloid antigens, or lymphoid antigens is determined from the appropriate FCM graphics to establish the phenotype of the blasts. To facilitate this visual review, it is usually preferable to limit the data on these dot plots to either mononuclear cells (i.e., granulocytes excluded) or the blast cluster only by appropriate gating on the SSC/CD45 dot plot. In addition to evaluating the blast population, the myeloid maturation curves and CD10 expression on granulocytes also need to be assessed, especially if the blast cluster is of myeloid lineage. In myeloid disorders, abnormalities in the CD13/CD16 and/or CD11b/CD16 maturation curves or altered CD10 expression are common (Figure 4.29).

4.2.1 Blasts of lymphoid lineage

If the blast population is of lymphoid origin, either precursor T-cell or precursor B-cell, then the diagnosis is ALL/lymphoblastic lymphoma irrespective of the body site and the relative proportion of tumor cells. One notable exception is the thymus, as encountered in thymic hyperplasia or thymoma, in which the overall phenotype of normal thymocytes is superficially

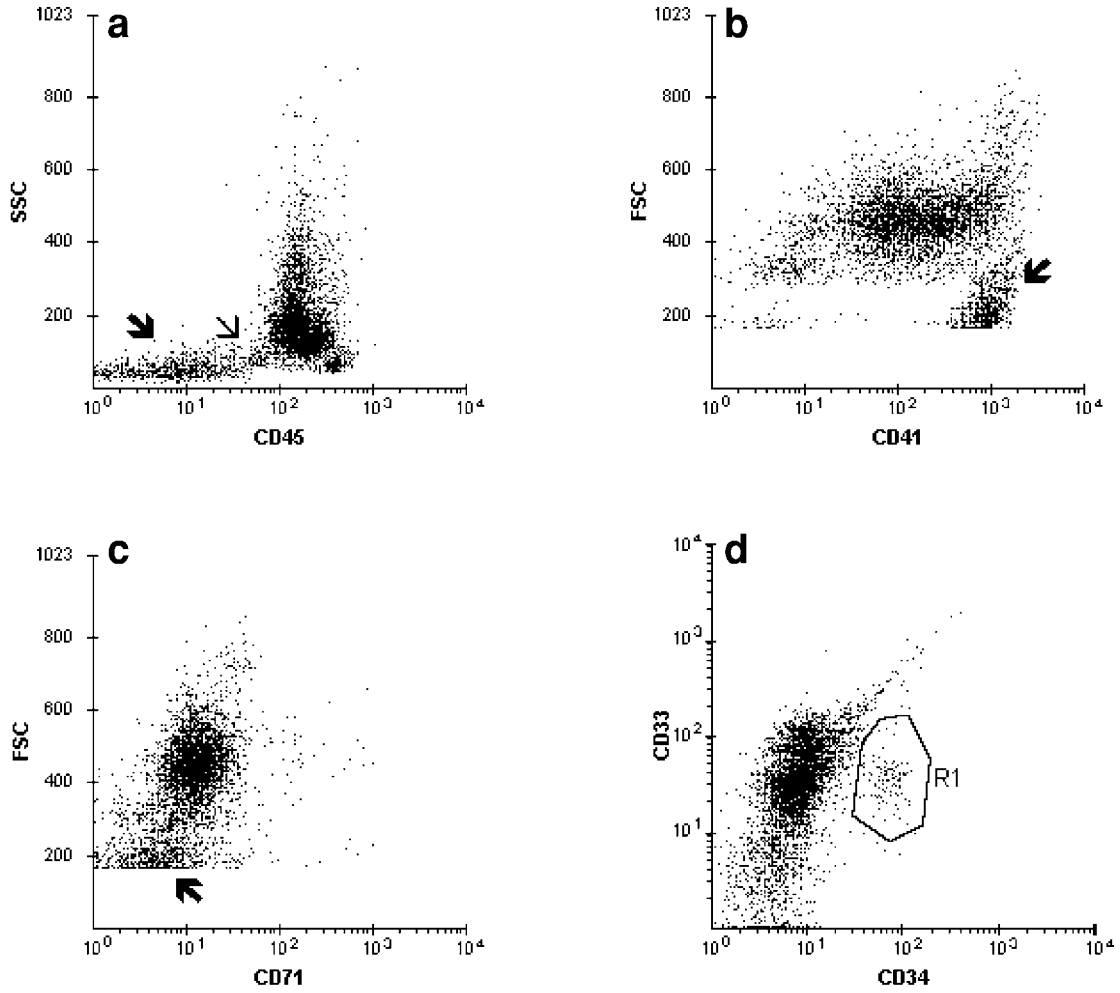

Figure 4.26 Peripheral blood with neoplastic thrombocytosis. (a–c) Giant platelets and platelet clumps form a conspicuous cluster in the CD45-negative to borderline region (arrow), with low FSC and brightest reactivity for CD41. CD71 is negative. A tiny blast cluster is also visible (thin arrow). The granulocytes display low SSC (*see* Figures 4.11b and 4.15a for comparison) and are not well separated from the monocytes. (d) Myeloblasts (R1) comprise 2% of the total cell population.

Case studies 25, 41, and 42

similar to that of T-lymphoblasts. The graphical FCM data are quite dissimilar between thymocytes and T-ALL cells (Figures 3.11 and 3.67), however, with the latter being a more homogeneous population than the former. In those cases of ALL where the involved bone marrow still contains a substantial number of myeloid precursors, the granulocytic maturation curves appear essentially normal (Figure 4.30), unless the ALL originates from an underlying CML (Figure 4.31).

4.2.2 Blasts of myeloid lineage

The differential diagnosis is more complex if the blast population is of myeloid lineage, requiring morphologic correlation with the hemogram, blood, and bone marrow smears to subclassify the disorder (AML vs high-grade MDS vs MPD with increased blasts) according to the currently accepted criteria. This step is especially important if the FCM sample is the bone marrow, where, as already mentioned, hemodilution can artifactually lower the blast proportion. The bone marrow is generally the specimen of choice for analysis in neoplastic myeloid disorders, especially if a further classification of AML into the different FAB subtypes is

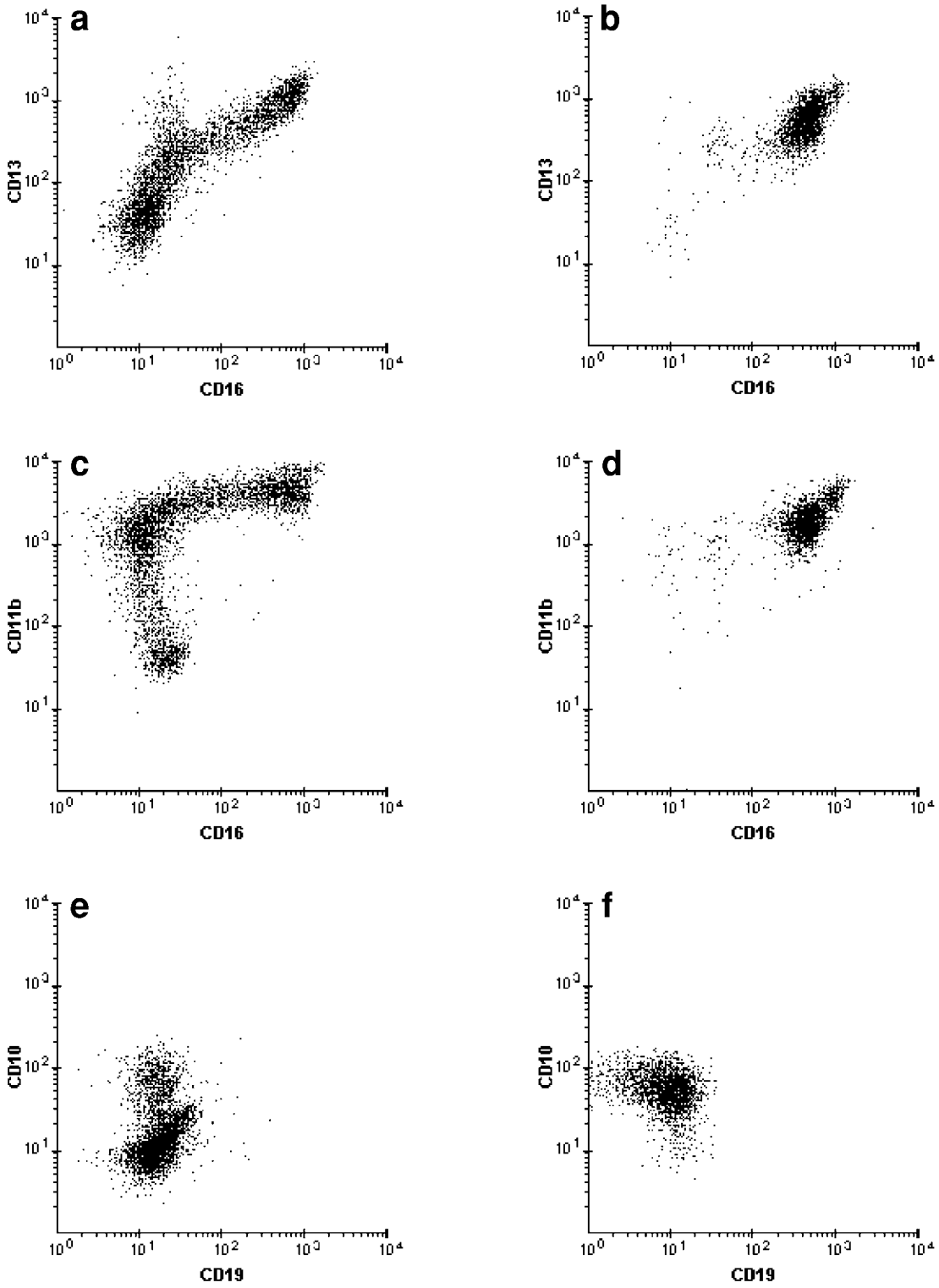

Figure 4.27 Antigenic features of normal myeloid cells in the bone marrow and peripheral blood. Gated on granulocytes: In the blood, the mature granulocytes form a single cluster with bright coexpression of CD13, CD16, and CD11b (b,d). CD10 is also well expressed (f). In the bone marrow, the variable coexpression of CD13, CD16, and CD11b reflect myeloid maturation and differentiation (a,c). CD10 is bimodal, being present on the more mature cells (e).

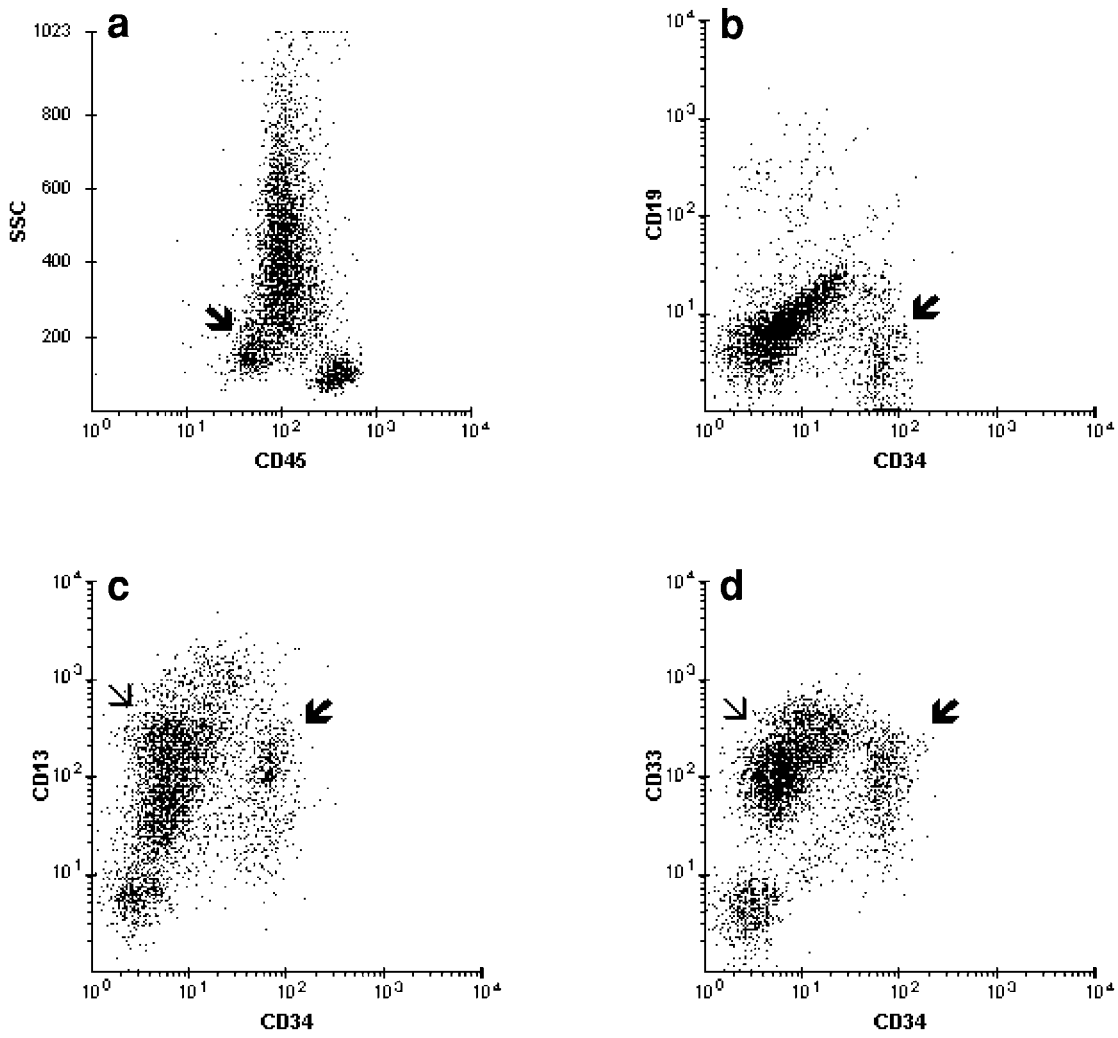

Figure 4.28 Bone marrow with high-grade MDS. (a) A small distinct blast cluster (arrow) is present. (b–d) Ungated data: Blasts coexpress CD34, CD13, and CD33 and are distinct from the myeloid precursors (thin arrow). The intensity of CD13 and CD33 on the blasts is relatively heterogeneous. CD19 is negative. Blasts comprise 12% of the cells analyzed.

required. Otherwise, if the blast level in the peripheral blood is that of an overt leukemia (the current criteria fluctuates between 20% and 30%), then FCM analysis of a blood sample is sufficient for establishing the diagnosis of non-M3 AML. A more precise interpretation of AML with monocytic differentiation can be achieved if the monocytic cluster is also prominent (Figure 3.36a,b). However, if both the monocytic and blast clusters in the blood are conspicuous and the proportion of blasts is below the threshold for acute leukemia but higher than that accepted for CMMoL (e.g., in the 10–15% range), then the distinction between AML with monocytic differentiation and CMMoL "accelerated phase" cannot be made with certainty in the peripheral blood.

4.2.2.1 AML

A heterogeneous bone marrow picture, in which blasts are admixed with other maturing hematopoietic elements at the time of the initial presentation, is seen primarily in AMLs with evidence of maturation. The main FAB subtypes of AML that fall into this category include

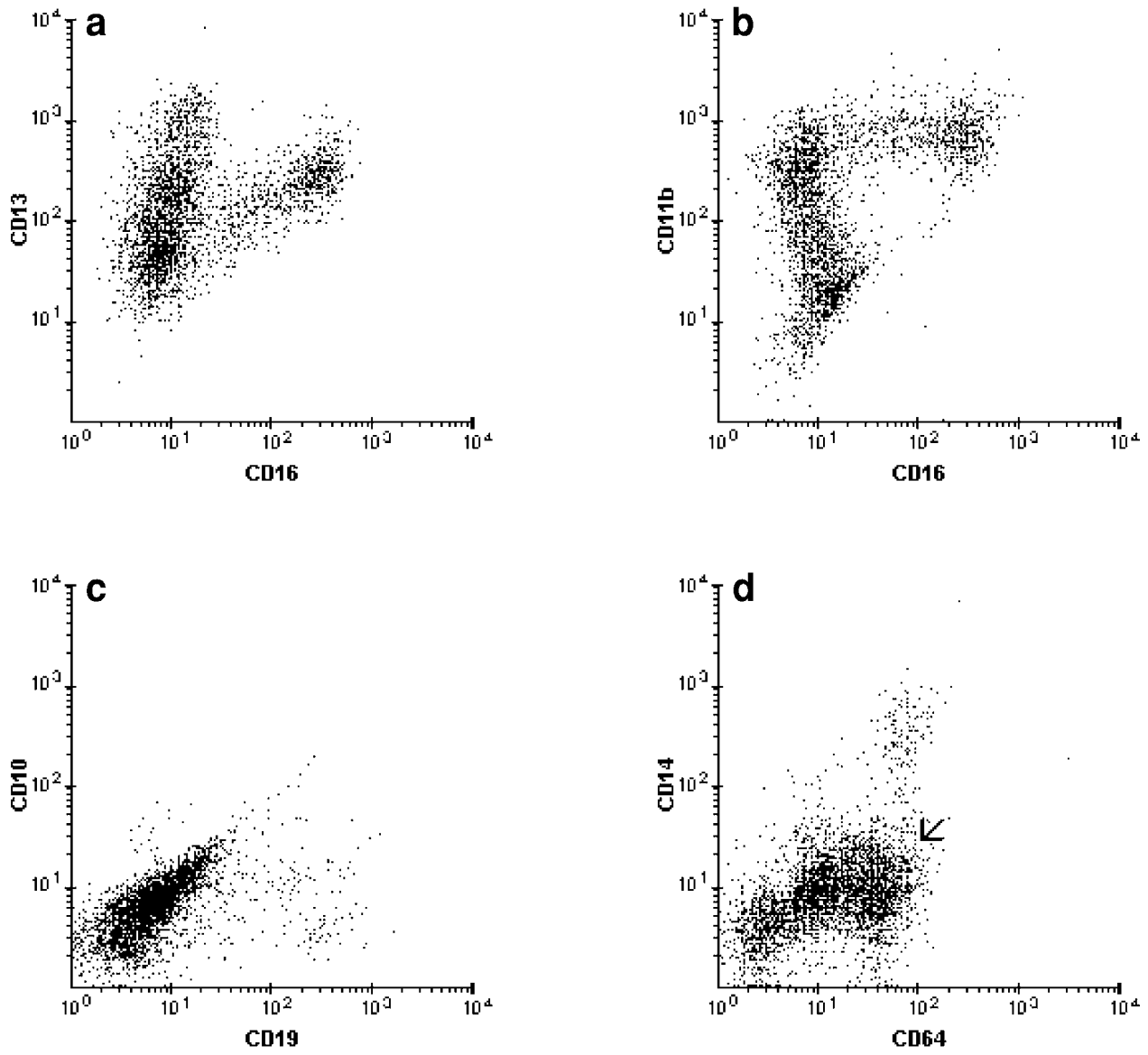

Figure 4.29 Bone marrow with high-grade MDS (continuation of Figure 4.28). (a–c) Gated on granulocytes: Altered myeloid maturation curves with downregulated CD16. There is also loss of CD10 expression. (d) Data ungated: No abnormalities noted in the CD14/CD64 expression on granulocytes (thin arrow).

Case study 43

M2 and M6, as well as M4 and M4E. In AML-M6, the blast population is accompanied by a conspicuous erythroid cluster (Figure 4.32). The relative proportion of erythroid cells by FCM is often not as dramatic as the degree of erythroid hyperplasia seen on the aspirate smears, as many of the late precursors are likely to be eliminated at the red lysis stage during specimen preparation. Inspection of the CD71/Gly-A or CD71/CD45 dot plots may disclose evidence of abnormal antigenic maturation in the erythroid precursors.

The appearance of the FCM dot plots in AML-M4 and M4E varies widely from case to case depending on the relative proportion of the blasts, granulocytic and monocytic components, and whether or not the blast and monocytic populations merge with each other. In many cases, the number of myeloid precursors is minimal, and the blasts and monocytic elements produce a single large merging cluster, as seen on the SSC/CD45 dot plot (*see* Section 3.4.1).

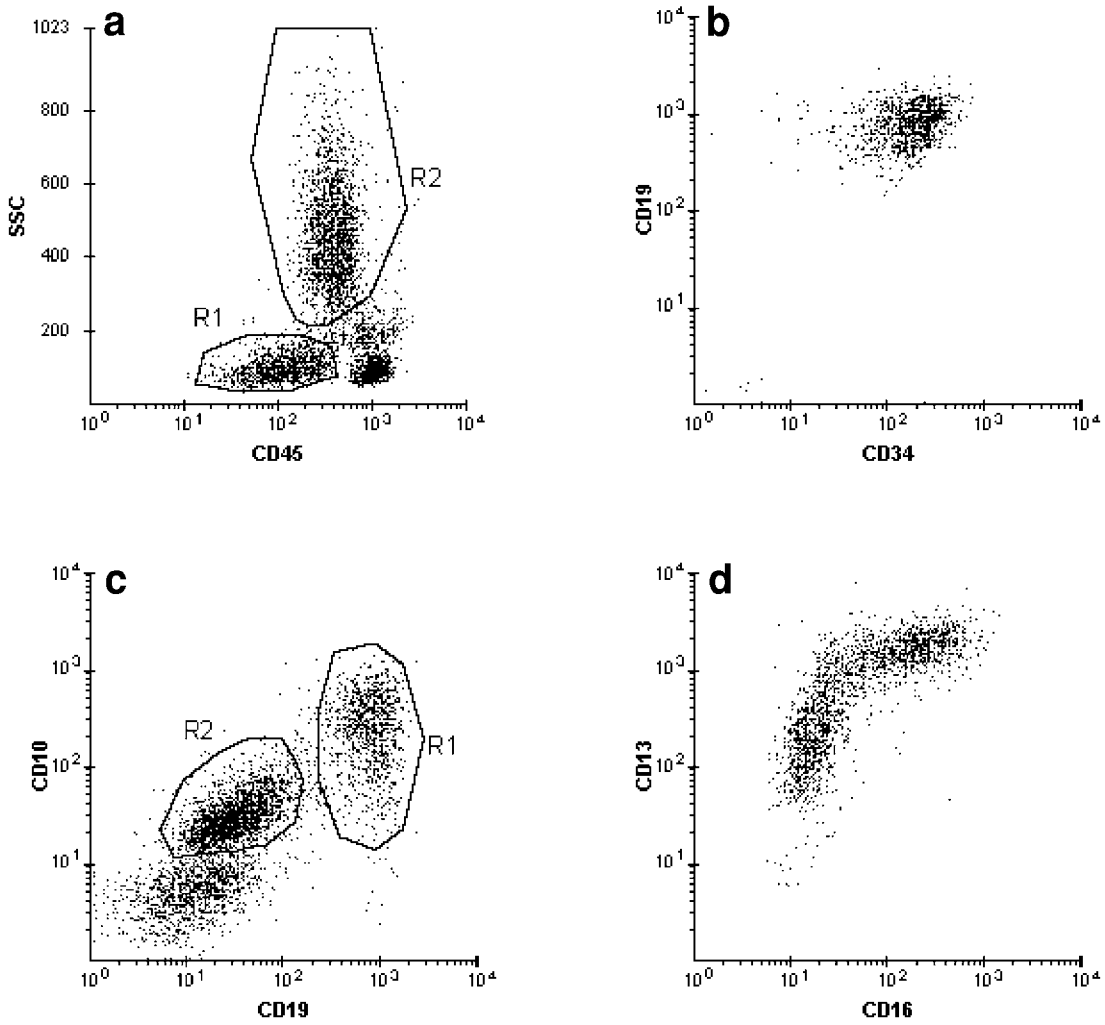

Figure 4.30 Precursor B-ALL. (a,b) Blasts (R1) comprise 20% of the cells analyzed and coexpress bright CD34 and CD19 (CD19/CD34 dot plot gated on R1). (c): Blasts coexpress bright CD10 and CD19. Granulocytes (R2) display weaker CD10 expression and are negative for CD19 (there is higher background fluorescence associated with PE). (d) Gated on R2: Essentially normal CD13/CD16 myeloid maturation curve.

Cases of AML-M4 with a substantial number of granulocytic elements may appear morphologically similar to AML-M2, especially if the monocytic component is not cytologically obvious. Furthermore, the NSE stain in AML-M4E is often negative and the abnormal eosinophils (Plate 12) may not be conspicuous. The FCM graphics in such instances are most helpful, as the monocytic cluster on the SSC/CD45 dot plot is insignificant in AML-M2, but more prominent in M4 and M4E (Figures 4.33 and 4.34). Occasionally, the SSC/CD45 display in AML-M2 may mimic that seen in monocytic disorders, however, as a result of the unusual location and shape of the blast cluster (Figure 4.35). Another useful feature pointing toward AML-M4 is the "trail" pattern on the CD14/CD64 dot plot, which corresponds to the spectrum of immature and mature monocytes (Figure 4.33) showing heterogeneous CD14 expression. The blast population itself may not express any monocytic associated antigen, however (e.g., in AML-M4E, *see* Section 3.5.1).

Case studies 44–46

The eosinophilic component in AML-M2Eo (Figure 4.36) or M4E may be visible on the SSC/CD45 and FSC/SSC dot plots, as well as on the bivariate displays of FSC vs myeloid antigens.

Case study 47

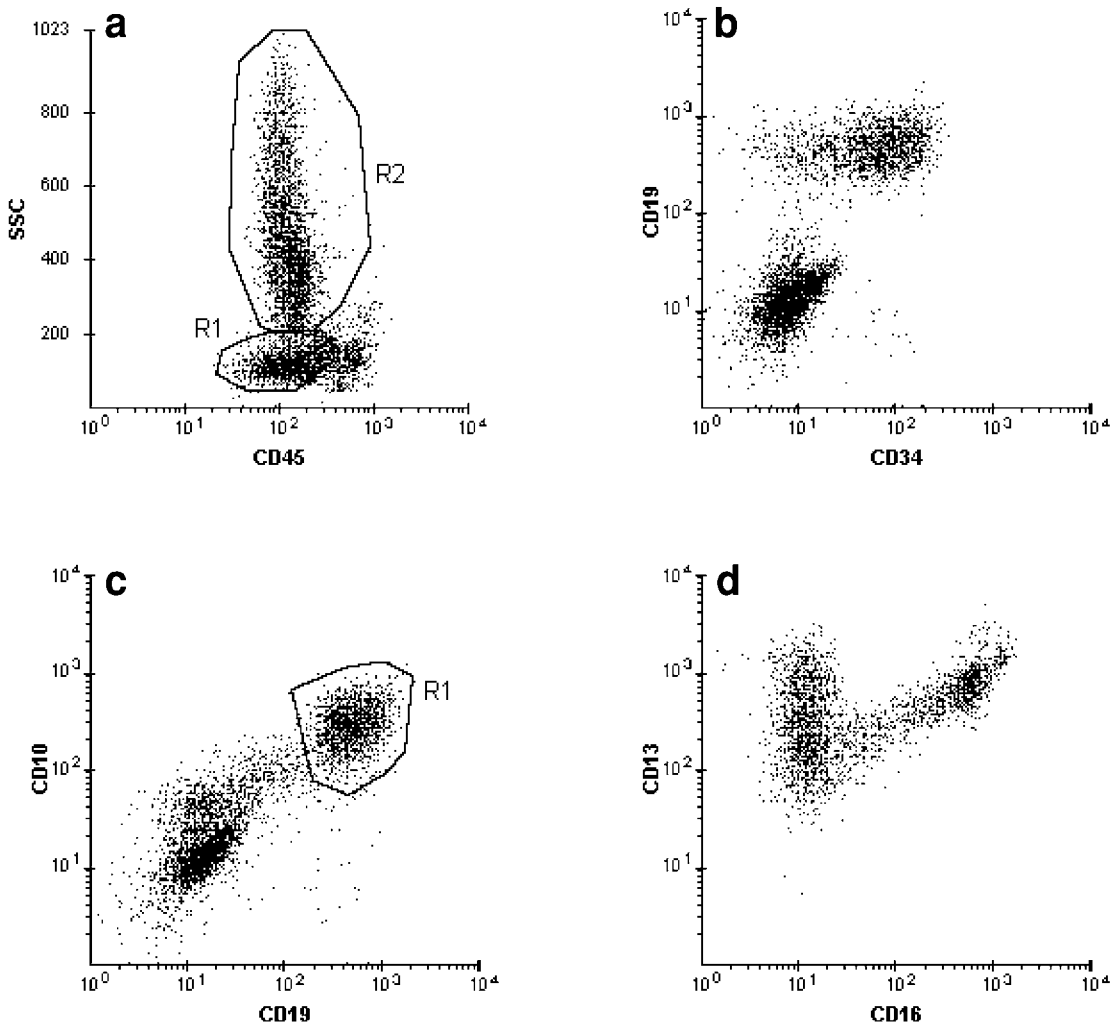

Figure 4.31 CML with lymphoid blast crisis. (a–c) Blasts (R1) comprise 35% of the cells analyzed and coexpress bright CD19, CD34, and CD10. Weak CD10 is present on a proportion of the myeloid precursors. (d) Gated on R2: Abnormal myeloid maturation curve similar to that in Figure 4.29a.

The phenotypic profile of the blast population in non-M3 AML varies widely from case to case. Other myeloid antigens besides CD13 or CD33 may be expressed. In some cases, a lymphoid-associated antigen or CD56 may also be present. As a result, a given combination of antigenic features present at the time of diagnosis can serve as a "fingerprint" for the FCM analysis of subsequent bone marrow samples to assess the patient's disease status and response to therapy (*see* Section 3.5.1.1).

In any of the above-described non-M3 AMLs, the myeloid elements may also display phenotypic abnormalities such as downregulated CD16, CD11b (Figures 4.32 and 4.35), or CD10 expression (Figure 4.36), especially when the leukemia is preceded by a myelodysplastic process.

4.2.2.2 High-grade MDS and MPD with increased blasts

The graphical FCM data in high-grade MDS (Figures 4.28 and 4.37), where the blast count is, by current criteria, between the threshold accepted for clinical remission and that for overt acute leukemia, are closely similar to that observed in AML. The blast cluster is smaller, how-

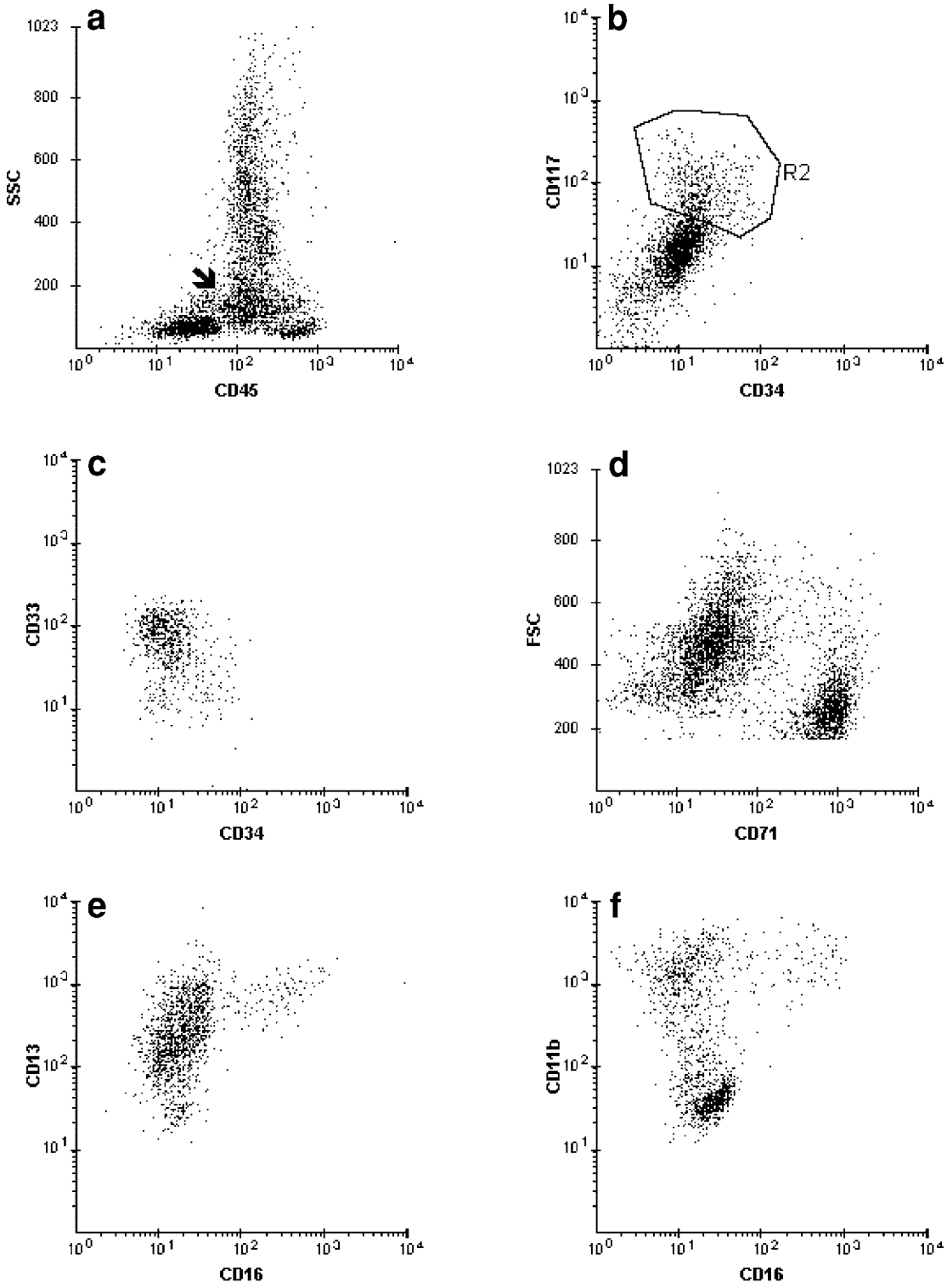

Figure 4.32 AML with erythroid hyperplasia. (a) Conspicuous erythroid cluster. The blast cluster (arrow) is poorly separated from the granulocytic cluster. (b) Gated on MNCs: Blasts (R2) are weakly positive for CD117; a subset expresses dim CD34. (c) Gated on blasts: CD33 and CD13 (not shown) are expressed. Blasts comprise 15% of the cells analyzed. (d) Increased erythroid precursors: Intense CD71 expression. (e,f) Gated on granulocytes: Abnormal maturation curves with downregulated CD16 and CD11b.

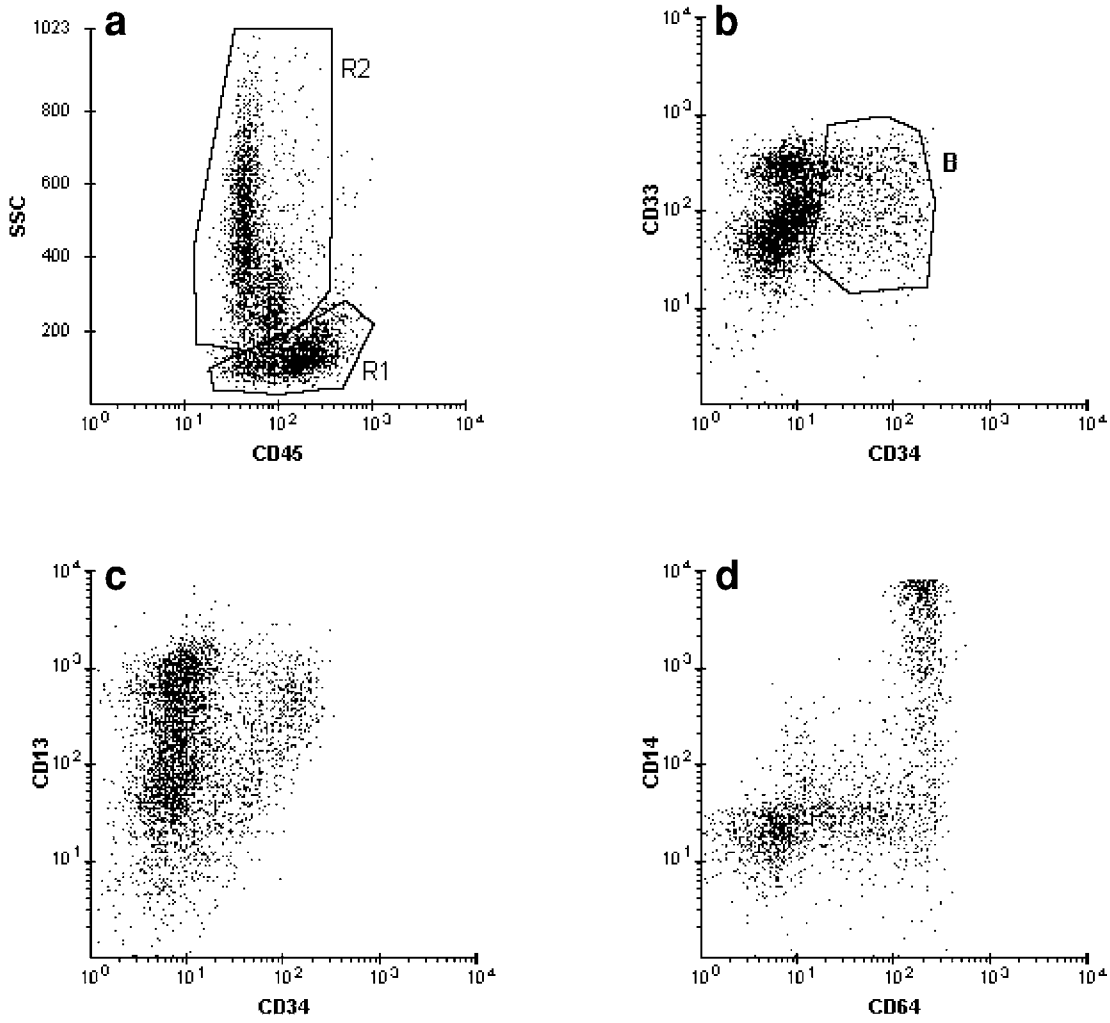

Figure 4.33 AML with a monocytic component. (a) Merging blast and monocytic clusters. (b,c) CD34-positive blasts (B) comprise 20% of the cells analyzed. CD13 and CD33 are expressed. (d) Gated on R1: CD14/CD64 trail pattern reflecting the heterogeneity of monocytic cells at various stages of maturation. When compared to the isotype-matched negative control (not shown), blasts are CD14-negative. CD64 is partially expressed.

ever. Abnormalities in the granulocytic maturation curves are common. The myeloid cluster may display abnormally low SSC signals (Figure 4.37). The corresponding aspirate smears demonstrate abnormal morphology with an excess of blasts and left-shifted myeloid maturation along with qualitative abnormalities such as hyposegmentation and hypogranulation. CD10 may also be downregulated. Because both the FCM and morphologic pictures of the bone marrow in high-grade MDS can closely resemble that of residual disease/impending relapse of AML, knowledge of the antecedent clinical history or availability of prior FCM and bone marrow data is critical.

An overt blast cluster of myeloid lineage, along with abnormal myeloid maturation curves similar to that seen in AML and MDS may also be observed in certain MPDs with increased blasts such as CML in accelerated phase. The bone marrow morphology may not be distinguishable from that of high-grade MDS. Knowledge of the peripheral blood data becomes important to discriminate between these two groups of disorders. The diagnosis of CML with increased blasts is made straightforward by the conspicuous presence of basophils on the SSC/CD45 dot plot, a finding more easily appreciated in the blood than in the bone marrow

Case studies 48 and 49

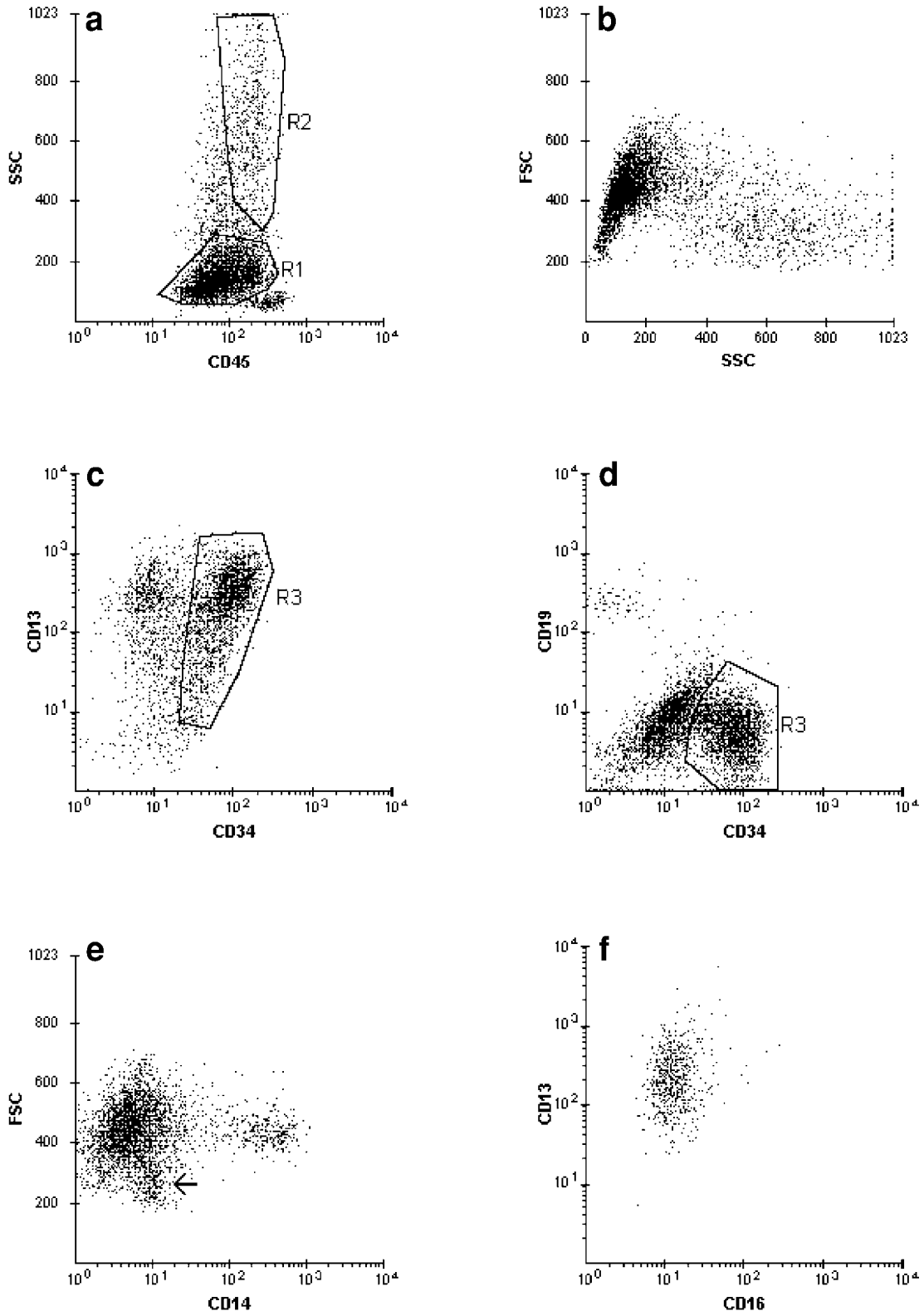

Figure 4.34 AML-M4E (morphology shown in Plate 12). (a,b) Merging blast and monocytic clusters (R1). Eosinophils (R2) are conspicuous, best seen on the FSC/SSC dot plot by their low FSC. (c,d) Blasts (R3) comprise 49% of the cells analyzed and express CD34, CD13, and CD33 (not shown). CD13 is of variable intensity. CD19 is negative. (e) Blasts and eosinophils (arrow) are negative for CD14 and CD64 (not shown). (f) Gated on R2: CD16 is absent on eosinophils.

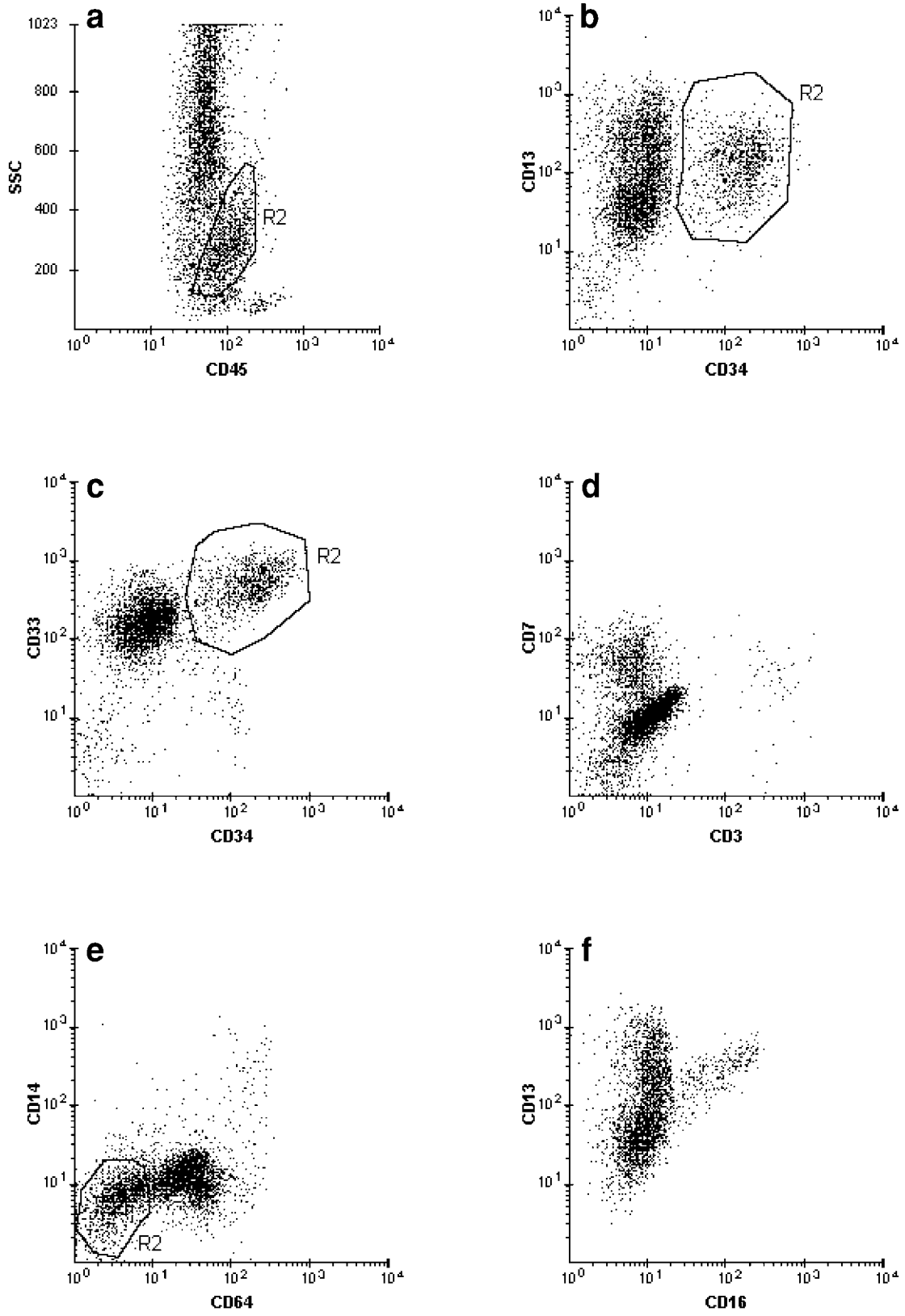

Figure 4.35 AML with maturation. (a) The SSC/CD45 picture is reminiscent of a monocytic disorder because of the shape of the blast cluster (R2). (b–e) Blasts comprise 24% of the cells analyzed and are positive for CD34, CD13, CD33, and CD7. CD14 and CD64 are not expressed. (f) Gated on granulocytes: Altered CD13/CD16 myeloid maturation curve with downregulated CD16.

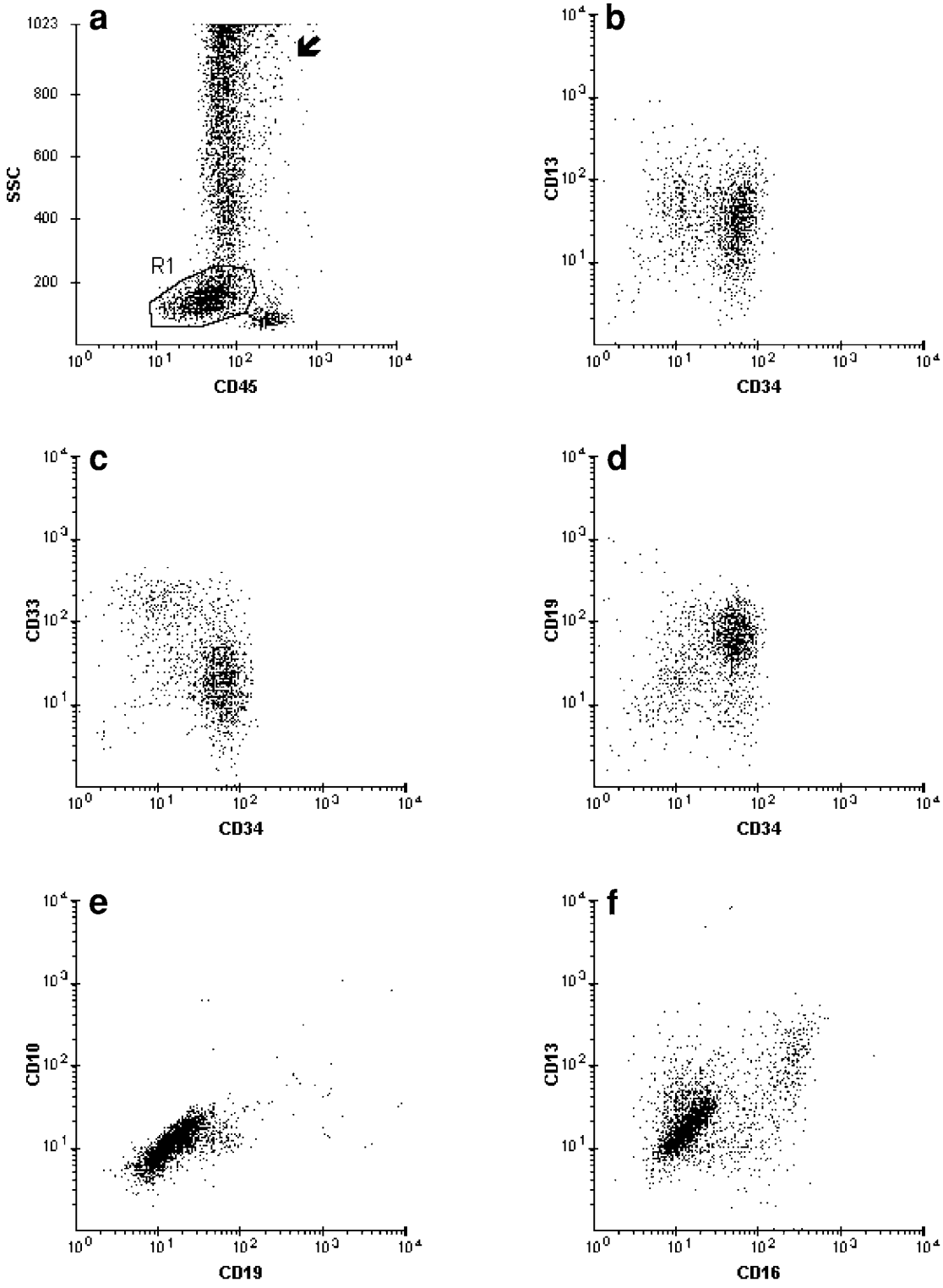

Figure 4.36 AML-M2Eo (morphology shown in Plate 20). (a) A conspicuous blast cluster (R1) and an ill-defined population of eosinophils (arrow). (b–d) Gated on R1: Blasts comprise 30% of the cells analyzed and coexpress CD34, CD13, CD33, and CD19. A small portion of the blasts lack CD34. (e,f) Gated on granulocytes: Myeloid precursors are antigenically abnormal, with loss of CD10 and downregulated CD13, CD16, and CD11b (not shown). Cytogenetics revealed t(8;21).

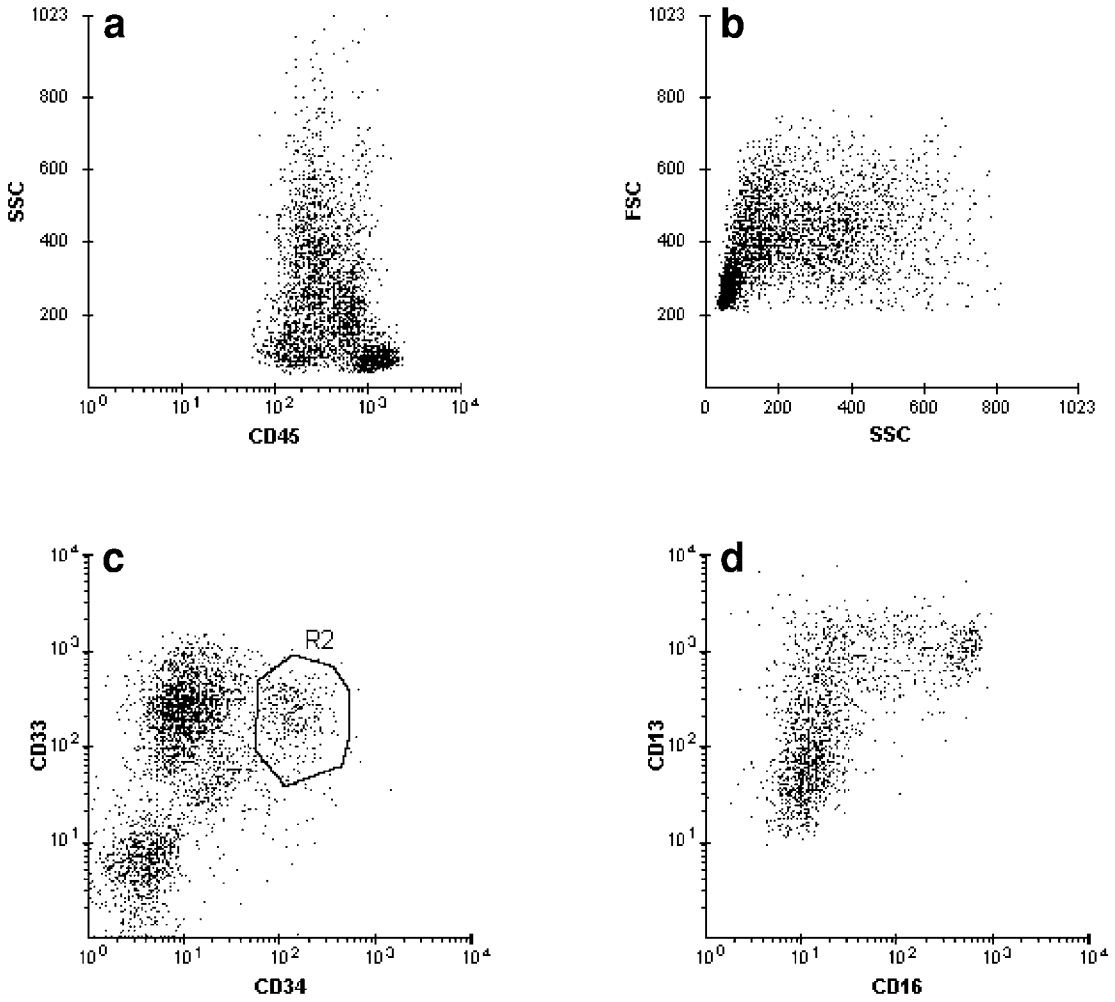

Figure 4.37 Bone marrow with high-grade MDS. (a,b) Decreased SSC on granulocytes. There is poor separation of the granulocytic, monocytic, and blast clusters on the SSC/CD45 dot plot. (c) Blasts (R2) comprise 8% of the cells analyzed and express CD34, CD33, and CD13 (not shown). (d) Gated on granulocytes (using the FSC/SSC dot plot): Altered myeloid maturation curve with downregulated CD16 and CD13 (partially).

(Figure 4.38). The manifestation of MPD/CML in the peripheral blood, with abundant circulating immature myeloid precursors, may produce an FCM and morphologic picture similar to that of the bone marrow.

4.3 Minimal residual disease

The study of MRD has been focused on disorders with blastic proliferations, namely acute leukemias. The evaluation of MRD by FCM analysis requires (1) knowledge of the detailed antigenic features present on the leukemic cells at the time of the initial diagnosis and (2) data acquisition on a large number of events (in the range of one million) using a limited antibody panel tailored to the phenotype sought after. FCM data analysis, in turn, is centered on those dot plots and histograms most useful for showing the known antigenic characteristics of the leukemic blasts and, where applicable, separating these from the normal cells with a similar phenotype. A typical example is the evaluation of MRD in precursor B-ALL, whereby the dot

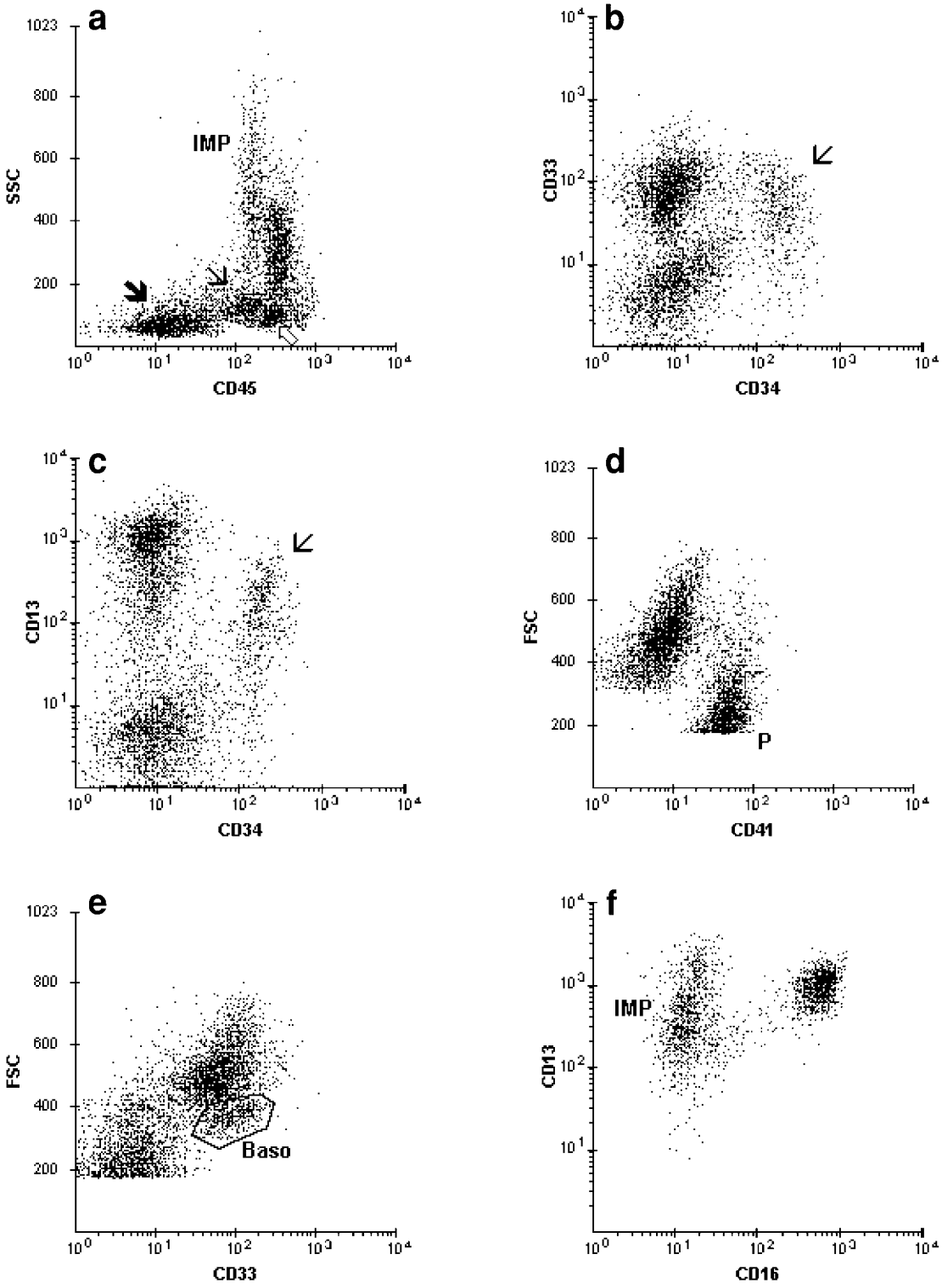

Figure 4.38 Peripheral blood: CML with 14% blasts. (a–f) Blasts (thin arrow) express CD34, CD13, and CD33. Platelet clumps/giant platelets (arrow) display dim CD45, but intense CD41 (P). Basophils (open arrow), located between the lymphoid and hematogone regions on the SSC/CD45 dot plot, express CD33 (and other myeloid markers) similar to granulocytes, but display lower FSC (Baso). (f) Gated on granulocytes: CD16 is downregulated on the circulating intermediate myeloid precursors (IMP).

plots TdT/DNA content, CD10/CD20, and CD58/CD19 are some of the most useful graphics (Figures 2.14, 3.39, and 3.41) for differentiating leukemic blasts from bone marrow B-cell precursors (*see* Section 3.5.2). In AML, the detection of residual disease relies on the presence of phenotypic aberrancies identified at the time of diagnosis (*see* Section 3.5.1.1). When such aberrancies are not observed, molecular genetics may be helpful if the AML is associated with certain specific genetic abnormalities for which molecular probes are currently available.

4.4 Abnormal samples with detectable mature neoplastic populations

The finding of an abnormal mature B- or T-cell population is virtually synonymous with involvement by an LPD/NHL. In patients with overt systemic involvement by LPD/NHL, the disease in the lymph node may progress to a higher-grade large cell lymphoma while the bone marrow involvement remains unchanged and composed of small neoplastic cells. This asynchronous picture is a well-known phenomenon in FCC lymphomas. Similarly, in CLL/SLL, the relative proportion of activated cells in the lymph node is higher than that present in the blood or bone marrow.

In the bone marrow or blood involved by LPD/NHL, the SSC/CD45 dot plot can appear deceptively normal, especially if the tumor cells are small (Figures 4.39 and 4.40). In disorders such as HCL, involvement by small cell lymphoma, Sezary syndrome, and the early stages of CLL or LGL leukemia, benign cells in the background may obscure a small population of tumor cells. If the neoplastic cluster is relatively conspicuous, subtle abnormalities such as slightly downregulated CD45 expression in the lymphoid cells can be appreciated (*see* Section 3.4.3). In such instances, the lymphoid cluster may extend toward the left into the hematogone region. In involvement by large cell LPD/NHL, the neoplastic cluster is usually more easily discerned on the FSC/SSC or FSC vs fluorescence displays (Figures 2.9 and 3.64).

4.4.1 Abnormal mature B-cells

The most efficient way to detect abnormal B-cells in a heterogeneous sample is by dual-parameter staining of surface light chains and pan B-cell antigens. Heterogeneous specimens, especially those derived from solid tissue, usually contain a substantial number of benign reactive B-cells in addition to malignant B-cells. In some cases, the benign component predominates. In the authors' experience, CD20 has proven to be most useful in separating the malignant and benign B-cell populations from each other. Depending on the type of lymphoma, the neoplastic cells often display either brighter or weaker CD20 than the benign cells (Figures 1.1, 3.19, 4.10, 4.39, and 4.41). On the dot plots that correlate CD20 and surface light chains, this differential in CD20 intensity permits the identification of the monoclonal cluster. In most cases, the picture is less clear-cut on the light chain/CD19 dot plots, as both the malignant and benign populations often display similar CD19 intensities (Figures 3.19, 4.39, and 4.41). The sensitivity of dual parameter staining with CD20 is sufficient for detecting very low numbers of abnormal B-cells, such as in HCL, "T-cell rich B-cell" lymphoma, or minimal involvement by FCC lymphoma in which the corresponding cytologic or histologic preparations are negative by light microscopy.

The heterogeneity of the B-cell component in B-cell LPD/NHL may also be appreciated on the FSC/CD20 or FSC/CD19 dot plots, which often show several B-cell clusters differing by cell size and CD20 (or CD19) intensity (Figures 1.1 and 4.41). By evaluating the FSC/CD20 and light chain/CD20 dot plots together, it is possible to deduce which B-cell cluster(s) is neoplastic and calculate its relative proportion. Alternatively, a gate is drawn systematically around each of the B-cell clusters present on the FSC/CD20 (and/or FSC/CD19) dot plot, and the neoplastic cluster(s) is identified based on the pattern of light chain distribution seen on the

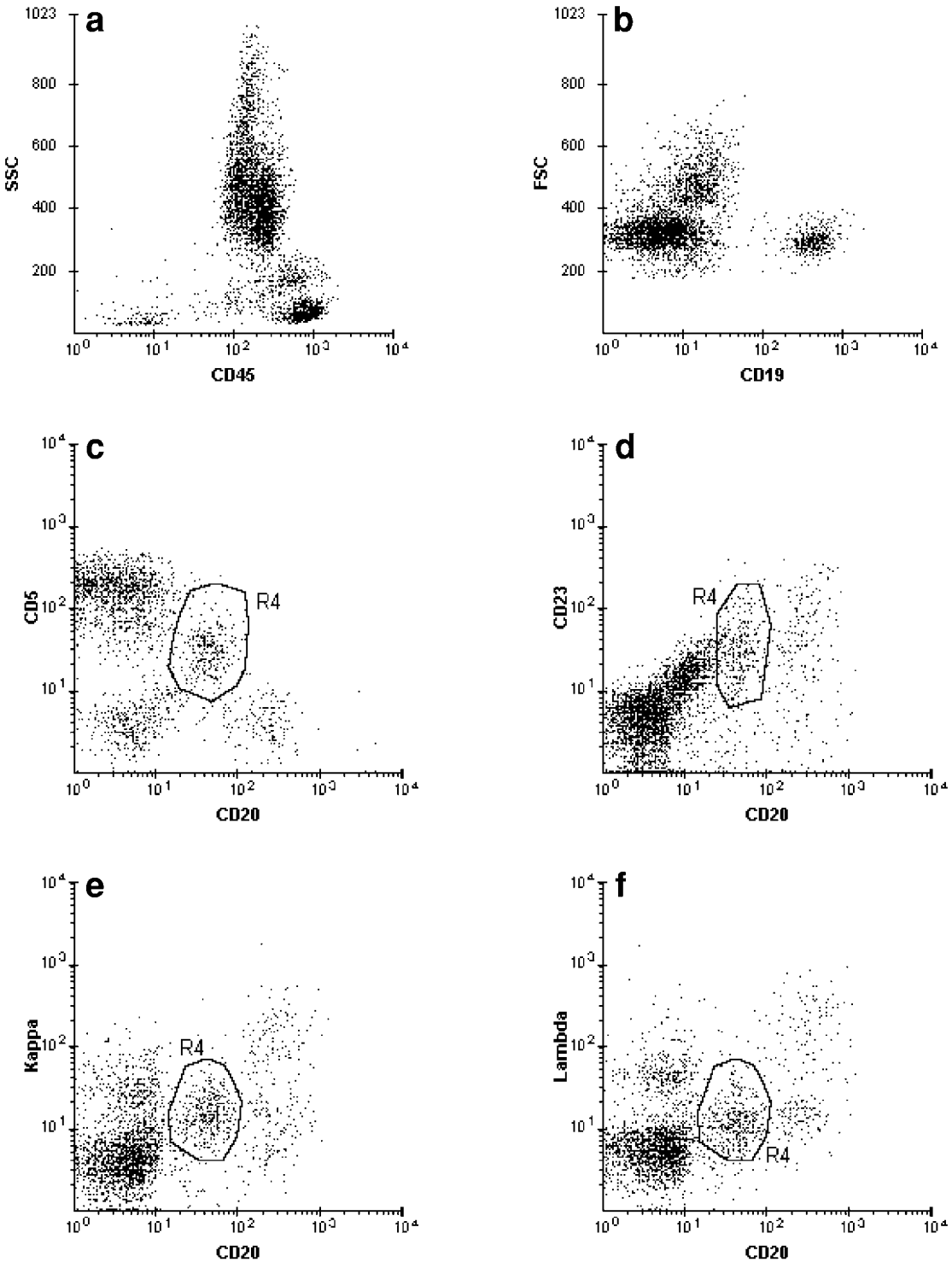

Figure 4.39 Bone marrow with 2% residual CLL. (a) Essentially normal SSC/CD45 picture. (b–f) Gated on MNCs: The small population of small B-cells with homogeneous CD19 expression is actually composed of two populations differing in CD20 intensity. The population with dimmer CD20 (R4) coexpresses CD5 and CD23 but has no detectable light chain. CD20 intensity is also less than CD19. The population with brighter CD20 is polyclonal.

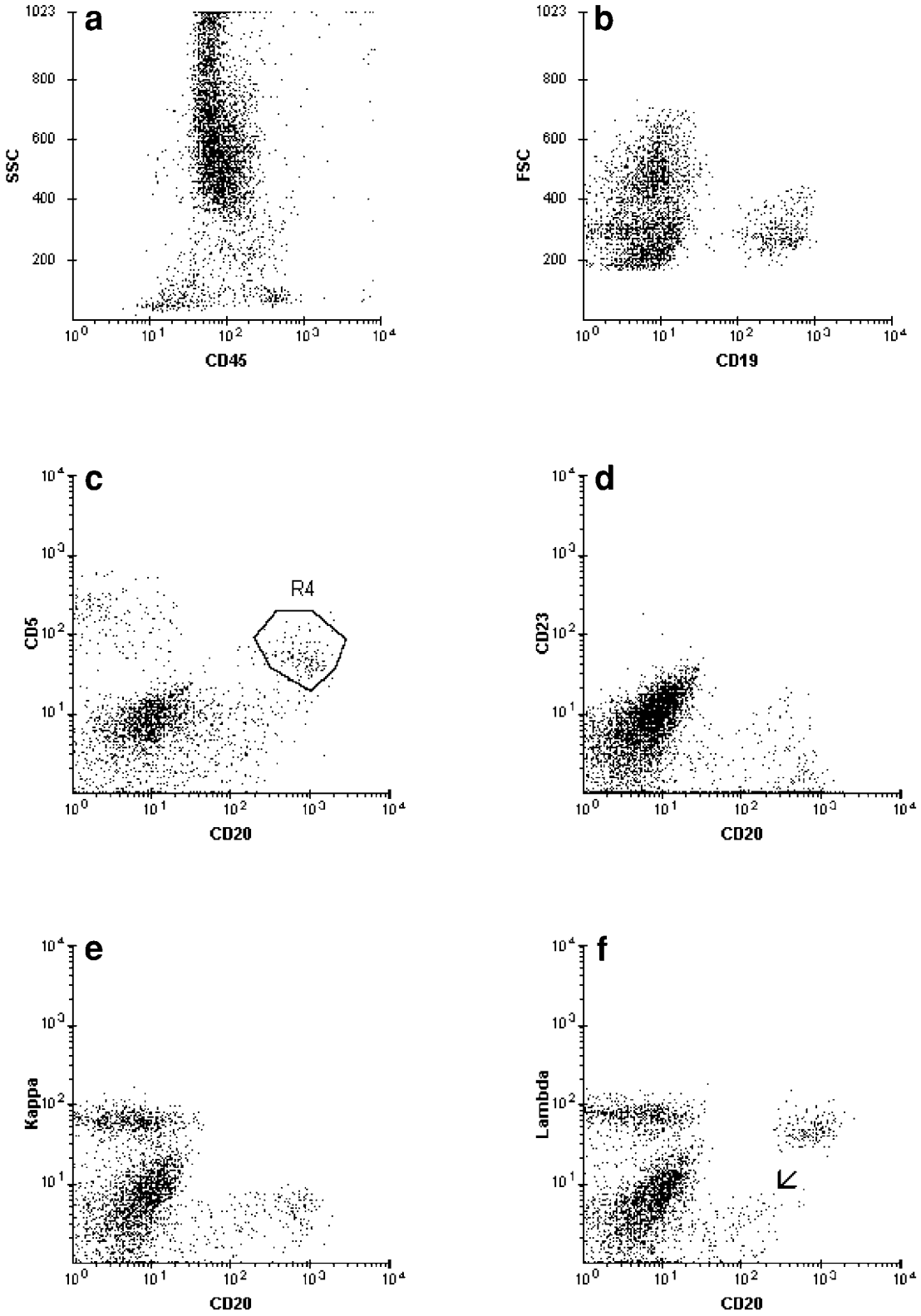

Figure 4.40 Bone marrow with minimal involvement by MCL (negative morphology on the corresponding aspirate smears and core biopsy). (a) Essentially normal SSC/CD45 picture. The small population of B-cells with homogeneous CD19 expression (b) consists of two populations differing in CD20 intensity. (c–f) Gated on MNCs: The brighter CD20 (R4) cells are $CD5^{+}$ $CD23^{-}$. Lambda is well expressed and CD20 slightly brighter than CD19. Cells with variable and weaker CD20 are hematogones (arrow).

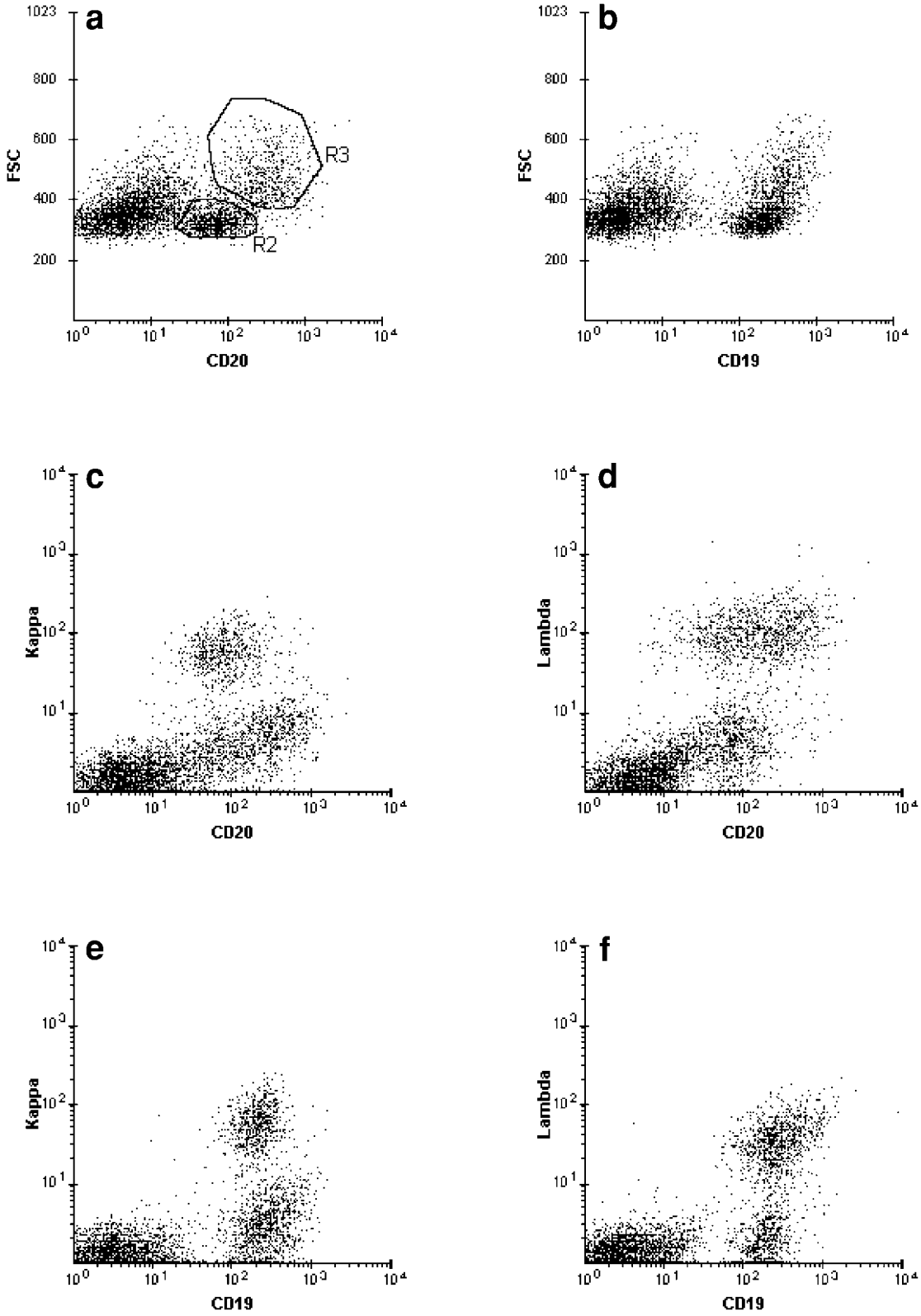

Figure 4.41 Lymph node with low-grade B-cell NHL NOS, morphologically monocytoid B-cell lymphoma (MBCL) (morphology shown in Plates 39 and 40). (a–f) Two populations of B-cells (R2 and R3) differing in cell size and CD20 expression but with overlapping CD19 intensity. The larger cells (medium size) with brighter CD20 are monoclonal for lambda. The smaller cells with dimmer CD20 are polyclonal. Monoclonality is better appreciated in (c,d) than (e,f).

single parameter histograms (Figures 4.41 and 4.42). The finding of superimposed unimodal distributions of kappa and lambda in the negative region indicates no detectable light chain expression. With the exception of benign $CD10^+$ B-cells in marked FRFH (*see* Section 4.1.1), the absence of both light chains on $CD20^+$ cells or on $CD19^+$ cells outside the bone marrow implies a neoplastic B-cell process.

Once the presence of a monoclonal B-cell population or a B-cell population negative for light chains is established, then graphics displaying the key antigens CD10, CD11c, CD25, and CD103 (*see* Section 3.6.3), along with CD5 and CD23 are evaluated (Figure 4.43). This permits the characterization of the B-cell LPD/NHL immunophenotypically, while the cell size and S-phase fraction are assessed for grading the tumor.

4.4.1.1 Evaluation of CD5 and CD23

The presence or absence of CD23 in monoclonal B-cells is only meaningful when CD5 is expressed, especially if the neoplastic population is of small cell size. In this context, the fluorescence intensity of the surface light chain, the pattern of CD20 intensity within the tumor population, and the relationship of CD20 and CD19 also need to be evaluated carefully (*see* Section 3.6.2). The various combinations of findings frequently encountered are described next.

Six combined features represent the FCM "fingerprint" of CLL/SLL (Figures 3.13, 3.15, 3.32, and 4.39). These are (1) downregulated CD20, (2) CD20 intensity < CD19 (provided they are conjugated with the same fluorochrome), (3) broad CD20 expression within the tumor population, (4) weak to absent surface light chain (i.e., the difference between the mean fluorescence intensity for kappa and lambda does not exceed one decalog), (5) CD20 (or CD19), CD5, and CD23 coexpression, and (6) small cell size. This FCM "fingerprint," being highly specific, is most useful for detecting MRD in CLL, especially since more aggressive therapy is now being applied to this group of patients. Recent studies have shown that in this setting, FCM analysis is much more sensitive for the detection of minimal disease than PCR-based methodologies.


Case study 50

Where the pattern of CD20 or surface light chain expression departs from the above description (i.e., either becomes brighter), a close inspection of the FSC parameter may reveal an increase in larger and more activated cells (*see* Section 3.6.2). Cases of CLL with an increased number of activated cells usually present with an overwhelming number of neoplastic cells in the blood or bone marrow and suppression of other hematopoietic elements. The resulting picture on the SSC/CD45 dot plot is that of a nearly homogeneous specimen, in which a predominant cluster occupies the lymphoid region (Figures 3.45 and 3.46).

Six FCM features in combination, (1) bright CD20, (2) CD20 intensity > CD19, (3) CD5 positive, (4) CD23 absent, (5) bright single surface light chain expression, and (6) small cell size (in most instances), are a virtual fingerprint of MCL (Figures 3.47 and 4.40). However, if CD20 and CD19 are similar in intensity (both bright), other LPD/NHLs with antigenic features similar to MCL need to be considered in the differential diagnosis (*see* Section 5.2.1.4). Correlation with the morphologic picture (including cyclin D1 expression by immunohistochemistry), serum immunoelectrophoresis results, and bcl-1 rearrangement or (11;14) translocation, is warranted in such cases. The disorder is unlikely to be MCL if the surface light-chain expression is weak or CD20 is dim and less intense than CD19 (Figure 4.44). The latter two features favor a LPC disorder.

The combination of medium/high FSC, $CD5^+$, and $CD23^-$ occurs infrequently (Figure 4.45). The diagnostic possibilities include $CD5^+$ high-grade B-cell lymphoma, PLL, and, less likely, the "blastic" variant of MCL. CD20 and a monoclonal surface light chain are well expressed in the latter, but may be variable in the other two disorders.

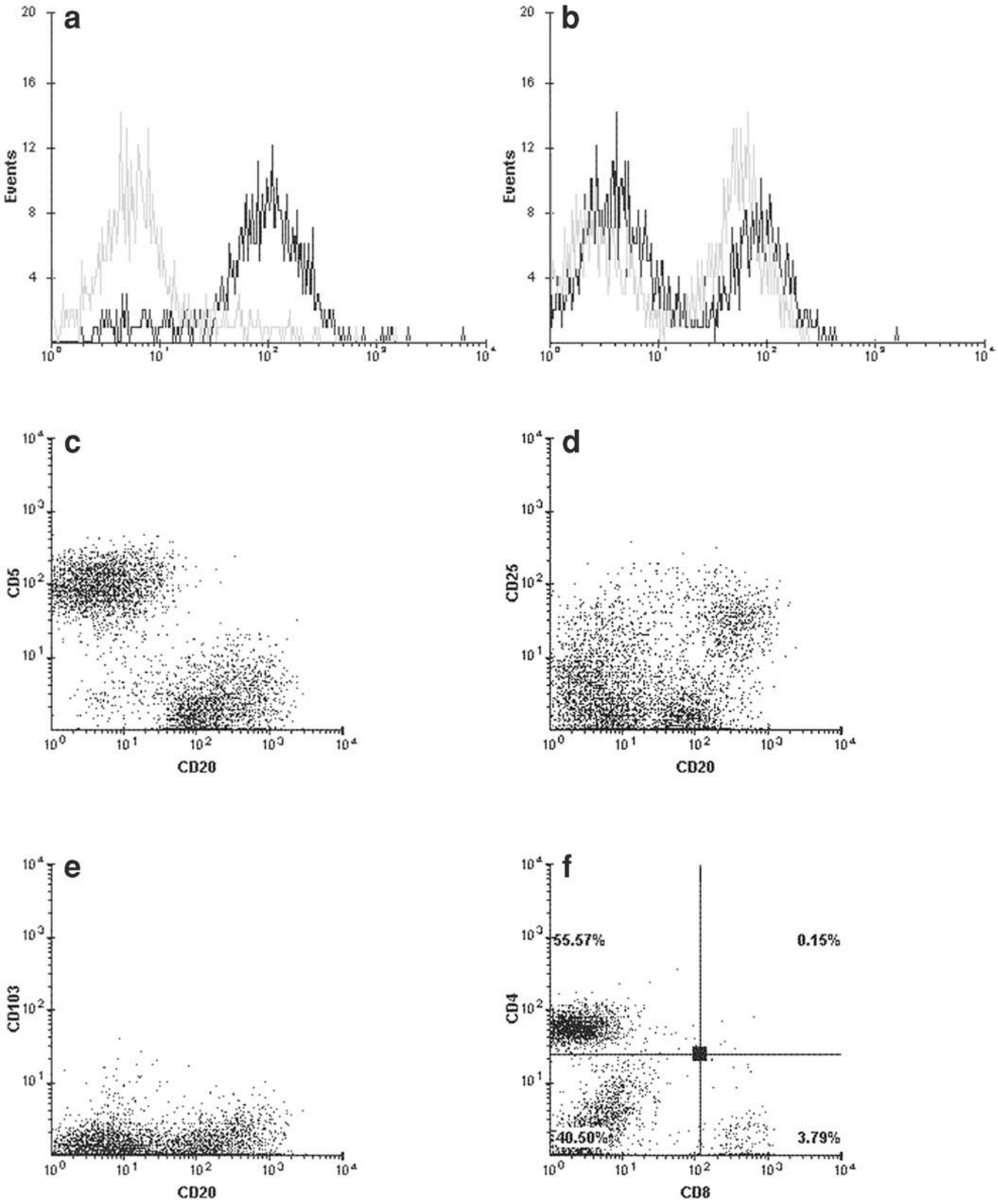

Figure 4.42 Lymph node with low-grade B-cell NHL NOS (continuation of Figure 4.41). (a) Gated on R3 (of Figure 4.41): Monoclonal lambda is well expressed. (b) Gated on R2 (of Figure 4.41): A polyclonal pattern. (c–f) The tumor is negative for CD5, CD10 (not shown), and CD103, but positive for CD25. CD25 is also present on some T-cells. Interestingly, the CD4;CD8 ratio is markedly increased (no evidence of TCR gene rearrangement or aberrant T-cell phenotype).

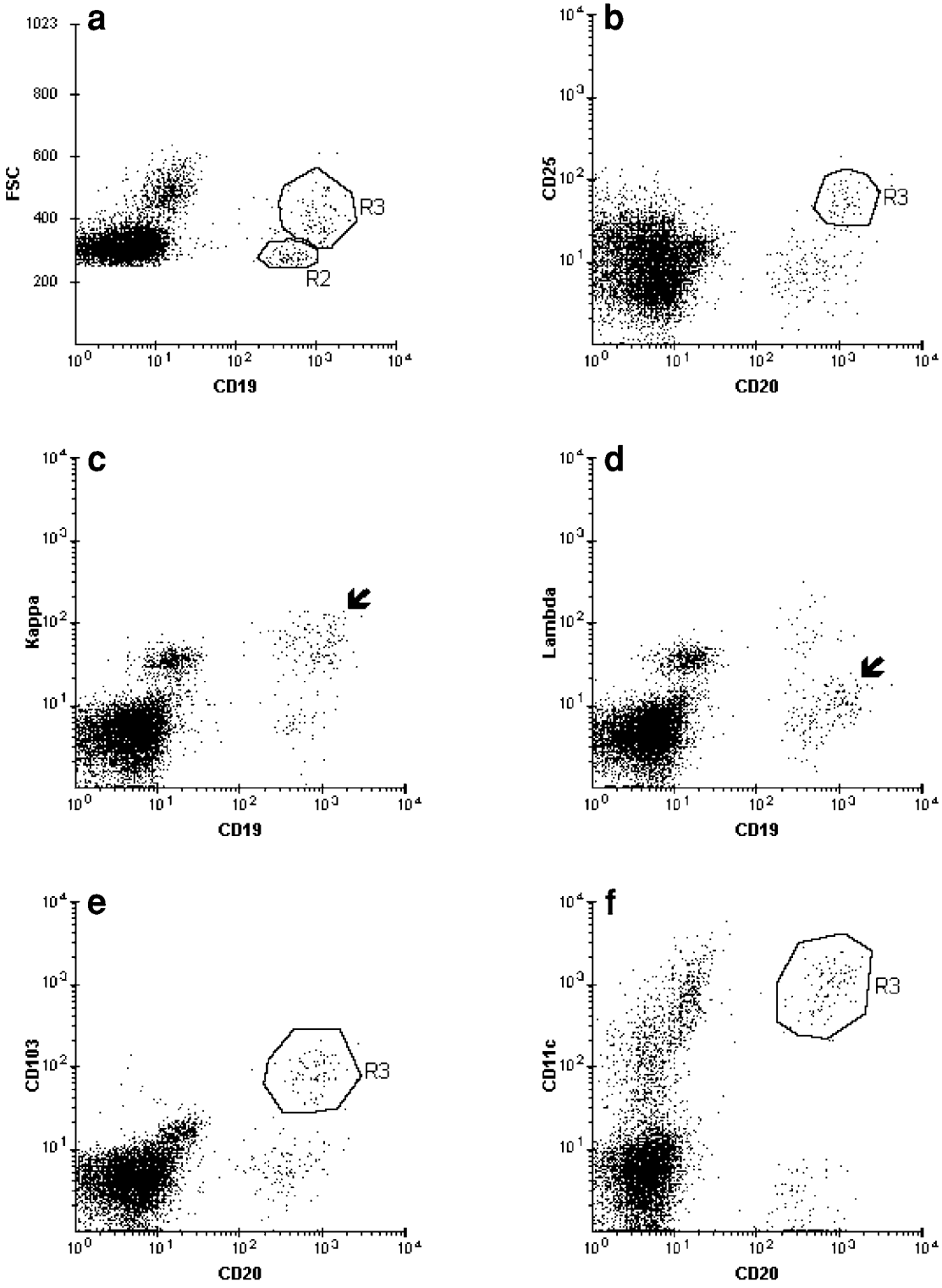

Figure 4.43 Peripheral blood with less than 1% hairy cells. (a–f) Gated on MNCs: Two B-cell populations differing in cell size. The larger cells (R3) display medium FSC, brighter CD19 and CD20, distinct expression of CD25 and CD103, intense CD11c, and monoclonal kappa light chain (arrow). The smaller CD20-positive cells (R2) are polyclonal.

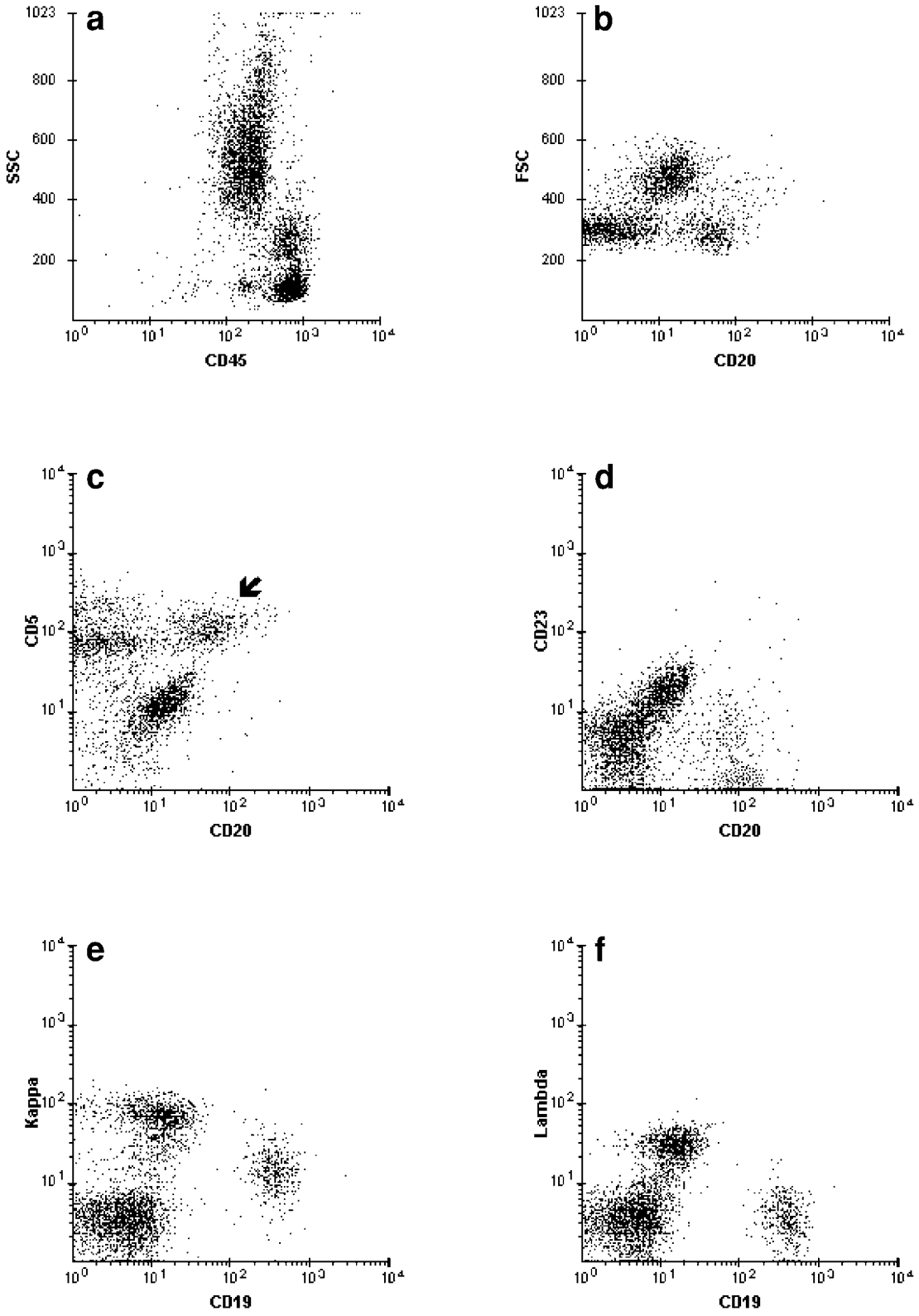

Figure 4.44 Bone marrow with low involvement by $CD5^+$ $CD23^-$ B-cell LPD, morphologically LPC lymphoma–leukemia. (a) A conspicuous lymphoid cluster. (b–f) Gated on MNCs: The lymphocytes are of small cell size and consist mostly of T-cells. B-cells are $CD5^+$ (arrow), $CD23^-$ and express weak monoclonal kappa. CD20 is less intense than CD19. The tumor comprises 4% of the cells analyzed.

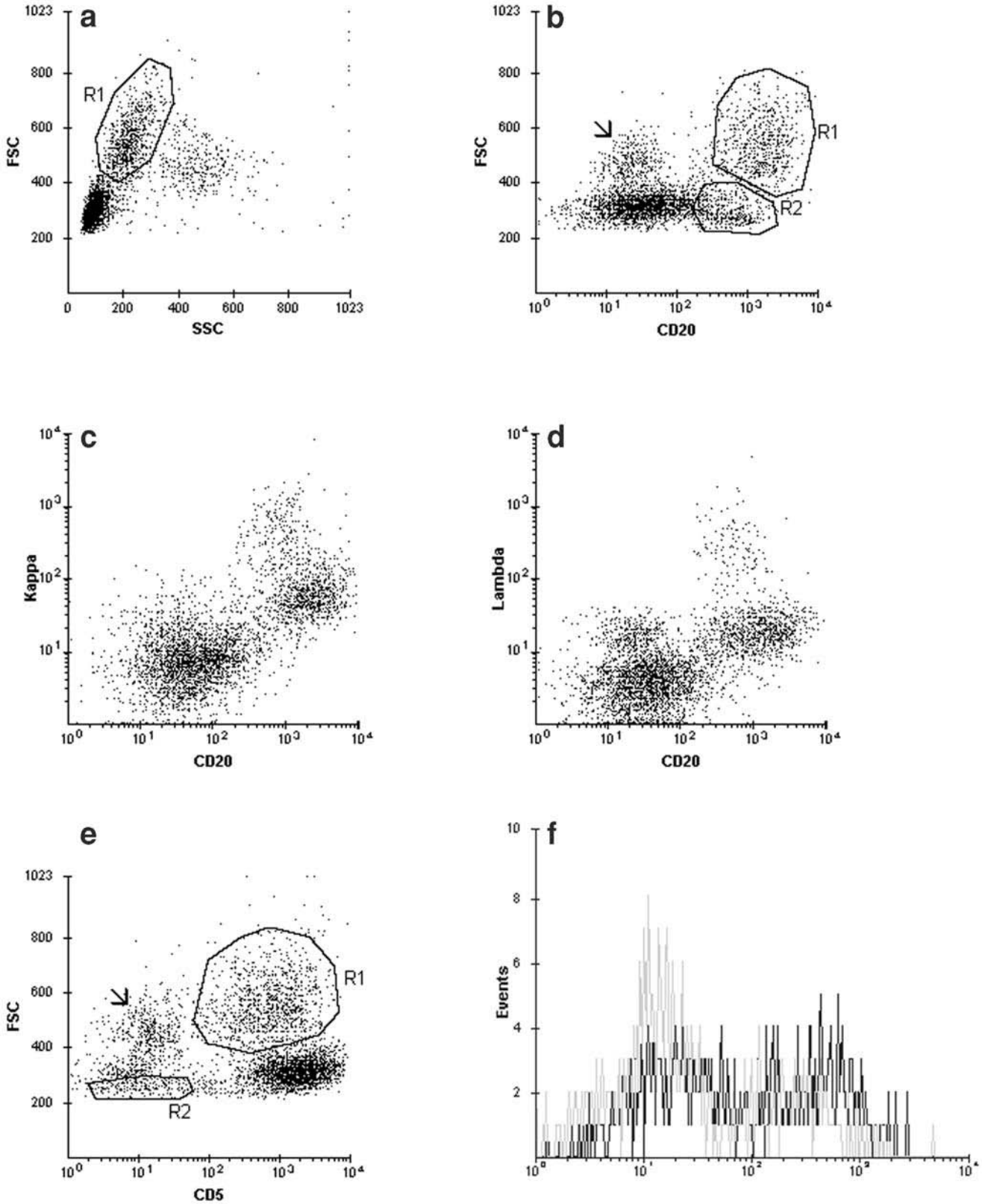

Figure 4.45 Lymph node FNA with CD5-positive LCL. (a–e) The neoplastic B-cells are large and (R1) comprise 18% of the cells analyzed. The tumor expresses CD5 and weak kappa light chain. A small number of granulocytes (arrow) represent blood contamination. (f) Gated on R2: The population of small B-cells (R2) is polyclonal for kappa and lambda. The tumor has a DI of 1.07 and an S-phase fraction of 21% (data not shown).

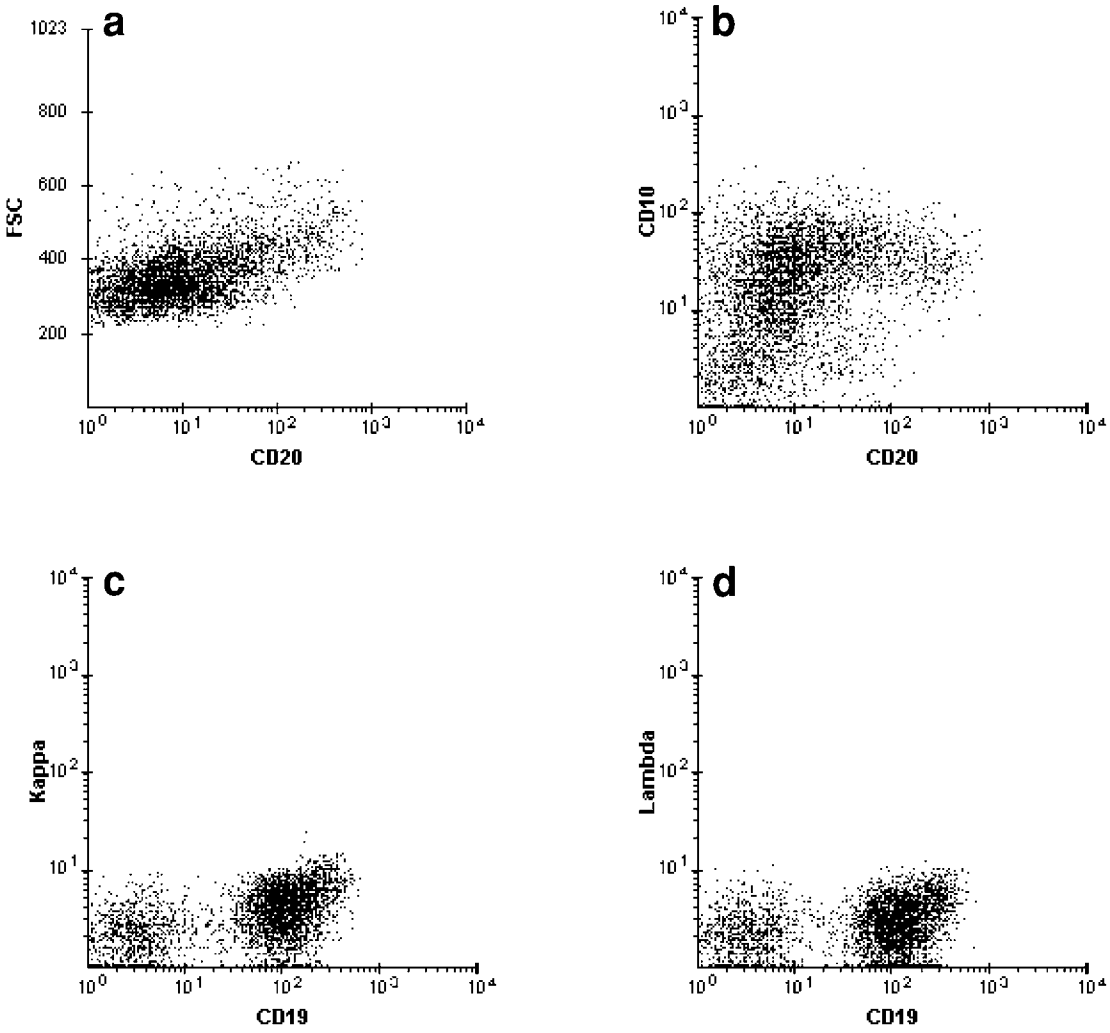

Figure 4.46 Lymph node with residual FCC lymphoma following anti-CD20 therapy. (a–d) The neoplastic cells are of variable cell size. CD20 (which in FCC lymphoma is normally more intense than CD19) is downregulated and dimmer than CD19. CD10 is well expressed. The tumor displays no detectable light chain.

4.4.1.2 FCM features suggestive of anti-CD20 therapy

While evaluating the expression of CD20, it is possible to suspect the effect of anti-CD20 therapy if the pattern of CD20 reactivity is incongruous with the remaining FCM data (Figure 4.46). Although a history of anti-CD20 therapy should be provided when submitting the specimen to the FCM laboratory, it is unfortunately not always available. Following anti-CD20 administration, the content of neoplastic cells in many cases, mainly those with bright CD20 expression, can be dramatically reduced. In the follow-up specimens, the interaction between the therapeutic chimeric anti-CD20 antibody and the residual B-cells masks the detection of CD20, resulting in an apparent decrease to absence of CD20 expression. This finding, when seen in the context of an abnormal B-cell population with either (1) CD10 expression, (2) small cell size, $CD5^+$, $CD23^-$, and bright surface light chain, or (3) small cell size, $CD5^-$, $CD23^-$, $CD10^-$ and bright surface light chain, should raise the suspicion of anti-CD20 therapy. If the neoplastic B-cells are large, however, then it is unclear whether the downregulated CD20 is inherent or secondary to anti-CD20 unless a prior FCM study is available for comparison.

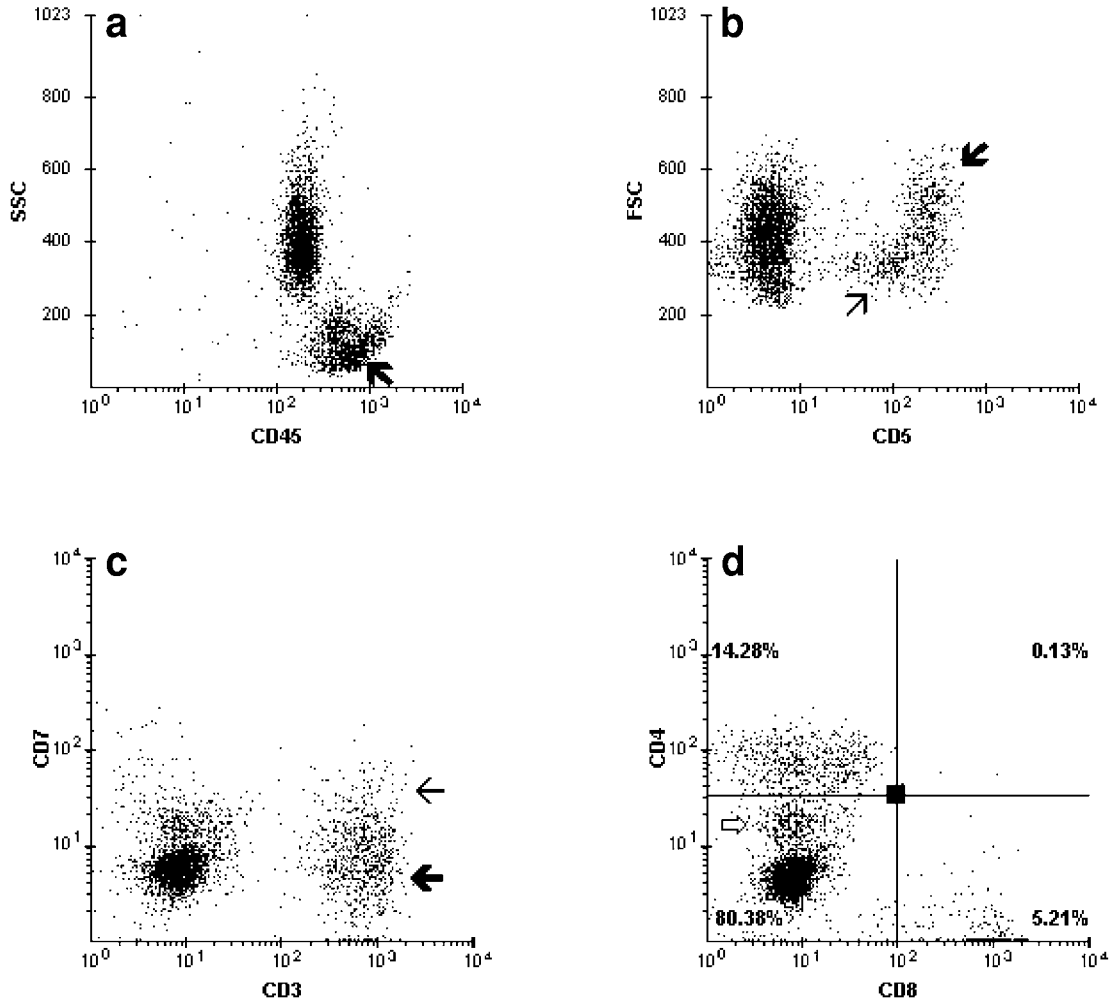

Figure 4.47 Peripheral blood involvement by PTCL. (a) The tumor (arrow) is part of the lymphoid cluster, but displays slightly increased SSC. (b,c) The neoplastic cells comprise 15% of the cells analyzed and display variable cell size, upregulated CD5, and downregulated CD7. A tiny population of residual small benign T-cells (thin arrow) is present. (d) The CD4;CD8 ratio is 2.7;1. Monocytes (open arrow) display dim CD4.

When CD20 is markedly downregulated, such as in some cases of CLL/SLL or following anti-CD20 therapy, the proportion of neoplastic cells may not be easily determined based on CD20, surface light chains, or FSC, especially if the tumor cells are of small cell size. Because benign and malignant B-cells often share similar CD19 intensities, examination of CD19 may not be helpful in this regard either. In such instances, the problem can often be resolved by analyzing the surface light chain expression (FITC) in conjunction with CD5 (PE) or CD10 (PE).

4.4.2 Abnormal mature T-cells

Case studies 51 and 52

A small population of abnormal mature T-cells can be detected based on one or more of the findings mentioned in Section 3.6.4. Most useful is the downregulation or upregulation (however slight) of one or more T-cell markers, which causes the neoplastic T-cells to be visibly separated from the normal T-lymphocytes (Figures 3.63, 3.64, and 4.47).

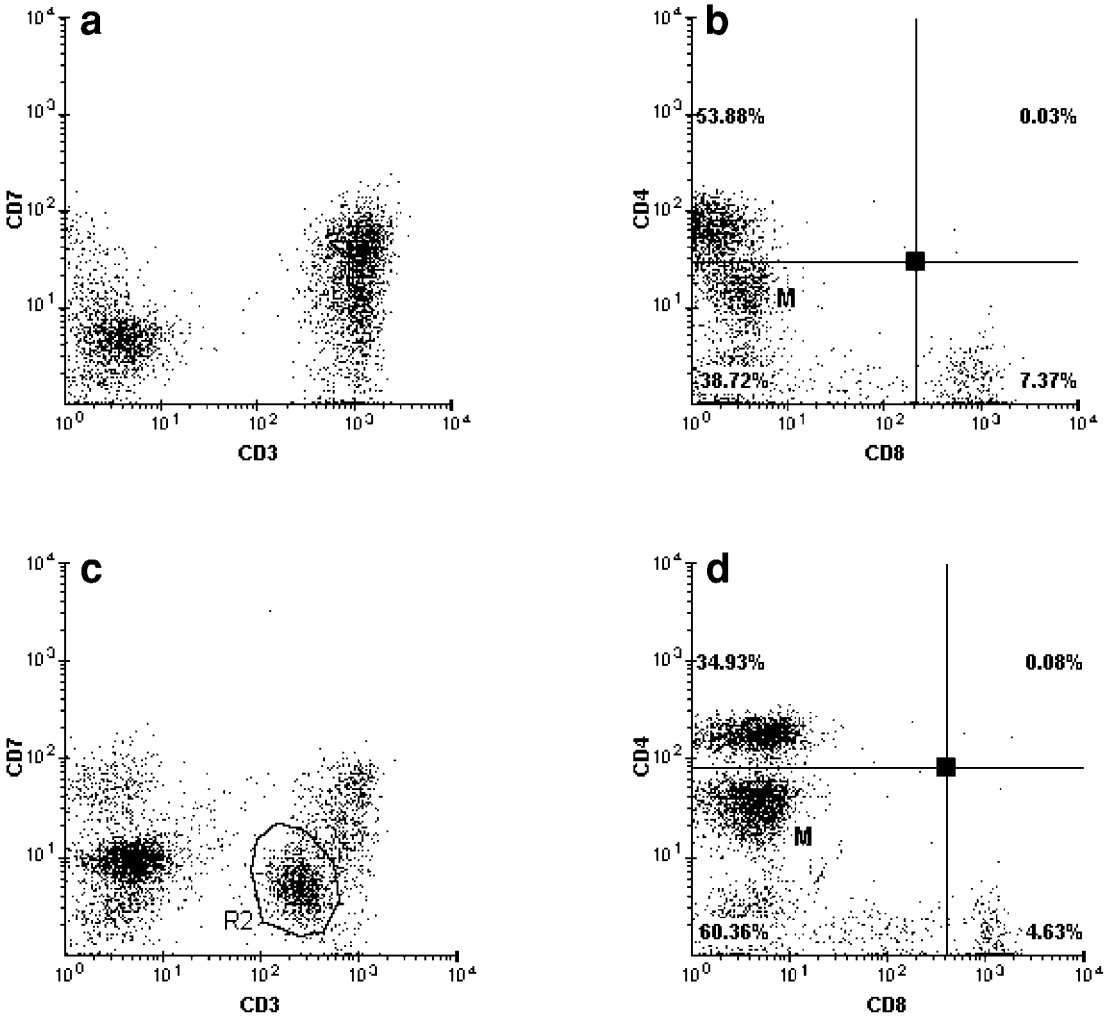

Figure 4.48 Peripheral blood with Sezary cells. Gated on MNCs. (a,b) Case 1: Sezary cells are not well separated from normal T-cells and are located at the lower end (i.e., with dimmer CD7) of the CD3/CD7 cluster. CD4;CD8 ratio is 7.3;1. The level of Sezary cells is about 5%. (c,d) Case 2: Sezary cells comprise 10% of the cells analyzed and are distinct (R2) from normal T-cells with loss of CD7 and down-regulated CD3 expression. CD4 intensity is similar to that on normal T-cells. CD4;CD8 ratio is 7.5;1. Monocytes (M) are CD4-positive.

Case study 53

In the early stages of mycosis fungoides/Sezary syndrome, the fluorescence pattern of T-cell markers on the tumor cells in the peripheral blood varies from case to case (Figure 4.48) and may be identical to that of normal T-cells. On the FCM displays, the malignant and benign cells are merged into one single cluster (Figure 4.48a). The CD4;CD8 ratio may be markedly increased, however, with the Sezary cells contributing to the excess of CD4 cells (Figure 4.48b). This is a rare instance where the "percent-positives" approach (otherwise applicable only for the enumeration of B- and T-cell subsets) may be useful for the identification of a T-cell malignancy.

More difficult to assess are the early stages of low-grade $CD8^+$ T-cell malignancies, the majority of which are large granular lymphocytes morphologically. The FSC signals, as well as the fluorescence intensity patterns of CD8, NK-cell markers, and other T-cell antigens are closely similar between the benign and low-grade malignant LGL proliferations. Furthermore, the blood and bone marrow involvement by indolent LGL leukemia is usually not overwhelming, in contrast to the aggressive NK disorders (*see* Section 3.6.5). The most commonly


Case studies 54 and 55

encountered phenotypic combination is that of an NK-like T-cell, with a TCR-αβ phenotype (i.e., positive CD3/TCR-αβ, $CD57^+$, downregulated CD8 and CD5, TCR-γδ$^-$, and $CD4^-$) (Figure 4.49). Other antigenic combinations such as $CD3^+$, TCR-γδ$^+$, $CD4^-$/$CD8^-$/TCR-αβ$^-$ occur much less frequently. Indolent CD3-negative LGL (i.e., true NK) proliferations are rare (Figure 4.50). For the latter group, establishment of the clonal nature of the proliferation is a challenging task because NK cells do not have rearrangements of the TCR genes.

4.4.3 Abnormal plasma cells present

Abnormal plasma cells are defined by the expression of a monoclonal cytoplasmic light chain, which, in most instances, can be evaluated by a side-by-side comparison of cKappa/CD38 and cLambda/CD38 (Figure 4.51). In addition, bright CD56 expression is frequently observed (Figure 4.51b). Other antigenic features include intense CD38 expression and down-regulation or absence of CD45, pan B-cell antigens, and HLA-DR. As in normal plasma cells, CD138 is usually well expressed. Plasma cells, benign or malignant, may also express a myeloid antigen, usually CD14 or CD13.

The immunophenotypic characteristics of neoplastic plasma cells can be best contrasted with that of their benign counterparts in conditions where the two coexist, namely in patients with monoclonal gammopathy of undetermined significance (MGUS). Clonal plasma cells often display one or more of the following abnormalities:

1. Higher FSC and SSC than that produced by reactive plasma cells. In many cases of plasma cell dyscrasia, the heterogeneous mixture of small to large neoplastic cells imparts a variable distribution to the FSC parameter.
2. Lack of CD19 reactivity.
3. The expression of one or more antigens (e.g., CD138, CD56) varies from case to case. Although intense, the expression of CD38 on clonal plasma cells is often lower than that on normal counterparts (Figure 4.52). Occasionally, CD38 may even be absent. In some cases, the tumor may have no detectable cytoplasmic light chain although the cytoplasmic heavy chain (IgG/IgA) is present. Some plasma cell tumors lack all antigenic reactivity except for CD38 and CD56.
4. Variable reactivity for markers normally not present on plasma cells such as CD117, CD20, and monoclonal surface light chain (of the same clone as the cytoplasmic light chain) (Figure 4.53). CD45 may also be brightly expressed. As a result, the neoplastic plasma cell cluster may be seen occupying the blast or monocytic region of the SSC/CD45 dot plot. Bright CD45 and high FSC tend to correlate with an "immature" plasma cell morphology.


Case study 56

The finding of coexisting residual polyclonal and neoplastic cells has been found to be a strong discriminating feature to separate MGUS from the early stages of multiple myeloma.

On the SSC/CD45 dot plot, the plasma cell cluster and erythroid precursors share the same CD45 negative to borderline region. However, plasma cells can be separated from erythroid elements on the FSC/CD45 plot since plasma cells are about the size of monocytes or even larger. Plasma cells can also be spotted on the FSC/SSC plot, seen as a cluster with medium/high FSC and with lower SSC than monocytes. This cluster location is not unique to plasma cells, but it can be observed in any large lymphoid malignancy (which may also lack CD45) involving the blood or bone marrow.


Case study 57

Because of hypergammaglobulinemia in multiple myeloma, the nonspecific coating of M-protein to cell surfaces is often not completely washed off during specimen processing. This nonspecific binding is most pronounced on monocytes, but it can also be seen on other cells (e.g., activated T-cells, NK cells). As a result, the monocytic cluster appears as an artifactual monoclonal B-cell population, which can be best appreciated when the kappa/CD20 and lambda/CD20 (or kappa/CD19 and lambda/CD19) dot plots are inspected side by side (Figure 4.52). The presence of monoclonal surface light chains on cells other than B-cells is therefore highly suggestive of a plasma cell dyscrasia.

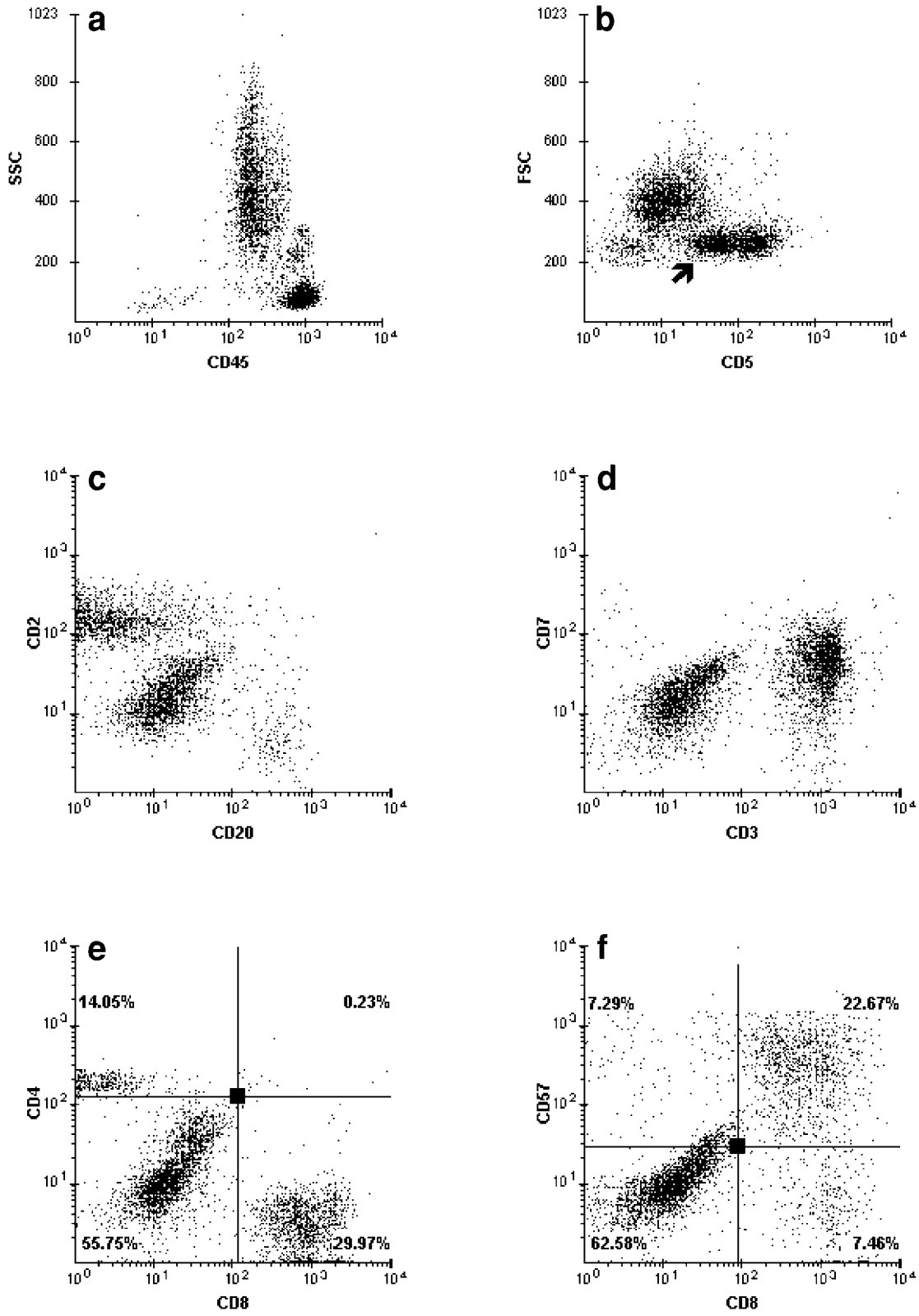

Figure 4.49 Bone marrow with indolent CD3+ LGL. (a) A conspicuous lymphoid cluster. (b–f) The neoplastic cells comprise 23% of the cells analyzed and display small cell size and normal expression of CD2, CD3, and CD7, but weaker CD5 (arrow) than normal T-cells. CD8 and CD57 are expressed. The intensity of CD8 is dimmer than that on suppressor T-cells.

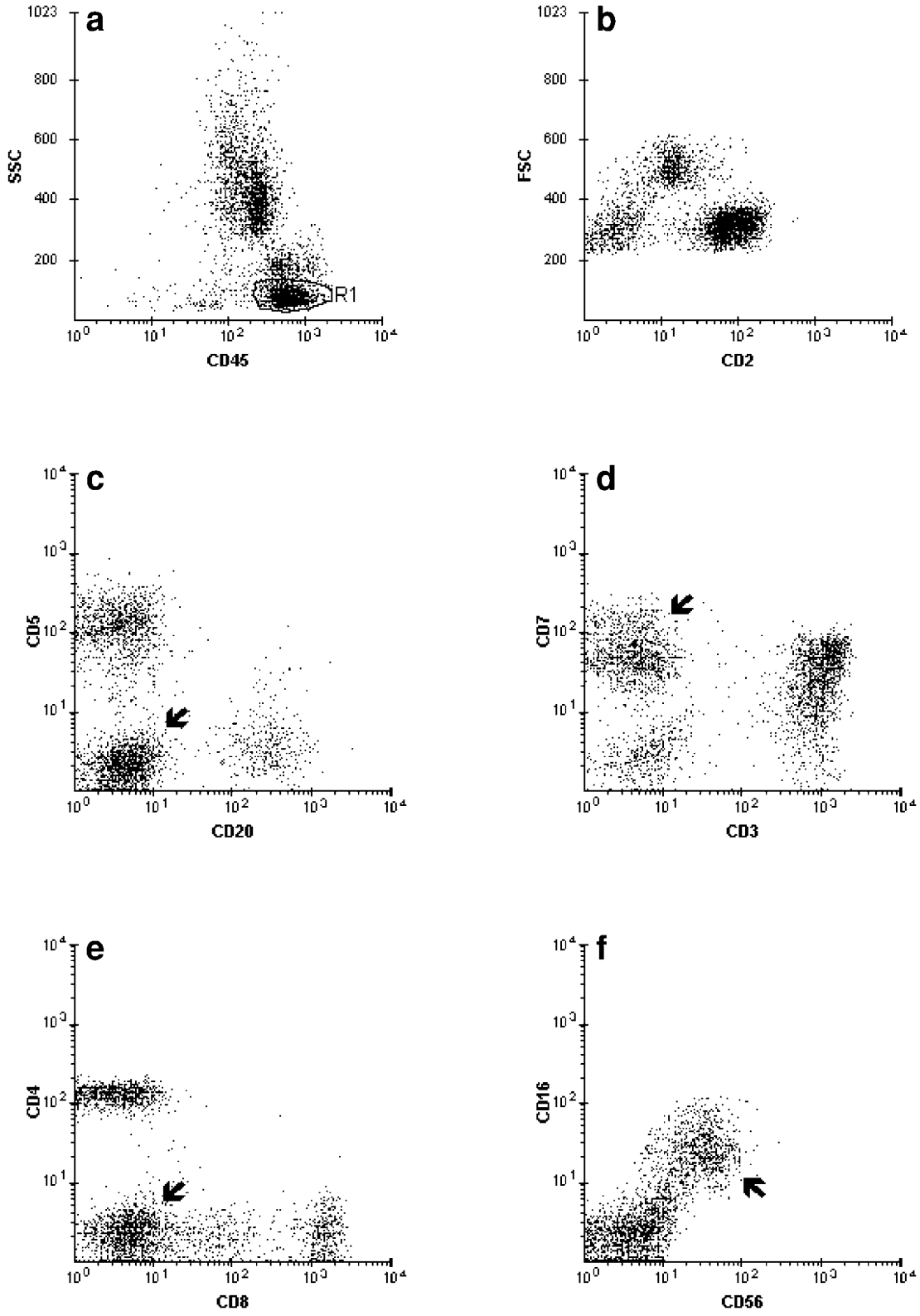

Figure 4.50 Indolent CD3-negative LGL (true NK cells). (a) Hemodilute bone marrow with a sizable lymphoid cluster (R1). (b) Gated on MNCs: The neoplastic cells have identical CD2 intensity to normal T-cells. (c–f) Gated on R1: Neoplastic cells (arrow) comprise 14 % of the cells analyzed and lack CD5, CD3, CD4, and CD8 but express CD7, CD16, and CD56.

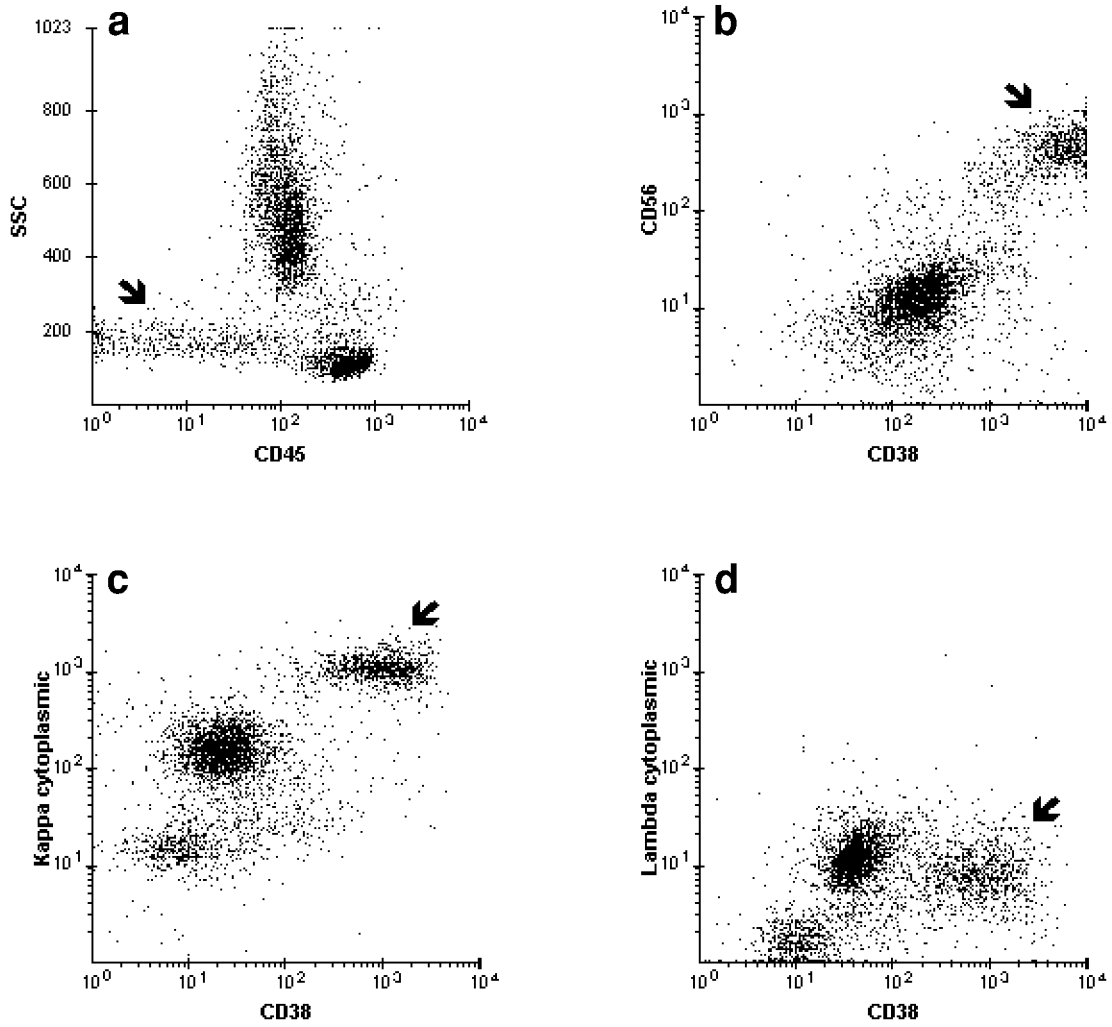

Figure 4.51 Bone marrow with plasma cell dyscrasia. (a–d) The intensity of CD45 on the neoplastic plasma cells (arrow) ranges from negative to weak. The tumor cells comprise 15% of the cells analyzed and coexpress intense CD38 and CD56. Monoclonal cytoplasmic kappa is present. There is indirect evident of kappa hypergammaglobulinemia.

4.5 Abnormal blood or bone marrow samples with no detectable neoplastic cells

Samples with no detectable neoplastic cells as referred to in this section are those in which (1) the percentage of myeloblasts is within normal limits, (2) blasts have no detectable phenotypic aberrancies, and (3) no abnormal (or suspicious) mature lymphoid cells or plasma cells are present. However, the relative cellular composition (mainly granulocytes or monocytes) of the blood or bone marrow is altered. The antigenic maturation of the hematopoietic elements may also be abnormal. Neoplastic disorders with such phenotypic abnormalities are predominantly MPDs in the chronic phase (in particular, CML and CMMoL) or low-grade MDS. Certain benign conditions such as a vigorous response to G-CSF therapy or myeloid maturation arrest from different underlying causes can also demonstrate similar findings.

Most clinical laboratories are not concerned about the FCM data from the above-mentioned conditions. This is especially true in those laboratories where morphology screening is employed as a method for selecting antibodies to be tested on any given sample. Although FCM analysis is not recommended in MPD or MDS unless there is a suspicion of progression

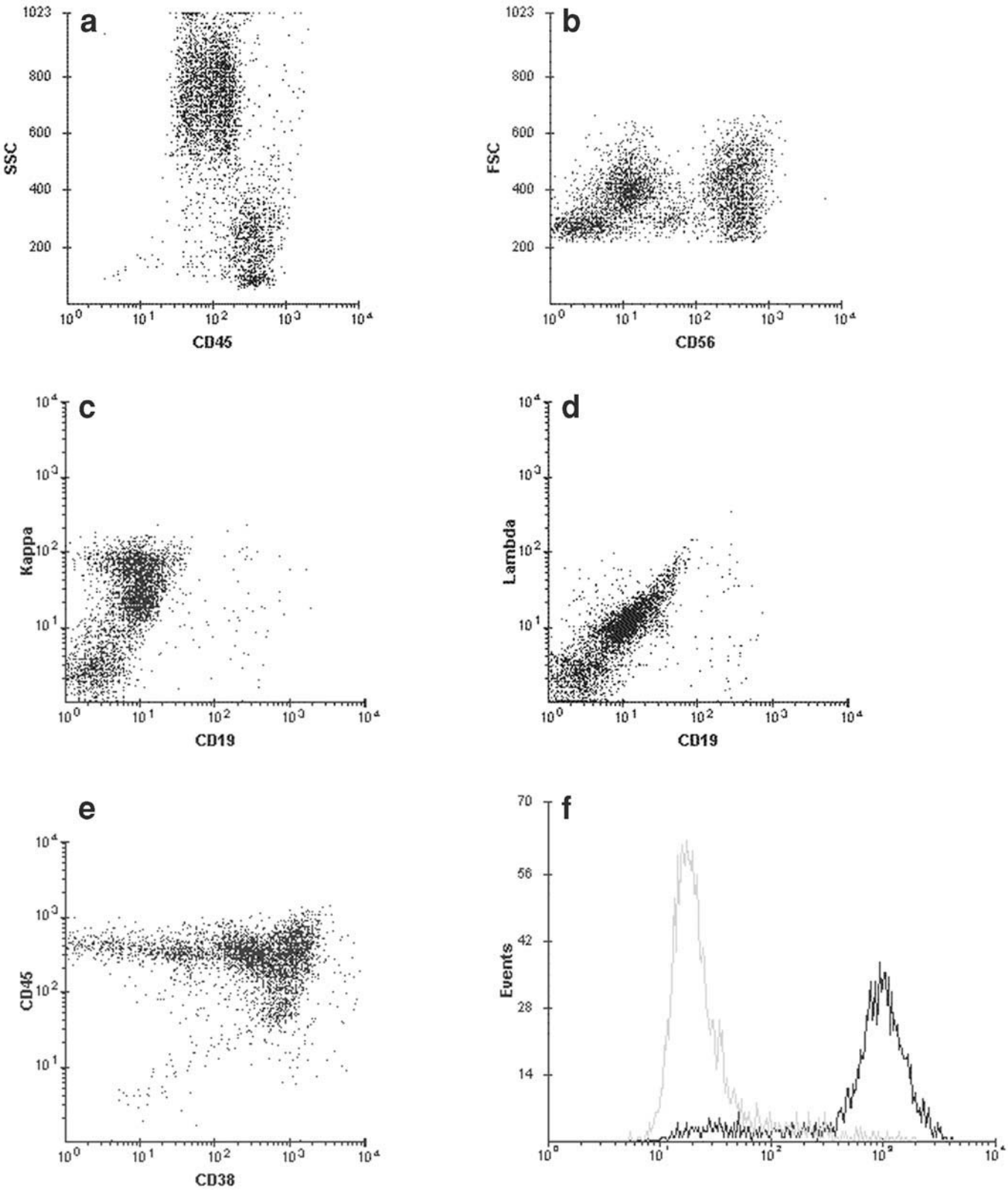

Figure 4.52 Bone marrow with plasma cell dyscrasia. (a) The neoplastic plasma cells comprise 17% of the cells analyzed and display bright CD45 (thus simulating a monocytic cluster). (b–e) Gated on MNCs: The tumor cells display variable FSC and express CD56. CD38 is downregulated compared to normal plasma cells. There is indirect evidence of kappa hypergammaglobulinemia. (f) Gated on the brightest CD38 cells: Cytoplasmic kappa is expressed.

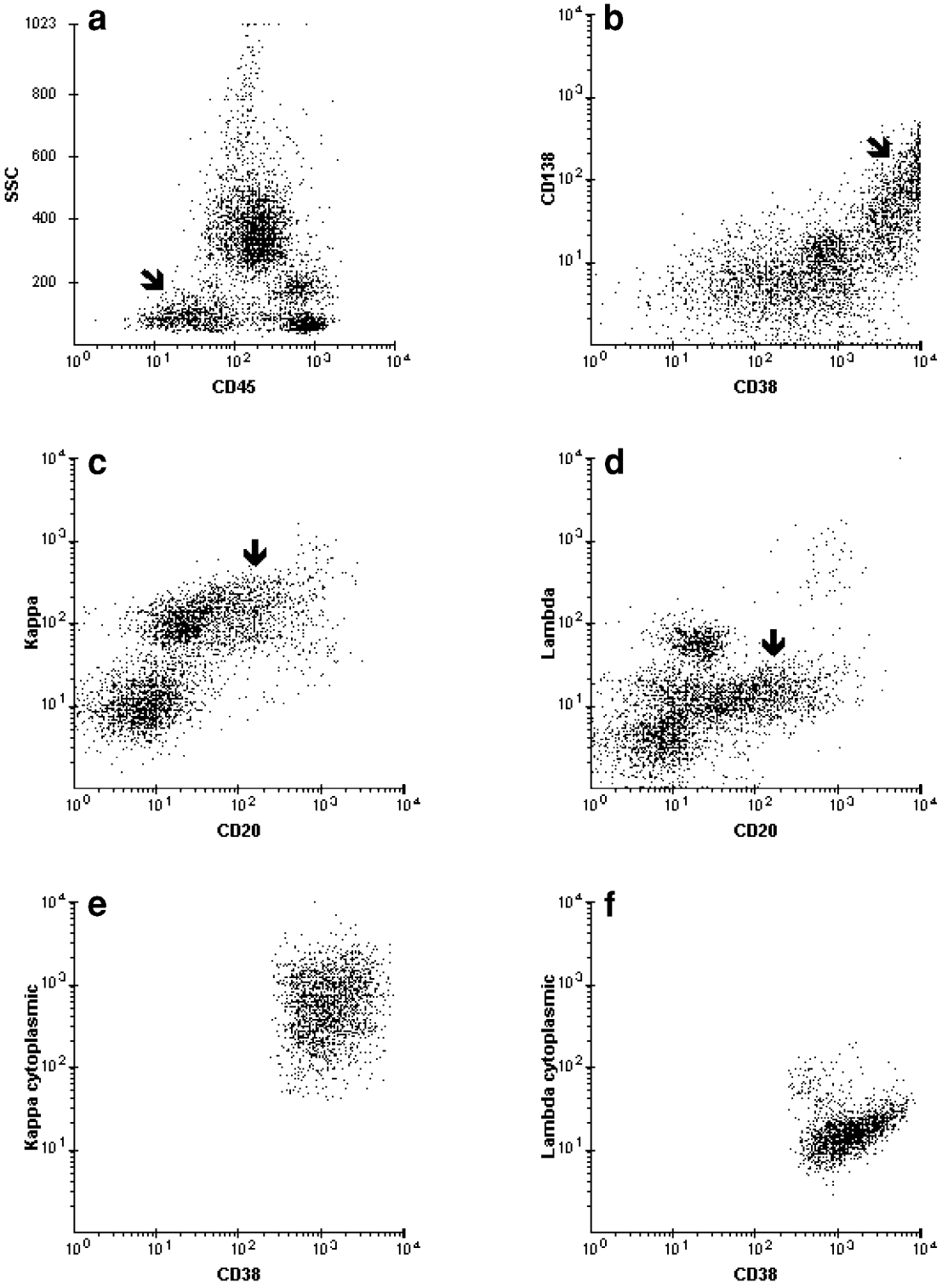

Figure 4.53 Bone marrow with plasma cell dyscrasia. (a,b) The tumor cells (arrow): Seventeen percent of the cells analyzed display dim CD45, intense CD38, and reactivity for CD138 and CD56 (not shown). (c,d) CD20 and surface light chain (kappa) are unusually well expressed. A minute population of polyclonal B-cells is present. (e,f) Gated on the brightest CD38 cells: The tumor cells contain cytoplasmic kappa.

to an acute leukemia, the visual FCM data can still be of interest, at least academically. In addition, if the bone marrow sample is representative, a more objective determination of the blast percentage can be obtained by FCM studies (in lieu of a manual differential count), which facilitates the distinction between the chronic phase and the accelerated phase of the disease.

Because the abnormalities are found mainly in the myeloid or monocytic population, the SSC/CD45, CD14/CD64, CD13/CD16, and CD11b/CD16 dot plots (the latter two gated on granulocytes) are the main FCM graphics for assessing the altered cellular composition and abnormal myeloid maturation. In those cases with increased erythroid elements, the graphics displaying CD71 and Gly-A are also closely inspected.

4.5.1 Altered cellular composition and abnormal SSC

The most obvious finding in specimens with an altered cellular composition is the increased prominence of the monocytic cluster observed on the SSC/CD45 dot plot, usually accompanied by a corresponding decrease in the size of the granulocytic cluster. This picture, when seen in the bone marrow, is quite suggestive of CMMoL. In the peripheral blood, however, this interpretation cannot be made with certainty since reactive or compensatory monocytosis may yield a similar picture. The presence of an elevated WBC count (via correlation with the hemogram data) or a small blast cluster (blast level well below 10%) on the SSC/CD45 display will point toward CMMoL. CD56, when expressed by the monocytes, is another helpful clue for confirming CMMoL (Figure 4.54).

In some cases of CMMoL, the bone marrow granulocytic component is markedly diminished (Figure 3.35). The resulting pattern of the cell clusters on the SSC/CD45 dot plot resembles that observed in AML with monocytic differentiation (Figure 3.36). These are cases in which the distinction between an AML (usually M5b) and CMMoL based on the bone marrow morphology is also problematic. Helpful clues for differentiating these two disorders include CD117 expression in AML and the difference in the patterns of CD14/CD64 coexpression (Figures 3.35c, 3.36, and 4.55), which reflect the difference in the relative distribution of blasts, promonocytes, and monocytes between the two diseases. Either disorder can produce a vertical "trail" pattern on the CD14/CD64 dot plot. CMMoL, in contrast to AML with monocytic differentiation (*see* Section 3.5.1), has a much higher proportion of mature elements, however. The mature elements are seen as a cluster expressing bright CD14 and CD64, located at the upper end of the vertical "trail" (Figure 4.55). Often the trail is insignificant, reflecting the low proportion of promonocytes in CMMoL.


Case study 58

An extremely prominent eosinophil population is a rare occurrence (Figure 4.56). Because of its low FSC, the cluster of eosinophils seen on the FSC/SSC display may be mistaken for degenerated granulocytes. The phenotype of eosinophils is best derived from the dot plots correlating the FSC parameter with the expression of various myeloid antigens. On these graphics, the eosinophil population stands out because of its characteristic low FSC signals (Figures 4.15d and 4.56c). The expressions of CD13, CD33, CD11b, and CD15 on eosinophils overlap with that of myeloid cells, however, at an intensity lower than that on the most mature granulocytes. CD16 is not expressed. Massive eosinophilia of the blood and bone marrow strongly suggests the hypereosinophilic syndrome, itself an MPD. Correlation with the clinical picture and cytogenetics is necessary, however, since this disorder is a diagnosis of exclusion.


Case study 59

On the SSC/CD45 dot plot, abnormalities of the myeloid cluster are usually not easily discernable, apart from hypogranularity or hypergranularity (Figures 4.57 and 4.58). For the observation to be valid, the instrument gain for the SSC parameter should be appropriately set (i.e., not excessively high). Low SSC signals can be observed in some cases of MDS in which the corresponding morphology displays extensive hypogranulation among the myeloid precursors, irrespective of whether the MDS is low- or high-grade. When present as the sole abnormality, low SSC is not a sufficient feature for identifying MDS, however, as hypogran-


Case study 39

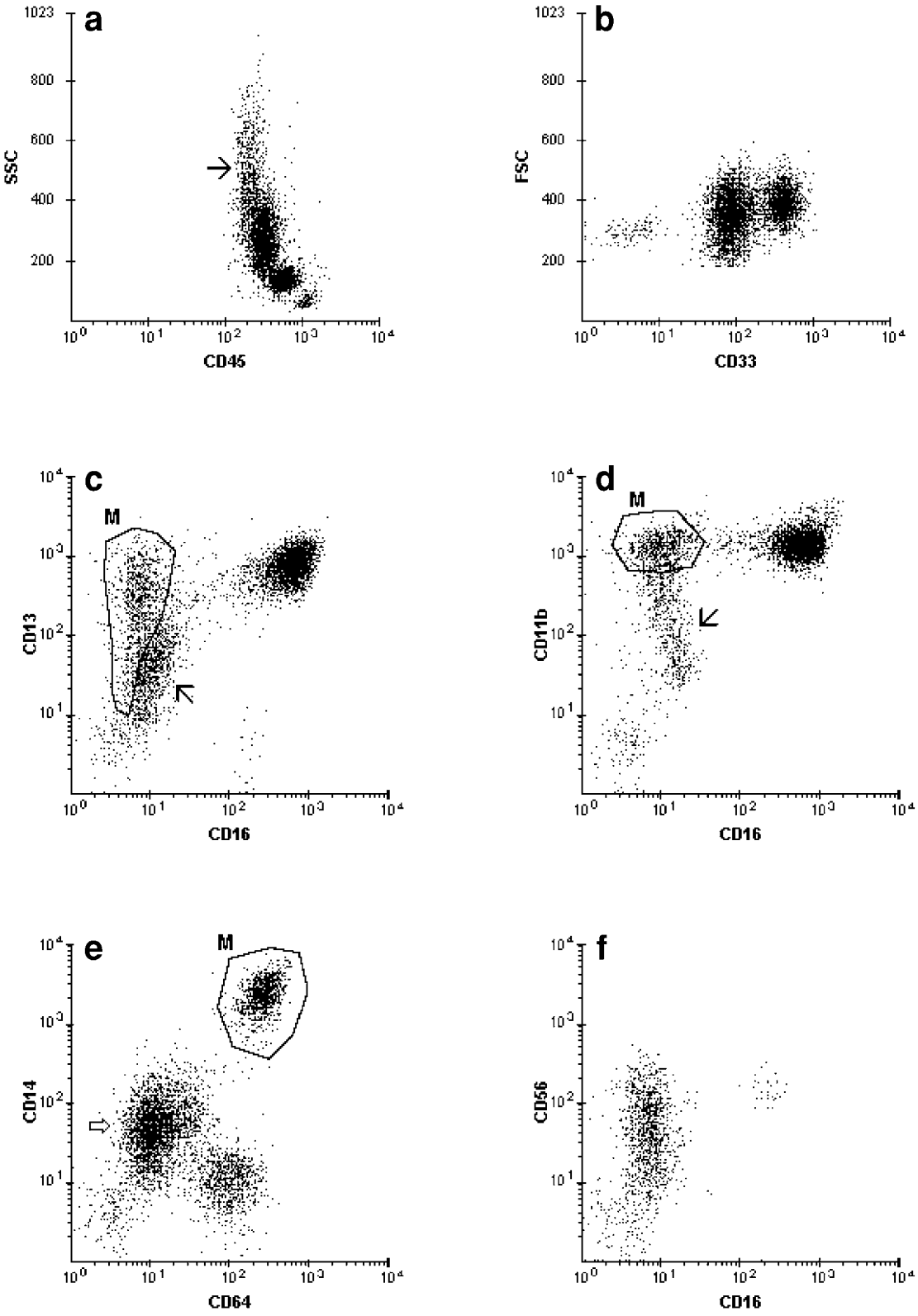

Figure 4.54 Peripheral blood with CMMoL. (a–e) The monocytic cluster is slightly enlarged (21% monocytes) and displays brighter CD33 than granulocytes. Monocytes (M) express CD13, CD11b, CD64, and intense CD14. Circulating myeloid precursors (arrow) are evident. The more mature granulocytes have a higher level of CD14 than usual (open arrow). (f) Gated on MNCs: The monocytic population is abnormal by its reactivity for CD56. A tiny cluster of CD16/CD56-positive NK-cells is present.

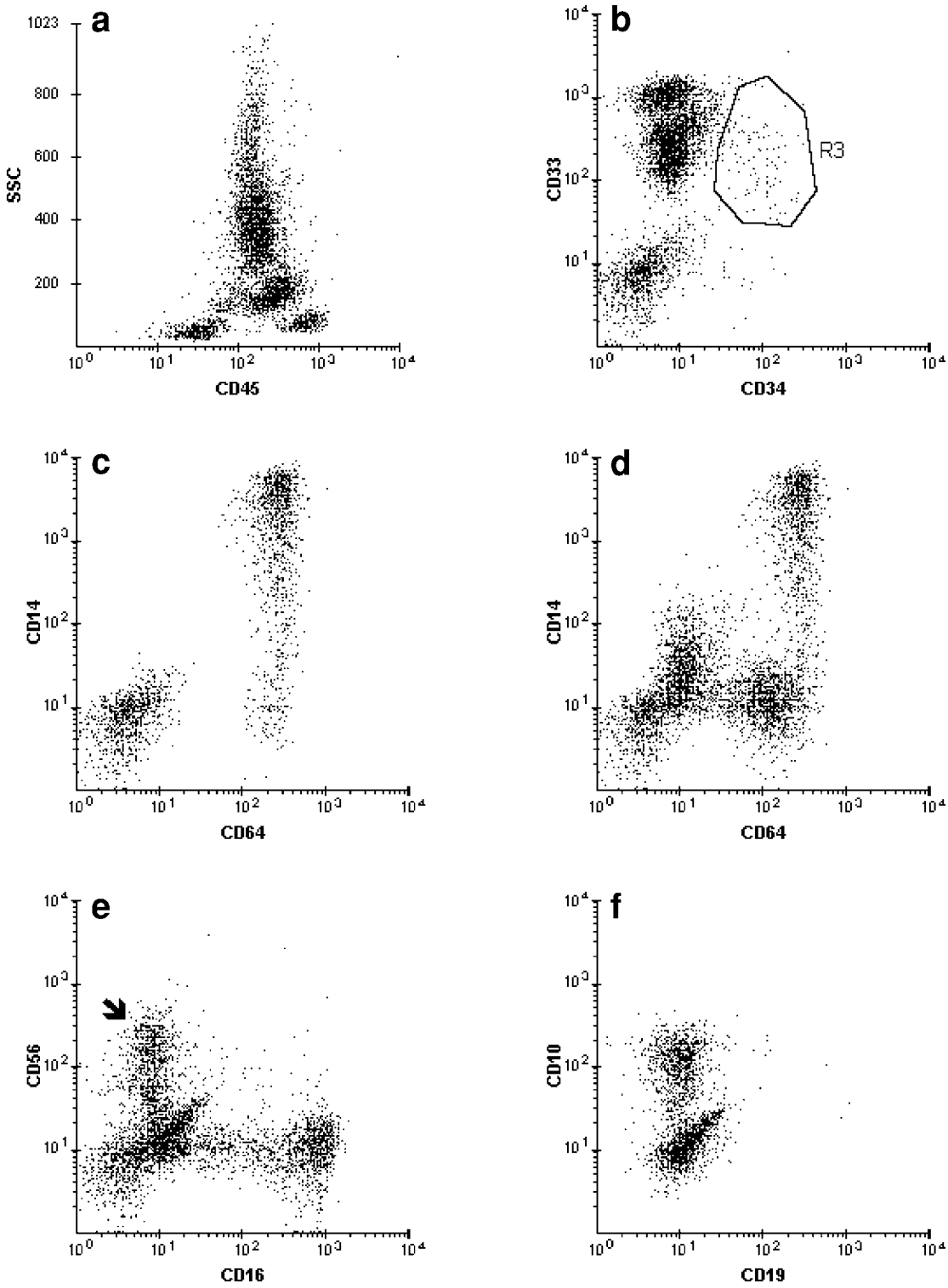

Figure 4.55 Bone marrow with CMMoL. (a,b) There are 2% blasts and 31% monocytes. Blasts (R3) are $CD34^{++}$, $CD33^{++}$. (c) Gated on MNCs: CD14/CD64 trail pattern reflecting the heterogeneity of monocytic cells at various stages of maturation; the more mature cells predominate. (d) The more mature granulocytes display a higher level of CD14 than usual. (e) Monocytes are CD56-positive (arrow) and thus neoplastic. (f) Normal pattern of CD10 expression on myeloid precursors.

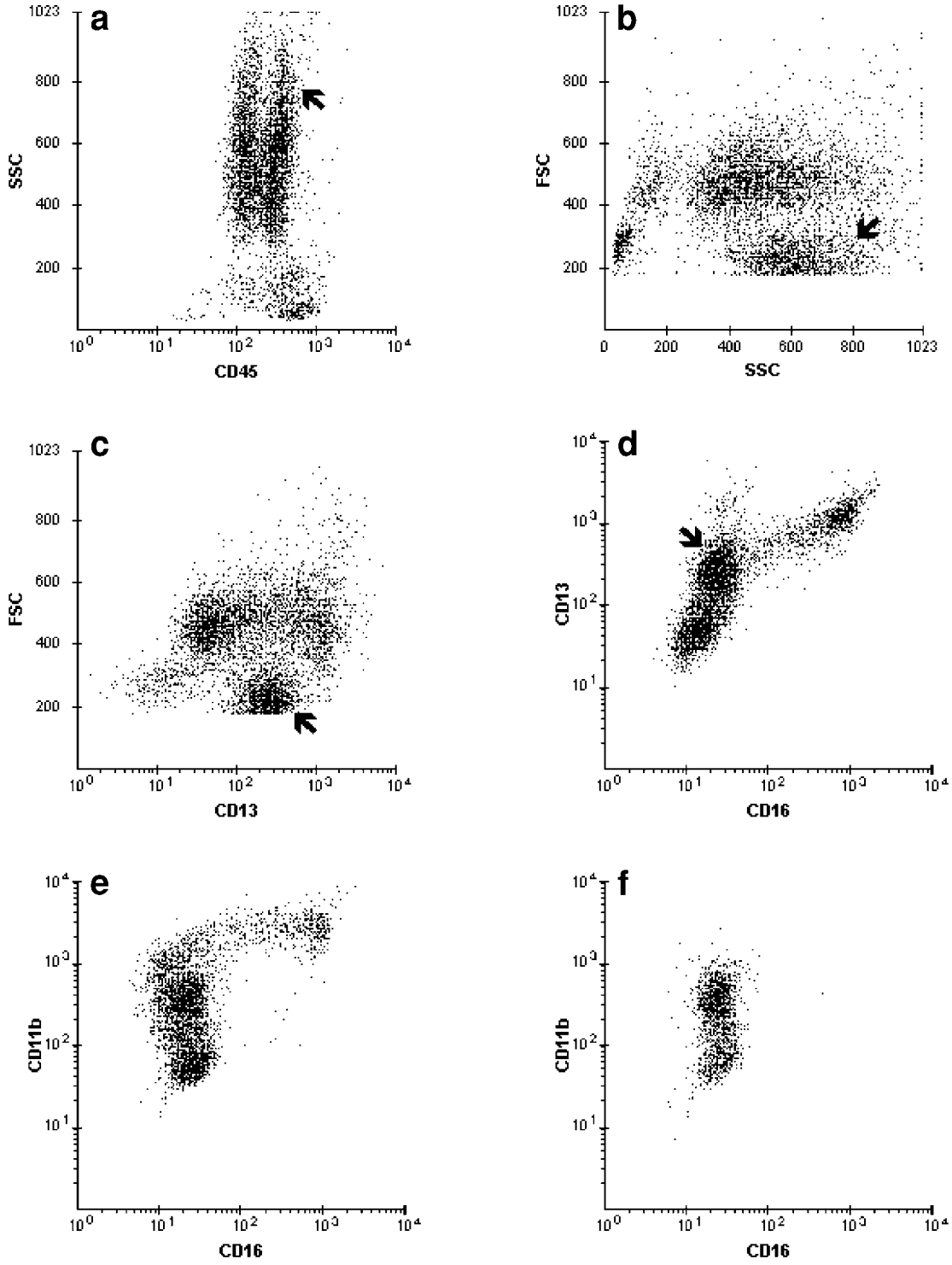

Figure 4.56 Bone marrow with hypereosinophilic syndrome. (a–c) Eosinophils (arrow) comprise 46% of the bone marrow cells and display the characteristic high SSC and low FSC. The expression of CD13 and CD33 (not shown) on eosinophils (arrow) overlaps with that of granulocytes. (d,e) Gated on cells with high SSC: Normal myeloid maturation curves. Similar CD11b expression on eosinophils and granulocytes. (f) Gated on eosinophils: Eosinophils are CD16-negative.

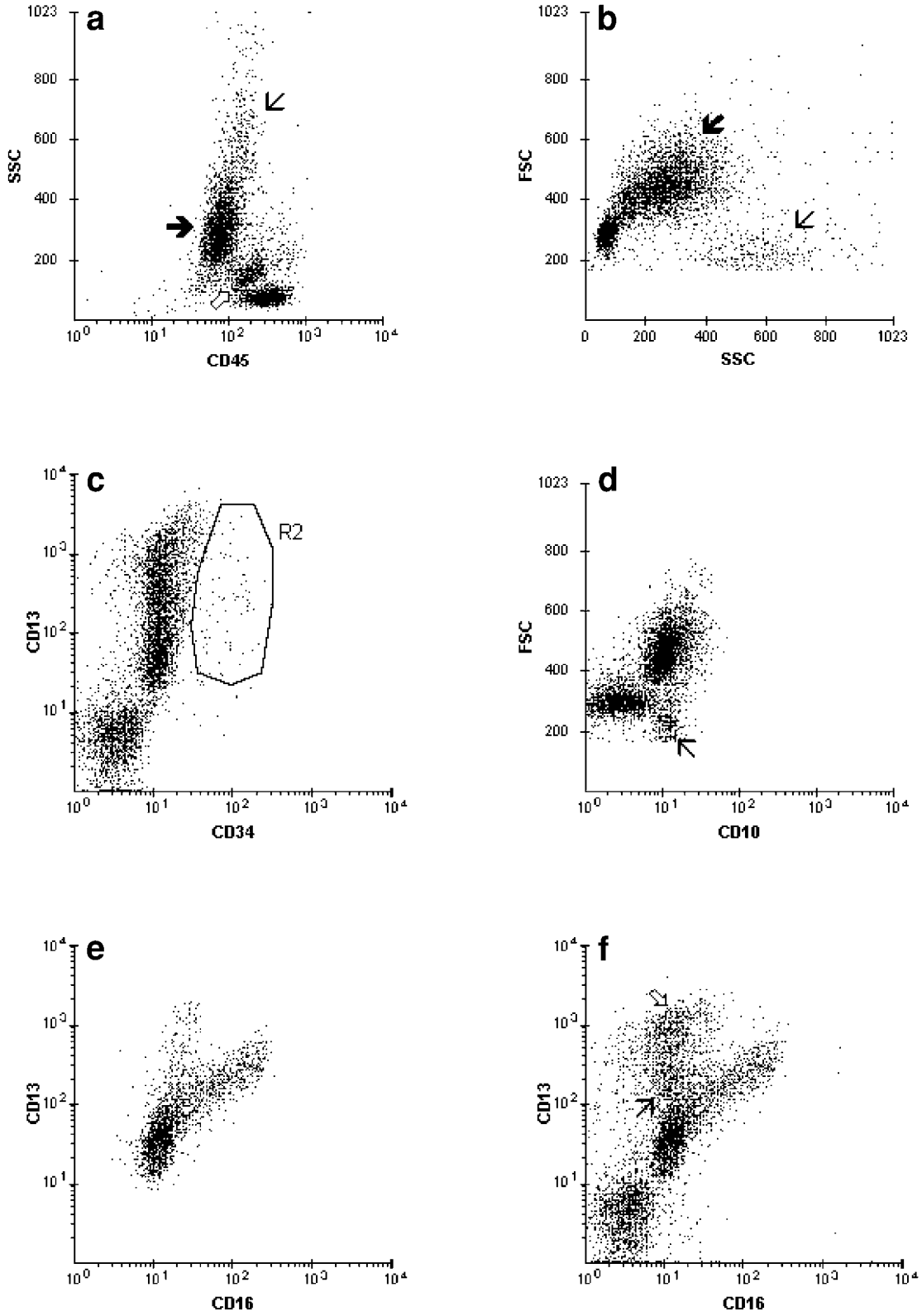

Figure 4.57 Bone marrow with low-grade MDS. (a,b) Hypogranular myeloid precursors (arrow) and a small number of eosinophils (thin arrow). (c) The blast content is 1% (R2). (d) Loss of CD10 expression on granulocytes. Eosinophils are CD10-negative. (e) Gated on granulocytes: abnormal CD13/CD16 maturation curve. (f) Ungated: Monocytes (open arrow) and eosinophils (thin arrow) are CD16-negative.

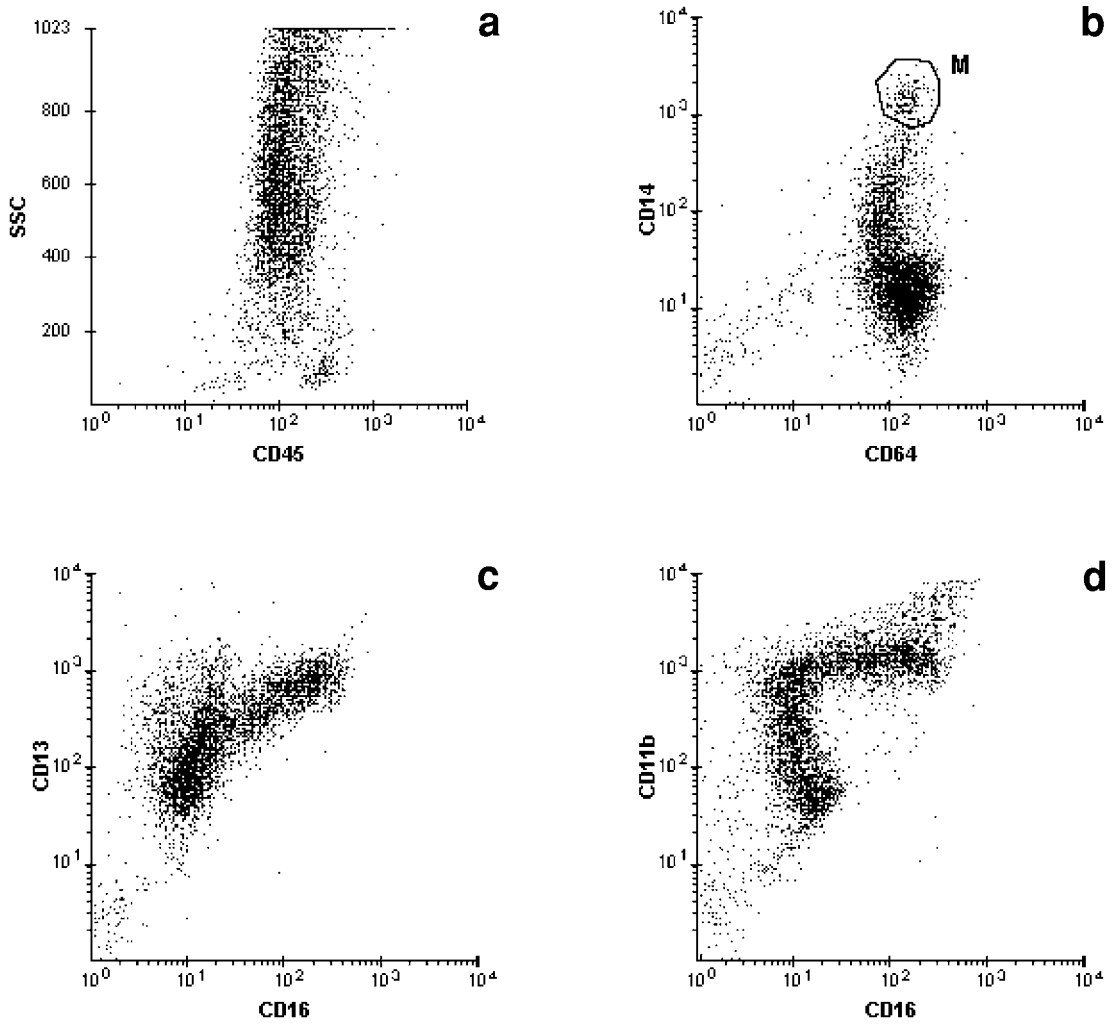

Figure 4.58 Bone marrow with G-CSF effect. (a) Myeloid precursors with increased SSC (hypergranulation). (b–d) Myeloid cells display increased levels of CD64 (as bright as that on monocytes) and CD14. The resulting CD14/CD64 picture nearly simulates the CD14/CD64 trail pattern seen in neoplastic monocytic proliferations. There are only 4% monocytes (M) in the sample analyzed. The myeloid maturation curves are nearly normal.

ularity can be encountered in other conditions such as HIV infection or some cases of MPD (Figure 4.26).

Increased granularity may be observed in an intense bone marrow response to G-CSF therapy (Figure 4.58), as well as some cases of CML or CML-like MPD (i.e., those MPDs with a blood and bone marrow picture similar to CML but different genotypic findings). The hypergranular myeloid cluster in these conditions occasionally simulates the SSC/CD45 picture of hypergranular AML-M3 (Figure 3.24). The findings on other FCM dot plots (e.g., CD13/CD16 and CD11/CD16, as well as the HLA-DR and CD15 results differ from those observed in AML-M3 (*see* Section 3.4.1), however.

In recent years, G-CSF has become part of the treatment regimen for acute leukemia. Because G-CSF is administered simultaneously with other chemotherapeutic agents, the bone marrow picture during the early follow-up period of a treated AML (2–6 weeks after the start of the induction) may be difficult to interpret. Under the effect of G-CSF, a large number of blasts can simultaneously undergo some attempt at (incomplete) maturation. As a result, the treated bone marrow contains a large cohort of intermediate myeloid precursors (mostly mye-


Case study 60

locytes) with a promyelocyte-like appearance due to the intense granulation. Although the morphology may simulate AML-M3 (Plate 13), these abnormal myeloid precursors differ from AML-M3 cells phenotypically (Figure 3.23). In rare cases, however, the large cohort of abnormal myeloid cells closely mimics AML-M3 antigenically (e.g., lacking both CD11b and CD16 expression) (Figure 4.59).

4.5.2 Abnormal antigenic maturation in myeloid or erythroid precursors

The main bone marrow antigenic abnormalities in maturing myeloid precursors are downregulated CD10 and CD16, including the rare congenital absence of CD16. As a result, the patterns of the maturation curves on the CD13/CD16 and CD11b/CD16 dot plots are altered to a variable extent when compared to that in the normal marrow. In most instances, the abnormal antigenic maturation is more easily visible on the CD13/CD16 rather than the CD11b/CD16 curve. These immunophenotypic abnormalities on the myeloid precursors were initially observed in MDS and, therefore, thought to be specific for myelodysplasia. However, similar abnormalities can also be found in some MPDs (especially CML and CML-like MPD) as well as certain non-neoplastic conditions, such as severe myeloid maturation arrest of various etiologies (e.g., drug-induced agranulocytosis) or intense G-CSF effect.


Case study 61

In all of the above-mentioned conditions, the common morphologic feature that appears to correlate with the abnormal antigenic maturation curves is a substantial degree of left-shifted myeloid maturation whereby the intermediate myeloid precursors exceed the mature elements. Where the myeloid series is normal appearing or just slightly left-shifted (e.g., low-grade MDS or MPD in chronic phase), the antigenic maturation curves are often essentially normal.

Increased levels of CD14 and/or CD64 on the granulocytes (Figures 4.58 and 4.60) is a helpful feature for identifying the G-CSF effect. The increased expression is similar to that seen in the neutrophilic response to infectious or inflammatory processes, which, in turn, suggests that the effect of G-CSF on myeloid cells is mediated by the tumor necrosis factor. Increased CD14 or CD64 may sporadically occur in MPDs, including CMMoL (Figures 4.54e and 4.55d), CML (Figure 4.61), or CML-like MPDs (Figure 4.62), however. The degree of G-CSF-associated phenotypic abnormalities (hypergranularity, altered maturation, upregulated CD14, downregulated CD10) on myeloid precursors varies from case to case depending on the extent of G-CSF therapy and when the bone marrow specimen is obtained. A vigorous response to G-CSF may yield a peripheral blood picture (with a low level of circulating blasts, Figure 4.60) mimicking that of CML. CML usually contains a conspicuous population of basophils (Figure 4.61), however.


Case study 62

Among the myelodysplastic syndromes, the abnormal myeloid maturation curves and/or loss of CD10 are less frequently observed in the low-grade than in the high-grade MDS. When present in low-grade MDS (Figure 4.57), however, they tend to correlate with abnormal cytogenetic findings, which, in turn, account for a more rapid progression to high-grade MDS and eventually acute leukemia.

The erythroid component, especially when increased, may also display altered antigenic maturation. The most frequent abnormality (as described in the literature) is downregulated CD71 expression. As a result, CD71 on the abnormal erythroid precursors is of heterogeneous distribution, ranging from very dim to bright intensity, in contrast to the homogeneously intense CD71 expression seen on normal erythroid elements. Other reported abnormalities include asynchronous expression of CD45 and CD71 or Gly-A and asynchronous expression of CD71 and Gly-A. Although downregulation of CD71 has been reported mainly in MDS, it has also been described in cases of aplastic anemia with morphologic evidence of dyserythropoiesis. It still remains to be elucidated if benign disorders with erythroid hyperplasia and dyserythropoiesis (namely B12/folate deficiency), also produce similar abnormal CD71 expression.

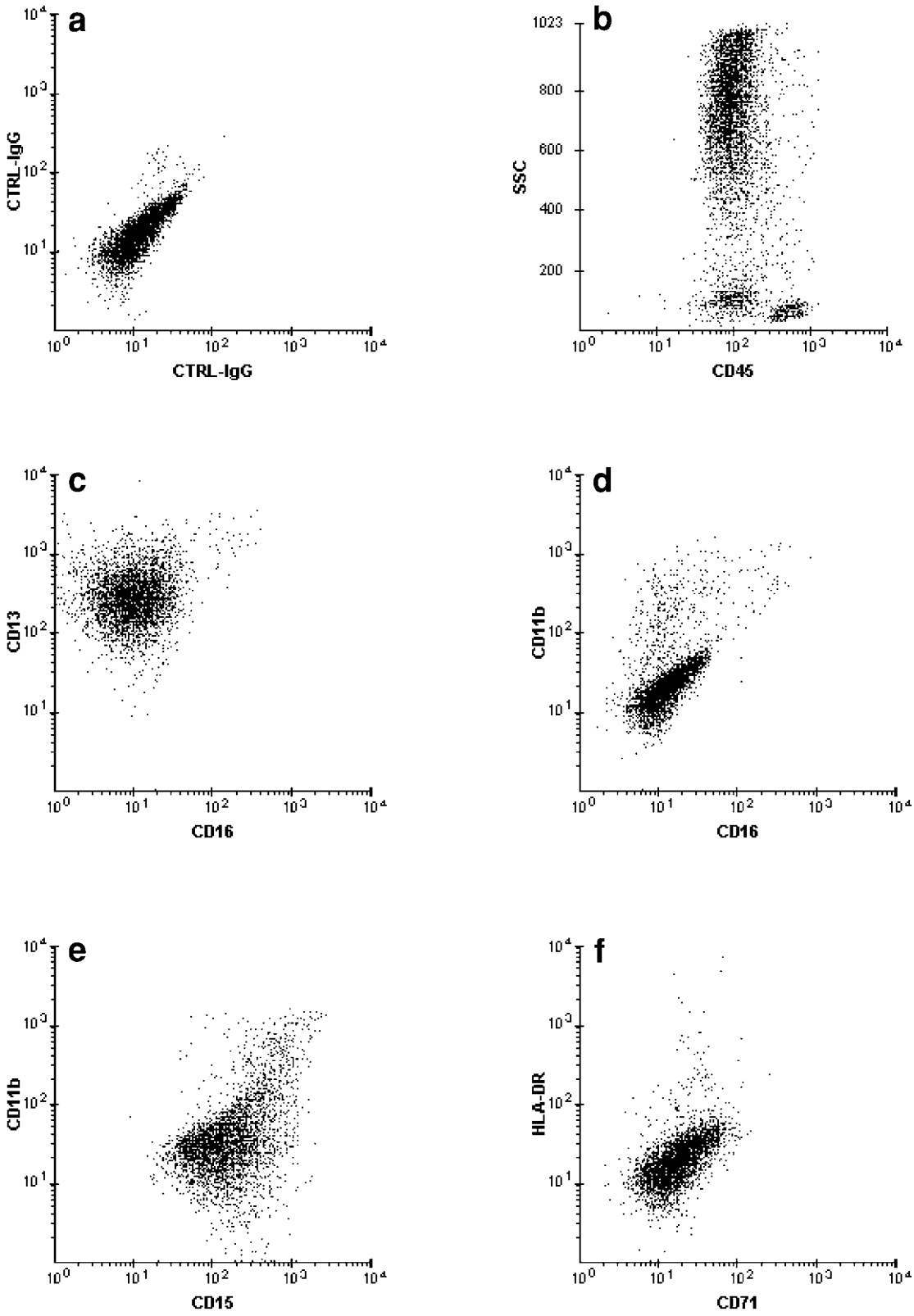

Figure 4.59 Bone marrow with residual AML and G-CSF effect (G-CSF was part of the induction chemotherapy regimen). (a) Isotype-matched negative control. (b) Myeloid cells with increased SSC and 9% residual blasts (AML-M1 at presentation). (c–f) Gated on granulocytes: The phenotypic features simulate that seen in AML-M3. Granulocytes are CD13-positive and CD33-positive (not shown) and lack CD11b, CD16, and HLA-DR. Differing from M3, however, is the bright expression of CD15.

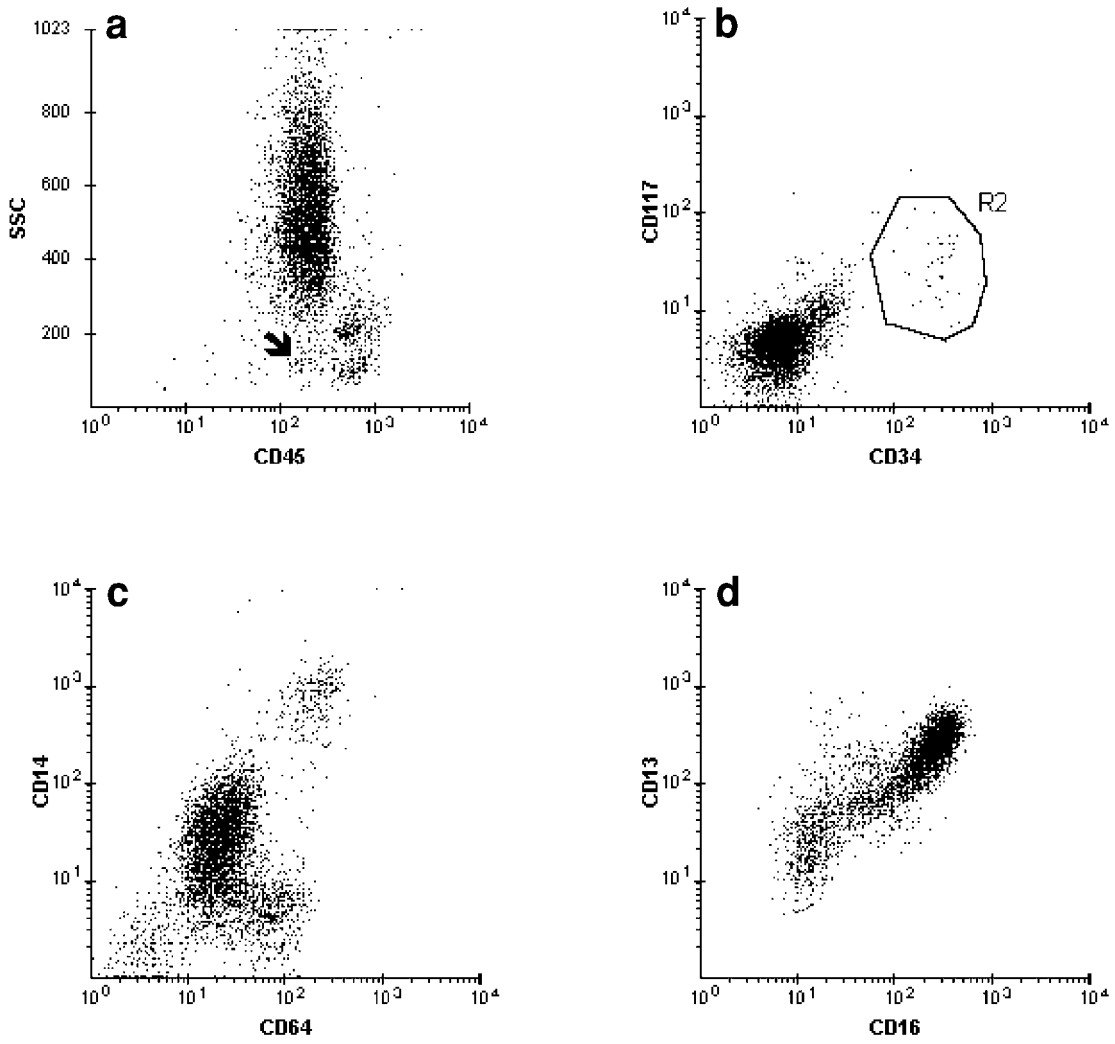

Figure 4.60 Peripheral blood with G-CSF effect. (a) The granulocytic cluster displays increased SSC. A tiny blast cluster (arrow) is present. (b) Blasts (R2), coexpressing CD34 and CD117, comprise less than 1% of the cells analyzed. CD13 and CD33 (not shown) are expressed. (c) CD14 is increased on most of the granulocytes. There are 4% monocytes. (d) Gated on granulocytes: The presence of circulating intermediate myeloid precursors yield a maturation curve similar to that seen in a hemodilute normal bone marrow (i.e., with an excess of mature granulocytes).


Case study 63

The diagnostic evaluation of low-grade MDS can be a difficult process, especially when clear-cut cytologic (e.g., ring sideroblasts) or cytogenetic abnormalities are not present. Furthermore, the patient may be treated with growth factors (namely G-CSF) to stimulate hematopoiesis. In such instances, it may not be possible to determine if the phenotypic abnormalities on the granulocytes are inherent to the MDS itself or secondary to G-CSF therapy. Otherwise, the combination of several of the following FCM abnormalities, when correlated with the peripheral blood (bicytopenia or pancytopenia) and bone marrow findings, may help to establish the diagnosis of MDS:

1. Altered myeloid maturation curves. The combination of this finding and pancytopenia is most useful, especially if the corresponding bone marrow is hypocellular and the differential diagnosis is hypocellular MDS vs aplastic anemia.
2. Downregulated CD10 expression.
3. Low SSC.

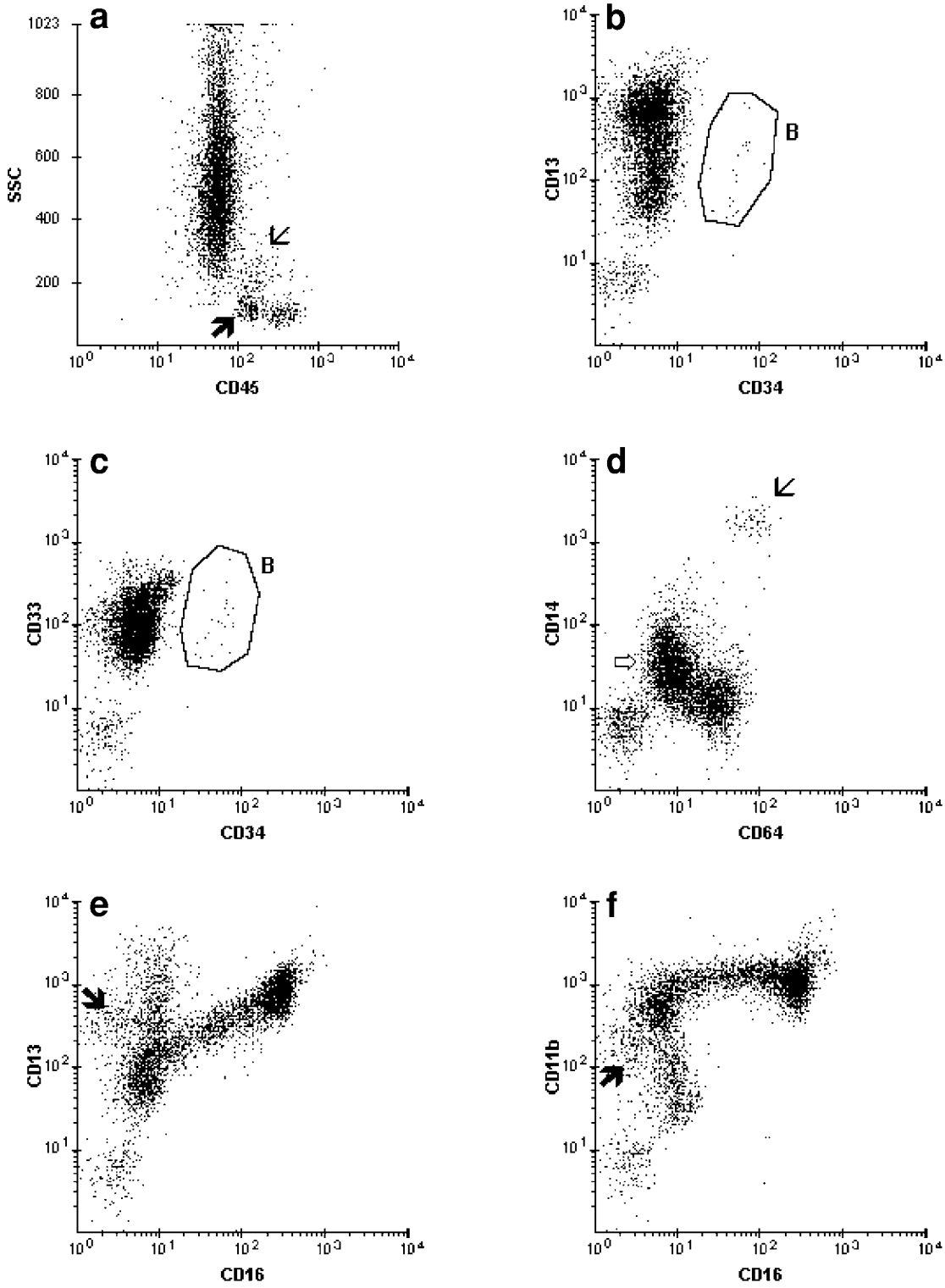

Figure 4.61 Peripheral blood with CML. (a) There are 4% basophils (arrow) and 1% monocytes (thin arrow). (b,c) Blasts (B), coexpressing CD34, CD13, and CD33, comprise 0.5% of the cells analyzed. (d) Upregulated CD14 expression on the more mature granulocytes (open arrow). (e,f) Basophils (arrow) express CD13 and CD11b, but lack CD16. Circulating myeloid precursors (*see* Figure 4.27b,d for comparison) are present, with an abnormal CD13/CD16 maturation curve.

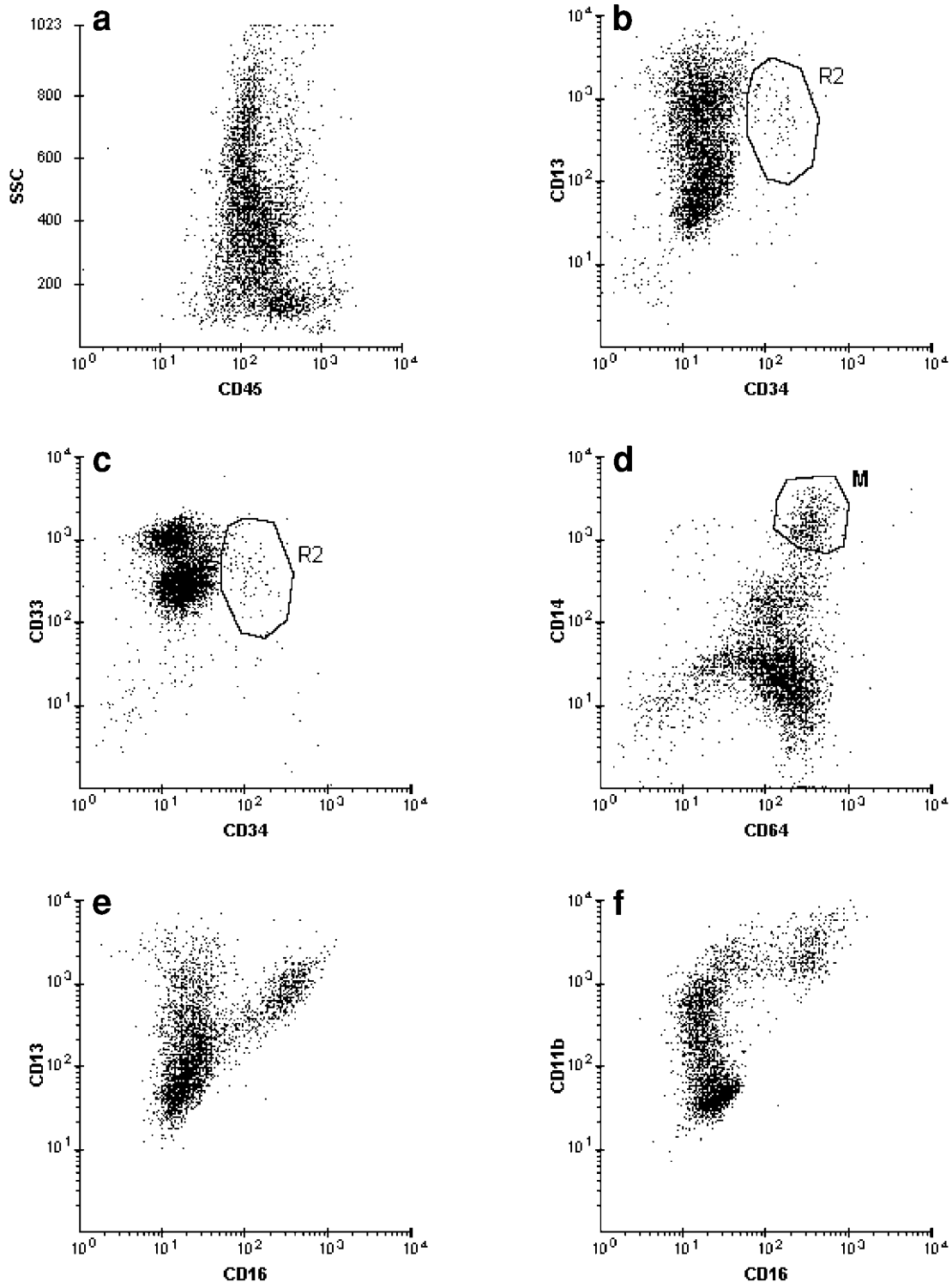

Figure 4.62 Bone marrow with a CML-like MPD (monosomy 7 syndrome). (a–c) Blasts (R2), which comprise less than 2% of the cells analyzed and coexpress CD34, CD13, and CD33, are not easily seen on the SSC/CD45 dot plot. (d) The myeloid precursors display increased CD64; CD14 is upregulated on the more mature cells. There are less than 8% monocytes (M) in the sample. (e–f) Gated on granulocytes: Abnormal myeloid maturation curves with downregulated CD16 and CD11b.

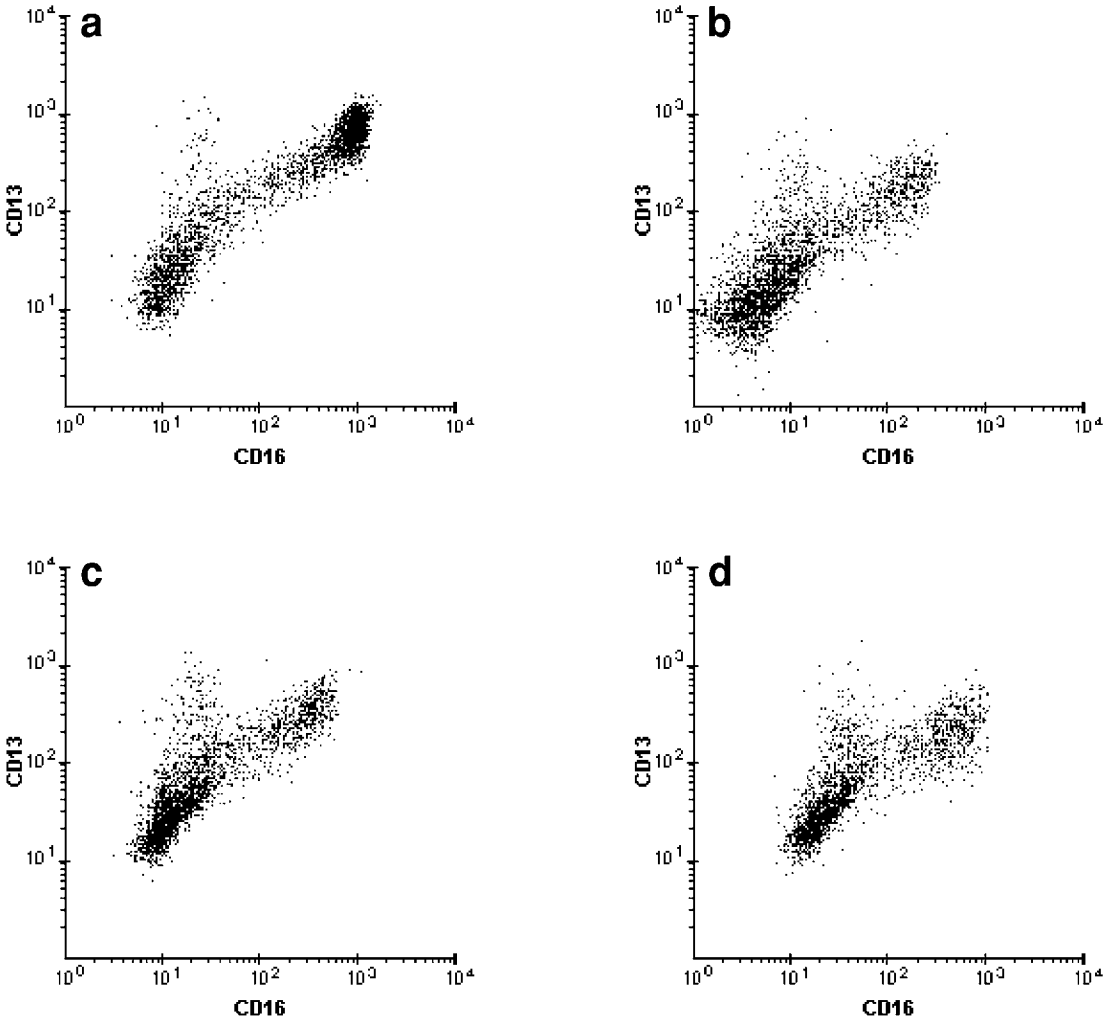

Figure 4.63 CD13/CD16 myeloid maturation curves from remission to relapse in a patient with AML. (a) In remission, 10 months prior to relapse: Normal CD13/CD16 maturation curve. (b) Still in clinical remission (bone marrow blasts < 5%), 4 months prior to relapse. Abnormal CD13/CD16 curve with down-regulated CD16. (c) Impending relapse (6% bone marrow blasts), 1 month prior to full-blown relapse: The abnormal CD13/CD16 curve is essentially identical to that in the diagnostic sample (not shown) and the relapse sample (d), which contains 23% blasts.

4. A discrete blast cluster on the SSC/CD45 dot plot, albeit not exceeding the accepted normal range. Any phenotypic aberrancy on the blast population, if present, confirms its neoplastic nature.
5. Abnormal CD71 expression and increased erythroid precursors.

The abnormal myeloid maturation curves can also be useful when evaluating the follow-up bone marrow specimens of AML patients in clinical remission. In the early post-treatment phase, it is unclear whether the maturational abnormalities, both antigenically and morphologically, reflect residual disease or are secondary to chemotherapy/G-CSF effect. If the patient remains in stable remission, the maturation curves will become essentially normal. When evaluating later follow-up bone marrow samples, it is helpful to compare the maturation curves from one specimen to the next. Via this exercise, it is possible to detect a trend toward an impending relapse even though the blast proportion still remains below the threshold level for clinical remission. During the 3–6 months preceding the relapse, the maturation curves may change from normal to abnormal (Figure 4.63).

4.6 Coexisting malignancies

The occurrence of two (or sometimes more) coexisting malignancies, although infrequent, is not rare. One of the neoplastic populations may comprise a very small component in the specimen analyzed and, thus, may escape FCM detection if a large antibody panel was not applied initially. The systematic approach to FCM data analysis, as thus far described, is applied to establish the phenotype of each individual neoplastic process. The various combinations of coexisting malignancies encountered in the FCM–hematopathology laboratory can be broadly grouped as follows:


Case study 64


Case study 65


Case study 66

1. A mature B-cell neoplasm, usually CLL or plasma cell dyscrasia, coexisting with a myeloid disorder (Figure 4.64) that can be an MPD, high-grade MDS, or AML. In the context of a low-grade LPD/NHL, the superimposed high-grade MDS or AML is likely to be associated with a history of aggressive chemotherapy.
2. Two or more coexisting LPDs/NHLs of different subtypes (e.g., CLL and HCL), which may or may not share the same light chain isotype. A high-grade B-cell malignancy occurring in the context of CLL suggests Richter's syndrome.
3. Two different clones within the same type of LPD/NHL (e.g., biclonal CLL). This is a very rare occurrence.
4. Biclonal acute leukemia (i.e., coexisting AML and ALL) (Figure 4.65).
5. Hematopoietic neoplasms coexisting with a nonhematopoietic malignancy. The metastatic tumor cells, individually and in clusters, may be too large to pass through the flow cytometer and may be seen only on the morphologic preparations.

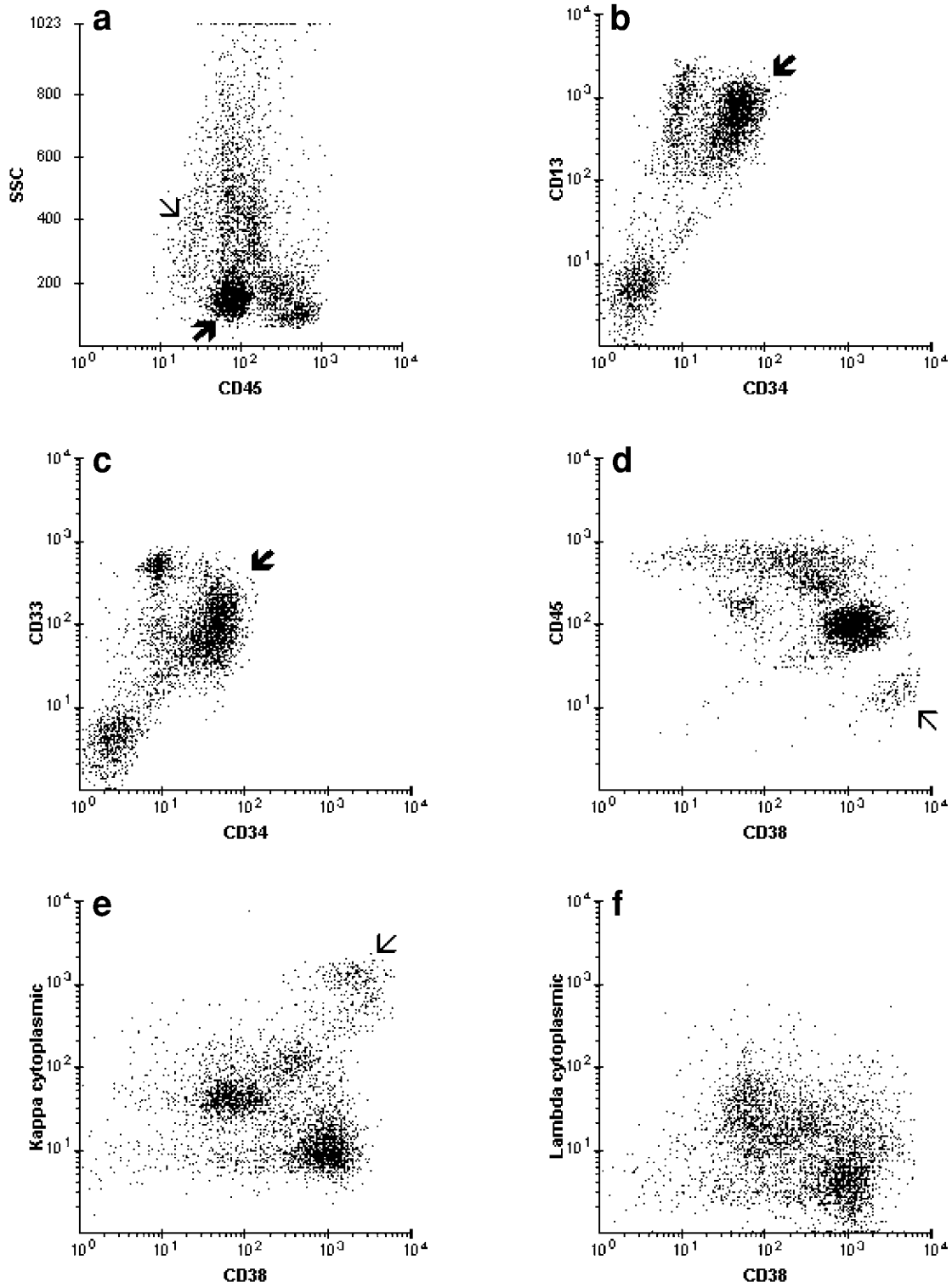

Figure 4.64 Bone marrow with AML and plasma cell dyscrasia. (a) A prominent blast cluster (arrow) and an ill-defined plasma cell cluster (thin arrow). (b–d) Gated on MNCs: Blasts, coexpressing CD34, CD13, and CD33, comprise 25% of the cells analyzed. There are 16% plasma cells with dim CD45 and bright CD38. (e,f) Monoclonal cytoplasmic kappa is expressed. There is kappa hypergammaglobulinemia.

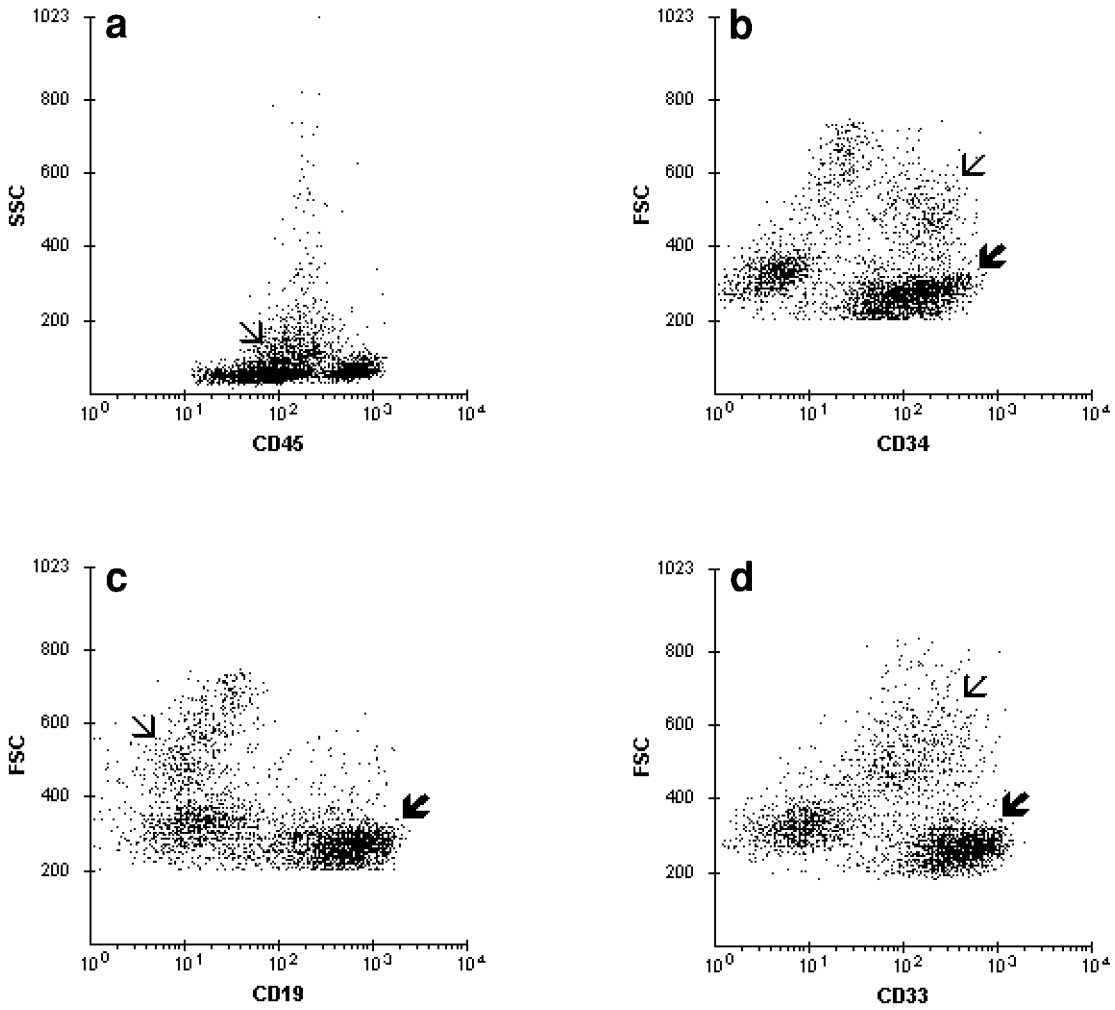

Figure 4.65 Biclonal acute leukemia (AML + ALL). (a–d) The two leukemic processes are best appreciated on the FSC vs fluorescence correlated displays. The major blast population (arrow) demonstrates low FSC and extremely low SSC and expresses CD34, CD19, and CD33. The minor blast population (thin arrow) displays slightly higher SSC and higher FSC and expresses CD34 and CD33. CD19 is negative.

CHAPTER

5 FCM interpretation and reporting

The previous chapters focus on analyzing FCM data by evaluating the location, shape, density, and size of the cell clusters observed on the various FCM graphics produced by light scatter signals and antigenic expression of the cells analyzed. In this chapter, the focus is on the last step of FCM analysis (i.e., FCM data interpretation and result reporting) which requires the integration of FCM results and other relevant laboratory and clinical information, including the correlation of the FCM and morphologic data.

Similar to data analysis, FCM interpretation is best carried out using a pattern approach. Each of the major immunophenotypic patterns (presented in detail in *Diagnostic Hematology: A Pattern Approach*) corresponds to a cell lineage and maturation, as inferred from the combination of relevant results derived from the FCM graphics. The antigenic patterns, similar to the leukemias and lymphomas they represent, can be segregated into two broad categories according to the maturity status of the critical cells. The mature group includes neoplasms with a mature B-cell, mature T-cell, NK cell, or plasma cell phenotype. The immature group consists of blastic proliferations, which can be of myeloid, immature B-cell, or immature T-cell differentiation, or, less commonly, a bilineage myeloid–lymphoid differentiation. A leukemic blast population with no evidence of lineage commitment (i.e., a stem cell phenotype) is an extremely rare occurrence.

Correlation of the FCM results and morphologic material is greatly facilitated in institutions where the FCM and hematopathology laboratories are integrated together as one single diagnostic service. For this exercise to be worthwhile, the air-dried preparations and tissue sections should be of optimal quality. The traditional approach in the literature has been to describe the immunophenotypes of hematologic neoplasms according to the accepted morphologic categories of that era, using morphology as the "gold standard." There are many flaws associated with a morphologic "gold standard," however. Morphologically-based categories suffer from serious subjectivity and reproducibility drawbacks and may not all represent distinct clinical entities. The incorporation of newer analytical techniques such as immunology, cytogenetics, and molecular genetics in recent classification schemes (WHO) has alleviated this problem. However, even with these additions, morphologic interpretations still remain subjective and dependent on optimally prepared histologic sections or cytologic smears. Therefore, in this chapter, the FCM/morphologic correlation departs from the traditional approach. The conventional terminology is employed when there is reasonable certainty that a given disorder is distinctive enough to be identified in a reproducible manner.

5.1 Immature hematopoietic malignancies

The immature status of the critical cells can be identified by the downregulation of CD45 and the presence of early markers, such as CD34, CD117, TdT, and/or CD1a. The expression of early antigens is most important in the lymphoid lineage because mature and immature lymphoid cells can simulate each other morphologically (e.g., small lymphoblasts can be mistaken for lymphocytes, and large lymphoma cells misidentified as blasts). In contrast, myeloid

blasts are cytologically different from maturing myeloid precursors and, therefore, can be more easily recognized as immature elements.

On air-dried preparations such as peripheral blood or bone marrow, the only lineage-specific cytologic feature is the presence of Auer rods. In the majority of cases, the leukemic blasts display a high nuclear/cytoplasmic (N/C) ratio, scant to moderately abundant pale blue cytoplasm, fine nuclear chromatin, a visible nucleolus, and variable degree of heterogeneity in cell size. These morphologic features are nondescript, however, and give no hint to the associated phenotype. Furthermore, some cases of T-ALL demonstrate conspicuous azurophilic granules, simulating the appearance of myeloblasts (Plate 14). Occasionally, the appearance of lymphoblasts closely mimics that of a mature lymphoid disorder (Plate 15).

Biopsies of lymph node specimens involved by any leukemic process usually reveal a diffuse pattern of infiltration. A less frequent morphologic manifestation is the interfollicular pattern of involvement, in which residual follicles are widely separated by an expanded interfollicular zone containing the neoplastic infiltration. On routine tissue sections, the morphology of AMLs can be easily mistaken for that of large cell lymphoma (Plate 16), whereas the cytology of lymphoblasts, with their medium-sized nuclei with a stippled ("salt and pepper") chromatin, may be simulated by the "blastic" variant of MCL (Plate 17). In the authors' experience, such diagnostic confusion is not an uncommon occurrence in institutions where FCM immunophenotyping or extensive immunohistochemistry studies are not applied to the workup of solid tissue specimens with suspected hematopoietic malignancies.

5.1.1 ALL/lymphoblastic lymphoma

The immature lymphoid malignancies are best designated according to their immunophenotypes (i.e., as precursor T-ALL/LL [lymphoblastic lymphoma] or precursor B-ALL/LL). Currently, it is still considered prognostically useful to further subclassify the precursor-B leukemias, especially in the pediatric age group, into "common" ALL ($CD10^+$) and "null" ALL ($CD10^-$). The latter is highly associated with adverse cytogenetic (chromosome 11) abnormalities and occurs more commonly in infants. The usefulness of identifying a third subgroup, pre-B-ALL, by testing for cytoplasmic IgM is questionable, since a substantial number of pre-B leukemias are not associated with specific chromosomal abnormalities.

Case studies 1, 10, and 12

Among the precursor-T malignancies, the phenotypic variations (e.g. $CD3^+$ vs $CD3^-$, $CD4^+CD8^+$ vs $CD4^-CD8^-$ vs $CD4^+CD8^-$) have no demonstrable prognostic significance. Therefore, it is not necessary to subdivide precursor T-ALL/LL according to the stages of thymocyte differentiation. CD10 expression, present in a substantial number of precursor T-ALL/LL, does not affect the prognosis either.

Case study 67

Rare cases of ALL/LL may display a very complex phenotype whereby antigens of several lineages are coexpressed. The clinical history or genotypic studies may disclose an underlying CML or an association with the (9;22) translocation.

5.1.2 Myeloid malignancies

In the myeloid lineage, the most useful antigens for recognizing myeloblasts include CD13 and CD33, CD117, and MPO. Other antigens, such as CD11b and CD16, are less useful because their expressions vary highly among AMLs and they may appear or disappear at relapse (and, therefore, may not be useful for follow-up purposes). Using a combined FCM and morphologic evaluation of the bone marrow, several subtypes of AML can be identified.

5.1.2.1 AML-M3

Case studies 2–4

The characteristic finding of bundles of Auer rods or dense granulation facilitates the morphologic recognition of typical AML-M3. The cytology of M3v may simulate that of other hematologic malignancies (Plates 6 and 18), however. In either instance, inspection of the FCM dot plots reveals the characteristic pattern of antigenic expression associated with AML-M3. CD13 and CD33 are well expressed and other antigens, namely CD34, CD117, HLA-DR, CD11b, CD15, and CD16, are absent or poorly expressed (Figure 3.23). As shown in Section 3.4.1, weak HLA-DR and/or weak CD34 (bimodal) may be observed in the severely hypogranular/agranular variant of AML-M3 (Figure 3.26).

5.1.2.2 AML with minimal maturation

Case studies 6, 7, and 68

In AML with minimal maturation, the neoplastic population is composed almost solely of myeloblasts. The leukemic blasts often share the phenotype of normal myeloblasts (i.e., CD13, CD33, and HLA-DR are expressed) with or without CD34. CD7 may be present. Whether this finding should be considered aberrant has been the subject of controversy. When expressed, CD7 may be used as a "fingerprint" to detect early relapse or residual disease. Other phenotypic aberrancies (*see* Section 3.5.1.1), when present, are also useful for follow-up purposes. A frequent aberrancy encountered in AML with minimal maturation is $CD13^{-}$, $CD33^{+}$. Some of the cases with this aberrant myeloid pattern also lack detectable CD34 and HLA-DR (Figure 5.1), which then may lead to a misinterpretation as AML-M3. If the institution still uses the FAB classification, then the distinction between AML-M0 and M1 can be made based on the finding of either Auer rods (Plate 19) or a positive myeloperoxidase cytochemistry (Plate 5) in AML-M1. AML with positive MPO antigen (or MPO cytochemistry) but lacking both CD13 and CD33 is a very rare occurrence.

5.1.2.3 AML with maturation

Case studies 45–47

In AML with maturation, the neoplastic clone includes a substantial proportion of maturing myeloid precursors in addition to the blasts. Most of the AMLs preceded by MDS fall into this category, which corresponds to the FAB AML-M2. The phenotype of the blasts is similar to that mentioned in Section 5.1.2.2. When present, the aberrant coexpression of CD19 (Figure 4.36) is highly associated with the translocation (8;21), a favorable prognostic indicator. The corresponding bone marrow often demonstrates some increase in eosinophils (i.e., AML-M2Eo) (Plate 20). The latter is not be confused with AML-M4E (Plate 12), itself characterized by the presence of abnormal eosinophils and abnormalities of chromosome 16. Although the FAB classification considers M4E as a subtype of M4, the bone marrow morphology more often resembles M2 than M4. Although the blast and monocytic components may merge together as one cell cluster on the SSC/CD45 dot plot (Figure 4.34), they are seen as two distinct populations on the CD14/CD64 display since blasts in AML-M4E usually demonstrate no reactivity for the monocytic associated markers CD14 and CD64 (Figure 5.2). Furthermore, NSE staining is often negative in AML-M4E, and peripheral monocytosis is not always present.

5.1.2.4 AML with monocytic differentiation

The AMLs with monocytic differentiation can be identified by FCM based on the shape and location of the blast cluster on the SSC/CD45 dot plot and the pattern of CD14 and CD64 coex-

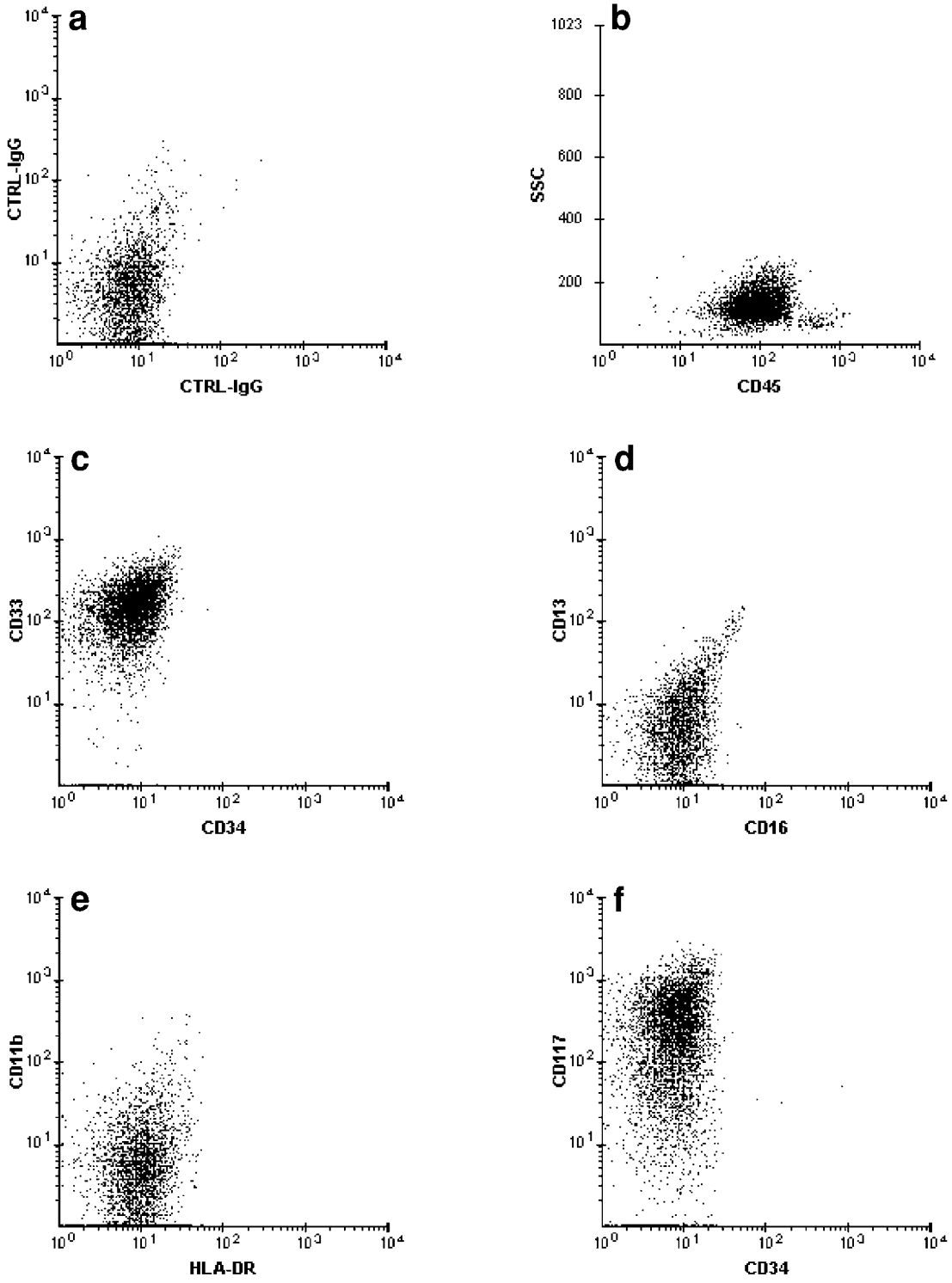

Figure 5.1 AML with minimal maturation (AML-M1). (a) Isotype-matched negative controls. (b–f) The sample is composed virtually entirely of blasts. The leukemic cells are $CD33^{++}$, $CD117^{++}$, $CD34^{-}$, $CD13^{-}$, $CD11b^{-}$, and $CD16^{-}$. HLA-DR is essentially negative. The phenotype superficially mimics that of AML-M3. However, the shape of the cluster on SSC/CD45, bright CD117 expression, and an aberrant CD13/CD33 pattern are features not supportive of the diagnosis of AML-M3.

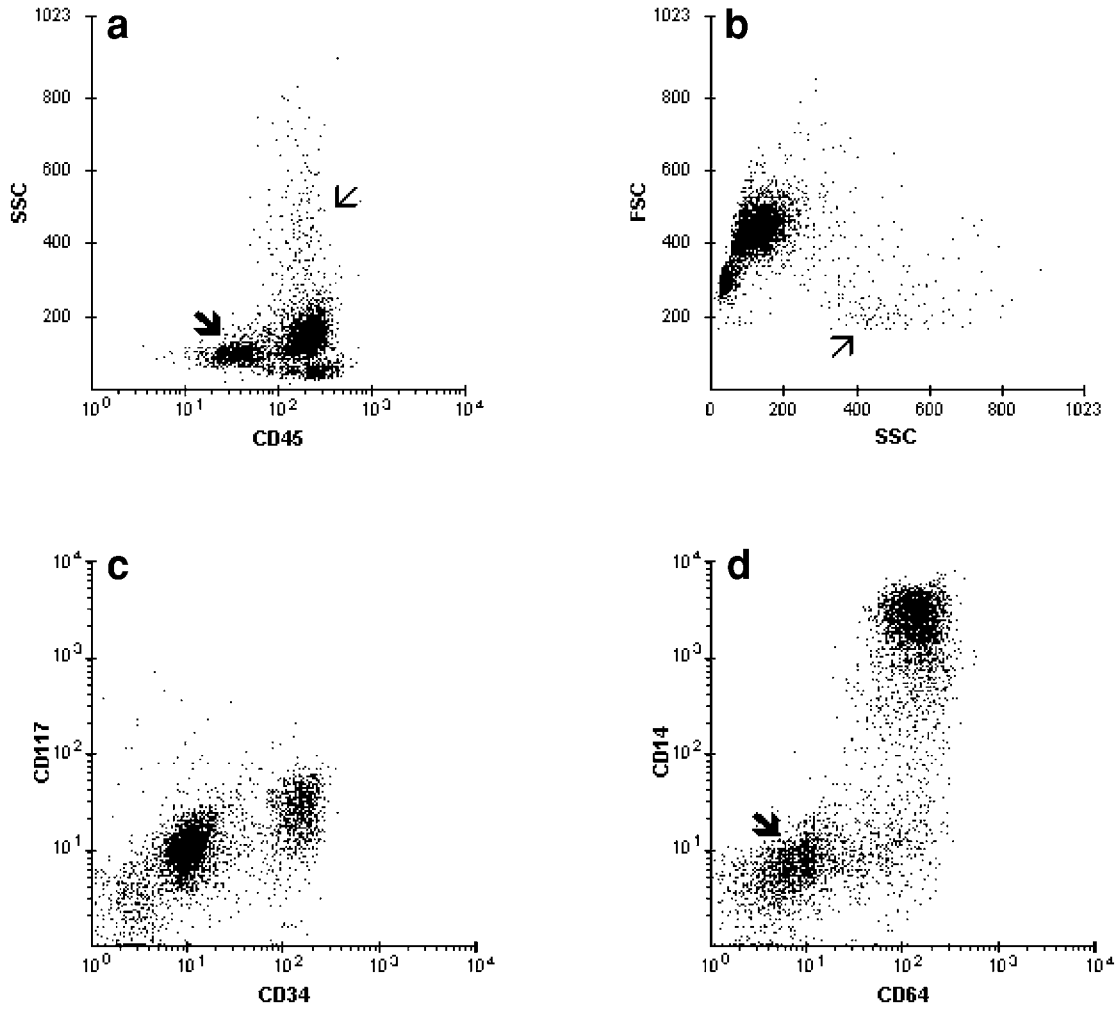

Figure 5.2 Bone marrow with AML-M4E. (a–d) The blast (arrow) and monocytic clusters are distinct from each other on the SSC/CD45 dot plot. Eosinophils (thin arrow) display the characteristic low FSC. Blasts coexpress CD34 and dim CD117 and lack both CD14 and CD64. The monocytic component is composed mostly of mature elements with bright CD14/CD64 coexpression. The CD14/CD64 trail is relatively attenuated, reflecting the lower number of immature monocytes.

pression (*see* Section 3.5.1). Cases composed predominantly of the most immature cells (so-called monoblasts) (i.e., AML-M5a [Plate 21]) can also be distinguished from those containing maturing monocytic elements according to the pattern of CD14/CD64 reactivity (Figures 3.36 and 3.37). Blasts in this group of AMLs may not express CD34. Further subclassification into AML-M4 and M5 according to the FAB criteria, if deemed necessary, is based on the results of the NSE cytochemistry using the recommended thresholds of 20% and 80%, respectively. The sensitivity of NSE staining varies with the type of substrate used, however. Furthermore, the relative proportion of the granulocytic and monocytic components fluctuate during the course of the disease. For instance, the bone marrow picture may be that AML-M5 at diagnosis, but residual/relapsed disease may resemble AML-M4.

Case studies 8, 9, 11, and 44

5.1.2.5 AML with erythroid hyperplasia

Acute myeloid leukemia with erythroid hyperplasia corresponds to AML-M6 if, on the bone marrow smear, the erythroid component exceeds the combined population of blasts and

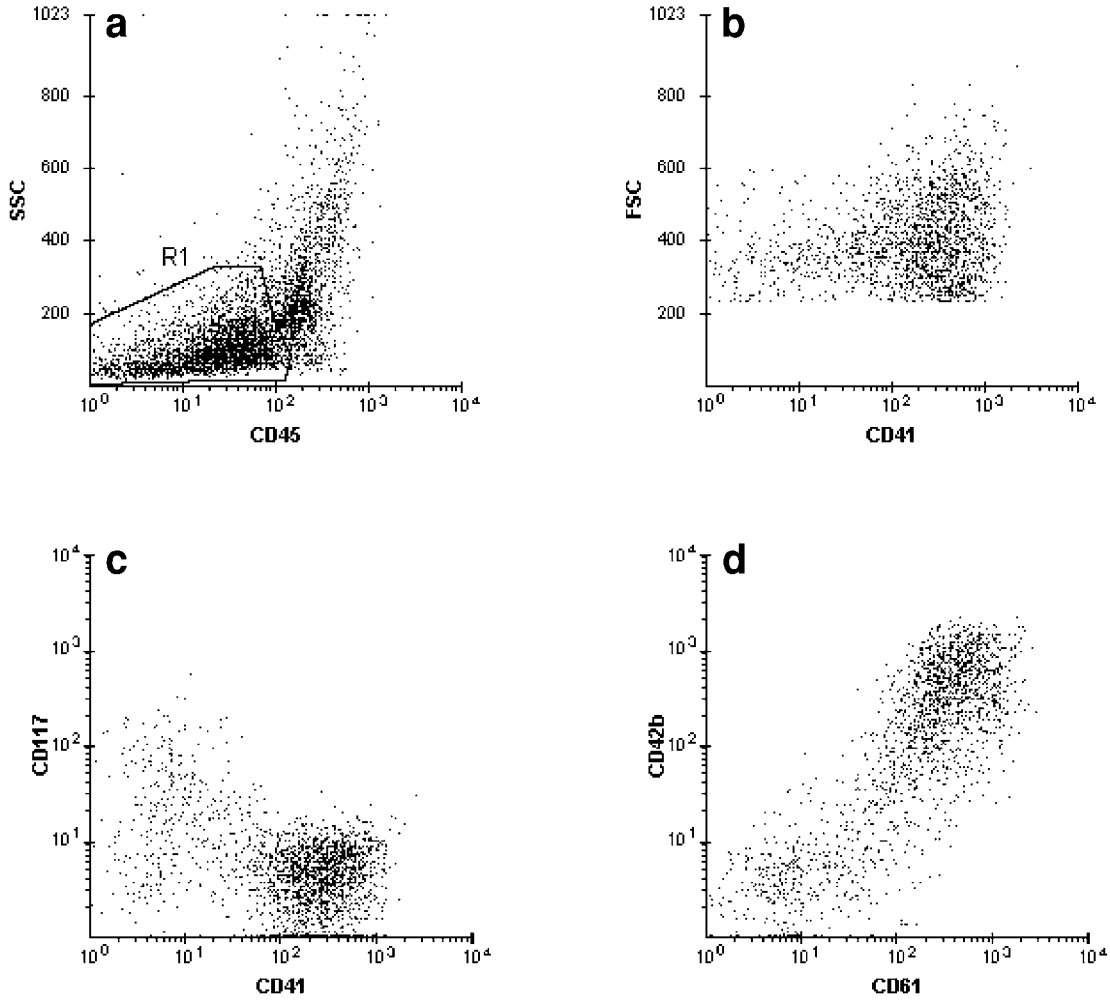

Figure 5.3 AML with megakaryocytic differentiation. (a) A prominent cluster (R1) with variable CD45 expression, ranging from negative to weak. (b–d) Gated on R1: Blasts are of medium to large cell size. Megakaryocytic markers (CD41, CD42b, and CD61) are well expressed. CD117 and CD34 (not shown) are present in a minute subset of the blasts.


Case study 43

myeloid precursors (Plate 22). Evidence of erythroid hyperplasia is best seen on the SSC/CD45 and FSC/CD71 dot plots (Figure 4.32). The antigenic profile of the blasts is similar to that of typical myeloblasts. In many instances, AML-M6 is a transient manifestation of either AML-M2 or AML with minimal maturation.

5.1.2.6 AML with megakaryocytic differentiation


Case study 69

The identification of the rare AML-M7 (AML with megakaryocytic differentiation, Figure 5.3) is based on megakaryocyte-associated antigen expression (e.g., CD41, CD61) and occasionally may require platelet peroxidase ultracytochemistry. Either CD13 or CD33 may also be expressed. The marrow aspirate is often aspicular because of severe reticulin fibrosis, thus necessitating examination of the bone marrow biopsy and corresponding imprints instead. Contrary to popular belief, the cytologic finding of blasts with cytoplasmic blebs does not necessarily imply megakaryocytic differentiation. Slow drying of the blood or bone marrow smears can induce bleb formation on cells with ample cytoplasm.

5.1.2.7 MPD and MDS

For myeloid disorders in which the blast component is below the currently accepted threshold for AML, a correlation of the blood and bone marrow findings is necessary to separate MPD from MDS. It is also necessary to distinguish the latter from residual/early-relapsed AML based on the appropriate clinical history. As a rule of thumb, in MDS, the blood and bone marrow pictures contrast with each other (i.e., the peripheral blood is cytopenic, while the bone marrow is hypercellular), whereas in MPD, the elevated WBC count parallels the bone marrow proliferative process. In the case of CMMoL, the FCM picture is relatively specific, such that a diagnosis can be made when the FCM dot plots are evaluated in the context of a peripheral leukocytosis or hyperplastic marrow (*see* Section 4.5.1). Some FCM abnormalities, such as altered myeloid maturation curves, can be seen in either MPD or MDS (*see* Section 4.5.2). Similarly, cytologic features that have been considered specific to MDS (e.g., hypogranulation) can be also present in MPD. An exception to the above rule of thumb is hypoplastic MDS, which morphologically may be difficult to differentiate from aplastic anemia (Plate 23). Abnormal FCM findings (e.g., altered myeloid maturation curves or a slight excess in blast content) or the presence of cytogenetic abnormalities are helpful clues for identifying hypoplastic MDS. The diagnosis can be further confirmed by a subsequent rapid progression to a typical hypercellular, high-grade MDS.


Case study 58

5.1.3 Acute leukemias with a multilineage antigenic profile

Expression of a myeloid antigen can be seen in some ALLs, especially those of precursor-B lineage. Conversely, some AMLs may express a lymphoid-associated marker (Figures 3.22, 4.35, and 4.36). Because of the variable criteria and lack of a standard uniform panel between different laboratories, there has been no clear definition regarding what constitutes aberrant antigenic expression in acute leukemia. In the authors' opinion, the label "aberrant myeloid antigen expression" or "aberrant lymphoid antigen expression" should take into account the relative specificity of the marker in question. For instance, CD13, CD33, CD19, and CD20 are relatively more specific than CD7, CD2, CD14, CD15, or CD56. Similar stringent criteria should be also applied in defining biphenotypic leukemia (Figure 5.4), a process characterized by the presence of blasts coexpressing lymphoid and myeloid antigens. In the literature, the frequency of this type of leukemia has varied widely, ranging from less than 1% to greater than 20% of acute leukemias. As a result of the lack of consistent criteria, it has been difficult to assess the clinical significance of the so-called biphenotypic leukemias. These leukemias may represent the neoplastic transformation of a stem cell at a stage prior to lineage commitment. Some studies have shown a high association with the presence of the Philadelphia chromosome. Biphenotypic leukemias should not be confused with biclonal (or multiclonal) acute leukemia (Figure 4.65), defined as the coexistence of two or more distinct leukemic populations with different phenotypes. This very rare process may also be associated with the (9;22) translocation.


Case study 70

5.2 Mature lymphoid malignancies

The mature lymphoid malignancies consist of mature B-cell, T-cell, and NK leukemias and lymphomas, as well as plasma cell dyscrasias. Most of the leukemias are chronic lymphoproliferative disorders and follow an indolent disease course. However, some of these mature neoplasias, such as ATLL, certain aggressive NK leukemias, and Burkitt's lymphoma–leukemia run a rapidly progressive course.

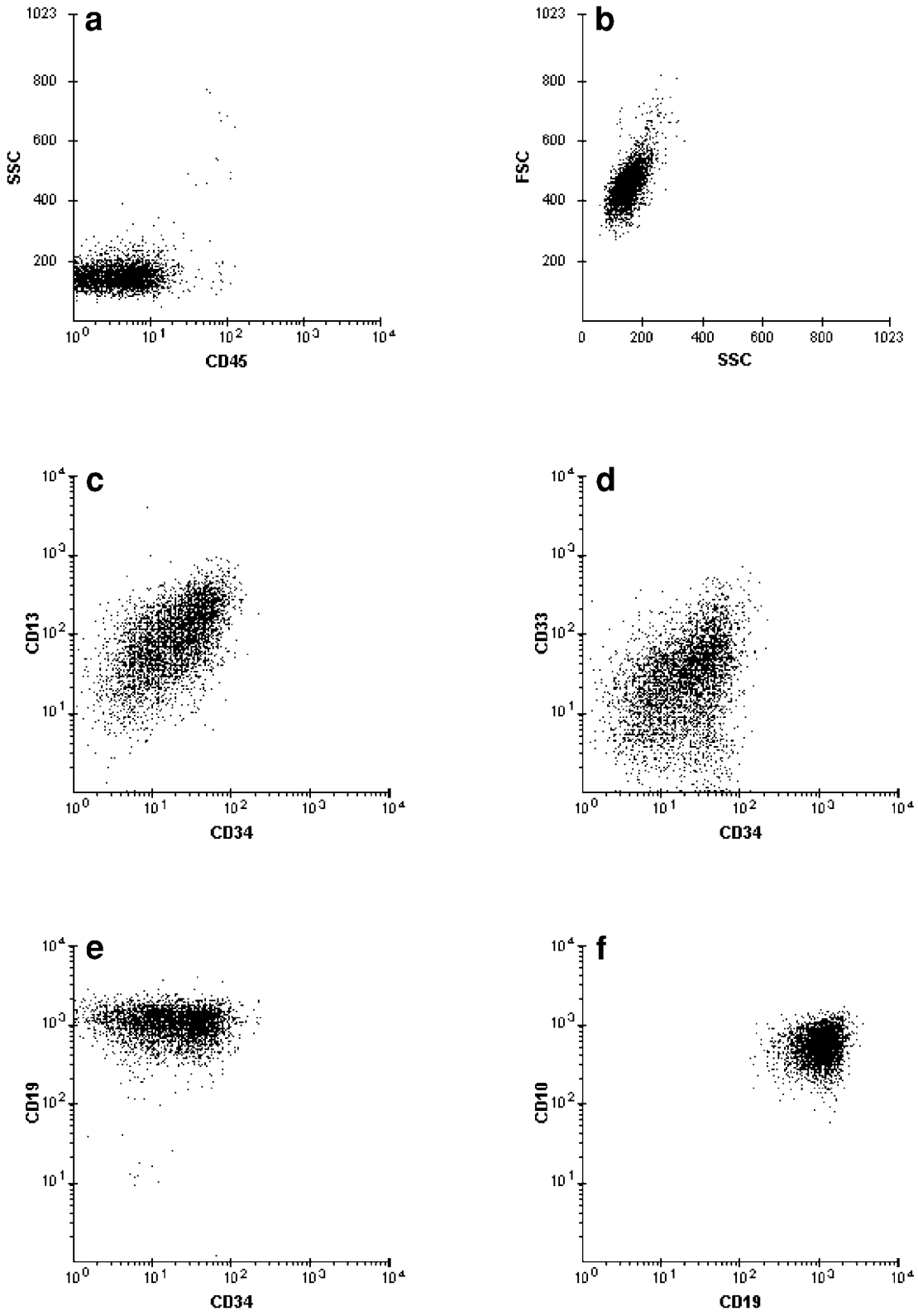

Figure 5.4 Biphenotypic acute leukemia. (a–f) The sample is essentially a pure cell culture of blasts. Blasts are of medium cell size and lack CD45. There is coexpression of CD34, CD13, CD33, CD10, and CD19. CD34 is weak and of variable distribution. Cytogenetics revealed t(9;22).

The diagnosis and classification of malignant lymphomas, which traditionally have relied mostly on morphology, have in recent years taken into account the results of immunologic studies. In most instances, the antigenic profiles of these neoplasms have been derived from immunohistochemistry, however, rather than from FCM immunophenotyping, which provides a much better delineation of antigen expression, as well as a better appreciation of antigen density and antigen coexpression. One of the main reasons is that in many institutions, including those with FCM laboratories (especially outside the United States), lymph nodes and other tissue specimens with suspected lymphoma are rarely submitted for FCM analysis. As a result, large amounts of valuable information contained in the rich data derived from the FCM analysis are not being taking into consideration in the current lymphoma classification schemes.

We have chosen to use the FCM immunophenotyping features, along with DNA and cell cycle analysis (*see* Section 2.10), as the basis for the discussion of the categorization of mature lymphoid malignancies.

5.2.1 B-cell LPD/NHL

The bulk of mature lymphoid malignancies passing through the FCM–hematopathology laboratory are of B-cell lineage. Several major categories can be identified with a high degree of accuracy and reproducibility based on their FCM patterns of antigenic expression and S-phase fraction.

5.2.1.1 CD10 expression

The correlation of CD10 expression with FCC lymphomas is straightforward (*see* Section 3.6.3.1 and Section 4.1.1.1). On histologic sections, the follicular pattern (however vague it may be) with back-to-back follicles in the lymph node and the paratrabecular pattern in a bone marrow biopsy are useful morphologic features for recognizing FCC lymphoma. Bone marrow involvement by other disorders (e.g., PTCL and mast cell disease) may also demonstrate a similar picture of paratrabecular infiltration (Plate 24). In some cases, the lymph node morphology is less clear-cut, as the neoplastic follicles are farther apart and still surrounded by an adequate mantle cuff. Occasionally, an FCC lymphoma adopts a so-called "floral" pattern on histologic sections (Plate 25). On air-dried preparations, the presence of deep nuclear indentations (e.g., "buttock" cells) facilitates the identification of the neoplastic cells, cytologically. Nuclear indentation is a cytologic feature common to lymphoma cells of various types and therefore does not imply an FCC origin, however. In addition, it is important to be aware that nuclear irregularities can be artifactually induced by prolonged storage (Plates 26 and 27).

Case studies 16–18

The subdivision of follicular center cell lymphomas into FCC I, II, and III (applicable to solid lymphoid tissue only) becomes more reproducible when taking the FSC parameter into account rather than based solely on the manual counting of the number of large cells per microscopic high-power field.

CD10 expression, common in FCC lymphomas, is also found in some DLCLs (Figure 3.53). Knowledge of the clinical history, along with the availability of previous lymph node biopsies and corresponding FCM analyses are helpful to determine if the $CD10^+$ DLCL is a *de novo* process or a progression of a previous FCC lymphoma.

The combined findings of a very high S-phase and CD10 expression in a mature B-cell proliferation is essentially pathognomonic of Burkitt's lymphoma (Figure 3.52). This diagnostic combination is most useful when analyzing fine needle aspirate specimens from deep-seated lesions where an adequate morphologic assessment is not possible.

5.2.1.2 Coexpression of CD11c, CD25, and CD103

When evaluated properly (*see* Section 3.6.3.2) coexpression of CD11c, CD25, and CD103 is the antigenic fingerprint of HCL. Hairy cells can be identified by diffuse tartrate-resistant acid phosphatase (TRAP) positivity, but this approach may not be useful because the number of hairy cells on the blood film or aspicular bone marrow smear is often very low. On optimal air-dried preparations, hairy cells demonstrate a characteristic bland ovoid/reniform nucleus and a voluminous amount of pale cytoplasm (Plate 28). A bone marrow procedure is rarely necessary nowadays, given the excellent sensitivity of FCM to detect hairy cells in the peripheral blood (Figure 4.43).


Case study 19

5.2.1.3 Coexpression of CD5 and CD23

Coexpression of CD5 and CD23 is associated with CLL/SLL and disorders closely related to CLL. Biologically the same disorder, SLL only differs from CLL by the presence of some adhesion molecules (CD11a, CD18). In most cases of CLL/SLL, the neoplastic population is composed mostly of small lymphoid cells; the larger and more activated cells (i.e., plasmacytoid lymphocytes and prolymphocytes) are essentially insignificant. On lymph node sections, the activated cells are loosely packed into scattered pseudofollicles (i.e., proliferation centers). Rarely, proliferation centers may be seen on the bone marrow biopsy. The typical morphology of CLL/SLL correlates with the classical antigenic profile of weak CD20, a weak monoclonal surface light chain, and coexpression of CD5 and CD23 (Figures 3.13, 3.15, and 3.32).

In the disorders closely related to CLL, the number of activated lymphoid cells is increased and occasional nuclear irregularities may be present (Plate 29), especially in long-standing disease resistant to chemotherapy. The cytology of the heterogeneous-appearing neoplastic cells, which range from small lymphoid cells to prolymphocytes, can be better appreciated on the blood film (Plate 8) than on bone marrow smears. Various terminologies have been used in the literature to designate these activated CLLs (e.g., "atypical" CLL or CLL/PL [Plate 8; Figures 3.6 and 3.46]). Traditionally, the arbitrary thresholds of 10% and 50% prolymphocytes in the peripheral blood have been used to define CLL, CLL/PL, and B-PLL. The solid tissue equivalent of "activated" CLL manifests as prominent proliferation centers showing a variable degree of merging with each other (Plate 30). The morphologic similarities to the blood picture are best appreciated on lymph node imprints (Plate 31).


Case study 13

In most instances, the coexpression of CD5 and CD23 is retained in the activated variants of CLL/SLL, although CD20 and/or surface light chain tend to be brighter and the FSC slightly higher (Figure 3.45) than that observed in classical CLL/SLL. Occasionally, CD23 may also be downregulated. Although most cases of LPC lymphoma–leukemia (Figures 5.5 and 5.6) express no specific markers (i.e., a nondescript B-cell phenotype), a small number display antigenic features similar to that of activated CLL. Because the terminology "LPC" is mostly based on morphology, other laboratory data, especially serum immunoglobulins, are helpful to confirm the diagnosis.

B-prolymphocytic leukemia occurs much less frequently than activated CLL. Because of the variability in the expression of CD5 and CD23, the leukemic cells can be $CD5^{+}CD23^{+}$ (as in CLL), $CD5^{+}CD23^{-}$, (similar to MCL), or CD5-negative and devoid of any specific antigenic characteristics (i.e., a nondescript mature B-cell profile). The proliferative fraction is variable though higher than in CLL. The clinical presentation and the blood picture, with its markedly high WBC count composed predominantly of prolymphocytes (Plate 32), are useful features for identifying B-PLL.


Case study 71

Lymph node biopsies have only been infrequently studied in PLL. The morphologic equivalent of PLL in the lymph node is known as paraimmunoblastic lymphoma (Plate 33). Richter's

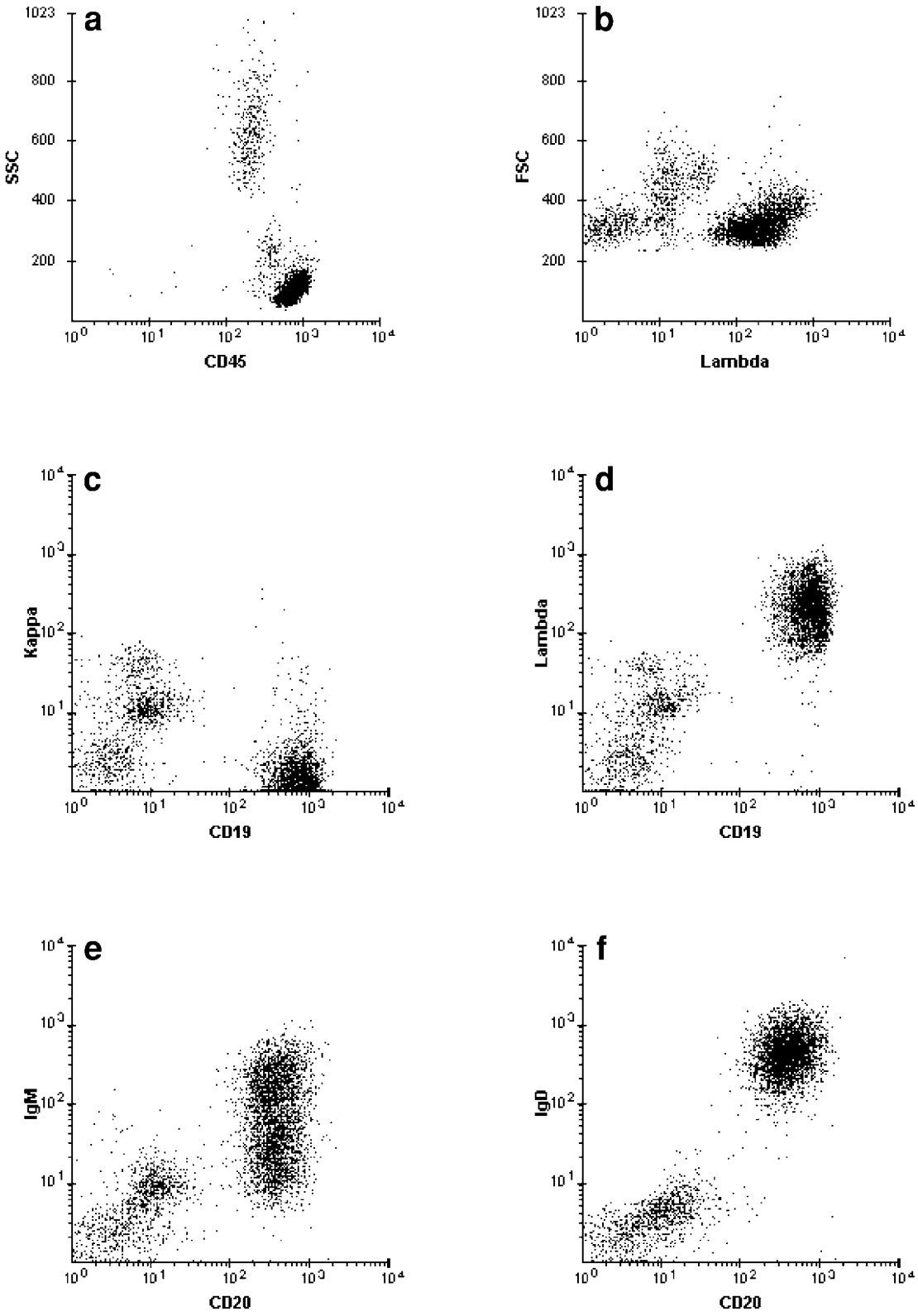

Figure 5.5 Peripheral blood with CD5+, CD23+ B-cell LPD, morphologically LPC lymphoma–leukemia. (a–f) The leukemic cells form a predominant lymphoid cluster with slightly increased FSC (the larger cells have brighter lambda). CD20 is bright (nearly as bright as CD19) and homogeneous. IgM and IgD are expressed. IgG and IgA (not shown) are negative. Lambda is brightly expressed.

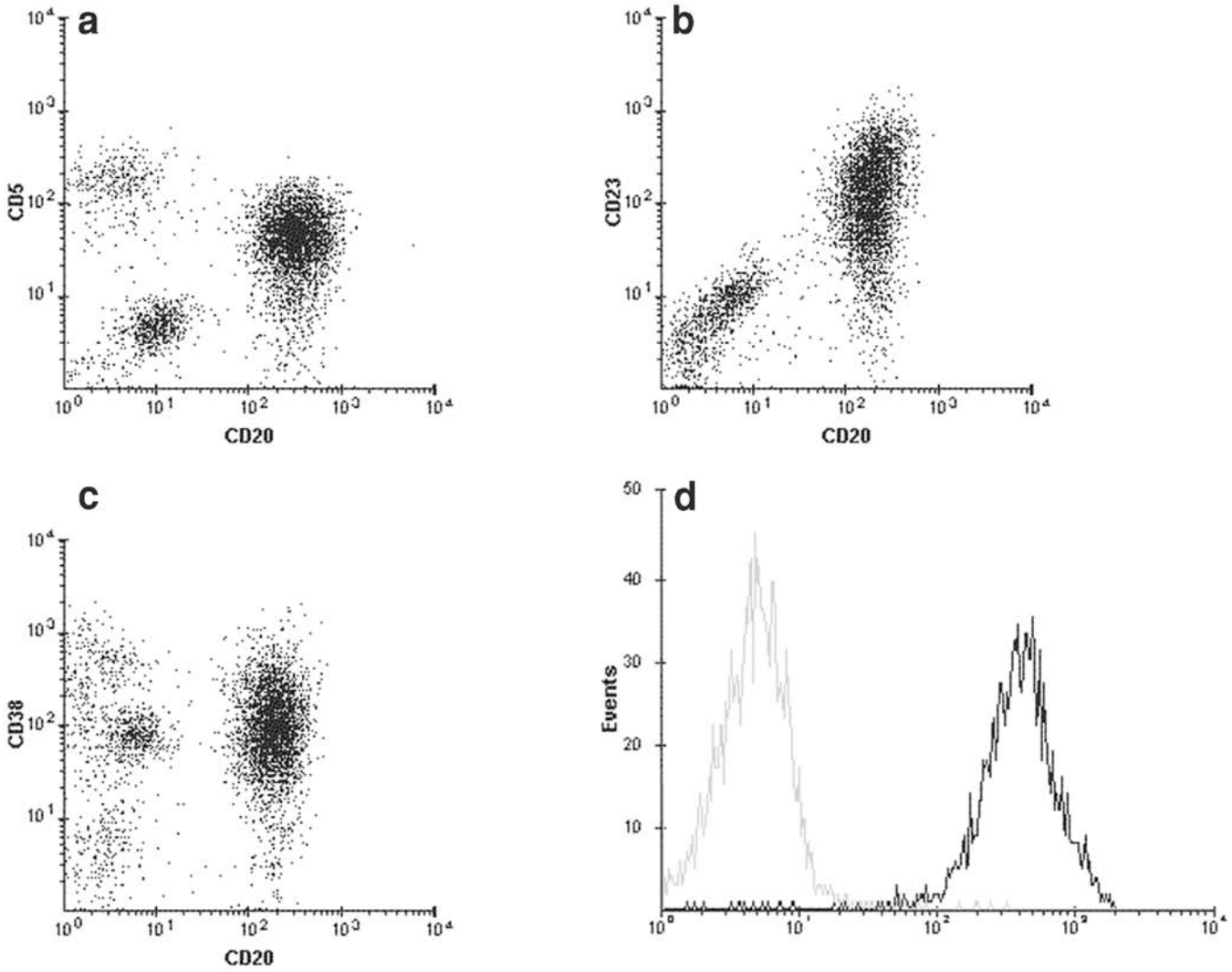

Figure 5.6 Peripheral blood with CD5+, CD23+ B-cell LPD (continuation of Figure 5.5). (a–c) The leukemic cells coexpress CD20, CD5, CD23, and CD38. (d) Gated on B cells: The difference between the mean peak fluorescence channels of the negative (kappa) and positive (lambda) histograms is greater than one decalog (i.e., lambda intensity is not weak).


Case study 65

syndrome, which refers to the transformation of CLL into a high-grade large cell lymphoma, is a rare occurrence and thus has been rather poorly defined. Therefore, it is unclear if a distinction between paraimmunoblastic lymphoma and Richter's syndrome can be made with certainty. In the former, the rather low number of mitotic figures is asynchronous with the large cell morphology. The large-cell lymphoma in Richter's syndrome, on the other hand, is expected to demonstrate a high mitotic rate and a corresponding elevated S-phase fraction similar to that seen in aggressive B-cell NHLs.

5.2.1.4 CD5+CD23– B-cell neoplasms

The antigenic profile of CD5+, CD23–, bright CD20, and bright surface light chain is very suggestive of MCL. However, some cases of activated CLL or lymphoplasmacytoid leukemia–lymphoma may exhibit a similar profile. The intensity of CD19 relative to that of

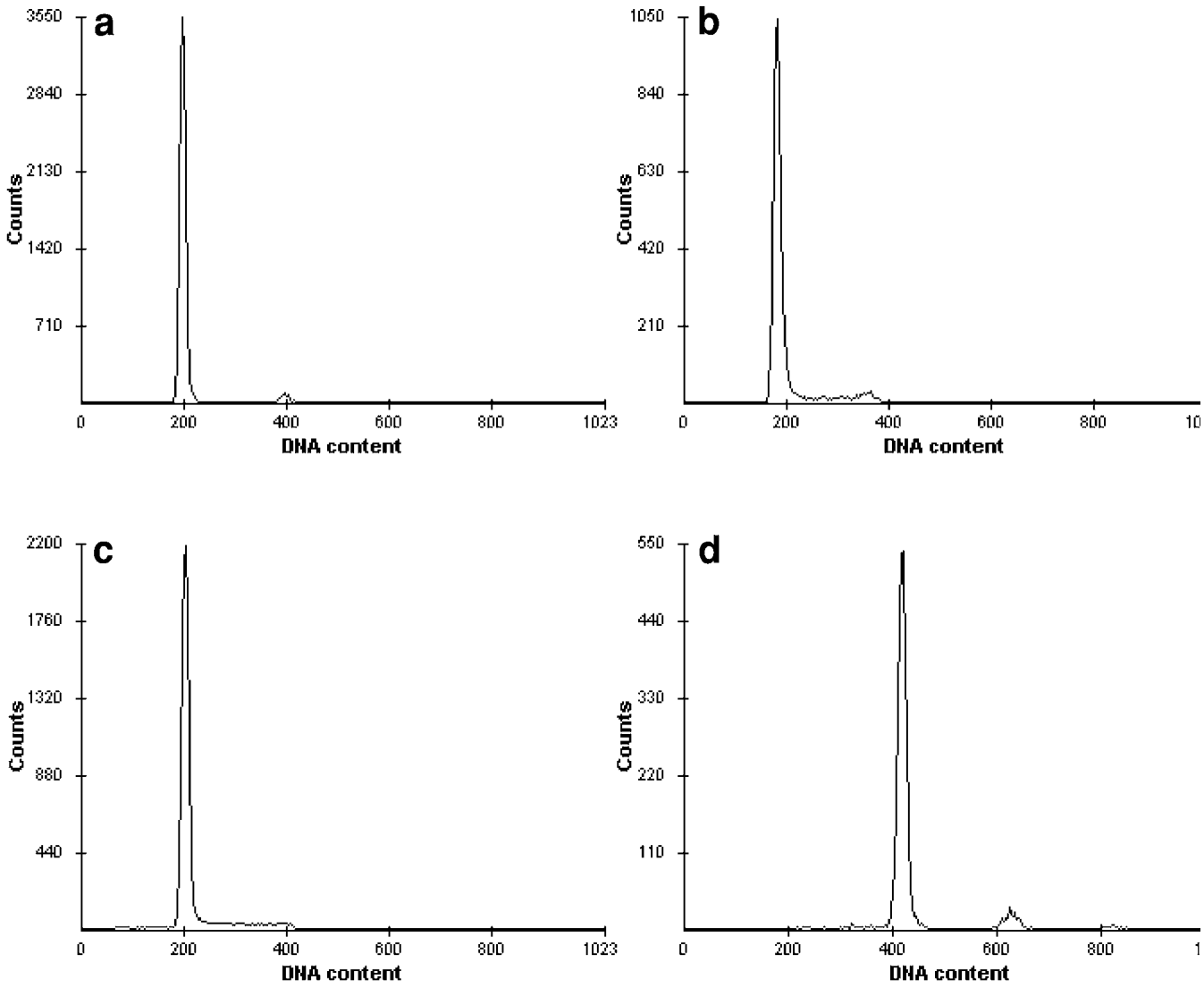

Figure 5.7 Proliferative fraction in MCL. (a) Case 1: The tumor is diploid; the S-phase fraction is low (S% 2.4). (b) Case 2: The tumor is diploid; the S-phase fraction is in the intermediate range (S% 10). (c) Case 3: The tumor is diploid; the S-phase fraction is high (S% 17). (d) Case 4: The tumor is near tetraploid (DI: 1.97) with a low S-phase fraction (S% 1.4).


Case study 72

CD20 (i.e., CD19 < CD20) (Figure 3.47) is an important clue for identifying MCL (*see* Section 3.6.2). Other findings useful for distinguishing MCL from other $CD5^+$,$CD23^-$ B-cell LPD/NHLs include (1) absence of serum monoclonal protein (IgM, IgA), (2) evidence of bcl-1 rearrangement [i.e., the (11;14) translocation (this abnormality may occur in a small number of lymphoplasmacytoid lymphomas and B-PLL, however)], (3) a mantle zone or a nodular growth pattern (even if focal) on lymph node/adenoid tissue sections (Plate 34), (4) lymphoid cells with cytologic features (e.g., indented nuclei) suggestive of lymphoma cells on air-dried smears, and/or (5) expression of cyclin D1. The nuclear indentations of the lymphoma cells can be better appreciated in uncrowded areas of the smears. The neoplastic cells in some cases may not display any nuclear indentations, however (Plate 35). The finding of nuclear irregularities, unless marked, is less meaningful on histologic sections because this feature may be artifactually induced by tissue fixation and processing.

Mantle cell lymphoma is considered to be a more aggressive disease than other small B-cell LPD/NHLs. In the authors' experience, the S-phase fraction varies widely between cases

(Figure 5.7), and not all patients have a limited survival. In some cases, the S-phase fraction is similar to that of low-grade lymphomas; in others, it is in the range seen in intermediate-grade lymphomas. The "blastic" variant of MCL (Plate 17b) is considered to represent a rapidly progressive stage of the disease. In laboratories that do not routinely perform FCM studies on solid tissue, this diagnosis is based mainly on the nuclear chromatin, which, in blastic MCL, appears finely stippled, similar to the chromatin of the lymphoblasts in ALL/LL. Blastic MCL can be recognized more reliably when taking the S-fraction, CD71 reactivity, and cell size into account rather than based solely on morphology, especially since the appearance of the nuclear chromatin can be easily affected by tissue processing and staining.

Case study 73

The immunophenotype $CD5^+$,$CD23^-$ may be found in a small number of large B-cell malignancies (Figure 4.45). Although some of these may be "blastic" MCL or PLL, most are high-grade B-cell lymphomas (Plate 36), which morphologically and genotypically bear no relationship to either PLL or MCL. Some may display an immunoblastic/plasmablastic appearance. Knowledge of the antecedent clinical history, or review of any available diagnostic material, may help to differentiate *de novo* $CD5^+$ large B-cell lymphoma from the other groups of disorders.

Case study 74

5.2.1.5 CD45 and/or pan B-cell antigens markedly downregulated

In addition to the decreased levels of CD45 or B-cell antigens (Figure 3.48), surface light chains may also be downregulated (Figure 3.60) in B-cell NHLs. These antigenic features are invariably associated with high-grade B-cell lymphoma with a variable degree of plasma cell differentiation. CD38 and CD56 may be present and light chain-restricted intracytoplasmic immunoglobulins can be detected in the majority of cases.

Case studies 20, 21, and 75

5.2.1.6 Nondescript B-cell phenotype and high FSC

Most large B-cell lymphomas display no specific antigenic characteristics. The aggressive nature of these lymphomas correlates with an increased S-phase fraction, high FSC signals, and bright CD71 expression (Figure 2.9). Occasionally, CD30 may be present. These lymphomas are heterogeneous, morphologically and genotypically. In lymphoid organs, several patterns of infiltration, such as interfollicular, sinusoidal, or diffuse, can be observed. The content of residual benign cells, especially T-cells, is highly variable. Simultaneous biopsies of several lymph nodes or sequential lymph node biopsies over the course of the disease may demonstrate the various morphologic manifestations of the same large cell lymphoma. For instance, the infiltration in one node may consist of scattered large neoplastic cells with a high content of benign T-cells (i.e., the so-called T-cell rich B-cell lymphoma), whereas in another node, the large cells predominate as sheets and clusters.

When faced with a DLCL, it may not be possible to distinguish a DLCL of FCC origin but lacking CD10 expression from a *de novo* DLCL. The distinction is based on the knowledge of previous lymph node studies or evidence of bcl-2 rearrangement.

5.2.1.7 Nondescript B-cell phenotype and low FSC

Small B-cell lymphomas with a so-called nondescript phenotype include the small number of FCC lymphomas without detectable CD10 and the heterogeneous group of small B-cell malignancies showing various morphologic manifestations and genotypic abnormalities. Several "entities" have been described, based primarily on morphologic features. However, the lack of uniform and well-defined morphologic criteria plus the lack of specific antigenic expression have very much hampered the reproducibility and accuracy of diagnosis in these low-grade B-cell neoplasms with a nondescript phenotype. Morphologic artifacts and the fact that the same disease may be given a different name depending on whether the specimen is blood/

bone marrow or solid lymphoid tissue further compound the diagnostic difficulties. The authors' approach to the diagnosis of these low-grade disorders is to append the morphologic name to the FCM interpretation (e.g., "low-grade B-cell LPD/NHL, morphologically LPC lymphoma–leukemia"). Some of the relatively common disorders are presented next.

Most lymphoplasmacytoid malignancies have a nondescript antigenic profile (Figures 3.55 and 5.8). There is a high degree of variability in the expression of several antigens, such as the following:

Case study 76

1. Surface light chain: From weak to bright, depending on the degree of differentiation toward the plasma cell stage. Cytoplasmic immunoglobulins can also be detectable. The laborious FCM procedure for cytoplasmic heavy chains is rarely called for, as a serum IEP will yield the same information.
2. CD20 may be downregulated.

Case studies 14 and 77

3. CD5 and CD23: Although most cases do not express CD5, some display the pattern of $CD5^{+}CD23^{-}$ (Figure 4.44) similar to that associated with MCL. Weak CD20 and/or weak surface light chain expression, if present, help to avoid a potential misinterpretation. An occasional case may be $CD5^{+}CD23^{+}$; however, CD20 or a monoclonal surface light chain is brightly expressed (Figure 5.5).

The plasmacytoid cytology of the neoplastic cells in lymphoplasmacytoid neoplasms is best appreciated on well-prepared blood films (Plate 37a) or in uncrowded areas of any air-dried preparation. Cellular crowding or slow drying of the air-dried smears often results in the formation of hairs and villous projections (Plate 37b). The degree of basophilia varies from case to case. A small number of larger lymphoid cells is usually present. Rouleaux are evident if the M-protein (IgM in most instances) is sufficiently elevated, and the disease is then called Waldenstrom's macroglobulinemia. In many instances, the M-protein level is much lower than the artificial threshold set for Waldenstrom's, however. Indirect evidence of monoclonal hypergammaglobulinemia may be visible on the FCM graphics (Figure 5.8). On histologic sections, recognition of the plasmacytoid cytology is often hampered by the many artifacts associated with tissue fixation and processing (Plate 38).

Splenic lymphoma with villous lymphocytes has been described in the literature as a distinct entity on the basis of hairy and villous projections on neoplastic lymphoid cells. It is in the group of LPC malignancies, however, as a large number of cases are associated with monoclonal gammopathy. Emphasis in the literature has been on distinguishing splenic lymphoma with villous lymphocytes (SLVL) from HCL because of the "hairy cytology," the expression of CD11c, and, occasionally, CD25 or CD103 (Figures 3.56 and 5.9) positivity. The distinction is straightforward, however, in view of the characteristic phenotypic fingerprint of HCL (*see* Section 3.6.3.2), and the marked differences in the hematologic pictures between the two diseases.

In solid tissue, entities described as monocytoid B-cell lymphoma, marginal zone lymphoma, and MALT lymphoma also have a nondescript B-cell phenotype (Figure 4.42). In the lymph node, a serpentine pattern of infiltration of the interfollicular zone by bland-appearing neoplastic cells with ample pale cytoplasm (a hairy-cell-like cytology) and some admixed neutrophils are the main features helpful for recognizing monocytoid B-cell lymphoma (MBCL) morphologically (Plates 39 and 40). The histology may appear deceptively non-neoplastic, as prominent residual hyperplastic follicles are not uncommon. The tumor cells may also encircle residual follicles, thus forming a marginal zone pattern.

The term "marginal zone" implies that the germinal center and its mantle zone (which may be attenuated) are surrounded by another ring (layer) of cells. The marginal zone pattern can be produced by various neoplastic proliferations such as monocytoid B-cells or plasmacytoid lymphocytes, as well as the proliferation centers of CLL (Plate 41). It is thus unclear if the entity labeled "marginal zone lymphoma" is related to the other small B-cell lymphomas with a nondescript phenotype.

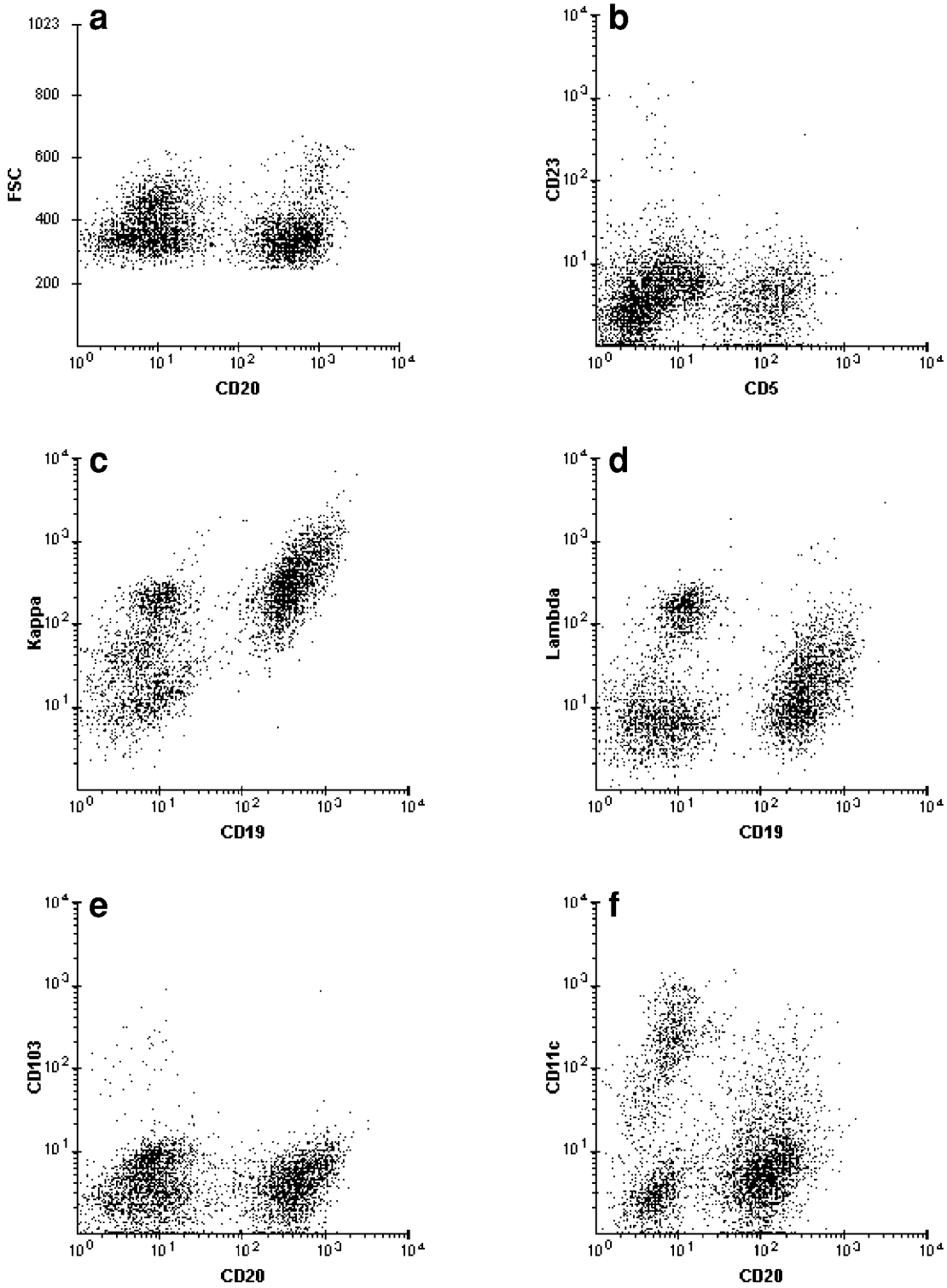

Figure 5.8 Peripheral blood with B-cell LPD/NHL NOS, morphologically LPC lymphoma–leukemia. (a–f) The cell size of the neoplastic cells is slightly larger than that of normal T-cells. A small subset displays higher FSC. The tumor cells lack CD5, CD23, and CD103. CD25 and CD10 are negative (not shown). CD11c is present in a small subset. Surface light chain (kappa) is well expressed. There is indirect evidence of hypergammaglobulinemia.

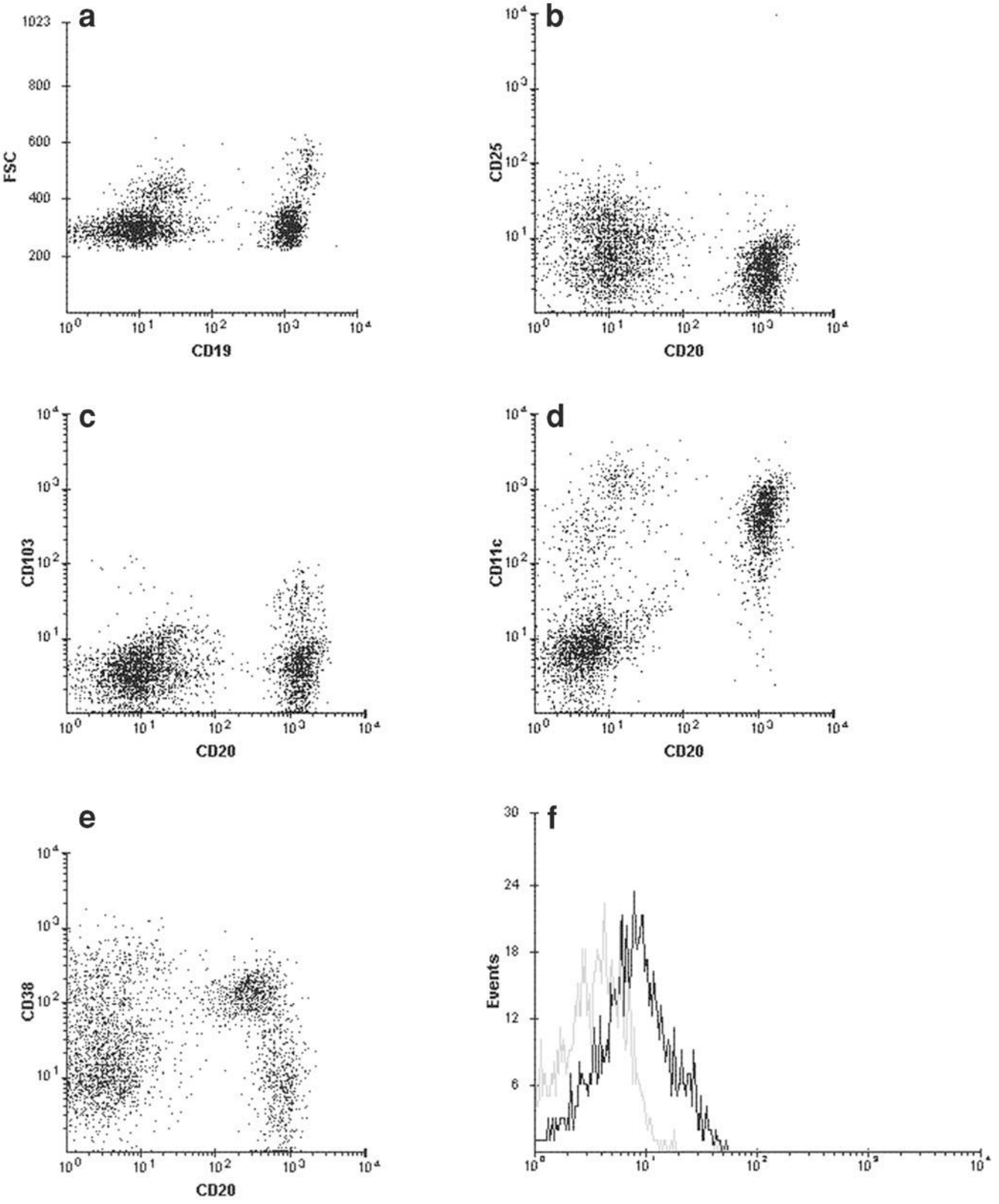

Figure 5.9 Peripheral blood with CD103-positive LPD NOS, morphologically LPC leukemia. Gated on MNCs: (a–f) Neoplastic cells comprise 20% of the cells in the sample. Most of the cells are of small cell size. CD25 is absent. A subset expresses CD103. CD11c is bright, but of variable distribution. The expression of CD38 is heterogeneous. Kappa is positive (weak) (f).

Small B-cell neoplasms in mucosal/glandular sites are known as MALT lymphomas. The minute size of the biopsies from these sites and the frequent dense inflammatory background are some of the factors precluding an optimal histologic assessment of these tumors, which, in turn, accounts for the difficulty of distinguishing MALT lymphoma from a reactive process morphologically. The clinical presentation and the ease of establishing the clonal (and thereby neoplastic) nature of the lymphoid cells by FCM immunophenotyping have made the diagnosis more straightforward, however.

5.2.1.8 Monoclonal B-cells of undetermined significance

An important issue in the bone marrow is the finding of a minute population of nondescript monoclonal B-cells in the range of 1–3% in elderly subjects. In the authors' experience, it is not infrequent for older individuals without any evidence of LPD/NHL to harbor a low level of monoclonal B-cells, asymptomatically and stable over the course of many years (10 years or more). The situation is analogous to MGUS. In these instances, knowledge of the clinical history is critical because the differential diagnosis is a low level of involvement by a B-cell LPD/NHL. Thus, in the absence of a positive clinical history, it is judicious to refrain from labeling the finding as lymphomatous involvement of the bone marrow. It is important, however, to review both the bone marrow aspirate smears and core biopsy sections to ensure that the low level of monoclonal cells in the FCM specimen is not due to sampling. Periodical clinical follow-up is also helpful.

5.2.2 Plasma cell dyscrasias

Case studies 56 and 57

The combined findings of a monoclonal cytoplasmic light chain and plasma cell morphology are adequate criteria for the diagnosis of a plasma cell dyscrasia. Other phenotypic characteristics include decreased CD45, downregulation or absence of pan B-cell antigens, and the expression of CD38 and CD56 (Figure 4.51). Phenotypic aberrancies (*see* Section 4.4.3) are not infrequent (Figures 4.52 and 4.53). The clinical diagnosis of multiple myeloma requires other clinical and laboratory data (e.g., the levels of the M-protein in the serum or urine) unless the bone marrow involvement is overt or neoplastic plasma cells are present in the peripheral blood (Plate 42).

Case study 78

Malignant plasma cells may be immature appearing (i.e., with dispersed chromatin and conspicuous nucleoli) and therefore referred to as plasmablasts (Plate 42). Extramedullary plasmacytomas with a high content of plasmablasts are referred to as anaplastic plasmacytomas. In some instances, the distinction between a plasmablastic proliferation, whether in the bone marrow or an extramedullary site, and a high-grade B-cell lymphoma with plasmablastic features may not be clear-cut. Plasmacytoma in the lymph node may present with an interfollicular pattern (i.e., containing residual reactive follicles). This morphology may be misinterpreted as the (infrequent) plasma cell variant of Castleman's disease.

5.2.3 T-Cell LPD/NHL

The systematic evaluation of T-cell antigens and DNA analysis by FCM can be applied to the diagnosis and grading of most mature T-cell neoplasms (*see* Section 3.6.4). The antigenic aberrancy can be subtle, such as a slight increase or decrease in the density of a pan-T-cell antigen (Figures 3.63, 3.64, 4.47, and 4.48). Where an aberrant phenotype is not evident (e.g., in indolent neoplastic LGL proliferations) molecular analysis of TCR gene rearrangements is helpful.

The majority of post-thymic T-cell neoplasms are CD4-positive. Many of the CD8-positive LPD/NHL also express one or more NK-associated antigens. The proportion of indolent vs aggressive mature T-cell neoplasms varies between different parts of the world.

Mature T-cell malignancies, especially those involving solid tissue, are currently classified into multiple subtypes. In many of these, the criteria for classification are primarily morphologic (e.g., angiocentric, angioimmunoblastic) or the names are derived from the sites of involvement (e.g., intestinal T-cell lymphoma). A biological classification of T-cell LPD/NHL, based on the antigenic characteristics and tumor grade, along with some very specific morphologic and/or clinical features would be more reproducible and less confusing. Using this approach, certain specific entities of mature T-cell malignancies can be recognized.

5.2.3.1 CD4+ T-cell LPD/NHL

Case studies 26 and 27

Adult T-cell leukemia–lymphoma (Plate 43 and Figure 3.69) and T-PLL (Plate 44; Figures 3.65 and 3.68) are the two most easily identifiable CD4+ T-cell disorders based on the combined immunologic and morphologic findings. The morphology of either disease is best appreciated in the peripheral blood, especially in ATLL, where the bone marrow involvement is invariably less obvious than the blood.

In contrast, recognition of Sezary syndrome may be less straightforward especially if the cerebriform cytology is not readily apparent and the level of abnormal lymphoid cells is low. On the other hand, cases with a large number of neoplastic cells and a high degree of nuclear irregularities may simulate the picture of ATLL (Plate 45). Circulating lymphoma cells from nodal based PTCL, although infrequent, can result in a blood picture similar to that in Sezary syndrome. Conversely, the lymph node picture in the advanced stages of mycosis fungoides/Sezary syndrome is that of a PTCL that cannot be distinguished from other nodal-based PTCLs. In addition to the loss of CD7 expression (the most frequent antigenic abnormality in Sezary syndrome), other corroborating laboratory/clinical data relating to the cutaneous lesions (Plate 46) are necessary to confirm the diagnosis.

Case studies 51–53

In addition to the above-mentioned disorders, the bulk of CD4+ T-cell malignancies consist of nodal-based PTCLs. The variability of several nonspecific features such as prominent vascularity, epithelioid histiocytes, and nuclear pleomorphism accounts for the diverse morphologic manifestations of PTCLs.

Case study 79

5.2.3.2 CD8+ disorders

CD8+ disorders can be further divided based on the expression of NK markers and the TCR/CD3 complex, into the subgroups of (1) suppressor T-cell (NK markers absent), (2) NK-like T-cell, and (3) true NK (TCR/CD3 complex absent) disorders. Each subgroup is heterogeneous and includes reactive conditions (*see* Section 4.1.2.3) as well as indolent and aggressive malignant disorders (*see* Section 3.6.5 and Section 4.4.2). The indolent neoplasms are found mainly in the blood and bone marrow and are composed of bland-appearing LGLs (Plate 47). The majority of cases display an NK-like T-cell, TCR-$\alpha\beta^+$, CD57+ phenotype (Figure 4.49). Similar to the reactive LGL proliferations, indolent CD3+ LGL leukemia has a high association with autoimmune disorders such as rheumatoid arthritis. Because of the similarities in phenotype, cytology and clinical picture, the differential diagnosis between indolent neoplastic and reactive LGL proliferations can be difficult, especially if the lymphocytosis is minimal. For those indolent cases in which the clinical and laboratory data (including molecular genetics) fail to establish the malignant nature of the process, a conservative approach of "watch and wait" is warranted.

Case studies 30, 54, and 55

As a group, aggressive CD8+ neoplasms are uncommon, although those with NK-associated antigens are found at high frequency in certain regions of the Far East and Central/South America, where the tumors also tend to be associated with EBV. The malignant nature of the

$CD8^+$ aggressive neoplasms can be easily recognized based on features such as aneuploidy, high S-phase, large cell size, or diffuse/extensive involvement. The cytology of the tumor cells on air-dried preparations is variable, depending on the quality of the cytoplasm (pale to basophilic) and the number and size of the azurophilic granules (Plate 48). As a result, the tumor cells often mimic the appearance of AML (especially AML-M5) when presenting in the blood or bone marrow (Plate 49). On tissue sections, the eye-catching feature is the ample pale cytoplasm (Plate 50). This is not a pathognomonic finding, however.

The current classification and terminology of $CD8^+$ neoplasms are confusing, especially for the tumors that express NK antigens. In many instances, a true NK or NK-like T-cell malignancy is referred to by different names (and therefore may be considered to be separate entities) depending on whether it presents in solid tissue sites (mostly extranodal) or the peripheral blood/bone marrow. Many of these tumors, such as angiocentric T-cell lymphoma, nasal lymphoma, panniculitis-like T-cell lymphoma, and aggressive LGL leukemia, share closely similar cytologic, biological, and clinical features, however. Furthermore, the neoplasm often quickly becomes systemic irrespective of its initial site of involvement. For these reasons, it would be preferable to designate these lymphomas/leukemias by their phenotypes (*see* Section 3.6.5) such as "true NK, $CD56^+$," or "NK-like T-cell, TCR-$\alpha\beta$, $CD56^+$," or "NK-like T-cell, TCR-$\gamma\delta$" (Figures 3.70, 3.71, and 3.72) instead of by the organ site or histologic features.

Case studies 28, 29, 31, and 32

5.2.3.3 $CD30^+$ lymphoma

Although the presence of CD30 (Figures 5.10 and 5.11) in a non-B-cell lymphoma suggests a so-called Ki-1 (CD30) lymphoma, this diagnosis needs to be rendered with caution. In some cases of CD30-lymphoma, the tumor cells have lost all pan T-cell antigens, thus displaying an apparent "null" phenotype. Tumors expressing this antigen are also referred to as anaplastic large cell lymphomas despite the fact that a substantial number of cases do not demonstrate a pleomorphic morphology (Plate 51). Because CD30 expression and pleomorphic features may occur in other post-thymic T-cell malignancies (e.g., in the late stages of mycosis fungoides [MF]) some other more specific criteria should be relied upon to define CD30 lymphoma. Currently, it appears that the diagnosis is best restricted to those lymphomas with the translocation (2;5). The advent of antibodies for detecting the expression of the chimeric NPM-ALK protein, a product of the t(2;5) associated with anaplastic large-cell lymphoma (ALCL), has facilitated the recognition of these tumors by immunohistochemistry.

Case study 80

5.3 FCM reporting

In the last critical step of the FCM study, the complexities of the FCM data are translated into a form that can be understood by clinicians and pathologists who may not always be familiar with hematopathology or flow cytometry. The goal is to package all of the relevant information in a short and concise report, so as to communicate the FCM data and diagnosis to other physicians most efficiently. The technical aspects (e.g., antibody–fluorochrome conjugation, three- vs four-color procedure) of FCM analysis as well as the FCM graphics can be omitted from the reports since few clinicians comprehend or care for these details. An example report is shown in Figure 5.12.

In addition to the information regarding the patient and the specimen, the FCM report for a hematologic neoplasm should include the following:

1. The proportion of the abnormal cells.
2. The cell size of the critical cells, especially for LPD/NHL.

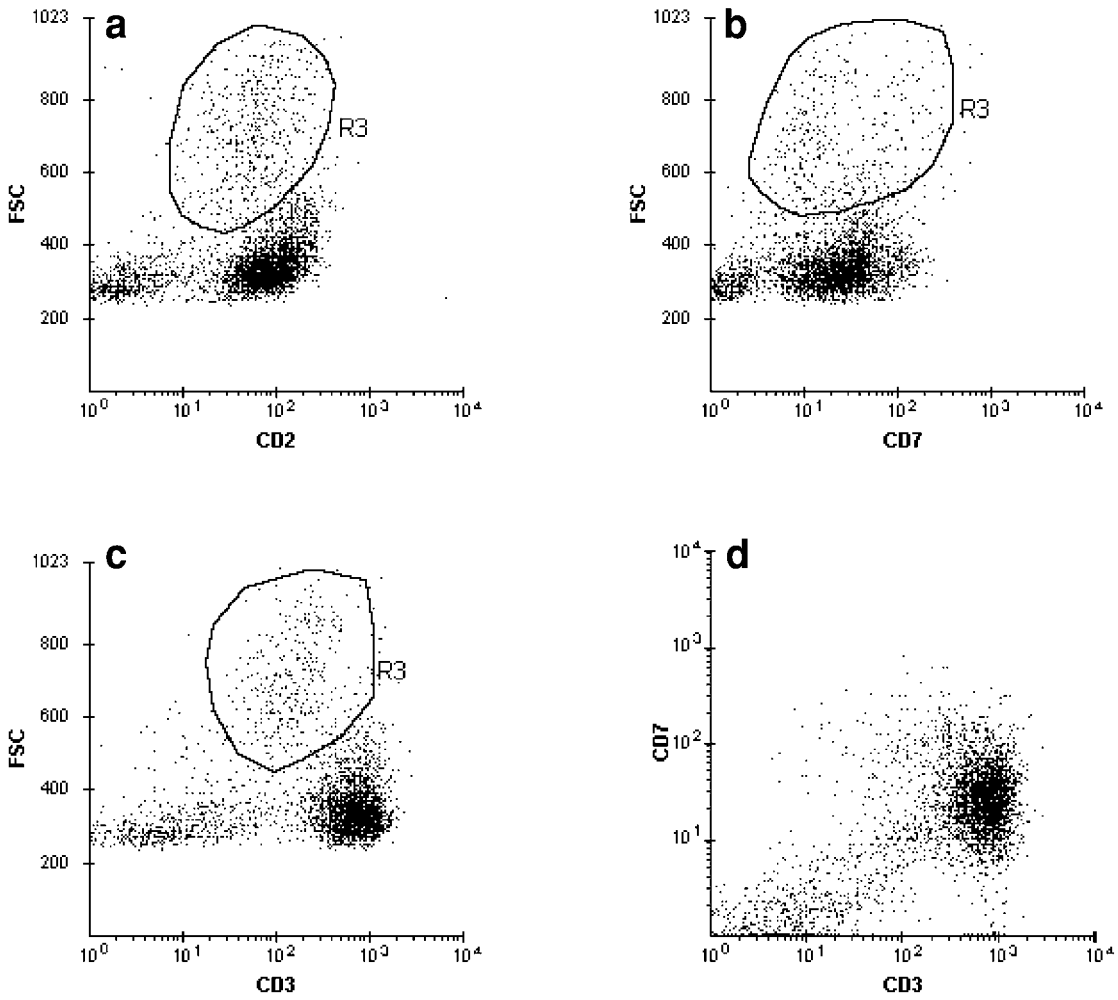

Figure 5.10 Lymph node with CD30⁺ lymphoma. (a–d) The tumor (R3) is of large cell size and comprises 12% of the cells analyzed. CD2 and CD7 are expressed. CD3 is slightly downregulated. The expression of CD7 and CD3 on the neoplastic cells can be better appreciated on the FSC/CD7 and FSC/CD3 displays. On CD7/CD3 dot plot, the neoplastic cells are obscured by the larger number of normal T-cells.

3. The ploidy and S-phase fraction (where applicable).
4. The markers evaluated.
5. The antigens expressed by the neoplastic cells, including the respective fluorescence intensities. This may be indicated in the form of a short textual description of the phenotype of the tumor.
6. A short description of the morphologic findings, including cytochemistry or immunohistochemistry results, if applicable.
7. The diagnosis or differential diagnosis based on the available FCM, morphologic, and clinical data.
8. Any additional comment if appropriate, such as in cases with low cell yield, poor viability, or when other additional laboratory tests are recommended.

For specimens without phenotypically abnormal cells, the FCM report can be a summary of the relative proportions of the various cell populations (e.g., granulocytes, monocytes, B-cells, T-cells). If present, qualitative abnormalities on the erythroid and myeloid precursors (e.g., altered myeloid maturation curves) should also be mentioned.

In general, the terminology employed for the diagnosis should reflect the lineage and maturation status of the neoplastic cells. In lymphomas, the grade (and thereby the proliferative

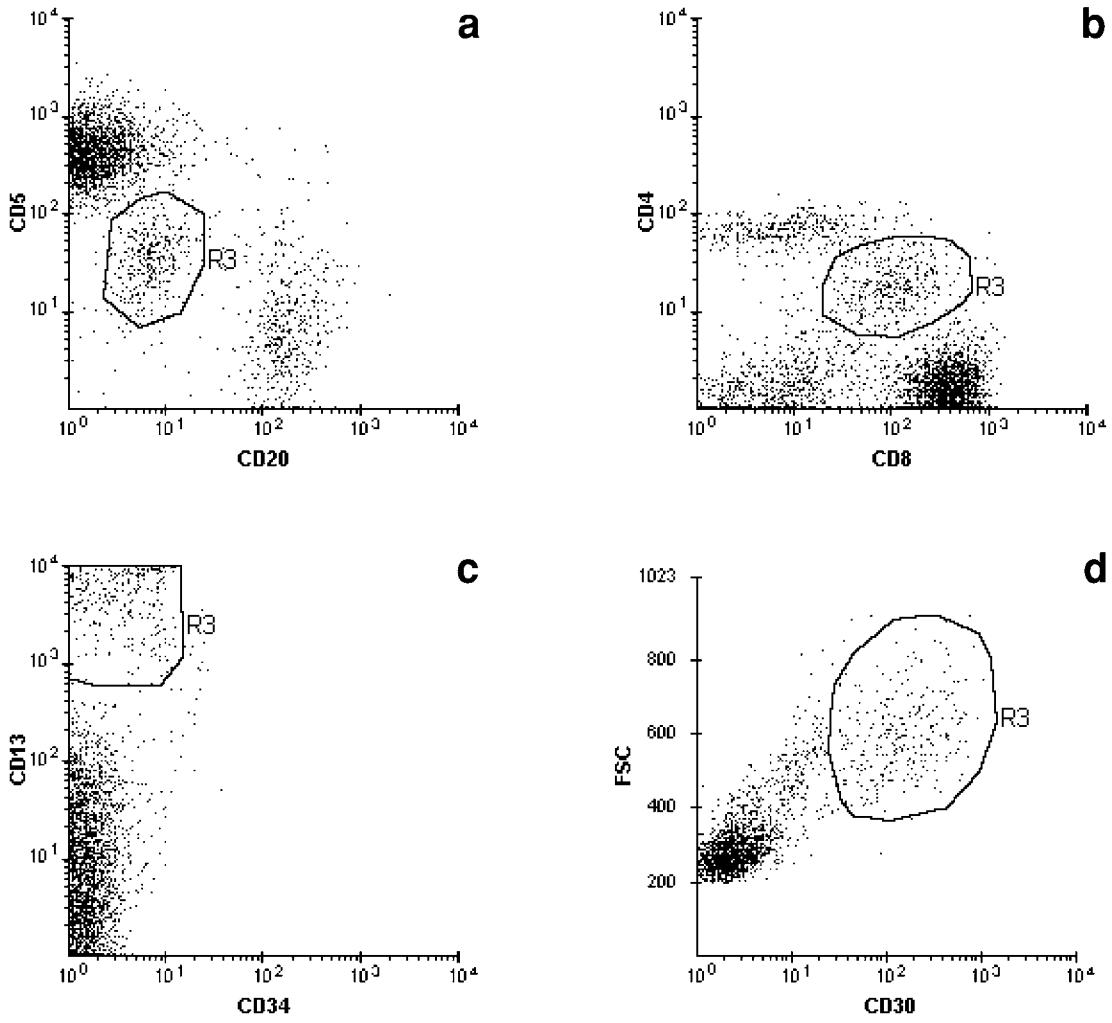

Figure 5.11 Lymph node with CD30+ lymphoma (continuation of Figure 5.10). (a–d) Neoplastic cells (R3) display downregulated CD5, and coexpression of CD4 and CD8. The intensity of CD4 and CD8 is less than that on normal CD4 and CD8 cells. The tumor cells express bright CD30. An unusual feature is the aberrant expression of CD13.

capacity) of the tumor as inferred from the cell size, CD71 reactivity, or the S-phase fraction should also be included. Where the conventional terminology is unsatisfactory, the authors prefer to use a more conservative and generic terminology instead. For instance, the statement "low-grade B-cell NHL with a nondescript B-cell phenotype" is preferred to "marginal zone lymphoma," especially if the specimen analyzed is the bone marrow or peripheral blood. This type of statement may not necessarily follow currently accepted (yet predictably volatile) classification schemes, but it reflects objectively the phenotype of the neoplastic cells.

FLOW CYTOMETRY IMMUNOPHENOTYPING ANALYSIS

Patient Name: Patient ID Number: Case Number:
Date of Birth: 11/14/1947 Gender: M Report Date:

Specimen Date: Specimen: Bone marrow

Clinical History: Follicular lymphoma treated with Rituxan.
? Bone marrow disease.

ANTIBODIES TESTED

Kappa	Negative	CD11b	Negative	CD34	Negative
Lambda	+ Moderate	CD11c	Negative	CD38	+ Dim
HLA-DR	+ Moderate	CD13	Negative	CD45	+ Bright
CD2	Negative	CD14	Negative	CD56	Negative
CD3	Negative	CD16	Negative	CD64	Negative
CD4	Negative	CD19	+ Moderate	CD103	Negative
CD5	Negative	CD20	Negative	CD117	Negative
CD7	Negative	CD23	Negative	CD138	Negative
CD8	Negative	CD25	Negative		
CD10	+ Dim	CD33	Negative		

Viability: 96% Cell yield: 20 million

Abnormal cells present by flow cytometry: Yes
Percentage of cells with abnormal phenotype: < 1%
Cell size: Small

PHENOTYPE: Monoclonal lambda CD10-positive B-cell population (0.3%).

MORPHOLOGY: Bone marrow aspirate and biopsy, normocellular with no overt abnormalities in the hematopoietic precursors.

DIAGNOSIS: A small population of monoclonal lambda B-cells is present in the bone marrow. The antigenic profile is consistent with follicular center cell lymphoma. In the context of the clinical history, the findings indicate minimal residual disease. The apparent "loss" of CD20 is secondary to anti-CD20 therapy.

NOTE: Molecular genetics pending.

Figure 5.12 An example of a FCM report. Information related to the patient has been omitted to preserve patient confidentiality. The clinical history was not provided initially and was obtained at the time when the FCM data and the bone marrow morphology were reviewed.

Suggested reading

Almasri NM, Iturraspe JA, and Braylan RC. CD10 expression in follicular lymphoma and large cell lymphoma is different from that of reactive lymph node follicles. Arch Pathol Lab Med 1998; 122:539–544.

Almasri NM, Duque RE, Iturraspe J, et al. Reduced expression of CD20 antigen as a characteristic marker for chronic lymphocytic leukemia. Am J Hematol 1992;40:259–263.

Arnulf B, Copie-Bergman C, Delfau-Larue M-H, et al. Nonhepatosplenic γδ T-cell lymphoma: a subset of cytotoxic lymphomas with mucosal or skin localization. Blood 1998;91:1723–1731.

Behm FG, Raimondi SC, Schell MJ, et al. Lack of CD45 on blast cells in childhood acute lymphoblastic leukemia is associated with chromosomal hyperdiploidy and other favorable prognostic features. Blood 1992;79:1011–1016.

Benharroch D, Meguerian-Bedoyan Z, Lamant L, et al. ALK-positive lymphoma: a single disease with a broad morphologic spectrum. Blood 1998;91:2076–2084.

Bennett JM, Catovsky D, Daniel M-T, et al. Proposals for the classification of chronic (mature) B and T lymphoid leukaemias. J Clin Pathol 1989;42:567–584.

Bogen SA, Pelley D, Charif M, et al. Immunophenotypic identification of Sezary cells in the peripheral blood. Am J Clin Pathol 1996;106:739–748.

Borowitz MJ, Bray R, Gascoyne R, et al. U.S.–Canadian consensus recommendations on the immunophenotypic analysis of hematologic neoplasia by flow cytometry: data analysis and interpretation. Cytometry (Commun Clin Cytometry) 1997;30:236–244.

Borowitz MJ, Shuster JJ, Civin CI, et al. Prognostic significance of CD34 expression in childhood B-precursor acute lymphoblastic leukemia: a Pediatric Oncology Group Study. J Clin Oncol 1990; 8:1380–1398.

Borowitz MJ, Guenther KL, Shults KE, and Stelzer GT. Immunophenotyping of acute leukemia by flow cytometric analysis. Use of CD45 and right-angle light scatter to gate on leukemic blasts in three color analysis. Am J Clin Pathol 1993;100:534–540.

Bouroncle BA. Thirty-five years in the progress of hairy cell leukemia. Leuk Lymphoma 1994;14(Suppl 1):1–12.

Bowen KL and Davis BH. Abnormal patterns of expression of CD16 (FCRgIII) and CD11b (CRIII) antigens by developing neutrophils in the bone marrow of patients with myelodysplastic syndrome. Lab Hematol 1997;3:292–298.

Braylan RC. Lymphomas. In: Bauer KD, Duque, RE, Shankey TV, eds. Clinical Flow Cytometry: Principles and Application. Philadelphia: Lippincott,Williams & Wilkins, 1993:203–234.

Braylan RC and Benson NA. Flow cytometric analysis of lymphomas. Arch Pathol Lab Med 1989;113:627–633.

Braylan RC, Benson NA, and Iturraspe J. Analysis of lymphomas by flow cytometry. Current and emerging strategies. Ann NY Acad Sci 1993;677:364–378.

Braylan RC, Atwater SK, Diamond LW, et al. U.S.–Canadian consensus recommendations on the immunophenotypic analysis of hematologic neoplasia by flow cytometry: data reporting. Cytometry (Commun Clin Cytometry) 1997;30:245–248.

Braylan RC, Orfao A, Borowitz MJ, and Davis BH. Optimal number of reagents required to evaluate hematolymphoid neoplasias: Results of an international consensus study. Cytometry (Commun Clin Cytometry) 2001;46:23–27.

Burke JS. Are there site-specific differences among the MALT lymphomas—morphologic, clinical? Am J Clin Pathol 1999;111(Suppl 1):S133–S143.

Campana D and Coutan-Smith E. Detection of minimal residual disease in acute leukemia by flow cytometry. Cytometry (Commun Clin Cytometry) 1999;38:139–152.

Carulli G, Gianfaldoni ML, Azzara A, et al. FcRIII (CD16) expression on neutrophils from chronic myeloid leukemia: a flow cytometric study. Leuk Res 1992;16:1203–1209.

Chen J-S, Coutan-Smith E, Suzuki T, et al. Identification of novel markers for monitoring minimal residual disease in acute lymphoblastic leukemia. Blood 2001;97:2115–2120.
Christensson B, Lindemalm C, Johansson B, et al. Flow cytometric DNA analysis: a prognostic tool in non-Hodgkin's lymphoma. Leuk Res 1989;13:307–314.
Cooke CB, Krenacs L, Tetler-Stevenson M, et al. Hepatosplenic T-cell lymphoma; a distinct clinicopathologic entity of cytotoxic γδ T-cell origin. Blood 1996;88:265–274.
Cornfield DB, Mitchell DM, Almasri NM, et al. Follicular lymphoma can be distinguished from benign follicular hyperplasia by flow cytometry using simultaneous staining of cytoplasmic bcl-2 and cell surface CD20. Am J Clin Pathol 2000;114:258–263.
Coutan-Smith E, Sancho J, Hankcock ML, et al. Clinical importance in minimal residual disease in childhood acute lymphoblastic leukemia. Blood 2000;96:2691–2696.
Damle RN, Wasil T, Fais F, et al. Ig V gene mutation status and CD38 expression as novel prognostic indicators in chronic lymphocytic leukemia. Blood 1999;94:1840–1847.
Davis BH, Foucar K, Szczarkowski W, et al. U.S.–Canadian consensus recommendations on the immunophenotypic analysis of hematologic neoplasia by flow cytometry: medical indications. Cytometry (Commun Clin Cytometry) 1997;30:249–263.
Delmer A, Ajchenbaum-Cymbalista F, Tang R, et al. Over-expression of cyclin D1 in chronic B-cell malignancies with abnormality of chromosome 11q13. Br J Haematol 1995;89:798–804.
Diamond LW, Bearman RM, Berry PK. et al. Prolymphocytic leukemia: flow microfluorometric, immunologic, and cytogenetic observations. Am J Hematol 1980;9:319–330.
Doherty PC. The function of γδ T-cells. Br J Haematol 1992;81:321–324.
Duque RE, Andreeff M, Braylan RC, et al. Consensus review of the clinical utility of DNA flow cytometry in neoplastic hematopathology. Cytometry 1993;14:492–496.
Dunphy CH, Dunphy FR, and Visconti JL. Flow cytometric immunophenotyping of bone marrow core biopsies. Report of 8 patients with previously undiagnosed hematologic malignancy and failed bone marrow aspiration. Arch Pathol Lab Med 1999;123:206–212.
Dworzak MN, Fritsch G, Fleischer C, et al. Multiparameter phenotype mapping of normal and post-chemotherapy B lymphopoiesis in pediatric bone marrow. Leukemia 1997;11:1266–1273.
Falini B, Pileri S, Zinzani PL, et al. ALK+ lymphomas: clinico-pathological findings and outcome. Blood 1999;93:2697–2706.
Gentile TC, Uner AH, Hutchison RE, et al. CD3+, CD56+ aggressive variant of large granular lymphocyte leukemia. Blood 1994;84:2315–2321.
Harada H, Kawano MM, Huang N, et al. Phenotypic difference of normal plasma cells from mature myeloma cells. Blood 1993;81:2658–2663.
Huebl W, Iturraspe J, and Braylan RC. FMC7 antigen expression on normal and malignant B-cells can be predicted by expression of CD20. Cytometry (Commun Clin Cytometry) 1998;34:71–74.
Hurwitz CA, Raimondi SC, Head D, et al. Distinctive immunophenotypic features of t(8,21)(q22;q22) acute myeloblastic leukemia in children. Blood 1992;12:3182–3188.
Jaffe ES. Classification of NK cell and NK-like T-cell malignancies. Blood 1996;87:1207–1210.
Jennings CD and Foon KA. Recent advances in flow cytometry: application to the diagnosis of hematologic malignancy. Blood 1997;90:2863–2892.
Kabutomori O, Iwatani I, Koh T, et al. CD16 antigen density on neutrophils in chronic myeloproliferative disorders. Am J Clin Pathol 1997;107:661–664.
Kita K, Nakase K, Miwa H, et al. Phenotypical characteristics of acute myelocytic leukemia associated with the t(8;21)(q22;q22) chromosomal abnormality: frequent expression of immature B-cell antigen CD19 together with stem cell antigen CD34. Blood 1992;80:470–477.
Koike T. Megakaryoblastic leukemia: the characterization and identification of megakaryoblasts. Blood 1984;64:683–692.
Koo CH, Rappaport H, Sheibani K, et al. Imprint cytology of non-Hodgkin's lymphomas. Based on a study of 212 immunologically characterized cases. Hum Pathol 1989;20(Suppl 1):1–138.
Krasinskas AM, Wasik MA, Kamoun M, et al. The usefulness of CD64, other monocyte-associated antigens, and CD45 gating in the subclassification of acute myeloid leukemias with monocytic differentiation. Am J Clin Pathol 1998;110:797–805.
Leclercq G and Plum J. Thymic and extrathymic T cell development. Leukemia 1996;10:1853–1859.
Loken MR, Shah VD, Dattilio KL, and Civin CI. Flow cytometric analysis of human bone marrow. II. Normal B lymphocyte development. Blood 1987;70:1316–1324.
Longacre TA, Foucar K, Crago S, et al. Hematogones: a multiparameter analysis of bone marrow precursor cells. Blood 1989;72:543–552.
Look AT, Roberson PK, Williams DL, et al. Prognostic importance of blast cell DNA content in childhood acute lymphoblastic leukemia. Blood 1985;65:1079–1086.

Loughran TP Jr. Clonal diseases of large granular lymphocytes. Blood 1993;82:1–14.
Macon WR, Williams ME, Greer JP, et al. Natural killer-like T-cell lymphomas: aggressive lymphomas of T-large granular lymphocytes. Blood 1996;87:1474–1483.
Malec M, Bjorklund E, Soderhall S, et al. Flow Cytometry and allele-specific oligonucleotide PCR are equally effective in detection of minimal residual disease in ALL. Leukemia 2000;15:716–727.
Matutes E, Brito-Babapulle V, Swansbury J, et al. Clinical and laboratory features of 78 cases of T-prolymphocytic leukemia. Blood 1991;78:3269–3274.
Matutes E, Oscier J, Garcia-Marco J, et al. Trisomy 12 defines a group of CLL with atypical morphology: correlation between cytogenetic, clinical and laboratory features in 544 patients. Br J Haematol 1996;92:382–388.
Nathwani BN. Diagnostic significance of morphologic patterns of lymphoid proliferations in lymph nodes. In: Knowles DM, ed. Neoplastic Hematopathology. Philadelphia: Lippincott Williams & Wilkins, 2000:507–536.
Nguyen D, Moskowitz FB, and Diamond LW. Potential diagnostic pitfalls caused by blood film artifacts in prolymphocytic leukaemia. Observations in two cases. Br J Biomed Sci 1994;51: 371–374.
Nguyen DT and Diamond LW. Diagnostic Hematology: A Pattern Approach. London: Arnold, 2000.
Nguyen DT, Diamond LW, Schwonzen M, et al. Chronic lymphocytic leukaemia with an interfollicular architecture: avoiding diagnostic confusion with monocytoid B-cell lymphoma. Leuk Lymphoma 1995;18:179–184.
Ocqueteau M, Orfao A, Almeida J, et al. Immunophenotypic characterization of plasma cells from monoclonal gammopathy of undetermined significance patients. Implications for the differential diagnosis between MGUS and multiple myeloma. Am J Pathol 1998;152:1655–1665.
Ocqueteau M, Orfao A, Garcia-Sanz R, et al. Expression of the CD117 on normal and myelomatous plasma cells. Br J Haematol 1996;95:489–493.
Orfao A, Chillon MC, Botolucci AM, et al. The flow cytometric pattern of CD34, CD15 and CD13 expression in acute myeloblastic leukemia is highly characteristic of the presence of PML-RARα gene rearrangements. Haematologica 1999;84:405–412.
Richards SJ, Sivakumaran M, Parapia LA, et al. A distinct large granular lymphocyte (LGL)/NK-associated (NKa) abnormality characterized by membrane CD4 and CD8 coexpression. Br J Haematol 1992; 82:494–501.
Robertson MJ and Ritz J. Biology and clinical relevance of human natural killer cells. Blood 1990;76:2421–2438.
San Miguel JF, Martinez A, Macedo A, et al. Immunophenotyping investigation of minimal residual disease is a useful approach for predicting relapse in acute myeloid leukemia patients. Blood 1997;90:2465–2470.
San Miguel JF, Vidriales MB, Lopez-Berges C, et al. Early immunophenotypical evaluation of minimal residual disease in acute myeloid leukemia identifies different patient risk groups and may contribute to postinduction treatment stratification. Blood 2001;98:1746–1751.
Shin SS and Sheibani K. Monocytoid B-cell lymphoma. Am J Clin Pathol 1993;99:421–425.
Smets LA, Homan-Blok J, Hart A, et al. Prognostic implication of hyperdiploidy as based on DNA flow cytometric measurement in childhood acute lymphocytic leukemia—a multicenter study. Leukemia 1987;1:163–166.
Spiekermann K, Emmendoerffer A, Elsner J, et al. Altered surface marker expression and function of G-CSF-induced neutrophils from test subjects and patients under chemotherapy. Br J Haematol 1996;87:31–38.
Spits H, Lanier LL, and Phillips JH. Development of human T- and natural-killer cells. Blood 1995; 85:2654–2670.
Steltzer GT, Shults KE, and Loken MR. CD45 gating for routine flow cytometric analysis of human bone marrow specimens. Ann NY Acad Sci 1993;677:265–279.
Stelzer GT, Marti G, Hurley A, et al. U.S.–Canadian consensus recommendations on the immunophenotypic analysis of hematologic neoplasia by flow cytometry: standardization and validation of laboratory procedures. Cytometry (Commun Clin Cytometry) 1997;30:214–230.
Stetler-Stevenson M, Arthur DC, Jabbour N, et al. Diagnostic utility of flow cytometric immunophenotyping in myelodysplastic syndrome. Blood 2001;98:979–987.
Stewart CC, Behm FG, Carey JL, et al. U.S.–Canadian consensus recommendations on the immunophenotypic analysis of hematologic neoplasia by flow cytometry: selection of antibody combinations. Cytometry (Commun Clin Cytometry) 1997;30:231–235.
Tefferi A, Li C-Y, Witzig TE, et al. Chronic natural killer cell lymphocytosis: a descriptive clinical study. Blood 1994;84:2721–2725.

Terstappen LWMM and Loken MR. Myeloid cell differentiation in normal bone marrow and acute myeloid leukemia assessed by multi-dimensional flow cytometry. Anal Cell Pathol 1990;2:229–240.

Terstappen LWMM, Huang S, and Picker LJ. Flow cytometric assessment of human T-cell differentiation in thymus and bone marrow. Blood 1992;79:666–677.

Terstappen LWMM, Safford M, and Loken MR. Flow cytometric analysis of human bone marrow III. Neutrophil maturation. Leukemia 1990;4:657–663.

Terstappen LWMM, Safford M, Koeemann S, et al. Flow cytometric characterization of acute myeloid leukemia . Part II. Phenotypic heterogeneity at diagnosis. Leukemia 1991;5:757–767.

The Non-Hodgkin's Lymphoma Classification Project. A clinical evaluation of the International lymphoma Study Group classification of non-Hodgkin's lymphoma. Blood 1997;89:3909–3918.

Vandersteenhoven AM, Williams JE, and Borowitz MJ. Marrow B-cell precursors are increased in lymphomas or systemic diseases associated with B-cell dysfunction. Am J Clin Pathol 1993;100:60–66.

Wells DA, Sale GE, Shulman HM, et al. Multidimensional flow cytometry of marrow can differentiate leukemic from normal lymphoblasts and myeloblasts after chemotherapy and bone marrow transplantation. Am J Clin Pathol 1998;110:84–94.

Appendix: Installing and using the case studies CD-ROM

This monograph, *Flow Cytometry in Hematopathology: A Visual Approach to Data Analysis and Interpretation*, is accompanied by a CD-ROM with 80 case studies.

The case studies are designed for computers running Windows 32-bit operating systems (Windows 95 or newer). They require a minimum screen resolution of 1024 × 768 and have been optimized for 16 million colors (24-bit). Your computer must be capable of displaying at least 65,000 colors (16-bit) at 1024 × 768 in order to view the photomicrographs properly.

The programs require the installation of the 32-bit Borland Database Engine (BDE). In addition, a database alias "FCMCaseData" must be created (instructions given below). A database alias tells the BDE which directory the databases are installed in (i.e., the path).

Note: To install the BDE, the install program must be able to write files to the Windows system directories. Therefore, the attributes of your system's C:\Windows and C:\Windows\System directories must not be "read only." You can check the attributes of these directories in Windows Explorer by right-clicking on the directory and choosing "properties."

To install the case studies, insert the CD-ROM and run setup.exe.

There are three installation options:

1. **Typical (recommended)**: This option installs the BDE, programs, and databases and automatically sets the database alias. This option requires approximately 580 MB of disk space on your hard disk drive.
2. **Compact**: This option installs the BDE only, allowing you to run the programs directly from the CD-ROM. This option requires approximately 10 MB of disk space on your hard disk drive.
   Note: You must modify/create the database alias (FCMCaseData) manually if you choose this option.
3. **Custom**: This option allows you to choose whether to install the BDE. If your computer already has the 32-bit version of the BDE installed (e.g., you are already using Paradox for Windows), you can deselect (uncheck) BDE installation and install only the programs and databases to your hard disk drive. *Note*: You must create the database alias manually if you choose this option. If the BDE is already installed and you choose to run the programs from the CD-ROM, then you do not have to run the installation program, but you still must create the database alias manually.

Make sure that you reboot your computer at the end of installation to ensure that the case studies program will run properly.

Instructions to create a database alias (FCMCaseData)

1. Run the BDE Administrator (BDEADMIN.EXE).
2. In the left panel, make sure that the Databases tab is selected.
3. Check the left panel to see if the alias "FCMCaseData" exists. If it exists, then skip to the section "Modifying an alias."
4. If the alias does not already exist, then select "New..." from the Object menu.
5. When the "New database alias" dialog appears, leave the Database driver name as STANDARD and click "OK."
6. In the left panel, change the name "STANDARD1" to "FCMCaseData" (without the quotes) and then hit the "Enter" key.
7. In the right panel, click on the field next to Path. Type in the directory where the database programs are installed. For example, if you are running the programs directly from the CD-ROM, then type

"F:\Databases" (where "F" is the drive letter of your CD-ROM). Make sure that the text you typed in (e.g., "F:\Databases") is selected by hitting the "Enter" key or clicking below the text.

8. From the Object menu, choose "Apply."
9. When the confirmation dialog appears, click on "OK."
10. Close the BDE Administrator.

Modifying an alias

To modify an existing FCMCaseData alias using the BDE Administrator, make sure that the case studies program is closed. Follow steps 1 and 2 above and then choose FCMCaseData from the databases list box in the left panel by clicking on the word "FCMCaseData". Do not click on the "+" sign. To modify the path, follow steps 7–10.

Troubleshooting: If, when you are editing the database alias, the text is locked or the setting will not save, check to see if the alias icon in the left panel has a yellow/green box around it. If it has, the database engine has locked the alias and it cannot be edited. Right-click on the alias icon and select "Close". This will clear the lock and allow the alias to be edited.

Using the case studies

The case studies are very simple to use. If you choose a compact installation and are running the program from the CD-ROM, you will find FCMCaseStudies.exe in the "Program" folder on the CD-ROM, and can use Explorer or "My Computer", to start the program. Once the program (FCMCaseStudies.exe) is running, simply choose the case study that you wish to open using the drop-down list in the tool bar at the top of the screen. Clicking on the microscope icons in the tool bar allows you to display any photomicrographs associated with the case. The FCM graphics and explanations for each case are presented in a series of tabbed pages with up to six graphics per page. Simply click on the tab (FCM Graphics 1, FCM Graphics 2, etc.) to see the graphics on that page.

Troubleshooting: With the latest Windows operating systems, setting the "Keep the taskbar on top of other windows" property can rob you of vertical space, causing the top of the program window to be partially cut-off. If you experience this difficulty, simply uncheck "Keep the taskbar on top of other windows" and/or check "Auto-hide the taskbar", which will restore the full vertical space to your screen.

Installing and running the case studies on a network

For network operation, the databases and program can exist on a server. Each client workstation needs its own copy of the BDE. To install on a network, do the following:

1. On the server: Install according to the instructions shown above but choose a "Custom" installation and uncheck the BDE option to install only the databases and program.
2. On each client workstation: Install according to the instructions shown above but choose a "Compact" installation to install only the BDE on the client workstations.
3. On each client, map a drive letter to the root directory of the server (or make note of the drive letter if it already exists).
4. Using the earlier instructions to create a database alias, create an alias to "FCMCaseData" on each client workstation.

> **Example**. If the databases and programs were installed with the default options, they exist in the directory "C:\FCM Case Studies" on the server. If the server's root directory ("C:\") is mapped to drive "K:" on the client workstation, then the path that you would enter for the "FCMCaseData" alias would be "K:\FCM Case Studies."

5. The BDE installation (using the default parameters) will create an "FCM Case Studies" folder on each workstation. Add a shortcut to the program located on the server (e.g., "K:\FCM Case Studies\FCMCaseStudies.exe") to the "FCM Case Studies" folder on each client workstation.

Limited warranty and disclaimer

Humana Press Inc. warrants the CD-ROM contained herein to be free of defects in materials and workmanship for a period of thirty days from the date of the book's purchase. If within this thirty day period Humana Press receives written notification of defects in materials or workmanship, and such notification is determined by Humana Press to be valid, the defective disk will be replaced. In no event shall Humana Press or the contributors to this CD-ROM be liable for any damages whatsoever arising from the use or inability to use the files contained therein.

The authors of this book have used their best efforts in preparing this material. Neither the authors nor the publisher make warranties of any kind, express or implied, with regard to these programs or the documentation contained within this CD-ROM, including, without limitation, warranties of merchantability or fitness for a particular purpose. No liability is accepted in any event, for any damages including incidental or consequential damages, lost profits, costs of lost data or program material, or otherwise in connection with or arising out of the furnishing, performance, or use of the files on this CD-ROM.

Index

Flow Cytometry in Hematophathology

A Visual Approach to Data Analysis and Interpretation

Doyen Nguyen, MD
Lawrence W. Diamond, MD
Raul C. Braylan, MD
University of Florida College of Medicine, Gainesville, FL

Although instrumentation and laboratory techniques for flow cytometry (FCM) immunophenotyping of hematologic malignancies are well documented, there is relatively little information on how best to perform data analysis, a critical step in FCM testing. In *Flow Cytometry in Hematopathology: A Visual Approach to Data Analysis and Interpretation*, three physicians highly experienced in laboratory hematopathology and FCM offer a unique systematic approach to FCM data analysis and interpretation based on the visual inspection of dual parameter FCM graphics. This step-by-step approach to optimal FCM data analysis is demonstrated by means of numerous FCM graphics derived from actual well-documented clinical cases. The authors include notes on "tricks of the trade" and pitfalls to avoid. The discussion, covering leukemias, lymphomas, and other conditions, moves from simple to complex specimens, with an emphasis on visual pattern analysis. The companion CD-ROM with 80 detailed case studies provides additional opportunities to gain a deeper understanding of FCM data analysis.

Richly illustrated and highly instructive, *Flow Cytometry in Hematopathology: A Visual Approach to Data Analysis and Interpretation* offers clinical pathologists, hematopathologists, and specialists in laboratory medicine a much-needed guide with a practical and logical approach for sharpening their FCM data analysis skills on a wide spectrum of hematologic disorders.

- **Step-by-step methods for flow cytometry data analysis and interpretation**
- **Emphasis on visual pattern analysis**
- **Coverage of both acute leukemias and malignant lymphomas**
- **CD-ROM with 80 case studies illustrating a wide variety of hematologic disorders**
- **Extensive FCM graphics, including DNA content determinations in malignant lymphomas**

CONTENTS

Flow Cytometry in Hematopathology
A Visual Approach to Data Analysis and Interpretation
ISBN: 1-58829-212-6
humanapress.com

ISBN 1-58829-212-6
9 0 0 0 0
9 781588 292124